eCAM
Evidence-Based Complementary and Alternative Medicine

History and Current Status of Evidence-Based Korean Medicine

Guest Editors: Seong-Gyu Ko, Bharat B. Aggarwal, Mingyao Liu, Chang Shik Yin, Dong Hoon Jin, and Bo-Hyoung Jang

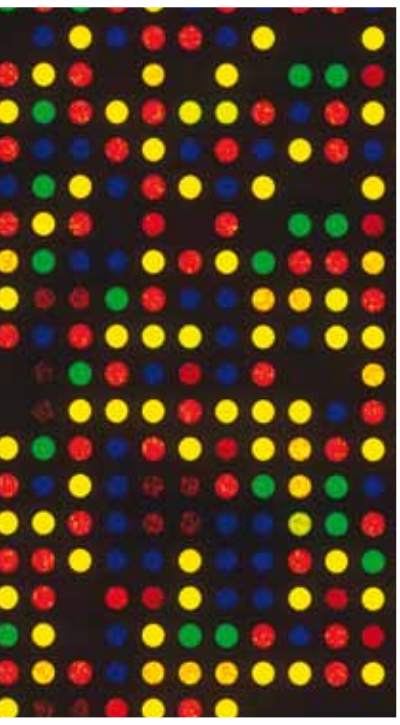

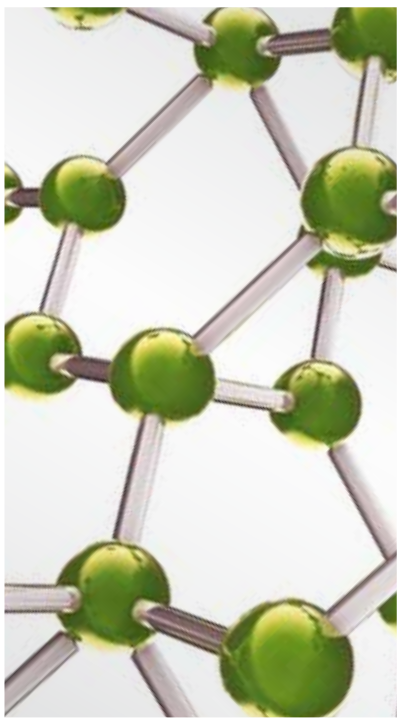


History and Current Status of Evidence-Based Korean Medicine

Evidence-Based Complementary and Alternative Medicine

History and Current Status of Evidence-Based Korean Medicine

Guest Editors: Seong-Gyu Ko, Bharat B. Aggarwal, Mingyao Liu, Chang Shik Yin, Dong Hoon Jin, and Bo-Hyoung Jang

Editorial Board

Contents

Hindawi Publishing Corporation
Evidence-Based Complementary and Alternative Medicine
Volume 2014, Article ID 503867, 2 pages
http://dx.doi.org/10.1155/2014/503867

Editorial

History and Current Status of Evidence-Based Korean Medicine

Seong-Gyu Ko,[1] Bharat B. Aggarwal,[2] Mingyao Liu,[3] Chang Shik Yin,[4] Dong Hoon Jin,[5] and Bo-Hyoung Jang[6]

[1] *Laboratory of Clinical Biology and Pharmacogenomics and Center for Clinical Research and Genomics, Kyung Hee University, Seoul 130-701, Republic of Korea*
[2] *Department of Experimental Therapeutics, The University of Texas M. D. Anderson Cancer Center, 1901 East Road, Houston, TX 77054, USA*
[3] *School of Life Science and Institute of Biomedical Science, East China Normal University, Shanghai 200241, China*
[4] *Acupuncture and Meridian Science Research Center, Kyung Hee University, Seoul 130-701, Republic of Korea*
[5] *Institute for Innovative Cancer Research, Asan Institute for Life Sciences, Asan Medical Center, University of Ulsan College of Medicine, Seoul 138-736, Republic of Korea*
[6] *Office of Health Services Research, National Evidence-Based Healthcare Collaborating Agency, Seoul 110-450, Republic of Korea*

Correspondence should be addressed to Seong-Gyu Ko; epiko@khu.ac.kr

Received 15 January 2014; Accepted 15 January 2014; Published 15 April 2014

The biomedical effects of natural products have been increasingly identified. Korean medicine originates from prehistoric times and shares its origin with Chinese medicine. However, Korean medicine, compared with the Chinese medicine, is not well known relatively. Though Korean medicine and Chinese medicine have a lot in common, Korean medicine has developed its own realm by developing unique approaches and research—"Four-Constitution (Sasang Constitutional) Medicine" as one of the diagnostic tools and Saam acupuncture as one of the treatments. In recent years, Korean medicine expanded its usages, thus, by integrating both traditional and modern approaches. Korean medicine covers many complementary and alternative approaches that are actively validated and developed. These efforts in the field of Korean medicine have been, and will be, an important contribution to the evidence-based complementary and alternative medicine.

This special issue will introduce you to the history and current status of evidence-based Korean medicine with a focus on the recent developments. The following is a brief overview of the articles in this special issue.

Biological activities of a compound or a mixture of herbal medicines in Korean medicine are explored on such conditions as nephrotoxicity, experimental colitis, vasoconstriction, cancer cell growth, multidrug resistant cancer cell growth, neutropenia, obesity and adipogenesis, adipocyte differentiation, cartilage degradation in arthritis, and inflammatory neuronal damage or on such an effect as stimulating osteogenic differentiation of bone marrow mesenchymal stem cells. For the sake of safe and effective use of herbal medicine in Korean medicine, potential interaction has to be cleared. Interaction between herb and herb or between herb and drug was investigated. Traditional rules on combining herbs for synergistic effect were validated. Effects on cytochrome P450 enzyme mediated drug metabolism were investigated in relation to herbal mixture. Randomized controlled trials were reported on the effect of Korean herbal medicine on dysmenorrhea and obesity.

A new real-time measurement system using a wireless inertial measurement unit was developed and reported to be reliable and effective in measuring three-dimensional cervical spine movements. As an effort to explore the diagnostic concept of Korean medicine, conceptual perception on pattern identification was explored with regard to a phlegm pattern. Recent developments on voice-based approach to Four-Constitution Medicine were reviewed. Tinnitus patients treated in Korean medicine clinic were shown to be on sympathetic overactivity with chronic tinnitus more affecting the autonomic indices.

In this special issue, several newly developed treatments are also introduced. The effect of cosmetic acupuncture was explored on facial elasticity in an open-label, single-arm pilot study. The effect of newly developed temporomandibular joint therapy targeting the postural Yin-Yang balance of the whole body was documented in a case series study. Detoxification program involving fasting, fluid administration, acupuncture, and herbal wet wrap dressing was reported to be positive for refractory cases of atopic dermatitis. As an exploration on varied application of herbal medicine, it was found to be safe and effective in hypertensive blood pressure when applied as enema agent. These therapies warrant further study with more rigid study design.

Seong-Gyu Ko
Bharat B. Aggarwal
Mingyao Liu
Chang Shik Yin
Dong Hoon Jin
Bo-Hyoung Jang

Hindawi Publishing Corporation
Evidence-Based Complementary and Alternative Medicine
Volume 2014, Article ID 740515, 6 pages
http://dx.doi.org/10.1155/2014/740515

Review Article

Introduction to the History and Current Status of Evidence-Based Korean Medicine: A Unique Integrated System of Allopathic and Holistic Medicine

Chang Shik Yin[1] and Seong-Gyu Ko[2]

[1] *Acupuncture and Meridian Science Research Center, Kyung Hee University, Seoul 130-701, Republic of Korea*
[2] *Department of Preventive Medicine, Center for Clinical Research and Drug Development, Institution for Korean Medicine, Kyung Hee University, Seoul 130-701, Republic of Korea*

Correspondence should be addressed to Seong-Gyu Ko; epiko@khu.ac.kr

Received 3 December 2013; Revised 9 January 2014; Accepted 10 January 2014; Published 14 April 2014

Academic Editor: Bo-Hyoung Jang

Objectives. Korean medicine, an integrated allopathic and traditional medicine, has developed unique characteristics and has been active in contributing to evidence-based medicine. Recent developments in Korean medicine have not been as well disseminated as traditional Chinese medicine. This introduction to recent developments in Korean medicine will draw attention to, and facilitate, the advancement of evidence-based complementary alternative medicine (CAM). *Methods and Results*. The history of and recent developments in Korean medicine as evidence-based medicine are explored through discussions on the development of a national standard classification of diseases and study reports, ranging from basic research to newly developed clinical therapies. A national standard classification of diseases has been developed and revised serially into an integrated classification of Western allopathic and traditional holistic medicine disease entities. Standard disease classifications offer a starting point for the reliable gathering of evidence and provide a representative example of the unique status of evidence-based Korean medicine as an integration of Western allopathic medicine and traditional holistic medicine. *Conclusions*. Recent developments in evidence-based Korean medicine show a unique development in evidence-based medicine, adopting both Western allopathic and holistic traditional medicine. It is expected that Korean medicine will continue to be an important contributor to evidence-based medicine, encompassing conventional and complementary approaches.

1. Introduction

Korean medicine originates from prehistoric times and shares its origins with Chinese and Japanese medicine. However, compared with traditional Chinese medicine, Korean medicine is much less well-known. Although Korean and Chinese medicine have much in common, Korean medicine has developed on its own as a whole-person-centered medicine system [1], developing unique concepts and research, with "Four Constitution" (Sasang constitutional) medicine [2] and Saam acupuncture [3] being representative of genuinely Korean developments. In recent years, Korean medicine has become part of a national health system and its use has expanded [4]. Thus, by integrating traditional and modern approaches, Korean medicine constitutes an exemplary case of a national health system that encompasses many complementary and alternative approaches and has been active in validating and developing them.

What follows is a brief introduction to the characteristics of Korean medicine with a focus on evidence-based approaches, along with a historical review of a standard disease classification in Korean medicine as a representative example of the efforts being made to implement evidence-based medicine.

2. Korean Medicine: Tailored, Simple, and Practical

As indicated previously, the tradition of Korean medicine features an individualized approach based on constitutional

energy traits of healthy qi [3], with simple and practical solutions, based on these underlying energy traits or core principles [5]. Qi and tao are the core principles that the body and the environment are composed of and by which both of them function [6]. Korean medicine places importance on self-discipline, a constitutional approach, and the three treasures (essence, qi, and spirit) deep in the axis of life [7] and focuses on the power and active response of the healthy qi as innate intelligence, intricately linked with constitutional characteristics and human dignity, which may be reflected and evaluated differentially in a pattern of systemic manifestations, including disease-specific ones that are directly linked to the pathology and nonspecific ones that may be remote from the lesion, with no apparent linkage to the pathology. These nonspecific characteristics may reflect the response of the body to the pathology rather than the pathology itself.

3. Challenges in Evidence-Based Approaches to CAM

Evidence-based medicine is about the best decision-making based on the best available evidence [8] and highlights a science and practice of medicine with a firm basis of evidence [9]. The evidence may vary in its hierarchical status and extent, but there may not be any strong opposition to the concept of a medicine being established and practiced based on stronger evidence. The evidence-based approach is rapidly gaining acceptance and expanding its realm, not only in academic [10, 11] or clinical activities but also with regard to regulation and insurance issues [12]. Complementary and integrative medicine is not an exception, even though there are many barriers, like the prioritization of classical books and practice as evidence sources [13].

In addition to the idea that traditional knowledge itself is an important source of evidence [14], the issue of evidence-based medicine is considered to be more challenging in the field of complementary and integrative medicine than in the field of the conventional allopathic medicine. Although a lack of research evidence for efficacy is said not to be evidence of a lack of efficacy [15], the main challenge is, of course, primarily due to the relative scarcity of evidence in the field of complementary and integrative medicine. However, in addition to the scarcity, it may be partially due to differences in the theoretical context and philosophical perspectives between complementary and integrative medicine and conventional allopathic medicine. This conceptual difference is accompanied naturally by differences in clinical practice. The theoretical context and clinical practice of complementary and integrative medicine have been handed down from the past or have developed from clinical experience rather than from the widely accepted current knowledge of modern biology, science, and technology, as is the case in orthodox allopathic medicine in which measurements are devised and performed on the basis of theoretical context, clinical practice, and technology and are linked directly with the production of high-quality scientific evidence [16]. Differences in the theoretical context, clinical practice, and measurements, in addition to the scarcity of evidence, complicate the issue of an evidence-based approach in the fields of complementary and integrative medicine.

4. Korean Medicine: An Exemplary Case in Evidence-Based Medicine

In the history of complementary and integrative medicine, Korea's situation may be a unique and exemplary case. Although many countries still lack national regulation of CAM, Korea established the parallel operation of two independent medical systems (Western medicine and Korean medicine) [17] in 1951, a rare instance whereby complementary and integrative approaches have been officially part of the national health system from the very start. In Korea, there is no generalist equivalent to a general physician in other countries. Each physician belongs to one of the two specialty professions: Western allopathic medicine or Korean medicine. Korean medicine is a specialty profession in which modern allopathic medicine and traditional, complementary approaches are integrated into a profession of modern holistic medicine. Only a few physicians satisfy the required educational and regulatory processes for both professions and receive both licenses from the government. Each is fully licensed to diagnose and treat patients and is independent in practicing medicine.

Korean medicine may be described as a form of integration of Western allopathic medicine and traditional medicine by considering the following points. (1) Educational programs for Korean medicine students and practitioners cover not only traditional knowledge but also the same basic and clinical medical sciences and research as in Western medicine. (2) Korean medicine practitioners are fully licensed to diagnose both disease entities of Western medicine origin and those of traditional medicine origin. (3) Treatment modalities provided by Korean medicine practitioners include those common in both Western and traditional medicine, as well as those specific to traditional medicine, such as acupuncture and yinyang balance concepts.

The Korean government has been promoting the evidence-based development of the national health system, especially with regard to Korean medicine, by means of standardization, research funding, and new drug development from herbal medicines. The Korean government has been expanding its research funding for such projects as Korean medicine diagnosis [18, 19] and new drug development from traditional herbal medicines [20, 21]. The Korean government invested a total of about 400 million US dollars during the first period to foster and develop Korean traditional medicine (2006–2010), with 63% invested in research and development projects, and planned to invest a total of about 1 billion US dollars during the 2nd period (2011–2015), with 34% invested in research and development projects [4].

As a fundamental platform for an evidence-based approach in modern Korean medicine, the history of a standard disease classification is briefly examined here. A standard disease classification alone does not mean, and cannot justify, the notion that Korean medicine is an evidence-based

approach. However, a standard disease classification may be an indispensable fundamental basis for evidence-based medicine.

5. Standard Disease Classification in Korean Medicine

If any evidence of medical practice is collected, interpreted, and incorporated into evidence-based medicine, the clinical pictures of that medicine have to be captured, classified, and documented. A clinical picture that has not been captured and documented may not be used as evidence. If we are to capture the clinical picture of different systems of medicine, we may need different classification systems of the clinical entities targeted, evaluated, and treated with each system of medicine.

In an effort to capture the clinical picture and produce statistics on allopathic medicine and Korean medicine, different disease classification systems have been developed and stipulated as national standards in Korea. In the allopathic medicine field, a Korean adaptation of the World Health Organization (WHO) international classification of diseases (ICD) has been stipulated as the allopathic medicine volume for the Korean standard classification of diseases (KCD). The first edition of KCD appeared in 1952. It was revised in 1972, 1979, 1993, 2002, 2007, and 2010. In the Korean medicine field, the Korean medicine volume of KCD was first published in 1973 and was revised in 1979, 1995, and 2009. Recently, the KCD allopathic medicine volume and the KCD Korean medicine volume were integrated into one volume, "KCD6" in 2010 [22].

Although pattern identification for the overall analysis of symptoms and signs is a core component of the theoretical context and clinical practice of Korean medicine as well as traditional medicine in China [23] and Japan, the traditional way of pattern identification is still being developed as a standardized, validated diagnostic tool. A recent revision of the KCD Korean medicine volume (2009), which was then integrated into KCD6 in 2010, differed from previous revisions in several aspects. First, the hierarchy and appropriateness of the classification were thoroughly revised and improved. Second, the issue of possible overlap between allopathic medical entities and Korean medical entities was addressed in great detail and every effort was made to remove possible overlap. Possibly overlapping Korean medicine entities were replaced with existing KCD allopathic medicine entities. The remaining entities of genuine Korean medicine were classified under "U" codes. The genuine Korean medicine entities were classified into three categories: 97 diseases, 191 patterns/syndromes, and 18 diseases-patterns/syndromes from "Four Constitution" medicine. This may have been the first attempt in the history of disease classification in which a national standard successfully integrated allopathic medicine entities and genuine traditional medicine entities into one classification that is widely applicable to all major regulations, such as the national health insurance system, national health statistics, and the traffic accident insurance system.

In the Joseon dynasty, about four centuries ago, there was already a comprehensive disease classification, which was usually composed of descriptions on related anatomy, physiology, etiology, manifestations, pattern differentiation, self-discipline, qigong, and the simple herbs prescribed. However, the concepts of diseases, disorders, and patterns were not so clearly defined or differentiated [24]. Over the course of serial revisions to Korean medicine disease classifications in the 20th and 21st centuries, the concepts of diseases, disorders, and patterns have been differentiated more explicitly, with the differentiation concepts embodied in the classification structure and entities classified. In a recent revision, many traditional medicine codes were replaced with allopathic medicine codes, with the remaining classification of genuine traditional medicine diseases, disorders, and patterns fully and systematically integrated with the allopathic medicine classification.

Recently, WHO has also sought to integrate the International Classification of Traditional Medicine (ICTM) [25] into its standard classification of diseases (ICD) when revising ICD-10 to ICD-11 with the concept of ontology-based disease classification by 2015 [26]. KCD, the integrated classification of diseases encompassing allopathic medicine codes and genuine Korean medicine codes, was a valuable source for the WHO project. Indeed, it is an important issue in the ICD revision project that ICD categories are listed in a mutually exclusive and jointly exhaustive way to make them useful for such purposes as mortality statistics and morbidity statistics [27], which were also considered in the revision of KCD.

The standard classification of diseases will be an essential part of capturing the clinical pictures of medicine and a systematically organized classification will facilitate objective documentation, production of related statistics, and the contribution of complementary and integrative approaches to the general health of world citizens. In that sense, Korea's experiences in revising the national standard disease classification may well be an exemplary case to support and embody an evidence-based approach in institutionalizing complementary and integrative approaches and integrating them with conventional allopathic medicine.

6. Disorder and Pattern Coding in Korean Medicine

According to the coding guidelines for the WHO ICD-10, a main condition is defined as the condition primarily responsible for the patient's need for treatment or investigation. A main condition is diagnosed at the end of the episode of health care. If there is more than one condition that may be considered as a "main condition," the one that was most responsible for the greatest use of resources is selected as a "main condition." If no diagnosis was considered to be made, the main symptom or problem may be selected as a "main condition" [28].

Disease codes of Korean medicine are a combined form of Western medicine codes and traditional Korean medicine codes. Korean medicine codes are regulated by the law.

According to the existing guideline for Korean medicine classifications [29], the followings are generally recommended.

In the first place, a "main condition" code is selected. Disease classification codes may be selected from the conventional Western medicine codes based on the conditions that patients appeal most or the amount of resources consumed in the clinical management. If the practicing physician does not consider the conventional Western medicine codes to be appropriate for the clinical picture of the patient, then the traditional Korean medicine codes, that is, U-codes in KCD, are used. When traditional Korean medicine codes in the U-codes are considered to be appropriate, the practicing physician should decide which category codes in the traditional Korean medicine codes are appropriate for the clinical picture of the patient: disorder codes, pattern codes, or "Four Constitution" medicine-related codes [29]. In addition to the "main condition," other conditions that coexist or develop during the episode of health care and affect the management of the patient may also be listed [28]. In Korean medicine, codes for other conditions, as well as a code for a main condition, may be selected from both areas of Western medicine classification codes and traditional Korean medicine classification codes.

By following this practice, the practicing physician in Korean medicine may select a code that is considered to be most appropriate for the clinical picture of the patient, not only from the conventional Western medicine codes, but also from the traditional Korean medicine codes. Thus, selected disease coding may reflect the body of knowledge in Western medicine disease classification and traditional Korean medicine disease classification. In this sense, Korean medicine may be considered as an integration of conventional allopathic medicine and traditional holistic medicine.

A disease may be a set of dysfunctions in any of the body systems that may be defined by symptomatology, etiology, course and outcome, treatment response, linkage to genetic factors, and linkage to interacting environmental factors. A disorder/syndrome may be defined as a common pattern of similar symptoms in clinical practice. As to a disorder/syndrome, the etiology is not known or multiple etiologies are related in the clinical manifestations [27].

Disorders and patterns in traditional Korean medicine that are coded in the clinical practice of Korean medicine are the health care conditions that are responsible for the patient's need for treatment or investigation. Both the disorder and the pattern are diagnosed for the sake of treatment or investigation by practicing physician. Both are similar in that they are named after the body structures, causes, properties, severity, and so forth. However, the naming and concept of the disorder and the pattern in traditional Korean medicine usually deal with differential aspects of clinical pictures based on the theories of traditional medicine:

(i) A disorder in traditional medicine is a clinical picture that is relatively constant throughout the duration of that disorder. A pattern in traditional medicine is relatively temporary (constant/temporary).

(ii) A disorder in traditional medicine usually delivers information reflecting the local manifestation of the pathology. A pattern in traditional medicine usually delivers information reflecting the systemic manifestation or the systemic response of the patient (local/systemic, pathology/patient).

(iii) A disorder in traditional medicine is a concept that summarizes findings that are specific to the pathologic process under investigation. A pattern in traditional medicine means the pattern of combination of the manifestations that encompasses both specific symptoms/signs and nonspecific findings such as pulse diagnosis and tongue diagnosis (specific/nonspecific).

(iv) A disorder may be applied for a time span. A disorder coding may be based on the main pathologic process which may show a causal relationship with the main manifestations in the patient. A pattern may be applied for a specific time span too. However, a pattern coding is based on the summarized whole picture that may be observed in the patient based on the perspectives of traditional medicine theories. A pattern is recognized based on the analysis of the systemic findings in the patient's body and mind which reflect the pathologic processes, responses to the pathologic processes, other concomitant findings, and innate or acquired constitutional traits of the patient (linear/multifactorial).

(v) A disorder in traditional medicine is usually described with general terms of anatomy-physiology together with terms of signs and symptoms. A pattern in traditional medicine is usually described in terms of the traditional medicine theories that are used to summarize the whole picture findings in the patients such as yin and yang balance, cold and heat, meridian, or constitution (general/theoretical).

(vi) A disorder in traditional medicine is used to describe the general characteristics considered to be relatively common to general population. A pattern in traditional medicine is used to describe the individual characteristics considered to be relatively specific to the patient at that time (commonality/individuality).

The concept of a pattern may reflect constitutional characteristics of the patient in addition to the disease or disorder characteristics. In other words, the systemic active response and individual characteristics of the patient's body and mind may be the target of the concept of a pattern diagnosed in traditional Korean medicine. However, the disorder in traditional Korean medicine and the disorder or disease in conventional Western medicine primarily target the disordered or pathologic process itself disregarding the patient that is actively trying to recover from that disordered process and to maintain balanced state of health. Considering the abovementioned concepts, the pattern and the disorder-disease may be considered as two complementary aspects that may be targeted when trying to capture the clinical picture of health care conditions.

7. Conclusions

Korean medicine has been an active player, at the forefront, in the implementation of evidence-based medicine. Korean medicine, an integrated conventional allopathic medicine and traditional holistic medicine, is exemplary in developing complementary and integrative approaches into an essential part of evidence-based mainstream medicine, implementing a national standard disease classification encompassing both allopathic and genuine traditional concepts. In this paper, recent developments regarding the biological activities of herbal medicines, diagnostic evaluations, and clinical applications are introduced. Korean medicine is expected to be an important contributor to the establishment and implementation of evidence-based, tailored medicine, integrating complementary and conventional approaches.

Conflict of Interests

There is no conflict of interests in this study.

Acknowledgment

This study was supported by a Grant of the Korea Healthcare Technology and Korean Medicine R&D Project, Ministry of Health & Welfare, Republic of Korea (A120642 and B120014).

References

[1] W. S. Cha, J. H. Oh, H. J. Park, S. W. Ahn, S. Y. Hong, and N. I. Kim, "Historical difference between traditional Korean medicine and traditional Chinese medicine," *Neurological Research*, vol. 29, supplement 1, pp. S5–S9, 2007.

[2] J. Lee, Y. Jung, J. Yoo, E. Lee, and B. Koh, "Perspective of the human body in sasang constitutional medicine," *Evidence-Based Complementary and Alternative Medicine*, vol. 6, supplement 1, pp. 31–41, 2009.

[3] C. Yin, H. J. Park, Y. Chae et al., "Korean acupuncture: the individualized and practical acupuncture," *Neurological Research*, vol. 29, supplement 1, pp. S10–S15, 2007.

[4] Ministry of Health & Welfare, *2nd 5-Year Comprehensive Plan to Foster and Develop Korean Traditional Medicine*, Ministry of Health & Welfare, 2011.

[5] J.-H. Won, "A study on the value of Donguibogam in medical science," *Korean Journal of Jangseogak Royal Library*, vol. 24, pp. 39–57, 2010.

[6] M.-L. Kim, "A study on the view of nursing life in the Donguibogam," *Philosophy and Culture*, vol. 18, pp. 63–106, 2009.

[7] N. I. Kim, "A study on the bodily perspective of Donguibogam," *The Journal of Humanities*, vol. 18, pp. 39–61, 2010.

[8] P. Squara, "Systematic approach: an evidence management strategy for better decision-making," *Journal of Evidence-Based Medicine*, vol. 6, no. 2, pp. 109–114, 2013.

[9] X. Liao and N. Robinson, "Methodological approaches to developing and establishing the body of evidence on post-marketing Chinese medicine safety," *Chinese Journal of Integrative Medicine*, vol. 19, no. 7, pp. 494–497, 2013.

[10] L. Steenfeldt and J. Hughes, "An evidence-based course in complementary medicines," *The American Journal of Pharmaceutical Education*, vol. 76, no. 10, article 200, 2012.

[11] P. F. Kotur, "Introduction of evidence-based medicine in undergraduate medical curriculum for development of professional competencies in medical students," *Current Opinion in Anaesthesiology*, vol. 25, no. 6, pp. 719–723, 2012.

[12] S. Yuan, Y. Liu, N. Li et al., "Impacts of health insurance benefit design on percutaneous coronary intervention use and inpatient costs among patients with acute myocardial infarction in Shanghai, China," *PharmacoEconomics*, vol. 32, no. 3, pp. 265–275, 2014.

[13] W. Spence and N. Li, "An exploration of traditional Chinese medicine practitioners' perceptions of evidence based medicine," *Complementary Therapies in Clinical Practice*, vol. 19, no. 2, pp. 63–68, 2013.

[14] A. Helmstadter and C. Staiger, "Traditional use of medicinal agents: a valid source of evidence," *Drug Discovery Today*, vol. 19, no. 1, pp. 4–7, 2014.

[15] M. Yakoot, "Bridging the gap between alternative medicine and evidence-based medicine," *Journal of Pharmacology and Pharmacotherapeutics*, vol. 4, no. 2, pp. 83–85, 2013.

[16] L. McClimans, "The role of measurement in establishing evidence," *Journal of Medicine and Philosophy*, vol. 38, no. 5, pp. 520–538, 2013.

[17] G. Bodeker, "Lessons on integration from the developing world's experience," *The British Medical Journal*, vol. 322, no. 7279, pp. 164–167, 2001.

[18] B. K. Kang, T. Y. Park, J. A. Lee et al., "Reliability and validity of the Korean standard pattern identification for stroke (K-SPI-Stroke) questionnaire," *BMC Complementary and Alternative Medicine*, vol. 12, article 55, 2012.

[19] M. M. Ko, J. A. Lee, B. K. Kang, T. Y. Park, J. Lee, and M. S. Lee, "Interobserver reliability of tongue diagnosis using traditional Korean medicine for stroke patients," *Evidence-Based Complementary and Alternative Medicine*, vol. 2012, Article ID 209345, 6 pages, 2012.

[20] J. Choi, J. Lee, S. H. Kim, J. Kim, and S. Kim, "PG201 downregulates the production of nitrite by upregulating heme oxygenase-1 expression through the control of phosphatidylinositol 3-kinase and NF-E2-related factor 2," *Nitric Oxide*, vol. 33, pp. 42–55, 2013.

[21] S. S. Shin, M. Jin, H. J. Jung et al., "Suppressive effects of PG201, an ethanol extract from herbs, on collagen-induced arthritis in mice," *Rheumatology*, vol. 42, no. 5, pp. 665–672, 2003.

[22] Statistics Korea, "Introduction to the Classification of Diseases," http://kostat.go.kr.

[23] B. C. Shin, S. Kim, and Y. H. Cho, "Syndrome pattern and its application in parallel randomized controlled trials," *Chinese Journal of Integrative Medicine*, vol. 19, no. 3, pp. 163–171, 2013.

[24] W. Y. Chung, "Study of basic theory on the name of disease and the standardization of disease classification," *Korean Journal of Oriental Medical Pathology*, vol. 12, no. 1, pp. 82–95, 1998.

[25] P. Gao and K. Watanabe, "Introduction of the World Health Organization project of the international classification of traditional medicine," *Journal of Chinese Integrative Medicine*, vol. 9, no. 11, pp. 1161–1164, 2011.

[26] World Health Organization, "The International Classification of Diseases 11th Revision is due by 2015," http://www.who.int/classifications/icd/revision/icd11faq/en/index.html.

[27] World Health Organization, *ICD-11 Alpha Content Model Reference Guide, 11th Revision*, World Health Organization, Geneva, Switzerland, 2011.

[28] World Health Organization, *International Statistical Classification of Diseases and Related Health Problems, 10th Revision*, vol. 2 of *Instruction Manual*, 2010.

[29] Statistics Korea, *Diseases Coding Guidelines—Korean Standard Classification of Diseases (KCD)*, 2012.

Hindawi Publishing Corporation
Evidence-Based Complementary and Alternative Medicine
Volume 2013, Article ID 475386, 10 pages
http://dx.doi.org/10.1155/2013/475386

Research Article

Rubi Fructus (*Rubus coreanus*) Inhibits Differentiation to Adipocytes in 3T3-L1 Cells

Mi-Young Jeong,[1] Hye-Lin Kim,[2] Jinbong Park,[2] Hyo-Jin An,[3] Sung-Hoon Kim,[2] Su-Jin Kim,[4] Hong-Seob So,[5] Raekil Park,[5] Jae-Young Um,[2] and Seung-Heon Hong[1]

[1] *Department of Oriental Pharmacy, College of Pharmacy, Wonkwang-Oriental Medicines Research Institute, Wonkwang University, Jeonbuk 570-749, Republic of Korea*
[2] *College of Korean Medicine, Institute of Korean Medicine, Kyung Hee University, 1 Hoegi-Dong, Dongdaemun-gu, Seoul 130-701, Republic of Korea*
[3] *Department of Pharmacology, College of Oriental Medicine, Sangji University, Wonju-si, Gangwon-do 220-702, Republic of Korea*
[4] *Department of Cosmeceutical Science, Daegu Hanny University, Yugok-dong, Kyungsan 712-715, Republic of Korea*
[5] *Center for Metabolic Function Regulation, Wonkwang University, Iksan, Jeonbuk 570-749, Republic of Korea*

Correspondence should be addressed to Jae-Young Um; jyum@khu.ac.kr and Seung-Heon Hong; jooklim@wku.ac.kr

Received 2 April 2013; Revised 14 August 2013; Accepted 21 August 2013

Academic Editor: Seong-Gyu Ko

Rubi Fructus (RF) is known to exert several pharmacological effects including antitumor, antioxidant, and anti-inflammatory activities. However, its antiobesity effect has not been reported yet. This study was focused on the antidifferentiation effect of RF extract on 3T3-L1 preadipocytes. When 3T3-L1 preadipocytes were differentiating into adipocytes, 10–100 μg/mL of RF was added. Next, the lipid contents were quantified by Oil Red O staining. RF significantly reduced lipid accumulation and downregulated the expression of peroxisome proliferator-activated receptor γ (PPARγ), CCAAT0-enhancer-binding proteins α (C/EBPα), adipocyte fatty acid-binding protein 2 (aP2), resistin, and adiponectin in ways that were concentration dependent. Moreover, RF markedly upregulated liver kinase B1 and AMP-activated protein kinase (AMPK). Interestingly, pretreatment with AMPKα siRNA and RF downregulated the expression of PPARγ and C/EBPα protein as well as the adipocyte differentiation. Our study shows that RF is capable of inhibiting the differentiation of 3T3-L1 adipocytes through the modulation of PPARγ, C/EBPα, and AMPK, suggesting that it has a potential for therapeutic application in the treatment or prevention of obesity.

1. Introduction

Obesity is associated with many diseases inducing diabetes, dyslipidemia, and atherosclerosis, which are risk factors for metabolic syndrome [1]. Obesity is a condition in which excess body fat has accumulated due to lipids changing into adipocytes and an increase in the number of differentiated mature cells which are regulated by genetic and environmental factors such as nutrients [2–4]. Understanding the mechanism through which a particular nutrient affects the differentiation to adipocytes would help to prevent the initiation and progression of obesity. The 3T3-L1 cell line is one of the best-characterized and reliable models for studying the conversion of preadipocytes into adipocytes. Adipocyte differentiation is a complex process involving coordinated expression of specific genes and proteins associated with each stage of adipogenesis [5, 6].

Peroxisome proliferator-activated receptor γ (PPARγ) and CCAAT-enhancer-binding protein α (C/EBPα) have been known to play a key role in the regulation of adipogenesis and in the modulation of fat cell function in adipose tissue. PPARγ, a member of the PPAR subfamily of nuclear hormone receptors, was identified as a component of a differentiation-dependent regulatory factor and a far-cell-specific enhancer of the adipocyte fatty acid-binding protein (aP2) gene [7, 8]. Another major protein in obesity regulation, C/EBPα, a member of a large family of leucine zipper transcription factors, plays an important role in induction of terminal adipocyte differentiation [9, 10]. PPARγ and C/EBPα are not

expressed in preadipocytes but are activated during adipocyte differentiation. PPARγ and C/EBPα are expressed prior to the expression of most adipocyte genes and regulate the expression of genes involved in creating and maintaining adipocytes, including aP2 and resistin [11, 12].

AMP-activated protein kinase (AMPK) is a serine/threonine protein kinase that is widely expressed in eukaryotes. AMPK, composed of α, β, and γ subunits, is a key player in energy homeostasis. The α subunit is the catalytic subunit, and its activation via the phosphorylation of the threonine residue 172 by the upstream liver kinase B1 (LKB1) is crucial for AMPK activation under ATP-depleted conditions [13]. When the intracellular AMP/ATP ratio increases because of the metabolic stress, AMPK is phosphorylated. Subsequently, downstream target molecules are activated, promoting catabolism. When the intracellular AMP/ATP ratio decreases, AMPK increases the anabolism. AMPK is associated with adipocyte differentiation via AMPK activation in 3T3-L1 adipocytes [14, 15]. In addition, AMPK inhibits the accumulation of fat by modulating downstream substrate acetyl-CoA carboxylase (ACC) [16].

Rubi Fructus (RF), the fruit of *Rubus coreanus* Miquel (Rosaceae), is a type of red raspberry from southern Korea. The dried fruit are used in traditional herbal medicine for the treatment of impotence, spermatorrhea, enuresis, and asthma [17]. RF includes functional constituents that include flavonoids, anthocyanin, polyphenols, niga-ichigoside F1, 23-hydroxytormentic acid, and gallic acid [18, 19]. It has been found that these constituents show anticarcinogenic, antinociceptive, antioxidant, and anti-inflammatory effects [20, 21]. Even though numerous biological activities of RF have been reported, there is limited evidence for its antiobesity effect. In this study, we evaluated the inhibitory effect of the water extract of RF and investigated how it acts to reduce differentiation to adipocytes in 3T3-L1 mouse fibroblasts.

2. Materials and Methods

2.1. Preparation of RF. Dried and ground powder of RF, the fruit of *Rubus coreanus* Miquel (Rosaceae), was kindly provided by Kyung Hee Oriental Hospital (Seoul, Republic of Korea). To prepare the aqueous extract, the water-soluble components of the RF powder were extracted with water (100 g/L of water) by heating at 100°C for 3 h. The boiled solution was filtered through Whatman filter paper, and the filtrates were lyophilized. The resulting powder was used as the crude total extract of the fruit. Total extracts were dissolved in water for cell treatment. The crude extract (10 g) was subsequently partitioned between ethyl acetate (EtOAc) and distilled water. The EtOAc fraction was concentrated under reduced pressure in a rotary evaporator and lyophilized. The EtOAc fractions were dissolved with DMSO, filtered using sterilized syringe filter through a 0.22 μm membrane pore, and stored at −20°C before use.

2.2. Reagents. Dulbecco's modified Eagle's medium (DMEM), penicillin-streptomycin, fetal calf serum (FCS), and fetal bovine serum (FBS) were from Gibco BRL (Grand Island, NY, USA). Insulin, 3-isobutylmethylxanthine (IBMX), and dexamethasone (DEX) were purchased from Sigma Chemical Co. (St. Louis, MO, USA). Anti-C/EBPα, anti-resistin, and anti-GAPDH antibodies were purchased from Santa Cruz Biotechnology (Santa Cruz, CA, USA). Anti-PPARγ, anti-aP2, anti-adiponectin, anti-phospho LKB1, anti-phospho AMPKα anti-AMPKα, and anti-ACC antibodies were purchased from Cell Signaling Technology (Beverly, MA, USA).

2.3. Cell Culture and Adipocyte Differentiation. 3T3-L1 mouse embryo fibroblasts were obtained from the American Type Culture Collection (Rockville, MD, USA). Cells were grown in DMEM plus 10% calf serum and plated for final differentiation in DMEM plus 10% FBS with 100 units/mL of penicillin-streptomycin solution at 37°C, in 5% CO_2, at 95% humidity until confluence. Two days after confluence (Day 0), the cells were stimulated to differentiate with differentiation inducers (1 μM dexamethasone, 500 μM 3-isobutyl-1-methylxanthine, and 1 μg/mL insulin, MDI) that were added to DMEM containing 10% FBS for two days (Day 2). Preadipocytes were then cultured in DMEM, 10% FBS supplemented with 1 μg/mL insulin for another two days (Day 4), followed by culturing with 10% FBS/DMEM medium for an additional two days (Day 6), at which time more than 90% of cells were mature adipocytes with accumulated fat droplets. On Day 2, RF was prepared in a differentiation medium at concentrations of 10 μg/mL, 50 μg/mL, and 100 μg/mL.

2.4. Cell Cytotoxicity Assay. Cell viability was measured with a CellTiter 96 Aqueous One Solution Cell Proliferation Assay Kit (Promega Corporation, Madison, USA) according to the manufacture's instruction. Briefly, The cells (5×10^3 per 96 well) were incubated at 37°C in 5% CO_2 and 95% air with different concentrations of RF. After 48 h for 3T3-L1 preadipocytes, 20 μL of MTS [3-(4,5-dimethylthiazol-2-yl)-5-(3-carboxymethoxyphenyl)-2(4-sulfophenyl)-2H-tetrazolium, inner salt] solution was added to each well, incubated for 4 h, and absorbance at 490 nm was measured using a VERSAmax microplate reader (Molecular Devices, Sunnyvale, CA, USA) to determine the formazan concentration, which is proportional to the number of live cells.

2.5. Oil Red O Staining. Intracellular lipid accumulation was measured using Oil Red O. The Oil Red O working solution was prepared as described by Ramirez-Zacarias et al. [22]. The 3T3-L1 cells were washed twice with phosphate-buffered saline (PBS) and were then fixed in 10% formaldehyde in PBS for 1 h. After washing with 60% isopropanol, the cells were stained with Oil Red O solution for 30 min at room temperature. The cells were washed with water four times to remove the unbound dye. The stained cells were observed with an Olympus IX71 Research Inverted Phase microscope (Olympus Co., Tokyo, Japan). Following the microscopic observation, 100% isopropanol was added as an extraction solution to extract the excess staining dye from the cells. The absorbance of the extracted dye was measured spectrophotometrically at 500 nm in a VERSAmax microplate reader (Molecular Devices, Sunnyvale, CA, USA).

Table 1: The primer sequences used for real-time PCR.

Target gene	Primer sequences
PPARγ	5′-TTTTCAAGGGTGCCAGTTTC-3′ (sense)
	5′-TTATTCATCAGGGAGGCCAG-3′ (antisense)
C/EBPα	5′-GCCGAGATAAAGCCAAACAA-3′ (sense)
	5′-CCTTGACCAAGGAGCTCTCA-3′ (antisense)
aP2	5′-CGTAAATGGGGATTTGGTCA-3′ (sense)
	5′-TCGACTTTCCATCCCACTTC-3′ (antisense)
Adiponectin	5′-AGACCTGGCCACTTTCTCCTCATT-3′ (sense)
	5′-AGAGGAACAGGAGAGCTTGCAACA-3′ (antisense)
Resistin	5′-TTCCTTGTCCCTGAACTGCT-3′ (sense)
	5′-AGCTCAAGACTGCTGTGCCT-3′ (antisense)
GAPDH	5′-AACTTTGGCATTGTGGAAGG-3′ (sense)
	5′-GGATGCAGGGATGATGTTCT-3′ (antisense)

PPARγ: peroxisome proliferator-activated receptor γ; C/EBPα: CCAAT-enhancer-binding protein α; adipocyte fatty acid-binding protein 2; GAPDH: Glyceraldehyde-3-phosphate dehydrogenase.

2.6. RNA Isolation and Real-Time RT-PCR. Total RNA was extracted using a GeneAll RiboEx Total RNA extraction kit (GeneAll Biotechnology, Seoul, Republic of Korea) and QIAzol lysis reagent (QIAZEN sciences, Maryland, USA). RNA (2 μg) was used as a template for first-strand cDNA synthesis performed using a Power cDNA Synthesis Kit (INTRON Biotechnology, Seoul, Republic of Korea) according to the manufacturer's instructions. Newly synthesized cDNA from 3T3-L1 control cells and RF-treated cells was amplified using specific primers and the Fast SYBR Green PCR Master Mix (Applied Biosystems, Foster City, CA, USA). PCR products were measured with a StepOnePlus Real-Time RT-PCR System, and the relative gene expression was calculated based on the comparative CT method using a StepOne software v2.1 (Applied Biosystems, Foster City, CA, USA). The expression of Glyceraldehyde-3-phosphate dehydrogenase (GAPDH) mRNA was used as an endogenous control. The primers used in the experiments are shown in Table 1.

2.7. Western Blot Analysis. T3-L1 cells were harvested and washed with PBS and then collected by centrifugation at 13,000 rpm for 1 min at 4°C. To obtain the cellular lysate, cells were lysed on ice for 30 min in RIPA buffer (50 mM Tris-HCl, pH 7.5, 0.15 M NaCl, 1% NP-40, 0.1% sodium dodecyl sulfate (SDS), 1 mM DTT, and 1 mM PMSF), which contained a mixture of protease inhibitors (Sigma, Mannheim, Germany). Insoluble materials were removed by centrifugation at 13,000 rpm for 15 min at 4°C. A total of 20 μg of the supernatants were separated using 10% sodium dodecyl sulfate-polyacrylamide gel electrophoresis (SDS-PAGE) and transferred to polyvinylidene difluoride (PVDF) membranes. After blocking with 10 mM Tris, 150 mM NaCl, and 0.05% Tween-20 (TBST) (pH 7.6) containing 5% skim milk for 1 h at room temperature, the membranes were washed with TBST. The membranes were incubated overnight with anti-PPARγ, anti-pAMPK, anti-AMPK, anti-C/EBPα, and GAPDH at 4°C. After washing with TBST, the blots were subsequently incubated with horseradish peroxidase (HRP)-conjugated affinipure Goat anti-rabbit IgG or Goat anti-mouse IgG (Jackson ImmunoResearch Laboratory, USA) in 5% skim milk-TBST at room temperature for 1 h. Protein signals were developed using the ECL Western Blotting Detection Reagent (Amersham Bioscience, Piscataway, NJ, USA). All experiments were repeated at least three times. Representative Western blots are shown along with the graphs of the quantitative data. The chemiluminescent intensities of protein signals were quantified using Quantity One software (Bio-Rad Laboratories, Hercules, CA, USA).

2.8. AMPKa siRNA Transfection. The transfection of siRNAs was performed according to the manufacturer's instructions. Preadipocytes were seeded in 6-well plates, and siRNA transfection was carried out 2 days after the confluence of preadipocytes. Lipofectamine 2000 (5 μL) and 10 μL siRNA (10 pmol) were individually diluted and incubated in 250 μL Opti-MEM medium (Invitrogen, Carlsbad, CA, USA) for 20 min. Next, these were mixed and incubated for 30 min before being added to each well. The initial medium was removed and replaced with induction medium 48 h after transfection.

2.9. Statistical Analysis. Results are expressed as the mean ± SEM of independent experiments, and statistical analyses were performed using Student's t-test to determine differences between groups. All statistical analyses were performed using SPSS statistical analysis software version 11.5 (SPSS Inc., Chicago, IL, USA). Values with $^{*}P < 0.05$ were considered to indicate statistical significance.

3. Results

3.1. Effects of RF on Cytotoxicity and Inhibition of Adipogenesis in 3T3-L1 Adipocytes. To determine the cytotoxicity of RF, 3T3-L1 cells were treated with various concentrations (10–500 μg/mL) of RF, and the cell viability was measured by the MTS assay. As shown in Figure 1(a), treatment with 10–100 μg/mL of RF did not cause significant cytotoxic effects

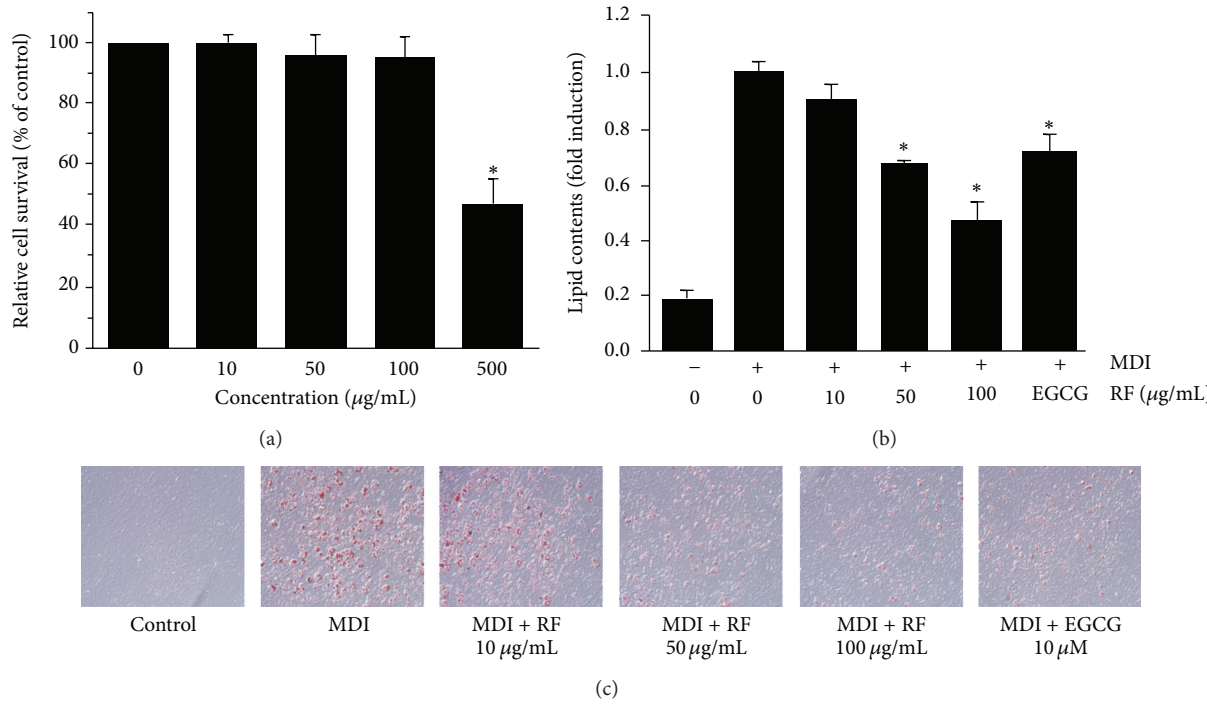

Figure 1: Effect of RF on cell viability and lipid accumulation in 3T3-L1 cells. (a) 3T3-L1 cells were treated with RF at various concentrations (10–500 μg/mL) for 48 h. Cell viability was determined by the MTS assay. Postconfluent 3T3-L1 cells were differentiated in the absence or in the presence of RF (0, 10, 50, and 100 μg/mL) for 6 days. (b) Triglyceride content was quantified by measuring absorbance. EGCG was used as positive control. Assays were performed in duplicate for each concentration, and experiments were repeated at least three times. Data are expressed as means ± S.D. where $P < 0.05$ was considered a statistically significant difference from the differentiated control. (c) Lipid droplets were measured by Oil Red O staining.

on 3T3-L1 cells. Next, we measured the effect of RF on adipocyte differentiation. We used a differentiation mixture (MDI) to induce the differentiation of 3T3-L1 cells. The 3T3-L1 cells were treated with 10, 50, and 100 μg/mL of RF during differentiation; after 6 days, cells were stained with Oil Red O. As shown in Figures 1(b) and 1(c), RF suppressed adipocyte differentiation in a dose dependent manner in 3T3-L1 cells, and adipogenesis was compared with the treatment of epigallocatechin gallate (EGCG), which is a known differentiation blocker. The cells treated with 50 and 100 μg/mL of RF showed a significant reduction in lipid accumulation through the inhibition of differentiation of 3T3-L1 preadipocytes.

3.2. Comparative Effects of RF Extraction Fraction on Inhibition of Adipogenesis in 3T3-L1 Adipocytes. To determine the comparative effects of RF extraction fraction, total water-soluble extract was sequentially extracted with ethyl acetate (EtOAC fraction, RFE) and water (water fraction, RFW). The 3T3-L1 cells were treated with three extracts together with MDI, and then the extent of adipocyte differentiation was determined by the Oil Red O staining method. As shown in Figures 2(a) and 2(b), among the three extracts, total water-soluble extract of RF (RF) was most effective in inhibiting adipocyte differentiation indicating that antiadipogenic activities might have been enriched RF. Troglitazone, one of the antidiabetic drugs and a ligand for PPARγ, was used as a positive control, and 2-chloro-5-nitro-N-phenylbenzamide GW9662, an antagonist for PPARγ, was used as a negative control.

3.3. Effect of RF on the Expression of PPARγ and C/EBPα in 3T3-L1 Adipocytes. To investigate whether RF suppresses adipogenesis through a PPARγ pathway, gene expressions of PPARγ and C/EBPα were evaluated by quantitative real-time RT-PCR and Western blot analysis, respectively, after the treatment of fully differentiated cells with 10–100 μg/mL of RF. We observed that the expressions of PPARγ and C/EBPα were strongly inhibited by RF at the mRNA level (Figures 3(a) and 3(b)). We also demonstrated that RF treatment resulted in a dose-dependent suppression of PPARγ and C/EBPα at the protein level. PPARγ and C/EBPα protein levels were reduced up to 68% by treatment with 100 μg/mL of RF (Figures 3(c) and 3(d)).

3.4. Effect of RF on Expression of aP2, Resistin, and Adiponectin in 3T3-L1 Adiposity. We next examined the effects of RF on the expression of adipogenic genes such as aP2, resistin, and adiponectin in 3T3-L1 cells. Fully differentiated cells were treated with 50 or 100 μg/mL of RF, followed by extraction of total RNA for analysis using quantitative real-time PCR. RF treatment with 0.05 mg/mL or 0.1 mg/mL significantly decreased the expression of aP2, resistin, and adiponectin (Figures 4(a), 4(b), and 4(c)). In particular, the resistin mRNA level was reduced up to 53% by treatment with

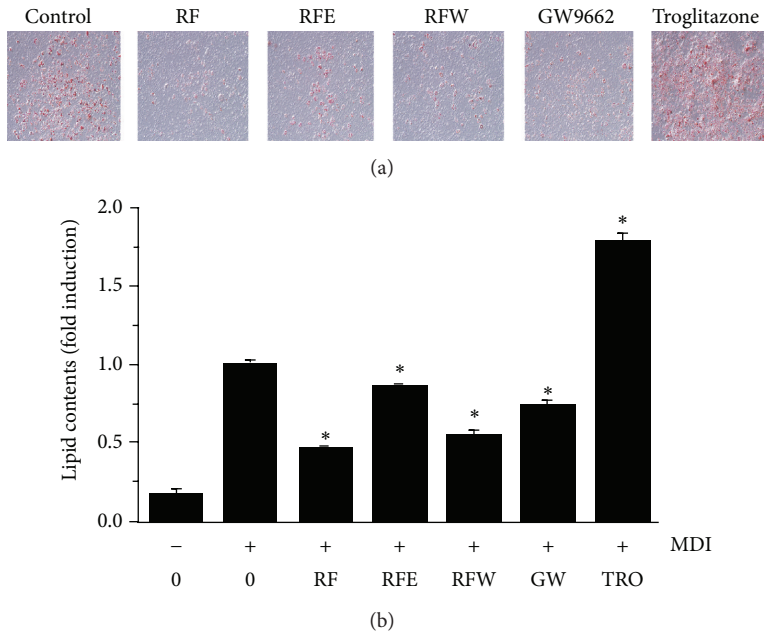

Figure 2: Effect of RF fraction on lipid accumulation of 3T3-L1 adipocyte differentiation. Postconfluent 3T3-L1 cells were differentiated in the absence or presence of RF, RF ethyl acetate fraction (RFE), and RF water fraction (RFW) for 6 days. (a) Lipid droplets were measured by Oil Red O staining. (b) Lipid content was quantified by measuring absorbance. Troglitazone was used as positive control, and GW9662 was used as negative control. Data are expressed as the means ± S.D. where $P < 0.05$ was considered a statistically significant difference from the differentiated control.

100 μg/mL of RF (Figure 4(b)). Consistent with the mRNA results, Western blot analysis revealed that RF markedly reduced the protein levels of aP2, resistin, and adiponectin (Figure 4(d)). These results suggest that RF effectively inhibited adipocyte differentiation through the downregulation of adipogenic genes.

3.5. The Effect of RF and AMPK siRNA Pretreatment on the Expression and Phosphorylation of Proteins Related to Adipogenesis. LKB1, which is an upstream kinase of AMPK, activates AMPK protein in adipose tissue [23]. To investigate whether AMPK, a key player in energy homeostasis [7], is activated by RF during 3T3-L1 differentiation, the protein levels of p-LKB1, p-AMPKα, and ACC were analyzed. When compared with the control group, LKB1 and AMPKα phosphorylation was increased by treatment with RF. The observed increase in the phosphorylation of LKB1 by RF suggests that RF might upregulate AMPK activity via LKB1. However, the expression of ACC, a downstream target protein of AMPK, was significantly suppressed (Figures 5(a) and 5(b)). To further confirm the above results, adipocytes were pretreated with AMPKα siRNA and then treated with 100 μg/mL of RF, and the relative intracellular fat content of each group was determined. AMPKα siRNA pretreatment effectively decreased the relative intracellular fat content when compared with the control group suggesting that AMPKα siRNA can inhibit adipocyte differentiation with or without RF treatment (Figure 5(c)). Figure 5(d) shows that the AMPKα expression was decreased at the protein level after the siRNA treatment. In addition, both RF and AMPKα siRNA treatments decreased the expression of PPARγ and C/EBPα proteins.

4. Discussion

Obesity is caused by the accumulation of lipid through adipogenesis in adipose tissue, and adipogenesis is the process by which undifferentiated precursor cells differentiate into fat storage cells. Numerous studies have demonstrated that adipocyte differentiation and the amount of fat accumulation are associated with the occurrence and development of obesity. Therefore, the inhibition of adipocyte differentiation is one of the strategies for the treatment of obesity. Recent studies have attempted to investigate the beneficial effects of natural products on obesity. The present study demonstrates the novel effect of RF extract on the inhibition of adipocyte differentiation. Our results show that RF did not cause significant cytotoxic effects in 3T3-L1 cells and significantly inhibited lipid accumulation and adipocyte differentiation in a concentration-dependent manner. These results indicate that RF inhibited adipogenesis during adipocyte differentiation and may have potential antiobesity effects (Figure 1). We also demonstrated that treatment with total water-soluble extract of RF strongly inhibited adipogenesis during adipocyte differentiation relative to an ethyl acetate-soluble fraction of RF (RFE) or water fraction of RF (RFW) (Figure 2).

PPARγ and C/EBPα are known to play a role in fat cell function and adipocyte differentiation of preadipocytes [24]. PPARγ induces C/EBPα and also increases its own expression. Similarly, C/EBPα induces PPARγ expression as

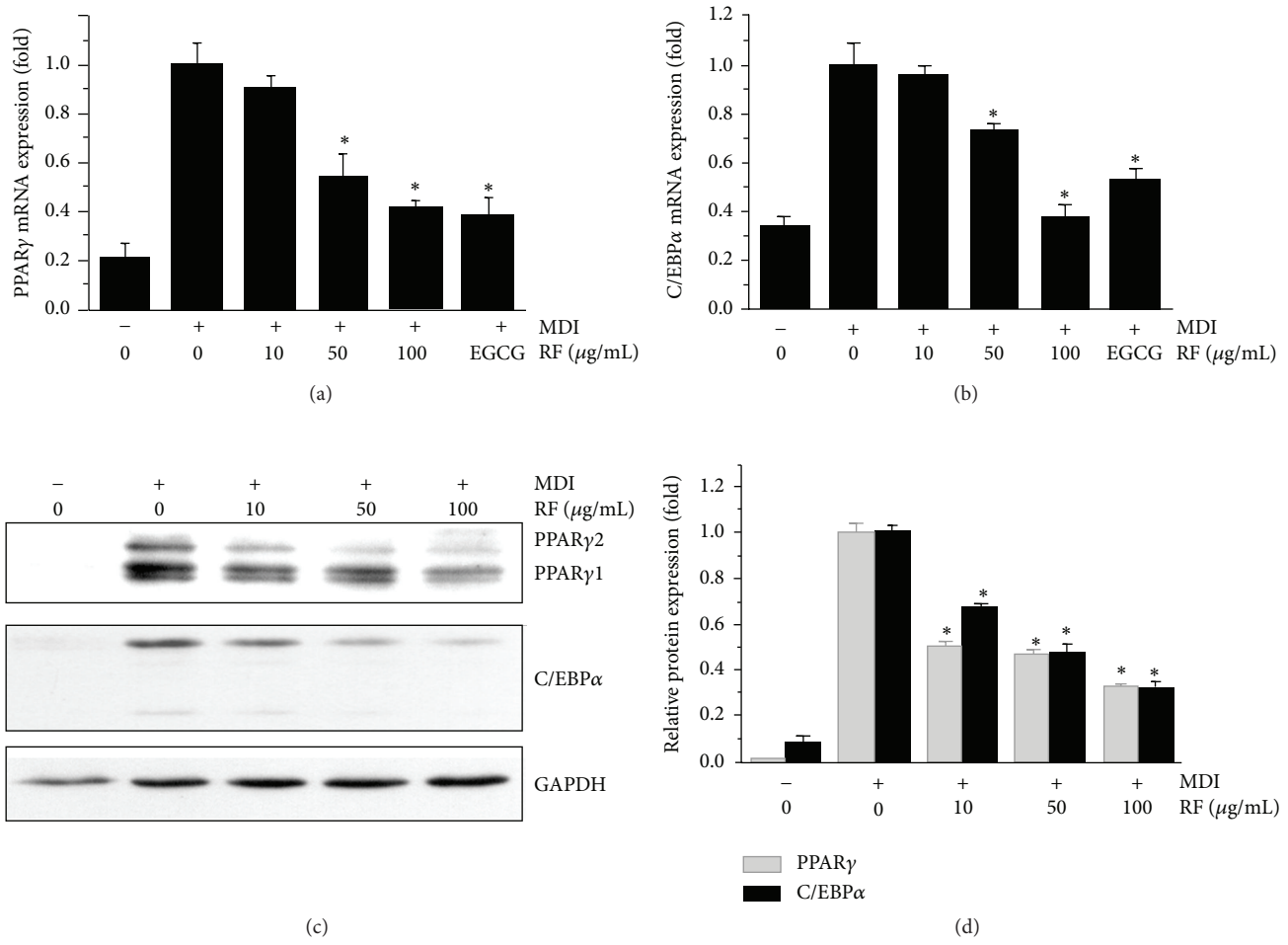

Figure 3: Effect of RF on the expression of PPARγ and C/EBPα in 3T3-L1 cells. Postconfluent 3T3-L1 cells were differentiated in the absence or presence of RF (0, 10, 50, and 100 μg/mL) for 6 days. (a) PPARγ and (b) C/EBPα mRNA expressions were evaluated by quantitative real-time RT-PCR. (c) PPARγ and (d) C/EBPα protein expressions were analyzed by Western blot analysis. Data are expressed as the means ± S.D. where $P < 0.05$ was considered a statistically significant difference from the differentiated control.

well as its own expression. These cooperative functions help in maintaining high levels of PPARγ and C/EBPα, and then PPARγ stimulates adipocyte differentiation. Rosen et al. [25] reported that C/EBPα can support adipocyte-specific gene expression in the presence of PPARγ at the level of cell morphology and lipid accumulation. In this study, we investigated whether RF can inhibit adipocyte differentiation through the suppression of related transcription factors such as PPARγ- and C/EBPα. As a result, RF treatment resulted in reduced expression of PPARγ and C/EBPα at both the mRNA and protein levels in 3T3-L1 cells (Figure 3). These results indicate that RF suppresses adipocyte differentiation through a PPARγ and C/EBPα-mediated adipogenesis mechanism. We also observed that 3T3-L1 cells treated with RF showed a decreased protein expression as well as mRNA expression of several adipogenesis-related genes including aP2, resistin, and adiponectin, in a dose-dependent manner (Figure 4). A member of the cytoplasmic fatty acid-binding protein family, aP2, was detected in adipose tissue, and its expression was highly regulated during the differentiation of adipocytes [26]. PPARγ binding is required for the function of the fat-selective enhancer for the aP2 gene, in cultured fat cells [24]. Resistin, an adipocyte-secreted molecule, serves as a critical link between obesity and insulin resistance and plays a role in the regulation of glucose homeostasis and hepatic glucose production [27, 28]. Acute administration of recombinant resistin to rats results in impaired glucose tolerance and hepatic insulin resistance [28]. Previous studies have demonstrated that compounds with antiobesity activity inhibit adipocyte differentiation in 3T3-L1 cells through the downregulation of PPARγ, C/EBPα, aP2, and resistin [29, 30]. Adiponectin is an adipocyte-derived hormone that plays a role in insulin sensitivity and energy homeostasis [31]. Previous studies have demonstrated that PPARγ agonists can induce an increase in adiponectin levels in 3T3-L1 adipocytes, and that this effect is associated with adipocyte differentiation *via* PPAR response element [32, 33].

AMPK, a central sensor of cellular energy, is a eukaryotic heterotrimeric serine/threonine kinase, and it has emerged as a therapeutic target for metabolic disorders including obesity. The activation of AMPK is essential for the inhibition of 3T3-L1 adipocyte lipogenesis by phytochemicals [34]. To

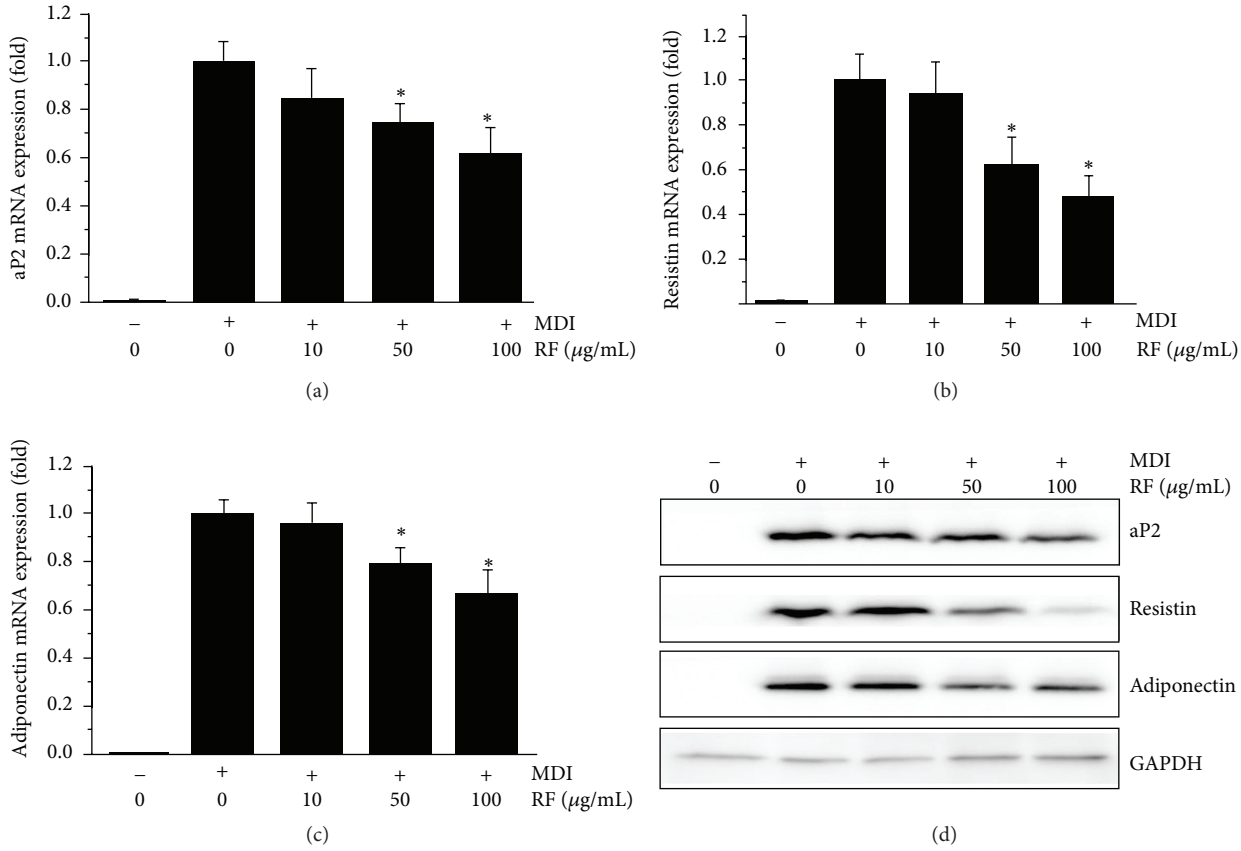

Figure 4: Effect of RF on the expression of aP2, resistin, and adiponectin in 3T3-L1 cells. Postconfluent 3T3-L1 cells were differentiated in the absence or presence of RF (0, 10, 50, and 100 μg/mL) for 6 days. (a) aP2, (b) resistin, and (c) adiponectin mRNA expression were evaluated by the quantitative real-time PCR. (d) aP2, resistin, and adiponectin protein levels were analyzed by Western blot analysis. GAPDH was used as internal controls. Data are expressed as means ± S.D. where $P < 0.05$ was considered a statistically significant difference from the differentiated control.

determine whether RF inhibits adipocyte differentiation by activating AMPK, the levels of LKB1/AMPK phosphorylation were determined. The results show that the levels of LKB1/AMPK phosphorylation are elevated significantly after RF treatment (Figures 5(a) and 5(b)). Furthermore, RF treatment inactivates the downstream substrate ACC, which is a key enzyme of lipogenesis. This result indicates RF inhibited adipocyte differentiation via the activation of LKB1/AMPK. It was reported that AMPK regulates PPARγ and C/EBPα, which are the critical regulators of adipogenesis and fat accumulation in adipocytes [35]. For example, AMPK activator A-769662 inhibits adipocyte differentiation by downregulating PPARγ, C/EBPα, FAS, and aP2 [6]. It has been also reported that the treatment of 3T3-L1 preadipocytes with an AMPK activator, AICAR, could inhibit the differentiation process [36].

Conversely, Compound C, which is an inhibitor of AMPK, significantly inhibited the adipogenic differentiation of 3T3-L1 cells in a dose-dependent manner, and this inhibitory effect was primarily effective in the initial stage of differentiation [37, 38]. The fact that AMPK signaling might be associated with an adipocyte differentiation program is still controversial, but we found that preadipocyte 3T3-L1 cells were not able to develop to mature adipocytes in the presence of RF and that this effect was promoted when the cells were pretreated with AMPK siRNA (Figure 5(c)). In addition, the expression of PPARγ and C/EBPα was markedly decreased by AMPKα siRNA pretreatment (Figure 5(d)). Although the downregulation of p-AMPK decreased the protein levels of PPARγ and C/EBPα, a direct correlation has not been understood. It has been also reported that AICAR was able to inhibit differentiation either at early or late stages of differentiation [36]. We therefore infer that RF is able to inhibit differentiation with an increasing level of AMPK activity at the late stage of differentiation and not the early stage of differentiation.

5. Conclusion

In conclusion, the objective of this study was to elucidate the effect of RF on adipogenesis in 3T3-L1 cells. This study demonstrated that the extract of RF inhibited adipocyte differentiation of 3T3L-1 and fat accumulation. The antiadipogenic mechanism of RF involves the downregulation of the adipogenic transcription factors, PPARγ and C/EBPα, which are related to the expression of aP2, resistin, and adiponectin. In addition, we observed that RF increases

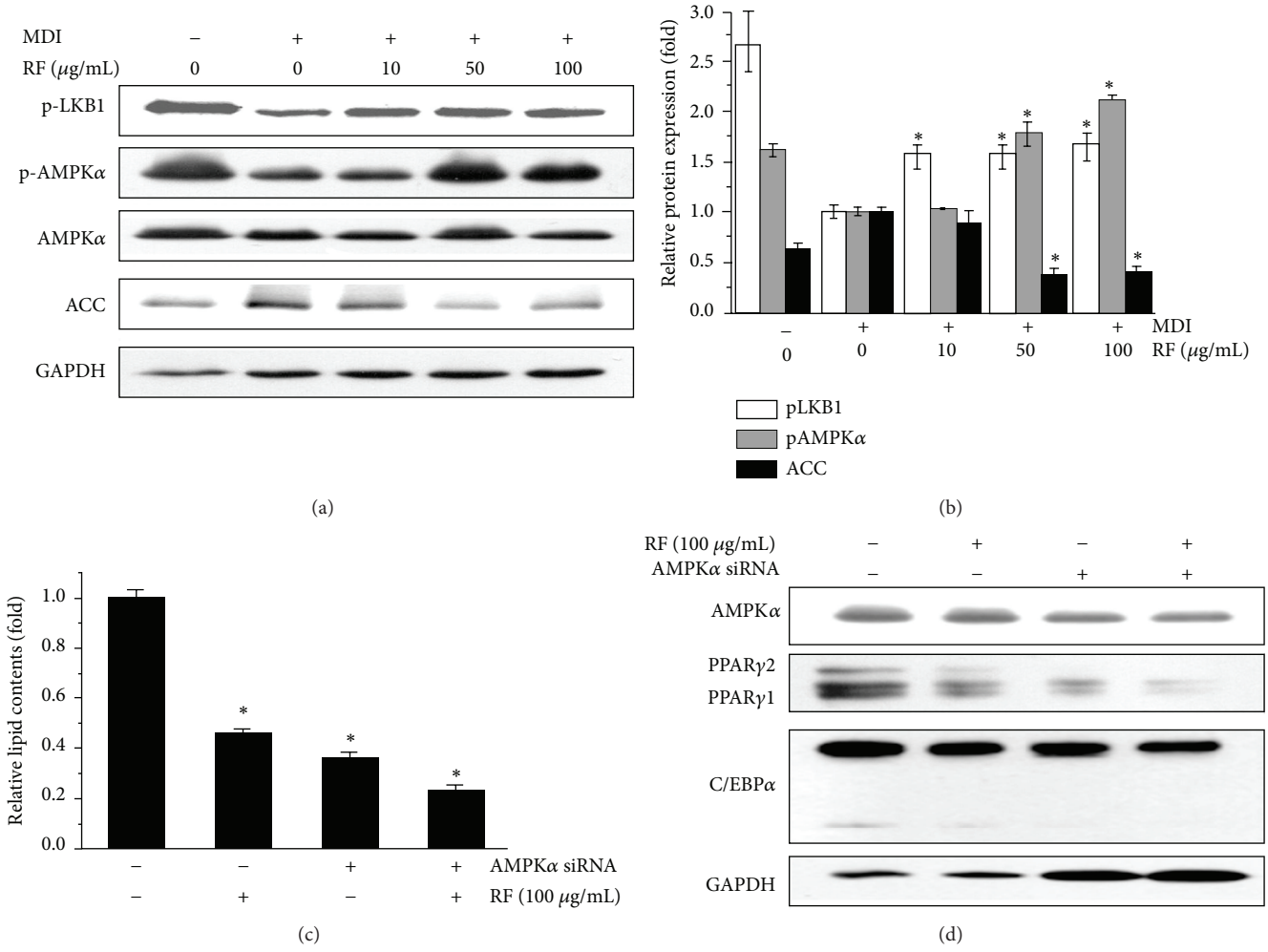

Figure 5: Effects of RF on the phosphorylation of AMPK during 3T3-L1 differentiation. 3T3-L1 preadipocytes were differentiated in the presence of RF (0, 10, 50, and 100 μg/mL) for 6 days. (a) p-LKB1, p-AMPK, and ACC protein levels were analyzed by Western blot analysis. (b) Densitometry analyses were presented as relative ratios of p-LKB1/GAPDH, p-AMPK/AMPK, and ACC/GAPDH. (c) 3T3-L1 cells were treated with RF (Day 4) in AMPKα siRNA pretreatment (Day 0). Cells were stained with Oil Red O at 6 days, and lipid contents were quantified. These experiments were conducted as independent experiments in triplicate. Data represent the mean ± S.D. where $P < 0.05$ was considered a statistically significant difference from the differentiated control. (d) After AMPKα siRNA pretreatment and RF-treated differentiation, the protein expressions of AMPKα, PPARγ, and C/EBPα were determined by Western blot analysis.

AMPK phosphorylation, which plays major roles in the expression of PPARγ and C/EBPα. These findings suggest that RF might have a therapeutic effect in the prevention of adipogenesis-related obesity and may be a potential natural drug candidate for the treatment of obesity.

Acknowledgment

This work was supported by the National Research Foundation of Korea (NRF) Grant funded by the Korean Government (MSIP) (no. 2011-0030717, no. 2011-0006220, and no. 2012-0007669).

References

[1] N. Abate, "Obesity and cardiovascular disease: pathogenetic role of the metabolic syndrome and therapeutic implications," *Journal of Diabetes and its Complications*, vol. 14, no. 3, pp. 154–174, 2000.

[2] S. R. Farmer and J. Auwerx, "Adipose tissue: new therapeutic targets from molecular and genetic studies–IASO stock conference 2003 report," *Obesity Reviews*, vol. 5, no. 4, pp. 189–196, 2004.

[3] J. Fu, F. Oveisi, S. Gaetani, E. Lin, and D. Piomelli, "Oleoylethanolamide, an endogenous PPAR-alpha agonist, lowers body weight and hyperlipidemia in obese rats," *Neuropharmacology*, vol. 48, no. 8, pp. 1147–1153, 2005.

[4] R. H. Unger and Y. T. Zhou, "Lipotoxicity of beta-cells in obesity and in other causes of fatty acid spillover," *Diabetes*, vol. 50, no. 1, pp. S118–S121, 2001.

[5] J. M. Ntambi and K. Young-Cheul, "Adipocyte differentiation and gene expression," *Journal of Nutrition*, vol. 130, no. 12, pp. 3122–3126, 2000.

[6] Y. Zhou, D. Wang, Q. Zhu et al., "Inhibitory effects of a-769662, a novel activator of AMP-activated protein kinase, on 3T3-L1 adipogenesis," *Biological and Pharmaceutical Bulletin*, vol. 32, no. 6, pp. 993–998, 2009.

[7] B. B. Lowell, "PPARgamma: an essential regulator of adipogenesis and modulator of fat cell function," *Cell*, vol. 99, no. 3, pp. 239–242, 1999.

[8] P. Tontonoz, E. Hu, R. A. Graves, A. I. Budavari, and B. M. Spiegelman, "mPPAR gamma 2: tissue-specific regulator of an adipocyte enhancer," *Genes and Development*, vol. 8, no. 10, pp. 1224–1234, 1994.

[9] R. P. Brun, J. B. Kim, E. Hu, S. Altiok, and B. M. Spiegelman, "Adipocyte differentiation: a transcriptional regulatory cascade," *Current Opinion in Cell Biology*, vol. 8, no. 6, pp. 826–832, 1996.

[10] R. F. Morrison and S. R. Farmer, "Hormonal signaling and transcriptional control of adipocyte differentiation," *Journal of Nutrition*, vol. 130, no. 12, 2000.

[11] E. D. Rosen, C. J. Walkey, P. Puigserver, and B. M. Spiegelman, "Transcriptional regulation of adipogenesis," *Genes and Development*, vol. 14, no. 11, pp. 1293–1307, 2000.

[12] T. Jeon, S. G. Hwang, S. Hirai et al., "Red yeast rice extracts suppress adipogenesis by down-regulating adipogenic transcription factors and gene expression in 3T3-L1 cells," *Life Sciences*, vol. 75, no. 26, pp. 3195–3203, 2004.

[13] J. T. Hwang, D. Y. Kwon, and S. H. Yoon, "AMP-activated protein kinase: a potential target for the diseases prevention by natural occurring polyphenols," *New Biotechnology*, vol. 26, no. 1-2, pp. 17–22, 2009.

[14] S. K. Kim and C. S. Kong, "Anti-adipogenic effect of dioxinodehydroeckol via AMPK activation in 3T3-L1 adipocytes," *Chemico-Biological Interactions*, vol. 186, no. 1, pp. 24–29, 2010.

[15] B. Huang, H. D. Yuan, D. Y. Kim, H. Y. Quan, and S. H. Chung, "Cinnamaldehyde prevents adipocyte differentiation and adipogenesis via regulation of peroxisome proliferator-activated receptor-gamma (PPARgamma) and AMP-activated protein kinase (AMPK) pathways," *Journal of Agricultural and Food Chemistry*, vol. 59, no. 8, pp. 3666–3673, 2011.

[16] Q. Qian, X. Liu, W. He et al., "TG accumulation inhibitory effects of Jinqi formula by AMPK signaling pathway," *Journal of Ethnopharmacology*, vol. 143, no. 1, pp. 41–48, 2012.

[17] G. S. Moon, "Constituents and Uses of Medicinal Herbs," 1991.

[18] J. W. Lim, J. T. Jeong, and C. S. Shin, "Component analysis and sensory evaluation of Korean black raspberry (*Rubus coreanus* Mique) wines," *International Journal of Food Science and Technology*, vol. 47, no. 5, pp. 918–926, 2012.

[19] J. W. Lim, H. J. Hwang, and C. S. Shin, "Polyphenol compounds and anti-inflammatory activities of Korean black raspberry (*Rubus coreanus* Miquel) wines produced from juice supplemented with pulp and seed," *Journal of Agricultural and Food Chemistry*, vol. 60, no. 20, pp. 5121–5127, 2012.

[20] J. Choi, K. T. Lee, J. Ha et al., "Antinociceptive and antiinflammatory effects of niga-ichigoside F1 and 23-hydroxytormentic acid obtained from *Rubus coreanus*," *Biological and Pharmaceutical Bulletin*, vol. 26, no. 10, pp. 1436–1441, 2003.

[21] J. E. Lee, E. Park, J. E. Lee et al., "Effects of a *Rubus coreanus Miquel* supplement on plasma antioxidant capacity in healthy Korean men," *Nutrition Research and Practice*, vol. 5, no. 5, pp. 429–434, 2011.

[22] J. L. Ramirez-Zacarias, F. Castro-Munozledo, and W. Kuri-Harcuch, "Quantitation of adipose conversion and triglycerides by staining intracytoplasmic lipids with oil red O," *Histochemistry*, vol. 97, no. 6, pp. 493–497, 1992.

[23] M. Daval, F. Foufelle, and P. Ferré, "Functions of AMP-activated protein kinase in adipose tissue," *Journal of Physiology*, vol. 574, part 1, pp. 55–62, 2006.

[24] P. Tontonoz, E. Hu, J. Devine, E. G. Beale, and B. M. Spiegelman, "PPAR gamma 2 regulates adipose expression of the phosphoenolpyruvate carboxykinase gene," *Molecular and Cellular Biology*, vol. 15, no. 1, pp. 351–357, 1995.

[25] E. D. Rosen, C. H. Hsu, X. Wang et al., "C/EBPalpha induces adipogenesis through PPARgamma: a unified pathway," *Genes & Development*, vol. 16, no. 1, pp. 22–26, 2002.

[26] J. F. C. Glatz, T. Börchers, F. Spener, and G. J. Van Der Vusse, "Fatty acids in cell signalling: Modulation by lipid binding proteins," *Prostaglandins Leukotrienes and Essential Fatty Acids*, vol. 52, no. 2-3, pp. 121–127, 1995.

[27] C. M. Steppan, S. T. Bailey, S. Bhat et al., "The hormone resistin links obesity to diabetes," *Nature*, vol. 409, no. 6818, pp. 307–312, 2001.

[28] M. W. Rajala, S. Obici, P. E. Scherer, and L. Rossetti, "Adipose-derived resistin and gut-derived resistin-like molecule-beta selectively impair insulin action on glucose production," *Journal of Clinical Investigation*, vol. 111, no. 2, pp. 225–230, 2003.

[29] M.J. Yim, M. Hosokawa, Y. Mizushina, H. Yoshida, Y. Saito, and K. Miyashita, "Suppressive effects of amarouciaxanthin A on 3T3-L1 adipocyte differentiation through down-regulation of PPARgamma and C/EBPalpha mRNA expression," *Journal of Agricultural and Food Chemistry*, vol. 59, no. 5, pp. 1646–1652, 2011.

[30] E. J. Cho, A. Rahman, S. W. Kim et al., "Chitosan oligosaccharides inhibit adipogenesis in 3T3-L1 adipocytes," *Journal of Microbiology and Biotechnology*, vol. 18, no. 1, pp. 80–87, 2008.

[31] T. Kadowaki and T. Yamauchi, "Adiponectin and adiponectin receptors," *Endocrine Reviews*, vol. 26, no. 3, pp. 439–451, 2005.

[32] T. Yamauchi, J. Kamon, H. Waki et al., "The fat-derived hormone adiponectin reverses insulin resistance associated with both lipoatrophy and obesity," *Nature Medicine*, vol. 7, no. 8, pp. 941–946, 2001.

[33] N. Maeda, M. Takahashi, T. Funahashi et al., "PPARgamma ligands Increase expression and plasma concentrations of adiponectin, an adipose-derived protein," *Diabetes*, vol. 50, no. 9, pp. 2094–2099, 2001.

[34] H. S. Moon, C. S. Chung, H. G. Lee, T. G. Kim, Y. J. Choi, and C. S. Cho, "Inhibitory effect of (−)-epigallocatechin-3-gallate on lipid accumulation of 3T3-L1 cells," *Obesity*, vol. 15, no. 11, pp. 2571–2582, 2007.

[35] M. Daval, F. Foufelle, and P. Ferré, "Functions of AMP-activated protein kinase in adipose tissue," *Journal of Physiology*, vol. 574, part 1, pp. 55–62, 2006.

[36] S. Giri, R. Rattan, E. Haq et al., "AICAR inhibits adipocyte differentiation in 3T3L1 and restores metabolic alterations in diet-induced obesity mice model," *Nutrition & Metabolism*, vol. 3, article 31, 2006.

[37] Y. Gao, Y. Zhou, A. Xu, and D. Wu, "Effects of an AMP-activated protein kinase inhibitor, compound C, on adipogenic differentiation of 3T3-L1 cells," *Biological and Pharmaceutical Bulletin*, vol. 31, no. 9, pp. 1716–1722, 2008.

[38] M. Nam, W. H. Lee, E. J. Bae, and S. G. Kim, "Compound C inhibits clonal expansion of preadipocytes by increasing p21 level irrespectively of AMPK inhibition," *Archives of Biochemistry and Biophysics*, vol. 479, no. 1, pp. 74–81, 2008.

Hindawi Publishing Corporation
Evidence-Based Complementary and Alternative Medicine
Volume 2013, Article ID 453096, 9 pages
http://dx.doi.org/10.1155/2013/453096

Research Article

Relationships between Pathological Patterns and Quality of Life: Pathway Analysis

Shin-Woong Cho,[1] Young-Jae Park,[1,2,3] Sang-Chul Lee,[4] Jaemin Ryu,[2] Young-Bae Park,[1,2] and Hwan-Sup Oh[1,5]

[1] *Interdisciplinary Programs, Department of Human Informatics of Oriental Medicine, Kyung Hee University, Seoul 130-701, Republic of Korea*
[2] *Department of Diagnosis and Biofunctional Medicine, College of Korean Medicine, Kyung Hee University, Seoul 130-701, Republic of Korea*
[3] *Department of Diagnosis and Biofunctional Medicine, Kyung Hee University Hospital at Gangdong, Seoul 134-727, Republic of Korea*
[4] *Department of Business Administration, Korea Christian University, Seoul 157-722, Republic of Korea*
[5] *Department of Mechanical Engineering, Kyung Hee University, Yongin, Gyeonggi-do 446-701, Republic of Korea*

Correspondence should be addressed to Young-Jae Park; bmpomd@khu.ac.kr

Received 27 March 2013; Revised 6 September 2013; Accepted 7 September 2013

Academic Editor: Bo-Hyoung Jang

Purpose. The purpose of our study was to examine the relationships between pathological patterns and self-rated quality of life (QoL). *Methods.* A total of 426 Korean subjects participated in this study (male : female = 154 : 272). The subjects were asked to complete Yin Deficiency (YD), Qi Deficiency (QD), Food Stagnation (FS), Blood Stasis (BS), Phlegm, and Seven Emotions Impairment (SEI) pattern Questionnaires and the General Health Questionnaire (GHQ). We formed a pathway model consisting of pathological patterns and QoL questionnaire scores and examined which pathological patterns resulted in decreased QoL using path analysis. *Results.* Our pathway model had satisfactory fitness levels (GFI = 0.975, NFI = 0.984, and CFI = 0.984) and showed that Phlegm and SEI patterns directly resulted in decreased QoL, whereas QD, YD, FD, and BS indirectly resulted in decreased QoL. The pathway model suggested that the severity or stage of decreased QoL may be estimated by pathological patterns: QD and YD patterns are associated with the early stage; FS and BS patterns are associated with the middle stage; Phlegm and SEI are associated with the later stage of decreased QoL. *Conclusion.* Our results suggest that pathological patterns directly or indirectly affect decreases in QoL.

1. Introduction

In East Asian medicine (EAM), the notion of pathological patterns refers to the cause, nature, and location of pathogens at a certain stage of disease or condition of healthy Qi, Blood, Yin, or Yang affected by those pathogens [1]. In addition to being used for diagnostic purposes, pattern diagnosis guides the practitioner toward a treatment principle, whereby specific acupoints and herbal formulae are selected for treatment, using a holistic approach [2]. According to the results of pattern diagnosis, specific treatments can be prescribed to maximize effectiveness [3–5]. When conducting pattern diagnosis, self-reported symptoms are the main clues used for determining pathological patterns. For example, symptoms of fatigue and a feeling of heaviness in the limbs are important clues for determining a deficiency pattern of the Qi. However, these symptoms are subjective and difficult to evaluate objectively. Therefore, a few pathological pattern questionnaires including the Yin Deficiency Questionnaire (YDQ) [6], Qi Deficiency Questionnaire (QDQ) [7], Food Stagnation Questionnaire (FSQ) [8], Blood Stasis Questionnaire (BSQ) [9], Phlegm Pattern Questionnaire (PPQ) [10], and Seven Emotions Impairment Questionnaire (SEIQ) [11] were developed based on self-reported symptoms.

It is interesting that quality of life (QoL) is evaluated mainly by self-rated symptoms, similarly to pathological

pattern questionnaires. QoL is an individual's perception of his or her position in life in the context of the culture and value systems in which he or she lives and in relation to his or her goals, expectations, standards, and concerns [12]. QoL is a broadly ranging concept, comprised of domains such as emotional well-being, social functioning, physical health, patient environment and personal beliefs, and can be assessed with both generic and condition-specific instruments [13]. QoL is particularly useful as an outcome measure in studies of diseases that have no obvious biological or clinical markers [14]. In these conditions, alleviation of symptom becomes a treatment priority, and, in the absence of objective clinical criteria, treatment efficacy should be evaluated by self-reported symptoms as well as based on patient well-being and functioning [15–17]. QoL generally correlates well with symptom severity scores in untreated patients, and improvement in QoL consequent to effective treatment has been reported [18]. The General Health Questionnaire (GHQ) is a measure of current mental health and has been widely used in different settings and different cultures [19]. As GHQ score increases, psychological QoL level decreases.

Many studies have addressed the relationships between QoL and frequently manifesting symptoms such as pain [20–22], fatigue [23], displeasure [24], disorder of emotions [25–27], and indigestion [28]. These symptoms are also associated with pathological patterns and serve as items on the pathological pattern questionnaires. Therefore, it is plausible that pathological pattern questionnaire scores are related to the QoL level. However, few studies have addressed the relationship between QoL and pathological patterns.

Cho et al. reported that SEIQ subscale scores extracted by principal component analysis (PCA) were associated with QoL, rated on a visual analog scale (VAS) [29]. However, to our knowledge, there are no studies that examined the relationships between pathological pattern scores and self-rated QoL. In this study, we used path analysis to examine these relationships. Path analysis is a straightforward extension of multiple regression models. Its aim is to provide estimates of the magnitude and significance of hypothesized causal connections between sets of variables [30]. Using path analysis, both the direct effects and indirect effects of pathological patterns on self-rated QoL can be estimated.

We formed a pathway model consisting of six pathological patterns and QoL questionnaire scores and hypothesized that the pattern scores would directly or indirectly affect the self-rated QoL scores. We examined the model-to-data fitness of our model and its effective power of the pathological patterns on QoL using path analyses.

2. Subjects and Methods

2.1. Subjects. A total of 426 Korean outpatients visiting four EAM clinics between July and August 2011 for pain-related problems including shoulder pain, low back pain, and ankle sprain, as well as headache, dizziness, indigestion, and chronic fatigue problems, participated in this study (male : female = 154 : 272). Table 1 lists the age distribution of subjects by gender. After the purpose of this study was presented to the subjects and informed consent was obtained from all subjects, they were asked to complete YDQ, QDQ, FSQ, BSQ, PPQ, SEIQ, and GHQ questionnaires. Table 2 lists questionnaire items of the YDQ, QDQ, FSQ, BSQ, PPQ, and SEIQ.

Table 1: Age distribution of the participants.

Age	Male (*n*)	Female (*n*)	Total (*n*)
20–29	37	42	79
30–39	33	48	81
40–49	24	51	75
50–59	39	85	124
60–64	21	46	67
Total	154	272	426

2.2. Questionnaires. To estimate decreases in QoL, we used the Korean version of the GHQ (K-GHQ) [31]. The K-GHQ consists of 28 items and is categorized into four domains: somatic symptoms, anxiety/insomnia, self-dysfunction, and severe depression. As mentioned in the introduction, increased total score of the GHQ leads to decreased QoL. Each item of the K-GHQ was rated on a 4-point Likert scale: 0 = not at all; 1 = no more than usual; 2 = rather more than usual; 3 = much more than usual. The GHQ scoring system transforms Likert scores of 0 and 1 to 0 points and Likert scores of 2 and 3 to 1 point. This dichotomous scoring method has the advantage of eliminating errors due to end users and middle users. Therefore, the 28 dichotomous total scores of the K-GHQ were summed in this study.

Yin Deficiency (YD) is a pattern resulting from deficiency of Yin fluid and essence and usually manifests as emaciation, dizziness, tinnitus, dryness of the mouth and throat, afternoon fever, and night sweats [1]. YDQ consists of 30 items related to YD [6]. The QDQ is a 22-item questionnaire relating to spleen Qi Deficiency (QD) [7]. Food Stagnation (FS) manifests as epigastric and abdominal distention, dyspepsia, water brash, anorexia, offensive odor of stools, and curd-like and slimy tongue coating [1]. The FSQ consists of 20 items to estimate symptoms related to FS [8]. Blood Stasis (BS) is defined as a pathological product of blood stagnation, including extravasated blood and sluggishly circulating blood or blood congested in a viscus, all of which may result in pathology [1]. The BSQ consists of 14 items to estimate symptoms related to BS [9]. Phlegm is the viscous turbid pathological product that can accumulate in the body, causing a variety of diseases [10]. The PPQ consists of 26 items to estimate self-rated symptoms related to Phlegm Pattern (PP) [10]. Seven Emotions Impairment (SEI) is a collective term for joy, anger, thought, anxiety, sorrow, fear, and fright, taken as endogenous factors causing diseases if in excess [1]. The SEIQ consists of 22 items to evaluate SEI [11]. The YDQ, QDQ, FSQ, BSQ, PPQ, and SEIQ were rated on a 7-point Likert scale: 1 = disagree very strongly; 2 = disagree strongly; 3 = disagree; 4 = neither agree nor disagree; 5 = agree; 6 = agree strongly; and 7 = agree very strongly. When conducting path analysis, the total scores of the six pattern questionnaires were subtracted from the number of total items to moderate the mean values.

Table 2: Yin Deficiency, Qi Deficiency, Food Stagnation, Blood Stasis, Phlegm, and Seven Emotions Impairment Questionnaires items.

Yin Deficiency Questionnaire (n = 30)	Qi Deficiency Questionnaire (n = 22)	Food Stagnation Questionnaire (n = 20)	Blood Stasis Questionnaire (n = 14)	Phlegm Pattern Questionnaire (n = 26)	Seven Emotions Impairment Questionnaire (n = 22)
I urinate frequently	I usually feel tired or languid	I feel pain in the pit of my stomach	I recently sprained my ankle or waist	I feel unclear in the head	I am often angry
My urine is dark yellow	I feel heavy or weak in the limbs	I have a feeling of fullness in the stomach after eating	I recently was hurt in a fall or traffic accident	I have a headache	I have alternating chills and fever
I feel residual urine	I have trouble standing or walking for a long time	I often have an upset stomach	I was operated on ( ) times	I feel dizzy	I feel dizzy
I cannot contain my urine	I have a heavy feeling in my anus	I feel stomach pain immediately after eating	I have dull pain that lasts for a long time	I have ringing in the ears	I feel heavy in the chest
I wake to urinate in the night	My memory has gone from bad to worse	I often belch	I have joint pain	I feel my heart palpitates	I have tightening in the chest
My stool is hard	I often catch common colds	I have water brash	I have lower abdominal pain	I am startled by faint noise	I have chest pain
My hair falls out	My colds last for a long time	I feel sick to my stomach	I have flank pain	I feel heavy in the chest	I often sigh
I have a rough skin	My voice easily becomes hoarse after talking	I have a bowel movement immediately after eating	I have pain that disturbs my sleep in the night	I have a cough	I taste bitter tastes
I have an itch in the night	I often have a weak voice	I am very fond of eating	I often have a bruise	I have sputum in my throat	I feel my heart palpitates
I have a dry mouth	I sweat spontaneously	I feel heavy in the body	My lips or tongue is dark blue	I feel a foreign body present in the throat, neither swallowed nor ejected	I am sleepless
My heel is dry and cracked	I often have a fever	I feel languid after eating	My face is dark blue	I feel short of breath	I am forgetful
I do not gain weight despite eating fully	I often experience nosebleeds	I swell in the face or limbs	I have dark circles under the eyes	I feel fatigued	I am startled by faint noise
I have a fever in the night	I overwork myself	I gained weight recently	My stool is black	I feel heavy or weak in the limbs	I feel down and uninterested in everything
I have a fever in the afternoon	My work hours are irregular	I often urinate	I feel a lump in my abdomen	I have a poor appetite	I feel like lying because of fatigue

Table 2: Continued.

Yin Deficiency Questionnaire (n = 30)	Qi Deficiency Questionnaire (n = 22)	Food Stagnation Questionnaire (n = 20)	Blood Stasis Questionnaire (n = 14)	Phlegm Pattern Questionnaire (n = 26)	Seven Emotions Impairment Questionnaire (n = 22)
I have a flush in the afternoon	I am under stress because of my work	My stool is mucousy		I feel sick to the stomach	I have indigestion despite a normal appetite
My soles are hot in the night	I feel pain after working	I have pain in the joints		I have indigestion	I feel uneasy
I feel hot deep in the body, for example, in the bone	I feel short of breath after working	I have a water-change-related diarrhea or abdominal pain		I have a feeling of fullness in the stomach with just a little food	I sweat during sleep
I prefer cold beverages to warm beverages	My mealtimes are irregular	I have a food-related allergy		My stomach or intestine rumbles	I have many things worrying me
I am susceptible to heat and cold	I feel weak after skipping meals	I have abdominal fullness or diarrhea after drinking		My stool is mucousy	I have trouble with my family
I sweat during sleep	I feel drowsy or languid after meals	(for women) I have vaginal discharge		I have a lump somewhere on my body	I have vaginal bleeding during sex
My ear rings	I have indigestion			My face is yellowish	My menstrual bleeding volume is irregular
I have a cough in the afternoon	I have a poor appetite			I have dark circles under the eyes	My menstrual period is irregular
I have a cough in the night				I feel itchy	
My cough lasts for a long time				I have pain in the joints	
I feel tired or languid				I have flank pain	
I feel tired in the morning				I gained or lost weight recently	
I feel low back pain					
I feel dull pain in my ankle or knee					
I feel heavy or weak in my lower limbs					
I feel dull pain in my heel					

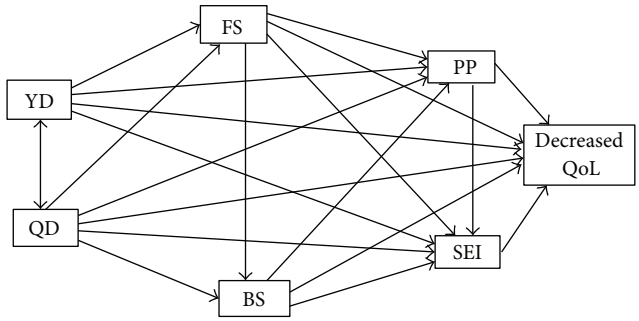

Figure 1: Research model for relationships between pathological patterns and quality of life.

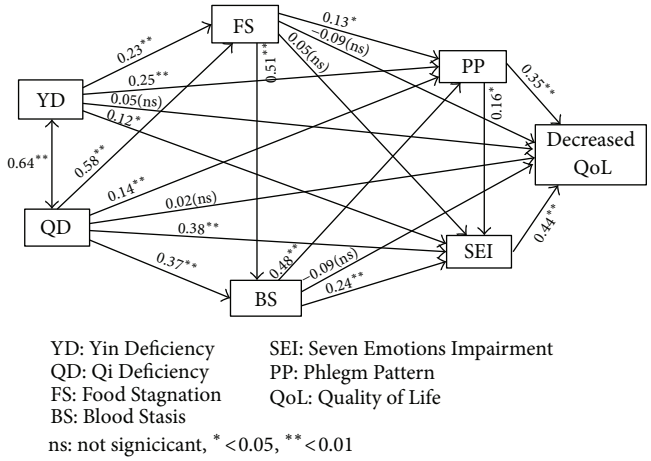

Figure 2: Results of path analysis. The model provided a good fit (GFI = 0.975, NFI = 0.984, CFI = 0.984). Note that the correlation between YD and QD is located on a two-directional arrow, whereas standard estimates of each pathological pattern to other patterns or QoL are located on the corresponding one-directional arrows.

2.3. Research Model. The relationships between the six pathological patterns were formed based on the EAM theory; the research model is depicted in Figure 1. YD affects FS because fluid, a source of Yin, is necessary when digesting food [32]. Deficiency fire resultant from YD burns and concentrates fluid and may form Phlegm [33]. Deficiency fire resultant from YD occurs in the upper body and results in palpitation, insomnia, and burning in the chest. Therefore, YD may affect SEI [32].

Digestion is conducted by spleen Qi, and QD may affect FS, which manifests as dyspepsia [32]. It is generally accepted that fluid cannot be transported to all parts of the body in the QD condition, and it may be deformed to Phlegm [32]. Spleen QD and heart QD are the main factors of SEI [33]. Blood circulates through the meridians with the assistance of the Qi. However, blood may stagnate in QD conditions, and BS may occur [32].

FS and BS have some related symptoms including abdominal lumps, nosebleeds, and bloody stools. FS also shares some SEI-related symptoms such as flank pain, chills and fever, and chest pain. These symptoms may be due to the effects of FS on BS and SEI [33–35]. FS, like QD, results in deformation of the fluid and may affect the formation of Phlegm. BS facilitates the formation of tumors or lumps, which in EAM theory are considered to be combinations of BS and Phlegm [33]. Therefore, it is possible that BS may affect PP. BS affects emotions, especially in women. For example, BS in the lower abdomen during menstruation may result in severe irritability [33, 36]. Thus, BS may affect SEI. Finally, Phlegm stagnated in the upper body results in neurophysiological symptoms such as palpitation, dizziness, chest discomfort, and sensitivity to noise [9]. Therefore, PP may affect SEI [33]. After forming the 12 pathways consisting of the six pathological patterns, the six direct pathways of the pathological patterns for decreased QoL estimated by GHQ scores were added to the pathway model.

2.4. Statistical Analysis. In our study, path analysis was used to examine whether the pathway model was acceptable and to examine which pathways among direct and indirect effects were more influential on QoL. We calculated three model fitness indexes, Goodness-of-Fit Index (GFI), Normed Fit Index (NFI), and Comparative Fit Index (CFI), to strictly evaluate the fitness of the proposed model [37–40]. Standardized estimates were calculated to compare the relative predictive powers of pathological patterns to decreases in QoL. Squared multiple correlations (SMC) were calculated to examine the percentage of pathological patterns contributing to decreases in QoL or were explained by other pathological patterns. All statistical analyses were performed with AMOS 18. In the model fitness tests, GFI > 0.950, 0 < NFI < 1, and CFI > 0.90 indicated statistical significance [37, 41, 42]. In examining standardized estimates of the direct and indirect effects, $P < 0.05$ indicated statistical significance.

3. Results

The results of the research model are presented in Figure 2. Correlation appears as a two-directional arrow, and standardized path coefficients appear as one-directional arrows. Three fitness indices showed that our research model possessed a satisfactory model-to-data fitness level (GFI = 0.975, NFI = 0.984, and CFI = 0.984).

Table 3 lists SMC and standardized estimates of the pathological patterns and decreases in QoL. The SMC values of FS, BS, Phlegm, SEI, and K-GHQ were 0.555, 0.667, 0.775, 0.726, and 0.437, respectively, indicating that Phlegm and SEI patterns result from other pathological patterns. Decreases in QoL were significantly affected by two pathological patterns: SEI ($\beta = 0.444$) and Phlegm patterns ($\beta = 0.350$). The highest estimate for the standardized regression weight was found in the path from the QD to FS ($\beta = 0.576$), and both the path from FS to BS ($\beta = 0.507$) and the path from BS to Phlegm ($\beta = 0.481$) showed higher estimates than other pathways.

Table 3: Results of path analysis.

Regression weight or correlation	Pathological pattern or QoL	SMC	Standardized estimate	Estimate	S.E.	C.R.	*P* value
Regression weight	Yin Deficiency → Food Stagnation	0.555	0.230	0.266	0.049	5.457	<0.001
	Qi Deficiency → Food Stagnation		0.576	0.436	0.032	13.668	<0.001
	Food Stagnation → Blood Stasis	0.667	0.507	0.449	0.036	12.500	<0.001
	Qi Deficiency → Blood Stasis		0.372	0.250	0.027	9.173	<0.001
	Food Stagnation → Phlegm	0.775	0.129	0.135	0.042	3.236	0.001
	Blood Stasis → Phlegm		0.481	0.564	0.047	12.037	<0.001
	Yin Deficiency → Phlegm		0.253	0.305	0.037	8.145	<0.001
	Qi Deficiency → Phlegm		0.143	0.113	0.031	3.682	<0.001
	Yin Deficiency → Seven Emotions Impairment	0.726	0.121	0.174	0.053	3.284	0.001
	Food Stagnation → Seven Emotions Impairment		0.052	0.065	0.055	1.168	0.243
	Qi Deficiency → Seven Emotions Impairment		0.382	0.359	0.041	8.762	<0.001
	Blood Stasis → Seven Emotions Impairment		0.239	0.335	0.071	4.692	<0.001
	Phlegm → Seven Emotions Impairment		0.163	0.195	0.064	3.052	0.002
	Seven Emotions Impairment → quality of life	0.437	0.444	1.739	0.273	6.379	<0.001
	Qi Deficiency → quality of life		0.019	0.072	0.250	0.287	0.774
	Blood Stasis → quality of life		−0.089	−0.489	0.411	−1.190	0.234
	Food Stagnation → quality of life		−0.088	−0.430	0.312	−1.379	0.168
	Yin Deficiency → quality of life		0.050	0.281	0.301	0.935	0.350
	Phlegm → quality of life		0.350	1.637	0.362	4.521	<0.001
Correlation	Yin Deficiency ↔ Qi Deficiency		0.641	0.511	0.046	11.122	<0.001

SMC: squared multiple correlations, S.E: standard error, C.R.: critical ratio.

Table 4 lists direct, indirect, and total standardized estimates of the pathological patterns and decreases in QoL. YD, QD, BS, PP, and SEI all showed significant total effects (β = 0.233, 0.389, 0.220, 0.423, and 0.444, resp.). Interestingly, YD, QD, and BS pathological patterns had only indirect effects on decreases in QoL. QD was a strong determinant of the FS, BS, Phlegm, and SEI patterns (β = 0.576, 0.664, 0.537, and 0.658, resp.). FS was a strong effector of BS (β = 0.507), indicating that QD has an indirect effect on decreases in QoL via other pathological patterns such as BS, FS, SEI, or PP.

4. Discussion

In this study, we hypothesized that pathological patterns would affect decreases in QoL, and we formed a pathway model according to the EAM theory. Our pathway model had satisfactory model-to-data fitness levels (GFI = 0.975, NFI = 0.984, and CFI = 0.984). As hypothesized, pathological patterns affected decreases in QoL. The influence of pathological patterns on decreases in QoL could be classified into direct and indirect pathological pattern determinants. For example, Phlegm and SEI directly affected decreases in QoL, and the total path estimates of the two patterns were similar, indicating that progressive Phlegm and SEI patterns directly induce decreases in QoL. Interestingly, the total effects of SEI on QoL decrease consist of only direct effects, whereas those of Phlegm consist of both direct and indirect effects, suggesting that the Phlegm pattern has a direct effect on decrease in QoL or an indirect effect on the aggravation of SEI followed by a decrease in QoL.

It is noteworthy that QD, YD, and BS patterns only indirectly affected decreases in QoL. For example, QD and BS patterns resulted in the formation or progression of PP and SEI, and, thereafter, formed or progressive Phlegm and SEI patterns decreased QoL. Especially, QD was a strong and general effector of the BS, Phlegm, SEI, and FS patterns. Although YD was also a general effector of the Phlegm, SEI, BS, and FS patterns, its efficacy was not as strong as that of QD. It is interesting that FS induces an increase in the Phlegm, BS, and SEI patterns, although it had a weak indirect effect on decreases in QoL, suggesting that FS, like other pathological patterns, should be considered and managed for the purpose of improving QoL. According to our pathway model, QD and YD patterns should be preferably estimated and managed in order not to result in decreases in QoL. When QD and YD were not managed, the FS or BS pattern occurred. In this stage, FS and BS formed secondarily from QD and YD induced Phlegm or SEI formation, which directly lowers the QoL. Taken together, our study results suggest that pathological patterns can be categorized into three levels from the QoL-etiological perspective: increased QD and YD patterns refer to the early stage of decreases in QoL, FS and BS patterns refer to the middle stage, and increases in Phlegm and SEI patterns refer to the latter stage of decreases in QoL. Therefore, in individuals with Phlegm or SEI patterns, QoL issues should be more intensively managed.

Table 4: Results of total, direct, and indirect effects.

Dependent variable	Standardized effect	Independent variable					
		Qi Deficiency	Yin Deficiency	Food Stagnation	Blood Stasis	Phlegm	Seven Emotions Impairment
Food Stagnation	Total	0.576*	0.230*				
	Direct	0.576*	0.230*				
	Indirect	0.000	0.000				
Blood Stasis	Total	0.664*	0.117**	0.507**			
	Direct	0.372*	0.000	0.507**			
	Indirect	0.292*	0.117**	0.000			
Phlegm	Total	0.537**	0.339*	0.373**	0.481**		
	Direct	0.143**	0.253*	0.129*	0.481**		
	Indirect	0.394*	0.086**	0.244**	0.000		
Seven Emotions Impairment	Total	0.658**	0.216*	0.234*	0.318**	0.163*	
	Direct	0.382**	0.121*	0.052	0.239*	0.163*	
	Indirect	0.276*	0.095*	0.182**	0.078*	0.000	
Decreases in quality of life	Total	0.389**	0.233*	0.101	0.220**	0.423*	0.444*
	Direct	0.019	0.050	−0.088	−0.089	0.350*	0.444*
	Indirect	0.370**	0.184**	0.189**	0.309**	0.072**	0.000

*$P < 0.05$, **$P < 0.01$.

In summary, we hypothesized that pathological patterns may affect decreases in QoL and form a pathway model consisting of YDQ, QDQ, FSQ, BSQ, PPQ, SEIQ, and K-GHQ scores. Our pathway model had satisfactory model-to-data fitness level and suggested that pathological patterns could be categorized into direct and indirect pathological pattern determinants of QoL decrease. Moreover, the severity or stage of QoL problems could be estimated by the pathological patterns, and therefore, suitable treatments to alleviate each pathological pattern can be conducted to improve QoL. Although, in this study, we proposed a pathway model with a satisfactory model-to-data fitness and presented the causalities of pathological patterns to decreases in QoL, our study had some limitations. First, our study was conducted only in Seoul, Korea, and, as a result, has limited population validity. Second, GHQ has the inherent limitation of examining QoL only from the psychological point of view. Further studies are required in order to overcome these limitations with respect to population validity and psychological QoL.

5. Conclusions

In this study, we hypothesized that pathological patterns would affect QoL. We formed a pathway model consisting of YDQ, QDQ, FSQ, BSQ, PPQ, SEIQ, and K-GHQ scores according to the EAM theory and examined the model-to-data fitness of our pathway model; our proposed pathway model had satisfactory fitness levels (GFI = 0.975, NFI = 0.984, and CFI = 0.984). The pathway model showed that Phlegm and SEI patterns were direct effectors on QoL, whereas QD, YD, FD, and BS were indirect effectors on QoL. The pathway model results also suggested that the severity or stage of decreased QoL could be estimated by the pathological patterns: QD and YD patterns were linked to the early stage; FS and BS patterns were linked to the middle stage; Phlegm and SEI patterns were linked to the latter stage of decreased QoL. A suitable pattern treatment should be conducted to improve QoL according to stage. Further studies are required in order to overcome the study limitations with respect to population validity and psychological QoL.

Abbreviations

EAM: East Asian medicine
YDQ: Yin Deficiency Questionnaire
QDQ: Qi Deficiency Questionnaire
SEIQ: Seven Emotions Impairment Questionnaire
PPQ: Phlegm Pattern Questionnaire
FSQ: Food Stagnation Questionnaire
BSQ: Blood Stasis Questionnaire
QoL: Quality of life
GHQ: General Health Questionnaire
PCA: Principal component analysis
VAS: Visual analog scale
K-GHQ: The Korean version of the GHQ
YD: Yin Deficiency
QD: Qi Deficiency
SEI: Seven Emotions Impairment
FS: Food Stagnation
BS: Blood Stasis
PP: Phlegm Pattern
GFI: Goodness-of-fit Index
NFI: Normed fit index

CFI: Comparative fit index
SMC: Squared multiple correlations.

Conflict of Interests

The authors have no personal or financial conflict of interests associated with this work.

References

[1] World Health Organization, *WHO International Standard Terminologies on Traditional Medicine in Western Pacific Region*, WHO Western Pacific Regional Office, Manila, Philippines, 2007.

[2] C. A. Berle, D. Cobbin, N. Smith, and C. Zaslawski, "A novel approach to evaluate traditional chinese medicine treatment outcomes using pattern identification," *Journal of Alternative and Complementary Medicine*, vol. 16, no. 4, pp. 357–367, 2010.

[3] A.P. Lu and K.J. Chen, "Integrative medicine in clinical practice: from pattern differentiation in traditional chinese medicine to disease treatment," *Chinese Journal of Integrative Medicine*, vol. 15, no. 2, p. 152, 2009.

[4] C. Lu, Q. Zha, A. Chang, Y. He, and A. Lu, "Pattern differentiation in traditional chinese medicine can help define specific indications for biomedical therapy in the treatment of rheumatoid arthritis," *Journal of Alternative and Complementary Medicine*, vol. 15, no. 9, pp. 1021–1025, 2009.

[5] S. P. Yun, W. S. Jung, S. U. Park et al., "Hwangryunhaedogtang (huanglianjiedutang) treatment for pathological laughter after stroke and importance of patterns identification: a preliminary study," *American Journal of Chinese Medicine*, vol. 35, no. 5, pp. 725–733, 2007.

[6] S. W. Cho, Y. J. Park, M. Y. Kim et al., "Development of questionnaires for pathogenesis analysis of Yukmijiwhangtang," *Journal of Korea Institute of Oriental Medical Diagnostics*, vol. 12, no. 2, pp. 61–73, 2008.

[7] T. D. Yoon, Y. J. Park, S. C. Lee et al., "Development of questionnaires for pathogenesis analysis of bojungikgitang symptom," *Journal of Korea Institute of Oriental Medical Diagnostics*, vol. 11, no. 2, pp. 45–58, 2007.

[8] B. H. Lee, Y. B. Park, Y. J. Park et al., "A study on reliability and validity of the guibi-tang patternization questionnaire," *Journal of Korea Institute of Oriental Medical Diagnostics*, vol. 13, no. 1, pp. 45–53, 2009.

[9] Y.-J. Park, J.-S. Park, M.-Y. Kim, and Y.-B. Park, "Development of a valid and reliable phlegm pattern questionnaire," *Journal of Alternative and Complementary Medicine*, vol. 17, no. 9, pp. 851–858, 2011.

[10] J. S. Lim, Y. B. Park, Y. J. Park et al., "A study on reliability and validity of the pyungweesan patternization questionnaire by the pathogenesis analysis," *Journal of Korea Institute of Oriental Medical Diagnostics*, vol. 11, no. 2, pp. 59–67, 2007.

[11] D. H. Yang, Y. J. Park, Y. B. Park et al., "Development of questionnaires for Blood Stasis pattern," *Journal of Korea Institute of Oriental Medical Diagnostics*, vol. 10, no. 1, pp. 141–152, 2006.

[12] D.-S. Tzeng, W.-C. Chung, P.-L. Fan, F.-W. Lung, and C.-Y. Yang, "Psychological morbidity, quality of life and their correlations among military health care workers in taiwan," *Industrial Health*, vol. 47, no. 6, pp. 626–634, 2009.

[13] The WHOQOL Group, "The World health organization quality of life assessment (WHOQOL): position paper from the world health organization," *Social Science & Medicine*, vol. 41, pp. 1403–1409, 1995.

[14] N. J. Talley, M. Haque, J. W. Wyeth et al., "Development of a new dyspepsia impact scale: the nepean dyspepsia index," *Alimentary Pharmacology and Therapeutics*, vol. 13, no. 2, pp. 225–235, 1999.

[15] G. H. Guyatt, D. H. Feeny, and D. L. Patrick, "Measuring health-related quality of life," *Annals of Internal Medicine*, vol. 118, no. 8, pp. 622–629, 1993.

[16] G. H. Guyatt and R. Jaaeschke, "Assessment in the clinical trials," in *Measurement in Clinical Trials: Choosing the Appropriate Approach*, B. Spilker, Ed., p. 37, Raven Press, NewYork, NY, USA, 1990.

[17] G. H. Guyatt, R. A. Deyo, M. Charlson, M. N. Levine, and A. Mitchell, "Responsiveness and validity in health status measurement: a clarification," *Journal of Clinical Epidemiology*, vol. 42, no. 5, pp. 403–408, 1989.

[18] G. H. Guyatt, D. H. Feeny, and D. L. Patrick, "Measuring health-related quality of life," *Annals of Internal Medicine*, vol. 118, no. 8, pp. 622–629, 1993.

[19] D. P. Goldberg and P. Williams, *A USer's Guide to the General Health Questionnaire*, NFER-Nelson, Windsor, UK, 1988.

[20] G. I. J. M. Kempen, J. Ormel, E. I. Brilman, and J. Relyveld, "Adaptive responses among dutch elderly: the impact of eight chronic medical conditions on health-related quality of life," *American Journal of Public Health*, vol. 87, no. 1, pp. 38–44, 1997.

[21] E. A. Schlenk, J. A. Erlen, J. Dunbar-Jacob et al., "Health-related quality of life in chronic disorders: a comparison across studies using the MOS SF-36," *Quality of Life Research*, vol. 7, no. 1, pp. 57–65, 1998.

[22] A. L. Stewart, S. Greenfield, R. D. Hays et al., "Functional status and well-being of patients with chronic study. results from the medical outcomes study," *Journal of the American Medical Association*, vol. 262, no. 7, pp. 907–913, 1989.

[23] A. L. Schwartz, "Fatigue mediates the effects of exercise on quality of life," *Quality of Life Research*, vol. 8, no. 6, pp. 529–538, 1999.

[24] R. L. Schalock and D. Felce, "Quality of life and subjective well-being: conceptual and measurement issues," in *The International Handbook of Applied Research in Intellectual Disabilities*, E. Emerson, C. Hatton, and T. Thompson, Eds., pp. 261–279, John Wiley & Sons, West Sussex, UK, 2004.

[25] L. Berkman, C. Berkman, S. Kasl et al., "Depressive symptoms in relation to physical health and functioning in the elderly," *American Journal of Epidemiology*, vol. 124, pp. 372–388, 1986.

[26] D. G. Blazer, "Depression in late life: review and commentary," *Journals of Gerontology: Series A*, vol. 58, no. 3, pp. 249–265, 2003.

[27] D. G. Blazer, C. F. Hybels, and C. F. Pieper, "The association of depression and mortality in elderly persons: a case for multiple, independent pathways," *Journals of Gerontology: Series A*, vol. 56, no. 8, pp. M505–M509, 2001.

[28] H. J. Schünemann, F. Sperati, M. Barba et al., "An instrument to assess quality of life in relation to nutrition: item generation, item reduction and initial validation," *Health and Quality of Life Outcomes*, vol. 8, article 26, 2010.

[29] S. W. Cho, H. S. Oh, M. Y. Kim et al., "The effects of the Seven Emotions on self-awareness quality of life," *Journal of Korea Institute of Oriental Medical Diagnostics*, vol. 15, no. 1, pp. 87–94, 2011.

[30] P. Webley and S. Lea, "Multivariate analysis II: manifest variables analyses," http://www.exeter.ac.uk/~SEGLea/multvar2/pathanal.html.

[31] K. S. Song, "The factor analytical study of general health questionnaire in neurotic outpatients," *Psychiatry Investigation*, vol. 25, no. 1, pp. 92–100, 1986.

[32] C. K. Park, *Cause and Mechanism of Disease*, Traditional Medicine Research Institute Press, Seoul, Republic of Korea, 1992.

[33] J. Heo, *An Oriental Medical Treasure*, Nam San Dang Press, Seoul, Republic of Korea, 2003.

[34] K. W. Lee, J. K. Jung, and M. H. Ahn, Eds., *Yellow Emperor'S Suwen*, Yeo Kang Press, Seoul, Republic of korea, 2000.

[35] Y. W. Hwang and J. H. Kim, *Psychiatry of Oriental Medicine*, Hyun Dai Ui Hak Seo Jeok Press, Seoul, Republic of korea, 1987.

[36] J. H. Park, J. J. Moon, G. S. Ahn et al., "A philological study on the pathology of syndromes of stagnated blood & water," *Journal of Oriental Medical Pathology*, vol. 9, pp. 129–152, 1994.

[37] L.-T. Hu and P. M. Bentler, "Fit indices in covariance structure modeling: sensitivity to underparameterized model misspecification," *Psychological Methods*, vol. 3, no. 4, pp. 424–453, 1998.

[38] K. Joreskog and D. Sorbom, *LISREL 8: Structural Equation Modeling with the SIIMPLIS Command Language*, Scientific Software International, Skokie, Ill, USA, 1993.

[39] P. M. Bentler and D. G. Bonett, "Significance tests and goodness of fit in the analysis of covariance structures," *Psychological Bulletin*, vol. 88, no. 3, pp. 588–606, 1980.

[40] X. Fan, B. Thompson, and L. Wang, "Effects of sample size, estimation methods, and model specification on structural equation modeling fit indexes," *Structural Equation Modeling*, vol. 6, no. 1, pp. 56–83, 1999.

[41] M. Shevlin and J. N. V. Miles, "Effects of sample size, model specification and factor loadings on the GFI in confirmatory factor analysis," *Personality and Individual Differences*, vol. 25, no. 1, pp. 85–90, 1998.

[42] S. A. Mulaik, L. R. James, J. Van Alstine, N. Bennett, S. Lind, and C. D. Stilwell, "Evaluation of goodness-of-fit indices for structural equation models," *Psychological Bulletin*, vol. 105, no. 3, pp. 430–445, 1989.

Hindawi Publishing Corporation
Evidence-Based Complementary and Alternative Medicine
Volume 2013, Article ID 975350, 9 pages
http://dx.doi.org/10.1155/2013/975350

Research Article

Trichosanthes kirilowii Ethanol Extract and Cucurbitacin D Inhibit Cell Growth and Induce Apoptosis through Inhibition of STAT3 Activity in Breast Cancer Cells

Soon Re Kim, Hye Sook Seo, Han-Seok Choi, Sung-Gook Cho, Yong Kuk Kim, Eun Hee Hong, Yong Cheol Shin, and Seong-Gyu Ko

Laboratory of Clinical Biology and Pharmacogenomics, Department of Preventive Medicine, College of Oriental Medicine, Kyung Hee University, Seoul 130-701, Republic of Korea

Correspondence should be addressed to Seong-Gyu Ko; epiko@khu.ac.kr

Received 4 April 2013; Revised 3 August 2013; Accepted 13 August 2013

Academic Editor: Bo-Hyoung Jang

Trichosanthes kirilowii tuber is a traditional medicine which exhibits various medicinal effects including antidiabetic and anticancer activities in several cancer cells. Recently, it was reported that Cucurbitacin D (CuD) isolated from *Trichosanthes kirilowii* also induces apoptosis in several cancer cells. Constitutive signal transducer and activator of transcription 3 (STAT3), which is an oncogenic transcription factor, is often observed in many human malignant tumor, including breast cancer. In the present study, we tested whether *Trichosanthes kirilowii* ethanol extract (TKE) or CuD suppresses cell growth and induces apoptosis through inhibition of STAT3 activity in breast cancer cells. We found that both TKE and CuD suppressed proliferation and induced apoptosis and G2/M cell cycle arrest in MDA-MB-231 breast cancer cells by inhibiting STAT3 phosphorylation. In addition, both TKE and CuD inhibited nuclear translocation and transcriptional activity of STAT3. Taken together, our results indicate that TKE and its derived compound, CuD, could be potent therapeutic agents for breast cancer, blocking tumor cell proliferation and inducing apoptosis through suppression of STAT3 activity.

1. Introduction

Breast cancer is the most common disease in women and the leading cause of cancer death. The cause of breast cancer involves a genetic disorder, life style, or dietary factors. There are effects in breast cancer therapy that have improved the survival period and quality of life. However, breast cancer patients continue to die, and thus new therapeutic strategies of breast cancer are required. Signal transducer and activator of transcription3 (STAT3) is an oncogenic transcription factor which is constitutively activated in more than 50% of primary breast tumor and tumor-derived cell lines [1, 2].

Apoptosis plays a crucial role during embryonic development and tissue homeostasis [3]. It is related to the activation of the family of central components of the apoptotic machinery known as Caspases [4, 5]. To date, research indicates that there are two main apoptotic pathways: the extrinsic or death receptor pathway and the intrinsic or mitochondrial pathway. The extrinsic and intrinsic pathways converge on the same terminal execution pathway. This pathway is initiated by the cleavage of caspase-3 and results in DNA fragmentation, degradation of cytoskeletal and nuclear proteins, cross-linking of proteins, formation of apoptotic bodies, expression of ligands for phagocytic cell receptors, and finally uptake by phagocytic cells. Apoptotic cell death is controlled by diverse signaling pathways, which may activate either extrinsic inducers (caspase-8) or intrinsic inducers (caspase-9). The extrinsic signaling pathways that initiate apoptosis involve transmembrane receptor-mediated interactions. The intrinsic signaling pathways that initiate apoptosis involve a diverse array of non-receptor-mediated stimuli that produce intracellular signals that act directly on targets within the cell and are mitochondrial-initiated events. Bcl-2 family members (Bcl-2, Bcl-XL, BAX, Bak, Bad, and Bid) are associated with mitochondrial death pathway and cell cycle progression [6].

Trichosanthes kirilowii tuber extract (TKE) is a traditional medicine used in East of Asia for patients with diabetes symptoms. Trichosanthin (TCS), which is also known as type 1 ribosome-inactivating protein, is a chemical component derived from TKE [7]. TCS acts as a potent inhibitor of HIV-1 replication and is known to have various antitumor functions [8, 9]. Recently, it was reported that Cucurbitacin D, isolated from TKE, induces apoptosis in human hepatocellular carcinoma cells [10].

Cucurbitacins refer to a group of tetracyclic triterpenoids initially identified in the plant family of Cucurbitaceae. In traditional medicine, cucurbitacin-containing plants have been known for their anti-inflammatory, antimicrobial, and antitumor activities [11, 12]. There are 17 main molecules from cucurbitacin A to cucurbitacin T and hundreds of derivatives from them. Among those, cucurbitacin B, D, E, I, and their derivatives have been studied extensively for their strong anticancer activities. Also, cucurbitacin F, O, P, Q, and their derivatives are known to have modest anticancer activities [11]. JAK-STAT pathway, AKT-PKB pathway, and MAPK pathway are significantly associated with cancer and action of cucurbitacin family [13, 14].

In this study, we hypothesized that TKE and its derived compound, CuD, may modulate the STAT3 signaling pathway and sensitize breast cancer cells to apoptosis. To confirm this hypothesis, we treated MDA-MB-231 cells with TKE or CuD and performed experiments to observe the changes in STAT3 expression and its transcriptional activity.

2. Material and Method

2.1. Reagents. 4′,6-diamidino-2-phenylindole (DAPI), (3-(4, 5-dimethylthiazol-2-yl)-2,5-diphenyltetrazolium bromide (MTT), and dimethyl sulfoxide (DMSO) were purchased from Sigma-Aldrich (St. Louis, MO, USA). Propidium Iodide (PI) and Alexa Flour 488 goat anti-rabbit antibody were purchased from Invitrogen (Carlsbad, CA, USA). Cucurbitacin D was purchased from Extrasynthese (Genay Cedex, France). Antibodies against phospho-STAT3 (Tyr 705) and total STAT3 were obtained from Cell signaling (Danvers, MA, USA). Antibodies against pro-caspase-9, cleaved-caspase-9, cleaved-caspase-8, pro-caspase-3, cleaved-caspase-3, and PARP/p85 were obtained from Santa Cruz Biotechnology (Santa Cruz, CA, USA).

2.2. Preparation of Trichosanthes kirilowii Alcohol Extract (TKE). *Trichosanthes kirilowii* was purchased from Omniherb (Yeongcheon, Republic of Korea). A ground powder (a mass of 100 g) was extracted twice with 80% (V/V) ethanol by using an ultrasonicator (Branson Ultrasonics, Danbury, CT, USA) for 30 min at room temperature. The alcohol extract was evaporated at 40°C (Evaporator, Eyela, Japan) and then freeze-dried for 72 h (Freezedryer, Matsushita, Japan). The powder from the extract was dissolved in distilled water to make a concentration of 200 mg/mL and centrifuged at 13,000 rpm at 4°C for 5 min. The supernatant TKE was stored in aliquots at −80°C until further analysis.

2.3. Cell Culture. MCF7, SK-BR3, and MDA-MB-231 breast cancer cells obtained from American Type Culture Collection (ATCC) were maintained in RPMI1640 supplemented with 10% heat-inactivated fetal bovine serum (Invitrogen, Carlsbad, CA, USA) and 100 U/mL antibiotic-antimycotic (Invitrogen). Cells were maintained at 37°C in a humidified incubator with 5% CO_2.

2.4. Cell Viability Assay. Cell viability was measured using MTT assay. Cells were plated in 96-well flat bottom tissue culture plates at a density of 5×10^3 cells/well and incubated for 24 h. Cells were cultured for additional 24 h with TKE (10–200 μg/mL) or CuD (0.1–10 μg/mL). After incubation, MTT reagents (0.5 mg/mL) were added to each well, and the plates were incubated in the dark at 37°C for another 2 h. Medium was removed, formazan was dissolved in DMSO, and optical density was measured at 570 nm using an ELISA plate reader.

2.5. Flow Cytometric Analysis. Flow cytometry was used to analyze cell cycle distribution. Cells (3×10^5) were seeded in 60 mm dishes. After 24 h, cells were cultured for additional 6 or 24 h in the absence (control) or presence of 60 μg/mL TKE. Trypsinized cells were washed with phosphate-buffer saline (PBS), fixed in 95% ethanol containing 0.5% Tween-20 overnight at −20°C. After washing with PBS, cells were then incubated with 1 U/mL of RNase A and 10 μg/mL of PI for 30 min at room temperature in the dark. DNA content in each cell nucleus was determined by a FACScalibur flow cytometer (Becton-Dickinson, San Jose, CA, USA), and cell cycle was analyzed using a ModFit LT V2.0 software.

2.6. Western Blot Analysis. Cells were harvested, and cell pellets were incubated in one volume of lysis buffer [50 mM Tris-Cl pH 7.4, 1% NP-40, 0.25% sodium deoxycholate, 0.1% SDS, 150 mM NaCl, 1 mM EDTA, and protease inhibitor] for 20 min and centrifuged at 13,000 rpm at 4°C for 20 min. Aliquots containing 20 μg of protein were separated by SDS-polyacrylamide gel electrophoresis using 8–12% gels and transferred to nitrocellulose membranes (Protran nitrocellulose membrane, Whatman, UK). Membranes were blocked with 5% nonfat milk and probed with specific primary antibodies. Membranes were then incubated with horseradish peroxidase-conjugated secondary IgG antibody (Calbiochem, San Diego, CA, USA) and visualized using the enhanced chemiluminescence detection system (Amersham ECL kit, Amersham Pharmacia Biotech Inc. Piscataway, NJ, USA).

2.7. Immunocytofluorescence. Cells were plated in 8-well chamber slide at a density of 2×10^4 cells/well and incubated for 24 h. Cells were cultured for additional 24 h with 20 μg/mL of TKE or culture medium alone (control). After incubation, cells were fixed with 4% paraformaldehyde for 30 min, and the slides were incubated with 5% BSA for 1 h. After overnight incubation with rabbit polyclonal anti-human STAT3 antibody (dilution, 1 : 500), the slides were washed with PBS and then incubated with FITC-conjugated secondary antibody (dilution, 1 : 500) at room temperature

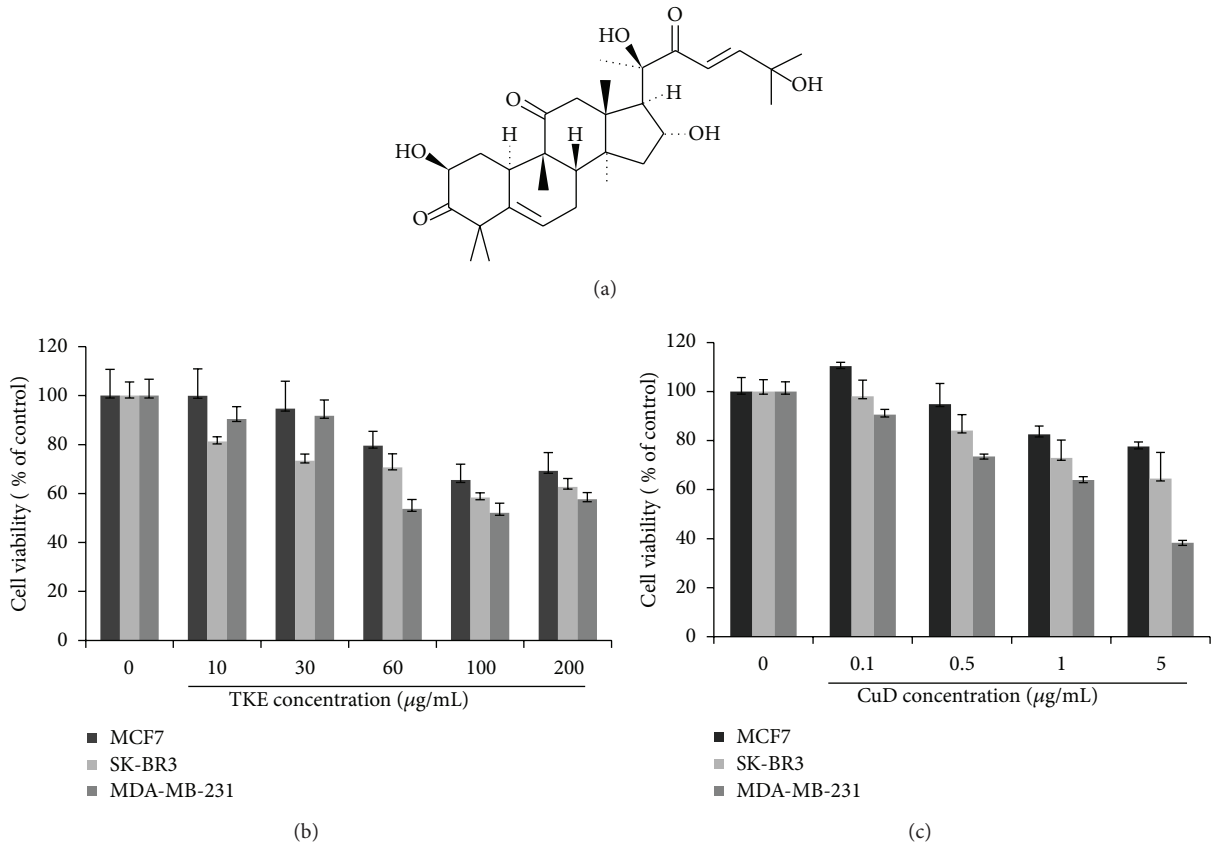

Figure 1: TKE and CuD inhibits cell proliferation in MCF7, SK-BR3, and MDA-MB-231 breast cancer cells. (a) Chemical structure of CuD. ((b), (c)) Different breast cancer cells were seeded into 96-well plates and treated with different concentrations of TKE (0, 10, 30, 60, 100, 200 μg/mL) or CuD (0, 0.1, 0.5, 1, 5 μg/mL) for 24 h. Cell viability measured by MTT assay. Data was reported as the percentage change in comparison to the 0 μg/mL concentration group, which were assigned 100% viability. The error bars represent the mean ± standard deviation (SD).

for 1 h. After a brief washing in PBS, the slides were incubated with DAPI solution at room temperature for 5 min for counter staining. The slides were then washed with H_2O and mounted by antifade mounting solution. The immunofluorescence staining of the cells was observed with confocal microscope (Zeiss, Germany).

2.8. Terminal Nucleotidyl Transferase-Mediated Nick End Labeling (TUNEL) Assay. Cells were plated in 8-well chamber slide at a density of 2×10^4 cells/well and incubated for 24 h. Cells were cultured for additional 24 h with 20 μg/mL of TKE or culture medium alone (control). After incubation, cells were fixed with 4% paraformaldehyde and incubated with 1% Triton X-100 in PBS for 2 min on ice for permeabilization. TUNEL staining was performed using TUNEL-label, enzyme kit (Roche) according to the manufacturer's instructions. The immunofluorescence staining of the cells was observed with confocal microscope.

2.9. Luciferase Assay. For the assay, MDA-MB-231 cells were plated and allowed to attach by overnight incubation. Next day, cells were transfected with control siRNA (Qiagen, Venlo, Netherlands) and STAT3 siRNA (SanTa Cruz, CA, USA) in the presence of STAT3-luciferase reporter using lipofectamine 2000 (Invitrogen, Carlsbad, CA, USA). Cells were then treated with TKE or CuD for 24 h. Luciferase assays were performed using a dual-luciferase assay kit (Promega, Madison, WI, USA) according to the manufacturer's instructions. Briefly, cells were lysed using a passive lysis buffer. Cell lysates were then centrifuged, and the supernatant was saved for analysis. Finally, luciferase activities were determined using a luminometer (BMG Labtech, Ortenberg, Germany).

2.10. Liquid Chromatography-Mass Spectrometry Analysis. An Agilent 1100 series liquid chromatography-mass spectroscopy (LC-MS) with an atmospheric pressure chemical ionization interface was used in negative and positive ionization modes. Data were collected using Chemstation software version A.09.03. A Shiseido capcell-pak UG120 column (4.6 mm × 250 mm, 5 μm) was used with an injection volume of 10 μL for the HPLC separation. The mobile phases consisted of (A) water and (B) methanol at a flow rate of 0.7 mL/min. The gradient of the mobile phases (A : B) for separation was 0–60 min (95 : 5 to 10 : 90). CuD was used as standard. Mass spectrometry was operated with an electrospray ionization source and positive mode.

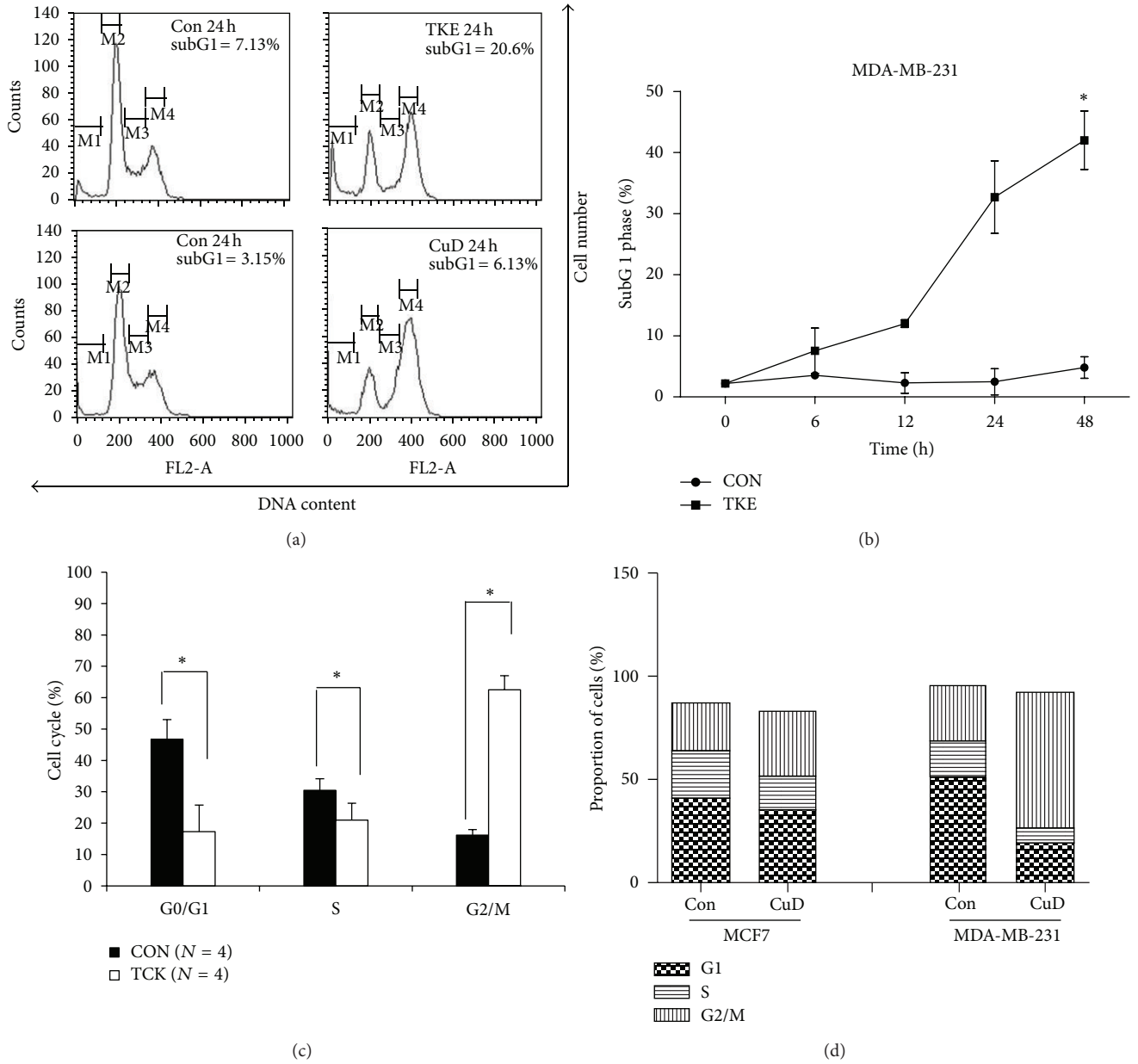

Figure 2: TKE and CuD cause apoptosis and G2/M cell cycle arrest in MDA-MB-231 cells. (a) MDA-MB-231 cells were treated with 60 μg/mL of TKE or 1 μg/mL of CuD for 24 h. Cell cycle distribution was analyzed using a FACStar flow cytometer. (b) Graphs shows FACS-based subG1 phase distribution of MDA-MB-231 cells incubated with 60 μg/mL TKE for 24 h. (c) Bar graphs show FACS-based cell cycle distribution of MDA-MB-231 cells incubated with 60 μg/mL TKE for 24 h. (d) Bar graphs show FACS-based cell cycle distribution of MCF7 cells and MDA-MB-231 cells incubated with 60 μg/mL TKE or 1 μg/mL of CuD for 24 h. The error bars represent the mean ± standard deviation (SD).

2.11. Statistical Analysis. All experiments were expressed as the mean ± standard deviation (SD) of at least three separate tests. Student's t-test was used for single variable comparisons, and a P value < 0.05 was considered statistically significant.

3. Results

3.1. TKE and CuD Inhibits Proliferation of Human Breast Cancer Cell Lines. Figure 1(a) shows the chemical structure of CuD. We investigated whether TKE and CuD exhibit antiproliferative activity in MCF7, SK-BR3, and MDA-MB-231 cells. For that purpose, cells were treated with various concentrations of TKE (10, 30, 60, 100, 200 μg/mL) or CuD (0.1, 0.5, 1, 5 μg/mL), and cell growth rate was determined using MTT assay at 24 h. We found that both TKE and CuD significantly inhibited growth of all breast cancer cell lines (Figures 1(b) and 1(c)).

3.2. TKE and CuD Cause Apoptosis and G2/M Cell Cycle Arrest in MDA-MB-231 Cells. To further characterize the inhibitory effect of TKE and CuD on cell proliferation, we monitored

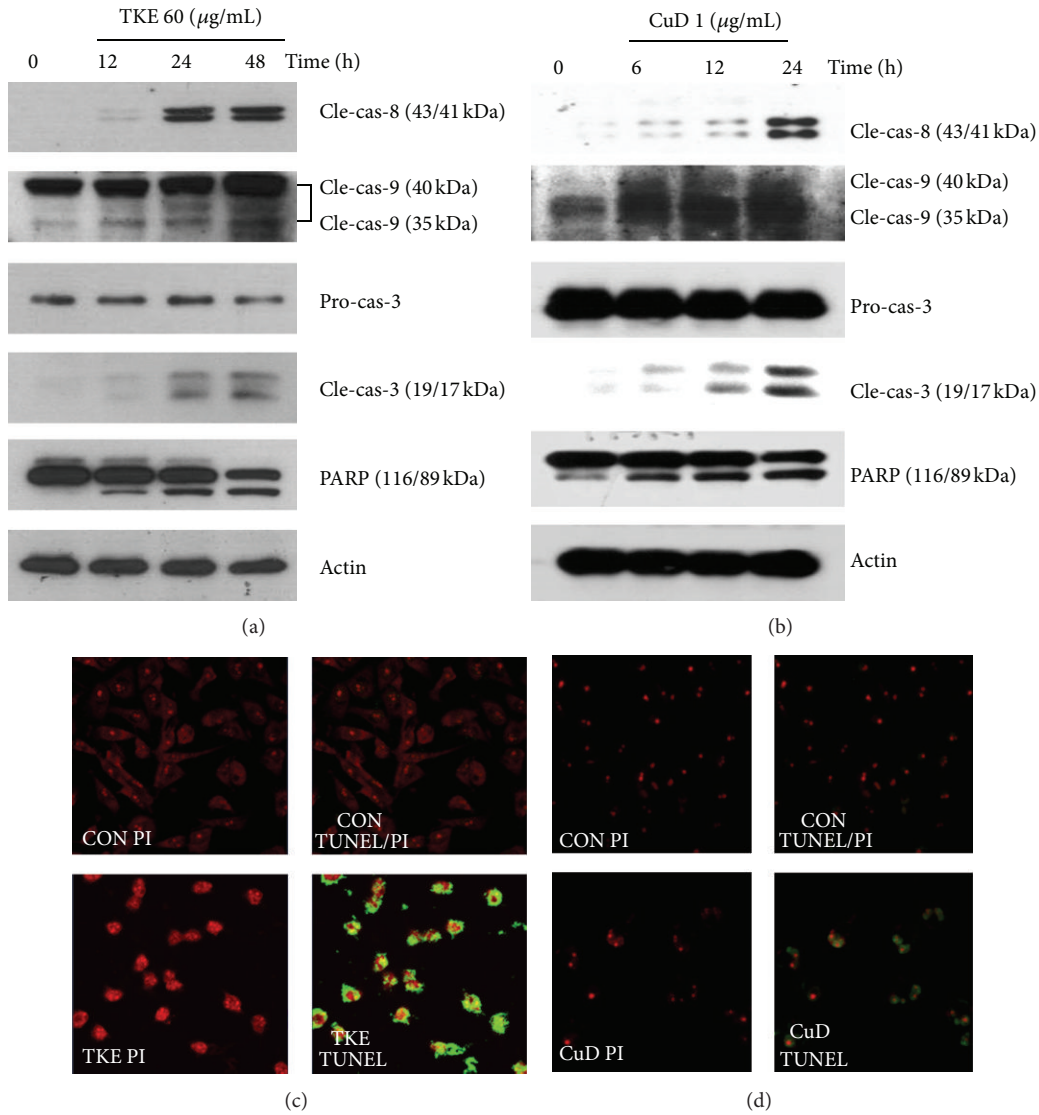

Figure 3: Effect of TKE and CuD on the expression of apoptosis-related molecules. ((a), (b)) MDA-MB-231 cells were treated with 60 μg/mL TKE or 1 μg/mL CuD for the indicated time periods, and the cell lysates were subjected to western blot analysis using specific antibodies. ((c), (d)) MDA-MB-231 cells were incubated in the absence or presence of TKE or CuD and submitted to TUNEL assay. For the TUNEL assay, cells were fixed, permeabilized, and visualized for DNA degradation using dUTP-labeling. Red fluorescence: nuclei stained with PI. Green or yellow (resulting from merged red and green) fluorescence: apoptotic nuclei containing fragmented DNA.

cell cycle progression using flow cytometry. Both TKE and CuD induced the increase of sub G1 apoptotic cell fractions in MDA-MB-231 cells suggesting that antiproliferative activity of TKE and CuD resulted from apoptosis (Figures 2(a) and 2(b)). Moreover, exposure to TKE and CuD resulted in an increase in G2/M phase cells, accompanied by a decrease in G1 phase cells in MDA-MB-231 cells (Figures 2(c) and 2(d)).

3.3. TKE and CuD Regulate Apoptotic Molecules in MDA-MB-231 Cells. To examine the effect of TKE and CuD on the apoptotic signaling pathway, the levels of apoptosis-related molecules were measured in MDA-MB-231 cells by western blot using specific antibodies. We found that TKE and CuD upregulated levels of cleaved caspase-8, cleaved caspase-9, and cleaved caspase-3 and induced the cleavage of PARP in MDA-MB-231 cells (Figures 3(a) and 3(b)). These results indicate that TKE and CuD induce apoptosis in MDA-MB-231 cells producing the cleavage of caspases and PARP. On the other hand, TUNEL assay demonstrated that both TKE and CuD induced apoptotic cell death increasing many apoptotic green and yellow nuclei (Figures 3(c) and 3(d)).

3.4. TKE and CuD Inhibit Constitutive STAT3 Phosphorylation. High expression of STAT3 has been found to be involved in cancer progression. Knowing that STAT3 is activated in MDA-MB-231 cells, we investigated whether

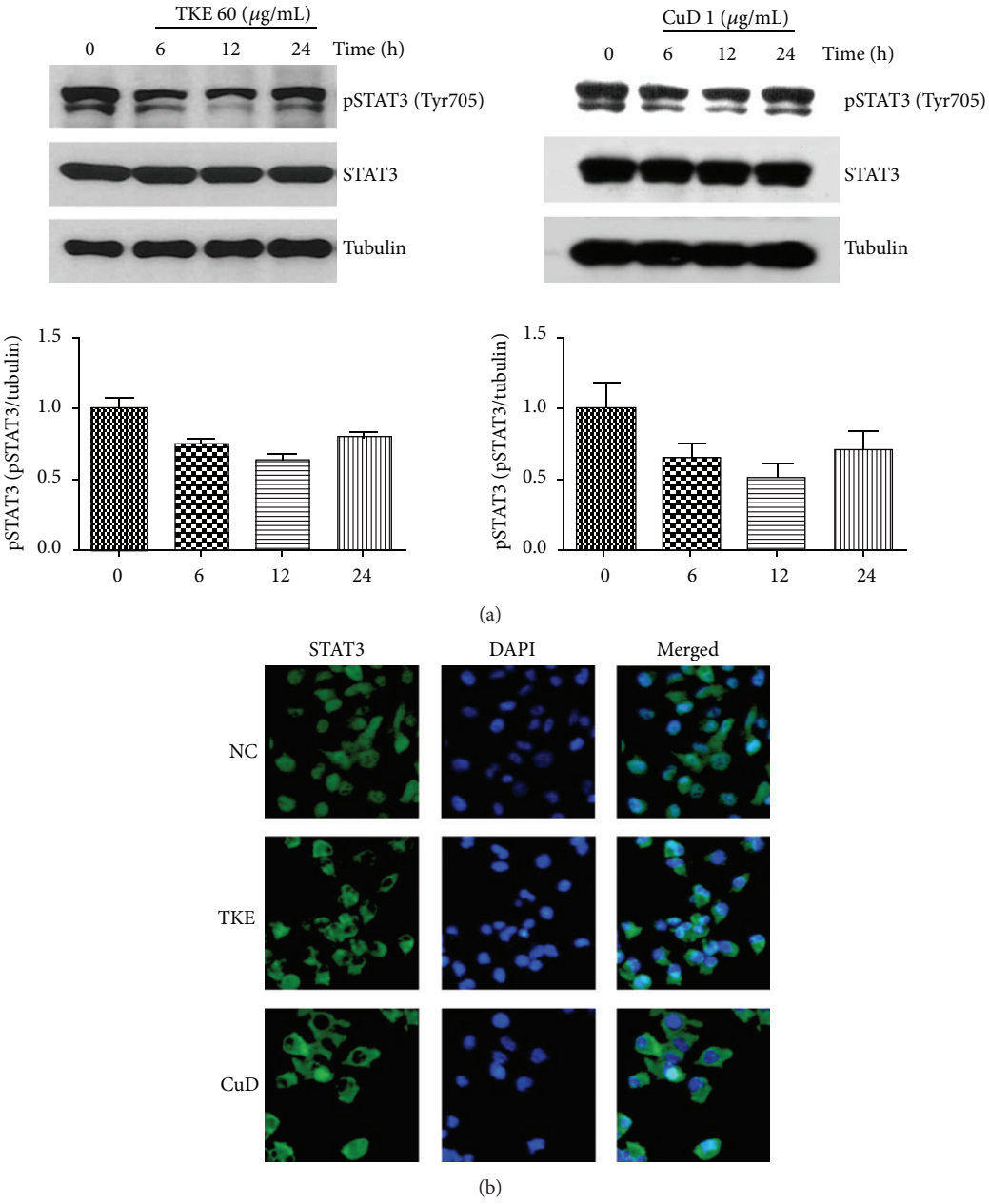

Figure 4: TKE and CuD suppress STAT3 phosphorylation and inhibit the translocation of STAT3 to the nucleus. (a) Cells were treated with 60 μg/mL TKE or 1 μg/mL CuD for different time periods (0–24 h). Total cell lysates were subjected to western blot analysis using specific antibodies (upper part) and the relative level of pSTAT3 as measured from the western blot analysis by densitometry (lower part). (b) MDA-MB-231 cells were plated in 8-well chamber slide. The next day, cells were incubated with 60 μg/mL TKE or 1 μg/mL CuD for 12 h and submitted to immunocytofluorescence assay. STAT3 distribution was exhibited by green fluorescence, and nuclei were counter-stained by DAPI.

TKE and CuD suppress STAT3 phosphorylation. Figure 4(a) demonstrates that both TKE and CuD suppress constitutive activation of STAT3 within 6 to 12 h.

3.5. TKE and CuD Suppress STAT3 Nuclear Translocation in MDA-MB-231 Cells. Normally, the active STAT3 homodimer translocates to the nucleus from the cytoplasm and induces specific target gene expression [15, 16]. Thus, we determined whether TKE and CuD suppress STAT3 nuclear translocation using immunofluorescence analysis. We found that TKE and CuD blocked the translocation of STAT3 into the nucleus in MDA-MB-231 cells (Figure 4(b)).

3.6. TKE and CuD Repress STAT3-Dependent Reporter Gene Expression. Although TKE and CuD has been shown to exhibit growth-inhibitory effect on MDA-MB-231 cells, it is not known whether it can modulate STAT3 signaling pathway. It should be noted that the constitutive activation

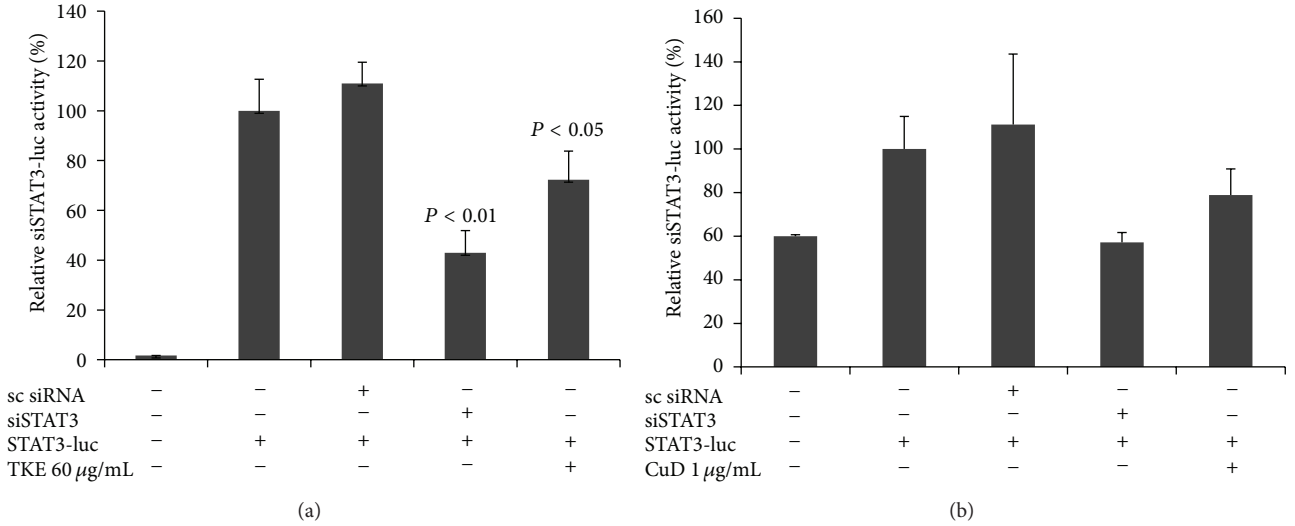

Figure 5: TKE and CuD suppress the STAT3 transcription activity. MDA-MB-231 cells were transfected with the indicated siRNA or plasmid and then treated with each drug for 24 hours and submitted to dual-luciferase reporter assay.

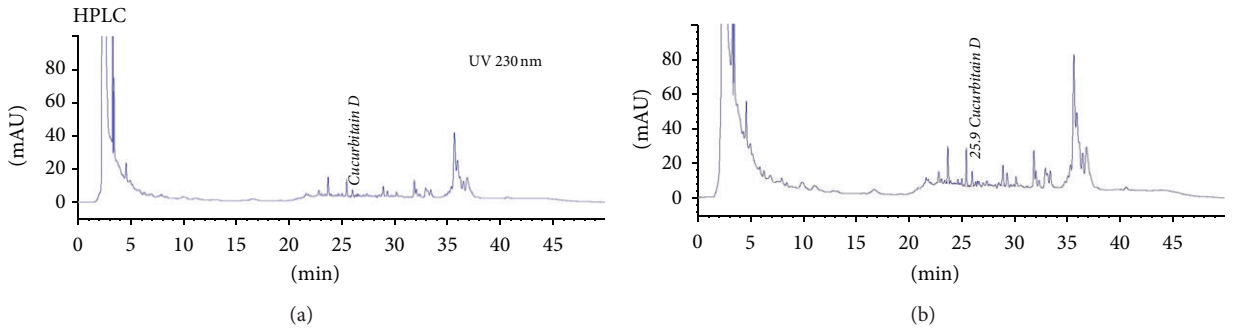

Figure 6: LC-MS chromatogram. (a) Identification of CuD from TKE. (b) Mass spectrum peak at 25.9 min.

of STAT3 is frequently detected in breast cancer tissues and cell lines. Therefore, we performed STAT3-dependent luciferase reporter gene assay to detect STAT3 transcriptional activity. We found that TKE and CuD significantly repressed STAT3-dependent reporter gene activity in MDA-MB-231 cells (Figures 5(a) and 5(b)).

3.7. CuD Is Extorted from TKE. We employed LC-MS analysis to confirm that CuD is extorted from TKE. Through analysis, chromatograms were acquired at 230 nm by UV detection (Figure 6(a)), and retention times of CuD were 25.9 min (Figure 6(b)).

4. Discussion

The roots of *Trichosanthes kirilowii* have been used as a traditional herbal remedy and are an attractive medical resource. In addition, recent paper reported that CuD is an active compound of *Trichosanthes kirilowii*, and CuD induces apoptosis via activation of caspases and JNK in hepatocellular carcinoma cells [10]. Here, we found that TKE and its derived compound, CuD, inhibit cell proliferation and induce G2/M phase cell cycle arrest in MDA-MB-231 cells. In addition, we found that antiproliferative activity induced by TKE was associated with reduction of STAT3 phosphorylation.

STAT3 promotes inflammation, survival, immunity, proliferation, and angiogenesis of tumor cells [17–19]. It was reported that constitutive STAT3 activation was significantly and inversely related to overall 5-year survival in a cohort of breast cancer patients [2, 20]. Therefore, the inhibition of constitutive STAT3 activity is important for the prevention and treatment of breast cancer. The STAT3 phosphorylation at Tyr705 causes its nuclear translocation and DNA binding to specific DNA sequences in the promoter of target genes. In the present study, we found that TKE inhibited nuclear translocation of STAT3 as revealed by immunofluorescence assay resulting in the inhibition of expression of STAT3 target genes (data not shown).

Several earlier studies indicated that Cucurbitacin and their derivatives are triterpenoids found in TKE [21]. Recently, it was reported that Cucurbitacin induces apoptosis in human cancer cells by targeting JAK-STAT pathway [13, 14]. Many studies confirmed that Cucurbitacin I is

a powerful JAK-STAT inhibitor by blocking the tyrosine phosphorylation of STAT3 and JAK2 in various human cancers [22–25]. Also, Cucurbitacin I chemical structure is similar to that of CuD [11]. In our study, both TKE and CuD inhibited phosphorylation and nuclear translocation of STAT3 in MDA-MB-231 cells. In addition, endogenously activated transcriptional activity of STAT3 was inhibited by TKE and CuD in MDA-MB-231 cells.

5. Conclusions

TKE and its derived compound, CuD, inhibit cell proliferation and induce apoptosis through inhibition of STAT3 activity in breast cancer cells. Therefore, our results suggest that TKE and CuD might be a potential anticancer agent which inhibits breast cancer associated with STAT3 activation.

Acknowledgment

This study was supported by a Grant from the Traditional Korean Medicine R&D Project of the Ministry of Health & Welfare, Republic of Korea (B110043).

References

[1] B. B. Aggarwal, G. Sethi, S. A. Kwang et al., "Targeting signal-transducer- and-activator-of-transcription-3 for prevention and therapy of cancer: modern target but ancient solution," *Annals of the New York Academy of Sciences*, vol. 1091, pp. 151–169, 2006.

[2] F.-C. Hsieh, G. Cheng, and J. Lin, "Evaluation of potential Stat3-regulated genes in human breast cancer," *Biochemical and Biophysical Research Communications*, vol. 335, no. 2, pp. 292–299, 2005.

[3] M. C. Maiuri, E. Zalckvar, A. Kimchi, and G. Kroemer, "Self-eating and self-killing: crosstalk between autophagy and apoptosis," *Nature Reviews Molecular Cell Biology*, vol. 8, no. 9, pp. 741–752, 2007.

[4] S. Kothakota, T. Azuma, C. Reinhard et al., "Caspase-3-generated fragment of gelsolin: effector of morphological change in apoptosis," *Science*, vol. 278, no. 5336, pp. 294–298, 1997.

[5] G. Nuñez, M. A. Benedict, Y. Hu, and N. Inohara, "Caspases: the proteases of the apoptotic pathway," *Oncogene*, vol. 17, no. 25, pp. 3237–3245, 1998.

[6] J. M. Adams and S. Cory, "The Bcl-2 protein family: arbiters of cell survival," *Science*, vol. 281, no. 5381, pp. 1322–1326, 1998.

[7] N. Bhatia, K. A. McDonald, A. P. Jackman, and A. M. Dandekar, "A simplified procedure for the purification of trichosanthin (a type 1 ribosome inactivating protein) from *Trichosanthes kirilowii* root tubers," *Protein Expression and Purification*, vol. 7, no. 2, pp. 143–146, 1996.

[8] Y. Cai, S. Xiong, Y. Zheng, F. Luo, P. Jiang, and Y. Chu, "Trichosanthin enhances anti-tumor immune response in a murine Lewis lung cancer model by boosting the interaction between TSLC1 and CRTAM," *Cellular and Molecular Immunology*, vol. 8, no. 4, pp. 359–367, 2011.

[9] J. Zhao, L.-H. Ben, Y.-L. Wu et al., "Anti-HIV agent trichosanthin enhances the capabilities of chemokines to stimulate chemotaxis and G protein activation, and this is mediated through interaction of trichosanthin and chemokine receptors," *Journal of Experimental Medicine*, vol. 190, no. 1, pp. 101–111, 1999.

[10] N. Takahashi, Y. Yoshida, T. Sugiura, K. Matsuno, A. Fujino, and U. Yamashita, "Cucurbitacin D isolated from *Trichosanthes kirilowii* induces apoptosis in human hepatocellular carcinoma cells in vitro," *International Immunopharmacology*, vol. 9, no. 4, pp. 508–513, 2009.

[11] J. C. Chen, M. H. Chiu, R. L. Nie, G. A. Cordell, and S. X. Qiu, "Cucurbitacins and cucurbitane glycosides: structures and biological activities," *Natural Product Reports*, vol. 22, no. 3, pp. 386–399, 2005.

[12] B. Jayaprakasam, N. P. Seeram, and M. G. Nair, "Anticancer and antiinflammatory activities of cucurbitacins from *Cucurbita andreana*," *Cancer Letters*, vol. 189, no. 1, pp. 11–16, 2003.

[13] C. Sun, M. Zhang, X. Shan et al., "Inhibitory effect of cucurbitacin E on pancreatic cancer cells growth via STAT3 signaling," *Journal of Cancer Research and Clinical Oncology*, vol. 136, no. 4, pp. 603–610, 2010.

[14] N. H. Thoennissen, G. B. Iwanski, N. B. Doan et al., "Cucurbitacin B induces apoptosis by inhibition of the JAK/STAT pathway and potentiates antiproliferative effects of gemcitabine on pancreatic cancer cells," *Cancer Research*, vol. 69, no. 14, pp. 5876–5884, 2009.

[15] J. Turkson and R. Jove, "STAT proteins: novel molecular targets for cancer drug discovery," *Oncogene*, vol. 19, no. 56, pp. 6613–6626, 2000.

[16] C.-L. Yu, D. J. Meyer, G. S. Campbell et al., "Enhanced DNA-binding activity of a Stat3-related protein in cells transformed by the Src oncoprotein," *Science*, vol. 269, no. 5220, pp. 81–83, 1995.

[17] G. Niu, K. L. Wright, M. Huang et al., "Constitutive Stat3 activity up-regulates VEGF expression and tumor angiogenesis," *Oncogene*, vol. 21, no. 13, pp. 2000–2008, 2002.

[18] H. Yu, D. Pardoll, and R. Jove, "STATs in cancer inflammation and immunity: a leading role for STAT3," *Nature Reviews Cancer*, vol. 9, no. 11, pp. 798–809, 2009.

[19] J. Bromberg and T. C. Wang, "Inflammation and cancer: IL-6 and STAT3 complete the link," *Cancer Cell*, vol. 15, no. 2, pp. 79–80, 2009.

[20] S.-M. Sheen-Chen, C.-C. Huang, R.-P. Tang, F.-F. Chou, and H.-L. Eng, "Prognostic value of signal transducers and activators of transcription 3 in breast cancer," *Cancer Epidemiology Biomarkers and Prevention*, vol. 17, no. 9, pp. 2286–2290, 2008.

[21] H. Oh, Y.-J. Mun, S.-J. Im et al., "Cucurbitacins from *Trichosanthes kirilowii* as the inhibitory components on tyrosinase activity and melanin synthesis of B16/F10 melanoma cells," *Planta Medica*, vol. 68, no. 9, pp. 832–833, 2002.

[22] M. A. Blaskovich, J. Sun, A. Cantor, J. Turkson, R. Jove, and S. M. Sebti, "Discovery of JSI-124 (cucurbitacin I), a selective Janus kinase/signal transducer and activator of transcription 3 signaling pathway inhibitor with potent antitumor activity against human and murine cancer cells in mice," *Cancer Research*, vol. 63, no. 6, pp. 1270–1279, 2003.

[23] X. Shi, B. Franko, C. Frantz, H. M. Amin, and R. Lai, "JSI-124 (cucurbitacin I) inhibits Janus kinase-3/signal transducer and activator of transcription-3 signalling, downregulates nucleophosmin-anaplastic lymphoma kinase (ALK), and induces apoptosis in ALK-positive anaplastic large cell lymphoma cells," *British Journal of Haematology*, vol. 135, no. 1, pp. 26–32, 2006.

[24] T. Tannin-Spitz, S. Grossman, S. Dovrat, H. E. Gottlieb, and M. Bergman, "Growth inhibitory activity of cucurbitacin glucosides isolated from *Citrullus colocynthis* on human breast cancer cells," *Biochemical Pharmacology*, vol. 73, no. 1, pp. 56–67, 2007.

[25] M. S. van Kester, J. J. Out-Luiting, P. A. von dem Borne, R. Willemze, C. P. Tensen, and M. H. Vermeer, "Cucurbitacin I inhibits Stat3 and induces apoptosis in Sézary cells," *Journal of Investigative Dermatology*, vol. 128, no. 7, pp. 1691–1695, 2008.

Hindawi Publishing Corporation
Evidence-Based Complementary and Alternative Medicine
Volume 2013, Article ID 424730, 6 pages
http://dx.doi.org/10.1155/2013/424730

Research Article

Effects and Safety of Gyejibongnyeong-Hwan on Dysmenorrhea Caused by Blood Stagnation: A Randomized Controlled Trial

Jeong-Su Park,[1,2] Sunju Park,[3] Chun-Hoo Cheon,[1,2] Seong-Cheon Jo,[2] Han Baek Cho,[4] Eun-Mee Lim,[5] Hyung Ho Lim,[6] Bo-Hyoung Jang,[2] Yong-Cheol Shin,[2] and Seong-Gyu Ko[1,2]

[1] *Center for Clinical Research and Drug Development, College of Korean Medicine, Kyung Hee University, Seoul 130-701, Republic of Korea*
[2] *Department of Preventive Medicine, College of Korean Medicine, Kyung Hee University, Seoul 130-701, Republic of Korea*
[3] *Department of Preventive Medicine, College of Korean Medicine, Daejeon University, Daejeon 300-716, Republic of Korea*
[4] *Department of Obstetrics and Gynecology, College of Korean Medicine, Won-Kwang University, Iksan 570-749, Republic of Korea*
[5] *Department of Obstetrics and Gynecology, College of Korean Medicine, Gachon University, Seongnam 461-701, Republic of Korea*
[6] *Department of Korean Medicine Rehabilitation, College of Korean Medicine, Gachon University, Seongnam 461-701, Republic of Korea*

Correspondence should be addressed to Seong-Gyu Ko; epiko@khu.ac.kr

Received 5 April 2013; Revised 16 August 2013; Accepted 19 August 2013

Academic Editor: Chang-Sik Yin

Objective. This study was a multicenter, randomized, double-blind, and controlled trial with two parallel arms: the GJBNH group and the placebo group. This trial recruited 100 women aging 18 to 35 years with primary dysmenorrhea caused by blood stagnation. The investigational drugs, GJBNH or placebo, were administered for two menstrual periods (8 weeks) to the participants three times per day. The participants were followed up for two menstrual cycles after the administration. *Results*. The results were analyzed by the intention-to-treat (ITT) dataset and the per-protocol (PP) dataset. In the ITT dataset, the change of the average menstrual pain VAS score in the GJBNH group was statistically significantly lower than that in the control group. Significant difference was not observed in the SF-MPQ score change between the GJBNH group and the placebo group. No significant difference was observed in the PP analyses. In the follow-up phase, the VAS scores of the average menstrual pain and the maximum menstrual pain continually decreased in the placebo group, but they increased in the GJBNH group. *Conclusion*. GJBNH treatment for eight weeks improved the pain of the dysmenorrhea caused by blood stagnation, but it should be successively administered for more than two menstrual cycles. *Trial Registration*. This trial is registered with Current Controlled Trials no. ISRCTN30426947.

1. Background

Dysmenorrhea is a common medical complaint in reproductive women worldwide. The prevalence varies from 45% to 95% depending on the definition [1]. In Korea, 78.3% of all adolescent girls have dysmenorrhea during their menstrual periods [2].

The first option for the treatment of dysmenorrhea is an over-the-counter drug, such as Ibuprofen, Naproxen, and Mefenamic [3, 4]. However, these medications have not been effective in 20% to 25% of women. Some adverse events such as digestive disorders were reported [5].

Alternative therapies were reported to treat primary dysmenorrhea. These treatments include acupuncture [6], auricular acupressure [7], infrared-emitting sericite belt [8], and single oral dose of vitamin D [9] and vitamin E [10]. The effectiveness was observed in the treatments, but most studies were pilot trials with small sample sizes. Large-scale clinical trials are needed to clarify the efficacy.

In Korean Medicine, the main factor causing menstrual abdominal pain is blood stagnation. If the flow of blood or *qi* is interrupted, it may cause pain. The signs of blood stagnation are being easily bruised, tender abdominal pain, loaf in the menstrual blood, and so forth. Gyejibongnyeong-hwan (GJBNH) is one of the most popular Korean Medicine formulas for periodical pain due to dysmenorrhea. GJBNH fluidifies blood to induce smooth blood flow and reduce pain [6]. However, the effectiveness was reported mostly in

the form of case reports or noncontrolled one-group clinical trials [11, 12]. The well-designed clinical trial is mandatory to prove the effect of GJBNH in primary dysmenorrhea.

The purpose of this trial is to identify the efficacy of GJBNH in dysmenorrhea caused by blood stagnation.

2. Methods

2.1. Hypothesis. The hypothesis was that GJBNH would reduce menstrual pain more effectively than placebo after taking the intervention—the GJBNH or the placebo—for two menstrual cycles.

2.2. Design. This was a multicenter, randomized, double-blind, parallel group, and placebo-controlled phase IV trial. This study was conducted from June 2009 to October 2012. Three investigational sites involved the trial: Korean Medicine Obstetrics and Gynecology Clinic of Kyung Hee Medical Center in Seoul, Obstetrics and Gynecology Clinic of Won-Kwang Korean Medicine Hospital in Gunpo, and Obstetrics and Gynecology Clinic of Gil Korean Medical Hospital of Gachon in Incheon, Republic of Korea. The institutional review boards (IRBs) of three investigational sites had approved the trial before the participants recruitment. Participants were treated as outpatients in these sites. The first visit was the screening. Participants were screened for entry into the trial. Medical, medication, and gynecologic histories were obtained. The second visit was the baseline. At the baseline, the participants were randomly assigned into two groups: the GJBNH group or the placebo group. Eligible participants had taken the investigational drugs for eight weeks. The 3rd visit was after one menstrual cycle from the baseline, and the 4th visit was after two menstrual cycles from the baseline. The 5th visit was after one menstrual period from the 4th visit, and the 6th visit was after two menstrual periods from the 5th visit. At the routine visit, patients returned to the clinic for assessment of the clinical improvement. The trial was conducted over five menstrual cycles. The treatment phase was after two menstrual periods from the baseline (about eight weeks). The participants were followed up three menstrual cycles after the treatment phase. Figure 1 is a flow diagram of this trial.

2.3. Participants. This trial recruited 100 women aging 18 to 35 years with primary dysmenorrhea. We used the 100 mm visual analogue scale (VAS) to measure the menstrual pain. The women enrolled were those whose pain intensity was more than 60 mm. Two Korean Medicine gynecology specialists diagnosed the participants to determine whether dysmenorrhea was caused by blood stagnation or not.

Inclusion criteria were for those with a period cycle of 30 ± 3 days during the last 3 months, for those with a VAS score over 60 mm of VAS at screening, and for those diagnosed with blood stagnation.

Exclusion criteria were for those having major neuropsychiatric disorders, planning to have a baby, or taking antidepressant, antiserotonin, barbiturate, or psychotropic drugs. Other inclusion criteria and exclusion criteria were described in the study protocol [13].

2.4. Intervention. Gyejibongnyeong-hwan (GJBNH) is one of the Korean Medicine formulas for dysmenorrhea caused by blood stagnation. The participants had taken the investigational drug, GJBNH or placebo, three times per day for two menstrual periods (eight weeks). GJBNH consists of *Cinnamomiramulus, Poria, Moutan cortex, Persicae semen,* and *Paeoniae radix*. The placebo medicine was made of lactose, corn starch, and food coloring and had a similar appearance, shape, weight, taste, and color as GJBNH. As rescue medication, ten pain-killer pills were provided during each treatment cycle.

2.5. Randomization. Participants were divided into two groups at Visit 2. The randomization process was commissioned to the independent institution. The random number was produced by a computer random number generator. The central web-site was used to perform the randomization procedure. The investigators, participants, and monitors were blinded to the study purpose and hypothesis.

2.6. Outcomes. The primary outcome was the change in the visual analogue scale (VAS) of the average menstrual pain after the baseline (Visit 2) and after the treatment (Visit 4). The secondary outcome measures included the VAS (the maximum pain during the menstrual period) and the Short-Form McGill Pain Questionnaire (SF-MPQ) [14].

2.7. Statistical Analyses. We carried out efficacy analyses on ITT (intention-to-treat: all were randomly assigned participants) and PP (per-protocol: participants completed the trial without any protocol violations). For ITT analysis, missing data were imputed by last-observation carried forward (LOCF) method. We used SPSS version 20.0 (IBM, Inc., Chicago, IL, USA) to perform the data analysis. The descriptive statistics were used to compare the demographic characteristics. We performed Student's t-test to evaluate the efficacy of GJBNH in the VAS and the SF-MPQ. For categorical outcome variables, the Chi-square test was used to test the difference. The significance level was $P = 0.05$.

2.8. Ethical Consideration. The trial is conducted according to the Declaration of Helsinki 2008 and/or the regulations of the "Good Clinical Practice" principles of the Korea Food & Drug Administration.

The institutional review boards (IRBs) have approved this clinical trial at all investigational sites before the participants recruitment. The reference numbers are KOMC IRB 2008-07 (IRB of Kyung Hee Oriental Medical Center approved it on the 18th of August 2008), WONSBHB IRB 2009-02 (IRB of Won-Kwang University Sanbon Oriental Medical Center approved it on the 24th of February 2009), and 09-101 (IRB of Kyungwon Gil Oriental Medical Hospital approved it on the 2nd of February 2009). Prior to undertaking any study-related procedures, all participants were fully informed and signed consent forms.

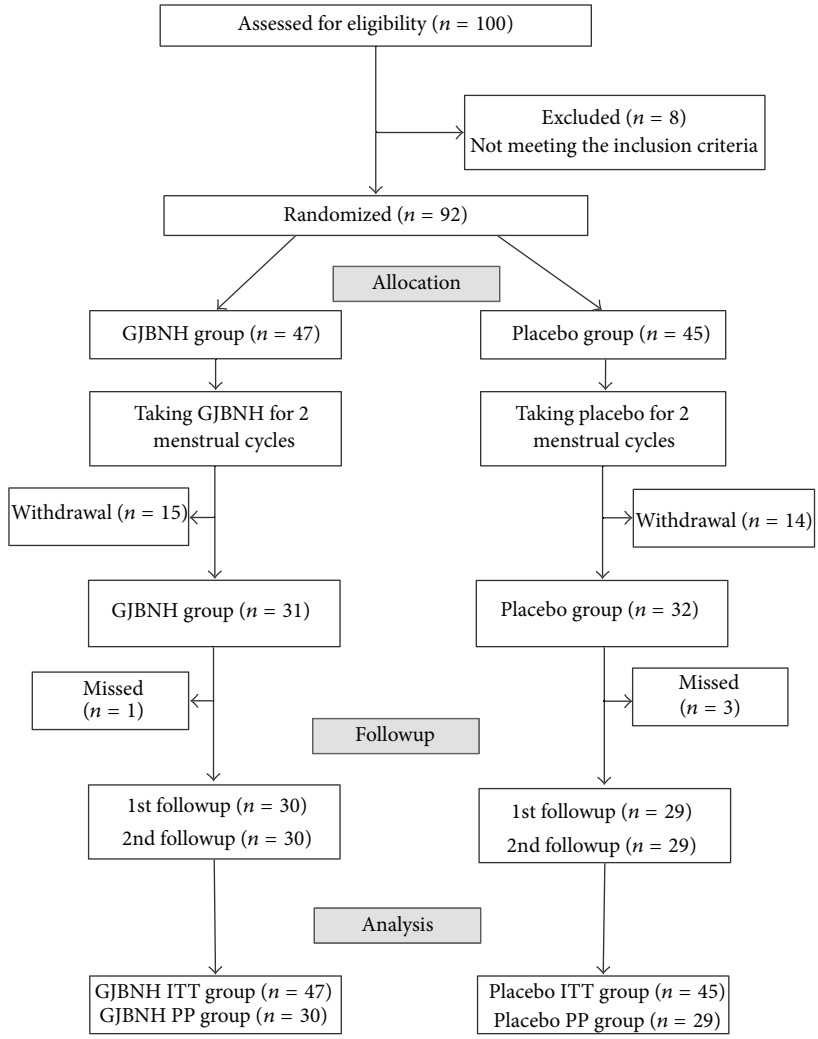

Figure 1: Study flowchart.

3. Results

A total of 100 women were screened. Eight women did not meet the inclusion criteria, and 92 participants were enrolled. Forty-seven subjects were allocated to the GJBNH group, and forty-five subjects were allocated to the placebo arm. After the eight weeks of treatment, 15 participants in the GJBNH group and 14 patients in the control group were dropped out. Two of the most common reasons for dropout were the irregular menstrual periods, under 27 days and over 33 days, and being due to compliance. Adverse events were rare. The most common compliant was the digestion problem.

The demographic characteristics of the two groups are described in Table 1. The mean age at randomization for the GJBNH group was 23.36 years, and it was 23.76 years for the control group. The mean Short-Form McGill Pain Questionnaire at baseline for the GJBNH group was 21.23, and it was 22.98 for the placebo group. The mean VAS scores of the average menstrual pain were 7.05 and 6.86 for the GJBNH group and the placebo group, respectively. The mean VAS of the maximum menstrual pain of the GJBNH group was 7.74, and that of the control group was 7.65. There was no statistical significant difference between the two groups in most of the variables assessed at the baseline.

In the ITT analysis, after the eight weeks of treatment, the change of the average menstrual pain VAS score in the GJBNH group was significantly lower than that of the control group (GJBNH group 1.75 ± 2.06, control group 0.88 ± 1.64; $P = 0.027$). But the difference was not statistically significant. The VAS scores of the maximum menstrual pain decreased by 1.03 ± 1.84 and 0.44 ± 2.05 in the GJBNH and the placebo groups, respectively. But the difference was not statistically significant ($P = 0.155$). Significant difference was not observed in the SF-MPQ score change between the GJBNH group and the placebo group: 4.11 ± 8.61 and 2.60 ± 8.86 in the GJBNH group and the placebo group, respectively ($P = 0.410$). Table 2 described the details of the ITT analysis results.

In the PP analysis, after the eight weeks of treatment, the change of the average menstrual pain VAS score in the GJBNH group was lower than that of the control group (GJBNH group 1.99 ± 2.18, control group 1.09 ± 1.84;

Table 1: Baseline demographics of the GJBNH group and the control group.

	GJBNH (n = 47) Mean (SD)	Control (n = 45) Mean (SD)	P value
Age (years)	23.36 (3.90)	23.76 (3.77)	0.623
Height (cm)	163.21 (5.58)	161.22 (6.21)	0.109
Weight (kg)	55.06 (7.44)	54.36 (7.13)	0.643
BMI (kg/m^2)	20.62 (2.18)	21.01 (3.33)	0.512
SBP (mmHg)	117.30 (17.08)	116.00 (14.66)	0.699
DBP (mmHg)	69.13 (11.03)	70.36 (13.58)	0.478
Menarche	12.61 (1.18)	12.71 (1.42)	0.710
Interval of cycles (days)	29.62 (1.33)	29.36 (1.51)	0.380
Dysmenorrhea begins (n, %)*			0.873
Under 2 years from menarche	17 (36.2)	17 (37.8)	
Over 2 years from menarche	30 (63.8)	28 (62.2)	
Severity of pain (VAS)	7.29 (1.01)	7.42 (1.1)	0.553

*Means the numbers in that domain indicates n (%), not mean (SD).

Table 2: Comparison of the outcomes of the GJBNH group and the control group (ITT).

Variables	GJBNH group (n = 47) Mean (SD)	Control group (n = 45) Mean (SD)	P value
Short-Form McGill Pain Questionnaire			
Baseline	21.23 (7.88)	22.98 (7.97)	
After treatment	17.13 (10.37)	20.38 (9.32)	
Difference	4.11 (8.61)	2.60 (8.86)	0.410
Visual analog scale (average pain)			
Baseline	7.05 (1.13)	6.86 (1.25)	
After treatment	5.30 (1.97)	5.98 (1.55)	
Difference	1.75 (2.06)	0.88 (1.64)	0.027
Visual analog scale (maximum pain)			
Baseline	7.74 (1.14)	7.65 (1.40)	
After treatment	6.72 (1.83)	7.20 (1.89)	
Difference	1.03 (1.84)	0.44 (2.05)	0.155

P = 0.094). But the difference was not statistically significant. The VAS scores of the maximum menstrual pain decreased by 1.26 ± 2.07 and 0.47 ± 2.44 in the GJBNH and the placebo groups, respectively. But the difference was not statistically significant (P = 0.188). Significant difference was not observed in the SF-MPQ score change between the GJBNH group and the placebo group: 5.03 ± 9.24 and 3.69 ± 9.81 in the GJBNH group and the placebo group, respectively (P = 0.590). The details of the PP analysis were shown in Table 3.

The effect of GJBNH maintained one cycle of the menstrual period. Figures 2 and 3 showed the tendency of the VAS of the average menstrual pain. The first followup was after one menstrual cycle after the treatment, and the second followup was after three menstrual cycles after the treatment. The score of the GJBNH group was the lowest at the first followup, but it increased at the second followup. The VAS score of the placebo group decreased continually through the trial. The difference at the first followup between the two groups was more considerable than that after the treatment. But, at the second followup, after the two menstrual cycles after the first followup, the difference tendency disappeared.

3.1. Safety. A total of 16 adverse events occurred. The adverse events were mild digestive disorder, breast stabbing pain, menstrual cycle shortage, urticaria, diarrhea, skin itchiness, and nausea. There were eight adverse events in the GJBNH group and eight adverse events in the placebo group. The adverse events rates were not statistically significant (P = 0.924). Table 4 showed the details.

4. Discussion

There are several study reports to treat dysmenorrhea. Acupuncture is a recommendable therapy. Acupuncture was as effective as nonsteroidal anti-inflammatory drug (NSAID) therapy [6]. A randomized controlled trial has shown the effectiveness of acupuncture in primary dysmenorrhea [15]. But there were no significant differences between the groups. Other therapies were effective in primary dysmenorrhea, auricular acupressure [7], infrared-emitting sericite belt [8], single oral doses of vitamin D [9] and vitamin E [10], and so forth. But the statistically significant differences were rare.

Table 3: Comparison of the outcomes of the GJBNH group and the control group (PP).

Variables	GJBNH group (n = 30) Mean (SD)	Control group (n = 29) Mean (SD)	P value
Short-Form McGill Pain Questionnaire			
Baseline	21.63 (7.67)	24.62 (7.38)	
After treatment	16.60 (9.72)	20.93 (9.83)	
Difference	5.03 (9.24)	3.69 (9.81)	0.590
Visual analog scale (average pain)			
Baseline	7.05 (0.97)	6.99 (1.18)	
After treatment	5.06 (2.08)	5.89 (1.60)	
Difference	1.99 (2.18)	1.09 (1.84)	0.094
Visual analog scale (maximum pain)			
Baseline	7.62 (1.14)	7.57 (1.43)	
After treatment	6.36 (1.90)	7.09 (2.08)	
Difference	1.26 (2.07)	0.47 (2.44)	0.188

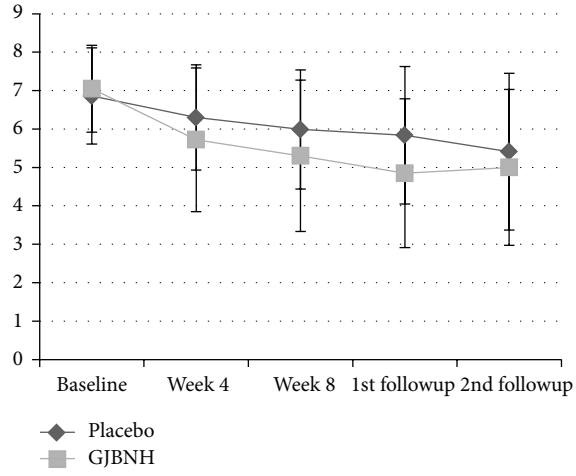

Figure 2: The trend of the GJBNH group and the control group in the VAS of the average menstrual pain—intention-to-treat (ITT) analysis.

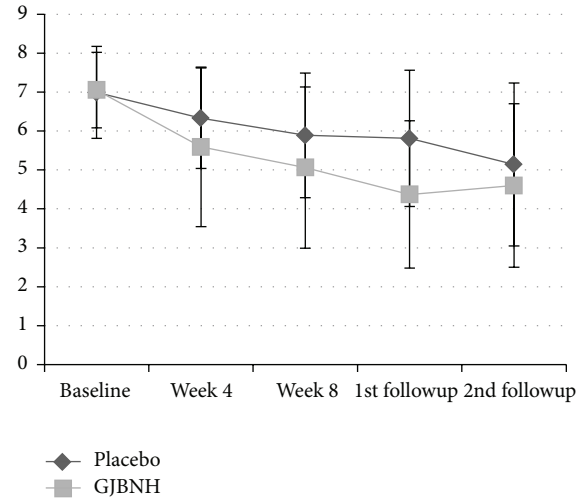

Figure 3: The trend of the GJBNH group and the control group in the VAS of the average menstrual pain—per-protocol (PP) analysis.

Table 4: The adverse events of the GJBNH group and the control group.

Event	GJBNH	Placebo
Mild digestive disorder	3	5
Breast stabbing pain	1	0
Menstrual cycle shortage	0	1
Urticaria	1	2
Diarrhea	1	0
Skin itchiness	1	0
Nausea	1	0
	8 (17%)	8 (18%)

This clinical trial aimed to identify the efficacy of GJBNH on dysmenorrhea caused by blood stagnation. The primary outcome was statistically significant in the ITT analysis. But the result was not significant in the PP analysis. But the result did not show the significant difference compared with the placebo. We discussed the reason for not detecting the difference in the PP analysis, and we concluded that it was due to the lack of sample size and the treatment period.

The first planned sample size was 100 participants. But the enrolled participants were 92 women. It was due to the pandemic break of influenza. In 2008, the influenza A virus subtype had spread in Korea. The enrolment was delayed. Although this study was supported by the National R&D Project, the study due date was inflexible. As a result, statistical power was lower than the planned.

There was the tendency of the pain decrease in the average menstrual pain between the GJBNH group and the placebo group. A decided difference was observed at Visit 4 and the first followup. This implied that GJBNH should be administered over two menstrual cycles and that the effect of GJBNH remains about one menstrual cycle after the cessation.

A total number of 18 adverse events occurred in this clinical trial. But of all the adverse events were mild and minor. The adverse events occurrence rates were not different between the groups. We considered that GJBNH was safe for clinical use.

This study assessed the other measurement. We analyzed only the primary endpoint and two secondary endpoints. More advanced analysis is needed for the other assessment.

The missing value imputation was planned by the multiple imputation (MI) method, but we used the LOCF method. The VAS scores continuously decreased throughout the trial, and the LOCF method was a conservative method. The dropout rates between the groups were not significantly different. Therefore, we inferred that the LOCF method was appropriate to analyze the data.

This study was valuable to show the effect of GJBNH by the randomized controlled trial. But still there were limitations. The most deficient point was the dropout rate. The participants were mostly young women in the university, and the dropout rate was high in the vacation season. The result was significant in the ITT analysis, but the significance was not shown in the PP analysis. We concluded that the lack of sample size was the main reason.

We expected that the results of this study would contribute to the practical use in the Korean Medicine clinics and the design of the clinical trial of the Korean Medicine for primary dysmenorrhea.

Conflict of Interests

The authors declare that they have no conflict of interests.

Authors' Contribution

Jeong-Su Park, Sunju Park, and Chun-Hoo Cheon had written the first draft paper for this trial and calculated the sample size. Han Baek Cho and Eun-Mee Lim had conducted the clinical trial and reviewed the draft paper. Bo-Hyoung Jang contributed to the analysis. Yong-Cheol Shin, Seong-Cheon Jo, Hyung Ho Lim, and Seong-Gyu Ko had edited the first version. Seong-Gyu Ko had conducted all of the procedures for this protocol. All authors read and approved the final version of this paper.

Acknowledgments

This study was supported by the Grant of the Traditional Korean Medicine R&D Project, Ministry of Health & Welfare, Republic of Korea (B120014). The authors also appreciate Hanpoong Pharm & Foods Co., Ltd., for the investigational product support.

References

[1] M. Proctor and C. Farquhar, "Diagnosis and management of dysmenorrhoea," *British Medical Journal*, vol. 332, no. 7550, pp. 1134–1138, 2005.

[2] H. O. Kim, S. W. Lim, H. Y. Woo, and K. H. Kim, "Premenstrual syndrome and dysmenorrhea in Korean adolescent girls," *Korean Journal of Obstetrics and Gynecology*, vol. 51, no. 11, pp. 1322–1329, 2008.

[3] K. O'Connell, A. R. Davis, and C. Westhoff, "Self-treatment patterns among Adolescent girls with dysmenorrhea," *Journal of Pediatric and Adolescent Gynecology*, vol. 19, no. 4, pp. 285–289, 2006.

[4] D. Durain, "Primary dysmenorrhea: assessment and management update," *Journal of Midwifery and Women's Health*, vol. 49, no. 6, pp. 520–527, 2004.

[5] X. Zhu, M. Proctor, A. Bensoussan, C. A. Smith, and E. Wu, "Chinese herbal medicine for primary dysmenorrhoea," *Cochrane Database of Systematic Reviews*, no. 4, Article ID CD005288, 2007.

[6] G. Kiran, Y. Gumusalan, H. C. Ekerbicer, H. Kiran, A. Coskun, and D. C. Arikan, "A randomized pilot study of acupuncture treatment for primary dysmenorrhea," *European Journal of Obstetrics & Gynecology and Reproductive Biology*, vol. 169, no. 2, pp. 292–295, 2013.

[7] M.-L. Yeh, Y. L. Hung, H. H. Chen, and Y. J. Wang, "Auricular acupressure for pain relief in adolescents with dysmenorrhea: a placebo-controlled study," *The Journal of Alternative and Complementary Medicine*, vol. 18, pp. 1–6, 2012.

[8] C. H. Lee, J.-W. Roh, C.-Y. Lim, J. H. Hong, J. K. Lee, and E. G. Min, "A multicenter, randomized, double-blind, placebo-controlled trial evaluating the efficacy and safety of a far infrared-emitting sericite belt in patients with primary dysmenorrhea," *Complementary Therapies in Medicine*, vol. 19, no. 4, pp. 187–193, 2011.

[9] A. Lasco, A. Catalano, and S. Benvenga, "Improvement of primary dysmenorrhea caused by a single oral dose of vitamin D: results of a randomized, double-blind, placebo-controlled study," *Archives of Internal Medicine*, vol. 172, no. 4, pp. 366–367, 2012.

[10] M. Kashanian, M. M. Lakeh, A. Ghasemi, and S. Noori, "Evaluation of the effect of vitamin E on pelvic pain reduction in women suffering from primary dysmenorrhea," *Journal of Reproductive Medicine*, vol. 58, pp. 34–38, 2013.

[11] D. Kim and D. Yoo, "Two cases report of the primary dysmenorrhea treated with Gamisoyosan-gagambang," *The Journal of Oriental Obstetrics & Gynecology*, vol. 24, no. 2, pp. 126–133, 2011.

[12] E. J. Nam, Y. K. Lee, D. N. Lee, and H. J. Kim, "Clinical study on the effect of Gyebongnyeong capsule in the treatment of primary dysmenorrhea," *Korean Journal Oriental Physiology & Pathology*, vol. 20, no. 5, pp. 1364–1368, 2006.

[13] J.-S. Park, S. Park, C.-H. Cheon et al., "Effects of Gyejibongnyeong-hwan on dysmenorrheacaused by blood stagnation: study protocol for arandomized controlled trial," *Trials*, vol. 13, no. 3, 2012.

[14] R. Melzack, "The short-form McGill pain questionnaire," *Pain*, vol. 30, no. 2, pp. 191–197, 1987.

[15] C. A. Smith, C. A. Crowther, O. Petrucco, J. Beilby, and H. Dent, "Acupuncture to treat primary dysmenorrhea in women: a randomized controlled trial," *Evidence-Based Complementary and Alternative Medicine*, vol. 2011, Article ID 612464, 2011.

Hindawi Publishing Corporation
Evidence-Based Complementary and Alternative Medicine
Volume 2013, Article ID 350964, 8 pages
http://dx.doi.org/10.1155/2013/350964

Research Article

Vasorelaxant Effect of Osterici Radix Ethanol Extract on Rat Aortic Rings

Kyungjin Lee, Geunyong Park, Inhye Ham, Gabsik Yang, Mihwa Lee, Youngmin Bu, Hocheol Kim, and Ho-Young Choi

Department of Herbology, College of Korean Medicine, Kyung Hee University, 26 Kyungheedae-ro, Dongdaemun-gu, Seoul 130-701, Republic of Korea

Correspondence should be addressed to Ho-Young Choi; hychoi@khu.ac.kr

Received 5 April 2013; Revised 17 August 2013; Accepted 19 August 2013

Academic Editor: Bo-Hyoung Jang

The root of *Ostericum koreanum* Maximowicz has been used as a traditional medicine called "Kanghwal" in Korea (or "Qianghuo" in China). The purpose of this study was to investigate the vasorelaxant activity and mechanism of action of an ethanol extract of the *O. koreanum* root (EOK). We used isolated rat aortic rings to assess the effects of EOK on various vasorelaxant or vasoconstriction factors. EOK induced vasorelaxation in phenylephrine hydrochloride (PE) or KCl precontracted aortic rings in a concentration-dependent manner. However, the vasorelaxant effects of EOK on endothelium-intact aortic rings were reduced by pretreatment with L-NAME or methylene blue. In Ca^{2+}-free Krebs-Henseleit solution, pretreatment with EOK (0.3 mg/mL) completely inhibited PE-induced constriction. In addition, EOK (0.3 mg/mL) also completely inhibited vasoconstriction induced by supplemental Ca^{2+} in aortic rings that were precontracted with PE or KCl. Furthermore, the EOK-induced vasorelaxation in PE-contracted aortic rings was inhibited by preincubation with nifedipine. These results indicate that the vasorelaxant effects of EOK are responsible for the induction of NO formation from L-Arg and NO-cGMP pathways, blockage of the extracellular Ca^{2+} entry via the receptor-operative Ca^{2+} channel and voltage-dependent calcium channel, and blockage of sarcoplasmic reticulum Ca^{2+} release via the inositol triphosphate pathway.

1. Introduction

Traditional Chinese medicine (TCM) was introduced to Korea in the 6th century [1]. Therefore, many Korean herbal medicines (KHMs) originated as traditional Chinese herbal medicines (TCHMs). However, many components of KHMs have developed independently from TCHMs because of differences in geography, climate, culture, and politics. Thus, many KHMs different from TCHMs have been used in Korean medicine clinics. Osterici Radix, the root of *Ostericum koreanum* Maximowicz (Umbelliferae), is an example of this type of herbal medicine.

The medicinal plant *O. koreanum* is a perennial herb widely distributed in Korea. The root of this plant has been used as a traditional medicine called "Kanghwal." However, the pharmacopoeias of Korea, China, and Japan describe this plant's origin differently. The Chinese and Japanese pharmacopoeias list only *Notopterygium incisum* and *Notopterygium forbesii* as being of "Kanghwal" origin ("Qianghuo" in Chinese), while the Korean pharmacopoeia includes *O. koreanum* as also being of "Kanghwal" origin [2–4].

Notopterygii Rhizoma et Radix, the rhizome and root of *N. incisum* and *N. forbesii*, has been used in China for the treatment of colds, headache, edema, arthritis, sores, and ulcers [5]. It is reported to have multiple effects including the elimination of fever, alleviation of pain, anti-inflammation, protection against heart palpitations and myocardial ischemia, antishock, antibacterial effects [5], and vasorelaxant effects [6].

Osterici Radix and Notopterygii Rhizoma et Radix have been used in Korea for the treatment of colds, fever, headache, swelling, arthritis, arthralgia, rhinitis [7], and cardiovascular diseases [6]. However, most doctors of Korean medicine have been using Osterici Radix more than Notopterygii Rhizoma et Radix as "Kanghwal" in clinics. However, there are fewer pharmacological studies and clinical data for Osterici Radix

than there are for Notopterygii Rhizoma et Radix. Therefore, many more pharmacological and clinical studies are needed to support the continued use of Osterici Radix as a beneficial medicine.

Osterici Radix is reported to have various pharmacological activities: antiinflammatory [8, 9], antitumor [10], antioxidant [11], antimicrobial [12], and antiasthmatic [13]. Further, the vasorelaxant effect of water extracts of Osterici Radix on 5-HT precontracted rat thoracic aorta rings has been reported [14]. However, there are no published studies on the exact mechanism underlying the vasorelaxant effects of Osterici Radix.

In cardiovascular diseases such as stroke, headache, and hypertension, vasoreactivity is of fundamental importance because it directly influences the arteries of the circulatory system. Accordingly, many researchers have investigated the vasorelaxant effects of various herbal medicines [15–18].

Therefore, we designed the present study to investigate the vasorelaxant activity and mechanism of action of the ethanol extract of the *O. koreanum* root (EOK). For this purpose, we used isolated rat thoracic aorta rings to assess the effects of EOK on various vasorelaxant or vasoconstriction factors.

2. Materials and Methods

2.1. Chemicals and Reagents. Phenylephrine hydrochloride (PE), acetylcholine (Ach), ethylene glycol-bis (β-aminoethyl ether)-N,N,N′,N′-tetraacetic acid (EGTA), potassium chloride, calcium chloride, Nω-nitro-L-arginine methyl ester (L-NAME), methylene blue (MB), Y-27632, nifedipine, tetraethylammonium (TEA), glibenclamide, 4-aminopyridine (4-AP), and caffeine were purchased from Sigma Aldrich (St Louis, USA). Barium chloride was purchased from Wako (Osaka, Japan). Isoimperatorin, imperatorin, oxypeucedanin, and oxypeucedanin hydrate were purchased from the Korean Food & Drug Administration. All other reagents were of analytical purity.

2.2. Plant Material and Extraction. *O. koreanum* was collected in Bongwha Alpine Medicinal Plant Experiment Station, Bongwha, Gyeongbook province, Republic of Korea, in October 2008. Plant identification was performed by Professor Chang Soo Yook of Kyung Hee University. A voucher specimen (KH001) of *O. koreanum* is deposited at the College of Korean Medicine, Kyung Hee University, Seoul, Pepublic of Korea. The dried root and rhizome of *O. koreanum* (1.0 kg) were extracted separately with 100% ethanol (3 times for 2 h at 60°C) in a reflux apparatus. After reflux and filtration, extracts were evaporated using a rotary evaporator at 60°C and lyophilized to yield 165.0 g of crude extract.

2.3. Preparation of Rat Aortic Ring. We used male Sprague-Dawley rats (weight, 240–260 g; Narabio, Seoul, Pepublic of Korea) to examine the vasorelaxant effect of EOK. All animal procedures were conducted according to the animal welfare guidelines issued by the Kyung Hee University Institutional Animal Care and Use Committee [KHUASP (SE)-09-006]. The rats were housed under controlled conditions (22 ± 2°C; lighting, 07:00–19:00), with food and water available *ad libitum*. Rats were anesthetized by exposure to ether; the thoracic aorta was removed and immersed in Krebs-Henseleit solution [K-H solution, composition (mM): NaCl, 118.0; KCl, 4.7; $MgSO_4$, 1.2; KH_2PO_4, 1.2; $CaCl_2$, 2.5; $NaHCO_3$, 25.0; and glucose, 11.1; pH 7.4], maintained at 37°C, and aerated with a mixture of 95% O_2 and 5% CO_2. After careful removal of the connective tissue and fat, approximately 2 mm long aortic rings were cut and suspended in organ chambers containing 10 mL K-H solution at 37°C and aerated with a mixture of 95% O_2 and 5% CO_2. The aortic rings were placed between 2 tungsten stirrups and connected to an isometric force transducer (Grass instrument Co., Rhode Island, USA). After incubation under no tension for 30 min, the vessel segments were allowed to equilibrate for 1 h at a resting tension of 1.0 g. During the equilibration period, the K-H solution was replaced every 20 min. Changes in tension were recorded by isometric transducers connected to a data acquisition system (PowerLab, ADI instrument Co., New South Wales, Australia). When required, the endothelium was removed by gentle rubbing of the vessel lumen with a thin cotton swab. The presence of functional endothelium was verified by the ability of Ach (10 μM) to induce more than 80% relaxation of rings precontracted by PE (1 μM). In endothelium-denuded rings, less than 10% relaxation due to Ach was seen. Ca^{2+}-free K-H solution was prepared by omission of $CaCl_2$ and addition of EGTA (1 mM).

2.4. Vasoactivities. In standard K-H solution, endothelium-intact aortic rings were precontracted by PE (1 μM) or KCl (60 mM). After the plateau was attained, EOK was added cumulatively (0.03–1.0 mg/mL). The vasorelaxant effect on the aortic rings was calculated as a percentage of contraction in response to PE or KCl. To determine whether the arterial endothelium pathways were involved in EOK-induced vasorelaxation, endothelium-intact aortic rings were preincubated with L-NAME (10 μM) or MB (10 μM) for 20 min before contraction by PE (1 μM) treatment. The relaxant effects of EOK on the aortic rings were compared with the control (not treated with L-NAME or MB). To investigate the effect of EOK on extracellular Ca^{2+}-induced contraction, we investigated the contractile responses induced by $CaCl_2$ (0.3–10 mM) addition on aortic rings pre-contracted by PE (1 μM) or KCl (60 mM) in Ca^{2+}-free K-H solution in the absence (control) and presence of a 10 min pre-incubation of EOK (0.3 mg/mL). $CaCl_2$-induced contractile responses were compared in the absence (control) and presence of EOK. To investigate the effect of EOK on L-type voltage-dependent calcium channel, K^+ channels, and Rho-kinase pathway, aortic rings were preincubated with nifedipine, 4-AP, glibenclamide, TEA, or Y-27632 (1 μM) for 20 min before the addition of PE (1 μM). After the plateau was attained, EOK was added cumulatively (0.01–0.8 mg/mL). The vasorelaxant effects on the aortic rings were calculated as a percentage of contraction in response to PE. To investigate the effect of EOK on intracellular Ca^{2+} release from sarcoplasmic reticulum- (SR-) induced contraction, we investigated the contractile responses induced by PE (1 μM) or caffeine

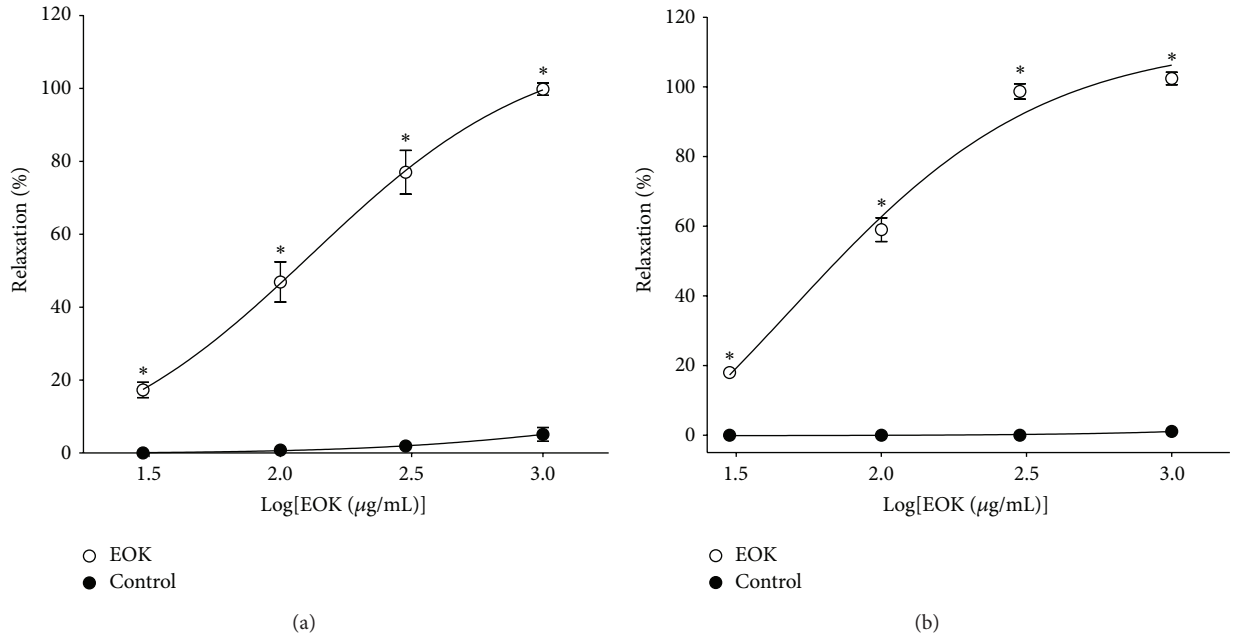

Figure 1: Concentration-dependent relaxant effects of EOK (0.03–1.0 mg/mL) on phenylephrine (PE, 1 μM) (a) or KCl (60 mM) (b) precontracted rat aortic rings. Control groups were not treated with EOK. The relaxant effects of EOK were calculated as a percentage of the contraction in response to PE or KCl. Values are expressed as mean ± SEM ($n = 4$). $^*P < 0.05$ versus control.

(5 mM) on endothelium-denuded aortic rings in Ca^{2+}-free K-H solution in the absence (control) and presence of a 10 min pre-incubation of EOK (0.3 mg/mL). Contractile responses induced by PE or caffeine were compared in the absence (control) and presence of EOK.

2.5. Qualitative and Quantitative HPLC Analysis of Standard Materials in EOK. Accurately weighted EOK (100.0 mg) was dissolved in 10 mL of methanol (HPLC reagent, J.T.Baker Co. Ltd, USA). And then it was filtered through a syringe filter (13 mm diameter with 0.45 μm pore size, Waters, MA, USA). Isoimperatorin, imperatorin, and oxypeucedanin hydrate were used as standard materials for the qualitative analysis of EOK. They were serially diluted (25, 50, 100, and 200 μg/mL), and HPLC chromatograms were obtained. The relationship between the concentration and the peak area was measured using the minimum square method (R^2 value). The HPLC chromatograms were obtained from Gilson System equipped with a 234 autoinjector, a UV/VIS-155 detector, and a 321 HPLC Pump (Gilson, WI, USA). A Luna 4.60 × 250 mm C18 reversed-phase column with 5 μm particles (Phenomenex, CA, USA) was used. Chromatographic separation was carried out using an isocratic solvent with acetonitrile (HPLC grade, J.T.Baker Co. LTD., U.S.A) water mixture in the ratio of 30 : 70 (v/v). The column eluent was monitored at UV 254 nm, following which all solvents were degassed with a micromembrane filter (PTFE, Advantec, Tokyo, Japan). Chromatography was performed at room temperature at a flow rate of 1.0 mL/min, and 10 μL was analyzed for 20 min. The quantity of the EOK standards was expressed as follows: the amount (mg) of standard material = the quantitative amount (mg) of standard materials $\times A_T/A_S/n$ ($n = 3$; A_T = the peak area of the test sample containing the standard; A_S = the peak area of the standard).

2.6. Statistical Analysis. Data were expressed as mean ± standard error of mean (SEM). Statistical comparisons were made using Student's t-test or one-way analysis of variance (ANOVA) followed by the Tukey's post hoc test. All statistical analyses were performed using SPSS v.13.0 statistical analysis software (SPSS Inc., USA). P values less than 0.05 were considered statistically significant.

3. Results

3.1. Effect of EOK on PE- or KCl-Induced Contraction. EOK (0.03–1.0 mg/mL) relaxed PE (1 μM) or KCl (60 mM) precontracted rings in a concentration-dependent manner. The maximal relaxant effects were up to 99.8 ± 1.7% and 102.4 ± 3.6% at the concentration of 1.0 mg/mL, respectively (Figure 1).

3.2. Vasorelaxant Effects of EOK on Endothelium-Dependent Pathways. Preincubation with L-NAME (10 μM) decreased EOK- (0.1, 0.2, and 0.4 mg/mL) induced relaxation of endothelium-intact aortic rings precontracted by PE (1 μM) treatment (Figure 2(a)). And, preincubation with MB (10 μM) also decreased EOK- (0.01–0.4 mg/mL) induced relaxation of endothelium-intact aortic rings (Figure 2(b)).

3.3. Effect of EOK on Extracellular Ca^{2+}-Induced Contraction. To investigate the effects of EOK on the receptor-operative Ca^{2+} channel (ROCC) pathway, PE (1 μM) was applied to induce stable contraction. $CaCl_2$ (0.3–10 mM) was then

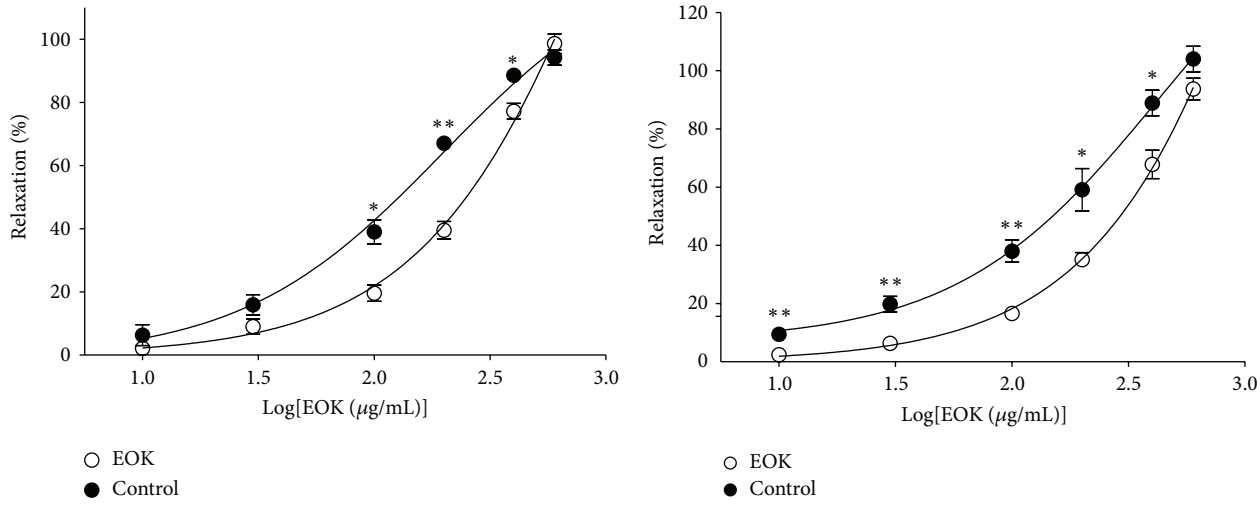

Figure 2: Relaxation responses induced by EOK (10–600 μg/mL) in endothelium-intact rat aortic rings precontracted with phenylephrine (PE, 1 μM) in the presence or absence (control) of Nω-nitro-L-arginine methyl ester (L-NAME, 10 μM) (a) or methylene blue (MB, 10 μM) (b) in Krebs-Henseleit solution. The relaxant effects of EOK on isolated rat aortic rings were calculated as a percentage of the contraction in response to PE. Control groups were not treated with L-NAME or MB. Values are expressed as mean ± SEM ($n = 4$). $^{*}P < 0.05$ and $^{**}P < 0.01$ versus control.

added cumulatively to induce a progressive increase in contraction of the aortic rings. EOK (0.3 mg/mL) preincubation significantly inhibited the contraction induced by extracellular $CaCl_2$ (0.3–10 mM) compared with the control group. And the contraction was decreased to −0.05±0.02 g, −0.07±0.02 g, −0.05 ± 0.02 g, and −0.05 ± 0.02 g, respectively (versus control group 0.09±0.01 g, 0.42±0.03 g, 1.34±0.15 g, and 1.67±0.14 g) (Figure 3(a)). To investigate the voltage-dependent calcium channel (VDCC) pathway, KCl (60 mM) was applied to induce a stable contraction. EOK (0.3 mg/mL) preincubation also significantly inhibited extracellular $CaCl_2$-induced (0.1–10 mM) contraction compared with the control group. Contraction decreased to 0.00 ± 0.02 g, −0.03 ± 0.02 g, −0.06 ± 0.02 g, −0.07 ± 0.03 g, and −0.08 ± 0.03 g, respectively (versus control group 0.22 ± 0.02 g, 0.22 ± 0.02 g, 0.83 ± 0.03 g, 1.19 ± 0.06 g, and 1.39 ± 0.06 g) (Figure 3(b)). In addition, preincubation with nifedipine (10 μM) for 20 min inhibited EOK-induced vasorelaxation on PE-contracted aortic rings (Figure 3(c)).

3.4. Effect of EOK on the Sarcoplasmic Reticulum Calcium Release Induced by PE or Caffeine. In the Ca^{2+}-free K-H solution, preincubation with EOK (0.3 mg/mL) for 10 min completely inhibited PE-induced (1 μM) contraction. However, preincubation with EOK (0.3 mg/mL) for 10 min did not alter caffeine-induced (5 mM) contraction (Figure 4).

3.5. Effect of EOK on the Rho-Kinase Pathway. Preincubation with Y-27632 (1 μM) for 20 min did not alter EOK-induced vasorelaxation on PE-contracted aortic rings (Figure 5).

3.6. Effect of EOK on the K^+ Channels. The vasorelaxant effects of EOK on PE (1 μM) precontracted aortic rings were not altered by preincubation of the rings with various K^+ channel blockers, including 4-AP (1 mM), glibenclamide (10 μM), or TEA (5 mM) (Figure 6).

3.7. Qualitative and Quantitative HPLC Analysis of Standard Materials in EOK. Figure 7 depicts the 6 principal peaks detected on the EOK HPLC chromatogram; the retention times of the peaks were as follows: peak 1, 2.04 min; peak 2 (oxypeucedanin hydrate), 3.26 min; peak 3, 5.35 min; peak 4, 6.57 min; peak 5 (imperatorin), 10.99 min; and peak 6 (isoimperatorin), 15.02 min. The standard curve was calibrated by using the linear regression derived from the peak area. The regression equation (correlation coefficient, R^2) of oxypeucedanin hydrate was $y = 201168.349x - 153935.071$ (0.999) and exhibited good linearity. The oxypeucedanin hydrate content in EOK was 1.80 ± 0.92%. The regression equation (correlation coefficient, R^2) of imperatorin was $y = 514722.569+153935.071$ (0.999) and exhibited good linearity. The imperatorin content in EOK was 0.42±0.02%. The regression equation (correlation coefficient, R^2) of isoimperatorin was $y = 301715.046x + 32227.015$ (0.998) and exhibited good linearity. The isoimperatorin content in EOK was 0.70 ± 0.02%.

4. Discussion

In the present study, we investigated the vasorelaxant effects of EOK on rat aortic rings and its related mechanisms. The vasorelaxant effects caused by EOK were both endothelium dependent and endothelium independent. And the vasorelaxant mechanisms of EOK were responsible for the induction of NO formation from L-Arg and NO-cGMP pathways,

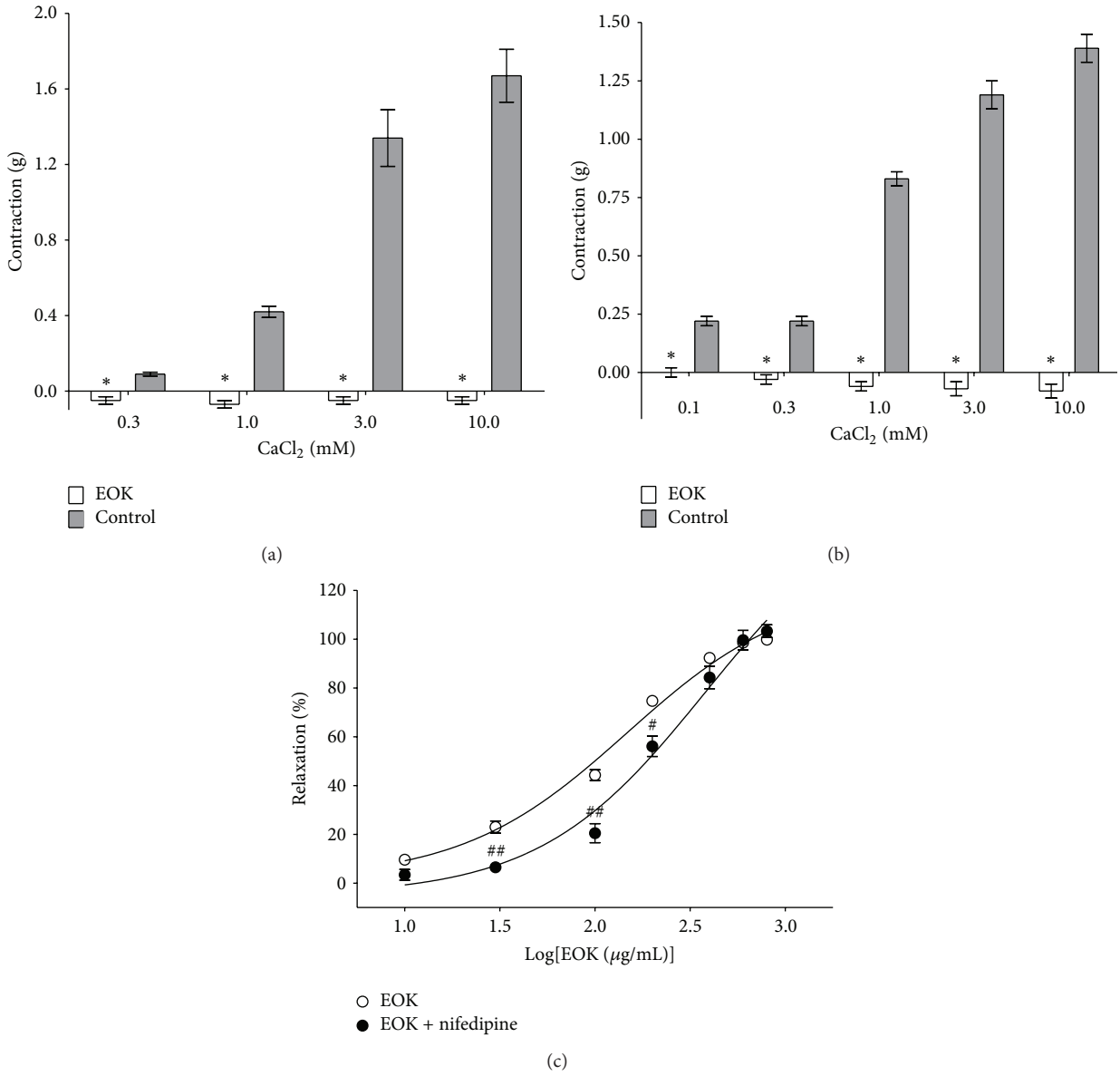

Figure 3: Inhibitory effect of EOK (0.3 mg/mL) on the contraction induced by extracellular Ca^{2+} addition (0.3–10 mM) in rat aortic rings precontracted with phenylephrine (PE, 1 μM) (a) or KCl (60 mM) (b) in Ca^{2+}-free Krebs-Henseleit solution and vasorelaxant responses induced by EOK (0.01–0.8 mg/mL) in rat aortic rings precontracted with PE (1 μM) in the presence or absence of nifedipine (10 μM). Values are expressed as mean ± SEM ($n = 4$). $^{*}P < 0.05$ versus control. $^{\#}P < 0.05$ and $^{\#\#}P < 0.01$ versus absence of nifedipine group.

blockage of the extracellular Ca^{2+} entry via the ROCC and VDCC, and blockage of SR Ca^{2+} release via the IP_3 pathway.

Vascular endothelium plays an important role in vasorelaxation. NO is one of the potent vasodilators secreted from vascular endothelium. And vascular smooth muscle is relaxed via NO-cGMP pathway [19]. In the present study, the vasorelaxant effect of EOK was reduced by pretreatment with L-NAME, an inhibitor of NOS. In addition, the vasorelaxant effect of EOK was reduced by pretreatment with MB, a soluble guanylate cyclase inhibitor. These results suggested that the vasorelaxant effect of EOK is related to the induction of NO formation from L-arginine and NO-cGMP pathways.

Vascular smooth muscle also plays an important role in vasorelaxation, which is regulated by extracellular Ca^{2+} influx via transmembrane Ca^{2+} channels and Ca^{2+} release from intracellular stores [20]. Ca^{2+} concentration in vascular cells is the most important factor of vascular contraction and relaxation. The factors that increase calcium in cells consist of stimulus by neurotransmitter, opened calcium channels by membrane potential, and calcium ion release from the SR. Ca^{2+} concentration in cells increases to combine with calmodulin, a protein that binds to calcium in cells. The bonded Ca^{2+}-calmodulin activates inactive myosin light chain kinase, which then phosphorylates myosin light.

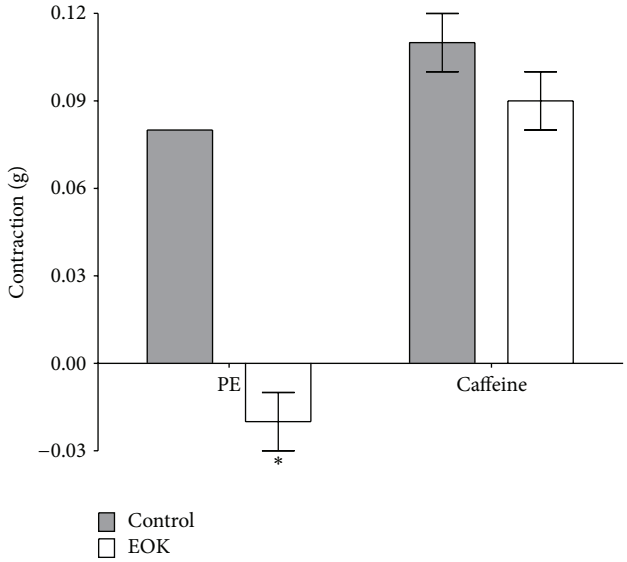

Figure 4: Inhibitory responses of EOK (0.3 mg/mL) preincubation on phenylephrine- (PE-, 1 μM)- or caffeine- (5 mM) induced contractions of rat aortic rings. Values are expressed as mean ± SEM ($n = 4$). Control groups were not treated with EOK. $^*P < 0.05$ versus control.

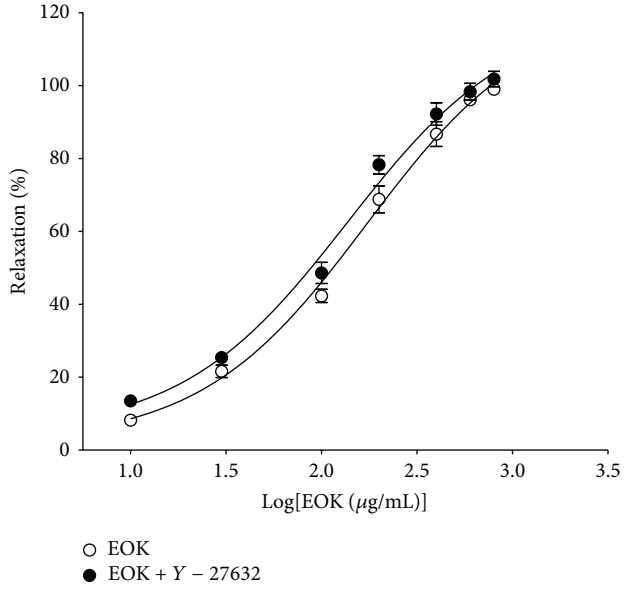

Figure 5: Vasorelaxant responses induced by EOK (0.01–0.8 mg/mL) in rat aortic rings precontracted with phenylephrine (1 μM) in the presence or absence of Y-27632 (1 μM). Values are expressed as mean ± SEM ($n = 4$).

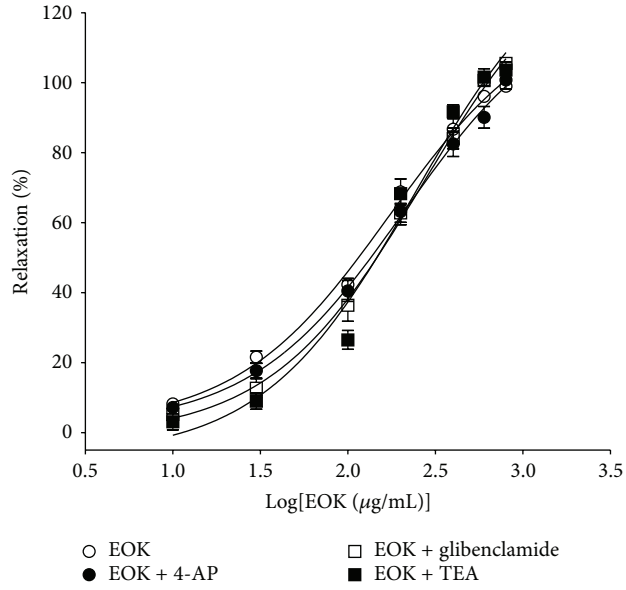

Figure 6: Vasorelaxant responses induced by EOK (0.01–0.8 mg/mL) in rat aortic rings precontracted with phenylephrine (1 μM) in the presence or absence of 4-aminopyridine (4-AP, 1 mM), glibenclamide (10 μM), or tetraethylammonium (TEA, 5 mM). Values are expressed as mean ± SEM ($n = 4$).

The phosphorylated myosin light chain then makes a phosphorylated crossbridge with actin to produce a contraction [20].

PE (an α-adrenergic agonist) contracts smooth muscle cells via extracellular Ca^{2+} influx through ROCC and by internal calcium release from specific IP_3 receptor (IP_3R) channels in the SR membrane [21]. In Ca^{2+}-free K-H solution, PE induced the contraction via the IP_3 pathway. In the present study, pretreatment with EOK (0.3 mg/mL) for 10 min completely inhibited PE-induced (1 μM) contraction. This result suggests that EOK could inhibit Ca^{2+}-induced vasoconstriction from specific IP_3R channels in the SR membrane. And EOK (0.3 mg/mL) completely inhibited vasoconstriction induced by Ca^{2+} supplementation in aortic rings that were precontracted with PE (1 μM). This result suggested that EOK could inhibit vasoconstriction induced by extracellular Ca^{2+} entry via the ROCC.

KCl contracts smooth muscle cells mainly by extracellular Ca^{2+} influx through depolarization of the cell membrane and subsequent opening of VDCC [22]. EOK (0.3 mg/mL) also completely inhibited vasoconstriction induced by Ca^{2+} supplementation in aortic rings that were precontracted with KCl (60 mM). This result suggests that EOK could also inhibit vasoconstriction induced by extracellular Ca^{2+} entry via the VDCC. L-type VDCC is the major mechanism of VDCC. In the present study, EOK-induced vasorelaxation on PE-contracted aortic rings was inhibited by preincubation with nifedipine (a typical L-type VDCC blocker). This result suggested that EOK could inhibit extracellular Ca^{2+} entry via blocking L-type VDCC.

Caffeine contracts smooth muscle cells by internal calcium release from ryanodine receptor (RyR) channels in the SR membrane [23]. EOK (0.3 mg/mL) did not inhibit caffeine-induced (5 mM) vasoconstriction, which suggested that EOK could not affect RyR channels.

Increase of K^+ efflux in vascular smooth muscle causes membrane potential hyperpolarization [22]. Thus, the opening of K^+ channels leads to vasorelaxation and the inhibition

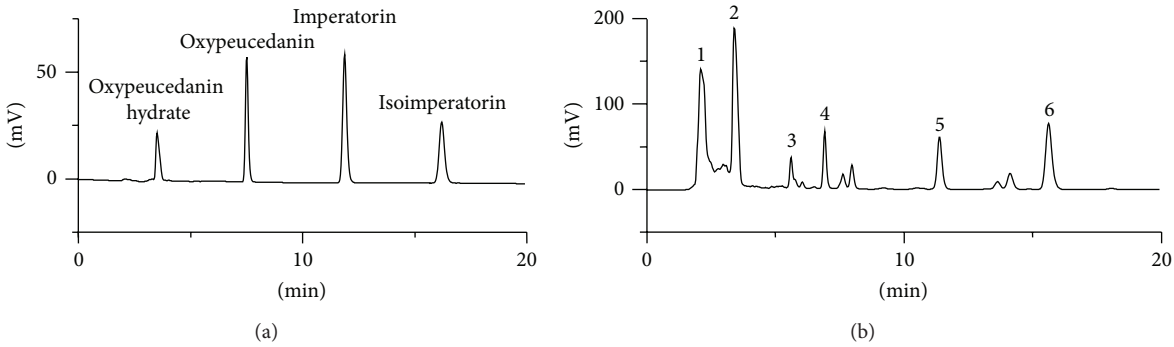

Figure 7: Qualitative and quantitative HPLC analysis of standard materials in EOK. The retention time of the peak 1, peak 2 (oxypeucedanin hydrate), peak 3, peak 4, peak 5 (imperatorin), and peak 6 (isoimperatorin) was 2.04 min, 3.26 min, 5.35 min, 6.57 min, 10.99 min, and 15.02 min, respectively.

of K^+ channels leads to vasoconstriction. Voltage-dependent K^+ (K_V) channels, Ca^{2+}-activated K^+ (BK_{Ca}) channels, and ATP-sensitive K^+ (K_{ATP}) channels are well-known distinct types of K^+ channels in vascular smooth muscle [22]. In the present study, the vasorelaxant effects of EOK were not affected by preincubation of 4-AP (K_V channel blocker), TEA (BK_{Ca} channel blocker), and glibenclamide (K_{ATP} channel blocker). These results indicated that the vasorelaxant effects of EOK on the rat aortic rings were not related to the opening of K^+ channels.

Rho kinase has been identified as one of the effectors of the small GTP-binding protein Rho. And Rho/Rho-kinase-mediated pathway has been implicated in the regulation of vascular tone [24]. Y-27632 is a Rho-kinase inhibitor that blocks agonist-induced Ca^{2+} sensitization of smooth muscle [25]. In this study, Y-27632 did not significantly affect the relaxant effect of EOK. This result indicated that the relaxant effect of EOK on rat aortic ring is not related to the Rho-kinase pathway.

Osterici Radix has been reported to contain several active compounds such as oxypeucedanin hydrate [11], oxypeucedanin, imperatorin, and isoimperatorin [26]. In the present study, we identified oxypeucedanin hydrate (1.80 ± 0.92%), imperatorin (0.42±0.02%), and isoimperatorin (0.70±0.02%) from EOK by using HPLC analysis. Imperatorin is reported to relax rat mesenteric arteries precontracted by KCl or endothelin-1 and human omental arteries precontracted by noradrenaline and U46619 [27]. And isoimperatorin is also reported to relax rat aortic rings precontracted by PE or KCl [28]. Therefore, vasorelaxant activities of EOK might result from these active compounds. However, vasorelaxant activity of oxypeucedanin hydrate has not yet been studied, and EOK possesses many other multiple known and unknown compounds. Thus, it is necessary to find more active compounds for the evidence of vasorelaxant activities of EOK.

In conclusions our findings suggest that Osterici Radix might be a useful herbal medicine for treating cardiovascular diseases such as hypertension. However, more detailed mechanism studies, *in vivo* studies, and chemical analyses may be necessary to establish the efficacy of Osterici Radix for treating hypertension.

Conflict of Interests

The authors declare that there is no conflict of interests.

Acknowledgment

This research was supported by a Grant (13172 a natural substance 418) from the Ministry of Food and Drug Safety in 2013.

References

[1] H. L. Park, H. S. Lee, B. C. Shin et al., "Traditional medicine in china, Korea, and Japan: a brief introduction and comparison," *Evidence-Based Complementary and Alternative Medicine*, vol. 2012, Article ID 429103, 9 pages, 2012.

[2] Korean Food & Drug Administration, *The Korean Pharmacopoeia Tenth Edition*, Korean Food & Drug Administration, Osong, Republic of Korea, 2013.

[3] Pharmacopoeia Commission of the Ministry of Health of the People's Republic of China, *Pharmacopoeia of the People's Republic of China 2010*, China Medical Science Press, Beijing, China, 2012.

[4] The Society of Japanese Pharmacopoeia, *The Japanese Pharmacopoeia, Fifteenth Edition*, Yakuji Nippo, Tokyo, Japan, 2006.

[5] Guo jia Zhong yi Yao Guan li ju Zhong hua ben cao bian wei hui bian, *Zhong Hua Ben Cao*, Shang Hai ke Xue ji Shu Chu Ban se, Shang hai, China, 1999.

[6] G. T. Chang and H. J. Kim, "The effect of Notopterygii Rhizoma on the carotid arterial tension in rabbit," *The Journal of Korean Oriental Pediatrics*, vol. 12, no. 1, pp. 163–181, 1998.

[7] K. Ryu and C. Yook, "Pharmacognostical study on the root of Angelica koreana," *Yakhakhoeji*, vol. 12, no. 3, pp. 50–58, 1968.

[8] H. W. Jung, R. Mahesh, J. H. Park, Y. C. Boo, K. M. Park, and Y. Park, "Bisabolangelone isolated from Ostericum koreanum inhibits the production of inflammatory mediators by down-regulation of NF-κB and ERK MAP kinase activity in LPS-stimulated RAW264.7 cells," *International Immunopharmacology*, vol. 10, no. 2, pp. 155–162, 2010.

[9] C. M. Kim and Y. K. Park, "The effects of different extracts of Ostericum koreanum on the production of inflammatory mediators in LPS-stimulated RAW264.7 cells," *Korean Journal of Herbology*, vol. 24, no. 1, pp. 169–178, 2009.

[10] T. J. Kang, S. Y. Lee, R. P. Singh, R. Agarwal, and D. S. Yim, "Anti-tumor activity of oxypeucedanin from Ostericum koreanum against human prostate carcinoma DU145 cells," *Acta Oncologica*, vol. 48, no. 6, pp. 895–900, 2009.

[11] Y. J. Park, H. J. Kim, S. J. Lee, H. Choi, C. Jin, and Y. S. Lee, "A new chromone, 11-hydroxy-sec-O-glucosylhamaudol from *Ostericum koreanum*," *Chemical and Pharmaceutical Bulletin*, vol. 55, no. 7, pp. 1065–1066, 2007.

[12] S. Shin, "*In Vitro* effects of essential oils from *Ostericum koreanum* against antibiotic-resistant Salmonella spp.," *Archives of Pharmacal Research*, vol. 28, no. 7, pp. 765–769, 2005.

[13] S. K. Lee, H. K. Cho, S. H. Cho, S. S. Kim, D. H. Nahm, and H. Park, "Occupational asthma and rhinitis caused by multiple herbal agents in a pharmacist," *Annals of Allergy, Asthma and Immunology*, vol. 86, no. 4, pp. 469–474, 2001.

[14] W. S. Yun, H. H. Kim, D. K. Ahn et al., "Effects of Angelicae korenae Radix on the vasomotor responses and focal cerebral ischemic damage by MCAO," *Korean Journal of Herbology*, vol. 19, no. 3, pp. 147–154, 2004.

[15] J. Y. Park, H. K. Shin, Y. J. Lee, Y. W. Choi, S. S. Bae, and C. D. Kim, "The mechanism of vasorelaxation induced by *Schisandra chinensis* extract in rat thoracic aorta," *Journal of Ethnopharmacology*, vol. 121, no. 1, pp. 69–73, 2009.

[16] M. Xia, L. Qian, X. Zhou, Q. Gao, I. C. Bruce, and Q. Xia, "Endothelium-independent relaxation and contraction of rat aorta induced by ethyl acetate extract from leaves of *Morus alba* (L.)," *Journal of Ethnopharmacology*, vol. 120, no. 3, pp. 442–446, 2008.

[17] L. M. de Oliveira, A. G. Rodrigues, E. F. da Silva et al., "Endothelium-dependent vasorelaxant effect of butanolic fraction from *Caryocar brasiliense* Camb. leaves in rat thoracic aorta," *Evidence-Based Complementary and Alternative Medicine*, vol. 2012, Article ID 934142, 9 pages, 2012.

[18] R. C. Devi, S. M. Sim, and R. Ismail, "Effect of *Cymbopogon citratus* and citral on vascular smooth muscle of the isolated thoracic rat aorta," *Evidence-Based Complementary and Alternative Medicine*, vol. 2012, Article ID 539475, 8 pages, 2012.

[19] E. Stankevicius, E. Kevelaitis, E. Vainorius, and U. Simonsen, "Role of nitric oxide and other endothelium-derived factors," *Medicina*, vol. 39, no. 4, pp. 333–341, 2003.

[20] H. Karaki, H. Ozaki, M. Hori et al., "Calcium movements, distribution, and functions in smooth muscle," *Pharmacological Reviews*, vol. 49, no. 2, pp. 157–230, 1997.

[21] I. McFadzean and A. Gibson, "The developing relationship between receptor-operated and store-operated calcium channels in smooth muscle," *British Journal of Pharmacology*, vol. 135, no. 1, pp. 1–13, 2002.

[22] M. T. Nelson and J. M. Quayle, "Physiological roles and properties of potassium channels in arterial smooth muscle," *American Journal of Physiology*, vol. 268, no. 4, pp. C799–C822, 1995.

[23] A. Lompré, "Sarcoplasmic reticulum in vascular cells in hypertension and during proliferation," *Clinical and Experimental Pharmacology and Physiology*, vol. 26, no. 7, pp. 553–557, 1999.

[24] G. P. Chen, Y. Ye, L. Li, Y. Yang, A. B. Qian, and S. Hu, "Endothelium-independent vasorelaxant effect of sodium ferulate on rat thoracic aorta," *Life Sciences*, vol. 84, no. 3-4, pp. 81–88, 2009.

[25] L. Luksha, S. Agewall, and K. Kublickiene, "Endothelium-derived hyperpolarizing factor in vascular physiology and cardiovascular disease," *Atherosclerosis*, vol. 202, no. 2, pp. 330–344, 2009.

[26] S. Kim, K. Y. Kim, C. S. Han et al., "Simultaneous analysis of six major compounds in Osterici Radix and Notopterygii Rhizoma et Radix by HPLC and discrimination of their origins from chemical fingerprint analysis," *Archives of Pharmacal Research*, vol. 35, no. 4, pp. 691–699, 2012.

[27] J. Y. He, W. Zhang, L. C. He, and Y. X. Cao, "Imperatorin induces vasodilatation possibly via inhibiting voltage dependent calcium channel and receptor-mediated Ca^{2+} influx and release," *European Journal of Pharmacology*, vol. 573, no. 1–3, pp. 170–175, 2007.

[28] L. Zhenkun, L. Meiqi, and Y. Hongjun, "The study of vasoactive of pungent herbs' chemical constituents in Umbelliferae," *Pharmacology and Clinics of Chinese Materia Medica*, no. 1, p. 018, 2009.

Hindawi Publishing Corporation
Evidence-Based Complementary and Alternative Medicine
Volume 2013, Article ID 423741, 11 pages
http://dx.doi.org/10.1155/2013/423741

Research Article

Corni Fructus Containing Formulation Attenuates Weight Gain in Mice with Diet-Induced Obesity and Regulates Adipogenesis through AMPK

Hye-Lin Kim,[1] Yong-Deok Jeon,[2] Jinbong Park,[1] Hong-Kun Rim,[3] Mi-Young Jeong,[2] Hara Lim,[1] Seong-Gyu Ko,[1] Hyeung-Jin Jang,[1] Byung-Cheol Lee,[1] Kyung-Tae Lee,[3] Kang-Min Lee,[4] Hyejung Lee,[1] Sung-Hoon Kim,[1] Su-Jin Kim,[5] Seung-Heon Hong,[2] and Jae-Young Um[1]

[1] *College of Korean Medicine, Institute of Korean Medicine, Kyung Hee University, Hoegi-Dong, Dongdaemun-Gu, Seoul 130-701, Republic of Korea*
[2] *Department of Oriental Pharmacy, College of Pharmacy, Wonkwang-Oriental Medicines Research Institute, Wonkwang University, Jeonbuk 570-749, Republic of Korea*
[3] *Department of Pharmaceutical Biochemistry, College of Pharmacy, Kyung Hee University, Hoegi-Dong, Dongdaemun-Gu, Seoul 130-701, Republic of Korea*
[4] *Department of Molecular Biology, College of Natural Science, Chonbuk National University, Jeollabuk-do 561-756, Republic of Korea*
[5] *Department of Cosmeceutical Science, Daegu Haany University, Yugok-dong, Kyungsan 712-715, Republic of Korea*

Correspondence should be addressed to Jae-Young Um; jyum@khu.ac.kr

Received 2 April 2013; Revised 9 August 2013; Accepted 19 August 2013

Academic Editor: Bo-Hyoung Jang

Obesity is a metabolic disorder characterized by chronic inflammation and dyslipidemia and is a strong predictor for the development of hypertension, diabetes mellitus, and cardiovascular disease. This study examined the antiobesity effect of an ethanol extract of Corni Fructus containing formulation (CDAP), which is a combination of four natural components: Corni Fructus, Dioscoreae Rhizoma, Aurantii Fructus Immaturus, and Platycodonis Radix. The cellular lipid content in 3T3-L1 adipocytes was assessed by Oil Red O staining. Expressions of peroxisome proliferator-activated receptor-γ (PPAR-γ), CCAAT/enhancer-binding protein-α (C/EBP-α), and lipin-1 were determined by real-time RT-PCR. Western blot was used to determine the protein levels of PPAR-γ, C/EBP-α, and AMP-activated protein kinase-α (AMPK-α). The CDAP extract suppressed the differentiation of 3T3-L1 adipocytes by downregulating cellular induction of PPAR-γ, C/EBP-α, and lipin-1. The CDAP extract also significantly upregulated phosphorylation of AMPK-α. An *in vivo* study showed that CDAP induced weight loss in mice with high-fat-diet-induced obesity. These results indicate that CDAP has a potent anti-obesity effect due to the inhibition of adipocyte differentiation and adipogenesis.

1. Introduction

Obesity is the main cause of metabolic syndrome, which can lead to various complications, including hardening of the arteries and an increased risk of cardiovascular diseases. Therefore, obesity has a large impact on healthcare in both developed and developing countries. Obesity is characterized by excessive fat deposition and is associated with morphological and functional changes in the adipocytes [1]. Accordingly, understanding the mechanisms by which particular herbal medicines affect adipocyte differentiation could help prevent obesity and its associated diseases [2].

Adipose tissue, an important depot for energy storage, regulates energy homeostasis. Excessive increases in the number and size of adipocytes result in obesity and metabolic syndrome. Adipogenesis, a differentiation process of

adipocytes, involves changes in gene expression and cellular morphology. Adipocyte hypertrophy results from an excessive accumulation of lipids from intake of excessive energy sources such as a high-fat (HF) diet. Changes in the number of adipocytes result from a complex interplay between proliferation and differentiation of preadipocytes [3]. Therefore, understanding the molecular mechanism of adipocyte differentiation is necessary for the efficient treatment of these diseases. To elucidate the molecular mechanisms of adipogenesis, 3T3-L1 cells have been generally used as an *in vitro* model. Differentiation of 3T3-L1 preadipocytes into mature adipocytes can be induced by upstimulation with 3-isobutyl-1-methylxanthine (IBMX), dexamethasone (Dex), and insulin and promotes the accumulation of large amounts of intracellular lipid droplets in mature adipocytes [4]. During adipogenesis of 3T3-L1 cells, peroxisome proliferator-activated receptor-γ (PPAR-γ) and CCAAT/enhancer-binding protein-α (C/EBP-α) play key roles as major transcription factors [5]. Expression of PPAR-γ, a transcription factor of the nuclear-receptor superfamily, and C/EBP-α, a member of the C/EBP family of basic-leucine zipper class of transcription factors, increased during differentiation of 3T3-L1 cells [6].

AMP-activated protein kinase (AMPK) is a "cellular fuel gauge" and acts to simultaneously shut down ATP-consuming biosynthetic processes and facilitate ATP-producing catabolic processes during periods of metabolic stress, leading to rapid changes in the control of fatty acid metabolism. AMPK stimulation of fatty acid metabolism occurs as a result of AMPK phosphorylation [7]. AMPK, composed of a, b, and g subunits, is a key player in energy homeostasis. When the intracellular AMP/ATP ratio increases because of metabolic stress, AMPK is phosphorylated. Subsequently, downstream target molecules are activated, promoting catabolism. When the intracellular AMP/ATP ratio decreases, AMPK increases anabolism. AMPK is associated with adipocyte differentiation via AMPK activation in 3T3-L1 adipocytes [8, 9]. Lipin is also a central regulator of adipose tissue development. Mammalian lipin proteins have been shown to control gene expression and to enzymatically convert phosphatidate to diacylglycerol, an essential precursor in triacylglycerol and phospholipid synthesis [10]. Previous studies established that lipin-1 is required at an early step in adipocyte differentiation for induction of the adipogenic gene transcription program, including the key regulator PPAR-γ [11].

In this study, we investigated the effect of CDAP, a modified prescription of "Supungsunki-hwan." This frequently prescribed Korean traditional medicine for the treatment of obesity was tested on humans as well as on an animal model subjected to HF diet-induced obesity [12, 13]. The CDAP is a combination of herbal extracts (i.e., Corni Fructus, Dioscoreae Rhizoma, Aurantii Fructus Immaturus, and Platycodonis Radix) at a ratio of 1 : 1 : 1 : 1. This new study investigated the effects of CDAP on the adipocyte differentiation process at the molecular level in 3T3-L1 cells and the effects of dietary CDAP on body weight changes, including physiological and metabolic variables, in HF diet C57BL/6 mice.

2. Materials and Methods

2.1. Preparation of CDAP. The oriental, medicinal, and herbal mixture used in this experiment (CDAP) is approved as a food ingredient. The herbal sample was prepared as described previously [13]. Briefly, 1 kg each of Corni Fructus, Dioscoreae Rhizoma, Aurantii Fructus Immaturus, and Platycodonis Radix was extracted with 80% ethanol (80% EtOH) for 2 h and 20 min using a heating mantle. The solvents were filtered and evaporated under reduced pressure (Rotary evaporator Model NE-1, Japan) and the remnant then freeze-dried (Freeze dryer FD-1, Japan) at −56°C and 9 mm Torr to acquire extracts of each herbal sample.

2.2. Animals and Diets. Male 4-week-old C57BL/6J mice were purchased from Daehan Biolink Co. (Eumsung, Korea) and maintained for one week prior to experiments. All animals were maintained in a C57Bl/6J background, on a 12 h light-dark cycle in a pathogen-free animal facility. Mice were provided with a laboratory diet and water *ad libitum*. All experimental protocols involving the use of animals were conducted in accordance with National Institutes of Health (NIH) guidelines. To induce obesity, the mice were fed a HF diet (Rodent Diet D12492, Research Diet, New Brunswick, NJ, USA) consisting of 60% fat in accordance with previously published reports [14]. Normal mice were fed a commercial standard chow diet (CJ Feed Co., Ltd., Seoul, Republic of Korea). Experimental mice were fed the HF diet for four weeks before administration of CDAP or Slinti, a green tea extract used as a positive control (Myungmoon Pharm. Co., LTD., Seoul, Republic of Korea). The mice were randomly divided into four groups ($n = 5$ per group) that were fed either a normal diet (ND), a HF diet, a HF diet plus CDAP, or a HF diet plus Slinti, for 16 weeks. Body weight and food intake were measured three times per week.

2.3. Cell Culture and Differentiation. 3T3-L1 mouse embryo fibroblasts were obtained from the American Type Culture Collection (Rockwill, MD, USA). Cells were grown in DMEM plus 10% calf serum and plated for final differentiation in DMEM plus 10% FBS with 100 units/mL of penicillin-streptomycin solution at 37°C, in 5% CO_2, at 95% humidity until confluence. Two days after confluence (Day 0), the cells were stimulated to differentiate with differentiation inducers (1 μM dexamethasone, 500 μM 3-isobutyl-1-methylxanthine, and 1 μg/mL insulin, MDI) that were added to DMEM containing 10% FBS for two days (Day 2). Preadipocytes were then cultured in DMEM, 10% FBS supplemented with 1 μg/mL insulin for another two days (Day 4), followed by culturing with 10% FBS/DMEM medium for additional two days (Day 6), at which time more than 90% of cells were mature adipocytes with accumulated fat droplets. On Day 2, CDAP was prepared in a differentiation medium at concentrations of 10 μg/mL, 50 μg/mL, and 100 μg/mL.

2.4. MTS Cell Viability Assay. On 96-well plates, the 3T3-L1 preadipocytes were seeded (2×10^4 cells/well) and incubated in 10% FBS/DMEM medium for 24 h. Then, the cells were incubated in 10% FBS/DMEM medium containing ethanol

extract of CDAP for an additional 48 h. Cell viability was monitored using the Cell Proliferation MTS Kit (Promega Corporation, Madison, WI, USA) as recommended by the manufacturer. Prior to measuring viability, treatment media were removed and replaced with 200 μL fresh 10% FBS/DMEM medium and 10 μL 3-(4,5-dimethylthiazol-2-yl)-5-(3-carboxymethoxyphenyl)-2-(4-sulfophenyl)-2H-tetrazolium (MTS) solution. Cells were then returned to the incubator for 4 h. The absorbance was measured at 490 nm in a VERSAmax microplate reader (Molecular Devices, Sunnyvale, CA, USA) to determine the formazan concentration, which is proportional to the number of live cells.

2.5. Oil Red O Staining. Intracellular lipid accumulation was measured using Oil Red O. The Oil Red O working solution was prepared as described by Ramirez-Zacarias et al. [15]. The 3T3-L1 cells were fixed with 10% formalin and then stained for 1 h with filtered solution of 60% Oil Red O in 100% aqueous 2-isopropanol. To quantify the intracellular lipids, the stained lipid droplets were dissolved in isopropanol (3 mL/well). The extracted dye was transferred into a 96-well plate and absorbance read with a VERSAmax microplate reader (Molecular Devices, Sunnyvale, CA, USA) at 500 nm.

2.6. RNA Extraction and Real-Time RT-PCR. Total RNA was extracted from the cells using a GeneAll^{R} RiboEx Total RNA extraction kit (GeneAll Biotechnology, Seoul, Republic of Korea) according to the manufacturer's instructions. From 2 μg of RNA, cDNA was reverse-transcribed using a Power cDNA synthesis kit (iNtRON Biotechnology, Seongnam, Kyunggi, Republic of Korea). The primers PPARγ, C/EBPα, and glyceraldehyde-3-phosphate dehydrogenase (GAPDH) were used for real-time PCR analysis. Real-time PCR was performed with SYBR Green Power Master Mix (Applied Biosystems, Foster City, CA, USA) using a Step One Plus Real-Time PCR System (Applied Biosystems, Foster City, CA, USA). The target cDNA was amplified using the sense and antisense primers described in Table 1.

2.7. Western Blot Analysis. Cultured and differentiated cells were harvested using a cell scraper and then lysed with ice-cold RIPA buffer. The total cell lysates were then centrifuged at 13,000 rpm for 20 min at 4°C to remove the insoluble materials. Next, the total concentration of extracted proteins was determined using the method of Bradford [16]. Western blottings were performed with polyclonal rabbit antibodies against PPAR-γ (Cell Signaling Technology, Beverly, MA, USA), C/EBP-α (Santa Cruz Biotechnology, Santa Cruz, CA, USA), Lipin-1 (Cell Signaling Technology, Beverly, MA, USA), AMPK-α (Cell Signaling Technology, Beverly, MA, USA), p-AMPK-α (Cell Signaling Technology, Beverly, MA, USA), and polyclonal mouse antibodies against GAPDH (Santa Cruz Biotechnology, Santa Cruz, CA, USA). The blots were subsequently incubated with horseradish peroxidase (HRP)-conjugated affinipure Goat anti-rabbit IgG (Jackson Immunoresearch Laboratory, USA) or HRP-conjugated affinipure Goat anti-mouse IgG (Jackson Immunoresearch Laboratory, USA). Polyvinylidene difluoride (PVDF) membrane was purchased from Millipore, and the protein assay reagent was obtained from Bio-Rad (Bio-Rad Laboratories, Hercules, CA, USA).

Table 1: Sequences of oligonucleotide primers (5′ to 3′) for real-time RT-PCR.

Genes	5′ to 3′ oligonucleotide sequences
Mouse PPAR-γ	
Sense (forward)	TTT TCA AGG GTG CCA GTT TC
Antisense (reverse)	TTA TTC ATC AGG GAG GCC AG
Mouse C/EBP-α	
Sense (forward)	GCC GAG ATA AAG CCA AAC AA
Antisense (reverse)	CCT TGA CCA AGG AGC TCT CA
Mouse lipin-1	
Sense (forward)	CGC CAA AGA ATA ACC TGG AA
Antisense (reverse)	TGA AGA CTC GCT GTG AAT GG
Mouse GAPDH	
Sense (forward)	AAC TTT GGC ATT GTG GAA GG
Antisense (reverse)	GGA TGC AGG GAT GAT GTT CT

PPAR-γ: peroxisome proliferator-activated receptor-γ; C/EBP-α: CCAAT/enhancer-binding protein-α; GAPDH: glyceraldehyde-3-phosphate dehydrogenase.

2.8. Serum Analysis. All mice were made to fast for 3 h prior to being sacrificed. Plasma was separated immediately after blood sampling by centrifugation at 4,000 ×g for 30 min. The serum was stored at −70°C until being used for assays. High-density lipoprotein (HDL-C) cholesterol, low-density lipoprotein (LDL-C) cholesterol, total cholesterol (TC), and fructosamine were assayed at the Seoul Medical Science Institute (Seoul Clinical Laboratories, Seoul, Republic of Korea).

2.9. Instrumentation. The HPLC was equipped with a vacuum degasser, a quaternary pump, and an automatic sample injection system. Chromatographic separation was performed on a Nucleosil C 18 (150 × 4.6 mm, 5 μm, Teknokroma, Barcelona, Spain). Samples were separated using acetonitrile and phosphate buffer (50 + 50 v/v), pH 5.5, as the mobile phase at a flow rate of 1.0 mL/min at ambient temperature. Initial elution was performed by acetonitrile-aqueous ammonium acetate 20 : 80 (v/v). After 10 min, the linear gradient reached 60% acetonitrile.

2.10. Statistical Analysis. All data, expressed as mean ± standard deviation, were processed statistically using the software SPSS 11.5 for Windows. Values with $^{*}P < 0.05$ were considered to indicate statistical significance.

3. Results

3.1. Effects of CDAP on Cytotoxicity and Inhibition of Adipogenesis in 3T3-L1 Adipocytes. To determine the cytotoxicity of CDAP, 3T3-L1 cells were treated with various concentrations (10–500 μg/mL) of CDAP and the cell viability measured

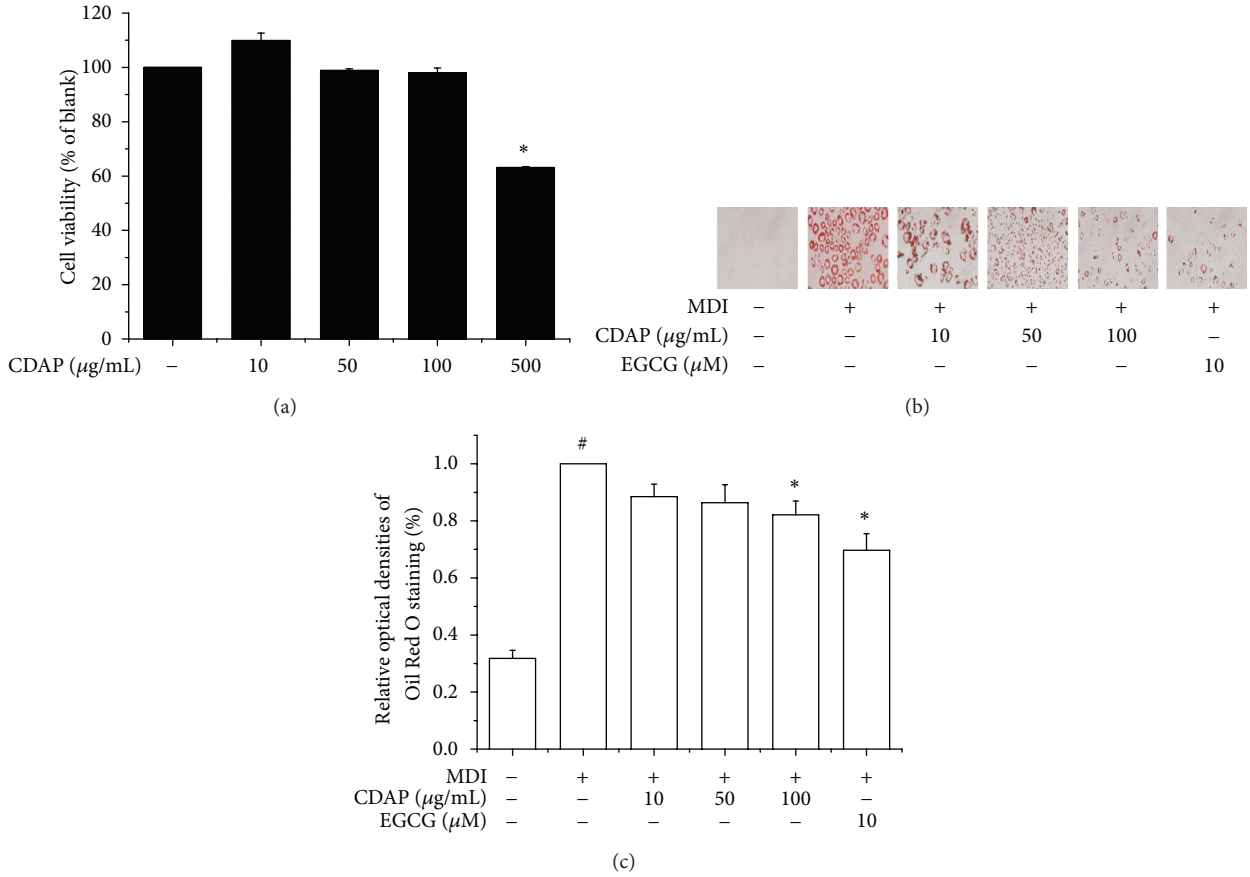

Figure 1: Effect of CDAP on cell viability and lipid accumulation in 3T3-L1 cells. (a) Cells were incubated with CDAP at the indicated concentration for 48 h. Cell viability was assessed by MTS assay. (b) Postconfluent 3T3-L1 cells were differentiated in the absence or in the presence of CDAP (0, 10, 50, and 100 μg/mL) for 6 days. Lipid droplets were measured by Oil Red O staining. EGCG was used as a positive control. All values are mean ± S.D. $^{\#}P < 0.05$ versus undifferentiated control cells; $^{*}P < 0.05$ versus differentiated control cells.

by the MTS assay. As shown in Figure 1(a), treatment with 10–100 μg/mL of CDAP did not cause significant cytotoxic effects on 3T3-L1 cells. Due to this result, further treatments proceeded at the concentrations of 10, 50, and 100 μg/mL. Next, to investigate the effects of CDAP on preadipocyte differentiation, the lipid accumulation was measured by an Oil Red O staining assay. As shown in Figure 1(b), 100 μg/mL of CDAP suppressed lipid accumulation in 3T3-L1 adipocytes at levels that were statistically significant ($P < 0.05$), suggesting that CDAP inhibits adipogenesis in 3T3-L1 cells. Epigallocatechin gallate (EGCG) was used as a positive control.

3.2. Effect of CDAP on the Expression of PPARγ, C/EBPα, and Lipin-1 in 3T3-L1 Adipocytes. Adipocyte differentiation accompanies the changes in expression of various adipogenic and lipogenic genes [17]. PPARγ and C/EBPα are well recognized adipogenic genes known to have roles in the early stage of adipogenesis [18]. Lipin-1 is also required at an early step in adipocyte differentiation for induction of the adipogenic gene transcription [11]. To investigate the antiadipogenic mechanism, the effect of CDAP on mRNA expression levels of PPARγ, C/EBPα, and lipin-1 were examined. Fully differentiated 3T3-L1 cells were exposed for 48 h to concentrations of 10, 50, and 100 μg/mL of CDAP. Expressions of both adipogenic genes PPARγ and C/EBPα were significantly decreased by CDAP (Figures 2(a) and 2(b)). In addition, CDAP significantly suppressed the expression of lipin-1 in a dose-dependent manner (Figure 2(c)). We also demonstrated that CDAP treatment resulted in a dose-dependent suppression of PPARγ, C/EBPα, and lipin-1 at the protein level (Figures 3(a), 3(b), and 3(c)). EGCG was used as a positive control.

3.3. The Effect of CDAP on the Expression and Phosphorylation of AMPK. To investigate whether AMPK, a key player in energy homeostasis [19], is activated by CDAP during 3T3-L1 differentiation, the level of phosphorylated AMPKα was analyzed and compared with the total level of AMPKα. When compared with the control group, AMPKα phosphorylation increased after treatment with 100 μg/mL of CDAP (Figure 4(c)). A western blot showed that total AMPKα was unchanged. In addition, the effect of CDAP on AMPK activation was also compared with naringin and platycodin D, since Aurantii Fructus Immaturus and Platycodonis Radix showed significant antiadipogenic effects on 3T3-L1

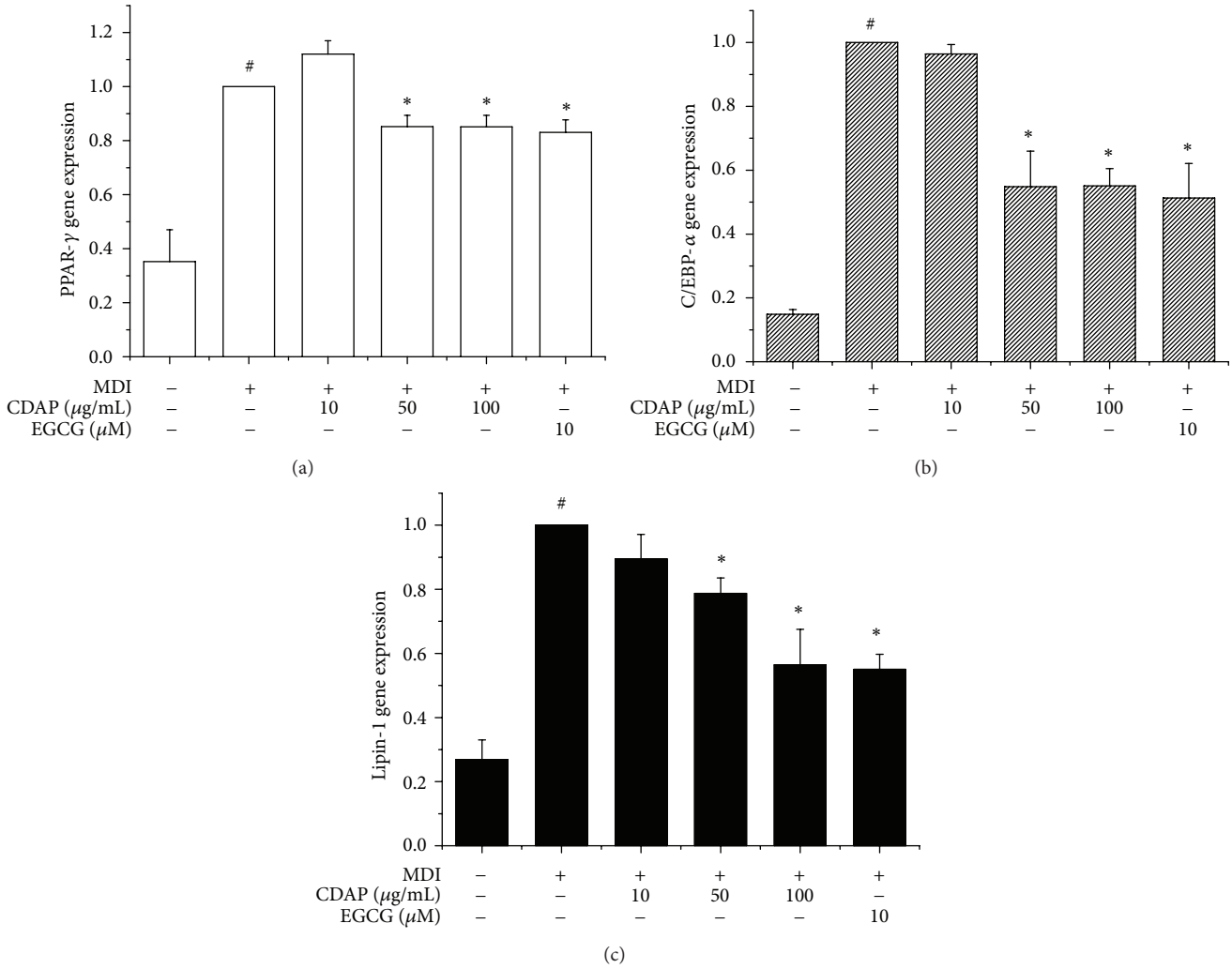

Figure 2: Effect of CDAP on the expression of transcription factors and adipocyte-specific genes in differentiation of 3T3-L1 cells. Postconfluent 3T3-L1 cells were differentiated in the absence or presence of CDAP (0, 10, 50, and 100 μg/mL) for 6 days. The mRNA of PPAR-γ (a), C/EBP-α (b), and lipin-1 (c) was analyzed by real-time RT-PCR. Results were expressed relative to untreated cells after normalization to GAPDH mRNA. EGCG was used as a positive control. Values are mean ± S.D. of data from three separate experiments; each experiment was performed in triplicate. $^{\#}P < 0.05$ versus undifferentiated control cells; $^{*}P < 0.05$ versus differentiated control cells.

differentiation compared to other herb components of CDAP (Figure 4(a)). The cytotoxicity of naringin and platycodin D, major constituents of Aurantii Fructus Immaturus and Platycodonis Radix, respectively, was examined using an MTS assay (Figure 4(b)). The result showed that CDAP had a higher effect on activation of AMPK than that of naringin but not higher than that of platycodin D.

3.4. Effects of CDAP Extract on HF Diet-Induced Obese C57BL/6J Mice. To examine the reduction of body weight by CDAP, mice were fed HFD for four weeks before administration of either CDAP or Slinti. After inducing obesity, the mice were subdivided into four groups: the normal diet group with vehicle treatment, the 60% HFD group with vehicle treatment, the 60% HFD group with Slinti (5 mg/kg/day) treatment as a positive control, and the 60% HFD group with CDAP (100 mg/kg/day). After inducing obesity with HFD for four weeks, there were significant differences in body weight between the HFD and normal diet groups. The weight gain of the group of mice administered with extract of CDAP (100 mg/kg/day) was significantly ($P < 0.05$) decreased compared with the HD diet group (Figures 5(a) and 5(b)). The level of daily food intake was unchanged, suggesting that the antiobesity effects of CDAP extract were not mediated by a reduction of food and water intake. The changes in the blood plasma parameter are shown in Figures 5(c)–5(f). The CDAP group showed significant decrease in LDL cholesterol compared to the HF diet group.

3.5. Chromatographic Separation. The HPLC chromatogram revealed that loganin (Corni Fructus), allantoin (Dioscoreae Rhizoma), naringin (Aurantii Fructus Immaturus), and

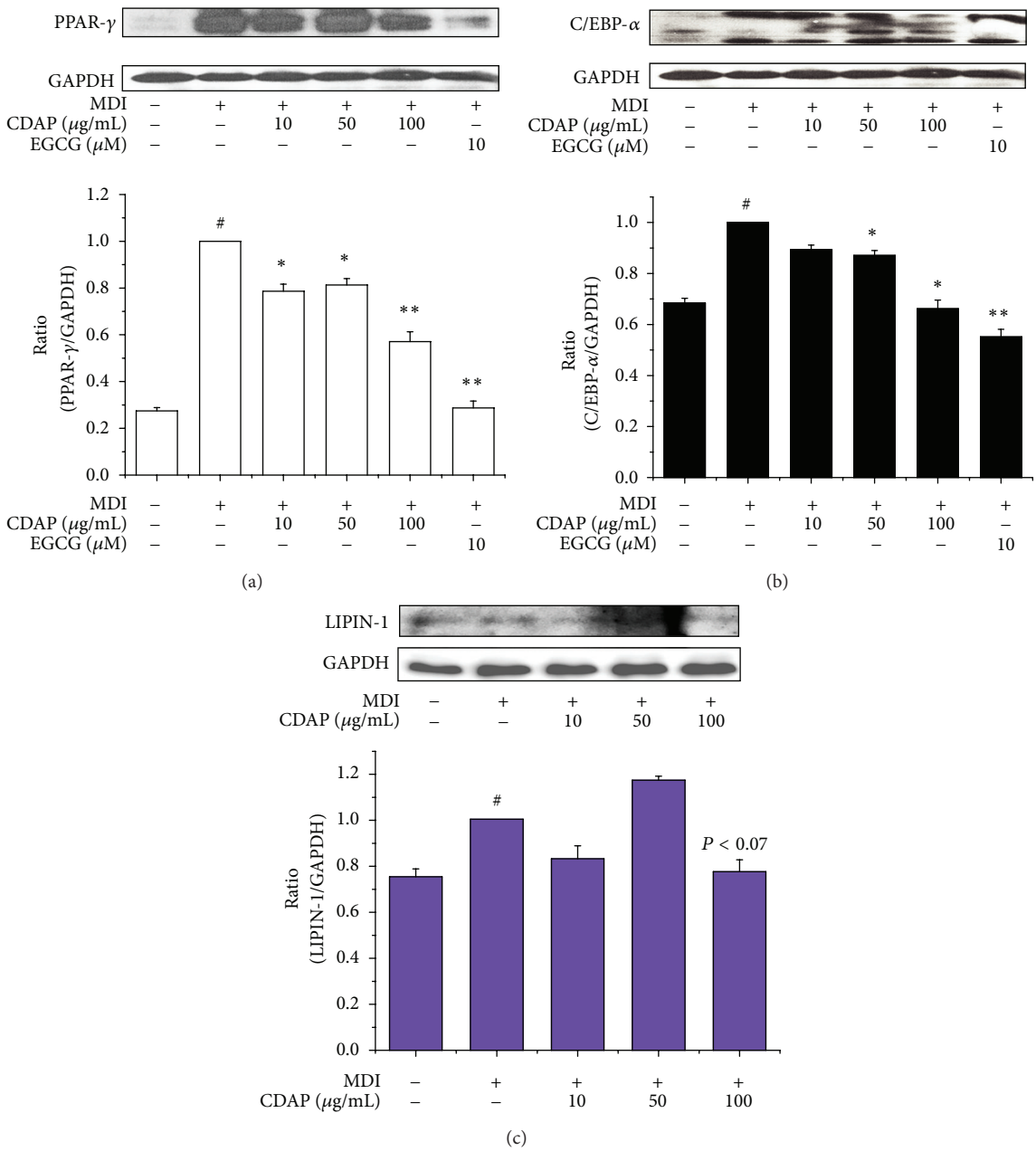

Figure 3: Effect of CDAP on the protein expressions of transcription factors in differentiation of 3T3-L1 cells. Postconfluent 3T3-L1 cells were differentiated in the absence or presence of CDAP (0, 10, 50, and 100 μg/mL) for 6 days. PPARγ (a), C/EBPα (b), and lipin-1 (c) protein expressions were analyzed by western blot analysis. EGCG was used as a positive control. Values are mean ± S.D. of data from three separate experiments; each experiment was performed in triplicate. $^{\#}P < 0.05$ versus undifferentiated control cells; $^{*}P < 0.05$ and $^{**}P < 0.01$ versus differentiated control cells.

platycodin D (Platycodonis Radix) were the major constituents in the organic molecules of the EtOH extract of CDAP (Figure 6).

4. Discussion

CDAP is a modified prescription of "Supungsunki-hwan", a frequently prescribed Korean traditional medicine for the treatment of obesity. The effects of Corni Fructus, Dioscoreae Rhizoma, and Aurantii Fructus Immaturus have been studied for reduction of blood glucose, as well as improving insulin sensitivity [12]. These three herbs are included in the original "Supungsunki-hwan" prescription, which consists of 12 herbal medicines. In addition, it has been reported that platycodin D, a major component of Platycodonis Radix, effectively inhibits triglyceride accumulation in adipocytes [16]. In this study, we examined the anti-obesity effect of ethanol extract of CDAP, a combination of four herbal components (i.e., Corni Fructus, Dioscoreae Rhizoma, Aurantii Fructus Immaturus, and Platycodonis Radix).

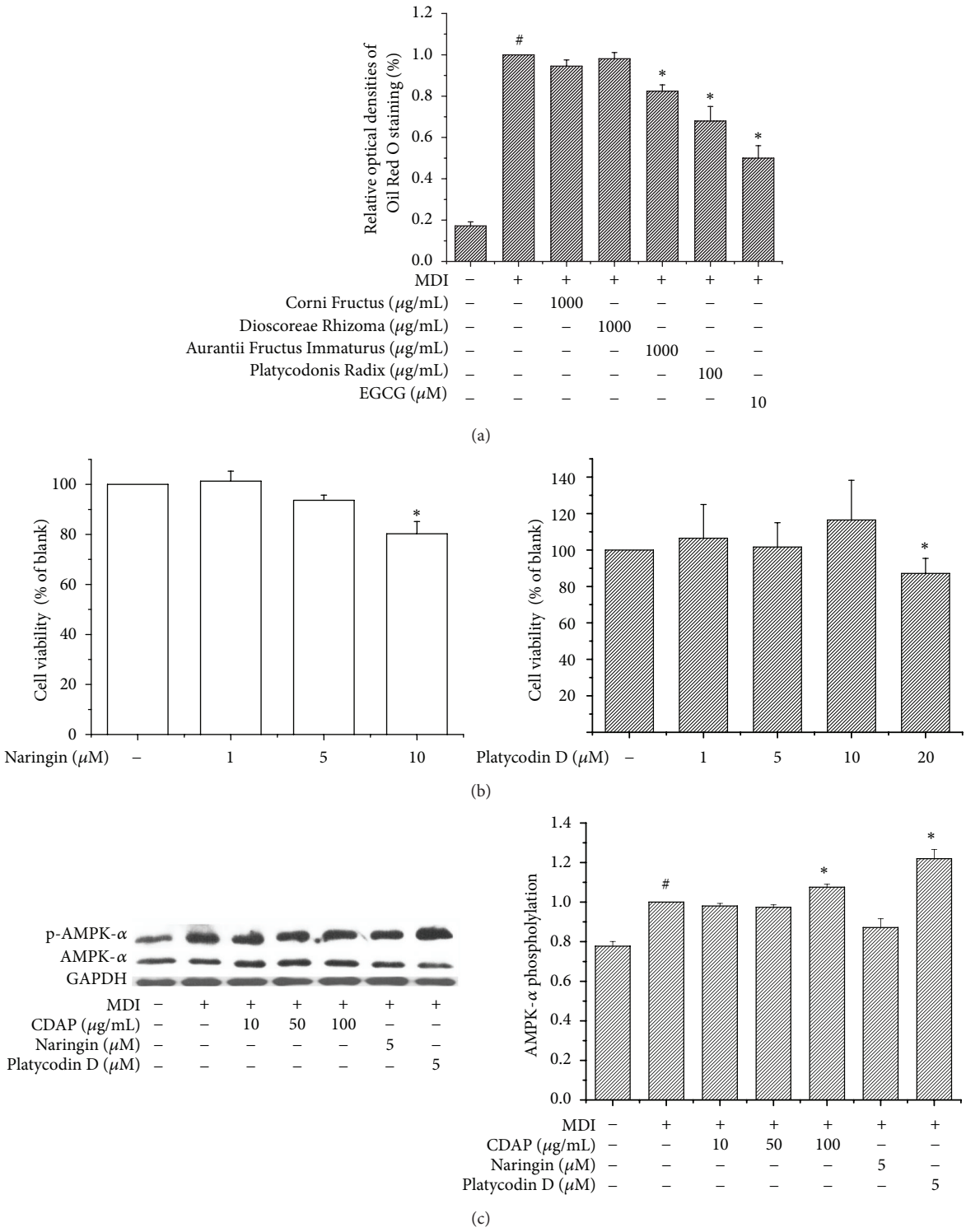

Figure 4: Effect of CDAP and its constituents on phosphorylation of AMPK during 3T3-L1 differentiation. Postconfluent 3T3-L1 cells were differentiated in the presence or absence of Corni Fructus, Dioscoreae Rhizoma, Aurantii Fructus Immaturus, and Platycodonis Radix for 6 days. (a) Lipid accumulation was measured by an Oil Red O staining assay. (b) The cytotoxicity of each constituent, naringin and platycodin D, which are more effective herb's constituents on lipid accumulation, was examined using an MTS assay. (c) Effect of CDAP on AMPK activation was compared with naringin and platycodin D, a major constituent of Aurantii Fructus Immaturus and Platycodonis Radix, respectively. Protein levels of phosphorylated AMPK (pAMPK) and total AMPK were determined by western blot analysis. The protein expression differences are normalized to AMPK-α. Values are mean ± S.D. of data from three separate experiments; each experiment was performed in triplicate. $^{\#}P < 0.05$ versus undifferentiated control cells; $^{*}P < 0.05$ versus differentiated control cells.

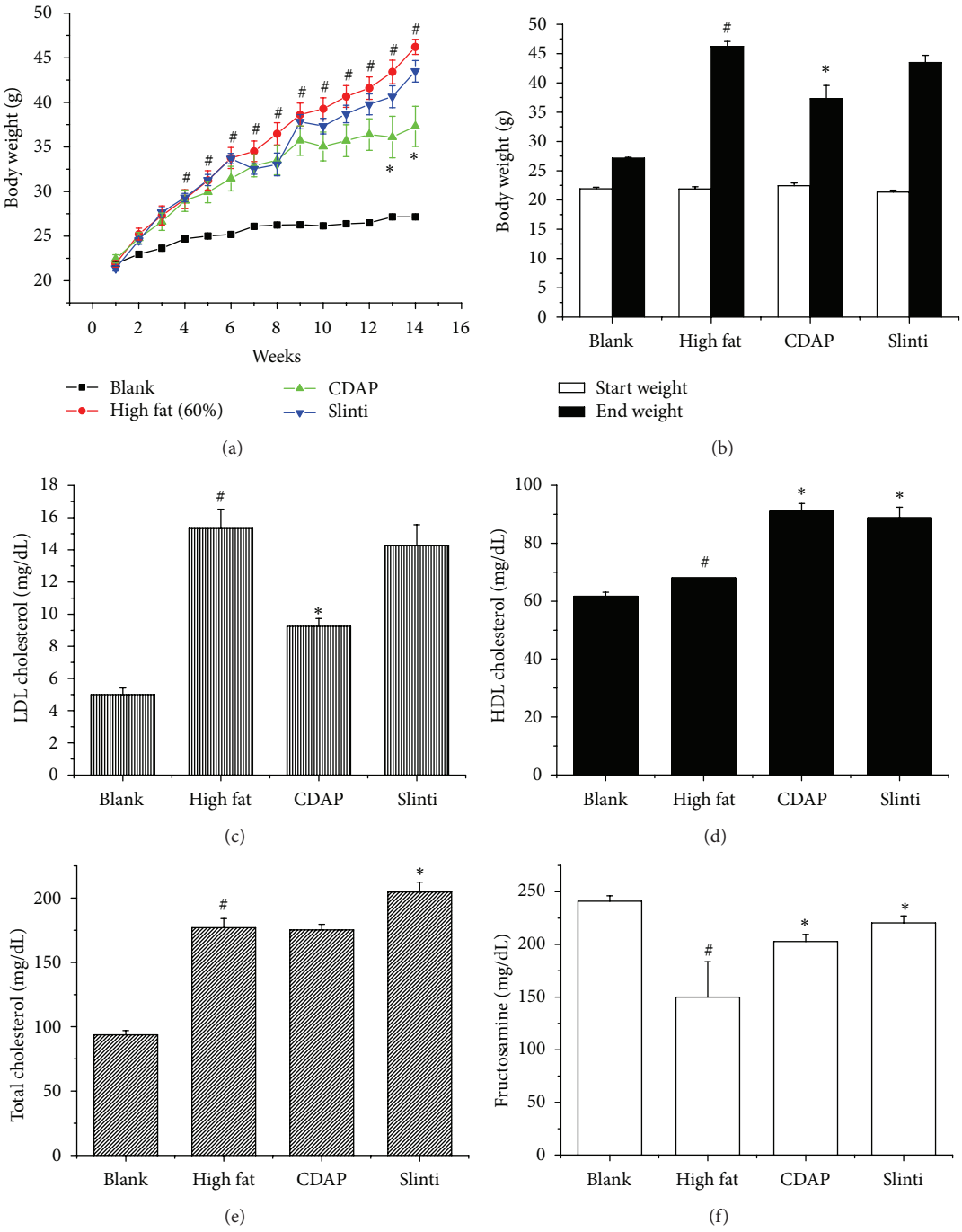

FIGURE 5: Effects of CDAP in HF diet-induced obesity mice. Mice ($n = 5$ per group) were administrated CDAP extract (100 mg/kg/day) with their HF diet for 16 weeks. Normal diet (blank) fed mice were administrated with vehicle. Slinti (5 mg/kg/day) was administrated as a positive control. Changes in body weight (a), the weight difference between the start weight and end weight of each group (b), LDL cholesterol (c), HDL cholesterol (d), total cholesterol (e), and fructosamine (f) of the mice were measured. All values are mean ± S.D. $^{\#}P < 0.05$ significantly different from blank (normal diet group); $^{*}P < 0.05$ significantly different from HF diet group (60%).

The present study demonstrates the effect of CDAP extract on inhibition of adipocyte differentiation. Our results show that CDAP did not cause significant cytotoxic effects in 3T3-L1 cells and significantly inhibited lipid accumulation and adipocyte differentiation in a concentration-dependent manner. These results indicate that CDAP inhibited adipogenesis during adipocyte differentiation and may have potential anti-obesity effects. As shown in Figure 4, Aurantii Fructus Immaturus and Platycodonis Radix were more effective than other herbs of CDAP to inhibit adipogenesis. In addition,

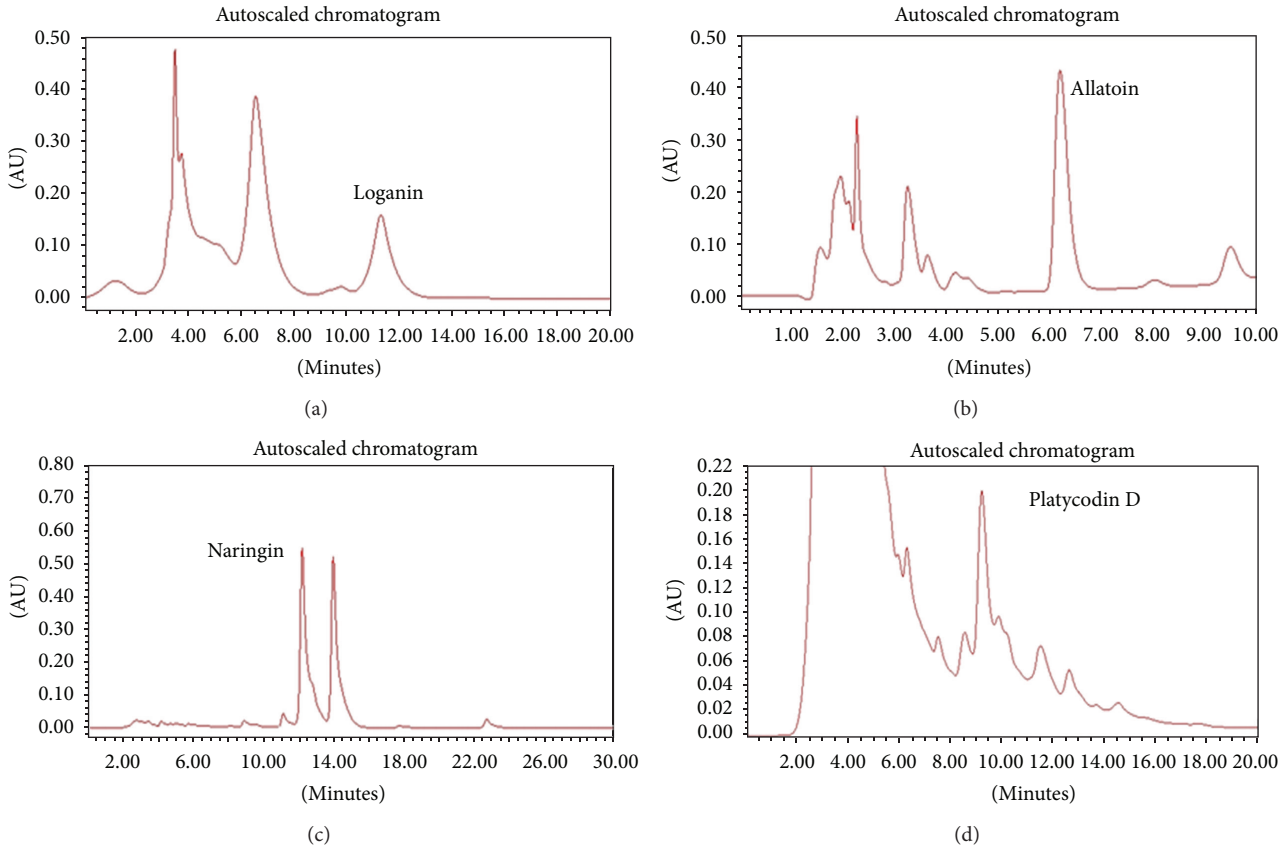

Figure 6: HPLC chromatogram of CDAP. The peaks were assigned based on the isolation of each compound. (a) Corni Fructus: logarnin; (b) Dioscoreae Rhizoma: allantoin; (c) Aurantii Fructus Immaturus: naringin; (d) Platycodonis Radix: platycodin D. The herbs were extracted with 80% ethanol (80% EtOH).

platycodin D, a major component of Platycodonis Radix, was more effective than CDAP to activate AMPK-α. However, CDAP reduced the serum levels of aspartate transaminase (AST) and alanine transaminase (ALT), compared to each individual herb (Supplementary Figure S1 available online at http://dx.doi.org/10.1155/2013/423741).

PPAR-γ, a transcription factor predominantly expressed in adipose tissue, plays an important role in adipocyte differentiation, lipid storage, and glucose homeostasis [20]. Also, adipogenesis is highly regulated by two primary adipogenic transcription factors, PPAR-γ and C/EBPs [21]. Among these, PPAR-γ is well known as the master of adipogenic transcription [22]. The expression of PPAR-γ leads to induced adipogenesis in mesenchyme stem cells and fibroblasts [23, 24]. PPAR-γ is also known to bind to the C/EBP-α promoter region that induces the expression of C/EBP-α [25]. C/EBP-α is a transcription factor of the C/EBP family, basic-leucine zipper class, and is regulated by C/EBP-β in adipocyte differentiation [26]. We found that CDAP significantly downregulates PPAR-γ and C/EBP-α mRNA and the protein levels induced by differentiation medium in 3T3-L1 cells. This could be explained in two ways: CDAP either inhibited PPAR-γ and C/EBP-α or suppressed the upstream molecules. Lipin-1 is also required in adipocyte differentiation for induction of the adipogenic gene transcription [11]. We found that CDAP can inhibit adipocyte differentiation through suppression of lipin-1.

AMPK, a central sensor of cellular energy, is a eukaryotic heterotrimeric serine/threonine kinase, and it has emerged as a therapeutic target for metabolic disorders including obesity. The activation of AMPK is essential for the inhibition of 3T3-L1 adipocyte lipogenesis by phytochemicals [27]. The anti-obesity effects of many natural compounds are mediated through the regulation of fat cells. Genistein, EGCG, and capsaicin, in particular, were shown to inhibit adipogenesis by activating AMPK-α [28, 29]. To determine whether CDAP inhibits adipocyte differentiation by activating AMPK, the level of AMPK phosphorylation was determined. The results show that the level of AMPK phosphorylation was elevated significantly after CDAP treatment. This result indicates that CDAP inhibited adipocyte differentiation via activation of AMPK. AMPK activator A-769662 inhibits adipocyte differentiation by downregulating PPARγ, C/EBPα, FAS, and aP2 [30]. It has been also reported that treatment of 3T3-L1 preadipocytes with an AMPK activator, AICAR, inhibited the differentiation process [31]. Therefore, our result suggests therapeutic potential for using CDAP as an activator of AMPK.

5. Conclusion

The results of this study show anti-obesity effects of CDAP both *in vivo* and *in vitro*. CDAP inhibited adipocyte differentiation of 3T3-L1 and reduced weight gain in mice with HF-diet-induced obesity. CDAP significantly decreased lipid accumulation and the expressions of the major adipogenesis factors PPAR-γ, C/EBP-α, and lipin-1. CDAP also upregulated phosphorylation of AMPK-α. These antiobesity effects of CDAP support its potential as a therapeutic substance or as a source of therapeutic substances.

Acknowledgment

This work was supported by the National Research Foundation of Korea (NRF) Grant funded by the Korean government (MSIP) (no. 2011–0006220).

References

[1] S.-I. Kang, H.-C. Ko, H.-S. Shin et al., "Fucoxanthin exerts differing effects on 3T3-L1 cells according to differentiation stage and inhibits glucose uptake in mature adipocytes," *Biochemical and Biophysical Research Communications*, vol. 409, no. 4, pp. 769–774, 2011.

[2] R. Suzuki, M. Tanaka, M. Takanashi et al., "Anthocyanidins-enriched bilberry extracts inhibit 3T3-L1 adipocyte differentiation via the insulin pathway," *Nutrition and Metabolism*, vol. 8, article 14, 2011.

[3] Y. H. Hsieh and S. Y. Wang, "Lucidone from *Lindera erythrocarpa* Makino fruits suppresses adipogenesis in 3T3-L1 cells and attenuates obesity and consequent metabolic disorders in high-fat diet C57BL/6 mice," *Phytomedicine*, vol. 7113, no. 12, pp. 420–425, 2012.

[4] B. A. Jessen and G. J. Stevens, "Expression profiling during adipocyte differentiation of 3T3-L1 fibroblasts," *Gene*, vol. 299, no. 1-2, pp. 95–100, 2002.

[5] H. Lee, S. Bae, Y. S. Kim, and Y. Yoon, "WNT/β-catenin pathway mediates the anti-adipogenic effect of platycodin D, a natural compound found in *Platycodon grandiflorum*," *Life Sciences*, vol. 89, no. 11-12, pp. 388–394, 2011.

[6] D. H. Kwak, J. H. Lee, T. S. Kim et al., "Aristolochia manshuriensis kom inhibits adipocyte differentiation by regulation of ERK1/2 and akt pathway," *Plos ONE*, vol. 7, no. 11, Article ID e49530, 2012.

[7] H. Kim and S. Y. Choung, "Anti-obesity effects of boussingaulti gracilis miers var. pseudobaselloides bailey via activation of AMP-activated protein kinase in 3T3-L1 cells," *Journal of Medicinal Food*, vol. 15, no. 9, pp. 811–817, 2012.

[8] S.-K. Kim and C.-S. Kong, "Anti-adipogenic effect of dioxinodehydroeckol via AMPK activation in 3T3-L1 adipocytes," *Chemico-Biological Interactions*, vol. 186, no. 1, pp. 24–29, 2010.

[9] B. Huang, H. D. Yuan, D. Y. Kim, H. Y. Quan, and S. H. Chung, "Cinnamaldehyde prevents adipocyte differentiation and adipogenesis via regulation of peroxisome proliferator-activated receptor-γ (PPARγ) and AMP-activated protein kinase (AMPK) pathways," *Journal of Agricultural and Food Chemistry*, vol. 59, no. 8, pp. 3666–3673, 2011.

[10] R. Ugrankar, Y. Liu, J. Provaznik, S. Schmitt, and M. Lehmann, "Lipin is a central regulator of adipose tissue development and function in *Drosophila melanogaster*," *Molecular and Cellular Biology*, vol. 31, no. 8, pp. 1646–1656, 2011.

[11] P. Zhang, K. Takeuchi, L. S. Csaki, and K. Reue, "Lipin-1 phosphatidic phosphatase activity modulates phosphatidate levels to promote peroxisome proliferator-activated receptor γ (PPARγ) gene expression during adipogenesis," *The Journal of Biological Chemistry*, vol. 287, no. 5, pp. 3485–3494, 2012.

[12] T. Kimura, K. Nakagawa, H. Kubota et al., "Food-grade mulberry powder enriched with 1-deoxynojirimycin suppresses the elevation of postprandial blood glucose in humans," *Journal of Agricultural and Food Chemistry*, vol. 55, no. 14, pp. 5869–5874, 2007.

[13] K. S. Kim, H. J. Yang, E. K. Choi et al., "The effects of complex herbal medicine composed of *Cornus fructus*, *Dioscoreae rhizoma*, *Aurantii fructus*, and *Mori folium* in obese type-2 diabetes mice model," *Oriental Pharmacy and Experimental Medicine*, vol. 13, no. 1, pp. 69–75, 2012.

[14] Y. Liu, H. Dang, and D. Li, "Inhibition of soluble epoxide hydrolase attenuates high-fat-diet—induced hepatic steatosis by reduced systemic inflammatory status in mice," *Plos ONE*, vol. 7, no. 6, Article ID e39165, 2012.

[15] J. L. Ramirez-Zacarias, F. Castro-Munozledo, and W. Kuri-Harcuch, "Quantitation of adipose conversion and triglycerides by staining intracytoplasmic lipids with oil red-O," *Histochemistry*, vol. 97, no. 6, pp. 493–497, 1992.

[16] M. M. Bradford, "A rapid and sensitive method for the quantitation of microgram quantities of protein utilizing the principle of protein dye binding," *Analytical Biochemistry*, vol. 72, no. 1-2, pp. 248–254, 1976.

[17] L. Fajas, "Adipogenesis: a cross-talk between cell proliferation and cell differentiation," *Annals of Medicine*, vol. 35, no. 2, pp. 79–85, 2003.

[18] E. D. Rosen, C. J. Walkey, P. Puigserver, and B. M. Spiegelman, "Transcriptional regulation of adipogenesis," *Genes and Development*, vol. 14, no. 11, pp. 1293–1307, 2000.

[19] B. B. Lowell, "PPARγ: an essential regulator of adipogenesis and modulator of fat cell function," *Cell*, vol. 99, no. 3, pp. 239–242, 1999.

[20] Y. Y. Sung, T. Yoon, W. K. Yang et al., "The antiobesity effect of *Polygonum aviculare* L. ethanol extract in high-fat diet-induced obese mice," *Evidence-Based Complementary and Alternative Medicine*, vol. 2013, Article ID 626397, 11 pages, 2013.

[21] A. Soukas, N. D. Socci, B. D. Saatkamp, S. Novelli, and J. M. Friedman, "Distinct transcriptional profiles of adipogenesis *in Vivo* and *in Vitro*," *The Journal of Biological Chemistry*, vol. 276, no. 36, pp. 34167–34174, 2001.

[22] E. D. Rosen, C. J. Walkey, P. Puigserver, and B. M. Spiegelman, "Transcriptional regulation of adipogenesis," *Genes and Development*, vol. 14, no. 11, pp. 1293–1307, 2000.

[23] P. Tontonoz, E. Hu, R. A. Graves, A. I. Budavari, and B. M. Spiegelman, "mPPARγ2: tissue-specific regulator of an adipocyte enhancer," *Genes and Development*, vol. 8, no. 10, pp. 1224–1234, 1994.

[24] W.-C. Yeh, Z. Cao, M. Classon, and S. L. McKnight, "Cascade regulation of terminal adipocyte differentiation by three members of the C/EBP family of leucine zipper proteins," *Genes and Development*, vol. 9, no. 2, pp. 168–181, 1995.

[25] E. D. Rosen, C. H. Hsu, X. Wang et al., "C/EBPalpha induces adipogenesis through PPARgamma: a unified pathway," *Genes and Development*, vol. 16, no. 2, pp. 22–26, 2002.

[26] S. A. Habinowski and L. A. Witters, "The effects of AICAR on adipocyte differentiation of 3T3-L1 cells," *Biochemical and Biophysical Research Communications*, vol. 286, no. 5, pp. 852–856, 2001.

[27] H.-S. Moon, C.-S. Chung, H.-G. Lee, T.-G. Kim, Y.-J. Choi, and C.-S. Cho, "Inhibitory effect of (-)-epigallocatechin-3-gallate on lipid accumulation of 3T3-L1 cells," *Obesity*, vol. 15, no. 11, pp. 2571–2582, 2007.

[28] J.-T. Hwang, I.-J. Park, J.-I. Shin et al., "Genistein, EGCG, and capsaicin inhibit adipocyte differentiation process via activating AMP-activated protein kinase," *Biochemical and Biophysical Research Communications*, vol. 338, no. 2, pp. 694–699, 2005.

[29] S. Rayalam, M. A. Della-Fera, and C. A. Baile, "Phytochemicals and regulation of the adipocyte life cycle," *Journal of Nutritional Biochemistry*, vol. 19, no. 11, pp. 717–726, 2008.

[30] Y. Zhou, D. Wang, Q. Zhu et al., "Inhibitory effects of A-769662, a novel activator of AMP-activated protein kinase, on 3T3-L1 adipogenesis," *Biological and Pharmaceutical Bulletin*, vol. 32, no. 6, pp. 993–998, 2009.

[31] S. Giri, R. Rattan, E. Haq et al., "AICAR inhibits adipocyte differentiation in 3T3L1 and restores metabolic alterations in diet-induced obesity mice model," *Nutrition and Metabolism*, vol. 3, article 31, 2006.

Hindawi Publishing Corporation
Evidence-Based Complementary and Alternative Medicine
Volume 2013, Article ID 310989, 7 pages
http://dx.doi.org/10.1155/2013/310989

Research Article

Paeonol, a Major Compound of Moutan Cortex, Attenuates Cisplatin-Induced Nephrotoxicity in Mice

Hyojung Lee, Gihyun Lee, Hyunseong Kim, and Hyunsu Bae

Department of Physiology, College of Korean Medicine, Kyung Hee University, 1 Hoeki-Dong, Dongdaemoon-gu, Seoul 130-701, Republic of Korea

Correspondence should be addressed to Hyunsu Bae; hbae@khu.ac.kr

Received 4 April 2013; Accepted 21 August 2013

Academic Editor: Seong-Gyu Ko

Cisplatin is an effective chemotherapeutic agent that is used for the treatment of a variety of cancers; however, its nephrotoxicity limits the use of this drug. In the present study, we examined whether paeonol, a major compound of Moutan Cortex, has protective effects on cisplatin-induced acute renal failure in mice. To accomplish this, Balb/c mice (6 to 8 wk of age, weighing 20 to 25 g) were administered, Moutan Cortex (300 mg/kg) or paeonol (20 mg/kg) once a day. At day 4, mice received cisplatin (30, 20, or 10 mg/kg) intraperitoneally. The paeonol-treated group showed marked attenuation of serum creatine and blood urea nitrogen levels as well as reduced levels of proinflammatory cytokines and nitric oxide when compared to the control group. In addition, the paeonol-treated group showed prolonged survival and marked attenuation of renal tissue injury. Taken together, these results demonstrated that paeonol can prevent the renal toxic effects of cisplatin.

1. Introduction

Cisplatin (cis-diamminedichloroplatinum (II)) is a platinum compound that has revolutionized the treatment of various solid organ tumors. Because of its high effects, cisplatin is used for the treatment of a variety of malignancies, including testicular, head and neck, ovarian, cervical, non-small-cell lung carcinoma and many other types of cancer [1, 2]. However, nephrotoxicity, the most common adverse effect of cisplatin, often requires dose reduction or withdrawal of cisplatin [3]. Therefore, various studies have been investigated to reduce cisplatin-induced nephrotoxicity.

Cisplatin-induced nephrotoxicity is related to direct tubular toxicity, inflammation, vascular factors, and oxidative stress [2]. Oxidative stress and inflammation have been suggested as the major mechanisms in the pathogenesis of cisplatin-induced nephrotoxicity [4].

Moutan Cortex, the root bark of *Paeonia suffruticosa Andrews*, is widely used in traditional medicine to treat various diseases including atherosclerosis, infection, and inflammation [5]. Previous studies have revealed that the extracts of Moutan Cortex can inhibit nitric oxide and tumor necrosis factor-alpha (TNF-α) in activated mouse peritoneal macrophages [5]. Further, our recent studies suggested that Moutan Cortex exerted recovery effects on cisplatin-induced nephrotoxicity *in vitro* [6]. In the present study, we searched whether extract of Moutan Cortex could ameliorate cisplatin-induced upregulation of serum creatinine and blood urea nitrogen (BUN) *in vivo*. After the confirmation that Moutan Cortex has the potential to attenuate the nephrotoxicity of cisplatin, we hypothesized that paeonol, a major phenolic component of Moutan Cortex, could attenuate cisplatin-induced renal damage. Recent studies have suggested that paeonol has various biological activities such as antiaggregatory, antioxidant, anxiolytic-like, and anti-inflammatory functions [7–9]. Moreover, it has been shown that natural antioxidants and anti-inflammatory agents such as curcumin, licorice extract, and *Zingiber officinale* can attenuate cisplatin-induced nephrotoxicity [10, 11]. In this study, we investigated whether paeonol attenuates cisplatin-induced renal damage by inhibiting inflammation and nitrosative stress.

2. Materials and Methods

2.1. Animals. Balb/c male mice (6 to 8 wk of age, weighing 20 to 25 g) were purchased from Orient Bio (Seongnam, Republic of Korea). All mice were kept under pathogen-free

conditions with air conditioning and a 12 h light/dark cycle and had free access to food and water during the experiments. The study was approved by the Animal Care and Use Committee of Kyung Hee University.

2.2. Materials. Moutan Cortex extract was purchased from Sun Ten (Sun Ten Pharmaceutical Co., Ltd., Taiwan) and dissolved in distilled water to give a final concentration of 10% (w/v). The herb suspension supernatant (HSS) was then obtained by centrifugation at 300 ×g for 10 min at 4°C. Next, the HSS was passed through a sterile 0.20 μm pore size filter unit (Sartorius AG, Germany). Paeonol was purchased from Wako (Wako Pure Chemical Industries, Ltd., Japan) and dissolved in phosphate buffered saline (PBS) at a concentration of 1 mg/ml. Cisplatin (*cis*-diammineplatinum II dichloride; Sigma-Aldrich, St. Louis, MO) was dissolved in 0.9% saline at a concentration of 1 mg/ml. Paeonol is one of many active main compounds contained in Moutan Cortex. Our previous study showed that 1 g of Moutan Cortex contained 0.46 ± 0.01 mg of paeonol. [5]

2.3. Experimental Protocol. Each group of mice was administered Moutan Cortex (300 mg/kg body wt) or paeonol (20 mg/kg body wt) orally for three days. The control groups were only administered PBS. At day 4, the mice were given a single i.p. injection of either cisplatin (30, 20, or 10 mg/kg body wt) or an equal volume of saline. Mice were sacrificed at 48 or 72 h after the cisplatin administration for further evaluation.

2.4. Assessment of Renal Function and Histologic Examination. Blood samples were obtained from mice 0, 24, 48, and 72 h after cisplatin injection. Renal and liver function was assessed based on the BUN, creatinine, alanine aminotransferase, and aspartate aminotransferase, which were measured using a Fuji DRI-CHEM 3500i (Fuji Photo Film, Ltd., Japan). Kidney tissue was fixed in 4% paraformaldehyde and then embedded in paraffin, after which it was cut into 5 μm sections and stained with hematoxylin and eosin. Three pathologists who were blinded to the experiments scored the degree of tubular injury. Renal tubular injury was assessed using a semiquantitative score in which the percentage of cortical tubules showing epithelial necrosis was assigned a score of either 0, none; 1, <10%; 2, 10–25%; 3, 25–75%; or 4, >75% [12].

2.5. Kidney Proinflammatory Cytokines. To examine the proinflammatory cytokines after cisplatin administration, the levels of TNF-α and IL-1β were measured in the kidneys by enzyme linked immunosorbent assay (ELISA; BD Biosciences, USA). Briefly, snap-frozen kidney tissue was homogenized in a PRO-PREP protein extraction solution (iNtRON Biotechnology, Inc., Korea), after which it was incubated for 20 minutes in ice and then centrifuged at 13,000 rpm (4°C) for 15 minutes. The supernatant was then used for kidney proinflammatory cytokine detection, which was accomplished using a BCATH Protein Assay Kit (Thermo Scientific, USA). The protein levels of cytokines were corrected for the total amount of protein, and the results were expressed as pg/mg.

2.6. Nitrite Estimation. Tissue nitrite was estimated using Greiss reagent and served as an indicator of NO production. Briefly, 500 μL of Greiss reagent (1 : 1 solution of 1% sulfanilamide in 5% phosphoric acid and 0.1% naphthylamine diamine dihydrochloric acid in water) was added to 100 μL of kidney homogenates. The nitrite concentration was calculated using a standard curve for sodium nitrite. Nitrite levels were expressed as μM/mg.

2.7. Statistical Analysis. Statistical analysis of the data was conducted using Prism 4.02 software (GraphicPad Software Inc., USA). All data are presented as the means ± S.E.M. The significance of differences between the experimental groups and the control was assessed by a Student's *t*-test. Kaplan-Meier analysis was used for the mouse survival analyses. For multiple comparison, two-way ANOVA was conducted. A P value < 0.05 was taken to indicate significance.

3. Results

To ascertain whether paeonol could attenuate cisplatin-induced renal damage, we analyzed survival rate, serum creatinine, BUN, histologic change, proinflammatory cytokines, and nitrite production in cisplatin-injected mice.

3.1. Effects of Moutan Cortex on Cisplatin-Induced Renal Dysfunction. Both levels of the serum creatinine and BUN in cisplatin group were significantly increased at 48 h after cisplatin administration when compared with the saline group. The serum creatinine level in Moutan Cortex pretreatment group was significantly decreased at 48 h after cisplatin administration when compared with the cisplatin group (Figure 1(a)). In addition, BUN level was slightly reduced in Moutan Cortex pretreatment group at 48 h after cisplatin injection when compared with the cisplatin group (Figure 1(b)).

3.2. Effects of Paeonol on Kidney and Liver Dysfunction. Each group of mice was administered paeonol (20 mg/kg body wt) or saline via a single intraperitoneal injection for three days. At day 4, blood samples were obtained from mice to check the toxicity of paeonol. The dose of 20 mg/kg paeonol caused no harmful effects on kidney and liver dysfunction (Figure 2).

3.3. Effects of Paeonol on Survival after Cisplatin Administration. Both the paeonol-pretreated group and cisplatin group received three different doses of cisplatin (30, 20, or 10 mg/kg body wt) and were followed up for 78 h. At 78 h after injection of 30 mg/kg cisplatin, all of the cisplatin group mice had expired. However, the paeonol-pretreated mice had 28% survival. Moreover, at 72 h after 20 mg/kg of cisplatin administration, all of the paeonol-pretreated mice survived, but 42% of cisplatin group mice had expired. Taken together,

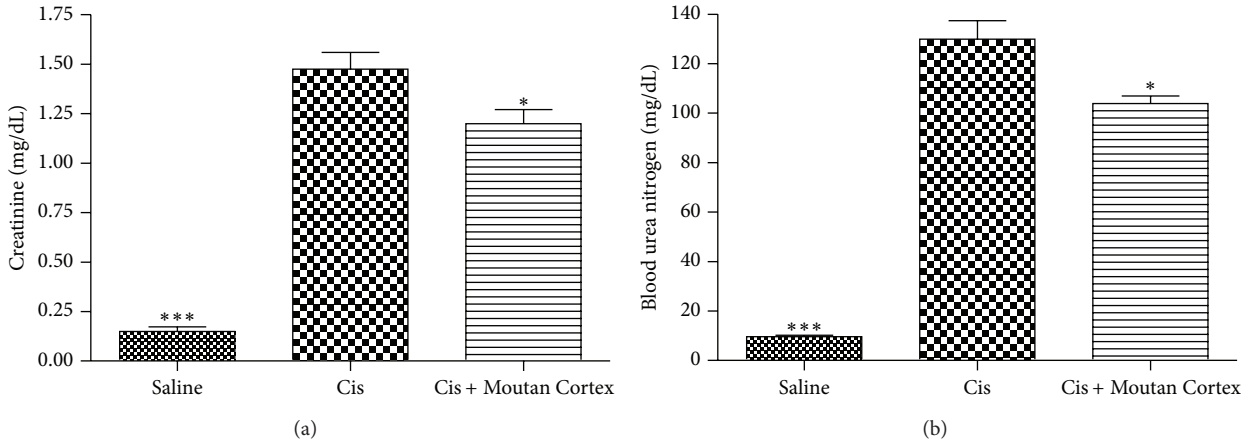

FIGURE 1: Effects of Moutan Cortex on creatinine and BUN production. All mice received a single dose of cisplatin intraperitoneally (30 mg/kg body wt). Serum creatinine (a) and BUN (b) were measured at 48 h after cisplatin injection. Saline: saline alone; Cis: cisplatin alone; Cis + Moutan Cortex: Moutan Cortex pretreatment and cisplatin treatment. Values shown are the mean ± S.E.M. Data were analyzed by a Student's t-test ($^{*}P < 0.05$, $^{***}P < 0.001$ versus Cis; $n = 4$).

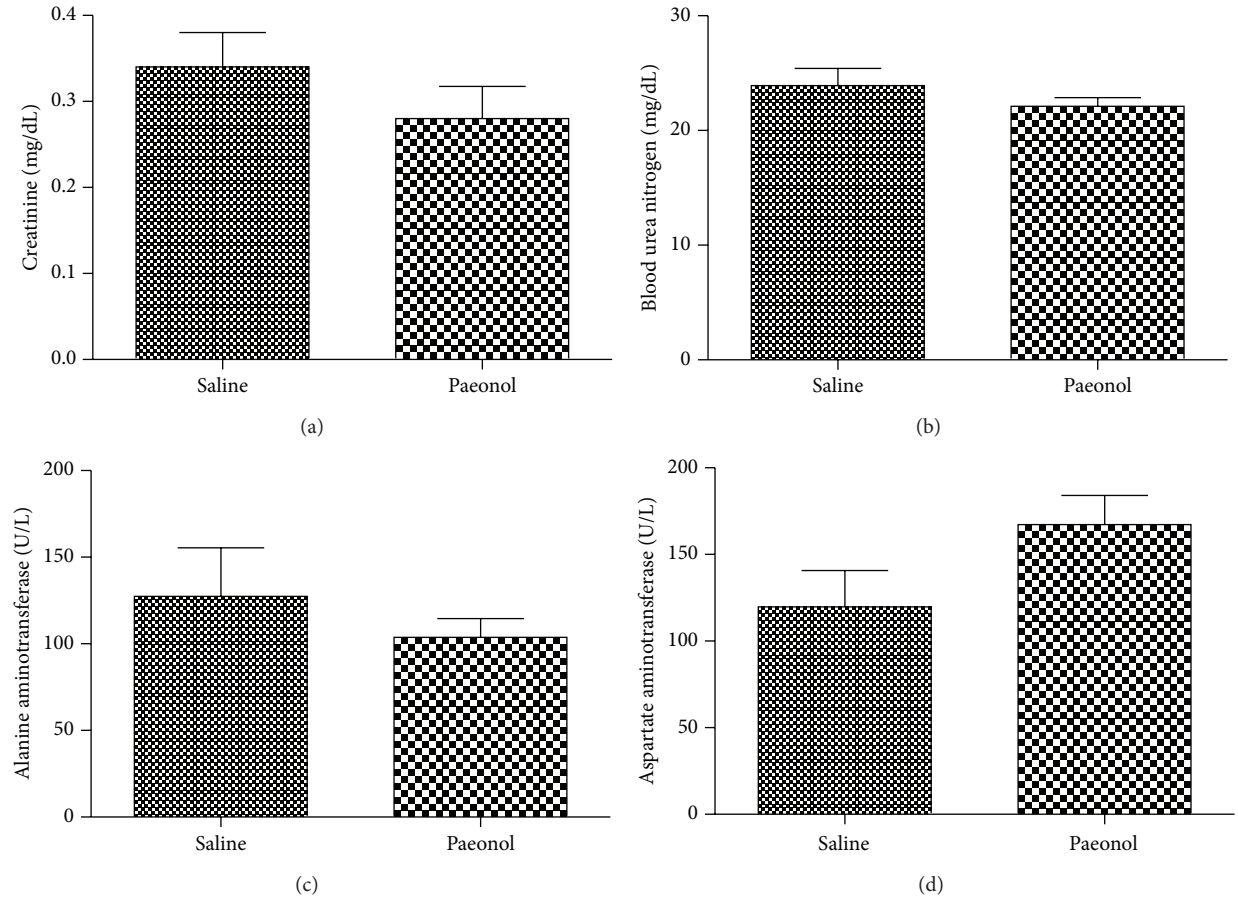

FIGURE 2: Effects of paeonol on kidney and liver dysfunction. Each group of mice was administered paeonol (20 mg/kg body wt) or saline via a single intraperitoneal injection for three days. At day 4, blood samples were obtained from mice to check the toxicity of paeonol. Serum creatinine (a), BUN (b), alanine aminotransferase (c), and aspartate aminotransferase (d) were measured. Values shown are the mean ± S.E.M. Data were analyzed by a Student's t-test ($n = 5$).

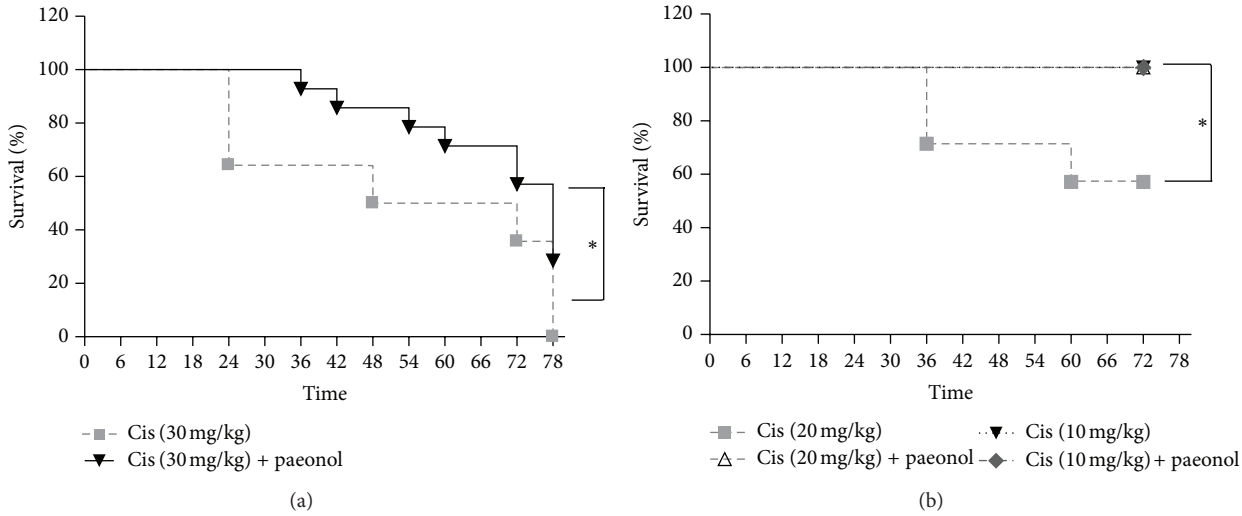

Figure 3: Survival in cisplatin-treated mice and paeonol-pretreated mice. (a) All mice received a single dose of cisplatin intraperitoneally (30 mg/kg body wt) and were followed up to 78 h. Compared with a 60 median survival time in cisplatin-treated group, paeonol-pretreated group had a 78 median survival time. Data were analyzed by a Kaplan-Meier test ($^*P < 0.05$ versus Cis; $n = 14$). (b) Mice received cisplatin intraperitoneally (20 or 10 mg/kg body wt) and were followed up to 72 h. Data were analyzed by a Kaplan-Meier test ($^*P < 0.05$ versus Cis; $n = 7$).

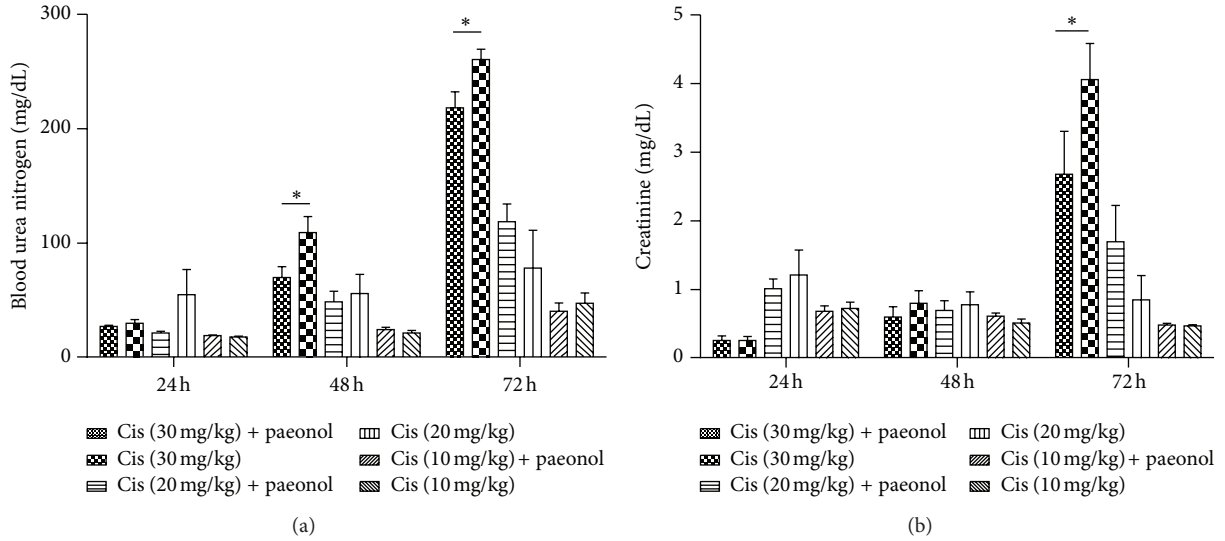

Figure 4: Effects of paeonol on cisplatin-induced renal dysfunction. Serum creatinine (a) and BUN (b) were measured at 24, 48, and 72 h after cisplatin injection (30, 20, or 10 mg/kg body wt). Data were analyzed by a two-way ANOVA test ($^*P < 0.05$ versus Cis (30 mg/kg); $n = 7$).

these results show that pretreatment with paeonol improved survival after cisplatin administration in mice (Figure 3).

3.4. Effects of Paeonol on Cisplatin-Induced Renal Dysfunction. The serum creatinine levels were significantly higher in the cisplatin group at 72 h after administration of 30 mg/kg of cisplatin when compared with the paeonol pretreatment group (Figure 4(a)). BUN level was also remarkably reduced in the paeonol pretreatment group at 48 h and 72 h after 30 mg/kg of cisplatin injection when compared with the group that only received cisplatin (Figure 4(b)). In 20 mg/kg of cisplatin-administered mice, creatinine and BUN levels were slightly decreased at 72 h by paeonol pretreatment. Besides, creatinine and BUN levels were not increased by 10 mg/kg of cisplatin treatment as previously reported [13, 14].

3.5. Effects of Paeonol on Cisplatin-Induced Renal Injury. The degree of renal tubular injury in the control- and paeonol-treated groups was observed at 72 h after cisplatin administration. Paeonol-treated groups showed slightly less renal injury than mice that received saline (Figure 5).

3.6. Effects of Paeonol on Cisplatin-Induced Proinflammatory Cytokines. To investigate the proinflammatory molecules

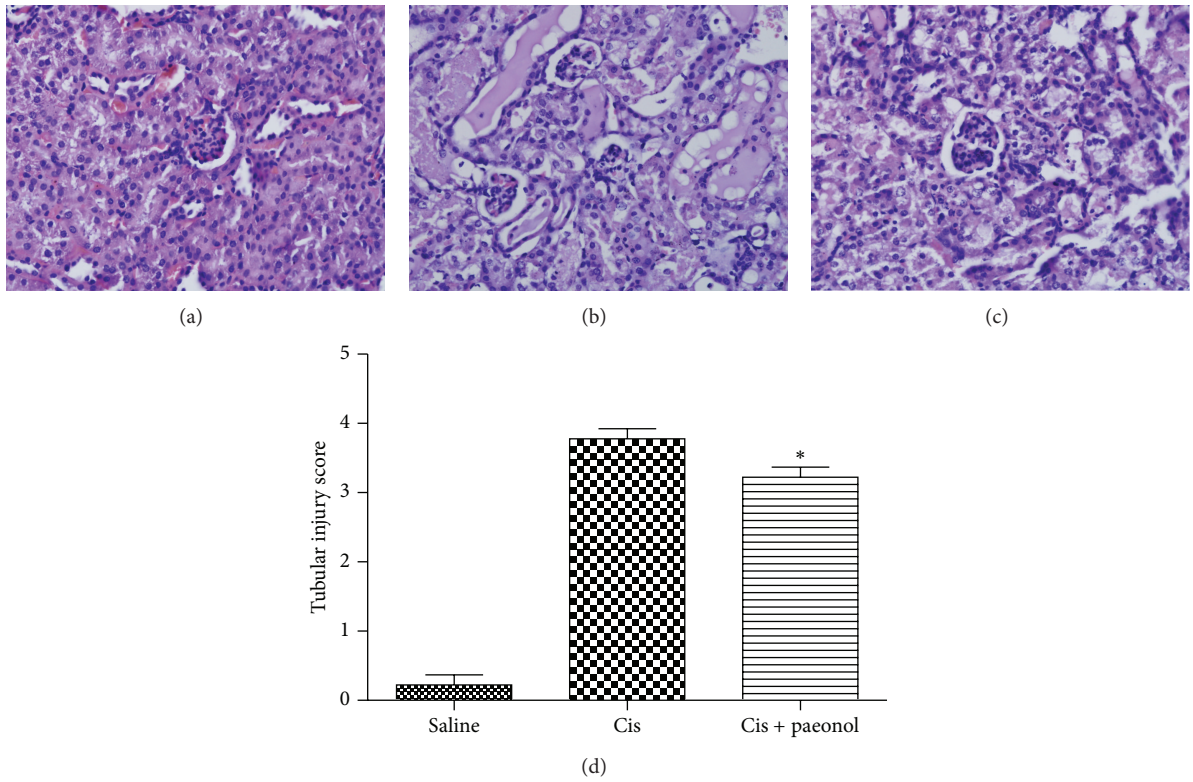

Figure 5: Effects of paeonol on renal histology in mice. Sections of kidney were stained with H&E 72 h after cisplatin injection. Saline treatment alone (a); cisplatin treatment alone (b); paeonol and cisplatin treatment (c). Renal tubular injury was assessed using a semiquantitative score in which the percentage of cortical tubules showing epithelial necrosis was assigned a score of either 0, none; 1, <10%; 2, 10–25%; 3, 25–75%; or 4, >75% (d). Saline: saline alone; Cis: cisplatin alone; Cis + paeonol: paeonol pretreatment and cisplatin treatment ($^{*}P < 0.05$ versus Cis, $n = 3$).

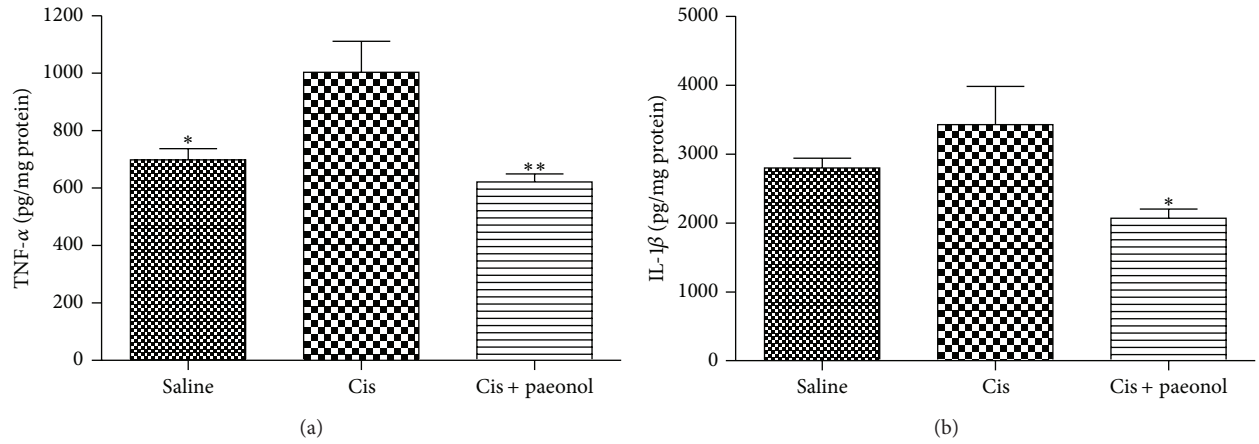

Figure 6: Effects of paeonol on cisplatin-induced proinflammatory cytokines. Kidneys were obtained at 72 h after cisplatin injection, and cytokine levels of TNF-α (a) and IL-1β (b) were determined by ELISA. Saline: saline alone; Cis: cisplatin alone; Cis + paeonol: paeonol pretreatment and cisplatin treatment. Values shown are the mean ± S.E.M. Data were analyzed by a Student's t-test ($^{*}P < 0.05$, $^{**}P < 0.01$ versus cis; $n = 4$ for saline; $n = 5$ for Cis or Cis + paeonol).

generated by cisplatin renal injury, the cytokine levels of TNF-α and IL-1β were measured at 72 h after cisplatin administration. Cisplatin-treated mice had significantly increased levels of TNF-α at 72 h after cisplatin injection, while paeonol pretreatment reduced expression of TNF-α in the kidney. IL-1β was increased by cisplatin treatment, but its increasing was not significant. However, paeonol significantly reduced IL-1β production by cisplatin treatment (Figure 6).

3.7. Effects of Paeonol on Cisplatin-Induced Nitric Oxide Production. Nitrite levels of kidney tissue homogenates were

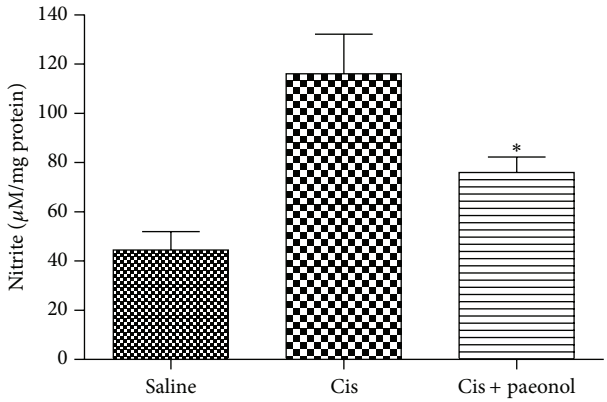

Figure 7: Effects of paeonol on cisplatin-induced nitric oxide production. Nitrate levels in kidney tissue were measured in control, cisplatin, and paeonol groups after a single dose of cisplatin (30 mg/kg body wt). Saline: saline alone; Cis: cisplatin alone; Cis + paeonol: paeonol pretreatment and cisplatin treatment. Values shown are the mean ± S.E.M. Data were analyzed by a Student's t-test ($^*P < 0.05$ versus cis; $n = 4$ for saline; $n = 5$ for Cis or Cis + paeonol).

measured at 72 h after cisplatin injection. Nitrite levels of kidney tissue were significantly elevated by cisplatin administration. The nitrite production in kidney tissue was slightly attenuated in paeonol-pretreated group compared with control group (Figure 7).

4. Discussion

Nephrotoxicity is a major side effect that limits the use of cisplatin in many cancer patients. Indeed, many studies have documented that apoptosis/necrosis, reactive oxygen species, and inflammation play a major role in the pathogenesis of cisplatin-induced acute renal failure [15, 16]. Therefore, various studies have been conducted to reduce the cisplatin-induced nephrotoxicity. Recent studies have suggested that natural antioxidants and anti-inflammatory agents such as curcumin, licorice extract, and *Zingiber officinale* can attenuate cisplatin-induced nephrotoxicity [10, 11]. Additionally, proinflammatory cytokines such as TNF-α, IL-6, and IL-1β have been shown to be associated with cisplatin-induced acute renal failure [17–19].

Moutan Cortex, the root bark of *Paeonia suffruticosa Andrews*, has been used extensively as a traditional medicine for treatment of various diseases such as atherosclerosis, infection, and inflammation. Previous studies have revealed that the extracts of Moutan Cortex can inhibit nitric oxide and TNF-α in activated mouse peritoneal macrophages [5].

A variety of compounds including paeonoside, paeonolide, apiopaeonoside, paeoniflorin, oxypaeoniflorin, benzoyloxypaeoniflorin, benzoylpaeoniflorin, paeonol, and sugars have been identified in Moutan Cortex [20]. Paeonol, a major phenolic component of Moutan Cortex, has various biological activities such as antiaggregatory, antioxidant, anxiolytic-like, and anti-inflammatory functions [8]. In this study, paeonol treatment significantly reduced the elevated levels of serum creatinine and BUN.

In addition, the role of proinflammatory cytokines in cisplatin-induced acute renal failure has been well documented [17, 18], and elevation of the proinflammatory cytokines TNF-α and IL-1β as well as that of IL-6 has been demonstrated in humans with acute renal failure [21]. Given that recent research has demonstrated that TNF-α plays a significant role in cisplatin-induced nephrotoxicity, we measured several proinflammatory cytokine levels in kidney tissue. We found that cisplatin administration increased the kidney tissue TNF-α level, whereas paeonol pretreatment led to a significant decrease in the TNF-α level. The increase in IL-1β level was also attenuated in paeonol-pretreated mice. Taken together, these results indicate that paeonol may reduce the production of TNF-α and IL-1β cytokines that is due to the direct anti-inflammatory effects of paeonol.

Nitric oxide (NO) is recognized as a mediator and regulator of inflammatory responses. NO is involved in host defense with cytotoxic properties against pathogenic microbes, but high levels of NO production in response to inflammatory stimuli can cause proinflammatory and destructive effects on host tissue [22]. Cisplatin treatment also causes significant increases in the activity of calcium-independent nitric oxide synthase (NOS) in rat kidney and liver, which leads to an increase in serum NO levels as well as tissue NO formation [23, 24]. Jung et al. reported that the upregulation of oxide mNOS and peroxynitrite formation in cisplatin treatment are key events that influence the development of harmful parameters that occur during cisplatin-associated kidney failure [25]. It is well known that selective iNOS inhibition reduces cisplatin-induced nephrotoxicity and nitrosative stress [26]. In the present study, paeonol treatment prevented the increases in kidney tissue nitric oxide when compared with cisplatin-treated mice. Recently, paeonol treatment was found to inhibit iNOS protein expression induced by TNF-α and iNOS mRNA expression *in vitro* [8, 27]. Therefore, our results indicate that paeonol has the potential to reduce nitrosative stress in cisplatin-induced nephrotoxicity.

In conclusion, our study provides evidence that Moutan Cortex has a potential to attenuate nephrotoxicity of cisplatin and its major constituent paeonol can be a therapeutic intervention for cisplatin-induced renal injury. However, what molecular mechanisms are related to the protective effects of paeonol on kidney and the influences of Moutan Cortex and paeonol on the therapeutic efficacy of cisplatin should be further studied.

Conflict of Interests

The authors have declared that there is no conflict of interests.

Acknowledgment

This work was supported by the National Research Foundation of Korea (NRF) grant funded by the Korean government

(Ministry of Education, Science and Technology, MEST) (No. 2011-0006220).

References

[1] D. Wang and S. J. Lippard, "Cellular processing of platinum anticancer drugs," *Nature Reviews Drug Discovery*, vol. 4, no. 4, pp. 307–320, 2005.

[2] N. Pabla and Z. Dong, "Cisplatin nephrotoxicity: mechanisms and renoprotective strategies," *Kidney International*, vol. 73, no. 9, pp. 994–1007, 2008.

[3] F. Ries and J. Klastersky, "Nephrotoxicity induced by cancer chemotherapy with special emphasis on cisplatin toxicity," *American Journal of Kidney Diseases*, vol. 8, no. 5, pp. 368–379, 1986.

[4] C. A. Davis, H. S. Nick, and A. Agarwal, "Manganese superoxide dismutase attenuates cisplatin-induced renal injury: importance of superoxide," *Journal of the American Society of Nephrology*, vol. 12, no. 12, pp. 2683–2690, 2001.

[5] H. S. Chung, M. Kang, C. Cho et al., "Inhibition of nitric oxide and tumor necrosis factor-alpha by moutan cortex in activated mouse peritoneal macrophages," *Biological and Pharmaceutical Bulletin*, vol. 30, no. 5, pp. 912–916, 2007.

[6] S. H. Sohn, H. Lee, J. Y. Nam et al., "Screening of herbal medicines for the recovery of cisplatin-induced nephrotoxicity," *Environmental Toxicology and Pharmacology*, vol. 28, no. 2, pp. 206–212, 2009.

[7] T. C. Chou, "Anti-inflammatory and analgesic effects of paeonol in carrageenan-evoked thermal hyperalgesia," *British Journal of Pharmacology*, vol. 139, no. 6, pp. 1146–1152, 2003.

[8] K. Ishiguro, T. Ando, O. Maeda et al., "Paeonol attenuates TNBS-induced colitis by inhibiting NF-κB and STAT1 transactivation," *Toxicology and Applied Pharmacology*, vol. 217, no. 1, pp. 35–42, 2006.

[9] J. M. Xiao, W. C. Si, J. W. Wen et al., "Anxiolytic-like effect of paeonol in mice," *Pharmacology Biochemistry and Behavior*, vol. 81, no. 3, pp. 683–687, 2005.

[10] T. A. Ajith, V. Nivitha, and S. Usha, "Zingiber officinale Roscoe alone and in combination with α-tocopherol protect the kidney against cisplatin-induced acute renal failure," *Food and Chemical Toxicology*, vol. 45, no. 6, pp. 921–927, 2007.

[11] A. Kuhad, S. Pilkhwal, S. Sharma, N. Tirkey, and K. Chopra, "Effect of curcumin on inflammation and oxidative stress in cisplatin-induced experimental nephrotoxicity," *Journal of Agricultural and Food Chemistry*, vol. 55, no. 25, pp. 10150–10155, 2007.

[12] H. Lee, D. Nho, H. S. Chung et al., "$CD4^+$ $CD25^+$ regulatory T cells attenuate cisplatin-induced nephrotoxicity in mice," *Kidney International*, vol. 78, no. 11, pp. 1100–1109, 2010.

[13] D. Z. Hsu, K. T. Chen, T. H. Lin, Y. H. Li, and M. Y. Liu, "Sesame oil attenuates cisplatin-induced hepatic and renal injuries by inhibiting nitric oxide-associated lipid peroxidation in mice," *Shock*, vol. 27, no. 2, pp. 199–204, 2007.

[14] E. A. Leite, C. D. S. Giuberti, A. J. A. Wainstein et al., "Acute toxicity of long-circulating and pH-sensitive liposomes containing cisplatin in mice after intraperitoneal administration," *Life Sciences*, vol. 84, no. 19-20, pp. 641–649, 2009.

[15] A. H. Lau, "Apoptosis induced by cisplatin nephrotoxic injury," *Kidney International*, vol. 56, no. 4, pp. 1295–1298, 1999.

[16] H. Matsushima, K. Yonemura, K. Ohishi, and A. Hishida, "The role of oxygen free radicals in cisplatin-induced acute renal failure in rats," *Journal of Laboratory and Clinical Medicine*, vol. 131, no. 6, pp. 518–526, 1998.

[17] S. Faubel, E. C. Lewis, L. Reznikov et al., "Cisplatin-induced acute renal failure is associated with an increase in the cytokines interleukin (IL)-1β, IL-18, IL-6, and neutrophil infiltration in the kidney," *Journal of Pharmacology and Experimental Therapeutics*, vol. 322, no. 1, pp. 8–15, 2007.

[18] G. Ramesh and W. B. Reeves, "TNF-α mediates chemokine and cytokine expression and renal injury in cisplatin nephrotoxicity," *Journal of Clinical Investigation*, vol. 110, no. 6, pp. 835–842, 2002.

[19] G. Ramesh and W. B. Reeves, "Inflammatory cytokines in acute renal failure," *Kidney International*, vol. 66, no. 91, supplement, pp. S56–S61, 2004.

[20] G. Chen, L. Zhang, and Y. Zhu, "Determination of glycosides and sugars in moutan cortex by capillary electrophoresis with electrochemical detection," *Journal of Pharmaceutical and Biomedical Analysis*, vol. 41, no. 1, pp. 129–134, 2006.

[21] E. M. Simmons, J. Himmelfarb, M. T. Sezer et al., "Plasma cytokine levels predict mortality in patients with acute renal failure," *Kidney International*, vol. 65, no. 4, pp. 1357–1365, 2004.

[22] R. Korhonen, A. Lahti, H. Kankaanranta, and E. Moilanen, "Nitric oxide production and signaling in inflammation," *Current Drug Targets*, vol. 4, no. 4, pp. 471–479, 2005.

[23] A. Kuhad, N. Tirkey, S. Pilkhwal, and K. Chopra, "6-gingerol prevents cisplatin-induced acute renal failure in rats," *Biofactors*, vol. 26, no. 3, pp. 189–200, 2006.

[24] R. C. Srivastava, A. Farookh, N. Ahmad, M. Misra, S. K. Hasan, and M. M. Husain, "Evidence for the involvement of nitric oxide in cisplatin-induced toxicity in rats," *Biometals*, vol. 9, no. 2, pp. 139–142, 1996.

[25] M. Jung, G. Hotter, J. L. Viñas, and A. Sola, "Cisplatin upregulates mitochondrial nitric oxide synthase and peroxynitrite formation to promote renal injury," *Toxicology and Applied Pharmacology*, vol. 234, no. 2, pp. 236–246, 2009.

[26] Y. I. Chirino, J. Trujillo, D. J. Sánchez-González et al., "Selective iNOS inhibition reduces renal damage induced by cisplatin," *Toxicology Letters*, vol. 176, no. 1, pp. 48–57, 2008.

[27] H. S. Chae, O. H. Kang, Y. S. Lee et al., "Inhibition of LPS-induced iNOS, COX-2 and inflammatory mediator expression by paeonol through the MAPKs inactivation in RAW 264.7 cells," *American Journal of Chinese Medicine*, vol. 37, no. 1, pp. 181–194, 2009.

Hindawi Publishing Corporation
Evidence-Based Complementary and Alternative Medicine
Volume 2013, Article ID 671281, 9 pages
http://dx.doi.org/10.1155/2013/671281

Research Article

Ixeris dentata NAKAI Reduces Clinical Score and HIF-1 Expression in Experimental Colitis in Mice

Dae-Seung Kim,[1] Jang-Ho Ko,[1] Yong-Deok Jeon,[1] Yo-Han Han,[1] Hyun-Ju Kim,[2] Amrit Poudel,[1] Hyun-Ju Jung,[1] Sae-Kwang Ku,[3] Su-Jin Kim,[4] Sang-Hyun Park,[5] Jin-Han Park,[6] Byung-Min Choi,[7] Sung-Joo Park,[8] Jae-Young Um,[2] and Seung-Heon Hong[1]

[1] *Department of Oriental Pharmacy, College of Pharmacy, Wonkwang-Oriental Medicines Research Institute, Wonkwang University, Iksan, Jeonbuk 570-749, Republic of Korea*
[2] *Department of Pharmacology, College of Korean Medicine, Institute of Korean Medicine, Kyung Hee University, Dongdaemun-gu, Seoul 130-701, Republic of Korea*
[3] *Department of Anatomy and Histology, College of Oriental Medicine, Daegu Hanny University, Yugok-Dong, Kyungsan 712-715, Republic of Korea*
[4] *Department of Cosmeceutical Science, Daegu Hanny University, Yugok-Dong, Kyungsan 712-715, Republic of Korea*
[5] *Isotope Sciences Lab, Korea Atomic Energy Research Institute, 1266 Shinjeong-dong, Jeongeup, Jeonbuk 580-185, Republic of Korea*
[6] *Department of Medicinal Herb, Gyeongju University, Gyeongbuk 780-712, Republic of Korea*
[7] *Department of Biochemistry, School of Medicine, Wonkwang University, Iksan, Chonbuk 570-749, Republic of Korea*
[8] *Department of Herbology, College of Oriental Medicine, Wonkwang University, Iksan 570-749, Republic of Korea*

Correspondence should be addressed to Jae-Young Um; jyum@khu.ac.kr and Seung-Heon Hong; jooklim@wku.ac.kr

Received 2 April 2013; Accepted 7 August 2013

Academic Editor: Seong-Gyu Ko

Ixeris dentata (ID) is an herbal medicine used in Asian countries to treat indigestion, pneumonia, hepatitis, contusions, and tumors; however, its effect on intestinal inflammation is unknown. Thus, we investigated the effect of ID in the dextran sulfate sodium (DSS) model of colitis in female BALB/c mice; animals were evaluated after seven days of DSS treatment. DSS-treated mice showed considerable clinical signs, including weight loss, reduced colon length, colonic epithelial injury, infiltration of inflammatory cells in the colon tissue, and upregulation of inflammatory mediators. However, administration of ID attenuated body weight loss, colon shortening, and the increase in disease activity index score. ID also significantly decreased the colonic mucosal injury and the number of infiltrating mast cells. Moreover, ID inhibited the expressions of cyclooxygenase-2 and hypoxia-inducible factor-1α in colon tissue. Taken together, the results provide experimental evidence that ID might be a useful therapy for patients with ulcerative colitis.

1. Introduction

Ulcerative colitis (UC) is a chronic inflammatory disorder of the colon and rectum with intervals of acute exacerbation. Its etiology remains unknown, although results from recent studies suggest that proinflammatory cytokines initiate the inflammatory response [1]. Patients with UC have been reported to have increased levels of interleukin- (IL-) 6 in the intestinal mucosa [2, 3] and of tumor-necrosis-factor- (TNF-) α in blood, colonic tissue, and stool [4]. Two cyclooxygenase (COX) isoenzymes have been recognized: COX-1, a constitutive enzyme, which generates prostaglandins (PGs) that protect the stomach and kidney against damage, and COX-2, an inducible enzyme induced by inflammatory stimuli, such as cytokines, and capable of generating PGs that contribute to the pain and swelling of inflammation [5, 6]. The expression of COX-2 is also elevated in the inflamed mucosa of patients with UC [7]. Moreover, metabolism is altered in inflamed mucosal tissues, secondary to decreased mucosal perfusion caused by infiltration of inflammatory cells. The resultant

hypoxia [8, 9] activates hypoxia-inducible-factor- (HIF-) 1, a transcription factor that links inflammatory pathways [10, 11].

Although corticosteroids are effective in bringing about clinical remission, severe adverse effects can sometimes lead to their discontinuation; thus, alternative treatments are needed. *Ixeris dentata* NAKAI (ID) is a traditional herbal medicine used in Korea to treat indigestion, pneumonia, hepatitis, and tumors [12]. It has also been reported to protect against kainic-acid-induced oxidative stress in the mouse brain by regulating glutathione concentration [13] and to inhibit the anaphylactic response induced by compound 48/80 or IgE [14]. Moreover, lactic acid fermentation of ID increased its potency against IgE-induced allergic diseases [15]. However, it is unknown whether ID can reduce intestinal inflammation.

The dextran sulfate sodium (DSS) model of UC has been well characterized morphologically and biochemically. DSS induces an acute colitis characterized by bloody stools, ulcerations, and infiltration of inflammatory cells [16]. Histologically, DSS produces submucosal erosions, crypt abscesses, and epithelioglandular hyperplasia. It is generally believed that DSS is directly toxic to gut epithelial cells of the basal crypts and affects the integrity of the mucosal barrier [17]. Hence, the DSS-induced colitis model is particularly useful for studying the contribution of inflammatory mechanisms in colitis. To provide experimental evidence that ID might be a useful therapy for patients with UC, we examined the effects of ID on DSS-induced colitis. The specific aims were to assess the effect of ID on clinical signs of colitis, including weight loss, colon shortening, diarrhea, and occult/gross bleeding, and to investigate the effect of ID on proinflammatory mediators in the colon of DSS-treated mice.

2. Materials and Methods

2.1. Animals and Reagents. Female BALB/c mice (6 weeks old) were obtained from Da-Mool Science (Taejeon, Republic of Korea). Mice were acclimatized in a specific pathogen-free environment under controlled conditions (22 ± 2°C under a 12 h light/dark cycle) for at least one week. All animal studies were carried out in accordance with the regulations issued by the Institutional Review Board of Wonkwang University (confirmation number: WKU11-10). DSS (mol wt: 36,000–50,000) was purchased from MP Biomedicals (Solon, OH, USA). Purified anti-mouse IL-6, recombinant mouse IL-6, and biotinylated anti-mouse IL-6 antibodies were obtained from BD-Pharmingen (San Diego, CA). Specific antibodies against COX-2, HIF-1α, and glyceraldehyde 3-phosphate dehydrogenase (GAPDH) were obtained from Santa Cruz Biotechnology (Santa Cruz, CA). All other chemical reagents were purchased from Sigma (St. Louis, MO).

2.2. Preparation of ID. ID extract was prepared by decocting with distilled water for three hours (100 g/L). The residue was filtered, lyophilized, and maintained at room temperature. The yield of dried extract from the starting materials was about 7.8%. Dried extract was diluted in saline and filtered through 0.22 μm syringe filter.

Table 1: Criteria for disease activity index.

Score	Weight loss (%)	Stool consistency	Bloodstain or gross bleeding
0	None	Normal	Negative
1	1–5	Loose stool	Negative
2	5–10	Loose stool	Positive
3	10–15	Diarrhea	Positive
4	>15	Diarrhea	Gross bleeding

2.3. Induction of Colitis by DSS. Acute colitis was induced by administering drinking water containing 5% (w/v) DSS to mice for seven days. Mice were checked daily for the body weight, stool consistency, and the presence of gross bleeding. Animals were randomized to four groups: control (no DSS), DSS, DSS plus ID (100 mg/kg), and DSS plus sulfasalazine (SFZ; 100 mg/kg) as a reference drug. ID and SFZ were diluted with purified water and orally administered once a day during the seven days of DSS treatment, after which time animals were killed.

2.4. Disease Activity Index (DAI). Intestinal disease activity was assessed based on the weight loss, the presence of diarrhea accompanied by blood and mucus, and colonic shortening [18]. DAIs were calculated by scoring weight loss, diarrhea, and rectal bleeding, based on the scoring system (Table 1) described by Murthy et al. [19]. Weight loss was defined as the difference between initial and final weights and diarrhea as the absence of fecal pellet formation and the presence of continuous fluid fecal material in the colon. Rectal bleeding was assessed based on the presence of diarrhea containing visible blood and on the presence of gross rectal bleeding. DAI values were calculated using the following formula: DAI = {(weight loss score) + (diarrhea score) + (rectal bleeding score)}/4. The DAI was determined by three investigators blinded to the protocol. The clinical parameters used in the present study were chosen to represent the subjective clinical symptoms observed in human UC.

2.5. Cytokine Assays. Levels of IL-6 and TNF-α in the serum and tissue were measured using an enzyme-linked immunosorbent assay (ELISA), as previously described [20]. Briefly, 96-well plates were coated with 100 μL of anti-mouse monoclonal antibodies (1.0 mg/mL at pH 7.4 in phosphate-buffered saline [PBS]) and incubated overnight at 4°C. After additional washes, 50 μL of sample or IL-6 and TNF-α standard was added and incubated at room temperature for two hours. Plates were then washed, and 0.2 μg/mL of biotinylated anti-mouse antibody was added and incubated at room temperature for two hours. After washing the plates, avidin-peroxidase was added, and plates were incubated for 30 min at 37°C. The plates were then washed again and ABTS substrate was added. Color development was measured at 405 nm using an automated microplate ELISA reader. Standard curves were prepared using serial dilutions of recombinant antibodies. Protein concentrations

Table 2: Criteria for assessment of microscopic rectal damage.

Score	Remarks
0	Normal colonic mucosa
1	Loss of one-third of the crypts
2	Loss of two-third of the crypts
3	Lamina propria covered with a single layer of epithelial cells with mild inflammatory cell infiltration
4	Erosions and marked inflammatory cell infiltration

were measured using bicinchoninic acid (BCA) protein assay reagent (Sigma).

2.6. Western Blot Analysis. Distal colons were homogenized in lysis buffer (iNtRON Biotech, Republic of Korea) and centrifuged at 13,000 rpm for five min. The supernatants were transferred to fresh tubes, and protein concentrations were determined using BCA protein assay reagent (Sigma). Lysates (50 μg of protein) were separated by 10% SDS-PAGE and transferred to membranes (Amersham Pharmacia Biotech, Piscataway, NJ), which were blocked with 5% skim milk in PBS-Tween-20 (PBST) for 1 h at room temperature. Membranes were incubated overnight with primary antibodies against COX-2 and HIF-1α and washed 3 times with PBST. Blots were incubated with secondary antibodies for one hour at room temperature; antibody-specific proteins were visualized using an enhanced chemiluminescence detection system (Amersham Corp. Newark, NJ, USA). Protein densities were quantified by densitometry.

2.7. Histological Processing. All trimmed rectums were fixed in 10% neutral buffered formalin. After paraffin embedding, 4 μm sections were prepared. Representative sections were stained with hematoxylin and eosin (H&E) for examination under light microscopy or with toluidine blue to detect mast cells.

2.8. Microscopic Scoring. The histological damage on the prepared, cross trimmed H&E stained samples were evaluated by two pathologist observers who were blinded to the experimental groups according to the modified criteria (Table 2) from Hamamoto et al. [21]. Briefly, the mucosa damages were scored 0–4 based on the loss of crypt (mucosa) and infiltration of inflammatory cells (max. score = 4).

2.9. Histomorphometry. Thickness of the rectal mucosa (μm/cross trimmed rectum) and numbers of infiltrating inflammatory cells (cells/mm^2 of mucosa) or mast cells (cells/mm^2 of mucosa, in toluidine blue stain) in the mucosa were calculated for individual histology samples using a digital image analyzer (DMI-300, DMI, Republic of Korea).

2.10. HPLC Analysis. The chromatographic system consisted of a pump (Gilson, 321 pump) and a UV detector (Gilson, 151 detector). For enhanced separation, a C_8 (4.6 × 250 mm) column (Watchers, Japan) was used. Acetonitrile : water : acetic acid (15 : 85 : 1.5) was used as the mobile phase in an isocratic manner. Peaks were detected at 254 nm. The injection volume was 10 μL, and flow rate was maintained at 1.0 mL/min. The sample and standard (3,4-dihydroxy cinnamic acid) were dissolved in 50% methanol/water. The sample was prepared with 10 mg/mL of ID. The stock solution at the concentration of 2 mg/mL of 3,4-dihydroxy cinnamic acid was prepared. The solutions were filtered through a 0.2 μm membrane filter.

2.11. Statistical Analysis. The results are presented as mean ± S.E.M of at least three independent experiments. Results were analyzed using PASW Statistics 18.0 program. The Student's*t* test was used to determine statistically significant differences. P values of <0.05 were considered significant.

3. Results

3.1. The Effects of ID on Clinical Signs in DSS-Induced Colitis. DSS caused a decrease in body weight (Figure 1(a)) and colon length (Figures 1(b) and 1(c)) at day 7 by 19.5% and 47.8%, respectively, compared to the control group. Both ID and SFZ alleviated the DSS effects on body weight loss and colon shortening (Figures 1(a)–1(c)). ID and SFZ also attenuated the DSS-mediated increase in DAI scores (Figure 1(d)).

3.2. The Effect of ID on Levels of IL-6 and TNF-α in DSS-Induced Colitis. Serum IL-6 level was significantly higher in the DSS group (0.193 ± 0.091 ng/mL) than in the control group (0.067 ± 0.018 ng/mL); IL-6 levels were significantly lower in ID (0.077 ± 0.014 ng/mL) or SFZ (0.041 ± 0.013 ng/mL) treatment group (Figure 2(a)). The serum TNF-α was also significantly increased in the DSS group (0.776 ± 0.045 ng/mL) compared to control (0.21 ± 0.025 ng/mL); serum TNF-α levels were significantly lower in ID (0.558 ± 0.070 ng/mL) or SFZ (0.435 ± 0.022 ng/mL) treatment group (Figure 2(b)). Furthermore, tissue IL-6 and TNF-α levels were significantly higher in the DSS groups (3.663 ± 0.585, 1.657 ± 0.140 ng/mL, resp.) than in the control groups (0.690 ± 0.346, 0.603 ± 0.046 ng/mL, resp.); tissue IL-6 and TNF-α levels were significantly lower in ID (2.373±0.461, 1.183 ± 0.191 ng/mL, resp.) or SFZ (2.050 ± 0.254, 0.760 ± 0.104 ng/mL, resp.) treatment groups (Figures 2(c) and 2(d)).

3.3. The Effect of ID on COX-2 and HIF-1α Expression in DSS-Induced Colitis. DSS markedly induced COX-2 and HIF-1α expression in colonic tissue versus controls (Figures 3(a)–3(c)); these increases were reduced by ID or SFZ administration. The effect of ID on COX-2 and HIF-1α expression was confirmed in colon tissues by immunohistochemical staining (Figure 3(d)).

3.4. The Effects of ID on Epithelial Injury and Mast Cells Infiltration in DSS-Induced Colitis. Mucosal thickness is regarded as a parameter of mucosal integrity. DSS treatment caused epithelial injury, as evidenced by an approximate 60% in mucosal thickness (Figures 4(a) and 4(c)). Mucosal infiltration of inflammatory cells, including mast cells (Figure 4(a); arrows), was also detected in the DSS-treated group as

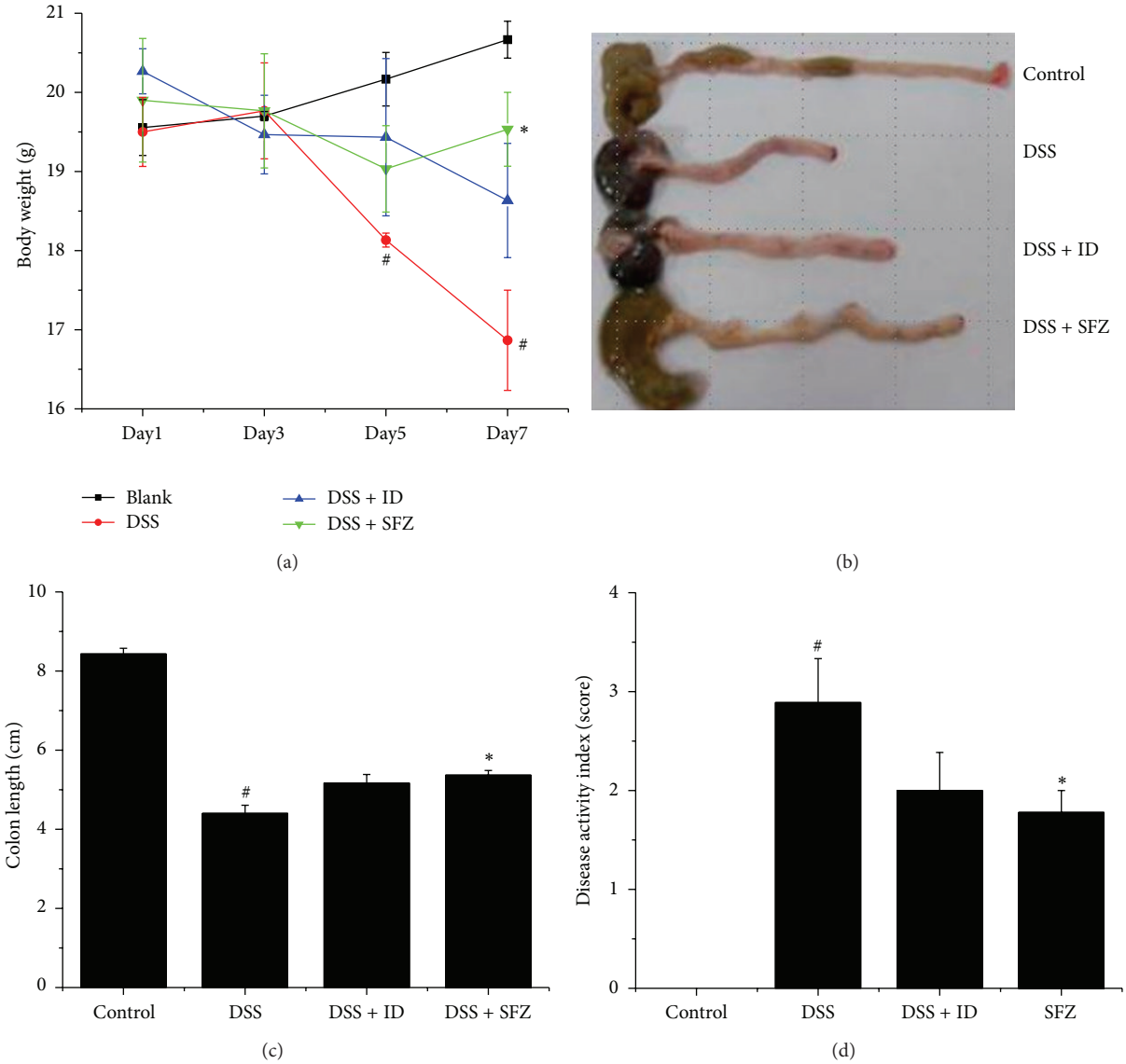

FIGURE 1: The effect of *Ixeris dentata* NAKAI (ID) on dextran-sodium-sulfate- (DSS-) induced clinical signs. Ulcerative colitis was induced in female BALC/c mice by administering 5% DSS in the drinking water for seven days. Over the same period, ID (100 mg/kg) and the reference compound sulfasalazine (SFZ; 100 mg/kg) were given orally once daily. (a) Body weights were measured at the same time of the experimental days. (b) Colons were harvested on day 7, and colon lengths were measured. (c) Colon lengths in the four study groups. (d) Disease activity index scores in the four study groups. Values represent mean ± S.E.M. ($n = 5$). Data were analyzed by Student's t test ($^{\#}P < 0.05$ versus control and $^{*}P < 0.05$ versus DSS alone).

compared with the control group (Figures 4(a) and 4(d)). ID and SFZ treatments attenuated these effects induced by DSS treatment (Figures 4(a), 4(c), and 4(d)). ID and SFZ treatments also reduced the DSS-mediated microscopic damage to the colonic tissue (Figure 4(b)).

3.5. Characterization of ID Constituents. A chromatogram of ID along with the standard 3,4-dihydroxy cinnamic acid is shown in Figure 5; the regression (R^2) of calibration curve was 0.9998. Based on the calibration curve, the content of 3,4-dihydroxy cinnamic acid in ID was estimated to be 4 mg/g of water extract of ID.

4. Discussion

UC is a type of inflammatory bowel disease (IBD), the symptoms of which include abdominal pain, weight loss, and bloody diarrhea [22–24]. Most therapies for UC include glucocorticosteroids, sulfasalazine, and immunomodulators (such as azathioprine) [25, 26]; however, these treatments can cause serious adverse effects. Although traditional herbal medicines have garnered much interest for their potential to treat inflammation, their pharmacological mechanisms of action have remained largely unresolved. Here it is demonstrated that ID alleviates the clinical signs—weight loss, colon shortening, diarrhea, and occult/gross

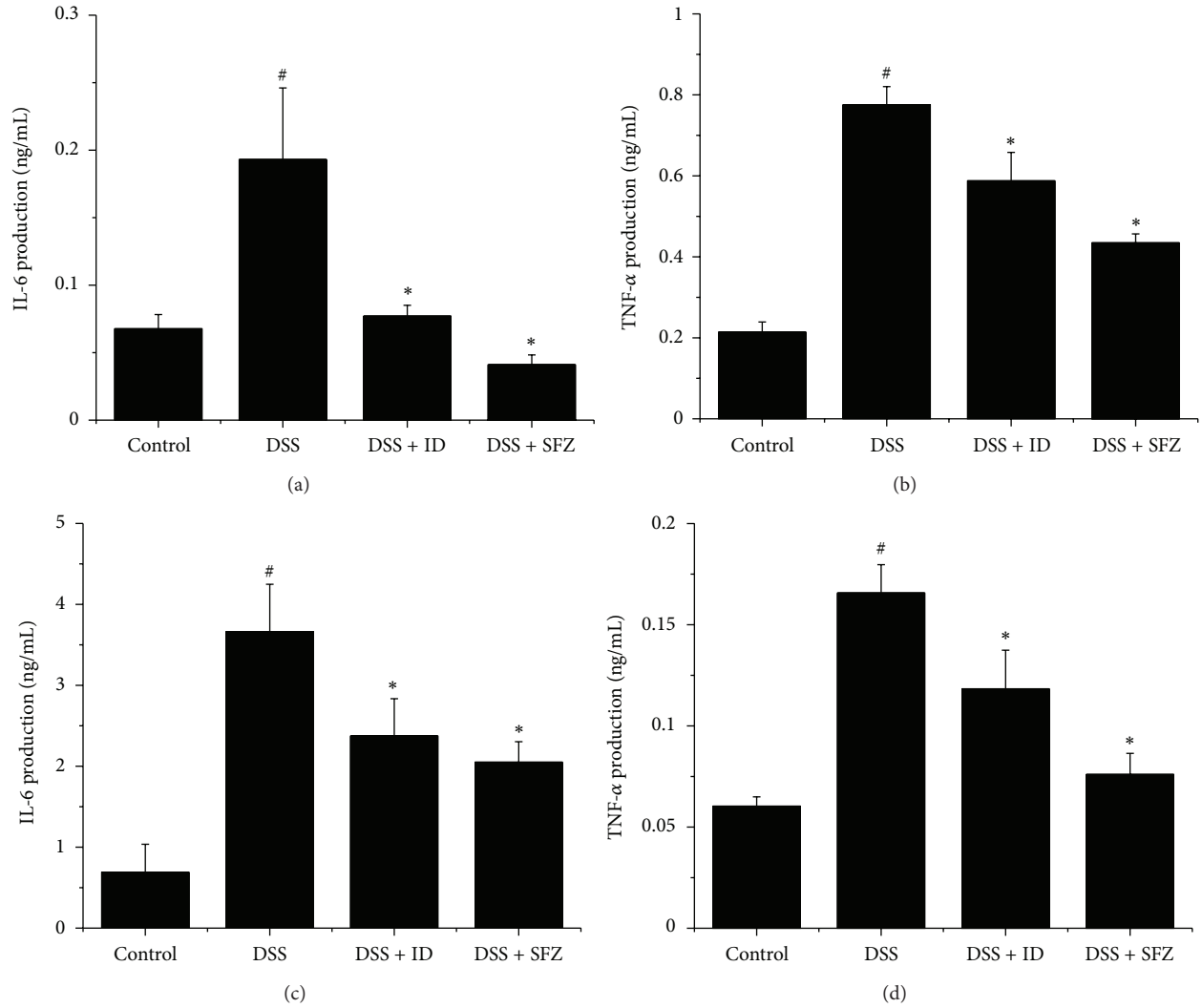

Figure 2: The effect of *Ixeris dentata* NAKAI (ID) on serum levels of interleukin- (IL-) 6 and tumor-necrosis-factor- (TNF-) α in DSS-induced colitis. Ulcerative colitis was induced by administering 5% DSS in the drinking water for seven days. Over the same period, ID (100 mg/kg) and the reference compound sulfasalazine (SFZ; 100 mg/kg) were given orally once daily. Cytokine production was determined by ELISA. (a) IL-6 production in mouse serum at day 7. (b) TNF-α production in mouse serum at day 7. (c) IL-6 production in colon tissue. (d) TNF-α production in colon tissue. Values represent mean ± S.E.M. ($n = 5$). Data were analyzed by Student's t test ($^{\#}P < 0.05$ versus control and $^{*}P < 0.05$ versus DSS alone).

bleeding—in the DSS-treated mouse model of UC. We also found that ID reduced epithelial injury, inflammatory cell infiltration into the colon tissue, and indices of microscopic injury. Moreover, ID prevented increases in the expression of COX-2 and HIF-1α and in the production of IL-6 and TNF-α. Thus, these results suggest that ID effectively inhibits symptoms of colitis caused by DSS.

Inflammatory cytokines such as IL-6, TNF-α, and interferon-γ mediate the pathogenesis of murine colitis [27–29]. Cytokines and chemokines are secreted by immune cells like T lymphocytes and macrophages that infiltrate the inflamed region. Studies in patients with UC have shown that gene [30] and protein expression [2–4] of IL-6 and TNF-α are similarly increased in the rectal mucosa. Consistent with the notion that IL-6 and TNF-α plays a causal role in the pathogenesis of UC, we found that ID suppressed the DSS-induced increase in IL-6 and TNF-α in mouse serum.

During the inflammatory process, the COX-1mRNA and protein activity do not change, whereas COX-2 levels increase dramatically, leading to the production of proinflammatory PGs [31]. However, Okayama et al. [32] found that both COX-1 and COX-2 inhibitors exacerbate inflammation and ulceration in the colon. Nevertheless, selective inhibitors like lumiracoxib have been developed as nonsteroidal anti-inflammatory drugs, many of which have been shown to be efficacious in a model of chemically induced colitis [33, 34]. 5-aminosalicylates, another drug class used to treat IBD, exert anti-inflammatory effects by inhibiting COX-2 activation [35]. Our study showed that ID inhibited the DSS-induced increase in COX-2 activation. These results suggest that the

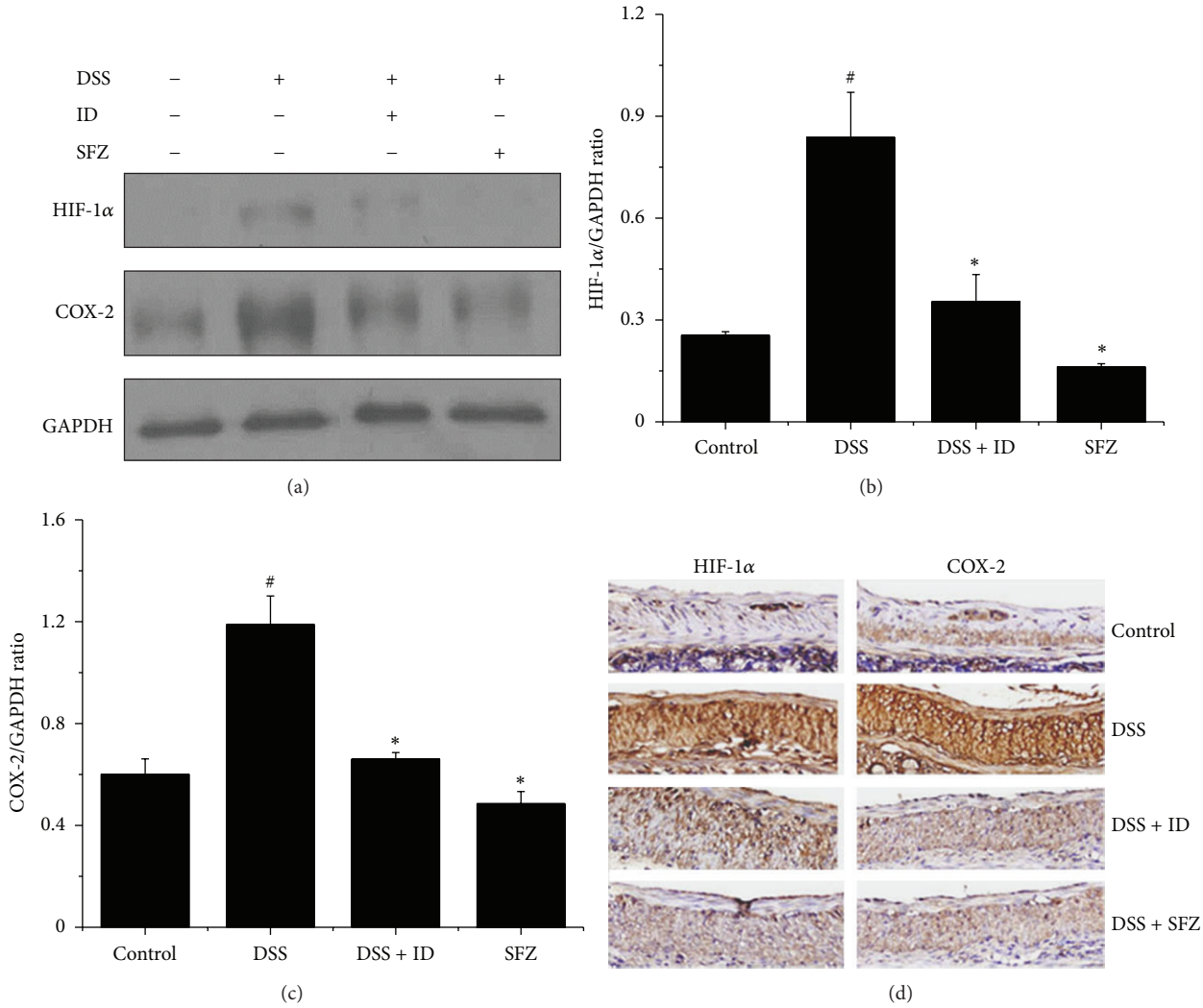

Figure 3: The effect of *Ixeris dentata* NAKAI (ID) on dextran-sodium-sulfate- (DSS-) induced cyclooxygenase- (COX-) 2 and hypoxia-inducible-factor- (HIF-) 1α levels in colonic tissues. Ulcerative colitis was induced in female BALC/c mice by administering 5% DSS in the drinking water for seven days. Over the same period, ID (100 mg/kg) and the reference compound sulfasalazine (SFZ; 100 mg/kg) were given orally once daily. COX-2 and HIF-1α levels were determined by western blot analysis. (a) Representative western blot (of three independent experiments) of COX-2 and HIF-1α expression in colonic tissue. (b) Ratios of COX-2/GAPDH and (c) HIF-1α/GAPDH were determined by densitometry. (d) Sections of colons of DSS-treated mice with or without ID treatment were subjected to immunohistochemical analysis. Values represent mean ± S.E.M. Data were analyzed by Student's t test ($^{\#}P < 0.05$ versus control and $^{*}P < 0.05$ versus DSS alone).

anti-inflammatory effect of ID is attributable to the regulation of COX-2 in DSS-induced colitis.

Inflamed mucosal tissue of colitic mice is highly hypoxic, leading to the overexpression of HIF-1α [36]. Clinical studies have also verified the upregulation of HIF-1α in colonic tissue from patients with IBD [37, 38]. And in HIF-1α overexpressing mice, Nuclear Factor-κB activity and the expression of pro-inflammatory genes were sequentially elevated [39]. Moreover, HIF-1α was shown to directly bind to the COX-2 promoter, thereby regulating the expression of COX-2 protein in two colorectal carcinoma cell lines, HCT116 and HT29 [40, 41]. It is therefore tempting to speculate that in the present study, the DSS-mediated increase in HIF-1α expression triggers the upregulation of COX-2. By virtue of its ability to inhibit the increased HIF-1α expression, ID therefore suppresses COX-2 activation and the ensuing inflammatory response.

5. Conclusions

We have shown that ID reduces the clinical signs and levels of inflammatory mediators in DSS-induced colitis in mice. This study provides experimental evidence to show that ID might be a useful therapy in the treatment of UC.

Authors' Contribution

Dae-Seung Kim and Jang-Ho Ko contributed equally to this work.

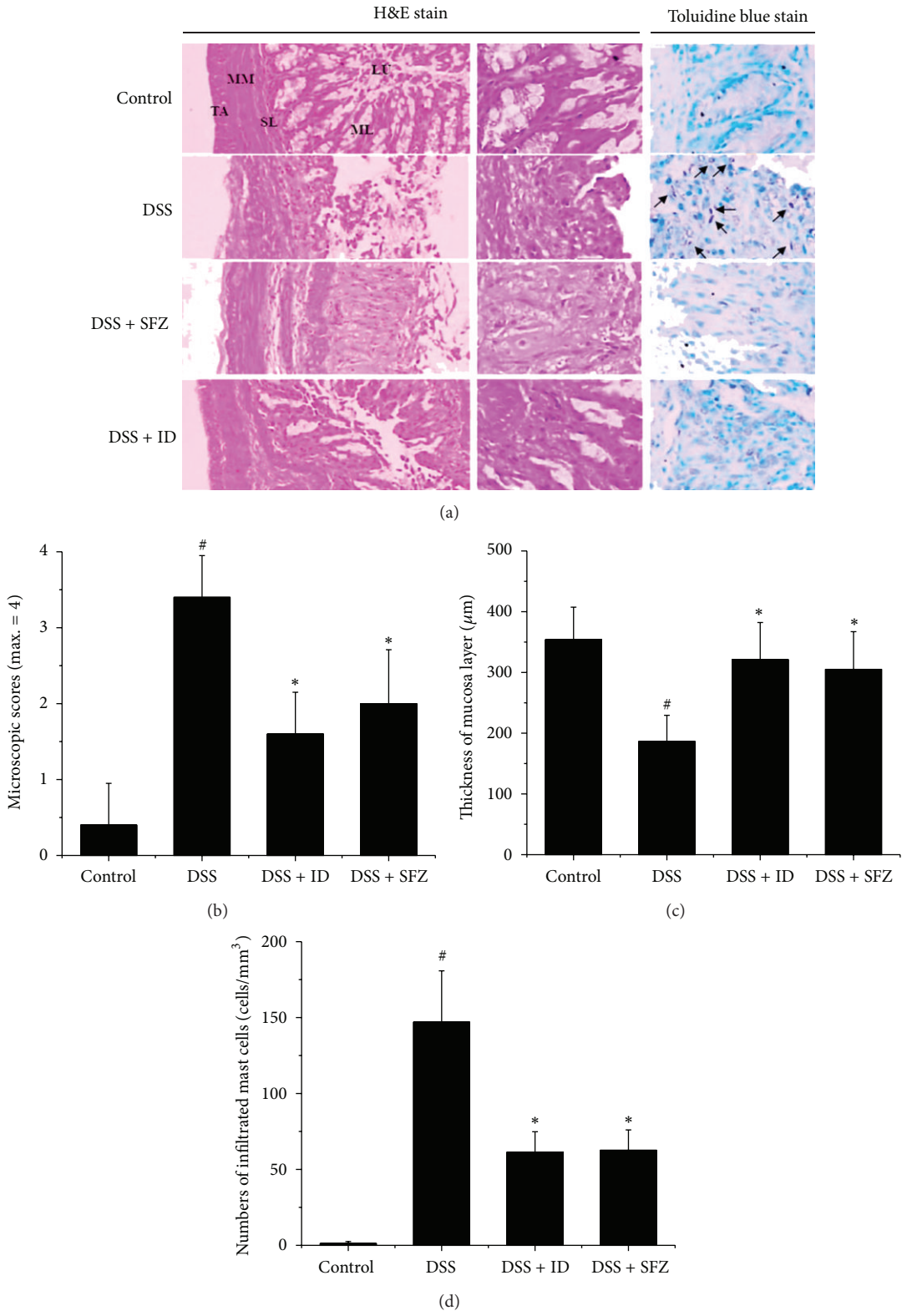

Figure 4: The effects of *Ixeris dentata* NAKAI on epithelial injury and mast cells infiltration in dextran-sodium-sulfate- (DSS-) induced colitis. Ulcerative colitis was induced in female BALC/c mice by administering 5% DSS in the drinking water for seven days. Over the same period, ID (100 mg/kg) and the reference compound sulfasalazine (SFZ; 100 mg/kg) were given orally once daily. (a) Paraffin sections of colonic tissue were stained with hematoxylin and eosin (100x) or with toluidine blue for mast cell identification. Mast cell infiltration is indicated by the arrows (structures: TA, tunica adventitia; MM, muscularis mucosa; SL, submucosa layer; ML, mucosa layer; LU, lumen). Microscopic scores (b), thickness of mucosal layer (c), and number of mast cells (d) were presented. Values represent mean ± S.E.M. ($n = 5$). Data were analyzed by Student's t test ($^{\#}P < 0.05$ versus control and $^{*}P < 0.05$ versus DSS alone).

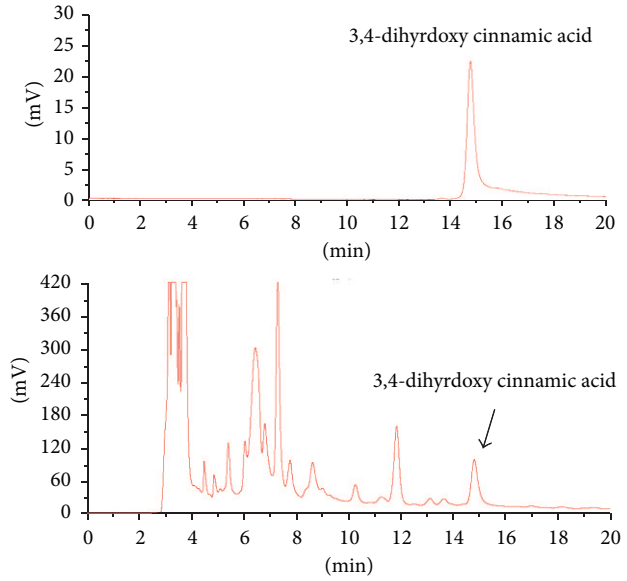

Figure 5: HPLC fingerprints of *Ixeris dentata* NAKAI (ID) and the standard 3,4-dihydroxy cinnamic acid. The mobile phase consisted of acetonitrile : distilled water : glacial acetic acid (15 : 85 : 1.5, isocratic manner). The injection volume was 10 μL of each sample, and flow rate was 1 mL/min. Wavelength was 254 nm. Retention time of 3,4-dihydroxy cinnamic acid was 14.3 min.

Acknowledgments

This work was supported by the National Research Foundation of Korea (NRF) Grant funded by the Korea government (MSIP) (no. 2012M2B2B1055244), and this work was also supported by the National Research Foundation of Korea (NRF) Grant funded by the Korea government (MSIP) (no. 2011-0030717).

References

[1] Y. Li, C. de Haar, M. Chen et al., "Disease-related expression of the IL6/STAT3/SOCS3 signalling pathway in ulcerative colitis and ulcerative colitis-related carcinogenesis," *Gut*, vol. 59, no. 2, pp. 227–235, 2010.

[2] H. Ogata and T. Hibi, "Cytokine and anti-cytokine therapies for inflammatory bowel disease," *Current Pharmaceutical Design*, vol. 9, no. 14, pp. 1107–1113, 2003.

[3] K. A. Papadakis and S. R. Targan, "Role of cytokines in the pathogenesis of inflammatory bowel disease," *Annual Review of Medicine*, vol. 51, pp. 289–298, 2000.

[4] C. Mueller, "Tumour necrosis factor in mouse models of chronic intestinal inflammation," *Immunology*, vol. 105, no. 1, pp. 1–8, 2002.

[5] S. A. McCartney, J. A. Mitchell, P. D. Fairclough, M. J. G. Farthing, and T. D. Warner, "Selective COX-2 inhibitors and human inflammatory bowel disease," *Alimentary Pharmacology and Therapeutics*, vol. 13, no. 8, pp. 1115–1117, 1999.

[6] P. J. Roberts, K. Morgan, R. Miller, J. O. Hunter, and S. J. Middleton, "Neuronal COX-2 expression in human myenteric plexus in active inflammatory bowel disease," *Gut*, vol. 48, no. 4, pp. 468–472, 2001.

[7] S. N. Agoff, T. A. Brentnall, D. A. Crispin et al., "The role of cyclooxygenase 2 in ulcerative colitis-associated neoplasia," *American Journal of Pathology*, vol. 157, no. 3, pp. 737–745, 2000.

[8] J. J. Haddad, "Science review: redox and oxygen-sensitive transcription factors in the regulation of oxidant-mediated lung injury: role for hypoxia-inducible factor-1α," *Critical Care*, vol. 7, no. 1, pp. 47–54, 2003.

[9] C. T. Taylor and S. P. Colgan, "Hypoxia and gastrointestinal disease," *Journal of Molecular Medicine*, vol. 85, no. 12, pp. 1295–1300, 2007.

[10] Y. Jung, J. S. Isaacs, S. Lee, J. Trepel, and L. Neckers, "IL-1beta-mediated up-regulation of HIF-1alpha via an NFkappaB/COX-2 pathway identifies HIF-1 as a critical link between inflammation and oncogenesis," *The FASEB Journal*, vol. 17, no. 14, pp. 2115–2117, 2003.

[11] A. Robinson, S. Keely, J. Karhausen, M. E. Gerich, G. T. Furuta, and S. P. Colgan, "Mucosal protection by hypoxia-inducible factor prolyl hydroxylase inhibition," *Gastroenterology*, vol. 134, no. 1, pp. 145–155, 2008.

[12] E. Ahn, M. Bang, M. Song et al., "Cytotoxic and ACAT-inhibitory sesquiterpene lactones from the root of *Ixeris dentata* forma albiflora," *Archives of Pharmacal Research*, vol. 29, no. 11, pp. 937–941, 2006.

[13] S. H. Oh, T. H. Sung, and M. R. Kim, "*Ixeris dentata* extract maintains glutathione concentrations in mouse brain tissue under oxidative stress induced by kainic acid," *Journal of Medicinal Food*, vol. 6, no. 4, pp. 353–358, 2003.

[14] J. Yi, S. Hong, H. Lee et al., "*Ixeris dentata* green sap inhibits both compound 48/80-induced aanaphylaxis-like response and IgE-mediated anaphylactic response in murine model," *Biological & Pharmaceutical Bulletin*, vol. 25, no. 1, pp. 5–9, 2002.

[15] E. Park, J. Sung, H. Trinh et al., "Lactic acid bacterial fermentation increases the antiallergic effects of *Ixeris dentata*," *Journal of Microbiology and Biotechnology*, vol. 18, no. 2, pp. 308–313, 2008.

[16] R. S. Blumberg, L. J. Saubermann, and W. Strober, "Animal models of mucosal inflammation and their relation to human inflammatory bowel disease," *Current Opinion in Immunology*, vol. 11, no. 6, pp. 648–656, 1999.

[17] I. Okayasu, S. Hatakeyama, M. Yamada, T. Ohkusa, Y. Inagaki, and R. Nakaya, "A novel method in the induction of reliable experimental acute and chronic ulcerative colitis in mice," *Gastroenterology*, vol. 98, no. 3, pp. 694–702, 1990.

[18] B. A. Hendrickson, R. Gokhale, and J. H. Cho, "Clinical aspects and pathophysiology of inflammatory bowel disease," *Clinical Microbiology Reviews*, vol. 15, no. 1, pp. 79–94, 2002.

[19] S. N. S. Murthy, H. S. Cooper, H. Shim, R. S. Shah, S. A. Ibrahim, and D. J. Sedergran, "Treatment of dextran sulfate sodium-induced murine colitis by intracolonic cyclosporin," *Digestive Diseases and Sciences*, vol. 38, no. 9, pp. 1722–1734, 1993.

[20] S. Kim, M. Kim, J. Um, and S. Hong, "The beneficial effect of vanillic acid on ulcerative colitis," *Molecules*, vol. 15, no. 10, pp. 7208–7217, 2010.

[21] N. Hamamoto, K. Maemura, I. Hirata, M. Murano, S. Sasaki, and K. Katsu, "Inhibition of dextran sulphate sodium (DSS)-induced colitis in mice by intracolonically administered antibodies against adhesion molecules (endothelial leucocyte adhesion molecule-1 (ELAM-1) or intercellular adhesion molecule-1 (icam-1))," *Clinical and Experimental Immunology*, vol. 117, no. 3, pp. 462–468, 1999.

[22] S. Ardizzone and G. B. Porro, "Biologic therapy for inflammatory bowel disease," *Drugs*, vol. 65, no. 16, pp. 2253–2286, 2005.

[23] P. A. Rufo and A. Bousvaros, "Current therapy of inflammatory bowel disease in children," *Pediatric Drugs*, vol. 8, no. 5, pp. 279–302, 2006.

[24] K. Sato, S. Ohkura, Y. Kitahara et al., "Involvement of CPI-17 downregulation in the dysmotility of the colon from dextran sodium sulphate-induced experimental colitis in a mouse model," *Neurogastroenterology and Motility*, vol. 19, no. 6, pp. 504–514, 2007.

[25] Y. Ishiguro, T. Ohkawara, H. Sakuraba et al., "Macrophage migration inhibitory factor has a proinflammatory activity via the p38 pathway in glucocorticoid-resistant ulcerative colitis," *Clinical Immunology*, vol. 120, no. 3, pp. 335–341, 2006.

[26] W. J. Sandborn and S. R. Targan, "Biologic therapy of inflammatory bowel disease," *Gastroenterology*, vol. 122, no. 6, pp. 1592–1608, 2002.

[27] K. J. Myers, S. Murthy, A. Flanigan et al., "Antisense oligonucleotide blockade of tumor necrosis factorα in two murine models of colitis," *Journal of Pharmacology and Experimental Therapeutics*, vol. 304, no. 1, pp. 411–424, 2003.

[28] Y. Naito, T. Takagi, K. Uchiyama et al., "Reduced intestinal inflammation induced by dextran sodium sulfate in interleukin-6-deficient mice," *International Journal of Molecular Medicine*, vol. 14, no. 2, pp. 191–196, 2004.

[29] F. Obermeier, G. Kojouharoff, W. Hans, J. Schölmerich, V. Gross, and W. Falk, "Interferon-gamma (IFN-γ)- and tumour necrosis factor (TNF)-induced nitric oxide as toxic effector molecule in chronic dextran sulphate sodium (DSS)-induced colitis in mice," *Clinical and Experimental Immunology*, vol. 116, no. 2, pp. 238–245, 1999.

[30] G. Fonseca-Camarillo, M. Villeda-Ramirez, F. Sanchez-Munoz et al., "IL-6 and TNF-a gene expression in the rectal mucosal of patients with chronic idiopathic ulcerative colitis and controls," *Revista de Gastroenterología de México*, vol. 74, no. 4, pp. 334–340, 2009.

[31] I. Morita, "Distinct functions of COX-1 and COX-2," *Prostaglandins and other Lipid Mediators*, vol. 68-69, pp. 165–175, 2002.

[32] M. Okayama, S. Hayashi, Y. Aoi, H. Nishio, S. Kato, and K. Takeuchi, "Aggravation by selective COX-1 and COX-2 inhibitors of dextran sulfate sodium (DSS)-induced colon lesions in rats," *Digestive Diseases and Sciences*, vol. 52, no. 9, pp. 2095–2103, 2007.

[33] K. Brune and B. Hinz, "Selective cyclooxygenase-2 inhibitors: similarities and differences," *Scandinavian Journal of Rheumatology*, vol. 33, no. 1, pp. 1–6, 2004.

[34] A. El-Medany, A. Mahgoub, A. Mustafa, M. Arafa, and M. Morsi, "The effects of selective cyclooxygenase-2 inhibitors, celecoxib and rofecoxib, on experimental colitis induced by acetic acid in rats," *European Journal of Pharmacology*, vol. 507, no. 1–3, pp. 291–299, 2005.

[35] K. Lauritsen, L. S. Laursen, J. Kjeldsen, K. Bukhave, T. K. Hansen, and J. Rask-Madsen, "Effects of mesalazine on the formation of lipoxygenase and cyclooxygenase products," *Advances in Experimental Medicine and Biology B*, vol. 371, pp. 1301–1306, 1995.

[36] J. Karhausen, G. T. Furuta, J. E. Tomaszewski, R. S. Johnson, S. P. Colgan, and V. H. Haase, "Epithelial hypoxia-inducible factor-1 is protective in murine experimental colitis," *The Journal of Clinical Investigation*, vol. 114, no. 8, pp. 1098–1106, 2004.

[37] A. Giatromanolaki, E. Sivridis, C. Kouskoukis, K. C. Gatter, A. L. Harris, and M. I. Koukourakis, "Hypoxia-inducible factors 1α and 2α are related to vascular endothelial growth factor expression and a poorer prognosis in nodular malignant melanomas of the skin," *Melanoma Research*, vol. 13, no. 5, pp. 493–501, 2003.

[38] F. Mariani, P. Sena, L. Marzona et al., "Cyclooxygenase-2 and Hypoxia-Inducible factor-1α protein expression is related to inflammation, and up-regulated since the early steps of colorectal carcinogenesis," *Cancer Letters*, vol. 279, no. 2, pp. 221–229, 2009.

[39] M. Scortegagna, C. Cataisson, R. J. Martin et al., "HIF-1α regulates epithelial inflammation by cell autonomous NFκB activation and paracrine stromal remodeling," *Blood*, vol. 111, no. 7, pp. 3343–3354, 2008.

[40] B. Agarwal, P. Swaroop, P. Protiva, S. V. Raj, H. Shirin, and P. R. Holt, "Cox-2 is needed but not sufficient for apoptosis induced by Cox-2 selective inhibitors in colon cancer cells," *Apoptosis*, vol. 8, no. 6, pp. 649–654, 2003.

[41] H. Zhong, M. Willard, and J. Simons, "NS398 reduces hypoxia-inducible factor (HIF)-1α and HIF-1 activity: multiple-level effects involving cyclooxygenase-2 dependent and independent mechanisms," *International Journal of Cancer*, vol. 112, no. 4, pp. 585–595, 2004.

Hindawi Publishing Corporation
Evidence-Based Complementary and Alternative Medicine
Volume 2013, Article ID 732126, 13 pages
http://dx.doi.org/10.1155/2013/732126

Research Article

Interaction of *Veratrum nigrum* with *Panax ginseng* against Obesity: A Sang-ban Relationship

Jinbong Park,[1] Yong-Deok Jeon,[2] Hye-Lin Kim,[1] Hara Lim,[1] Yunu Jung,[1] Dong-Hyun Youn,[1] Mi-Young Jeong,[2] Hyun-Ju Kim,[1] Sung-Hoon Kim,[1] Su-Jin Kim,[3] Seung-Heon Hong,[2] and Jae-Young Um[1]

[1] *College of Korean Medicine, Institute of Korean Medicine, Kyung Hee University, 26 Kyungheedae-ro, Dongdaemun-Gu, Seoul 130701, Republic of Korea*
[2] *Department of Oriental Pharmacy, College of Pharmacy, Wonkwang University, 460 Iksandae-ro, Iksan, Jeonbuk 570749, Republic of Korea*
[3] *Department of Cosmeceutical Science, Daegu Haany University, 1 Haanydaero, Gyeongsan-si, Gyeongsangbuk-Do 712715, Republic of Korea*

Correspondence should be addressed to Seung-Heon Hong; jooklim@wku.ac.kr and Jae-Young Um; jyum@khu.ac.kr

Received 2 April 2013; Revised 18 July 2013; Accepted 19 July 2013

Academic Editor: Seong-Gyu Ko

Obesity has become a major health threat in developed countries. However, current medications for obesity are limited because of their adverse effects. Interest in natural products for the treatment of obesity is thus rapidly growing. Korean Medicine (KM) is characterized by the wide use of herbal formulas. However, the combination rule of herbal formulas in KM lacks experimental evidence. According to *Shennong's Classic of Materia Medica*, the earliest book of herbal medicine, *Veratrum nigrum* (VN) has antagonistic features against *Panax ginseng* (PG), and the PG-VN pair is strictly forbidden. In this study, we have shown the effects of PG, VN, and their combination on obesity in high-fat (HF) diet-induced obese mice and in 3T3-L1 cells. PG, VN, and PG-VN combination significantly reduced weight gain and the fat pad weight in HF diet-induced obese mice. They also significantly decreased lipid accumulation and the expressions of two major adipogenesis factors, PPARγ and C/EBPα, in 3T3-L1 cells. In addition, the PG-VN combination had synergistic effects compared with the mixture of extracts of PG and VN on inhibition of PPARγ and C/EBPα expressions at lower doses. These results indicate a new potential anti-obese pharmacotherapy and also provide scientific evidence supporting the usage of herbal combinations instead of mixtures in KM.

1. Introduction

Obesity is a public health dilemma, especially in developed countries, and has steadily increased in recent years. The World Health Organization currently estimates that over 1 billion individuals worldwide are overweight. Almost one-third of these individuals are clinically obese, markedly raising their chances of suffering cardiovascular disease, type 2 diabetes, cancer, and stroke [1]. Over 1 billion adults are either overweight BMI > 25 or obese BMI > 30, and even more problematic is that about 25% of children in the USA are also now overweight or obese. These numbers are expected to increase by more than half again by the year 2025 worldwide, with especially severe impact in less developed countries [2].

The regulation of body fat content in animals results from the integration of multiple nutrient, sensory, and hormonal inputs, primarily at the level of the brain and adipose tissues [3]. The mechanisms underlying the development of obesity may include changes in skeletal muscle and adipose tissue enzymatic and/or receptor regulation (lipoprotein lipase, hormone sensitive lipase, and very low-density lipoprotein receptor) and/or hormonal regulation (i.e., insulin, growth hormone, catecholamine), resulting from physical inactivity and/or inappropriate macronutrient intake (i.e., high levels of saturated fat and/or refined carbohydrates) [4]. Thus, the integrative network of obesity, a complex, systemslevel disease, is influenced not only by genetics but also by circadian rhythm and physical and social environments [5].

The transcriptional regulation of adipocyte differentiation is known to rely on interplays between several adipogenic transcription factors. Among these, the peroxisome proliferator-activated receptor gamma (PPARγ) acts as a key regulator, both *in vitro* and *in vivo*, of the development of adipocytes and the only factor that can induce the adipocyte-like phenotype in nonadipogenic cell types [6]. The function of PPARγ is relatively close to members of the CCAAT-enhancer-binding protein (C/EBP) family, which have important functions at different time points during adipogenesis. C/EBPβ and C/EBPδ are expressed already in preadipocytes and are rapidly induced further [7], posttranslationally activated [8] by the adipogenic inducers cocktail. The expression of C/EBPβ is induced by the cAMP response element-binding protein and the glucocorticoid receptor (GR), and the phosphorylation and activation of C/EBPβ are induced by the extracellular-signal-regulated kinase 1/2 pathway [8]. On the other hand, C/EBPδ is induced by GR [9]. Both C/EBPβ and C/EBPδ are direct activators of the expression of PPARγ and C/EBPα [7, 10], the two major late-acting adipogenic transcription factors. These two factors are known to mutually induce the expression of each other and also cooperate to activate the adipogenesis gene program [11].

In contrast, according to "Huangdi's Internal Classic," one of the oldest Oriental Medicine's classics that describes the most basic theories of Oriental Medicine, obesity is a result of overeating [12]. In Korean Medicine (KM)'s most well-known classic *Treasured Mirror of Eastern Medicine*, obesity is explained in a similar manner to the description in *Huangdi's Internal Classic*, as it refers to obesity as a result of food overwhelming one's original qi and it notes that it can shorten one's life [13].

The root of *Panax ginseng* C. A. Meyer (Radix Ginseng) is one of the most popular Korean herbal medicines and has also gained popularity in Western countries recently [14]. In KM, *Panax ginseng* (PG) is known to improve "well-being" by highly restoring and enhancing qi and fluid at the same time, acting like a tonic, rather than a curative medication for specific types of patients. Modern therapeutic claims refer to vitality, immune function, cancer, and improvement of cognitive and physical performance and sexual function [15]. In dietary obese mice, ethanol extract of wild PG significantly inhibited body weight gain, decreased blood glucose, triglycerides, and free fatty acids levels, and improved insulin sensitivity [16]. Efficacy of PG on glucose metabolism has been confirmed in patients with type 2 diabetes also, showing reduced fasting blood glucose and body weight [17]. PG was also shown to regulate lipid metabolism. The lipid metabolism by PG was reported 30 years ago, in a chicken *in vivo* model [18]. In a clinical trial, PG extract administration reduced total cholesterol, triglycerides, and LDL and induced HDL [19]. In addition to these features, ginseng has been widely studied for treatment of diabetes, dyslipidemia, and obesity. Its berries and leaves were also demonstrated to reduce blood glucose in diabetic models [20].

The root of *Veratrum nigrum* Linné var. *ussuriense* Loes. fil. (Radix Veratri nigri), commonly known as Black False Hellebore, is a coarse, highly poisonous perennial herb native to Asia and Europe [21]. *Veratrum nigrum* (VN) is known to be highly toxic [22], and due to its ability to cause nausea and vomiting, it is applied to dyspnea in epilepsy or stroke patients. Studies have revealed that VN is a potential agonist of β2-adrenoceptor [23] and can decrease blood pressure and heart rate in a dose-dependent manner in hypertensive rats [24], and it affords significant protection against hepatic ischemia/reperfusion injury in rats [25]. However, to date, no study of VN on obesity has been reported.

According to *Shennong's Classic of Materia Medica*, VN has antagonistic features against PG [26]. This antagonism is one of the six types of "Chil-jeong." The "Chil-jeong" theory first appeared in *Shennong's Classic of Materia Medica*, a classic of oriental medicine that introduced 365 kinds of herbs and described their qi and flavors, meridian entries, and special features [26]. The six types of "Chil-jeong" can be sorted into three kinds considering their major features. "Sang-soo" and "Sang-sa" are combinations where two herbs reinforce and have synergistic effects. On the other hand, "Sang-oe" and "Sang-swae" are types that can neutralize the toxicity of combinations. And finally, "Sang-o" and "Sang-ban" are types that are not recommended because of weakened effects or occurrences of adverse effects. A representative example of "Sang-ban" is a combination of VN and PG. This combination was introduced in *Shennong's Classic of Materia Medica* as one of the herbal pairs that should not be used together.

In this study, because the effects of PG and VN co-treatment on obesity have not been proved scientifically, the effects of PG and VN extracts on obesity are investigated both *in vivo* and *in vitro*, and an investigation of the effects of their combination is followed to search the antagonistic effects between the two and compare them with those of the separate extracts.

2. Materials and Methods

2.1. Preparation of PG, VN, and Their Combination. 100 g of PG was chopped and soaked in 1000 mL of distilled water and extracted at 100°C for 3 hours. 100 g of VN was extracted by the same method. In order to prepare the combination extractions, 50 g of PG and 50 g of VN (1 : 1) or 90 g of PG and 10 g of VN (9 : 1) were extracted together by the same method. After filtering, the solvent was removed by evaporation. It was then freeze-dried to obtain the extracts. The samples were stored at −20°C.

2.2. Animal Experiments. Male C57BL/6J mice, weighing 17-18 g at the age of 4 weeks, were purchased from the Dae-Han Experimental Animal Center (Dae-Han Biolink, Eumsung, Republic of Korea). The animals were all maintained in conditions in accordance with the regulations issued by the Institutional Review Board of Kyung Hee University (confirmation number: KHUASP (SE)-13-012). The animals were housed under a 12-hour light/dark cycle at a humidity of 70% and a constant temperature of 23 ± 2°C. The animals were divided into six groups of five mice each. The six groups of mice were fed for 16 weeks with the following (1) a standard laboratory diet (CJ Feed Co., Ltd., Seoul, Korea); (2) a high-fat (HF) diet (60% fat); (3) a HF plus PG; (4) a HF plus VN; (5) a HF plus

Table 1: Composition of experimental diets (g/kg).

Compositions	Control	HFD*	PG*	VN*	1 : 1*	Slinti*
Casein	200.0	265.0	265.0	265.0	265.0	265.0
L-Cystine	3.0	4.0	4.0	4.0	4.0	4.0
Corn starch	397.486	—	—	—	—	—
Maltodextrin	132.0	160.0	160.0	160.0	160.0	160.0
Sucrose	100.0	90.0	90.0	90.0	90.0	90.0
Lard	—	310.0	310.0	310.0	310.0	310.0
Soybean oil	70.0	30.0	30.0	30.0	30.0	30.0
Cellulose	50.0	65.5	65.5	65.5	65.5	65.5
Mineral mix[a]	35.0	48.0	48.0	48.0	48.0	48.0
Calcium phasphate, dibasic	—	3.4	3.4	3.4	3.4	3.4
Vitamin mix[b]	10.0	21.0	21.0	21.0	21.0	21.0
Choline bitartrate	2.5	3.0	3.0	3.0	3.0	3.0
TBHQ, antioxidant[c]	0.014	—	—	—	—	—
Blue food color	—	0.1	0.1	0.1	0.1	0.1
PG	—	—	0.75	—	—	—
VN	—	—	—	0.75	—	—
PG-VN combination	—	—	—	—	0.75	—
Slinti	—	—	—	—	—	0.75

[a]Mineral mix, AIN-93G-MX (94046) containing (g/kg): calcium phosphate dibasic 500, sodium chloride 74, potassium citrate 220, potassium sulfate 52, magnesium oxide 24, manganous carbonate 3.5, ferric citrate 6, zinc carbonate 1.6, cupric carbonate 0.3, potassium iodate 0.0.1, sodium selenite 0.01, and chromium potassium sulfate 0.55. [b]Vitamin mix, AIN-93-VX (94047), containing (g/kg): thiamin HCl 0.6, riboflavin 0.6, pyridoxine HCl 0.7, niacin 3, calcium pantothenate 1.6, folic acid 0.2, biotin 0.02, vitamin B12 (0.1 % trituration in mannitol) 1, dry vitamin A palmitate (500,00 U/g) 0.25, and menadione sodium bisulfite complex 0.15. [c]TBHQ: tertiary butylhydroquinone. *60 % of total calories come from fat. HFD: high-fat diet; PG: *Panax ginseng*; VN: *Veratrum nigrum;* 1 : 1: PG-VN combination.

PGand VN combination; (6) a HF plus Slinti, a green tea extract used as a positive control (Myoungmoon Pharm. Co., LTD., Seoul, Republic of Korea). The components of the diets are described in Table 1. The diets were prepared according to the AIN-93G modified formulation. The animals were given free access to food and tap water. The body weight and food intake amount were recorded every week. At the end of this period, the animals were fasted overnight. The next day, they were anesthetized with ketamine and Rompun (5 : 3), and blood samples were collected by cardiac puncture. The organs and fat pads were immediately weighed.

2.3. Plasma Parameter Analysis. Plasma was separated immediately after blood sampling by centrifugation at 10,000 ×g for 10 min. Plasma concentrations of total cholesterol and high-density lipoprotein (HDL) cholesterol were determined using automated enzymatic methods [27], and low-density lipoprotein (LDL) cholesterol was calculated using the Friedewald formula [28]. The plasma concentration of triglyceride was measured enzymatically using a triglyceride assay kit (Asan Co., Seoul, Republic of Korea). Alanine aminotransferase (ALT) activity was determined with an ALT/GPT kit (Sigma-Aldrich, St. Louis, MO, USA).

2.4. Reagents. Dulbecco's modified Eagle's medium (DMEM), penicillin-streptomycin, fetal calf serum (FCS), and fetal bovine serum (FBS) were from Gibco BRL (Grand Island, NY). Insulin, 3-isobutylmethylxanthine (IBMX), and dexamethasone (DEX) were purchased from Sigma Chemical Co. (St. Louis, MO). Anti-C/EBPα and anti-GAPDH antibodies were purchased from Santa Cruz Biotechnology (Santa Cruz, CA). Anti-PPARγ antibody was purchased from Cell Signaling Technology (Beverly, MA).

2.5. Cell Culture and Adipocyte Differentiation. 3T3-L1 mouse embryo fibroblasts were obtained from the American Type Culture Collection (ATCC, Rockville, MD, USA). Cells were maintained in DMEM containing 10% FBS with 100 units/mL of penicillin-streptomycin solution at 37°C in 5% CO_2 at 95% humidity until confluence. Two days after confluence (day 0), the cells were stimulated to differentiate with differentiation inducers (1 μM dexamethasone, 500 μM 3-isobutyl-1-methylxanthine, and 1 μg/mL insulin) that were added to DMEM containing 10% FBS for 48 hours. On day 2, 3T3-L1 cells were then cultured in DMEM, 10% FBS supplemented with 1 μg/mL insulin, for another two days. At that time, water extract of PG, water extract of VN, and water extract of their combination were prepared in the differentiation medium at concentrations of 0.01 mg/mL, 0.1 mg/mL, and 1 mg/mL. And then, the cells were cultured with 10% FBS/DMEM medium for an additional two days, at which time more than 90% of cells were mature adipocytes with accumulated fat droplets. On day 6, the cells were harvested and prepared for further experiments.

2.6. MTS Cell Viability Assay. Tests were performed in 96-well plates. 3T3-L1 preadipocytes were seeded (2×10^4 cells/well) and incubated in 10% FBS/DMEM medium for 24

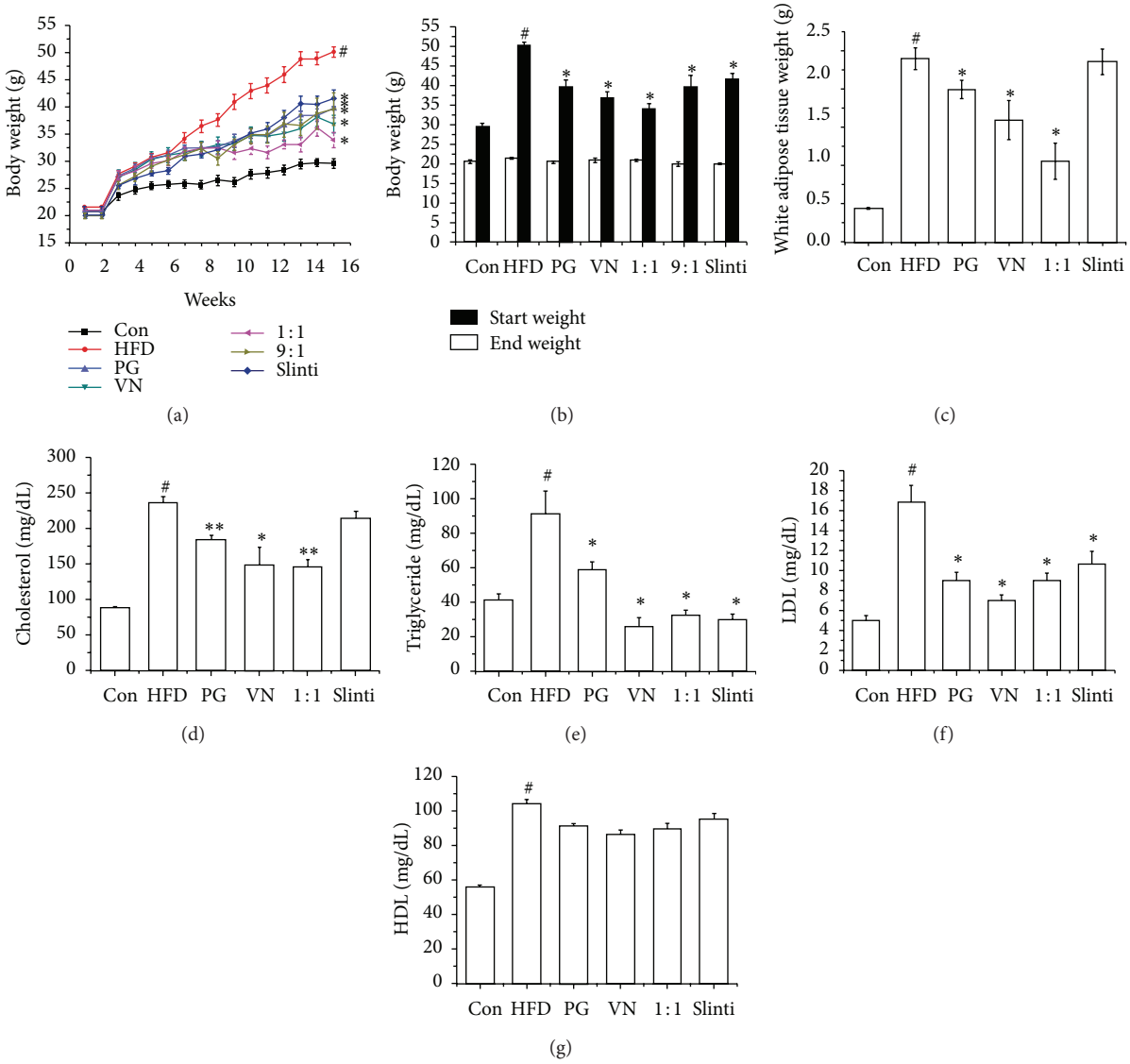

FIGURE 1: Effects of PG, VN, and their combinations in HF diet-induced obese mice. The weight changes of control, HF diet, PG, VN, PG-VN combination, and slinti groups were measured for 16 weeks (a). The weight difference between the start weight and end weight of each group was measured to evaluate the weight gain (b). The white adipose tissue weights (c), total cholesterol (d), triglyceride (e), LDL-cholesterol (f), and HDL-cholesterol (g) of the mice were also measured. All values are mean ± SD. $^{\#}P < 0.05$, significantly different from the Control; $^{*}P < 0.05$, significantly different from the HF diet group. Con, standard laboratory diet group; HFD, high-fat diet group; PG, HF diet plus PG group; VN, HF diet plus VN group; 1 : 1, HF diet plus PG-VN 1 : 1 combination group; 9 : 1, HF diet plus PG-VN 9 : 1 combination group; Slinti, HF diet plus slinti group. PG, *Panax ginseng*; VN, *Veratrum nigrum*.

hours. The cells were then incubated in 10% FBS/DMEM medium containing water extract of PG, water extract of VN, and water extract of their combination for an additional 48 hours. Cell viability was monitored by a Cell Proliferation MTS Kit as recommended by the manufacturer [29]. Prior to measuring viability, treatment media were removed and replaced with 200 μL of fresh 10% FBS/DMEM medium and 20 μL of 3-(4,5-dimethylthiazol-2-yl)-5-(3-carboxymethoxyphenyl)-2-(4-sulfophenyl)-2H-tetrazolium (MTS) solution. Cells were then returned to the incubator for 4 hours. The absorbance was measured at 490 nm in a VERSAmax microplate reader (Molecular Devices, Sunnyvale, CA, USA) to determine the formazan concentration, which is proportional to the number of live cells.

2.7. Oil Red O Staining. Intracellular lipid accumulation was measured using Oil Red O. The Oil Red O working solution was prepared as described by Ramirez-Zacarias et al. [30]. 3T3-L1 adipocytes were harvested 6 days after the initiation of differentiation. Cells were washed twice with phosphate buffered saline (PBS, pH 7.4) and then fixed with 10% neutral formalin for 2 hours at room temperature. After washing with 60% isopropanol, the cells were stained with Oil Red O working solution for 30 min and then washed 4 times with water

Table 2: Sequences of oligonucleotide primers (5′ to 3′) for real-time RT-PCR.

Genes	5′ to 3′ oligonucleotide sequences
Mouse PPARγ	
Sense (forward)	TTT TCA AGG GTG CCA GTT TC
Antisense (reverse)	TTA TTC ATC AGG GAG GCC AG
Mouse C/EBPα	
Sense (forward)	GCC GAG ATA AAG CCA AAC AA
Antisense (reverse)	CCT TGA CCA AGG AGC TCT CA
Mouse GAPDH	
Sense (forward)	AAC TTT GGC ATT GTG GAA GG
Antisense (reverse)	GGA TGC AGG GAT GAT GTT CT

PPARγ: peroxisome proliferator activated receptor γ; C/EBPα: CCAAT enhancer binding protein α; GAPDH: glyceraldehyde-3-phosphate dehydrogenase.

to remove the unbound dye. The stained cells were observed by an Olympus IX71 Research Inverted Phase microscope (Olympus Co., Tokyo, Japan). Following the microscopic observation, 100% isopropanol was added as an extraction solution to extract the staining dye of cells. The absorbance of the extracted dye was measured spectrophotometrically at 500 nm in a VERSAmax microplate reader (Molecular Devices, Sunnyvale, CA, USA).

2.8. RNA Isolation and Real-Time Reverse-Transcription Polymerase Chain Reaction (RT-PCR). Total cellular RNA was isolated from 3T3-L1 adipocytes using a GeneAll RiboEx Total RNA extraction kit (GeneAll Biotechnology, Seoul, Republic of Korea) and QIAzol lysis reagent (QIAZEN sciences, Maryland, USA). Total RNA was used as a template for first-strand cDNA synthesis performed using a Power cDNA Synthesis Kit (iNtRON Biotechnology, Seoul, Republic of Korea) according to the manufacturer's instructions. PCR products were measured with a StepOnePlus Real-time RT-PCR System (Applied Biosystems, Foster City, CA, USA), and the relative gene expression was calculated based on the comparative CT method using StepOne Software v2.1 (Applied Biosystems, Foster City, CA, USA). The expression of glyceraldehyde-3-phosphate dehydrogenase (GAPDH) mRNA was used as an endogenous control. The target cDNA was amplified using the sense and antisense primers described in Table 2.

2.9. Western Blot Analysis. After experimental treatment, cells were washed twice with ice-cold PBS and lysed with RIPA lysis buffer, which consisted of 50 mM Tris-HCl (pH 7.5), 0.1% sodium dodecyl sulphate (SDS), 0.1% Triton X-100, 1% Nonidet P-40, 0.5% sodium deoxycholate, 150 mM NaCl, and 1 mM phenylmethylsulfonyl fluoride. Insoluble materials were removed by centrifugation at 13,000 rpm for 20 min at 4°C. The total concentration of extracted proteins was determined using the method of Bradford [31]. The proteins in the supernatants were separated by 8% sodium dodecyl sulfate-polyacrylamide gel electrophoresis (SDS-PAGE) and transferred onto polyvinylidene difluoride (PVDF) membranes. After blocking with 10 mM Tris, 150 mM NaCl, and 0.05% Tween-20 (TBST) (pH 7.6) containing 5% skim milk for 1 hour at room temperature, the membranes were washed with TBST and then incubated with the appropriate primary antibodies against PPARγ (Cell Signaling Technology, Beverly, MA, USA), C/EBPα, or GAPDH (Santa Cruz Biotechnology, Santa Cruz, CA, USA) at 4°C overnight. After washing with TBST, the blots were subsequently incubated with horseradish peroxidase (HRP)-conjugated AffiniPure goat anti-rabbit IgG or Goat anti-mouse IgG (Jackson Immunoresearch Lab., USA) in 5% skim milk TBST at room temperature for 1 h. Protein signals were developed by using the ECL Western Blotting Detection Reagent (Amersham Bioscience, Piscataway, NJ, USA). All experiments were repeated at least three times. Representative Western blots are shown along with graphs of the quantitative data. The chemiluminescent intensities of protein signals were quantified using Quantity One software (Bio-Rad Laboratories, Hercules, CA, USA).

2.10. Statistical Analysis. Results are expressed as the mean ± SEM of independent experiments, and statistical analyses were performed using a Student's t-test to determine differences between groups. All statistical analyses were performed using SPSS statistical analysis software version 11.5 (SPSS Inc., Chicago, IL, USA). Values with $^{*}P < 0.05$ were considered to indicate statistical significance.

3. Results

3.1. Effects of PG, VN, and Their Combination on Body Weight in HF Diet-Induced Obese C57BL/6J Mice. Experimental animals appeared healthy, showing no pathological signs or abnormalities during the feeding period. As shown in Figures 1(a) and 1(b), the seven groups had similar body weights at the beginning of the study. However, mice fed the HF diet gained significantly more weight than those fed the standard diet mice ($P < 0.05$). On the other hand, weight gain in the PG, VN, PG-VN 1 : 1 combination, and PG-VN 9 : 1 combination groups was significantly less than that in the HF diet group ($P < 0.05$). The weight gain in the PG-VN 1 : 1 combination group also significantly decreased compared with the PG group ($P < 0.05$), but not with the VN group. The HF diet group gained 27.49 ± 1.01 g of weight, while the PG group gained 18.07 ± 1.13 g, the VN group gained 15.06 ± 1.07 g, the slinti (consisted of green tea powder 250 mg and orthosiphon powder 150 mg) group, which is the positive control group, gained 20.59 ± 1.25 g, and the PG-VN 1 : 1 combination group gained 12.17 ± 1.13 g of weight after 16 weeks. Antiobese effect of the PG-VN 1 : 1 combination group in weight gain was higher than that in the PG-VN 9 : 1 combination group. Therefore, further PG-VN combination studies were performed at the ratio of 1 : 1. Changes in the fat pads among the six groups are given in Figure 1(c). The results showed significant differences in the weight of the fat pad. The white adipose tissue weight of the PG, VN, and combination group was significantly lower than that of the HF diet group ($P < 0.05$). In addition, the PG-VN combination group showed a significant difference compared with PG ($P < 0.05$).

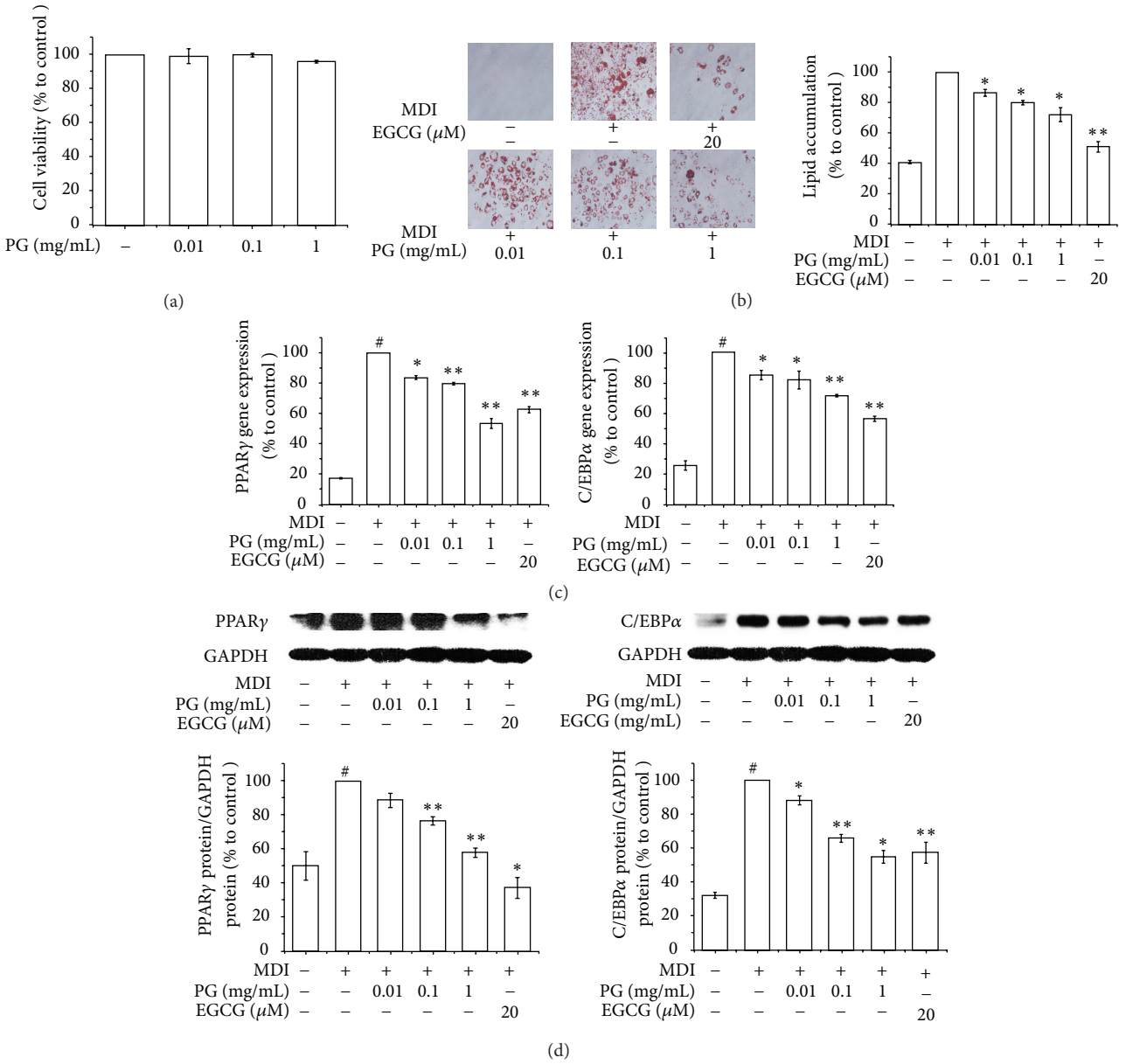

Figure 2: Effects of the water extract of PG on adipogenesis and transcription factors in 3T3-L1 cells. An MTS assay (a), Oil Red O staining assay (b), real-time RT-PCR assay (c), and Western blot assay (d) were performed to measure the effects of PG in 3T3-L1 cells. 3T3-L1 preadipocytes were induced to differentiate with 10% FBS/DMEM medium containing insulin, DEX, IBMX, and 0, 0.01, 0.1, or 1 mg/mL of PG extract for 2 days, and then the culture media were replaced with 10% FBS/DMEM medium containing insulin for the following 2 days. The control was treated with DW instead of extracts. EGCG was used as a positive control. Assays were performed in duplicates for each concentration, and experiments were repeated at least three times. Data represented are the relative expression. All values are mean ± SD. $^{\#}P < 0.05$, versus undifferentiated control cells; $^{*}P < 0.05$ and $^{**}P < 0.005$, versus differentiated control cells; DW, distilled water; PG, *Panax ginseng*; EGCG, epigallocatechin gallate.

3.2. Effects of PG, VN, and Their Combination on Lipid Level in HF Diet-Induced Obese C57BL/6J Mice. The blood plasma parameter changes are shown in Figures 1(d)–1(g). The level of total cholesterol in plasma is the major determinant of the risk of vascular disease, and lowering the LDL cholesterol level diminishes the risk of vascular diseases [32–34]. Furthermore, abdominal obesity is known to be associated with dyslipidemia, as characterized by increased triglyceride and decreased HDL cholesterol levels [35]. The total cholesterol level, triglyceride level, and LDL cholesterol level in the HF diet group were 2.8-fold, 2.5-fold, and 3-fold increased, respectively, compared with the standard chow diet group. The PG group, the VN group, and the PG-VN combination group all showed significant decreases in total cholesterol, triglyceride, and LDL cholesterol concentrations compared to the HF diet group (Figures 1(e)–1(g)). The HDL cholesterol level also showed an increase in the HF diet group compared with the standard chow diet group, but there were no significant differences in HDL cholesterol level between the HF diet group and the other four groups. In order to

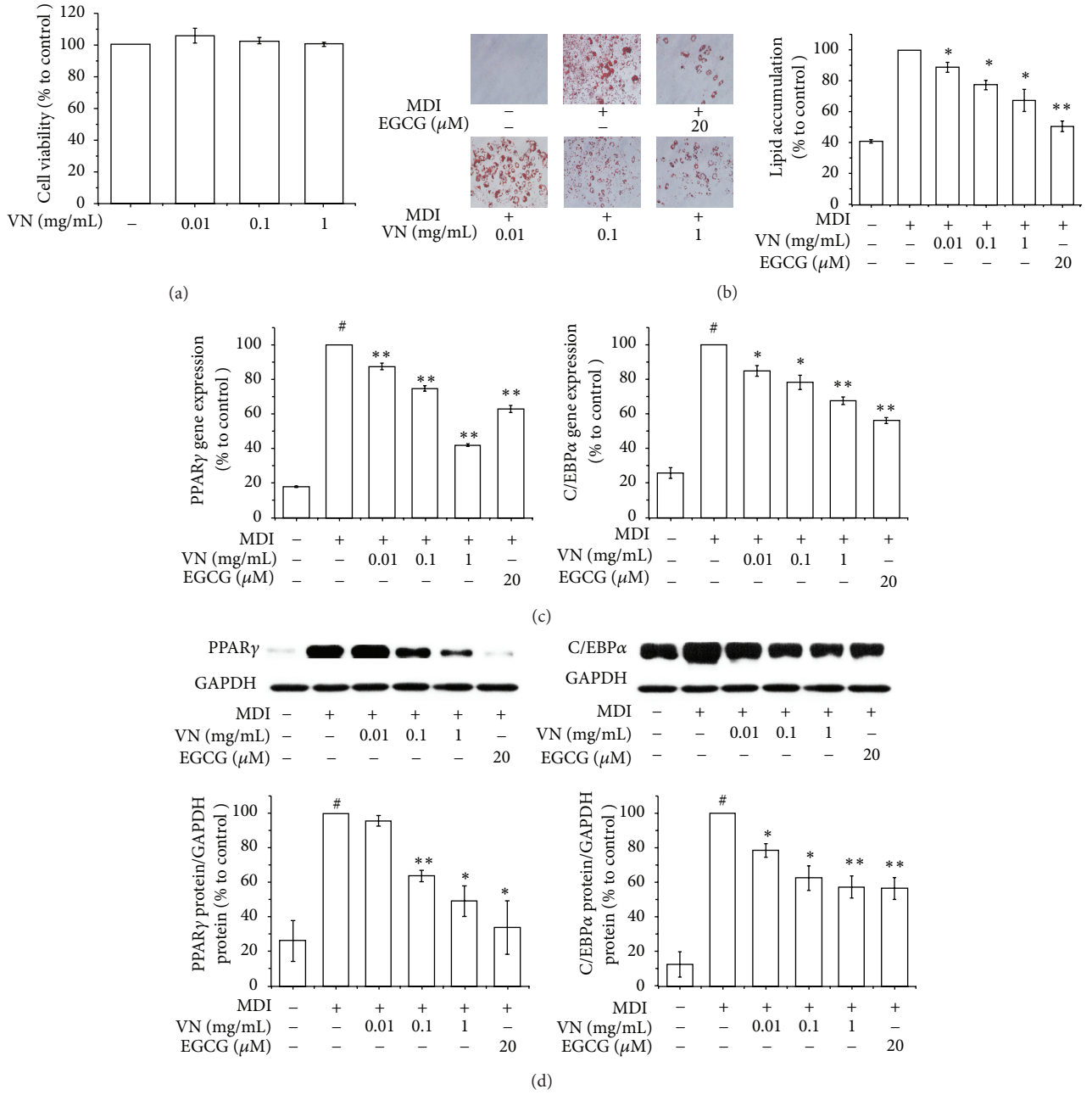

Figure 3: Effects of the water extract of VN on adipogenesis and transcription factors in 3T3-L1 cells. An MTS assay (a), Oil Red O staining assay (b), real-time RT-PCR assay (c), and Western blot assay (d) were performed to measure the effects of VN in 3T3-L1 cells. 3T3-L1 preadipocytes were induced to differentiate with 10% FBS/DMEM medium containing insulin, DEX, IBMX, and 0, 0.01, 0.1, or 1 mg/mL of VN extract for 2 days, and then the culture media were replaced with 10% FBS/DMEM medium containing insulin for the following 2 days. The control was treated with DW instead of extracts. EGCG was used as a positive control. Assays were performed in duplicates for each concentration, and experiments were repeated at least three times. Data represented are the relative expression. All values are mean ± SD. $^{\#}P < 0.05$, versus undifferentiated control cells; $^{*}P < 0.05$ and $^{**}P < 0.005$, versus differentiated control cells; DW, distilled water; VN, *Veratrum nigrum*; EGCG, epigallocatechin gallate.

investigate any possible internal toxicity, the serum levels of alanine transaminase (ALT), aspartate transaminase (AST), blood urea nitrogen (BUN), and creatinine were evaluated and the results are shown in Supplementary Figures S1(a)–S1(d) (Supplementary Material available online at http://dx.doi.org/10.1155/2013/732126).

3.3. Effects of the Water Extract of PG on Adipogenesis and Transcription Factors in 3T3-L1 Cells. Before investigating the antiobesity effects of PG *in vitro*, a cell viability test in 3T3-L1 preadipocytes was performed first. The MTS assay was performed to assess the effect of the water extract of PG on 3T3-L1 cell viability. As shown in Figure 2(a), the water extract

of PG showed no significant effect on viability after 48 h treatment at concentrations of 0.01, 0.1, and 1 mg/mL. Further investigations were hence carried out at concentrations of 0.01, 0.1, and 1 mg/mL. Next, to investigate the effects of PG on preadipocytes differentiation, the lipid accumulation was measured by an Oil Red O staining assay. As shown in Figure 2(b), PG suppressed lipid accumulation in 3T3-L1 adipocytes in a dose-dependent manner with statistical significance ($P < 0.05$), suggesting that PG inhibits adipogenesis in 3T3-L1 cells. Epigallocatechin gallate (EGCG), a green tea compound that accounts for 54–59% of total tea catechins [36], was used as a positive control. Adipocyte differentiation accompanies the changes in expression of various adipogenic and lipogenic genes [37]. PPARγ and C/EBPα, well-recognized adipogenic genes known to have roles in the early stage of adipogenesis [38], were examined. To investigate the inhibitory mechanism, the effects of PG on both mRNA and protein expression levels of PPARγ and C/EBPα were examined. Fully differentiated 3T3-L1 cells were exposed for 48 h to concentrations of 0.01, 0.1, and 1 mg/mL of PG. Expression of both adipogenic genes PPARγ and C/EBPα was significantly suppressed by PG in a dose-dependent manner. The results are shown in Figure 2(c). These results suggest that PG has inhibitory effects on PPARγ and C/EBPα, which are found almost exclusively in adipose tissues and play crucial roles in the induction of adipose-specific genes and in the manifestation of the mature adipose phenotype [39]. In order to confirm the effects of PG on PPARγ and C/EBPα, a Western blot analysis was carried out. Figure 2(d) shows that the expressions of PPARγ and C/EBPα significantly are suppressed by PG at concentrations of 0.1 and 1 mg/mL. Consistent with the results of the real-time RT-PCR assay shown above (Figure 2(c)), the Western blotting analyses confirm that PG has inhibitory effects on PPARγ and C/EBPα.

3.4. Effects of the Water Extract of VN on Adipogenesis and Transcription Factors in 3T3-L1 Cells. Ahead of any other investigation, a cell viability assay of VN was performed as well as PG. As shown in Figure 3(a), an MTS assay verified that VN had no cytotoxic effects in 3T3-L1 cells at the concentrations of 0.01, 0.1, and 1 mg/mL. Further investigations were performed at the concentrations that did not show cytotoxicity, and EGCG was used as a positive control. The effect of VN on lipid accumulation in 3T3-L1 cells was measured via an Oil Red O staining assay. Similar to the results of PG, Figure 3(b) indicates that VN suppressed lipid accumulation in 3T3-L1 cells in a dose-dependent manner ($P < 0.05$). In a real-time RT-PCR assay, the results showed that VN also had significant inhibitory effects on the expression of PPARγ and C/EBPα in a dose-dependent manner (Figure 3(c)). In addition, the results of the Western blot analysis implied that VN had inhibitory effects on expression of PPARγ and C/EBPα in a dose-dependent manner as well as on the protein levels (Figure 3(d)).

3.5. Comparison of the Effects of the Mixture and the Combination Extract of PG and VN on Differentiation of 3T3-L1 Cells. The cytotoxicity of the PG-VN combination extract was examined using an MTS assay. The MTS assay was performed to assess the effect of the water extract of the 1 : 1 PG-VN combination on 3T3-L1 cell viability. As seen in Figure 4(a), the water extract of the 1 : 1 PG-VN combination showed no significant effect on viability after 48 h treatment at concentrations of 0.5, 1, and 2 mg/mL. Because the highest concentration (2 mg/mL) of 1 : 1 combination extract did not have any toxic effects on 3T3-L1 adipocytes, further investigations were carried out at concentrations of 1 and 2 mg/mL, including PG and VN at a concentration of 1 mg/mL, respectively. Next, in order to identify the differences in adipogenic effects between the mixture (1 : 1 mixture of PG extract and VN extract) and the combination (1 : 1 PG and VN combination extract), a real-time RT-PCR analysis was performed to investigate whether the effects are clearly different. The mixture was prepared by mixing PG extract and VN extract at the same ratio, and the combination was prepared by water extraction of PG and VN as described above. The results of Figure 4(b) show that the combination formula of PG and VN had significantly higher effects on inhibition of PPARγ and C/EBPα than the mixture of PG and VN, possibly providing scientific evidence supporting the prescription of a combination of herbs in KM. Due to this result, further investigations were performed using the PG-VN combination rather than the PG-VN mixture.

3.6. Synergistic Effects of PG-VN Combination Extract on Differentiation of 3T3-L1 Cells. Next, in order to compare the effects of PG and VN with their combination under the same conditions, a real-time RT-PCR assay was carried out. As seen in Figure 5(a), the expressions of PPARγ and C/EBPα were significantly decreased by PG and VN. PG-VN combination at 1 and 2 mg/mL also showed a significant decrease compared with the control. PPARγ expression of the PG-VN combination at 1 and 2 mg/mL was significantly decreased compared with PG. Table 3 indicates that in both PPARγ and C/EBPα, the PG-VN combination may have synergistic action and exhibits enhanced effects at a concentration of 1 mg/mL, since the inhibition rates of PG-VN combination (PPARγ: 35.75 ± 2.07%, C/EBPα: 36.32 ± 4.34%) were higher than the sum of those of PG and VN at 1 mg/mL divided in half (PPARγ: 23.195 ± 3.155%, C/EBPα: 31.92 ± 3.165%), but at higher dose, it did not show any synergism. Instead, the PG-VN combination inhibition rates at 2 mg/mL (PPARγ: 30.19 ± 1.30%, C/EBPα: 39.88 ± 4.15%) were lower than the sum of the 1 mg/mL PG and VN inhibition rates (PPARγ: 46.39 ± 6.31%, C/EBPα: 63.84 ± 6.33%). This suggests the possibility of antagonistic features at higher concentrations. In the case of C/EBPα, the difference in the inhibition rate (23.96 ± 10.48%) was larger than that in PPARγ (16.20 ± 7.61%), and this indicates the antagonism at high concentration was expressed more strongly on C/EBPα than on PPARγ.

To confirm the results shown above regarding protein levels, we compared the effects of PG and VN with their combination using a Western blotting assay. PG and VN at 1 mg/mL showed significant differences compared with the control in both PPARγ and C/EBPα protein expressions (Figure 5(b)). In addition, the PG-VN combination

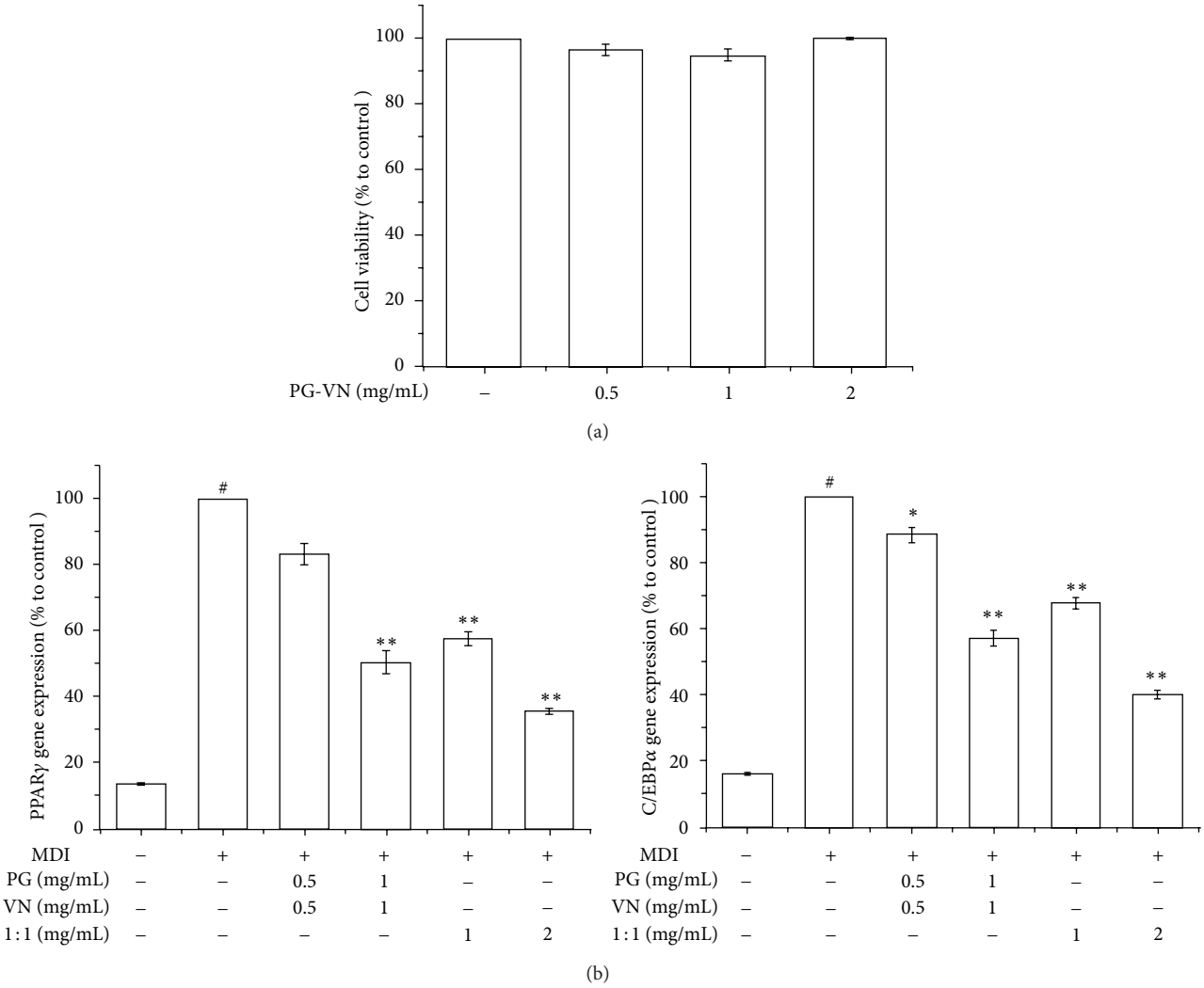

Figure 4: Comparison of the effects of the mixture and the combination extract of PG and VN on differentiation of 3T3-L1 cells. An MTS assay (a) was performed to measure the effects of PG-VN combination in 3T3-L1 cells. A real-time RT-PCR assay was performed to measure the difference between the effects of the combination and the mixture on PPARγ and C/EBPα mRNA expressions in 3T3-L1 cells (b). 3T3-L1 preadipocytes were induced to differentiate with 10% FBS/DMEM medium containing insulin, DEX, IBMX, and 0, 0.01, 0.1, or 1 mg/mL of PG-VN mixture or PG-VN combination for 2 days, and then the culture media were replaced with 10% FBS/DMEM medium containing insulin for the following 2 days. The control was treated with DW instead of extracts. EGCG was used as a positive control. Assays were performed in duplicates for each concentration, and experiments were repeated at least three times. Data represented are the relative expression. All values are mean ± SD. $^{\#}P < 0.05$, versus undifferentiated control cells; $^{*}P < 0.05$ and $^{**}P < 0.005$, versus differentiated control cells; DW, distilled water; PG, *Panax ginseng*; VN, *Veratrum nigrum*; 1 : 1, PG-VN combination.

also exerted a significant decrease on PPARγ and C/EBPα expressions at two different concentrations (1 and 2 mg/mL). Similar to the mRNA expression results (Table 3), the results regarding protein level of both PPARγ and C/EBPα (Table 4) also implied that the PG-VN combination may have synergistic interaction at the concentration of 1 mg/mL, since the inhibition rate of PG-VN combination on PPARγ (28.87 ± 2.25%) was higher than the sum calculation of those on PPARγ of PG and VN at 1 mg/mL divided in half (23.905 ± 4.375%), but the C/EBPα expression (39.61 ± 3.82%) showed antagonistic effects compared with the calculation (42.035 ± 4.44%). The PG-VN combination inhibition rates at 2 mg/mL (PPARγ: 45.22 ± 3.88%, C/EBPα: 59.94 ± 1.94%) were lower than the sum of the 1 mg/mL PG and VN inhibition rates (PPARγ: 47.81 ± 8.75%, C/EBPα: 84.07 ± 8.88%). The difference in the inhibition rate of C/EBPα (24.13 ± 10.82%) was larger than that of PPARγ (2.59±12.63%), suggesting that the antagonism at high concentration was expressed stronger on C/EBPα than on PPARγ, supporting the former gene expression results.

4. Discussion

Many of the most effective phytomedicines are provided on the drug market as whole extracts of herbs, and practitioners have always believed that synergistic interactions between the

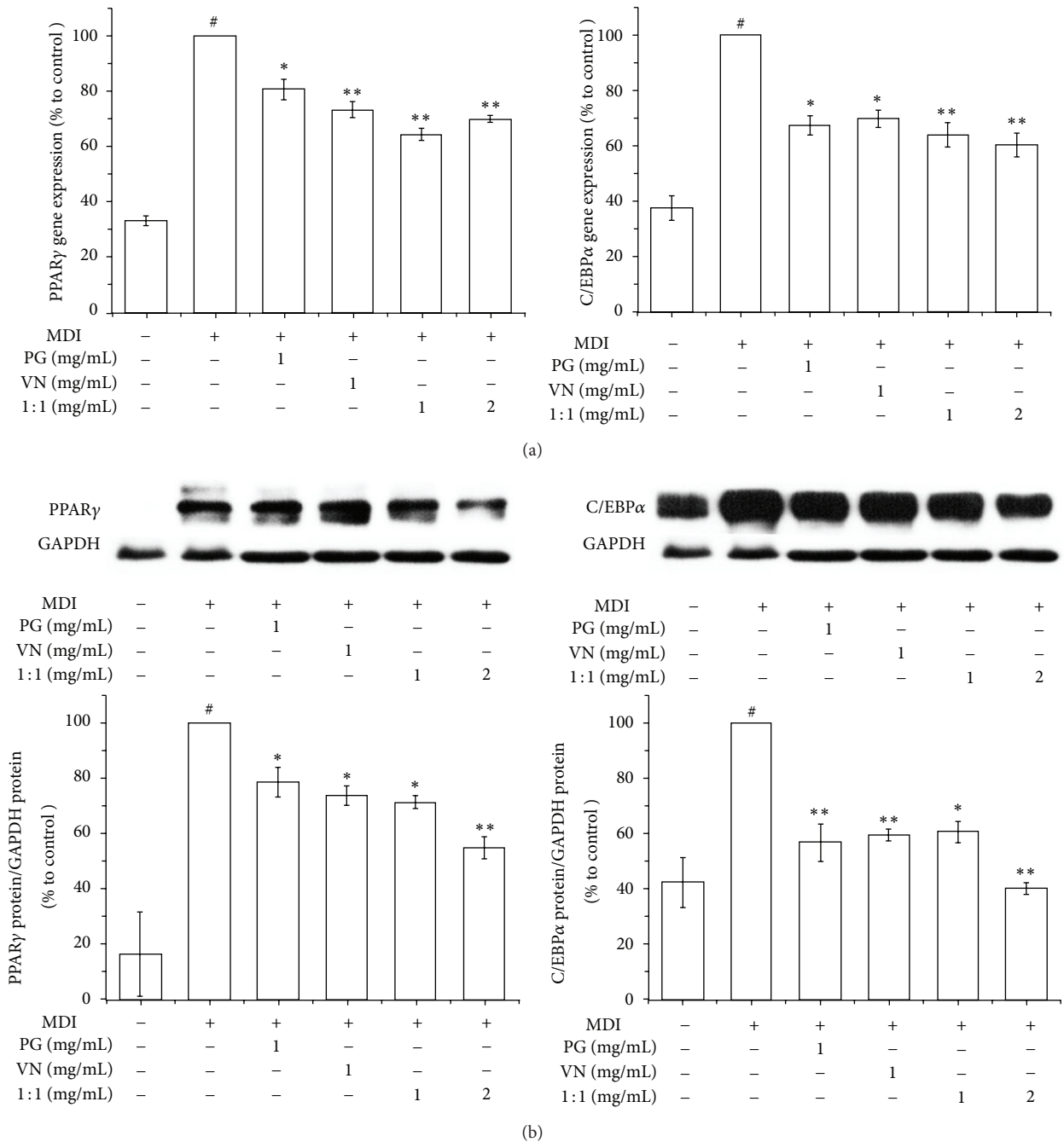

Figure 5: Synergistic effects of PG-VN combination extract on differentiation of 3T3-L1 cells. A real-time RT-PCR assay (a) and Western blot assay (b) were performed to measure the effects of PG-VN combination in 3T3-L1 cells. 3T3-L1 preadipocytes were induced to differentiate by 10% FBS/DMEM medium containing insulin, DEX, IBMX, and 0, 0.01, 0.1, or 1 mg/mL of PG-VN mixture or PG-VN combination for 2 days, and then the culture media were replaced with 10% FBS/DMEM medium containing insulin for the following 2 days. The control was treated with DW instead of extracts. EGCG was used as a positive control. Assays were performed in duplicates for each concentration, and experiments were repeated at least three times. Data represented are the relative expression. All values are mean ± SD. $^{\#}P < 0.05$, versus undifferentiated control cells; $^{*}P < 0.05$ and $^{**}P < 0.005$, versus differentiated control cells; DW, distilled water; PG, *Panax ginseng*; VN, *Veratrum nigrum*; 1:1, PG-VN combination.

components of individual or mixtures of herbs are a vital part of their therapeutic efficacy [40]. KM is characterized by the wide use of herbal formulas, which are capable of systematically treating disease determined by interactions among various herbs. However, the science underlying the combination rule of KM herbal formulas remains a mystery due to a lack of experimental evidence. Although some studies on the interaction between herbs have been performed, most focused on the synergistic interactions, that is, the "Sang-sa" or "Sang-o" relationship [40–46]; studies

Table 3: Inhibition rate of PG, VN, and their combination on gene expression of PPARγ and C/EBPα.

Treatment	PPARγ (%)	C/EBPα (%)
PG 1 mg/mL	$19.54 \pm 3.62^{*}$	$32.92 \pm 3.34^{*}$
VN 1 mg/mL	$26.85 \pm 2.69^{**}$	$30.92 \pm 2.99^{*}$
PG-VN combination 1 mg/mL	$35.75 \pm 2.07^{**a}$	$36.32 \pm 4.34^{**}$
PG-VN combination 2 mg/mL	$30.19 \pm 1.30^{**a}$	$39.88 \pm 4.15^{**}$
^{x}PG + VN	46.39 ± 6.31	63.84 ± 6.33
^{x}(PG + VN)/2	23.195 ± 3.155	31.92 ± 3.165

Values were expressed as means ± SD. $^{*}P < 0.05$, significantly different from the Control; $^{**}P < 0.005$, significantly different from the control; $^{a}P < 0.05$, significantly different from PG. ^{x}Calculated additive response (the sum of the effects of the individual PG and VN treatments). Control, expression of the differentiated 3T3-L1 cells was considered as 0%; PG: *Panax ginseng*; VN: *Veratrum nigrum*.

Table 4: Inhibition rate of PG, VN, and their combination on protein expression of PPARγ and C/EBPα.

Treatment	PPARγ (%)	C/EBPα (%)
PG 1 mg/mL	$21.52 \pm 5.28^{*}$	$43.42 \pm 6.80^{**}$
VN 1 mg/mL	$26.29 \pm 3.47^{*}$	$40.65 \pm 2.08^{**}$
PG-VN combination 1 mg/mL	$28.87 \pm 2.25^{*}$	$39.61 \pm 3.82^{*}$
PG-VN combination 2 mg/mL	$45.22 \pm 3.88^{**ab}$	$59.94 \pm 1.94^{**b}$
^{x}PG + VN	47.81 ± 8.75	84.07 ± 8.88
^{x}(PG + VN)/2	23.905 ± 4.375	42.035 ± 4.44

Values were expressed as means ± SD. $^{*}P < 0.05$, significantly different from the Control; $^{**}P < 0.005$, significantly different from the control; $^{a}P < 0.05$, significantly different from PG; $^{b}P < 0.05$, significantly different from VN. ^{x}Calculated additive response (the sum of the effects of the individual PG and VN treatments). Control, expression of the differentiated 3T3-L1 cells was considered as 0%; PG: *Panax ginseng*; VN: *Veratrum nigrum*.

focusing on antagonism, that is, "Sang-ban" or 'Sang-o," have not yet been published. According to *Shennong's Classic of Materia Medica*, the classic of herbs written in 5 C, VN has a "Sang-ban" relationship with PG. This text does not specify the exact effects when used together, but every herb classic since *Shennong's Classic of Materia Medica* has forbidden usage of PG and VN together [12]. In this study, we investigated the antiobese effects of PG and VN combination, the representative example of "Sang-ban." The effects of PG and VN extracts on obesity are investigated both *in vivo* and *in vitro*, and an investigation of the effects of their combination is followed.

Obesity is a chronic metabolic disorder caused by imbalance between energy intake and expenditure [47]. The prevalence of obesity is increasing in developed countries, and rates in the developing world are rapidly rising as well. The consequences of this are morbidity and mortality associated with other serious medical diseases, such as diabetes, hyperlipidemia, hypertension, cardiovascular diseases, osteoarthritis, and cancer [48]. Current medications for the treatment of obesity include mixed noradrenergic-serotonergic agents (sibutramine) [49] and absorption-reducing agents (orlistat) [50]. However, the usage is limited by their adverse effects. Sibutramine is known to increase blood pressure, which may cause cardiac arrhythmias, constipation, and headache with only minimum weight loss [49]. Orlistat, one of the most widely used obesity treatments, has also been reported to cause steatorrhea and deficiencies in lipid-soluble vitamins and essential fatty acids [50]. Furthermore, the first selective cannabinoid receptor CB1 blocker, rimonabant, was officially withdrawn from the market due to its serious side effects [51]. Interest in natural products for the treatment of obesity is thus rapidly growing. During the last decade, researchers have focused on the discovery of new drugs to reduce obesity, one of the most important health issues of modern society.

In the present study, we have shown the effects of PG, VN, and their combination on obesity in HF diet-induced obese mice and in 3T3-L1 cells. PG, VN, and PG-VN combination significantly reduced weight gain and the fat pad weight in HF induced obese mice. They also significantly decreased lipid accumulation and the expressions of two major adipogenesis factors, PPARγ and C/EBPα, in 3T3-L1 cells. Interestingly, the PG-VN combination had higher effects on PPARγ and C/EBPα than the mixture of postextracted PG and VN. We found that the PG-VN combination had synergistic effects compared with a mixture of the extracts of PG and VN on inhibition of PPARγ and C/EBPα expressions at lower doses. The PG-VN combination at 1 mg/mL showed stronger effects on gene and protein expressions of PPARγ and C/EBPα than the calculated sum of separate PG and VN at 1 mg/mL divided into half. This result may constitute scientific evidence supporting the prescription of a combination of herbs instead of separate herb extraction mixtures in KM. However, because the exact mechanism was not fully revealed in this study, analytical assays such as HPLC should be carried out to investigate the componential differences between the combination and the mixture.

The study also suggests a potentially contentious issue that is unknown and at the same time could be a potential area of KM: the forbidden herb pairs, "Sang-ban," known to have antagonistic effects when used together, introduced in *Shennong's Classic of Materia Medica*. The "Sang-ban" classification has been unquestioned until now, but the present study indicates the possibility of conflicting views. In *Shennong's Classic of Materia Medica*, the medical treatment of PG and VN pair is strictly forbidden [12]. But in this study on obesity, the PG and VN combination showed potential synergism. Obesity is a recently growing modern disease. In the past, weight loss may have been considered as an adverse effect, and this might partly explain the synergistic effects of PG-VN combination on obesity. However, further investigations must be followed. Although we have shown in this study that one of the representative "Sang-ban" pairs, PG and VN, shows synergism with regard to obesity, evidential verification of other pairs of the "Chil-jeong" theory is necessary.

5. Conclusion

In conclusion, the results of this study show the antiobese effects of PG and VN both *in vivo* and *in vitro*. PG, VN, and PG-VN combination significantly reduced weight gain and the fat pad weight in HF-induced obese mice. They also significantly decreased lipid accumulation and the expressions of two major adipogenesis factors, PPARγ and C/EBPα, in

3T3-L1 cells. In addition, PG-VN combination had synergistic effects compared with the mixture of the extract of PG and VN on inhibition of PPARγ and C/EBPα expressions at lower doses. These results show potential for a new pharmaceutical antiobese therapy and at the same time point toward a scientific basis for the usage of combinations in KM. Further investigations on combinations of various herbs should be carried out in future studies.

Authors' Contribution

Seung-Heon Hong and Jae-Young Um equally contributed as corresponding authors.

Acknowledgment

This work was supported by the National Research Foundation of Korea (NRF) Grant funded by the Korea government (MSIP) (nos. 2013R1A2A2A03006068, 2011-0006220, and 2011-0010435).

References

[1] WHO, "Global Strategy on Diet (Physical Activity and Health)," 2009.

[2] D. W. Haslam and W. P. T. James, "Obesity," *Lancet*, vol. 366, no. 9492, pp. 1197–1209, 2005.

[3] I. S. Farooqi and S. O'Rahilly, "Genetic factors in human obesity," *Obesity Reviews*, vol. 8, no. 1, pp. 37–40, 2007.

[4] J. Garrow, "Treatment for obesity," *Lancet*, vol. 351, no. 9115, p. 1590, 1998.

[5] J. A. Pospisilik, D. Schramek, H. Schnidar et al., "Drosophila genome-wide obesity screen reveals hedgehog as a determinant of brown versus white adipose cell fate," *Cell*, vol. 140, no. 1, pp. 148–160, 2010.

[6] P. Tontonoz and B. M. Spiegelman, "Fat and beyond: the diverse biology of PPARγ," *Annual Review of Biochemistry*, vol. 77, pp. 289–312, 2008.

[7] N. Salma, H. Xiao, and A. N. Imbalzano, "Temporal recruitment of CCAAT/enhancer-binding proteins to early and late adipogenic promoters in vivo," *Journal of Molecular Endocrinology*, vol. 36, no. 1, pp. 139–151, 2006.

[8] Q.-Q. Tang, M. Grønborg, H. Huang et al., "Sequential phosphorylation of CCAAT enhancer-binding protein β by MAPK and glycogen synthase kinase 3β is required for adipogenesis," *Proceedings of the National Academy of Sciences of the United States of America*, vol. 102, no. 28, pp. 9766–9771, 2005.

[9] Z. Cao, R. M. Umek, and S. L. McKnight, "Regulated expression of three C/EBP isoforms during adipose conversion of 3T3-L1 cells," *Genes and Development*, vol. 5, no. 9, pp. 1538–1552, 1991.

[10] J. K. Hamm, B. H. Park, and S. R. Farmer, "A role for C/EBPbeta in regulating peroxisome proliferator-activated receptor gamma activity during adipogenesis in 3T3-L1 preadipocytes," *Journal of Biological Chemistry*, vol. 276, no. 21, pp. 18464–18471, 2001.

[11] Z. Wu, E. D. Rosen, R. Brun et al., "Cross-regulation of C/EBP alpha and PPAR gamma controls the transcriptional pathway of adipogenesis and insulin sensitivity," *Molecular Cell*, vol. 3, no. 2, pp. 151–158, 1999.

[12] C. K. Park, "Huangdi's internal classic," 2005.

[13] J. Hur, "Dongeuibogam," 1991.

[14] A. S. Attele, J. A. Wu, and C.-S. Yuan, "Ginseng pharmacology: multiple constituents and multiple actions," *Biochemical Pharmacology*, vol. 58, no. 11, pp. 1685–1693, 1999.

[15] M. O'Hara, D. Kiefer, K. Farrell, and K. Kemper, "A review of 12 commonly used medicinal herbs," *Archives of Family Medicine*, vol. 7, no. 6, pp. 523–536, 1998.

[16] S. N. Yun, S. J. Moon, S. K. Ko, B. O. Im, and S. H. Chung, "Wild ginseng prevents the onset of high-fat diet induced hyperglycemia and obesity in ICR mice," *Archives of Pharmacal Research*, vol. 27, no. 7, pp. 790–796, 2004.

[17] E. A. Sotaniemi, E. Haapakoski, and A. Rautio, "Ginseng therapy in non-insulin-dependent diabetic patients. Effects of psychophysical performance, glucose homeostasis, serum lipids, serum aminoterminalpropeptide concentration, and body weight," *Diabetes Care*, vol. 18, no. 10, pp. 1373–1375, 1995.

[18] A. A. Qureshi, N. Abuirmeileh, and Z. Z. Din, "Suppression of cholesterogenesis and reduction of LDL cholesterol by dietary ginseng and its fractions in chicken liver," *Atherosclerosis*, vol. 48, no. 1, pp. 81–94, 1983.

[19] S.-H. Kim and K.-S. Park, "Effects of Panax ginseng extract on lipid metabolism in humans," *Pharmacological Research*, vol. 48, no. 5, pp. 511–513, 2003.

[20] V. Vuksan and J. L. Sievenpiper, "Herbal remedies in the management of diabetes: lessons learned from the study of ginseng," *Nutrition, Metabolism and Cardiovascular Diseases*, vol. 15, no. 3, pp. 149–160, 2005.

[21] A. R. Toogood, "Gardener's Encyclopedia of Perennials," 1989.

[22] D. G. Barceloux, "Medical Toxicology of Natural Substances," 2008.

[23] H. Wang, S.-Y. Li, C.-K. Zhao, and X. Zeng, "A system for screening agonists targeting β2- adrenoceptor from Chinese medicinal herbs," *Journal of Zhejiang University*, vol. 10, no. 4, pp. 243–250, 2009.

[24] L. Wang, W. Li, and Y. Liu, "Hypotensive effect and toxicology of total alkaloids and veratramine from roots and rhizomes of *Veratrum nigrum* L. in spontaneously hypertensive rats," *Pharmazie*, vol. 63, no. 8, pp. 606–610, 2008.

[25] Z.-Z. Wang, W.-J. Zhao, X.-S. Zhang et al., "Protection of *Veratrum nigrum* L. var. ussuriense *Nakai alkaloids* against ischema-reperfusion injury of the rat liver," *World Journal of Gastroenterology*, vol. 13, no. 4, pp. 564–571, 2007.

[26] R. Jin, B. Zhang, C.-M. Xue, S.-M. Liu, Q. Zhao, and K. Li, "Classification of 365 Chinese medicines in Shennong's Materia Medica Classic based on a semi-supervised incremental clustering method," *Journal of Chinese Integrative Medicine*, vol. 9, no. 6, pp. 665–674, 2011.

[27] B. Pitt, G. B. John Mancini, S. G. Ellis, H. S. Rosman, J.-S. Park, and M. E. McGovern, "Pravastatin limitation of atherosclerosis in the coronary arteries (PLAC I): reduction in atherosclerosis progression and clinical events," *Journal of the American College of Cardiology*, vol. 26, no. 5, pp. 1133–1139, 1995.

[28] W. T. Friedewald, R. I. Levy, and D. S. Fredrickson, "Estimation of the concentration of low-density lipoprotein cholesterol in plasma, without use of the preparative ultracentrifuge," *Clinical Chemistry*, vol. 18, no. 6, pp. 499–502, 1972.

[29] D. C. Woods, C. Alvarez, and A. L. Johnson, "Cisplatin-mediated sensitivity to TRAIL-induced cell death in human granulosa tumor cells," *Gynecologic Oncology*, vol. 108, pp. 632–640, 2008.

[30] J. L. Ramirez-Zacarias, F. Castro-Munozledo, and W. Kuri-Harcuch, "Quantitation of adipose conversion and triglycerides by staining intracytoplasmic lipids with oil red O," *Histochemistry*, vol. 97, no. 6, pp. 493–497, 1992.

[31] M. M. Bradford, "A rapid and sensitive method for the quantitation of microgram quantities of protein utilizing the principle of protein dye binding," *Analytical Biochemistry*, vol. 72, no. 1-2, pp. 248–254, 1976.

[32] J. Shepherd, S. M. Cobbe, I. Ford et al., "Prevention of coronary heart disease with pravastatin in men with hypercholesterolemia," *New England Journal of Medicine*, vol. 333, no. 20, pp. 1301–1307, 1995.

[33] F. M. Sacks, M. A. Pfeffer, L. A. Moye et al., "The effect of pravastatin on coronary events after myocardial infarction in patients with average cholesterol levels," *New England Journal of Medicine*, vol. 335, no. 14, pp. 1001–1009, 1996.

[34] J. R. Downs, M. Clearfield, S. Weis et al., "Primary prevention of acute coronary events with lovastatin in men and women with average cholesterol levels: results of AFCAPS/TexCAPS," *Journal of the American Medical Association*, vol. 279, no. 20, pp. 1615–1622, 1998.

[35] F. Paccaud, V. Schlüter-Fasmeyer, V. Wietlisbach, and P. Bovet, "Dyslipidemia and abdominal obesityan assessment in three general populations," *Journal of Clinical Epidemiology*, vol. 53, no. 4, pp. 393–400, 2000.

[36] N.-H. Kim, S.-K. Choi, S.-J. Kim et al., "Green tea seed oil reduces weight gain in C57BL/6J mice and influences adipocyte differentiation by suppressing peroxisome proliferator-activated receptor-γ," *Pflugers Archiv European Journal of Physiology*, vol. 457, no. 2, pp. 293–302, 2008.

[37] L. Fajas, "Adipogenesis: a cross-talk between cell proliferation and cell differentiation," *Annals of Medicine*, vol. 35, no. 2, pp. 79–85, 2003.

[38] E. D. Rosen, C. J. Walkey, P. Puigserver, and B. M. Spiegelman, "Transcriptional regulation of adipogenesis," *Genes and Development*, vol. 14, no. 11, pp. 1293–1307, 2000.

[39] D. Shao and M. A. Lazar, "Peroxisome proliferator activated receptor γ, CCAAT/enhancer-binding protein α, and cell cycle status regulate the commitment to adipocyte differentiation," *Journal of Biological Chemistry*, vol. 272, no. 34, pp. 21473–21478, 1997.

[40] E. M. Williamson, "Synergy and other interactions in phytomedicines," *Phytomedicine*, vol. 8, no. 5, pp. 401–409, 2001.

[41] G. Wei and X. Zheng, "A survey of the studies on compatible law of ingredients in Chinese herbal prescriptions," *Journal of Traditional Chinese Medicine*, vol. 28, no. 3, pp. 223–227, 2008.

[42] S. Li, B. Zhang, D. Jiang, Y. Wei, and N. Zhang, "Herb network construction and co-module analysis for uncovering the combination rule of traditional Chinese herbal formulae," *BMC Bioinformatics*, vol. 11, no. 11, supplement, article S6, 2010.

[43] S. Su, Y. Hua, Y. Wang et al., "Evaluation of the anti-inflammatory and analgesic properties of individual and combined extracts from *Commiphora myrrha*, and *Boswellia carterii*," *Journal of Ethnopharmacology*, vol. 139, no. 2, pp. 649–656, 2012.

[44] H. Wagner and G. Ulrich-Merzenich, "Synergy research: approaching a new generation of phytopharmaceuticals," *Phytomedicine*, vol. 16, no. 2-3, pp. 97–110, 2009.

[45] H. Wagner, "Synergy research: a new approach to evaluating the efficacy of herbal mono-drug extracts and their combinations," *Natural Product Communications*, vol. 4, no. 2, pp. 303–304, 2009.

[46] H. Wagner, "Synergy research: approaching a new generation of phytopharmaceuticals," *Fitoterapia*, vol. 82, no. 1, pp. 34–37, 2011.

[47] B. M. Spiegelman and J. S. Flier, "Obesity and the regulation of energy balance," *Cell*, vol. 104, no. 4, pp. 531–543, 2001.

[48] A. H. Mokdad, E. S. Ford, B. A. Bowman et al., "Prevalence of obesity, diabetes, and obesity-related health risk factors, 2001," *Journal of the American Medical Association*, vol. 289, no. 1, pp. 76–79, 2003.

[49] C. A. Luque and J. A. Rey, "Sibutramine: a serotonin-norepinephrine reuptake-inhibitor for the treatment of obesity," *Annals of Pharmacotherapy*, vol. 33, no. 9, pp. 968–978, 1999.

[50] A. M. Heck, J. A. Yanovski, and K. A. Calis, "Orlistat, a new lipase inhibitor for the management of obesity," *Pharmacotherapy*, vol. 20, no. 3, pp. 270–279, 2000.

[51] C. E. Leite, C. A. Mocelin, G. O. Petersen, M. B. Leal, and F. V. Thiesen, "Rimonabant: an antagonist drug of the endocannabinoid system for the treatment of obesity," *Pharmacological Reports*, vol. 61, no. 2, pp. 217–224, 2009.

Hindawi Publishing Corporation
Evidence-Based Complementary and Alternative Medicine
Volume 2013, Article ID 976270, 8 pages
http://dx.doi.org/10.1155/2013/976270

Research Article

Dangguijakyak-San Protects against 1-Methyl-4-phenyl-1,2,3,6,-tetrahydropyridine-Induced Neuronal Damage via Anti-Inflammatory Action

Deok-Sang Hwang,[1] Hyo Geun Kim,[2] Jun-Bock Jang,[1] and Myung Sook Oh[2]

[1] *Department of Oriental Gynecology, College of Korean Medicine, Kyung Hee University, No. 1 Hoegi-dong, Dongdaemun-gu, Seoul 130-701, Republic of Korea*
[2] *Department of Oriental Pharmaceutical Science and Kyung Hee East-West Pharmaceutical Research Institute, College of Pharmacy, Kyung Hee University, No. 1 Hoegi-dong, Dongdaemun-gu, Seoul 130-701, Republic of Korea*

Correspondence should be addressed to Myung Sook Oh; msohok@khu.ac.kr

Received 30 March 2013; Revised 30 July 2013; Accepted 31 July 2013

Academic Editor: Chang Shik Yin

Dangguijakyak-san (DJS), a famous traditional Korean multiherbal medicine, has been used to treat gynecological and neuro-associated disease. Recent studies demonstrated that DJS has multiple bioactivities including neuroprotection. In the present study, we were to investigate the effect of DJS and its mechanism in an *in vitro* and *in vivo* model of Parkinson's disease (PD). In primary mesencephalic culture system, DJS attenuated the dopaminergic cell damage induced by 1-methyl-4-phenylpyridine toxicity, and it inhibited production of inflammatory factors such as tumor necrosis factor α (TNF-α), nitric oxide (NO), and activation of microglial cells. Then, we confirmed the effect of DJS in a mouse PD model induced by 1-methyl-4-phenyl-1,2,3,6-tetrahydropyridine (MPTP). In the pole test, DJS at 50 mg/kg/day for 5 days showed increase of motor activity showing shortened time to turn and locomotor activity compared with the MPTP only treated mice. In addition, DJS significantly protected nigrostriatal dopaminergic neuron from MPTP stress. Moreover, DJS showed inhibition of gliosis in the substantia nigra pars compacta. These results have therapeutic implications for DJS in the treatment of PD via anti-inflammatory effects.

1. Introduction

One of most common neurodegenerative diseases is Parkinson's disease (PD), which is characterized pathologically by the selective, irreversible loss of dopaminergic (DA) neurons in the substantia nigra pars compacta (SNpc) and their terminals in the striatum and clinically by bradykinesia, resting tremor, rigidity, and disturbances in posture and gait [1].

The initial factors that cause neuronal death remain unclear. Studies have suggested that the pathology of PD involves oxidative stress [2, 3], apoptotic mechanisms [4], mitochondrial dysfunction [5], and the accumulation of toxic protein [6, 7]. Other studies have shown that dopaminergic neuronal death is related to inflammatory processes involving increases in inflammatory mediators, including tumor necrosis factor-α (TNF-α), interleukin-1β, and interferon-γ [8, 9], and the activation of glial cells [10]. Recent studies have suggested that anti-inflammatory therapy might be an effective therapeutic strategy for neuroprotection [11].

Dangguijakyak-san (DJS), also called Danggui-Shaoyao-San (DSS) or Toki-shakuyaku-san (TJ-23), is a widely used traditional Korean herbal medicine consisting of Paeoniae Radix, Cnidium Rhizome, Alismatis Rhizoma, Angelicae Gigantis Radix, Poria, and Atractylodis Rhizoma Alba. In biological studies, DJS has hormone-like [12], antianemia [13], and antihypertensive [14] effects. Also, DJS stimulated progesterone production in rat luteal cells and luteal steroidogenesis [15], improved the quality of life of postmenopausal women in Korea [16], and improved motor activity after peripheral facial nerve axotomy [17]. Additionally, studies have revealed that DJS has neuro-associated actions; DJS

attenuated cognition problems and had regulatory effects on the central cholinergic nervous system in scopolamine-treated mice [18], DJS protected cortical neurons against amyloid β-induced neurotoxicity [19], and DJS improved cognitive function and protected ultrastructure of brain cortex in aged mice [20]. Moreover, DJS protected dopaminergic cells from hydrogen peroxide and 6-hydroxydopamine-induced neurotoxicity *in vitro* and against 1-methyl-4-phenyl-1,2,3,6,-tetrahydropyridine- (MPTP-) induced damage in estrogen-deprived mice by inhibiting oxidative stress such as reactive oxygen species production and glutathione level depletion and suppressing apoptosis through mitochondria-mediated caspase pathway [21–23].

Based on those actions of DJS, we hypothesized that DJS might be a potent neuroprotective agent in PD model. However, the effect of DJS on neuroinflammation, one of therapeutic target for PD, has not been investigated yet in animal models. Therefore, we examined the protective effect of DJS against 1-methyl-4-phenylpyridinium- (MPP+-) induced neurotoxicity and explored its possible mechanisms by measuring inflammatory factors in rat primary dopaminergic cells. Then, we confirmed the protective effect of DJS in a mouse model of PD by performing behavioral tests and a histological analysis.

2. Materials and Methods

2.1. Materials. Minimal essential medium (MEM) and fetal bovine serum (FBS) were purchased from Gibco Industries (Auckland, New Zealand). Glucose, L-glutamine, paraformaldehyde (PFA), MPTP, MPP+, poly-L-lysine (PLL), 3,3-diaminobenzidine (DAB), Griess reagent, sodium chloride, sucrose, and phosphate-buffered saline (PBS) were purchased from Sigma-Aldrich (St. Louis, MO, USA). The rat tumor necrosis factor-alpha (TNF-α) ELISA kit was purchased from Invitrogen (Carlsbad, CA, USA). Affinity-purified rabbit anti-tyrosine hydroxylase (TH) polyclonal antibody, mouse and rat anti macrophage-1 antigen integrin alpha M (MAC-1) affinity-purified monoclonal antibody, and rabbit anti glial fibrillary acidic protein (GFAP) affinity-purified monoclonal antibody were obtained from Merck Millipore (Billerica, MA, USA). Biotinylated anti-rabbit, anti-mouse, and anti-rat antibodies, normal goat serum, and a standard avidin-biotin peroxidase complex (ABC) kit were purchased from Vector Laboratories (Burlingame, CA, USA). The DJS extract was the same as that used in previous studies [22, 23].

2.2. Primary Culture of Mesencephalic Dopaminergic Cells. Cultures were prepared from the mesencephalons of gestational day 14 embryos from Sprague-Dawley rats, obtained from Dae Han Biolink (Eumseong, Korea). The ventral mesencephalon was separated, dissected, pooled, dissociated, and plated on 24-well plates with coverslips precoated with PLL at a density of 1.5×10^5 cells per well. Cultures were maintained in a humidified incubator in an atmosphere of 5% CO_2 in air at 37°C in MEM with 6.0 g/L glucose, 2 mM glutamine, and 10% FBS. On the 6th day *in vitro* (DIV 6), the medium was changed to serum-free MEM, and the cells were treated with DJS (0.04 or 0.2 μg/mL) for 1 h and then stressed with MPP+ (15 μM) for 23 h. Then, the cells were fixed with 4% PFA at room temperature for 30 min. The cells were stored in PBS at 4°C for immunocytochemistry.

2.3. NO Assay. The accumulation of nitrite in the culture supernatant was determined with a colorimetric assay using Griess reagent (0.1% N-(1-naphthyl) ethylenediamine dihydrochloride, 1% sulfanilamide, and 2.5% H_3PO_4). Equal volumes of culture supernatant and Griess reagent were mixed and incubated for 10 min at room temperature in the dark. The absorbance at 540 nm was determined spectrophotometrically (SpectraMax Gemini EM; Molecular Devices, Sunnyvale, CA, USA). The NO concentration was determined from the sodium nitrite standard curve. Control cells were treated in the same way without DJS and MPP+, and the absorbances were expressed as percentages of the control.

2.4. TNF-α Assay. The TNF-α assay was performed in accordance with the manufacturer's instructions. Briefly, 50 μL of culture supernatant was mixed with 50 μL of incubation buffer. To all samples, 50 μL of standard diluent buffer was added. These samples were pipetted with 50 μL of biotin conjugate, and the side of the plate was tapped gently to mix it. The plates were incubated for 60 min with a plate cover at room temperature. After aspirating the liquid, all wells were washed four times. Then, 100 μL of streptavidin-horseradish peroxide working solution was added and incubated for 45 min with a plate cover at room temperature. After aspiration and washing, 100 μL of stabilized chromogen was added to the wells. The plates were allowed to stand for 30 min at room temperature in the dark. Next, 100 μL of stop solution was added, and the side of the plate was tapped gently to mix it. The plates were read using a spectrophotometer at 450 nm. The standard smooth curve was plotted with fitting software using a four-parameter algorithm, and the data are expressed as standard rat TNF-α (pg/μL).

2.5. Animals. Animal maintenance and treatment were carried out in accordance with the Principles of Laboratory Animal Care (NIH publication number 85-23, revised 1985) and the Animal Care and Use Guidelines of Kyung Hee University, Seoul, Korea. Eight-week-old male C57BL/6 mice were purchased from Dae Han Biolink. The animals were housed at an ambient temperature of 23 ± 1°C and relative humidity 60 ± 10% under a 12 h light/dark cycle and were allowed free access to water and food.

2.6. Drug Administration. Animals were assigned to three groups: (1) control (n = 9; intraperitoneal and intraoral vehicle); (2) MPTP (n = 9; intraperitoneal MPTP plus intraoral vehicle); and (3) MPTP + DJS (n = 9; intraperitoneal MPTP plus intraoral DJS) groups. DJS dissolved in saline was administered at 50 mg/kg/day for 5 days. MPTP (base form) in normal saline was injected at 20 mg × 4/kg/day at 2 h intervals for the last day of DJS treatment.

2.7. Behavioral Test and Brain Tissue Preparation. To measure motor coordination, we performed the pole test the day after the last MPTP injection. The mouse was placed head upward

near the top of a vertical rough-surfaced pole (diameter 8 mm, height 55 cm). The times it took for the mouse to turn completely downward (time to turn; T-turn) and then to reach the floor (locomotion activity time; T-LA) were recorded, with a cut-off limit of 30 s. Then, mice were sacrificed on the first and seventh days to quantify inflammatory and dopaminergic factors, respectively. The mice were anesthetized with 50 mg/kg Zoletil (intramuscularly) and rapidly perfused transcardially with PBS, followed by 4% PFA in 0.1 M phosphate buffer (PB). Then, the brains were removed rapidly, postfixed in 4% PFA solution, and processed for cryoprotection in 30% sucrose at 4°C. The frozen brains were cut into 30 μm coronal sections using a cryostat microtome (CM3000; Leica, Wetzlar, Germany). Finally, the tissues were stored in storing solution containing glycerin, ethylene glycol, and PB at 4°C for immunohistochemistry.

2.8. Immunocytochemistry and Immunohistochemistry. Primary cells on cover slips and free-floating sections were rinsed in PBS at room temperature before immunostaining. They were pretreated with 1% hydrogen peroxide in PBS for 15 min to remove endogenous peroxidase activity. Then, they were incubated overnight at room temperature with a rabbit anti-TH antibody (1 : 2,000 dilution) to detect dopaminergic neurons, a mouse or rat anti-MAC-1 antibody (1 : 1000 dilution) to detect microglial cells, and a rabbit anti-GFAP antibody (1 : 1000 dilution) to detect astrocytes. Next, they were incubated with a biotinylated antisecondary IgG for 90 min and then in ABC solution for 1 h at room temperature. The peroxidase activity was visualized with DAB for 4 min. After every incubation step, the cells and tissues were washed three times with PBS. Finally, the primary cells on cover slips were mounted on gelatin-coated glass slides, air dried, and photographed through a microscope (Axioskop 2; Carl Zeiss, Göttingen, Germany). The free-floating brain tissues were mounted on gelatin-coated slides, dehydrated, cleared with xylene, and cover slipped using Histomount medium. To quantify the effect of DJS on the mesencephalic dopaminergic and microglial cells, TH- and MAC-1-immunopositive cells were counted on at least four cover slips from independent experiments for each condition. The effect of DJS on brain tissues was quantified by counting the number of TH-immunopositive cells in the SNpc at ×100 magnification under a microscope. The TH-immunoreactivity in the striatum (ST) was measured at ×40 magnification using a Stereo Investigator (MBF Bioscience, Williston, ND, USA). The anti-inflammatory effects of DJS were visualized with MAC-1 and GFAP-immunopositivity in the SNpc at ×400 magnification under a microscope. Data are presented as percentages of control group values.

2.9. Statistical Analysis. The data are expressed as means ± standard errors of the mean (SEM). Data were analyzed by one-way analysis of variance (ANOVA) followed by the least significant differences (LSD) using SPSS 12.0 K for Windows (SPSS, Chicago, USA). For all statistical analyses, $P < 0.05$ was considered significant.

3. Results

3.1. DJS Protects Dopaminergic Cells against MPP+-Induced Toxicity in Rat Primary Mesencephalic Culture System. To investigate the effect of DJS on neuroprotection against MPP+ toxicity in mesencephalic neuronal cells, we counted dopaminergic cells. MPP+ neurotoxicity was defined as a 66.20% reduction in the survival rate compared with the control group. Treatment with 0.04 and 0.2 μg/m DJS L increased the survival of dopamine cells to 85.05 and 90.25%, respectively, compared with the control group (Figure 1).

3.2. DJS Inhibits Gliosis Induced by MPP+ in Rat Primary Mesencephalic Culture System. To determine the protective effect of DJS on MPP+-induced microglia activation, we counted MAC-1-positive cells. Treatment with 15 μM MPP+ increased active microglia cells by 211.76% compared with the control group, whereas treatment with 0.04 and 0.2 μg/mL DJS significantly inhibited it to 128.29 and 126.64%, respectively, compared with the controls (Figure 2).

3.3. DJS Inhibits Neuroinflammation Induced by MPP+ in Rat Primary Mesencephalic Culture System. To assess the protective effect of DJS on MPP+-induced neuroinflammation involving NO and TNF-α production, Griess reagent and a rat TNF-α ELISA kit were used, respectively. The incubation of cells with 15 μM MPP+ increased NO production by 134.48% compared with the control group, whereas treatment with 0.04 and 0.2 μg/mL DJS significantly decreased it to 119.37 and 118.44%, respectively, compared with the control (Figure 3(a)). Additionally, treatment with MPP+ increased the TNF-α level by 214.13% compared with the control, whereas the 0.04 and 0.2 μg/mL DJS treatments inhibited TNF-α production by 158.57 and 152.63%, respectively (Figure 3(b)).

3.4. DJS Protects Movement Impairment Induced by MPTP in a Mouse Model of PD. To examine whether DJS could relieve the motor symptoms in the MPTP-induced mouse PD model, we performed the pole test. In this test, the MPTP-only treated group showed bradykinesia, with the time to turn at the top (T-turn) and time to climb down (T-LA) prolonged by 254.90 and 187.90%, respectively, compared with the control. However, DJS treatment at 50 mg/kg/day for 5 days reduced this to 100.78 and 99.60%, respectively, compared to the control (Figure 4).

3.5. DJS Protects Dopaminergic Neuronal Damage and Gliosis Induced by MPTP in a Mouse Model of PD. The protective effects of DJS on dopaminergic neurons in a mouse PD model induced by MPTP were also investigated. Seven days after MPTP treatment, the number of TH-positive cell bodies in the SNpc was decreased by 35.91%, and the optical density of the TH-positive fibers in the ST was decreased by 41.45%. The administration of DJS at 50 mg/kg/day for 5 days protected the nigrostriatal dopaminergic neurons, reducing loss by 49.69 and 84.89% in the SNpc and ST, respectively, compared with the control (Figure 5). Additionally, we found that

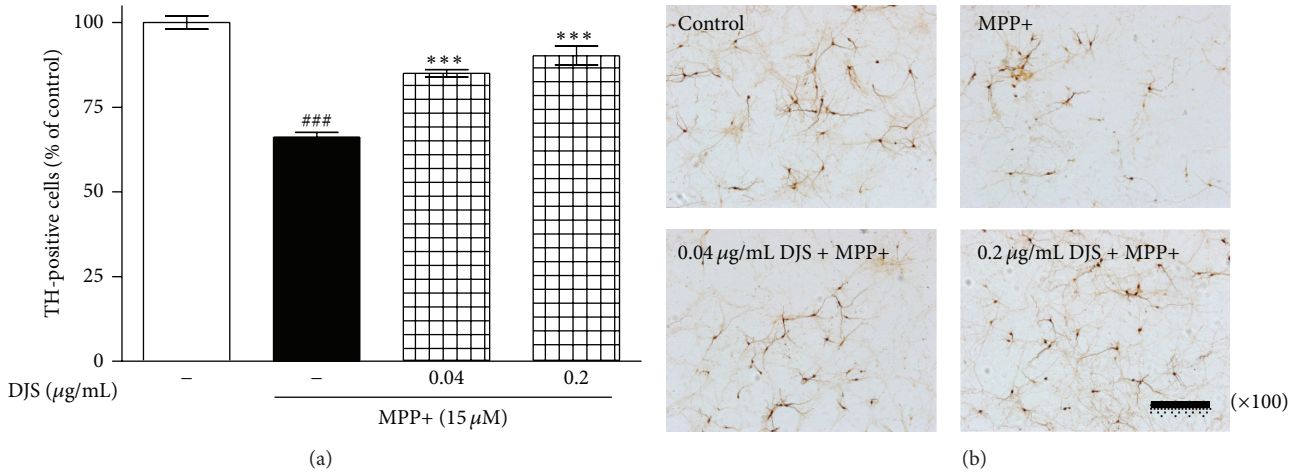

FIGURE 1: Protective effect of DJS against MPP+ neurotoxicity in primary mesencephalic cells. After cells were treated with DJS and 15 μM MPP+, dopaminergic neurons were stained with a TH antibody. The number of TH-positive cells was counted (a) and the representative images were shown (b). Scale bar = 100 μm. Each column represents the mean ± SEM from four replications. Data are expressed as percentages relative to the controls. $^{###}P < 0.001$ significantly different from the control group. $^{***}P < 0.001$ significantly different from the MPP+ only treated group.

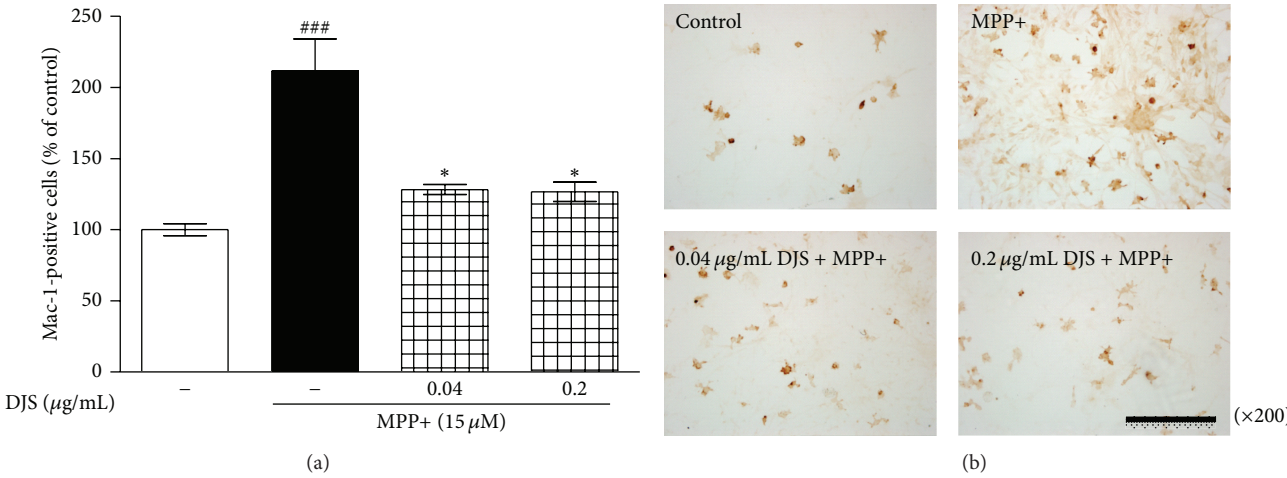

FIGURE 2: Inhibitory effect of DJS on MPP+-induced gliosis in primary mesencephalic cells. After cells were treated with DJS and 15 μM MPP+, microglia cells were stained with a Mac-1 antibody. The number of Mac-1-positive cells was counted (a), and the representative images were shown (b). Scale bar = 200 μm. Each column represents the mean ± SEM from four replications. Data are expressed as percentages relative to the controls. $^{###}P < 0.001$ significantly different from the control group. $^{*}P < 0.05$ significantly different from the MPP+ only treated group.

MAC-1- and GFAP-immunopositive cells were increased in the MPTP only treated group, whereas they were decreased in the DJS treatment group (Figure 6). These results show that DJS reversed the toxic effect of MPTP on neuronal cells by inhibiting inflammatory factors.

4. Discussion

This study evaluated the neuroprotective effects of DJS against MMP+/MPTP toxicity and the mechanism of the effect. The treatment of DJS led to significant neuroprotection of dopaminergic neurons against MMP+/MPTP-induced stress and inhibited microglia activation and inflammatory factor production *in vitro* and *in vivo*. To understand the mechanism of therapy, it is important to study microglial activation in the pathogenesis of PD. It has been reported that activated microglia cells actively participate in the pathogenesis of MPTP-induced PD via the release of cytotoxic factors [24]. We observed that exposure to MPP+ resulted in a significant increase in the proinflammatory factors MAC-1, NO, and TNF-α in the cultures and altered cell morphology. The elevation of MAC-1, which is expressed exclusively on microglia in the central nervous system, has been reported in the MPTP model of PD [25]. Furthermore, MAC-1 contributes to the MPP+/MPTP-induced reactive microgliosis and progressive dopaminergic neurodegeneration, so inhibiting microglial cells might constitute a novel microglia-suppressive therapy for the treatment of PD [26].

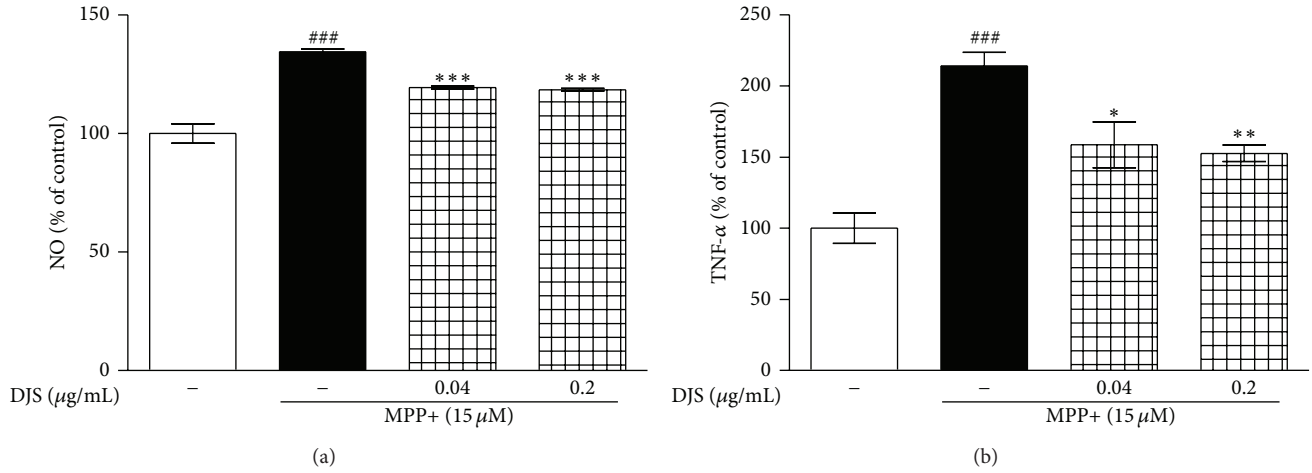

Figure 3: Inhibitory effects of DJS on MPP+-induced NO and TNF-α productions in primary mesencephalic cells. After cells were treated with DJS and 15 μM MPP+, the supernatants were activated with Griess reagent and rat TNF-α ELISA kit. The nitrite contents (a) and TNF-α level (b) were determined. Each column represents the mean ± SEM from four replications. Data are expressed as percentages relative to the controls. $^{###}P < 0.001$ significantly different from the control group. $^{***}P < 0.001$, $^{**}P < 0.01$, and $^{*}P < 0.05$ significantly different from the MPP+ only treated group.

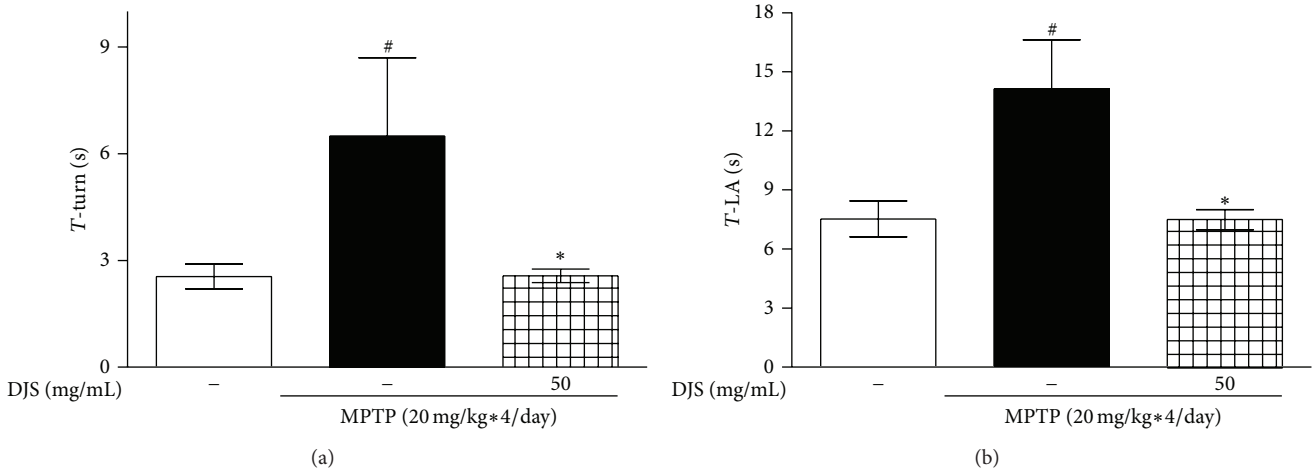

Figure 4: Inhibitory effect of DJS on MPTP-induced bradykinesia in a mouse model of PD. DJS at 50 mg/kg/day for 5 days was administered, and MPTP at 20 mg/kg was injected four times at 2 h interval on the day of last DJS treatment. On the first day of MPTP injection, the pole test was performed. The times to turn (T-LA) and the times to completely downward and to arrive at the floor (b) were recorded. Each column represents the mean ± SEM from ten replications. Data are expressed as percentages relative to the controls. $^{###}P < 0.001$ significantly different from the control group. $^{***}P < 0.001$, $^{*}P < 0.05$ significantly different from the MPTP only treated group.

In this study, DJS inhibited MAC-1 against MPP+-induced gliosis. We performed a TNF-α assay to investigate whether DJS exerts anti-inflammatory activity on mesencephalic dopaminergic cells. TNF-α might damage dopaminergic cells directly by activating an intracellular death pathway, leading to the production of toxic amounts of NO [11]. The NO levels were determined to assess the effects of DJS on NO generation. Mesencephalic dopaminergic cells exposed to MPP+ generated increased NO, whereas DJS treatment significantly reduced this enhancement. The pathogenesis of PD involves impaired mitochondrial function, inflammation, and oxidative damage [27]. Free radicals such as reactive oxidative species (ROS) and NO can cause oxidative damage, which can attenuate microglia proliferation [28]. Furthermore, excessive NO production in the brain contributes to the neuronal energy deficiency in PD [29]. In the primary mesencephalic culture treated with MPP+, DJS attenuated the loss of TH-positive neurons and decreased the generation of MAC-1-positive cells, TNF-α, and NO.

Furthermore, we performed the pole test to determine the effect of DJS on the behavior symptoms of PD. We used C57BL/6 mice, which are susceptible to MPTP toxicity and are useful for studying the protective and compensatory mechanisms of PD [30]. In the pole test, T-turn and T-LA were prolonged significantly in the MPTP-treated mice, whereas they were shortened significantly in the mice treated

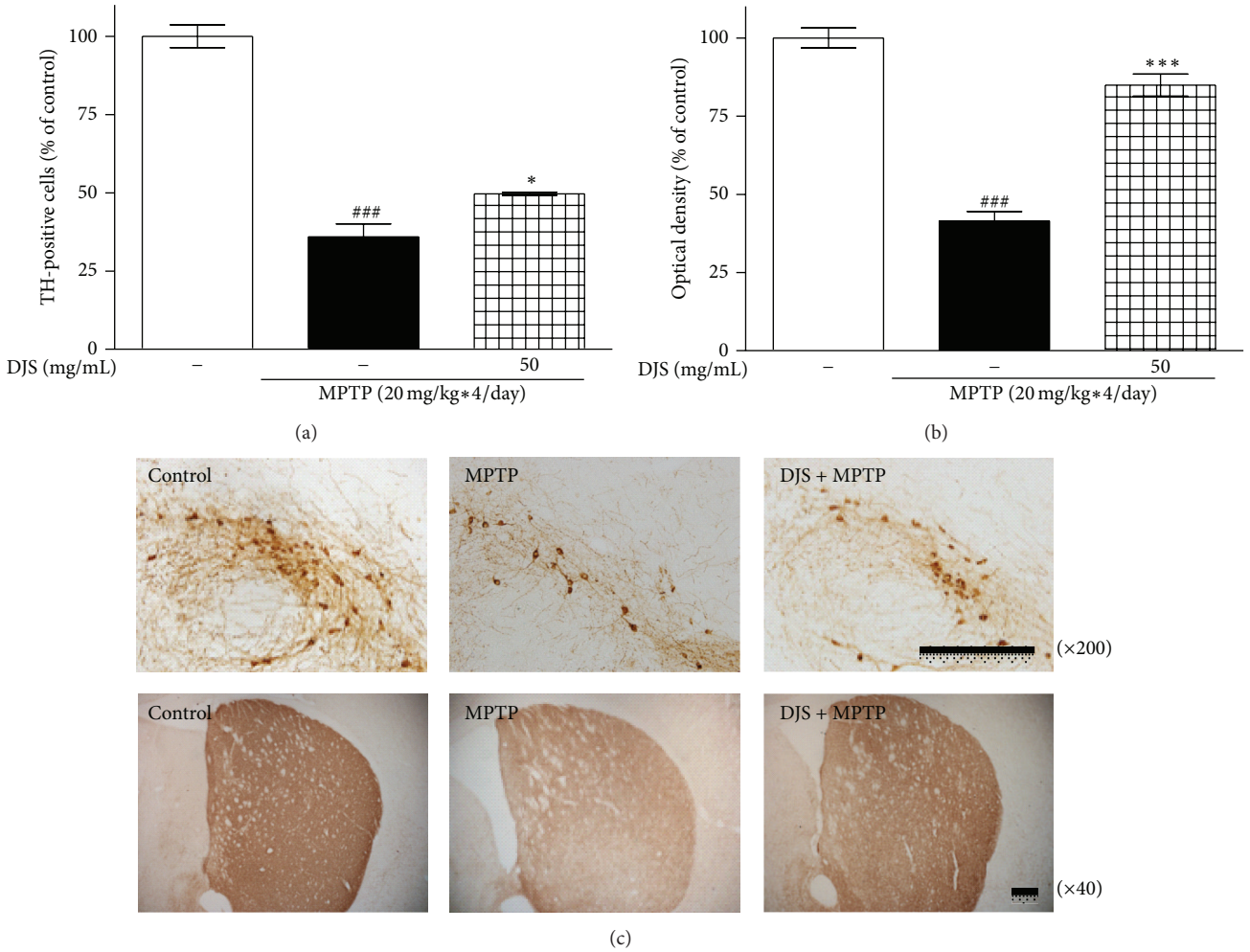

Figure 5: Protective effect of DJS on MPTP-induced dopaminergic neuronal damage in a mouse model of PD. DJS at 50 mg/kg/day for 5 days was administered, and MPTP at 20 mg/kg was injected four times at 2 h interval on the day of last DJS treatment. On the seventh day of MPTP injection, dopaminergic neurons and fibers in the SNpc and the ST, respectively, were stained with a TH antibody. The number of TH-positive cell bodies was counted (a), and the optical density of TH-positive fibers was measured (b). The representative images were shown (c). Scale bar = 100 μm. Each column represents the mean ± SEM from six replications. Data are expressed as percentages relative to the controls. $^{###}P < 0.001$ significantly different from the control group. $^{***}P < 0.001$, $^{*}P < 0.05$ significantly different from the MPTP only treated group.

with DJS before MPTP. The pole test is a measure of bradykinesia and is very sensitive to nigrostriatal dysfunction [31, 32]. We also demonstrated that DJS can protect against behavior problems in ovariectomized mice [23]. It was reported that herbs containing Paeoniae Radix improved the movement disorder [33]. As DJS contains Paeoniae Radix, DJS likely inhibited the toxic effect of MPTP, that is, bradykinesia. DJS improved behavior, which is in agreement with the findings using the Morris water maze test and step-down passive avoidance test [34].

In mice, the anti-inflammatory actions of DJS resulted in a significant decrease in dopaminergic cell death induced by MPTP. Activated microglia and reactive astrocytes to a lesser extent are found in the area associated with cell loss, possibly contributing to the inflammatory process by the release of proinflammatory prostaglandins or cytokines [31]. In the MPTP-treated mice, severe shrinkage of the cell bodies and a decrease in dopaminergic cells and optical density were observed in the SNpc and ST. By contrast, the dopaminergic cells in the DJS mice remained intact. Additionally, MPTP increased striatal astrocytes and microglial cells in the SNpc, whereas DJS treatment attenuated the two markers of activated microglia. These results show that DJS reversed the toxic effect of MPTP on neuronal cells in the SNpc.

Our study showed that DJS has a neuroprotective effect on dopaminergic cells via anti-inflammatory effects. Recently, it was reported that DJS has an antidiabetic effect via its antioxidative properties [35]. Previously, we showed that DJS protects against the glutathione decrease induced by 6-OHDA and inhibits ROS production [22]. We also reported that DJS has neuroprotective effects via antioxidant and antimitochondria-mediated apoptotic effects [22, 23]. In this study, we showed that the neuroprotective effect of DJS could be attributed to the inhibition of MPTP-stimulated microglial activation by inhibiting TNF-α and NO. Therefore,

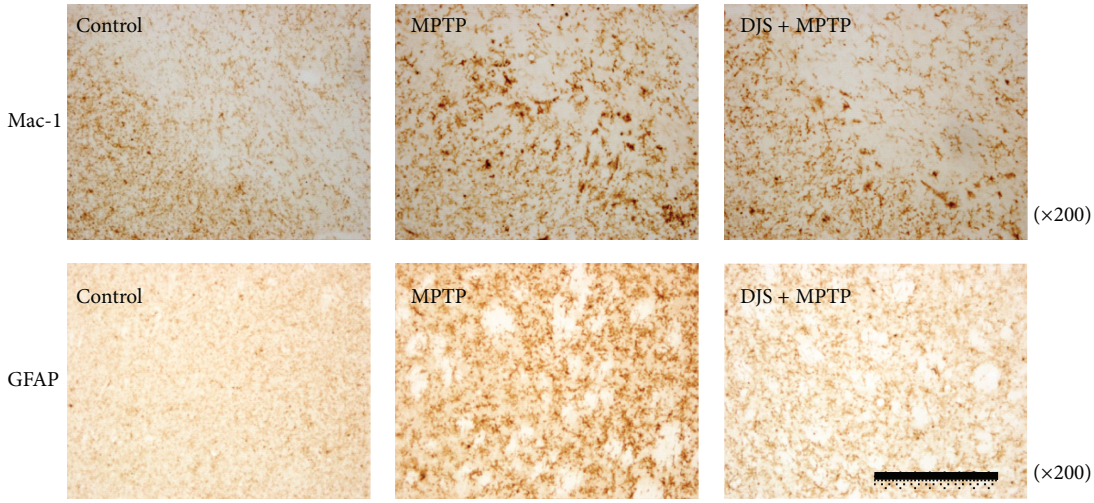

Figure 6: Inhibitory effect of DJS on MPTP-induced gliosis in a mouse model of PD. DJS at 50 mg/kg/day for 5 days was administered, and MPTP at 20 mg/kg was injected four times at 2 h interval on the day of last DJS treatment. On the first day of MPTP injection, microglia and astrocyte in the SNpc were stained with Mac-1 and GFAP antibodies, respectively, and the photographs were shown.

DJS has anti-inflammatory effects as well as antioxidant and antiapoptotic effects.

These anti-inflammatory effects of DJS may be related to the effects of each constituent herb. Angelicae Gigantis Radix has been reported to have anti-inflammatory activity and to inhibit the production of pro-inflammatory cytokines, including TNF-α, IL-6, and IL-8 [29]. Four compounds isolated from *Cnidium officinale* inhibited COX-2 and iNOS expressions in LPS-stimulated macrophages [27]. Paeoniflorin, a main component of Paeoniae Radix, has been reported to inactivate the inflammatory response by inhibiting activation of the NF-κ B pathway via the inhibition of IκB kinase activity [36]. The interactions of these effects might result in the anti-inflammatory effect of DJS. PD has been associated with many factors, including environmental toxins, genetic factors, mitochondrial dysfunction, and oxidative stress. Furthermore, neuroinflammation is recognized as a major factor in the pathogenesis and treatment of PD [37]. DJS is a potential candidate for treating PD via multiple mechanisms.

In conclusion, DJS significantly improved the movement disorder in MPTP-induced mice and protected dopaminergic neurons. Additionally, an anti-inflammatory effect of DJS was seen as the mechanism by which DJS treatment attenuated the loss of dopaminergic cells. We believe that the anti-inflammatory effect of DJS may be useful for treating PD patients.

Authors' Contribution

Deok-Sang Hwang and Hyo Geun Kim contributed equally to this study.

References

[1] W. Paulus and K. Jellinger, "The neuropathologic basis of different clinical subgroups of Parkinson's disease," *Journal of Neuropathology and Experimental Neurology*, vol. 50, no. 6, pp. 743–755, 1991.

[2] P. Jenner, H. Hunot, O. Olanow et al., "Oxidative stress in Parkinson's disease," *Annals of Neurology*, vol. 53, supplement 3, pp. S26–S38, 2003.

[3] A. H. Schapira, "Mitochondria in the aetiology and pathogenesis of Parkinson's disease," *The Lancet Neurology*, vol. 7, no. 1, pp. 97–109, 2008.

[4] C. W. Olanow and W. G. Tatton, "Etiology and pathogenesis of Parkinson's disease," *Annual Review of Neuroscience*, vol. 22, pp. 123–144, 1999.

[5] M. Orth and A. H. V. Schapira, "Mitochondria and degenerative disorders," *American Journal of Medical Genetics*, vol. 106, no. 1, pp. 27–36, 2001.

[6] D. J. Moore, A. B. West, V. L. Dawson, and T. M. Dawson, "Molecular pathophysiology of Parkinson's disease," *Annual Review of Neuroscience*, vol. 28, pp. 57–87, 2005.

[7] O. Halbach, A. Schober, and K. Krieglstein, "Genes, proteins, and neurotoxins involved in Parkinson's disease," *Progress in Neurobiology*, vol. 73, no. 3, pp. 151–177, 2004.

[8] G. Boka, P. Anglade, D. Wallach, F. Javoy-Agid, Y. Agid, and E. C. Hirsch, "Immunocytochemical analysis of tumor necrosis factor and its receptors in Parkinson's disease," *Neuroscience Letters*, vol. 172, no. 1-2, pp. 151–154, 1994.

[9] T. Nagatsu, M. Mogi, H. Ichinose, and A. Togari, "Cytokines in Parkinson's disease," *Journal of Neural Transmission, Supplement*, vol. 58, pp. 143–151, 2000.

[10] L. Qian, P. M. Flood, and J. Hong, "Neuroinflammation is a key player in Parkinson's disease and a prime target for therapy," *Journal of Neural Transmission*, vol. 117, no. 8, pp. 971–979, 2010.

[11] E. C. Hirsch and S. Hunot, "Neuroinflammation in Parkinson's disease: a target for neuroprotection?" *The Lancet Neurology*, vol. 8, no. 4, pp. 382–397, 2009.

[12] S. Usuki, E. Kotani, Y. Kawakura, M. Sano, Y. Katsura, and T. Kubo, "Tokishakuyakusan effect on DNA polymerase alpha activity in relationship to DNA synthesis before and/or after the LH/FSH surge in rats," *The American Journal of Chinese Medicine*, vol. 23, no. 3-4, pp. 231–242, 1995.

[13] T. Akase, T. Akase, S. Onodera et al., "A comparative study of the usefulness of Toki-shakuyaku-san and an oral iron preparation in the treatment of hypochromic anemia in cases of uterine myoma," *Yakugaku Zasshi*, vol. 123, no. 9, pp. 817–824, 2003.

[14] H. Takei, Y. Nakai, N. Hattori et al., "The herbal medicine Toki-shakuyaku-san improves the hypertension and intrauterine growth retardation in preeclampsia rats induced by N ω-nitro-L-arginine methyl ester," *Phytomedicine*, vol. 11, no. 1, pp. 43–50, 2004.

[15] S. Usuki and E. Kotani, "Tokishakuyakusan directly attenuates PACAP's luteolytic action on luteal function in the rat ovary," *American Journal of Chinese Medicine*, vol. 30, no. 4, pp. 521–531, 2002.

[16] J. Park, J. Yang, and D. Kim, "A clinical trial to verity the quality of life improvement efficacy of Dangguijakyak-san and Gyejibongnyeong-hwan granulation in postmenopausal women," *The Journal of Oriental Obstetrics and Gynecology*, vol. 20, pp. 213–228, 2007.

[17] M. Ito, M. Ohbayashi, M. Furukawa, and S. Okoyama, "Neuroprotective effects of TJ-23 (Tokishakuyakusan) on adult rat motoneurons following peripheral facial nerve axotomy," *Otolaryngology*, vol. 136, no. 2, pp. 225–230, 2007.

[18] T. Itoh, S. Michijiri, S. Murai et al., "Regulatory effect of danggui-shaoyao-san on central cholinergic nervous system dysfunction in mice," *American Journal of Chinese Medicine*, vol. 24, no. 3-4, pp. 205–217, 1996.

[19] N. Egashira, K. Iwasaki, Y. Akiyoshi et al., "Protective effect of Toki-shakuyaku-san on amyloid β_{25-35}-induced neuronal damage in cultured rat cortical neurons," *Phytotherapy Research*, vol. 19, no. 5, pp. 450–453, 2005.

[20] J. Kou, D. Zhu, and Y. Yan, "Neuroprotective effects of the aqueous extract of the Chinese medicine Danggui-Shaoyao-san on aged mice," *Journal of Ethnopharmacology*, vol. 97, no. 2, pp. 313–318, 2005.

[21] Y. Qian, H. Wang, W. Yao, and X. Gao, "Aqueous extract of the Chinese medicine, Danggui-Shaoyao-San, inhibits apoptosis in hydrogen peroxide-induced PC12 cells by preventing cytochrome c release and inactivating of caspase cascade," *Cell Biology International*, vol. 32, no. 2, pp. 304–311, 2008.

[22] D. Hwang, H. G. Kim, H. Kwon et al., "Dangguijakyak-san, a medicinal herbal formula, protects dopaminergic neurons from 6-hydroxydopamine-induced neurotoxicity," *Journal of Ethnopharmacology*, vol. 133, no. 2, pp. 934–939, 2011.

[23] J. Lee, D. Hwang, H. G. Kim, C. Lee, and M. S. Oh, "Dangguijakyak-san protects dopamine neurons against 1-methyl-4-phenyl-1,2, 3,6-tetrahydropyridine-induced neurotoxicity under postmenopausal conditions," *Journal of Ethnopharmacology*, vol. 139, no. 3, pp. 883–888, 2011.

[24] M. Delgado and D. Ganea, "Neuroprotective effect of vasoactive intestinal peptide (VIP) in a mouse model of Parkinson's disease by blocking microglial activation," *The FASEB Journal*, vol. 17, no. 8, pp. 944–946, 2003.

[25] G. T. Liberatore, V. Jackson-Lewis, S. Vukosavic et al., "Inducible nitric oxide synthase stimulates dopaminergic neurodegeneration in the MPTP model of Parkinson disease," *Nature Medicine*, vol. 5, no. 12, pp. 1403–1409, 1999.

[26] X. Hu, D. Zhang, H. Pang et al., "Macrophage antigen complex-1 mediates reactive microgliosis and progressive dopaminergic neurodegeneration in the MPTP model of Parkinson's disease," *Journal of Immunology*, vol. 181, no. 10, pp. 7194–7204, 2008.

[27] M. F. Beal, "Mitochondria, oxidative damage, and inflammation in Parkinson's disease," *Annals of the New York Academy of Sciences*, vol. 991, pp. 120–131, 2006.

[28] R. Mosley, E. J. Benner, I. Kadiu et al., "Neuroinflammation, oxidative stress, and the pathogenesis of Parkinson's disease," *Clinical Neuroscience Research*, vol. 6, no. 5, pp. 261–281, 2006.

[29] S. Moncada and J. P. Bolaños, "Nitric oxide, cell bioenergetics and neurodegeneration," *Journal of Neurochemistry*, vol. 97, no. 6, pp. 1676–1689, 2006.

[30] M. Sedelis, K. Hofele, G. W. Auburger, S. Morgan, J. P. Huston, and R. K. W. Schwarting, "MPTP susceptibility in the mouse: behavioral, neurochemical, and histological analysis of gender and strain differences," *Behavior Genetics*, vol. 30, no. 3, pp. 171–182, 2000.

[31] G. E. Meredith and U. J. Kang, "Behavioral models of Parkinson's disease in rodents: a new look at an old problem," *Movement Disorders*, vol. 21, no. 10, pp. 1595–1606, 2006.

[32] K. Matsuura, H. Kabuto, H. Makino, and N. Ogawa, "Pole test is a useful method for evaluating the mouse movement disorder caused by striatal dopamine depletion," *The Journal of Neuroscience Methods*, vol. 73, no. 1, pp. 45–48, 1997.

[33] R. Sakai, Y. Irie, T. Murata, A. Ishige, N. Anjiki, and K. Watanabe, "Toki-to protects dopaminergic neurons in the substantia nigra from neurotoxicity of MPTP in mice," *Phytotherapy Research*, vol. 21, no. 9, pp. 868–873, 2007.

[34] Z. Lan, J. Liu, L. Chen et al., "Danggui-Shaoyao-San ameliorates cognition deficits and attenuates oxidative stress-related neuronal apoptosis in d-galactose-induced senescent mice," *Journal of Ethnopharmacology*, vol. 141, no. 1, pp. 386–395, 2012.

[35] I. Liu, T. Tzeng, S. Liou, and C. J. Chang, "Beneficial effect of traditional chinese medicinal formula Danggui-Shaoyao-San on advanced glycation end-product-mediated renal injury in streptozotocin-diabetic rats," *Evidence-Based Complementary and Alternative Medicine*, vol. 2012, Article ID 140103, 10 pages, 2012.

[36] D. C. Wu, V. Jackson-Lewis, M. Vila et al., "Blockade of microglial activation is neuroprotective in the 1-methyl-4-phenyl-1,2,3,6-tetrahydropyridine mouse model of Parkinson disease," *The Journal of Neuroscience*, vol. 22, no. 5, pp. 1763–1771, 2002.

[37] P. S. Whitton, "Inflammation as a causative factor in the aetiology of Parkinson's disease," *British Journal of Pharmacology*, vol. 150, no. 8, pp. 963–976, 2007.

Hindawi Publishing Corporation
Evidence-Based Complementary and Alternative Medicine
Volume 2013, Article ID 498935, 10 pages
http://dx.doi.org/10.1155/2013/498935

Research Article

Efficacy and Safety of Taeeumjowi-tang in Obese Korean Adults: A Double-Blind, Randomized, and Placebo-Controlled Pilot Trial

Sunju Park,[1] Won Nahmkoong,[2] ChunHoo Cheon,[2,3] Jeong-Su Park,[2,3] Bo-Hyoung Jang,[2,3] Yongcheol Shin,[2] Kyung-Soo Kim,[4] Hoyeon Go,[5] Yun-Kyung Song,[6] and Seong-Gyu Ko[2,3]

[1] *Department of Preventive Medicine, College of Korean Medicine, Daejeon University, 62 Daehak-ro, Daejeon 300-716, Republic of Korea*
[2] *Department of Preventive Medicine, College of Korean Medicine, Kyung Hee University, 1 Hoegi-dong, Seoul 130-701, Republic of Korea*
[3] *Center for Clinical Research & Drug Development, Kyung Hee University, 1 Hoegi-dong, Seoul 130-701, Republic of Korea*
[4] *Family Medicine & Integrative Medicine, Seoul St. Mary's Hospital, Catholic University Medical Center, Seoul 137-701, Republic of Korea*
[5] *Department of Internal Medicine, College of Korean Medicine, Semyung University, Bongbang-dong, Chungju 380-960, Republic of Korea*
[6] *Department of Korean Rehabilitation Medicine, College of Korean Medicine, Gachon University, Seongnam 461-701, Republic of Korea*

Correspondence should be addressed to Yun-Kyung Song; lyricsong@kyungwon.ac.kr and Seong-Gyu Ko; epiko@khu.ac.kr

Received 4 April 2013; Accepted 5 July 2013

Academic Editor: Chang Shik Yin

Objective. The purpose of this study was to assess the efficacy and safety of Taeeumjowi-tang (TJ001) as well as to estimate obesity-related factors. *Methods*. This was a 12-week trial with 5 visits. A total of 102 participants of both genders were randomized to either TJ001 ($n = 57$) group or the placebo group ($n = 55$). Subjects were administered 7 g of either TJ001 or placebo 3 times a day. The primary outcome was a rate of subjects who lost 5% or more of initial weight. Secondary outcomes included anthropometric parameters, lipid profiles, and body fat composition. *Results*. The subject response rate of ≥5% weight loss compared to baseline was similar in both groups, and no statistically significant difference was observed ($P = 0.87$). Changes in anthropometric parameters were greater during the first 4 weeks in the treatment group ($P < 0.0001$). There were no significant changes in both within groups and between groups for lipid profile and body fat composition. No adverse event was reported in either group. *Conclusion*. Although the difference between the groups regarding a rate of subjects who lost 5% or more of initial weight did not show statistical significance, TJ001 appears to be beneficial in safely controlling weight.

1. Introduction

Obesity is defined as abnormal or excessive fat accumulation that threatens health. Obesity not only leads to physical and external complications but also causes various diseases, such as cardiovascular disease, musculoskeletal disease, endocrinopathy, and psychological disease [1]. The World Health Organization (WHO) considers obesity to be lifestyle-related disease and calls for its management. A high prevalence of obesity has become a global problem. If the current trend continues, the obese population will be 700 million in 2015 and one-third of the world population in 2025. The most recent Korean National Health and Nutrition Examination Survey (KNHANES) found that 35.2% of male adults, 28.6% of female adults, and 31.9% of adults aged over 19 were overweight according to BMI calculations [2]. Westernized

eating habits, such as an increased intake of fat, salt, and sugar, have played a large part in the increasing number of obese individuals in Korea.

Socioeconomic costs for obesity treatment in Korea were estimated to be approximately 205 billion won to 422.5 billion won in 1998 [3], and in 2005, this treatment incurred direct expenses of 177 billion won, an overhead cost of 715.2 billion won, and a total cost of 1792.2 billion won, four times the cost in 1998. The trend will continue with medical cost inflation and with the increasing number of obese individuals.

Over a period of many years, numerous medications have been developed and used to treat obesity. However, most of the drugs have been withdrawn because of serious adverse effects [4]. Recently, sibutramine was withdrawn due to an association with increased cardiovascular disease risk [5]. In this context, a demand for novel treatments exists, and herbal medicines have received considerable attention due to the perception that they have no adverse effects.

Taeeumjowi-tang (TJ001) is a traditional Korean medicine preparation for Tae-eumin exterior cold symptoms. It is recorded in I Je-ma's Donguisusebowon, which is considered to be the bible of Sasang constitutional medicine theory. Taeeumjowi-tang works as a treatment for dyspepsia, stuffiness and the sensation of fullness, diarrhea, and wind stroke [1, 6]. Taeeumjowi-tang tonifies the exhale-dispersing strength of the lung and represses the inhale-gathering strength of the liver. It is used to treat obesity by inducing weight loss through metabolic activation. Animal studies and case reports have already demonstrated weight loss success and the anorectic effect of Taeeumjowi-tang [7, 8]. Based on these research results, Taeeumjowi-tang has been suggested as an alternative treatment for obesity. The aims of the present study were to examine estimates of obesity-related variables, to obtain data to suggest an appropriate primary endpoint and treatment period, and to assess the clinical efficacy and safety of Taeeumjowi-tang as a viable treatment for obesity.

2. Methods

2.1. Study Design and Settings. This study was a 12-week randomised, double-blind, and placebo-controlled clinical trial conducted at four tertiary university hospitals in South Korea. The study was approved by the institutional review board (IRB) at the Catholic University of Korea Seoul St. Mary's Hospital, Dongguk University Ilsan Oriental Hospital, Semyung University Oriental Medicine Hospital, and Kyungwon Gil Oriental Medical Hospital. Subjects were randomized by a web-based randomization program that was developed by an independent biostatistician coded with a block size of 4. The program was designed to ensure concealment of the sequence as well as allocation to the treatment and placebo groups in a 1 : 1 ratio for each site. The research coordinator or the study staff assigned the subjects after the randomization, and the pharmacist provided the interventions to the subjects according to the randomization number. All study participants including the subjects were blinded to the group assignment. A sealed envelope copy of the code was kept to CRO in case of emergency and for the analysis. The study was conducted from December 2009 to June 2012, and the trial was registered in Current Controlled Trials (ISRCTN87153759) [9].

2.2. Subjects. The subjects were recruited by advertising on the bulletin board of each hospital. Written informed consent was obtained from each subject prior to participation. The subjects were obese Koreans of both genders with an age range of 18 to 65 years. In this trial, 102 subjects with BMI $\geq$ 30 kg/m^2 or BMI 27 to 30 kg/m^2 with properly controlled hypertension, noninsulin-dependent diabetes mellitus of fasting blood glucose <7.8 mmol/L (140 mg/dL), properly treated hyperlipidemia, ≥236 mg/dL total cholesterol, or ≥150 mg/dL triglycerides at the screening stage were included. The exclusion criteria consisted of the following: (1) endocrine disease except for type 2 diabetes mellitus; (2) heart diseases; (3) uncontrolled hypertension; (4) malignant tumor; (5) severe renal and liver disability; (6) history or existence of neurological or psychological disease including eating disorder; (7) use of medication affecting weight and blood pressure within the past 3 months; (8) forbidden treatments; (9) renal or hepatic disease; (10) inability to follow instructions; (11) pregnant, planning a pregnancy but not in agreement with proper contraception or lactating women.

2.3. Study Schedule. The study was conducted within a 1-week screening period followed by a 12-week treatment period with a total of 5 visits. Baseline measurements were carried out during the 1-week screening phase. After satisfying the inclusion criteria, the subjects were equally randomized into either the TJ001 group or the placebo group. Physical examinations (body weight, BMI, and waist and hip circumferences, waist and hip ratio (WHR)) were taken at every visit, throughout the 12-week period for the efficacy assessment. Lipid profiles (total cholesterol, low density lipoprotein cholesterol (LDL) cholesterol, and triglycerides), body fat composition (total fat area, visceral fat area, and subcutaneous fat area), C-reactive protein, and self-assessment questionnaires were measured at the 2nd and 5th visits.

Safety parameters were assessed by measuring changes in vital signs, general physical examinations, blood and urine test results, and self-reported symptoms.

The subjects were asked to record their diet in dietary planners and to maintain s hypocaloric diet (1,500 kcal/day for men and 1,200 kcal/day for women) during the course of the trial. Subjects were instructed to maintain their usual exercise but not to intensify their activities. Life style management factors, such as dietary intake and exercise, were recorded and counseled at every visit but were not strictly controlled.

Subjects received either 7 g of TJ001 or placebo extracts three times daily for 12 weeks. Both TJ001 and placebo extracts were provided by HANPOONG Pharm & Foods Co. Ltd (Jeonju-si, South Korea) produced by Good Manufacturing Practice (GMP) facilities. The ingredients of TJ001 were *Semen Coicis* 3.75 g, *Semen Castaneae* 3.75 g, *Semen Raphani* 2.5 g, *Schisandrae Fructus* 1.25 g, *Liriopis tuber* 1.25 g, *Herba Ephedrae* 1.25 g, *Radix platycodi* 1.25 g, and *Acori Tatarinowii*

Rhizoma 1.25 g. The placebo granules were identical to TJ001 in appearance, color, smell, and taste.

2.4. Screening. Body weight, height, waist and hip circumference, demographic characteristics, measurements of vital signs, medical and drug use history, smoking and drinking status, general physical examination, laboratory tests, electrocardiography, and pregnancy tests were included in the screening. Blood samples were analyzed at the central laboratory (Eone Reference Laboratory, Seoul, Korea).

2.5. Efficacy. The primary outcome was the rate of subjects who lost 5% or more compared with baseline body weight. The secondary outcomes were changes in body weight (kg), body mass index (BMI, kg/m^2), waist circumference (WC, cm), hip circumference (HC, cm), waist/hip circumference ratio (WHR), blood pressure (mmHg), lipid profile (total cholesterol (TC, mg/dL), HDL cholesterol (mg/dL), LDL cholesterol (mg/dL), and triglyceride (TG, mg/dL) levels. In addition, body fat composition such as total fat area (TFA, cm^2), visceral fat area (VFA, cm^2), and subcutaneous fat area (SFA, cm^2) was assessed by abdominal computed tomography. Subject body weight was measured in light clothing and without shoes. Weight and height were measured by a balance scale with a movable headpiece rod in the standing position to the nearest 0.1 cm and 0.1 kg, respectively. BMI was estimated by dividing weight in kilograms by height in square meters. Both WC and HC were recorded to the nearest 0.1 cm with a plastic tape. The WC was measured at the suprailiac line according to NIH protocol [10], and the HC was measured at the horizontal level of the largest part of the buttocks. Laboratory data (fasting plasma glucose concentration (mg/dL) and C-reactive protein (CRP, mg/L) were also included in the secondary outcomes. Korean Obesity-related Quality of Life (KOQOL) and Korean version of Eating Attitudes Test-26 (KEAT-26) questionnaires scores were evaluated. All measurements were taken by well-trained medical staffs by standard operating procedure (SOP).

2.6. Safety. Vital signs such as resting blood pressure, general physical examinations, and laboratory data (AST, ALT, BUN, and creatinine) were measured at every visit for the safety assessments. Adverse events were reported to the case report form regardless of their association with the intervention.

2.7. Statistical Analysis. All statistical analyses were done to achieve a statistical power of 80%, and a P value of <0.05 was considered statistically significant. The sample size was calculated based on the null hypothesis that the rate of subjects who lost 5% or greater of the baseline weight, that is, the primary endpoint in the TJ001 group, would be higher than that of the placebo group. As pilot studies have not been conducted for TJ001, the 5% or greater responder rate of the baseline weight in each group was set based on the other reference literature [11]. Allowing for a 20% dropout rate, the minimum sample size of 104 subjects with 52 subjects per group was estimated for the study.

Both efficacy and safety outcomes were analyzed by an intention-to-treat (ITT) analysis. All randomized subjects with at least one visit after the administration of the interventions were included in the ITT data set. Missing data were handled by the last-value-carried-forward (LOCF) method. Continuous variables were described as the mean ± SD, and categorical variable such as gender was presented as percentages. The normal distribution assumption was checked before the analysis was conducted. Data were log transformed when necessary.

As all data satisfied the normality assumption, the baseline characteristics of the efficacy and safety outcomes were compared by either Student's t-test for continuous variables or by the chi-square test (Fisher's exact test if the expected value was less than 5) for categorical data.

Efficacy parameters and vital signs were compared at every visit for analysis between groups. Student's t-test was applied to assess the difference between groups, while the paired t-test was used to examine differences within groups. Repeated measures ANOVA was used to assess time by group interaction in repeated measurements. ANCOVA was used to evaluate all efficacy outcomes to determine whether the between groups were significantly different at the end of the study using baseline measures as a covariate.

Data were analyzed using the SPSS Statistic software, version 19.0 for Windows (SPSS, Chicago, IL).

3. Results

3.1. Participant Flow. Participant flow is shown in Figure 1. A total of 139 participants were assessed for eligibility, 21 were disqualified, and 5 decided not to participate. One hundred and thirteen subjects were randomized, 58 to the treatment group and 55 to the placebo group. As one participant in the treatment group had allergic dermatitis after randomization, this subject was excluded from the ITT data set before receiving the intervention. Thus, 55 individuals treated with placebo and 57 treated with TJ001 were included in the ITT analyses. After 12 weeks, 45 completed the trial in the placebo group and 41 in the treatment group.

The baseline characteristics of the trial participants are described in Table 1. Subjects between groups were not different initially except for total cholesterol ($P = 0.0180$). Distribution of gender was also not significantly different between groups ($P = 0.3842$).

3.2. Efficacy Analysis

3.2.1. Primary Outcome. After the 12-week treatment period, the rate of subjects who lost at least 5% of baseline was similar in both groups with no statistically significant difference (TJ001 group and placebo group, 21.1% and 18.2%, resp., $P = 0.87$, Figure 2). However, the subject rates of at least 3% weight loss were significantly higher in the treatment group compared with the placebo group ($P = 0.01$, Figure 2).

3.2.2. Secondary Outcomes: Anthropometric Measurements. The mean weights at each time point are shown in Figure 3.

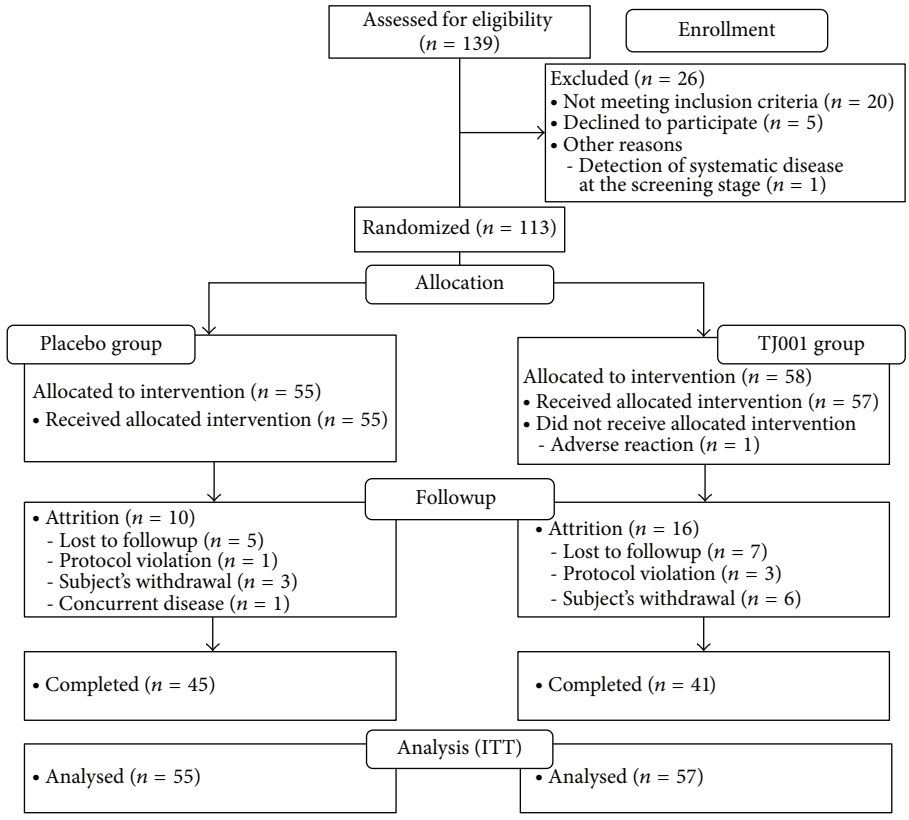

Figure 1: Disposition of the subjects in TJ001 trial.

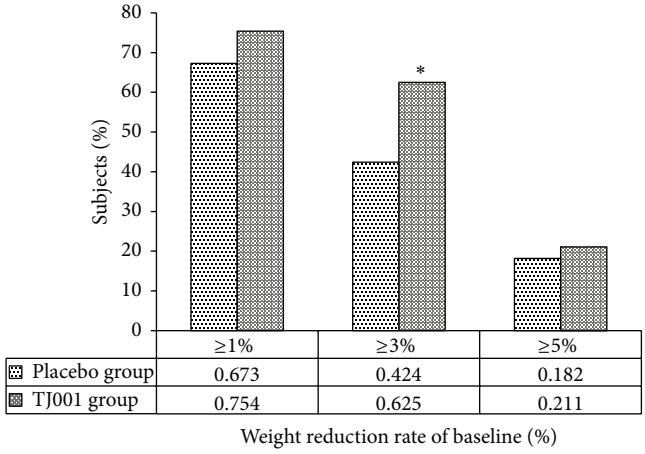

Figure 2: Percentage of subjects who had 1%, 3%, and 5% or more weight reduction (*: statistically significant between groups, $P < 0.05$).

The change patterns in BMI, WC, and HC paralleled those in weight change in the two groups (not shown). Weight, BMI, WC, and HC reductions for every 4th week were greater during the first 4 weeks in the treatment group compared with the other treatment period, showing a plateau between the 4th and 8th weeks. This pattern was more definite in the treatment group than in the placebo group. In contrast, the weight loss in the placebo group did not proceed after week 8.

A significant decrease in weight was observed in both groups but was greater in the treatment group (−1.95 ± 3.35 kg, $P < 0.0001$); however, it was not significant between groups (Table 2). The within-group changes in BMI, WC, and HC were also significant in each group but not significant for the between-group comparison. For WHR, the within-group changes were significant only in the treatment group ($P = 0.0108$). Repeated measures ANOVA results depicted that there were no significant visit and group interaction (time × treatment, Table 2).

3.2.3. Secondary Outcomes: Lipid Profile, Body Fat Composition, and CRP. There were no significant changes both within groups and between groups in regards to lipid profile and body fat composition (Table 3). Questionnaire scores were also not statistically significant for both the within-group and between-group assessments (not shown).

The distribution of Sasang constitution according to the Questionnaire for the Sasang Constitution Classification (QSCC) II in this study was as follows: 82 Tae-eum types, 2 So-yang types, 1 So-eum type, 1 Tae-yang type, and 20 unclassified subjects.

3.3. Safety Analyses. Mean systolic and diastolic blood pressure and creatinine were not different between groups at any week nor were they different from the baseline measurements within each group at the final visit of the study (Table 4). Systolic blood pressure increased from baseline to week 8

Table 1: Baseline characteristics of TJ001 trial subjects.

	Group		
	Placebo group ($N = 55$) mean ± S.D.	TJ001 group ($N = 57$) mean ± S.D.	P value*
Age, year	38.8 ± 10.1	39.2 ± 9.5	0.8475
Anthropometric measurements			
Height, cm	161.8 ± 9.2	160.8 ± 6.4	0.4998
Weight, kg	83.7 ± 14.4	82.2 ± 10.5	0.5458
BMI, kg/m^2	31.9 ± 3.8	31.8 ± 2.6	0.8598
Waist circumference, cm	100.4 ± 9.5	99.6 ± 7.0	0.6259
Hip circumference, cm	110.4 ± 8.8	109.9 ± 6.0	0.7096
Waist-to-hip ratio (WHR)	0.91 ± 0.05	0.90 ± 0.05	0.6934
Lipid profile			
Cholesterol			
Total cholesterol, mg/dL	207.3 ± 36.8	191.7 ± 31.5	0.0180
LDL cholesterol, mg/dL	160.39 ± 36.57	146.43 ± 30.37	0.0300
HDL cholesterol, mg/dL	46.9 ± 9.9	46.1 ± 10.6	0.7161
Triglyceride, mg/dL	152.2 ± 87.2	134.6 ± 66.9	0.2352
Abdominal computed tomography (CT)			
Total fat area (TFA), cm^2	402.8 ± 153.9	392.5 ± 134.6	0.7676**
Visceral fat area (VFA), cm^2	118.2 ± 58.1	110.1 ± 47	0.5073**
Subcutaneous fat area (SFA), cm^2	283.6 ± 116.3	282.1 ± 103	0.9149**
VFA/SFA	0.44 ± 0.21	0.40 ± 0.17	0.2524
C-reactive protein (CRP), mg/dL	0.19 ± 0.24	0.22 ± 0.36	0.6786**
Questionnaires			
KOQOL	33.7 ± 8.2	33.5 ± 6.8	0.8815
KEAT-26	13.5 ± 5.5	12.1 ± 4.8	0.1665
Energy intake, kcal/day	1859 ± 635.9	1823.1 ± 623	0.7671
Pulse, bpm	76.9 ± 9.3	75.3 ± 7.4	0.3072
Systolic blood pressure (SBP), mmHg	123 ± 13.9	122.7 ± 14.6	0.9175
Diastolic blood pressure (DBP), mmHg	77.8 ± 10.8	76.6 ± 9.2	0.5433
AST, IU/L	24.09 ± 10.97	27.86 ± 16.16	0.1395**
ALT, IU/L	30.22 ± 23.55	28.91 ± 18.92	0.9326**
BUN, mg/dL	13.39 ± 2.89	14.45 ± 10.42	0.8895**
Creatinine, mg/dL	0.83 ± 0.17	0.78 ± 0.18	0.1415**
Number of subjects (n)	n (%)	n (%)	P value†
Gender			
Male, n (%)	10 (18.2%)	7 (12.3%)	0.3842
Female, n (%)	45 (81.8%)	50 (87.7%)	

S.D.: standard deviation; BMI: body mass index; LDL: low-density lipoprotein; HDL: high-density lipoprotein CT: computed tomography; KOQOL: Korean Obesity-related Quality of Life, KEAT-26: Korean version of Eating Attitudes Test-26; BUN: blood urea nitrogen; AST: aspartate aminotransferase; ALT: Alanine transaminase. *Continuous variables were analyzed by independent samples t-test. **P values after log transformed, as they did not satisfy normality assumption. †Categorical variables were analyzed by chi-square test. $P < 0.05$: considered statistically significant.

(Figure 4). However, after the 8th week, systolic blood pressure decreased only in the treatment group. There was a significant change in pulse observed in the placebo group and in the between-group comparison ($P = 0.0058$ and $P = 0.018$, resp.).

Although changes in AST in either group (placebo group and treatment group $P = 0.0315$ and 0.0003, resp.) and in ALT in the treatment group were statistically significant ($P = 0.0038$) from baseline, they were not in the abnormal range. All variables of subjects in both groups were in the clinically normal range at end of the study.

3.4. Adverse Effects. One subject in the treatment group developed allergic dermatitis before the administration of the intervention. Therefore this can be ruled out as a potential treatment-related adverse effect. In this trial, no adverse effects were reported.

Table 2: Analyses of anthropometric parameters.

Secondary outcomes (Anthropometric parameters)	Period	Group				P^*	(P_{inter})
		Placebo group ($N = 55$)		TJ001 group ($N = 57$)			
		Mean ± S.D.	(P_{intra})	Mean ± S.D.	(P_{intra})		
Weight, kg	Baseline	83.7 ± 14.4		82.2 ± 10.5		0.5458	
	week 4	83.2 ± 14.8	—	80.9 ± 10.2	—	0.3272	—
	week 8	82.7 ± 13.8		80.7 ± 10.3		0.3900	
	week 12	82.8 ± 15.1		80.3 ± 10.5		0.3080	
	Δ0–12	−0.88 ± 3.05	0.0371	−1.95 ± 3.35	<0.0001	—	0.0708
	ANOVA	visit X group interaction: $P = 0.0816$					
Body mass index (BMI), kg/cm^2	Baseline	31.9 ± 3.80		31.8 ± 2.60		0.8598	
	week 4	31.6 ± 3.90	—	31.2 ± 2.60	—	0.5660	—
	week 8	31.4 ± 3.90		31.2 ± 2.80		0.7407	
	week 12	31.4 ± 4.10		31.0 ± 2.80		0.5420	
	Δ0–12	−0.45 ± 1.17	0.0061	−0.75 ± 1.27	<0.0001	—	0.1680
	ANOVA	visit X group interaction: $P = 0.3703$					
Waist circumference (WC), cm	Baseline	100.4 ± 9.50		99.6 ± 7.00		0.6259	
	week 4	99.7 ± 9.60	—	97.6 ± 7.40	—	0.1932	—
	week 8	98.6 ± 9.30		97.3 ± 7.70		0.3938	
	week 12	97.3 ± 11.70		96.3 ± 7.90		0.6056	
	Δ0–12	−3.09 ± 8.57	0.010	−3.29 ± 4.54	<0.0001	—	0.7665
	ANOVA	visit X group interaction: $P = 0.4725$					
Hip circumference (HC), cm	Baseline	110.4 ± 8.80		109.9 ± 6.00		0.7096	
	week 4	109.8 ± 8.30	—	108.4 ± 5.70	—	0.3027	—
	week 8	109.2 ± 8.40		108.1 ± 5.50		0.4026	
	week 12	108.6 ± 8.30		107.6 ± 5.70		0.4330	
	Δ0–12	−1.82 ± 3.48	0.0003	−2.35 ± 3.51	<0.0001	—	0.3183
	ANOVA	visit X group interaction: $P = 0.3456$					
Waist/hip ratio (WHR)	Baseline	0.91 ± 0.05		0.90 ± 0.05		0.6934	
	week 4	0.91 ± 0.05	—	0.90 ± 0.05	—	0.4217	—
	week 8	0.90 ± 0.04		0.90 ± 0.06		0.6775	
	week 12	0.90 ± 0.05		0.89 ± 0.05		0.4159	
	Δ0–12	−0.0073 ± 0.04	0.1307	−0.0114 ± 0.03	0.0108	—	0.4058
	ANOVA	visit X group interaction: $P = 0.7758$					

P^*: A P value for between-group comparison at each visit and visit X group interaction using ANOVA.
(P_{intra}): A P value for within-group comparison between baseline and 5th visit by paired t-test.
(P_{inter}): A P value for between-group comparison after 12-week treatment using ANCOVA (baseline as covariate).
Δ0–12: Changes between baseline and the 5th visit (after 12-week treatment).
$P < 0.05$ were considered statistically significant.

3.5. Compliance. Overall compliance of treatment was 24% with 70.7% in the TJ001 group and 81.8% in the placebo group.

4. Discussion

Up-to-date, safety, and efficacy matters are the main issues for human weight controlling agents [12–14]. Among the many efforts to evaluate the efficacy and safety of herbal antiobesity agents [15, 16], this pilot study is the first randomized clinical trial for Taeeumjowi-tang in the Korean population.

Because the beneficial effect of at least a 5% weight reduction of baseline has been previously studied [17], we set the rate of subjects who lost 5% or more of baseline weight for primary endpoint.

In this trial, groups did not achieved ≥5% weight reduction (18.2% and 21.1% in the placebo group and the TJ001 group, resp.). The difference between groups was only 2.9%, which was not statistically significant (Figure 2). The weight loss in both groups might be due to the large quantity of the extracts that result in a decrease in food intake. This result indicates that weight loss can be more efficient when accompanied with a strict diet and exercise counseling. However, a 3% or greater reduction rate from baseline weight is statistically significant between groups, suggesting that

Table 3: Analyses of lipid profile, body fat composition, and CRP.

Secondary outcomes (lipid profile, body fat composition, and CRP)	Period	Group				P^*	(P_{inter})
		Placebo group ($N = 55$)		TJ001 group ($N = 57$)			
		Mean ± S.D.	(P_{intra})	Mean ± S.D.	(P_{intra})		
Lipid profile							
Cholesterol							
Total cholesterol, mg/dL	Baseline	207.3 ± 36.8	0.1142	191.7 ± 31.5	0.0983	0.0180	0.8980
	week 12	201.9 ± 39.6		187.2 ± 34.3		0.0374	
HDL cholesterol, mg/dL	Baseline	46.9 ± 9.90	0.8695	46.1 ± 10.6	0.7240	0.7161	0.2717
	week 12	47.2 ± 10.9		45.9 ± 9.70		0.5249	
Triglyceride, g/dL	Baseline	152.2 ± 87.2	0.4709	134.6 ± 66.9	0.8306	0.2352	0.4977
	week 12	143.3 ± 87.9		133.3 ± 64.5		0.4963	
Body fat composition							
Total fat area (TFA), cm^2	Baseline	402.8 ± 153.9	0.2103	392.5 ± 134.6	0.1201	0.7105	0.5205
	week 12	387.9 ± 134.2		383.4 ± 137.0		0.8601	
Visceral fat area (VFA), cm^2	Baseline	118.2 ± 58.1	0.4255	110.1 ± 47.0	0.2669	0.4252	0.6621
	week 12	115.9 ± 58.5		105.4 ± 51.8		0.3253	
Subcutaneous fat area (SFA), cm^2	Baseline	283.6 ± 116.3	0.2898	282.1 ± 103.0	0.2582	0.9425	0.3767
	week 12	272.1 ± 102.1		278.2 ± 105.2		0.7579	
VFA/SFA	Baseline	0.44 ± 0.21	0.3921	0.40 ± 0.17	0.5682	0.2524	0.8109
	week 12	0.43 ± 0.21		0.39 ± 0.19		0.3055	
C-reactive protein (CRP), mg/dL	Baseline	0.83 ± 0.17	0.3766	0.78 ± 0.18	0.6834	0.1547	0.3731
	week 12	0.85 ± 0.19		0.79 ± 0.19		0.0721	

P^*: A P value for between-group comparison at each visit and visit X group interaction using ANOVA.
(P_{intra}): A P value for within-group comparison between baseline and 5th visit by paired t-test.
(P_{inter}): A P value for between-group comparison after 12-week treatment using ANCOVA (baseline as covariate).
$P < 0.05$ were considered statistically significant.

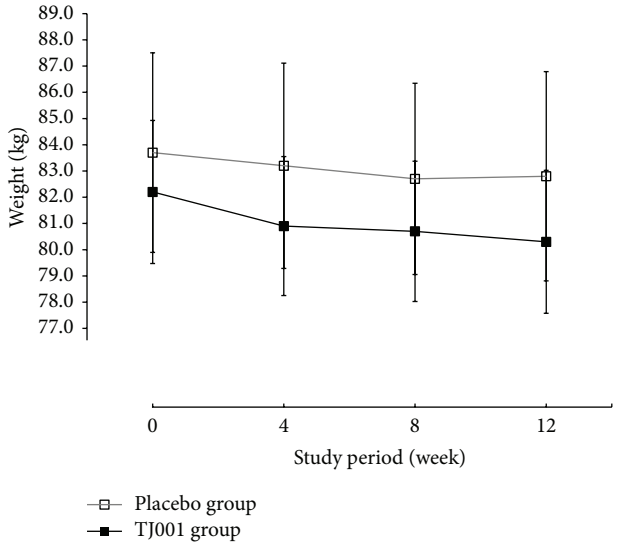

Figure 3: Changes in average body weight over time. Data are represented as the mean ± S.D. of weight at each week. The full squares with a solid line indicate the herbal treatment (TJ001) group, and the empty squares with a grey line depict the placebo group. No statistically significant differences were found between the groups at each week.

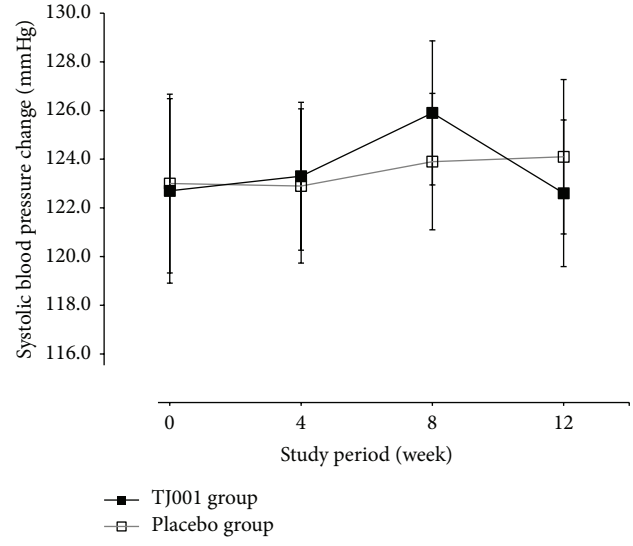

Figure 4: Changes in average systolic blood pressure (SBP) over time. Data are shown as mean ± S.D. of SBP at each week. Full squares with a solid line indicate the herbal treatment (TJ001) group, and empty squares with a grey line depict the placebo group. No statistically significant differences were found between groups at each week.

Table 4: Safety analyses of TJ001.

Safety parameters	Period	Group				P^*	(P_{inter})
		Placebo group ($N = 55$)		TJ001 group ($N = 57$)			
		Mean ± S.D.	(P_{intra})	Mean ± S.D.	(P_{intra})		
Blood pressure							
Systolic, mmHg	Baseline	123.0 ± 13.9	0.5360	122.7 ± 14.6	0.9712	0.9175	0.3607
	week 4	122.9 ± 12.0		123.3 ± 11.7		0.8620	
	week 8	123.9 ± 10.6		125.9 ± 11.4		0.3451	
	week 12	124.1 ± 12.0		122.6 ± 11.6		0.5248	
	ANOVA	visit X group interaction: $P = 0.4121$					
Diastolic, mmHg	Baseline	77.8 ± 10.8	0.9167	76.6 ± 9.20	0.4862	0.5433	0.7461
	week 4	76.2 ± 9.00		77.1 ± 8.10		0.5852	
	week 8	79.7 ± 16.20		78.8 ± 8.20		0.6966	
	week 12	77.9 ± 9.20		77.5 ± 7.60		0.7933	
	ANOVA	visit X group interaction: $P = 0.75$					
Pulse, bpm	Baseline	76.9 ± 9.30	0.0058	75.3 ± 7.40	0.7718	0.3072	0.0184
	week 4	76.3 ± 7.70		76.3 ± 8.00		0.9851	
	week 8	75.5 ± 7.70		76.9 ± 7.60		0.3108	
	week 12	73.6 ± 7.20		75.6 ± 8.50		0.1743	
	ANOVA	visit X group interaction: $P = 0.0475$					
AST, IU/L	Baseline	24.1 ± 11.0	0.0315	27.9 ± 16.2	0.0003	0.1505	0.0544
	week 12	22 ± 8.80		21.9 ± 12.3		0.9798	
ALT, IU/L	Baseline	30.2 ± 23.5	0.1236	28.9 ± 18.9	0.0038	0.7464	0.3573
	week 12	27.3 ± 21.7		22.1 ± 13.5		0.1327	
BUN, mg/dL	Baseline	13.4 ± 2.90	0.1252	14.5 ± 10.4	0.2556	0.4616	0.7000
	week 12	12.8 ± 2.60		12.7 ± 4.10		0.8953	
Creatinine, mg/dL	Baseline	0.83 ± 0.17	0.3766	0.78 ± 0.18	0.6834	0.1547	0.3731
	week 12	0.85 ± 0.19		0.79 ± 0.19		0.0721	

P^*: A P value for between-group comparison at each visit and visit X group interaction using ANOVA.
(P_{intra}): A P value for within-group comparison between baseline and 5th visit by paired t-test.
(P_{inter}): A P value for between-group comparison after 12-week treatment using ANCOVA (baseline as covariate).
$P < 0.05$ were considered statistically significant.

the appropriate primary endpoint for herbal preparation might be between a 3 and 5% reduction rates of initial weight. However, reduction patterns were different in each group (Figure 3). The weight, WC, and HC reductions were greater during the first 4 weeks in the treatment group, with a plateau between the 4th and 8th week and a subsequent decrease after 8 weeks. In contrast, the plateau was seen after 8 weeks in the placebo group. This pattern indicates that the weight reducing effect of TJ001 might be beneficial for relatively short-term or long-term use. Therefore, the appropriate treatment period of TJ001 would be less than 4 weeks or more than 12 weeks (long term).

A total of 62.5% subjects in the treatment group reduced at least 3% of their initial weight after 12 weeks, compared with those in the placebo group (42.4%, Figure 2), and the difference between the two groups was found to be statistically significant ($P = 0.015$). These results suggest that ≥3% weight loss might be an adequate primary endpoint for herbal preparation for less than 12 weeks. In Korean Medicine, obesity originates from the accumulation of body wastes and the congestion of qi. While the mechanism of actions of Taeeumjowi-tang is not fully understood, components of Taeeumjowi-tang and circulating effects, such as fat oxidation and thermogenic action, might promote weight reduction and other responses, such as a decrease in waist and hip circumference [12].

Ideally, any weight reducing agent should promote the loss of body fat as well as body weight. However, regardless of the reduction trend in the anthropometric parameters, the differences in lipid profile and body fat composition both within and between groups were not statistically significant (Table 3). The Korean Obesity-related Quality of Life (KOQOL) and Korean version of Eating Attitudes Test-26 (KEAT-26) questionnaires also showed no statistical significance in both within and between groups. Additionally, the Sasang distribution results suggest that obesity is diagnosed predominantly in Tae-eum types ($n = 82$, 77.4%), which support the Sasang constitutional medicine theory that obesity prevalence is higher in Tae-eum types than in the other three constitutional types.

For safety-related parameters, although some parameters such as AST and ALT were significant within the treatment group, all observed changes in the variables were in the clinically normal range. No significant adverse effects were

reported in the present study. Some participants withdrew themselves because of personal reasons but not due to treatment-related side effects.

The limitations of this study are as follows. First, as previously described, the trial included both genders, which might be a cause of heterogeneity, as the gender difference in weight loss pattern and magnitude are well known [18]. However, we could not perform subgroup analysis for gender because the number of male subjects was too small (Table 1). Second, a TJ001 efficacy assessment longer than 12 weeks could not be performed because of the limited study budget. Therefore, as these are relatively short-term results, it is unclear as to whether weight loss can be maintained, that is, no trajectory weight gain.

Third, the drop-out rate was exceeded in this study (Figure 1). The main reason for the high drop-out rate was lost to followup due to difficulty in managing subjects. The medical staff mostly covered role of the clinical research coordinator (CRC). This implies that the management of subjects with sufficient clinical research staffs is one of the major factors for controlling the drop-out rate.

Finally, the study was performed without strict lifestyle management, which might affect weight control. To identify true intervention effects, other variables, such as diet and exercise, should be controlled.

The strengths of the study include the implication that TJ001 is an effective treatment for weight control in the Korean population and that the results of this trial can be extended to other weight loss studies based on the measurements of obesity-related variables.

5. Conclusion

In conclusion, despite the several limitations and lack of statistical significance between the groups, the present study identified the possibility of and trend for the safe weight reducing effect of Taeeumjowi-tang. Additionally, results from this study will offer preliminary data for large-scale and precise antiobesity trials in the Korean population. Furthermore, the efficacy and safety of relatively long-term use needs to be validated.

Authors' Contribution

Sunju Park, Won Nahmkoong, and ChunHoo Cheon contributed equally to this work.

Acknowledgments

This study was supported by a grant of the Korean Health Technology R&D Project, Ministry of Health & Welfare, Republic of Korea (B080037). This research was also partially supported by a grant from the Traditional Korean medicine R&D Project, Ministry of Health and Welfare, Republic of Korea (B110068).

References

[1] Ministry of Health & Welfare Korea Centers for Disease Control and Prevention, *Korean National Health and Nutrition Examination Survey*, Ministry of Health & Welfare Korea Centers for Disease Control and Prevention, Seoul, Republic of Korea, 2011.

[2] S. M. Park, I. S. Ahn, D. S. Kim, S. Kang, D. Y. Kwon, and H. J. Yang, "Anti-obesity effects of Tae-Um-Jo-Wee-Tang and Do-Dam-Tang in female rats with diet-induced obesity," *Journal of Applied Biological Chemistry*, vol. 53, no. 1, pp. 44–50, 2010.

[3] B. G. Jeong, O. R. Moon, N. S. Kim et al., "Socioeconomic costs of obesity for Korean adults," *Journal of Preventive Medicine and Public Health*, vol. 35, no. 1, pp. 1–12, 2002.

[4] J. G. Kang and C. Y. Park, "Anti-obesity drugs: a review about their effects and safety," *Journal of Diabetes & Metabolism*, vol. 36, no. 1, pp. 13–25, 2012.

[5] W. P. James, I. D. Caterson, W. Coutinho et al., "Effect of sibutramine on cardiovascular outcomes in overweight and obese subjects," *The New England Journal of Medicine*, vol. 363, no. 10, pp. 905–917, 2010.

[6] WHO, "Obesity: preventing and managing the global epidemic," Report of a WHO Consultation 0512-3054, WHO, Geneva, Switzerland, 2000.

[7] K. S. Kim, D. U. Lee, Y. L. Kim et al., "Anti-obesity and anti-hyperlipidemic effects of Taeyeumjowee-tang and its modified prescription," *Journal of Oriental Neuropsychiatry*, vol. 18, no. 2, pp. 57–74, 2007.

[8] WHO International Standard Terminologies on Traditional Medicine in the Western Pacific Region, *WHO International Standard Terminologies on Traditional Medicine in the Western Pacific Region*, WHO, Geneva, Switzerland, 2007.

[9] S. Park, J. S. Park, C. Cheon et al., "A pilot study to evaluate the effect of Taeumjowi-tang on obesity in Korean adults: study protocol for a randomised, double-blind, placebo-controlled, multicentre trial," *Trials*, vol. 13, p. 33, 2012.

[10] A. V. Chobanian, G. L. Bakris, H. R. Black et al., "The seventh report of the Joint National Committee on Prevention, Detection, Evaluation, and Treatment of High Blood Pressure: the JNC 7 report," *Journal of the American Medical Association*, vol. 289, no. 19, pp. 2560–2572, 2003.

[11] C. Y. Park, Y. S. Kim, M. S. Ryu et al., "A phase 3 double-blind, parallel-group, placebo-controlled trial of the efficacy and safety of sibutramine (Reductil) in the treatment of obese patients," *The Korean Journal of Obesity*, vol. 10, no. 4, pp. 336–347, 2001.

[12] C. N. Boozer, P. A. Daly, P. Homel et al., "Herbal ephedra/caffeine for weight loss: a 6-month randomized safety and efficacy trial," *International Journal of Obesity*, vol. 26, no. 5, pp. 593–604, 2002.

[13] F. L. Greenway, "The safety and efficacy of pharmaceutical and herbal caffeine and ephedrine use as a weight loss agent," *Obesity Reviews*, vol. 2, no. 3, pp. 199–211, 2001.

[14] R. M. Hackman, P. J. Havel, H. J. Schwartz et al., "Multinutrient supplement containing ephedra and caffeine causes weight loss and improves metabolic risk factors in obese women: a randomized controlled trial," *International Journal of Obesity*, vol. 30, no. 10, pp. 1545–1556, 2006.

[15] S. Hasani-Ranjbar, N. Nayebi, B. Larijani, and M. Abdollahi, "A systematic review of the efficacy and safety of herbal medicines used in the treatment of obesity," *World Journal of Gastroenterology*, vol. 15, no. 25, pp. 3073–3085, 2009.

[16] G. B. Lenon, K. X. Li, Y. H. Chang et al., "Efficacy and safety of a Chinese herbal medicine formula (RCM-104) in the management of simple obesity: a randomized, Placebo-controlled clinical trial," *Evidence-Based Complementary and Alternative Medicine*, vol. 2012, Article ID 435702, 11 pages, 2012.

[17] National Heart, Lung, and Blood Institute, *Clinical Guidelines on the Identification, Evaluation, and Treatment of Overweight and Obesity in Adults*, National Heart, Lung, and Blood Institute, Bethesda, Md, USA, 1998.

[18] M. Sakurai, K. Miura, T. Takamura et al., "Gender differences in the association between anthropometric indices of obesity and blood presssure in Japanese," *Hypertension Research*, vol. 29, no. 2, pp. 75–80, 2006.

Hindawi Publishing Corporation
Evidence-Based Complementary and Alternative Medicine
Volume 2013, Article ID 761497, 11 pages
http://dx.doi.org/10.1155/2013/761497

Research Article

Multivariate Analysis as a Method for Evaluating the Conceptual Perceptions of Korean Medicine Students regarding Phlegm Pattern

Hyungsuk Kim,[1] Hyunho Kim,[2] Young-Jae Park,[2] and Young-Bae Park[2]

[1] *College of Korean Medicine, Kyung Hee University, Seoul 130-702, Republic of Korea*
[2] *Department of Biofunctional Medicine & Diagnostics, College of Korean Medicine, Kyung Hee University, Seoul 130-702, Republic of Korea*

Correspondence should be addressed to Young-Bae Park; bmppark@khu.ac.kr

Received 3 April 2013; Revised 20 July 2013; Accepted 22 July 2013

Academic Editor: Chang Shik Yin

Individuals may perceive the concepts in Korean medicine pattern classification differently because it is performed according to the integration of a variety of information. Therefore, analysis about individual perspective is very important for examining the cross-sectional perspective state of Korean medicine concepts and developing both the clinical guideline including diagnosis and the curriculum of Korean medicine colleges. Moreover, because this conceptual difference is thought to begin with college education, it is worthwhile to observe students' viewpoints. So, we suggested multivariate analysis to explore the dimensional structure of Korean medicine students' conceptual perceptions regarding phlegm pattern. We surveyed 326 students divided into 5 groups based on their year of study. Data were analyzed using multidimensional scaling and factor analysis. Within-group difference was the smallest for third-year students, who have received Korean medicine education in full for the first time. With the exception of first-year students, the conceptual map revealed that each group's mean perceptions of phlegm pattern were distributed in almost linear fashion. To determine the effect of education, we investigated the preference rankings and scores of each symptom. We also extracted factors to identify latent variables and to compare the between-group conceptual characteristics regarding phlegm pattern.

1. Introduction

In western medicine, the physiology, pathology, and concepts of disease are described using quantitative and objective descriptive terms of molecular biology, histophysiology, and natural science, whereas those of Korean medicine are depicted in relatively abstract terms based on old Chinese ideographic characters. Pattern classification, a unique diagnostic method of Korean medicine, is a significant holism-based tool used to extract and integrate the sign and symptom information of patients for diagnosis. However, pattern classification terms are in fact abstractive because since *Huangdi's Internal Classic*, which is acknowledged as having been written almost 2000 years ago, various terms of Korean medicine have been created, disappeared, or slightly changed by many medical groups. Therefore, practitioners could have different images about the same pattern concepts, and it is a challenging issue in professional education or in academic discussion in Korean medicine.

Many studies have been conducted to overcome these concept-related communication problems. For example, the World Health Organization project to derive consensus regarding the standardization of traditional medicine terminology [1] and the development of ontology by the Korea Institute of Oriental Medicine for medicinal materials based on Korean medicine [2] are studies to render abstract concepts more objective. In addition, there have been efforts towards objectification of tongue diagnosis [3] and pulse diagnosis [4] based on the use of diagnostic instruments. Questionnaires have also been developed to diagnose several patterns such as Yin-deficiency [5], phlegm pattern [6], food accumulation, 7 emotions, overexertion and fatigue, static

Table 1: Characteristics for participants.

	First year	Second year	Third year	Fourth year	Fifth year
Total students	107	113	100	123	99
Refusal	57	65	24	23	15
Participants	50	48	76	100	84
Missing value records	4	7	8	6	7
Finally included records	46	41	68	94	77
Included records					
Age, years (M ± SD)	21.1 ± 1.39	23.4 ± 4.76	23.0 ± 1.97	24.8 ± 3.48	25.4 ± 4.08
Male	25	25	38	63	49
Female	21	16	30	31	28
Response rate	43.0%	36.3%	68%	76.4%	77.8%

M: mean.
SD: standard deviation.

Table 2: Within-group distribution of conceptual perception of phlegm pattern.

Year of study	First year	Second year	Third year	Fourth year	Fifth year	P value
Mean PD_{ij}	6.79[a]	6.65[a]	5.98[b]	6.43[c]	6.36[c]	<0.001
SD of PD_{ij}	1.57	2.34	1.18	1.43	1.26	
Mean AD_i	4.72	4.62	4.18	4.49	4.44	0.093
SD of AD_i	1.24	1.19	0.92	1.12	1.00	

SD: standard deviation.
i, j: index of a student.
[abc]Indicators of the homogeneous subsets grouped by Dunnett's $T3$ test.

blood, and subhealth [7] using modern statistical methodology such as factor analysis, principal component analysis, or structural equation. Data from diagnostic devices or questionnaires, however, cannot present the corresponding pathologic concept perfectly. Thus, a practitioner's clinical decision is still the most important, and the decision of pattern classification generally comes from the conceptual perception formed by the college education [8]. For these reasons, it is necessary to measure the conceptual perception of individuals, especially students. To evaluate it, a new technique would be helpful to describe and compare these invisible conceptual perceptions.

Multidimensional scaling (MDS) is a statistical and visualization method used to project multidimensional variable objects into lower dimensions to analyze the association between the objects. It can also model objects and evaluators together in the same conceptual space, enabling analysis of the between- or within-evaluator difference of perception. There are two approaches in MDS. One is the similarity-analyzing method based on a similarity matrix, and the other is a method for evaluating the objects and ideal point (or ideal vector) simultaneously based on the preference matrix [9–11]. MDS has mainly been applied to the field of marketing to observe customer awareness and to conduct positioning of new products and is used in education as well because it visualizes the abstract perception of learners. Several studies on medical students have used this method to study students' perception of physical symptoms [12], students' personal and professional development [13], students' views on empathy in medical education [14], and to visualize the dimensional structure of medical students' perceptions of diseases [15]. There have also been MDS studies on traditional medicine: observation of the association between the cold and heat pattern of traditional tongue diagnosis and the tongue coating microbiome [16], and study of the similarity and dissimilarity of pattern analysis by physicians regarding patients' tongue diagnosis information [17]. Meanwhile, factor analysis explains the structure of items, finding latent variables that affect multivariable data. It is usually used when developing questionnaires, such as verifying the construct validity of a questionnaire and grouping variables according to latent factors. Some studies have used factor analysis in traditional medicine to study the attitudes and skills of Hong Kong Chinese medicine practitioners towards computerization in practice [18], the attitudes of Hong Kong Chinese medicine practitioners to traditional Chinese medicine and western medicine [19], the development of a stagnation questionnaire [20], factor analysis of the symptoms of unstable angina [21], chronic low back pain [22], dysfunctional uterine bleeding [23], and efficiency study of the cold and heat pattern in the symptoms of rheumatoid arthritis [24]. Nevertheless, there have been no studies to evaluate and compare their perceptions of concepts in Korean medicine.

Therefore, we conducted a study to evaluate and analyze the individual concepts of phlegm pattern numerically and visually and applied these methods to the Korean medicine students. Using an internationally published phlegm pattern questionnaire and the above mentioned methods, we could

Table 3: Symptom preference for phlegm pattern diagnosis.

Symptom	Ranking (score mean)				
	First year	Second year	Third year	Fourth year	Fifth year
Feeling heavy in the chest	1 (3.78)	5 (3.88)	4 (3.82)	3 (4.06)	8 (3.79)
Unclearness in the head*1	2 (3.61)[a]	9 (3.46)[a]	3 (3.85)[ab]	5 (3.91)[ab]	5 (4.18)[b]
Feeling of foreign body in the throat*2	3 (3.57)[a]	1.5 (4.07)[ab]	1 (4.32)[b]	2 (4.26)[b]	2 (4.27)[b]
Sputum*2	4 (3.54)[a]	1.5 (4.07)[ab]	2 (4.28)[b]	1 (4.36)[b]	3.5 (4.22)[b]
Fatigue	5 (3.39)	11.5 (3.39)	13 (3.25)	12 (3.45)	10 (3.58)
Headache	6 (3.35)	10 (3.44)	10 (3.46)	14 (3.35)	14 (3.29)
Yellow face	7 (3.33)	16 (3.22)	18 (3.00)	16 (3.24)	20 (3.05)
Sickness*2	8.5 (3.30)[a]	11.5 (3.39)[a]	5 (3.65)[ab]	4 (3.99)[bc]	3.5 (4.22)[c]
Indigestion*1	8.5 (3.30)[a]	6 (3.78)[b]	9 (3.50)[ab]	7.5 (3.80)[b]	7 (3.88)[b]
Feeling of abdominal fullness*1	10.5 (3.24)[a]	4 (3.95)[b]	8 (3.54)[ab]	7.5 (3.80)[b]	6 (3.90)[b]
Rumbling sound in the abdomen**	10.5 (3.24)	14 (3.29)	19.5 (2.91)	18.5 (3.18)	12 (3.40)
Dizziness*2	12 (3.22)[a]	17 (3.20)[a]	7 (3.56)[ab]	6 (3.86)[b]	1 (4.42)[c]
Cough**	13 (3.17)	8 (3.51)	6 (3.60)	15 (3.31)	16.5 (3.14)
Shortness of breath	14.5 (3.15)	13 (3.32)	11 (3.38)	20 (3.12)	18 (3.12)
Feeling heavy in the limbs	14.5 (3.15)	22.5 (2.88)	21 (2.81)	21 (3.06)	22 (2.94)
Lumps*1	16.5 (3.11)[a]	3 (3.98)[b]	12 (3.26)[a]	10.5 (3.46)[ab]	19 (3.08)[a]
Dark circles under the eyes**	16.5 (3.11)	15 (3.24)	15 (3.21)	17 (3.23)	9 (3.74)
Mucousy stool	18 (3.09)	21 (2.95)	19.5 (2.91)	18.5 (3.18)	21 (3.04)
Poor appetite**	19.5 (3.07)	19 (3.00)	14 (3.24)	9 (3.48)	11 (3.48)
Flank pain**	19.5 (3.07)	7 (3.59)	17 (3.03)	13 (3.39)	16.5 (3.14)
Startled by faint noise**	21.5 (2.89)	25 (2.59)	25 (2.29)	24 (2.54)	24 (2.55)
Joint pain**	21.5 (2.89)	18 (3.12)	16 (3.07)	10.5 (3.46)	13 (3.39)
Palpitation**	23 (2.87)	22.5 (2.88)	24 (2.41)	23 (2.76)	23 (2.87)
Tinnitus	24 (2.83)	20 (2.98)	22 (2.79)	22 (2.86)	15 (3.22)
Itching**	25 (2.59)	24 (2.73)	23 (2.51)	25 (2.28)	25 (2.40)

Symptoms of same ranking scored the median value.
Item that has statistically significant mean difference among groups by analysis of variance.
*$P < 0.05/25$ by the Bonferroni correction for the multiple comparisons.
**$P < 0.05$ for the exploratory analysis.
[1]Scheffe's test for the post hoc multiple comparisons of the equal variance assumed data.
[2]Dunnett's $T3$ test for the post hoc multiple comparisons of the unequal variance assumed data.
[abc]Indicators of the homogeneous subsets grouped by Scheffe's test or Dunnett's $T3$ test in a row.

compare the perceptive structure of the students' concepts regarding phlegm pattern and discuss the differences in the educational aspects.

2. Materials and Methods

2.1. Subjects. We tried to perform a complete enumeration survey of the first- to fifth-year students of the College of Korean Medicine, Kyung Hee University, Seoul, Korea. The College of Korean Medicine teaches a 6-year course: students are taught general education and introduction to Korean medicine during the first and second years, while full Korean medicine education begins in the third year. However, sixth year students does not take any classes, they only do practice in hospital. Thus, students from first to fifth year were included in this study. Data were acquired during December 2012, which is the period in which each year of study finishes. We provided proper gifts as rewards to encourage honest and sincere responses. The students were requested to judge the importance level of each symptom to diagnose phlegm pattern according to 5-point Likert scale: 1, "very insignificant"; 2, "insignificant"; 3, "moderate"; 4, "significant"; 5, "very significant." Three hundred and sixty four students answered the survey; the data of 38 students were excluded due to the missing values. Finally, 326 students' records were analyzed out of 542 students in the whole school excluding sixth-year students (60.1%). The characteristics for participants are listed in Table 1.

2.2. Phlegm Pattern Questionnaire. The phlegm pattern questionnaire was developed in 2011 to evaluate a patient's phlegm pattern score and consists of 25 items: 7 neuropsychologic,

Table 4: Factor Loadings for the items of the phlegm pattern questionnaire responded by the first-year students.

Item	Factor								
	1	2	3	4	5	6	7	8	9
Sputum	**0.849**	0.083	0.043	−0.180	0.004	−0.120	−0.255	0.132	0.201
Cough	**0.847**	−0.019	0.196	−0.092	−0.065	0.092	0.083	0.149	0.034
Feeling of foreign body in the throat	**0.799**	0.233	−0.053	0.226	−0.096	−0.149	−0.168	−0.041	0.076
Shortness of breath	**0.626**	0.116	−0.073	0.205	−0.055	0.156	**0.512**	−0.125	−0.104
Indigestion	0.130	**0.840**	0.105	−0.148	0.030	0.091	0.065	0.272	−0.008
Sickness	0.150	**0.788**	−0.071	0.226	−0.086	−0.268	0.035	−0.107	0.053
Lumps	−0.035	**0.605**	−0.031	**0.556**	0.029	0.064	−0.198	0.037	0.244
Poor appetite	−0.029	**0.585**	0.557	−0.013	−0.052	−0.009	0.186	0.179	0.064
Fatigue	0.042	−0.048	**0.830**	0.017	0.005	0.061	0.173	0.088	0.003
Feeling heavy in the limbs	0.030	0.052	**0.793**	0.050	0.194	−0.045	0.243	0.247	−0.151
Yellowish face	0.228	**0.433**	**0.582**	0.137	0.114	−0.124	−0.247	−0.227	−0.185
Tinnitus	0.025	0.012	−0.066	**0.792**	0.081	−0.067	0.299	0.097	−0.133
Dizziness	0.017	−0.038	0.243	**0.703**	0.017	**0.442**	0.085	−0.179	−0.212
Flank pain	−0.385	0.283	0.183	**0.453**	0.367	−0.166	0.110	0.215	0.298
Itching	−0.010	0.016	0.072	−0.121	**0.880**	−0.055	0.020	−0.198	−0.136
Joint pain	−0.183	−0.112	0.104	0.097	**0.811**	0.190	−0.119	−0.001	0.234
Dark circle under the eyes	0.010	0.013	−0.006	0.221	**0.735**	0.152	0.237	0.221	−0.266
Headache	−0.028	−0.008	0.080	0.183	0.051	**0.866**	−0.039	0.133	0.016
Unclearness in the head	0.015	−0.011	−0.083	−0.080	0.100	**0.820**	−0.127	−0.090	−0.005
Mucousy stool	0.148	0.304	0.203	**0.411**	−0.067	**−0.458**	−0.108	0.376	−0.023
Palpitation	−0.028	0.118	0.235	0.262	0.084	−0.132	**0.702**	−0.006	−0.022
Startled by faint noise	−0.235	−0.051	0.297	−0.025	0.022	−0.115	**0.687**	0.272	0.045
Rumbling sound in the abdomen	0.089	0.102	0.192	0.061	−0.014	−0.056	0.074	**0.863**	−0.019
Feeling of abdominal fullness	0.106	**0.529**	0.076	−0.081	−0.061	0.211	0.211	**0.572**	−0.313
Feeling heavy in the chest	0.218	0.067	−0.143	−0.142	−0.106	0.015	0.003	−0.093	**0.878**
Variance explained (%)	11.57	11.20	9.61	8.98	8.93	8.80	7.26	7.17	5.40

Symptoms with factor loading ≥0.4 are marked bold.

4 respiratory, 3 fatigue-related, 5 gastrointestinal, 4 dermatological, and 2 pain-related symptoms. The items of the phlegm pattern questionnaire are presented in the Supplementary Material (See Supplementary Material available online at http://dx.doi.org/10.1155/2013/761497). Cronbach's alpha was 0.919 and the item-total correlations of all items were >0.3 [6]. Structural validity was examined by factor analysis with varimax rotation, and the first 6 factors explained 58.9% of the total variance. According to the receiver operating characteristic curve, the cut-off point was calculated to be 5. At that level, the sensitivity was 83.78% and the specificity was 83.33%.

2.3. Statistical Parameters and Analysis

2.3.1. Distance Matrix and Parameters. To perform MDS analysis, the distance matrix between the subjects should be calculated to present them in perceptual space. Some types of distance are generally calculated according to the properties of the data, and thus we used Euclidean distance to obtain the distance matrix in this study

$$\mathrm{PD}_{ij} = \sqrt{\sum_{n=1}^{25} \left(A_{in} - A_{jn}\right)^2}, \quad (1)$$

PD_{ij} is the Euclidean pair distance between 2 arbitrary objects, i and j. A_{in} is the response score of the nth questionnaire item by object i. Based on these PD_{ij} values, we were able to calculate the mean value of all pair distances using the following equation, where N is the number of students of each year. We applied this equation to all 5 groups, which were defined by the year of study

$$\overline{\mathrm{PD}} = \frac{\sum_{i=1}^{N} \sum_{j=1}^{N} \mathrm{PD}_{ij}}{N\left(N-1\right)/2}. \quad (2)$$

Separately, absolute distance (AD), a student's perceptive distance from the average point of the corresponding year of study, was calculated using the following equation. $\overline{A}_n$ indicates the mean of the nth questionnaire item and i is the index of a student. The mean and standard deviation of the AD were assessed. These calculations were performed for each year of study

$$\mathrm{AD}_i = \sqrt{\sum_{n=1}^{25} \left(A_{in} - \overline{A}_n\right)^2}. \quad (3)$$

2.3.2. MDS and Factor Analysis. MDS is a statistical and visualization method used to map a set of multivariable data to

Table 5: Factor loadings for the items of the phlegm pattern questionnaire responded by the second-year students.

Item	Factor						
	1	2	3	4	5	6	7
Unclearness in the head	**0.815**	0.026	0.039	0.036	0.159	−0.013	0.136
Headache	**0.711**	−0.065	−0.027	0.006	0.097	0.394	0.248
Lumps	**0.705**	0.289	−0.087	0.283	0.008	0.098	−0.335
Joint pain	**0.703**	−0.115	−0.101	0.357	0.222	0.067	0.071
Flank pain	**0.641**	0.357	0.268	0.060	−0.144	−0.106	−0.287
Feeling heavy in the chest	**0.563**	0.184	**0.536**	0.034	0.257	−0.331	−0.082
Feeling of abdominal fullness	**0.400**	**0.808**	0.019	0.069	−0.038	0.013	0.123
Indigestion	−0.022	**0.710**	0.373	−0.129	−0.025	−0.046	0.240
Rumbling sound in the abdomen	0.023	**0.617**	−0.190	**0.535**	0.000	0.129	0.013
Sickness	−0.159	**0.584**	0.172	−0.082	0.385	**0.500**	0.162
Poor appetite	−0.228	**0.460**	**0.424**	−0.131	0.217	0.249	0.398
Startled by faint noise	0.081	0.107	**0.855**	0.138	0.063	0.276	−0.006
Palpitation	0.034	0.035	**0.721**	0.276	−0.183	0.310	0.034
Itching	−0.003	−0.110	0.191	**0.808**	−0.021	−0.104	0.085
Dark circles under the eyes	0.238	0.090	−0.013	**0.740**	−0.154	0.199	−0.139
Yellowish face	**0.425**	−0.115	0.240	**0.499**	0.067	0.144	0.323
Mucousy stool	0.297	0.156	0.168	**0.488**	0.157	0.269	0.186
Sputum	0.212	0.060	−0.012	0.036	**0.878**	−0.090	−0.002
Cough	0.004	−0.328	0.047	−0.007	**0.820**	−0.086	0.228
Feeling of foreign body in the throat	0.154	0.241	0.005	−0.081	**0.704**	0.189	0.085
Tinnitus	0.026	0.056	0.275	0.092	−0.034	**0.819**	0.277
Dizziness	0.156	0.052	0.168	0.150	−0.007	**0.810**	−0.076
Feeling heavy in the limbs	−0.011	0.118	0.004	0.015	0.113	0.135	**0.809**
Fatigue	0.230	0.176	−0.049	0.240	0.037	−0.023	**0.733**
Shortness of breath	−0.144	0.091	0.461	−0.174	0.201	0.101	**0.535**
Variance explained (%)	14.513	10.606	9.835	9.819	9.819	9.375	9.315

Symptoms with factor loading ≥0.4 are marked bold.

a lower dimensional space for the convenience of intuitive insight or understanding of the data. A 2- or 3-dimensional model is typical because of the limitation of man's spatial perception. MDS is divided into two approaches: one to visualize the similarity of the data, and the other to calculate the ideal point or ideal vector additionally using preference data. As we intended to present within- and between-group similarity, we used the ALSCAL algorithm, a dimension-lowering algorithm with conserving between-object distances. Factor analysis is a modern statistical method that allows the determination of latent variables from directly measurable variables. The Kaiser criterion was used and the factors with eigenvalues ≥ 1.00 were retained. After principal component extraction, varimax rotation was performed. All statistical calculations were performed using SPSS Statistics 19 (SPSS Inc., Chicago, IL, USA) and Excel 2007 (Microsoft Office Excel 2007; Microsoft, Redmond, WA, USA).

3. Results and Discussion

3.1. Within-Group and Between-Group Distribution of Conceptual Perception of Phlegm Pattern. As shown in Table 2, the mean within-group pair distance values of conceptual perception of phlegm pattern in the Euclidean system were 5.98–6.79. Analysis of variance (ANOVA) revealed that statistically significant differences exist among the 5 groups ($P < 0.001$). Dunnett's T3 test, a post hoc analysis of unequal-variance assumed data, was used to analyze the homogeneous subgroups indicated in Table 2. First- and second-year students belonged to one subset, and fourth- and fifth-year students belonged to another subset. Third-year students had a statistically narrow distribution in comparison with the other 4 groups. This means that some consensus regarding phlegm pattern was formed among third-year students possibly due to the beginning of full Korean medicine education. The within-group conceptual gap increased again from the fourth year. This may be owing to the influence of the various Korean medicine classics or various pattern classification systems, because Korean medicine theories emphasize diagnostic points in a slightly different manner. However, the distances were statistically shorter than that of the first- or second-year students.

$\overline{AD}$ value, the mean distance from the average point of each year of study, exhibited a similar tendency. As the statistical significance was not revealed ($P = 0.093$), this should be considered from the exploratory viewpoint.

Table 6: Factor loadings for the items of the phlegm pattern questionnaire responded by the third-year students.

Item	Factor							
	1	2	3	4	5	6	7	8
Feeling of foreign body in the throat	**0.688**	0.183	−0.285	−0.032	0.160	0.024	0.098	−0.085
Cough	**0.686**	−0.064	−0.081	−0.087	−0.210	−0.049	−0.052	0.338
Sputum	**0.640**	0.043	−0.171	**−0.415**	−0.180	0.110	0.071	0.227
Shortness of breath	**0.639**	0.141	0.104	**0.449**	0.004	−0.132	0.055	0.131
Feeling heavy in the chest	**0.628**	0.000	0.189	0.089	0.201	0.057	0.074	−0.288
Sickness	0.221	**0.796**	0.063	0.094	−0.045	−0.046	−0.192	−0.103
Indigestion	0.028	**0.774**	−0.081	−0.094	0.081	0.114	0.315	−0.127
Feeling of abdominal fullness	0.062	**0.676**	−0.248	−0.078	0.238	−0.017	**0.411**	−0.091
Poor appetite	−0.109	**0.634**	0.306	−0.211	−0.016	0.152	−0.127	0.171
Feeling heavy in the limbs	−0.167	−0.058	**0.835**	0.118	−0.055	0.131	0.113	−0.067
Fatigue	0.000	0.128	**0.738**	0.042	0.200	0.125	−0.075	−0.016
Palpitation	−0.092	−0.003	0.227	**0.727**	0.024	0.062	−0.114	0.180
Startled by faint noise	0.118	−0.221	−0.052	**0.712**	0.186	0.225	−0.077	−0.202
Tinnitus	0.013	−0.059	−0.040	**0.547**	−0.116	**0.542**	0.193	0.032
Yellowish face	−0.036	0.203	−0.154	−0.042	**0.747**	0.038	−0.086	0.012
Joint pain	−0.006	−0.060	0.366	0.083	**0.698**	−0.016	−0.124	0.156
Flank pain	0.144	−0.119	**0.444**	0.156	**0.567**	−0.062	−0.105	0.130
Dark circles under the eyes	−0.315	0.106	0.318	0.250	0.345	0.048	0.266	0.217
Unclearness in the head	0.033	0.011	0.164	0.015	0.046	**0.850**	−0.132	−0.051
Dizziness	−0.231	0.101	0.132	0.355	−0.133	**0.625**	0.055	0.120
Headache	0.227	0.323	0.252	0.119	0.236	**0.484**	−0.142	0.366
Lumps	0.252	0.113	−0.184	−0.329	0.330	**0.434**	0.313	−0.135
Mucousy stool	0.164	−0.097	−0.026	−0.071	−0.187	0.052	**0.794**	0.008
Rumbling sound in the abdomen	−0.069	0.358	0.099	0.000	−0.087	−.180	**0.696**	0.286
Itching	0.101	−0.168	−0.040	0.059	0.244	0.053	0.187	**0.791**
Variance explained (%)	10.421	10.337	8.951	8.654	8.285	8.147	7.259	5.524

Symptoms with factor loading ≥0.4 are marked bold.

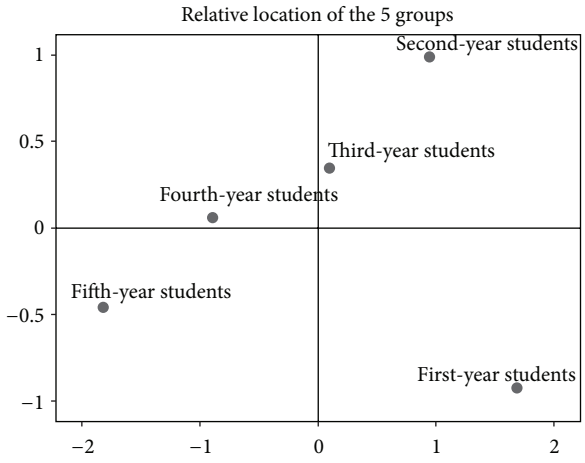

Figure 1: Between-group distribution of conceptual perception of phlegm pattern.

Figure 1 illustrates a 2-dimensional model of the mean points of phlegm pattern conceptual perception of the 5 groups according to the Euclidean distance matrix by ALSCAL algorithm. The stress value of this model was 0.00545 and the R^2 was 0.99978. This indicates that the goodness of fit of this model was very high. The important physical value is the relative distance between 2 arbitrary points; therefore, the 2 axes are physically meaningless. As shown in the figure, the first- and second-year students are furthest from the fifth-year students, and the distance between them is very long. The second- to fifth-year students are aligned in order in a relatively straight line. This figure expresses that the conceptual gap between the fourth- and the fifth-year students is small compared with that between the third- and fifth-year students or between the second- and fifth-year students. This also demonstrates that the conceptual perception of phlegm pattern is not formed correctly in the first and second year of study, but as the year of study increases, the average perceptive distance of each group from the fifth-year students' perception decreases. In other words, full Korean medicine education is believed to result in the average conceptual perception of each year of study resembling that of fifth-year students.

3.2. Symptom Preference for Phlegm Pattern Diagnosis according to Year of Study. Figure 2 depicts the average score of each questionnaire item according to year of study. A high score meant "this symptom is very important for diagnosing

Table 7: Factor loadings for the items of the phlegm pattern questionnaire responded by the fourth-year students.

Item	Factor							
	1	2	3	4	5	6	7	8
Indigestion	**0.713**	−0.145	0.388	0.114	0.120	0.041	−0.110	0.048
Feeling of abdominal fullness	**0.705**	0.091	0.312	0.050	0.082	0.056	0.054	−0.050
Rumbling sound in the abdomen	**0.669**	0.359	−0.072	0.250	0.063	0.204	−0.067	−0.022
Sickness	**0.607**	−0.038	0.025	0.072	−0.001	−0.220	0.229	0.336
Startled by faint noise	0.047	**0.866**	−0.133	0.044	0.075	0.012	−0.153	0.060
Palpitation	0.077	**0.834**	−0.104	0.066	0.147	0.093	0.057	0.104
Tinnitus	−0.045	**0.613**	0.281	−0.048	0.342	0.066	0.324	−0.092
Itching	0.034	**0.437**	0.353	0.381	−0.164	0.315	0.022	0.158
Feeling heavy in the limbs	0.175	−0.047	**0.769**	0.210	−0.136	0.186	0.048	0.102
Fatigue	0.251	−0.132	**0.744**	0.164	0.191	0.039	−0.038	−0.022
Poor appetite	**0.509**	−0.042	**0.548**	0.087	0.152	0.057	0.256	0.078
Shortness of breath	0.039	0.210	**0.548**	0.118	−0.011	−0.202	0.257	**0.430**
Dark circles under the eyes	0.128	0.181	0.180	**0.762**	0.192	−0.044	−0.060	0.034
Yellowish face	0.146	−0.121	0.248	**0.726**	0.061	0.181	−0.031	0.198
Lumps	0.233	0.087	0.161	**0.525**	−0.171	0.184	0.347	−0.036
Unclearness in the head	0.299	0.047	0.089	−0.081	**0.747**	0.127	−0.062	−0.056
Dizziness	0.112	0.280	0.031	0.037	**0.730**	−0.009	0.222	0.019
Headache	−0.083	0.128	−0.020	0.315	**0.678**	0.155	−0.051	0.279
Mucousy stool	0.348	0.109	0.034	0.389	**−0.453**	0.284	0.093	−0.001
Flank pain	−0.047	0.238	0.046	0.019	0.033	**0.854**	0.079	0.087
Joint pain	0.132	−0.036	0.121	0.194	0.143	**0.762**	0.199	0.094
Feeling of foreign body in the throat	0.022	0.103	0.115	0.020	0.026	0.064	**0.828**	−0.010
Sputum	0.080	−0.238	−0.065	0.001	0.074	**0.430**	**0.670**	0.201
Cough	0.036	0.100	0.043	0.226	0.053	0.168	0.074	**0.804**
Feeling heavy in the chest	0.165	0.021	0.278	**−0.438**	0.136	0.192	−0.094	**0.563**
Variance explained (%)	10.257	10.146	9.905	9.009	8.597	8.165	6.890	6.042

Symptoms with factor loading ≥0.4 are marked bold.

a patient as phlegm pattern." According to Figure 2, the difference of symptom importance becomes clearer as the year of study increases. The score difference between the most and least important symptoms was 2.01 (fifth-year students) and 1.20 (first-year students). The difference between the average scores of 5 most and 5 least important symptoms was 1.50 (fifth-year students) and 0.77 (first-year students). The difference had a tendency to increase with the year of study. We may consider that the weight value of symptoms differs largely based on the year of study; that is, some certain symptoms are believed to be more important than others as the year of study increases.

Table 3 lists the differences in preference of symptoms according to year of study for phlegm pattern diagnosis. ANOVA was used to test the statistical significance. Twenty-five symptoms were tested as independent events; therefore, we adjusted the alpha level as 0.05/25 by Bonferroni correction to compensate for accumulated alpha error. With this, we could guarantee that the total alpha error < 0.05. At this level, a statistically significant difference was observed for the symptoms: "unclearness in the head," "feeling of foreign body in the throat," "sputum," "sickness," "indigestion," "feeling of abdominal fullness," "dizziness," and "lumps." Then, we tested these symptoms again using Scheffe's or Dunnett's

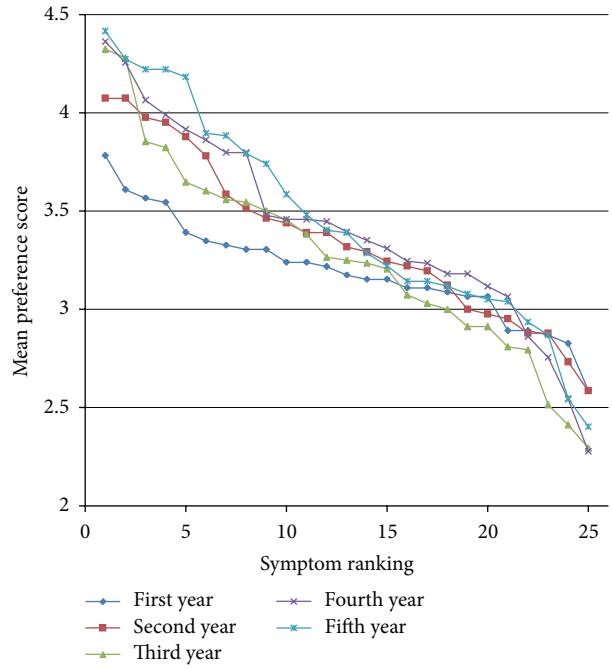

Figure 2: Symptom preference score for phlegm pattern diagnosis.

Table 8: Factor loadings for the items of the phlegm pattern questionnaire responded by the fifth-year students.

Item	Factor								
	1	2	3	4	5	6	7	8	9
Indigestion	**0.832**	0.030	0.172	−0.015	−0.100	0.032	−0.085	−0.054	0.077
Sickness	**0.784**	0.014	−0.190	0.038	0.046	−0.036	0.054	0.024	0.053
Feeling of abdominal fullness	**0.743**	0.102	0.180	0.069	−0.051	−0.014	−0.032	0.079	0.033
Rumbling sound in the abdomen	**0.598**	0.172	−0.083	0.024	**0.400**	0.092	−0.054	−0.316	−0.223
Poor appetite	**0.571**	−0.165	**0.436**	0.082	0.048	0.022	−0.155	0.194	0.027
Palpitation	−0.073	**0.850**	−0.085	−0.031	−0.029	0.012	0.154	−0.235	0.148
Startled by faint noise	0.011	**0.759**	0.107	0.131	−0.053	0.001	0.095	0.027	0.153
Dark circles under the eyes	0.279	**0.624**	−0.054	0.223	0.010	−0.043	−0.173	0.298	−0.321
Dizziness	0.265	**0.500**	0.034	−0.030	−0.051	0.037	**0.411**	0.110	−0.395
Fatigue	0.025	0.124	**0.877**	−0.020	0.003	0.002	0.047	0.117	0.001
Feeling heavy in the limbs	0.145	−0.204	**0.754**	0.144	0.143	0.149	0.214	−0.203	0.054
Shortness of breath	0.309	0.396	**0.495**	−0.153	0.282	0.154	−0.235	−0.048	0.075
Lumps	0.076	−0.008	−0.056	**0.830**	0.176	0.075	0.027	0.154	−0.127
Yellowish face	−0.087	0.244	0.060	**0.729**	−0.106	0.068	0.054	0.056	0.354
Mucousy stool	0.380	−0.017	0.163	**0.497**	0.058	0.078	−0.015	−0.299	−0.135
Cough	−0.146	−0.059	0.191	−0.007	**0.853**	0.140	0.004	0.049	0.120
Sputum	0.132	−0.054	0.011	0.196	**0.754**	−0.248	−0.056	0.243	−0.165
Headache	−0.076	0.006	0.186	−0.051	−0.136	**0.790**	0.095	0.030	−0.168
Joint pain	0.100	−0.019	−0.052	0.198	0.073	**0.706**	0.032	0.074	0.155
Itching	0.065	0.107	0.357	0.366	0.293	**0.401**	−0.050	−0.267	0.077
Unclearness in the head	−0.165	0.013	0.178	0.136	−0.074	−0.057	**0.797**	0.079	0.125
Tinnitus	−0.024	0.329	−0.089	−0.129	0.055	0.341	**0.635**	−0.029	0.022
Flank pain	−0.048	0.033	0.160	0.102	0.020	0.386	−0.187	**0.653**	0.292
Feeling of foreign body in the throat	0.075	−0.058	−0.100	0.035	0.310	−0.059	0.275	**0.645**	0.005
Feeling heavy in the chest	0.162	0.147	0.053	0.021	−0.013	0.025	0.120	0.156	**0.844**
Variance explained (%)	12.367	9.733	8.846	7.417	7.358	6.854	6.218	5.962	5.783

Symptoms with factor loading ≥0.4 are marked bold.

T3 post hoc analysis based on the variance homogeneity of the data. Homogeneous subsets were grouped by these statistical methods. Symptoms with $P < 0.05$ were also indicated for exploratory consideration even though they were unable to meet the adjusted P value condition of under 0.002.

"Feeling of foreign body in the throat" and "sputum" ranked highly in the average score and rank for all years of study. Moreover, there was a tendency for these items to score higher as the year of study increased. From this, we believe that all students had the impression that phlegm pattern is highly correlated with symptoms of the throat. "Phlegm" directly indicates a secretion, that is, "sputum". This might have been the reason for the high preference for "sputum" and "feeling of foreign body in the throat" in the diagnosis of phlegm pattern. "Fatigue" scores were similar for all years of study, but its ranking fell from the second year onwards. This indicates that the students similarly preferred this symptom, but came to believe that other symptoms were more important in evaluating phlegm pattern as the year of study increased. The scores and rankings for "sickness" and "dizziness" showed a tendency to increase, especially rapidly from the second to third year. Based on this, we may believe that third-year students have been taught that these symptoms are very important and featured in evaluating phlegm pattern.

All years of study felt that "Feeling heavy in the limbs," "startled by faint noise," "palpitation," and "itching" were not particularly important in phlegm pattern. Only the fifth-year students registered a high preference for "dark circle under the eye," whilst its score and ranking by the first- to fourth-year students were almost identically low.

There was a unique phase for "lumps," where it was scored and ranked very highly by the second-year students. It is possible there had been a lecture or event that had classified "lumps" as being very important and characterized in phlegm pattern. The third- to fifth-year students registered low scores and ranks for "lumps"; therefore, we believe that only the second-year students had this experience, or that the full Korean medicine education beginning in the third year corrected this overestimated importance.

Symptoms that scored a mean value <3.0 were thought to have "no or less significance" for evaluating or diagnosing phlegm pattern. Seven symptoms were scored <3.0 at least once by the third-, fourth-, or fifth-year students, and 3 symptoms were scored <3.0 in all of these 3 groups. We excluded the first- and second-year students in this discussion because they had not been taught full Korean medicine yet. There are 2 possible reasons for the low mean values.

Table 9: Factors of phlegm pattern questionnaire according to year of study and a previous study.

First year	Second year	Third year	Fourth year	Fifth year	Study by Park et al. [6]
Sputum, cough, feeling of foreign body in the throat, shortness of breath	Sputum, cough, feeling of foreign body in the throat	Sputum, cough, feeling of foreign body in the throat, shortness of breath, feeling heavy in the chest	Sputum, feeling of foreign body in the throat	Sputum, cough, rumbling sound in the abdomen	Sputum, cough, feeling of foreign body in the throat
Sickness, indigestion, poor appetite, lumps yellow face	Sickness, indigestion, Poor appetite, feeling of abdominal fullness, rumbling sound in the abdomen	Sickness, indigestion, poor appetite, feeling of abdominal fullness	Sickness, indigestion, poor appetite, feeling of abdominal fullness, rumbling sound in the abdomen	Sickness, indigestion, poor appetite, feeling of abdominal fullness, rumbling sound in the abdomen	Sickness, indigestion, poor appetite, feeling of abdominal fullness, rumbling sound in the abdomen
Rumbling sound in the abdomen, feeling of abdominal fullness		Mucousy stool, rumbling sound in the abdomen, feeling of abdominal fullness			
Headache, unclearness in the head, mucousy stool(−)	Headache, join pain, flank pain, unclearness in the head, lumps, feeling heavy in the chest feeling of abdominal fullness	Headache, unclearness in the head, lumps, dizziness, tinnitus	Headache, Unclearness in the head, dizziness, mucousy stool(−)	Headache, joint pain, itching	
Tinnitus, dizziness, flank pain, mucousy stool	Tinnitus, dizziness, sickness	Yellowish face, joint pain, flank pain	Joint pain, flank pain, sputum	Tinnitus, dizziness, unclearness in the head	
Fatigue, feeling heavy in the limbs, yellowish face	Fatigue, feeling heavy in the limbs, shortness of breath	Fatigue, feeling heavy in the limbs, flank pain	Fatigue, feeling heavy in the limbs, shortness of breath poor appetite	Fatigue, feeling heavy in the limbs, shortness of breath, poor appetite	Fatigue, feeling heavy in the limbs, headache, dizziness, unclearness in the head
Feeling heavy in the chest			Feeling heavy in the chest, cough, shortness of breath	Feeling heavy in the chest	
Palpitation, startled by faint noise	Palpitation, startled by faint noise, feeling heavy in the chest, poor appetite	Palpitation, startled by faint noise, tinnitus, sputum(−), shortness of breath	Palpitation, startled by faint noise, tinnitus, itching	Palpitation, startled by faint noise, dark circles under the eyes, dizziness	Palpitation, startled by faint noise, tinnitus, joint pain, flank pain, shortness of breath feeling, heavy in the chest
Itching, Joint pain, dark circles under the eyes	Itching, yellowish face, dark circles under the eyes, mucousy stool, rumbling sound in the abdomen	Itching	Dark circles under the eyes, yellowish face, lumps, feeling heavy in the chest(−)	Yellowish face, lumps, mucousy stool	Itching, lumps, mucousy stool
				Feeling of foreign body in the throat, flank pain	Dark circles under the eyes, yellow face

Only items with a factor loading ≥0.4 were extracted.
Factor order does not equal the order of variance explained.
(−) Factor loading is negative value.

First, it is possible that education regarding these symptoms is not conducted enough, although all 25 symptoms are almost equally significant for diagnosing phlegm pattern according to Park et al.'s study [6]. Second, it is also possible that, in practice, these symptoms have less significance than other symptoms for diagnosing phlegm pattern; thus, the teaching process places less emphasis on them. Further studies should be conducted to explain this phenomenon properly.

3.3. Factor Analysis. Tables 4, 5, 6, 7, and 8 present the factor loadings and results of factor analysis regarding the response of the phlegm pattern questionnaire according to the year of study. The factors were constructed using items with a factor loading ≥0.4 for the exploratory factor analysis.

Table 9 lists the extracted factors for the between-group comparison. For the convenience of comparison, the factors are listed with similar factors in a row regardless of their variance explained. The rightmost column contains the factors extracted from the health information of existing patients by Park et al. [6].

With the exception of the fourth-year students, "sputum" and "cough" were grouped together by all years of study. Similarly, with the exception of the fifth-year students, "feeling of foreign body in the throat" and "sputum" were extracted into the same factor. Hence, the students apparently consider "sputum," "cough," and "feeling of foreign body in the throat" as one factor, that is, a respiratory system problem. For all years of study, "sickness," "indigestion," and "poor appetite" were grouped together. We believe that this factor is digestive system problem. For all years of study, "fatigue" and "feeling heavy in the limbs" were grouped together. As these 2 symptoms are the typical symptoms of qi-deficiency pattern, one of the Korean medicine pattern classifications, they exhibit a high correlation. The fourth- and fifth-year students grouped "poor appetite" with "fatigue," "feeling heavy in the limbs," and "shortness of breath," and these symptoms are also related to qi-deficiency pattern. In other words, the fourth- and fifth-year students consider "poor appetite" a symptom of qi-deficiency pattern unlike the first- to third-year students. This may be the effect of the full Korean medicine education. Only the first-year students separated "feeling of abdominal fullness" from "sickness" and "indigestion." Perhaps these students have not yet formed the concept of relating "feeling of abdominal fullness" with the latter 2 symptoms as a digestive system problem. All years of study perceived "headache" and "unclearness in the head" as the same factor. "Palpitation" and "startled by faint noise" also fell within the same factor for all years of study. These 2 symptoms are known as symptoms of the mind in Korean medicine and are treated with similar prescriptions. Thus, this may have affected the students' conceptual perception.

Generally, the factor analysis results of the students' conceptual perception are similar to that of Park et al.'s [6]. Accordingly, we may believe the students' concept of phlegm pattern has a similar dimensional structure containing the manifesting pattern of symptoms in patients.

3.4. Limitation and Further Study. There are some limitations in this study. First, it could not demonstrate the time effect of education directly, because it was a cross-sectional study focusing on a certain point of time, and not a time-series study performed on the same group students from their entry into college to advancing higher years of study. Second, although the College of Korean Medicine of Kyung Hee University is the biggest Korean medicine college in Korea, it does not represent the dimensional structure of conceptual perception of all Korean medicine students in Korea, as each college possesses a certain amount of distinct educational characteristics and curricula. Further studies of a long-term, time-series study and comparison with students from other colleges should be performed in the future. Then, how the full Korean medicine education can affect the students' perceptions over time can be identified more precisely.

4. Conclusion

In this study, we attempted to observe the perceptive characteristics of Korean medicine students' concepts of phlegm pattern according to the year of study mainly by MDS and factor analysis. We found that third-year-student group had the narrowest within-group distribution of perceptions regarding phlegm pattern. Moreover, we were able to observe the difference in diagnostic preference regarding symptoms between years of study. We could witness the apparent effect of education from this study. Finally, by factor analysis, we found that the extracted conceptual factors have similar tendencies with a previously conducted clinical trial study. We expect that this study lends critical meaning to the study of the pattern classification system of Korean medicine and to the study of the structure of conceptual perception in Korean medicine students.

Conflict of Interests

The authors declare that no conflict of interests exists.

Authors' Contribution

Hyungsuk Kim and Hyunho Kim have equally contributed to this paper.

References

[1] World Health Organization, *WHO international standard terminologies on traditional medicine in the western pacific region*, WHO Western Pacific Regional Office, Manila, Philippines, 2007.

[2] H. Jang, J. Kim, S. K. Kim et al., "Ontology for medicinal materials based on traditional Korean medicine," *Bioinformatics*, vol. 26, no. 18, pp. 2359–2360, 2010.

[3] H. Zhang, W. Zuo, K. Wang, D. Zhang, and Y. Chen, "TDS and its application in computer aided TCM diagnostics education," in *Proceedings of the 2nd International Workshop on Education Technology and Computer Science (ETCS '10)*, vol. 3, pp. 260–263, March 2010.

[4] C. C. Tyan, W. M. Liang, H. Y. Shy et al., "How to standardize 3 finger positions of examiner for palpating radial pulses at wrist

in traditional Chinese medicine," *Acupuncture and Electro-Therapeutics Research*, vol. 32, no. 1-2, pp. 87–96, 2007.

[5] Y. J. Park, S. W. Cho, B. H. Lee, and Y. B. Park, "Development and validation of the Yin deficiency scale," *The Journal of Alternative and Complementary Medicine*, vol. 19, no. 1, pp. 50–56, 2013.

[6] Y. J. Park, J. S. Park, M. Y. Kim, and Y. B. Park, "Development of a valid and reliable phlegm pattern questionnaire," *The Journal of Alternative and Complementary Medicine*, vol. 17, no. 9, pp. 851–858, 2011.

[7] L. M. Wang, X. Zhao, X. L. Wu et al., "Diagnosis analysis of 4 TCM patterns in suboptimal health status: a structural equation modelling approach," *Evidence-Based Complementary and Alternative Medicine*, vol. 2012, Article ID 970985, 6 pages, 2012.

[8] T. Stuardi and H. MacPherson, "Acupuncture for irritable bowel syndrome: diagnosis and treatment of patients in a pragmatic trial," *The Journal of Alternative and Complementary Medicine*, vol. 18, no. 11, pp. 1021–1027, 2012.

[9] M. L. Davison, *Multidimensional Scaling*, John Wiley & Sons, New York, NY, USA, 1983.

[10] J. B. Kruskal and M. Wish, *Multidimensional Scaling*, Sage, Newbury Park, Calif, USA, 1978.

[11] S. S. Schiffman, M. L. Reynolds, and F. W. Young, *Introduction to Multidimensional Scaling: Theory, Methods, and Applications*, Academic Press, New York, NY, USA, 1981.

[12] L. C. Swartzman and M. C. Lees, "Causal dimensions of college students' perceptions of physical symptoms," *Journal of Behavioral Medicine*, vol. 19, no. 2, pp. 95–110, 1996.

[13] N. Lown, I. Davies, L. Cordingley, C. Bundy, and I. Braidman, "Development of a method to investigate medical students' perceptions of their personal and professional development," *Advances in Health Sciences Education*, vol. 14, no. 4, pp. 475–486, 2009.

[14] J. Winseman, A. Malik, J. Morison, and V. Balkoski, "Students' views on factors affecting empathy in medical education," *Academic Psychiatry*, vol. 33, no. 6, pp. 484–491, 2009.

[15] L. P. Schmelkin, A. B. Wachtel, B. E. Schneiderman, and D. Hecht, "The dimensional structure of medical students' perceptions of diseases," *Journal of Behavioral Medicine*, vol. 11, no. 2, pp. 171–183, 1988.

[16] B. Jiang, X. Liang, Y. Chen et al., "Integrating next-generation sequencing and traditional tongue diagnosis to determine tongue coating microbiome," *Scientific Reports*, vol. 2, article 936, 2012.

[17] L. C. Lo, J. Y. Chiang, T. L. Cheng, and P. S. Shieh, "Visual agreement analyses of traditional Chinese medicine: a multiple-dimensional scaling approach," *Evidence-Based Complementary and Alternative Medicine*, vol. 2012, Article ID 516473, 5 pages, 2012.

[18] M. F. Chan, M. C. Day, L. K. P. Suen, S. H. M. Tse, and T. F. Tong, "Attitudes and skills of Hong Kong Chinese medicine practitioners towards computerization in practice: a cluster analysis," *Medical Informatics and the Internet in Medicine*, vol. 30, no. 1, pp. 55–68, 2005.

[19] M. F. Chan, E. Mok, Y. S. Wong et al., "Attitudes of Hong Kong Chinese to traditional Chinese medicine and Western medicine: survey and cluster analysis," *Complementary Therapies in Medicine*, vol. 11, no. 2, pp. 103–109, 2003.

[20] S. Ng, C. L. W. Chan, D. Y. F. Ho, Y. Y. Wong, and R. T. H. Ho, "Stagnation as a distinct clinical syndrome: comparing '*Yu*' (stagnation) in traditional Chinese medicine with depression," *British Journal of Social Work*, vol. 36, no. 3, pp. 467–484, 2006.

[21] J. Wang, Q. Y. He, H. X. Li, and Y. T. Fang, "Factor analysis of traditional Chinese medicine syndromes in 815 patients with unstable angina," *Zhong Xi Yi Jie He Xue Bao*, vol. 6, no. 8, pp. 788–792, 2008.

[22] G. Xiong, C. Virasakdi, A. Geater, Y. Zhang, M. Li, and S. Lerkiatbundit, "Factor analysis on symptoms and signs of chronic low-back pain based on traditional Chinese medicine theory," *The Journal of Alternative and Complementary Medicine*, vol. 17, no. 1, pp. 51–55, 2011.

[23] N. N. Jin and K. Ma, "Study of traditional Chinese medicine syndrome factors of dysfunctional uterine bleeding based on cluster analysis and factor analysis," *Zhongguo Zhong Yao Za Zhi*, vol. 33, no. 13, pp. 1622–1625, 2008.

[24] C. Lu, Q. Zha, A. Chang, Y. He, and A. Lu, "Pattern differentiation in traditional Chinese medicine can help define specific indications for biomedical therapy in the treatment of rheumatoid arthritis," *The Journal of Alternative and Complementary Medicine*, vol. 15, no. 9, pp. 1021–1025, 2009.

Hindawi Publishing Corporation
Evidence-Based Complementary and Alternative Medicine
Volume 2013, Article ID 920384, 7 pages
http://dx.doi.org/10.1155/2013/920384

Research Article

Recent Progress in Voice-Based Sasang Constitutional Medicine: Improving Stability of Diagnosis

Jun-Su Jang, Young-Su Kim, Boncho Ku, and Jong Yeol Kim

KM Health Technology Research Group, Medical Research Division, Korea Institute of Oriental Medicine, 1672 Yuseongdae-ro, Yuseong-gu, Daejeon 305-811, Republic of Korea

Correspondence should be addressed to Jong Yeol Kim; ssmed@kiom.re.kr

Received 2 May 2013; Accepted 19 July 2013

Academic Editor: Seong-Gyu Ko

Sasang constitutional medicine is a unique form of tailored medicine in traditional Korean medicine. Voice features have been regarded as an important cue to diagnose Sasang constitution types. Many studies tried to extract quantitative voice features and standardize diagnosis methods; however, they had flaws, such as unstable voice features which vary a lot for the same individual, limited data collected from only few sites, and low diagnosis accuracy. In this paper, we propose a stable diagnosis model that has a good repeatability for the same individual. None of the past studies evaluated the repeatability of their diagnosis models. Although many previous studies used voice features calculated by averaging feature values from all valid frames in monotonic utterance like vowels, we analyse every single feature value from each frame of a sentence voice signal. Gaussian mixture model is employed to deal with a lot of voice features from each frame. Total 15 Gaussian models are used to represent voice characteristics for each constitution. To evaluate repeatability of the proposed diagnosis model, we introduce a test dataset consisting of 10 individuals' voice recordings with 50 recordings per each individual. Our result shows that the proposed method has better repeatability than the previous study which used averaged features from vowels and the sentence.

1. Introduction

Sasang constitutional medicine (SCM) is a unique form of tailored medicine in traditional Korean medicine. The origin of SCM was started by Lee, a Korean medical doctor [1]. In SCM theory, human beings can be categorized into one of the four Sasang constitutional (SC) types (Tae-Yang: TY, Tae-Eum: TE, So-Yang: SY, and So-Eum: SE) according to their inherited characteristics, such as temperament profile, physiological and pathological features, susceptibility to particular diseases, and responses to drugs [2, 3]. In the principle of SCM, treatment is to recover balance between hypoactive organs and hyperactive organs, based on one's constitution. Therefore, determining one's SC type is important and many attempts have been made for standardization of SC diagnosis [4–6].

Diagnosis using voice is one of the important parts in SCM. The relation between SC types and voice is referred in the literatures [1, 7]. TY type's voice is resonant, clear, and loud. It was derived from good respiratory organs. TE types have a load baritone voice, which sounds thick, heavy, and grave. SY types have clear, fast, and high-pitched voice. They are talkative, hasty, and vigorous. SE type's voice is clam and easy. It sounds gentle, slow, and lively. Some of the voice characteristics are described by using utterance quality and style, but personality term is also used to depict voice characteristics. Since the vague linguistic representation can be understood differently to each oriental medicine doctor, an objective and standardized voice diagnosis is needed.

To establish objective and scientific diagnosis of SC types, many studies used computerized voice analysis method. Early studies focused on finding correlation between SC types and various voice features such as fundamental frequency, formants, and energy of voice signal [8–10]. In 2004, Park and Kim found a significant difference between SE and SY in formant frequency and formant bandwidth [11]. Their result showed that SY voice was clearer than SE voice, which was coincident with the SCM literatures. Kim et al. developed a voice analysis system, namely, phonetic system for Sasang constitution (PSSC), and applied it to investigate

constitutional characteristics of Korean adult males and females [12, 13]. They used pitch, amplitude perturbation quotient, shimmer, octave, and energy as voice features. Choi et al. studied characteristics of the Korean adult male sound using PSSC with a sentence [14]. In 2009, Kang et al. analysed 144 voice features from 5 vowels and one sentence recorded from 473 people [15]. They developed a constitutional classification method using support vector machine; however, their classifier was able to apply correctly in only limited voice data [16].

Although many studies existed, they were not sufficient for practical use, because the diagnosis model was made by using a limited number of data gathered in few sites. To overcome the generalization problem, a set of large data, collected from 23 different oriental clinics, were established in the study of Do et al. [4]. They developed an integrative SC analysis tool (SCAT) using four individual diagnosis components: face, body shape, voice, and questionnaire. They trained four individual diagnosis models using logistic regression method, and the four models were combined into a final integrated model. They evaluated the integrated model to a test dataset which was not used in training stage, for confirming generalization ability. As a generalization test result, the diagnostic accuracies of the integrated model were 64.0% and 55.2% in the male and female patient groups, respectively. The accuracies of the voice component were 39.9% and 37.5% for male and female, respectively. Although the accuracies of voice component were low, voice information was still helpful to increase the performance of the integrated model. Another research using the same voice data of Do et al. was carried out by Kim et al. [5]. They employed linear discriminant analysis as a classifier, and the training accuracies were 51% and 47% for male and female, respectively. However, they only provided the training result, which is generally higher than generalization test result.

Most of the previous studies were tried to find voice features that were strongly correlated to SC types and developed SC classification model. A few weakly correlated features were found, and different types of classifier were developed; however, none of those studies mentioned the diagnostic stability of their method. Because of the natural variation in speech, diagnosis results can be different for the same individual speaker. To reduce a lot of unsystematic variation, speaker's utterance should be constrained by a strict standard operating procedure (SOP). Kim et al. studied about developing SOP for extracting stable voice features that can characterize individual's voice quality consistently [17] and also analysed stable voice features [18].

In this paper, we propose a method to improve stability of voice-based SC diagnosis. All of large database, strict SOP, stable voice features, and a robust classification method are required to obtain stability of diagnosis. We use the same voice data as in the previous study [4], since they are known as the largest data containing patients' SC type proved by herbal remedy [19]. The proposed method uses only sentence recordings, against many previous studies using vowels or both vowels and sentences. Most of recent speaker identification studies use words or sentences, rather than vowels, since words or sentences are better to distinguish each individual's voice characteristics [20, 21]. Our results also show that the detailed analysis using a sentence recording has better repeatability in SC classification than the previous approach [4], which used vowels and the sentence.

2. Materials and Methods

2.1. Voice Data for Sasang Constitution Diagnosis. Voice data were collected from 23 oriental medical clinics. The patient whose SC type was diagnosed to TY was excluded due to its small sample size compared with other three SC types. The total number of patients used in this study was 1,969, ranging in age 15–60 years in both genders. The patients did not suffer from any voice-related disease so that they could speak naturally with their own voice quality. Their SC type was examined by SCM practitioners, who had more than five years of experience in clinical practice. A more detailed procedure of data collection was described in Song et al. [19]. Original database included face, body shape, and questionnaire information; however, only voice data were considered in this study.

Recording environment and procedure was strictly controlled by an SOP. Environment noise kept below 40 dB for low-noise recording. Recording room temperature was controlled to $20^{\circ}\mathrm{C} \pm 5^{\circ}\mathrm{C}$, and humidity kept to $40\% \pm 5\%$. Sound Blaster Live 24 bit External Soundcard and Sennheiser e-835s Microphone with a microphone stand were equipped. The distance between the patient and microphone was 4–6 cm. Recording systems were controlled to avoid echoes of voice or irregular resonance. Recording was saved as a wav file with setting of mono 16 bit integer and 44.1 kHz sampling frequency.

Voice data consisted of five vowels (/a/, /e/, /i/, /o/, and /u/) and a sentence. The sentence was recorded twice. Since the all patients were Korean, the sentence was also composed of Korean words. As voice features should represent the natural characteristics of patients in short recordings, the patients were asked to pronounce their natural voice without tension as possible. Before actual recording, an operator instructed the patients about the recording contents and allowed them to rest for 1 hour. Each vowel was uttered at least 3 s. The sentence was uttered in their ordinary speed and tones. In this paper, we used only sentence part to diagnose constitution, and for comparison, the previous study [4] used both five vowels and sentence.

2.2. Voice Feature Extraction. Figure 1 shows how voice features are calculated from a voice signal. We should define the size of a frame window, which is the minimum length to process. Then, we can extract voice features in the frame. After processing the current frame window, the same feature extraction is applied to the next frame window. In this study, the size of a frame window was 46.4 ms, which mapped to 2^{11} audio samples in 44.1 kHz sampling frequency. Neighboring frame windows were overlapped by 50%.

There exist more than a hundred valid frames in each vowel or sentence. In the past studies, there were many candidate voice features, such as fundamental frequency

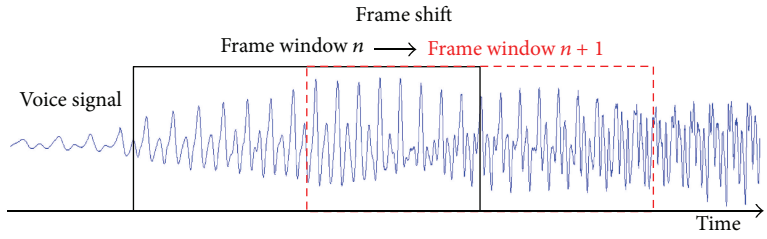

Figure 1: Frame window shift for extracting voice features for each frame.

(*F0*), formants, and jitter. Most of them were calculated by averaging the feature values obtained from the all valid frames in the voice signal. An averaged feature could be good for monotonic utterance like a vowel. For example, *F0* for a vowel is calculated by averaging all *F0* values from the valid frames. The vowel utterance is monotonic, which means that every single *F0* value from each frame should be similar. Therefore, averaging is appropriate for characterizing *F0* for a vowel. Most of the previously used features from a vowel are averaged features, which may represent quality of the vowel properly.

However, features from the vowel are not proper to characterize individual's stable voice quality. It can be easily verified that words or sentences are more suitable for characterizing individual's stable voice quality in the most of recent speaker identification application [20, 21]. To make a stable diagnosis model, which has a good repeatability for the same individual, we focus on the sentence rather than vowel. In contrast to the features for vowel, averaged features are hardly used for the sentence since the features vary a lot in many frames. When averaging, we may lose useful information of individual's voice characteristics. Therefore, we analyse the features from every single frame.

Let $\mathbf{y}_i$ be the feature vector extracted from the ith valid frame. Then, we define the feature vector as follows:

$$\mathbf{y}_i = \begin{bmatrix} \mathbf{x}_i \\ ts_i \end{bmatrix}, \tag{1}$$

where ts_i indicates the relative position of the ith frame in all valid frames, and it has a range between 0 and 1. When the feature vector comes from the first frame of the sentence, the value of ts_i is 0. The vector $\mathbf{x}_i$ is a column vector of candidate voice features. We use Mel-frequency cepstral coefficients (MFCCs) as the candidate voice features. MFCCs are coefficients of the short-term power spectrum of a sound, based on a linear cosine transform of a log power spectrum on a nonlinear mel scale of frequency [22]. The mel scale approximates the human auditory system's response more closely than the linearly spaced frequency bands. MFCCs are widely used in speech and speaker recognition systems [23]. Total 12 MFCCs were used in our study.

Finally, feature vector $\mathbf{y}_i$ is a 13-dimensional vector, and the total number of $\mathbf{y}_i$ is the same as the number of all valid frames, which is usually more than a hundred for a sentence. By defining the feature vector including relative position of the frame, each feature vector contains not only voice characteristics of a frame signal, but also the information where the voice features come from. The feature vector was extracted using C++ program combined with HTK [24].

Since the voice features showed nonlinear fluctuation according to the age in general, a process to reduce the effect of age was required. To eliminate the age effect to the voice features, a standardization process was performed the same as Do et al. [4]. All MFCCs were standardized by using their moving averages and standard deviations derived from the data within the length of age ±5 years for the specific age.

2.3. Gaussian Mixture Model-Based Classification. The problem of SC diagnosis is treated as three-class classification, since TY type is usually excluded due to its rareness. Many statistical pattern recognition methods were applied to SC classification, such as logistic regression [4], linear discriminant analysis [5], and support vector machine [16]. Although many attempts were made in the past, none of them analysed the features from each frame separately. We propose a detailed analysis method to deal with the features of each frame using Gaussian mixture model (GMM). It is widely used for speech analysis area, since it can effectively model voice characteristics. GMM is denoted as

$$p(\mathbf{y} \mid \lambda) = \sum_{j=1}^{M} w_j \cdot g\left(\mathbf{y} \mid \boldsymbol{\mu}_j, \boldsymbol{\Sigma}_j\right), \tag{2}$$

where λ is one of the SC classes, M is the total number of Gaussian models, w_j is the weight for the jth Gaussian model, and $g(\mathbf{y} \mid \boldsymbol{\mu}_j, \boldsymbol{\Sigma}_j)$ is Gaussian function with mean $\boldsymbol{\mu}_j$ and covariance matrix $\boldsymbol{\Sigma}_j$.

The basic idea of using GMM for SC classification is that we put each Gaussian model along the time axis to cover each part of the voice signal. Since we have to deal with a few feature vectors from all valid frames, it is important to use the relative position of each feature vector. In other words, someone's voice features extracted from a certain part of the sentence should be compared to a model that is generated by voice features extracted from similar parts. The feature vector $\mathbf{y}_i$ has 12-dimensional MFCCs and relative position information as the 13th element. Hence, each Gaussian model in GMM is 13-dimensional, and we can display the location of each Gaussian model along the time axis by using the 13th element. Figure 2 shows that GMM covers each part of the voice signal.

Since GMM is needed for each gender and SC type, total 6 groups of feature vectors extracted from training data are

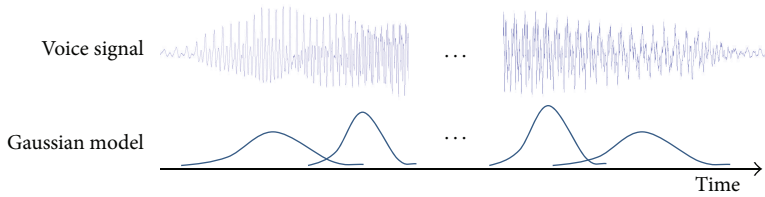

Figure 2: Gaussian mixture model along the time axis to cover each part of the voice signal.

prepared for making 6 GMMs. GMM is trained for each feature vector group using EM algorithm [25]. In training process, the feature vectors need to be assigned to one of the Gaussian models as an initial assignment. The initial assignment can be done by uniformly dividing the feature vectors using the ts_i value. For example, when the number of Gaussian model is 15 ($M = 15$), the feature vectors are extracted from the first 1/15 part of the sentence assigned to the first Gaussian model. This is just for initial assignment, and the assignment is automatically changed in learning process.

After GMM for each SC class is trained, we follow the basic maximum likelihood-based classification. Probability that input recording falls into class of λ is calculated as follows:

$$\overline{p}(\mathbf{y} \mid \lambda) = \prod_{i=1}^{N} p(\mathbf{y}_i \mid \lambda). \quad (3)$$

The total number of feature vectors is N, and the $p(\mathbf{y}_i \mid \lambda)$ is calculated using (2) for each feature vector. Then, the estimated probability for being in each SC type π_k can be denoted as

$$\pi_k = \frac{\overline{p}(\mathbf{y} \mid \lambda_k)}{\sum_{l=1}^{3} \overline{p}(\mathbf{y} \mid \lambda_l)}. \quad (4)$$

The index $k \in \{1, 2, 3\}$ indicates SC types, TE, SE, and SY, respectively. Finally, let $h \in \{1, 2, 3\}$ be the predicted SC types; then the classification rule for SC types using π_k is given by

$$h = \arg\max_{k \in \{1,2,3\}} (\pi_k). \quad (5)$$

This means that simply taking the class of maximum probability is the final decision.

3. Experimental Results

3.1. GMM-Based Classifier. Total 1,969 samples (1,263 females and 706 males) were used to train GMMs. Since the voice characteristics were different according to gender, GMMs were separately trained for each gender. Total 6 GMMs, representing 3 types of SC for each gender, were obtained. Each model had 15 Gaussians to cover the voice signal of a sentence. Table 1 shows the location of each Gaussian in time axis by summarizing the mean value of ts_j. The value of ts_j indicates the relative position of the jth Gaussian model.

Table 1: Mean values of ts_j in each Gaussian model.

No. of Gaussian	Female			Male		
	TE	SE	SY	TE	SE	SY
1	0.050	0.046	0.035	0.062	0.064	0.065
2	0.133	0.149	0.127	0.116	0.109	0.109
3	0.172	0.179	0.177	0.170	0.178	0.187
4	0.279	0.268	0.235	0.225	0.227	0.214
5	0.332	0.283	0.307	0.296	0.279	0.279
6	0.421	0.338	0.396	0.407	0.332	0.339
7	0.502	0.412	0.432	0.459	0.417	0.416
8	0.526	0.524	0.582	0.529	0.488	0.478
9	0.590	0.592	0.590	0.590	0.591	0.549
10	0.660	0.654	0.655	0.691	0.645	0.637
11	0.687	0.694	0.721	0.773	0.649	0.700
12	0.694	0.731	0.794	0.798	0.817	0.774
13	0.820	0.819	0.814	0.832	0.837	0.823
14	0.926	0.922	0.923	0.885	0.932	0.896
15	0.981	0.978	0.979	0.894	0.980	0.937

For example, the first Gaussian in female TE has the relative position value of 0.05. This means that the first Gaussian is located in the first 5% part of the sentence, and input feature vectors are extracted around 5% part of the sentence are mainly judged by the first Gaussian.

Although the purpose of this study is to improve repeatability of diagnosis, we shortly mention the accuracy of the classifier. To make a fair comparison, we used the same test dataset of previous study conducted by Do et al. [4]. The accuracies of the GMM-based classifier were 41.3% and 39.3% for male and female, respectively, which are slightly better than Do et al. It should be noted that the accuracies of voice diagnosis are still low and have to be improved further. However, improvement of accuracy is not the main point of this study. The proposed method has better repeatability (see the next section) than the previous study while maintaining the similar accuracy.

3.2. Diagnosis Repeatability Comparison. To evaluate the repeatability of the SC classification, we gathered voice data of 10 individuals. Total 50 recordings for each individual were prepared with the same way of gathering the training data explained in Section 2.1. It took more than a week to record

Table 2: Comparison results of diagnosis stability between the previous study and the proposed method.

Subject	Do et al. [4]			Proposed		
	Repeatability (%)	Probability mean	Probability standard deviation	Repeatability (%)	Probability mean	Probability standard deviation
1	68	0.561	0.098	100	0.460	0.016
2	76	0.632	0.119	100	0.434	0.039
3	100	0.732	0.090	98	0.406	0.027
4	54	0.500	0.059	100	0.397	0.025
5	98	0.735	0.112	100	0.451	0.031
6	100	0.672	0.090	70	0.381	0.020
7	84	0.603	0.100	82	0.362	0.013
8	56	0.567	0.082	76	0.381	0.013
9	70	0.689	0.130	90	0.384	0.019
10	76	0.629	0.140	100	0.408	0.017
Average	78.2	0.632	0.102	91.6	0.406	0.022

50 times for each individual, so that the recordings contained the intrapersonal voice variations enough. We used this data to compare the proposed method and the previous study conducted by Do et al.

We tested the repeatability and probability values (mean and standard deviation) as a measure of diagnosis stability. Repeatability was defined by the ratio of the number of majority decision to total number of tests. In every test, we also obtained the probability value of the current decision, that is, the maximum probability among π_k. Since the problem of SC diagnosis is three-class classification, the maximum probability is larger than 1/3. A stable classification has a high percentage of repeatability and a low probability standard deviation.

Table 2 shows the comparison results of diagnosis stability. For 10 individuals, the average repeatability of the proposed method was 91.6%, which clearly showed better repeatability than 78.2% of Do et al. And probability standard deviation was 0.022, which was much lower than 0.102 of Do et al. It means that the proposed method generated more consistent results in 50 times classification test of the same individual's voice than the previous study. Interpretation of the probability mean value might be controversial. However, we think that a low probability mean value is more appropriate, considering that the accuracy of the voice diagnosis is low around 40%.

Some of subjects, such as subjects 6 and 8, had low repeatabilities in our method. The subject whose voice feature vector is located close to decision boundary can have a low repeatability, because a small change of the feature vector can switch the final decision. In this case, the probability value is also close to 1/3, which means that the decision has less confidence. We may have a difficulty in determining one's constitution with high confidence when his/her voice does not have clear constitutional characteristics. This can drop the repeatability of diagnosis. However, even in this case, it is good to have similar probability values in repeated tests for the same subject. Our method shows stable diagnosis in probability sense, having low probability standard deviations even in low repeatability cases.

An improved repeatability is obtained from the proposed method that analyses every single frame of the sentence. The improvement is caused by not only analysis method but also recording contents. Our approach uses only sentence rather than both vowels and the sentence since the features from vowels have relatively large variations for the same subject. To examine the stability of each feature value itself, standard deviations of feature values from the sentence and vowels are summarized in Table 3. Some of the vowel features, used in the study of Do et al., are compared to the sentence features in this study. Table 3 shows that sentence features have smaller standard deviations than vowels. Standard deviations of the most sentence features are ranged from 0.2 to 0.7, while standard deviations of many vowel features are larger than 1. Therefore, stability of diagnosis with only sentence will outperform other cases, regardless of classification algorithms.

4. Discussion and Conclusions

In this study, a stable classification method for voice-based Sasang constitutional diagnosis was proposed. In contrast to the previous study, which used averaged features from vowels and one sentence, the proposed method used MFCCs extracted from the sentence only. Since we did not use averaged features to avoid losing useful information of individual's voice characteristics, features from every valid frame were required to be analysed separately. We defined a feature vector that contained MFCCs and relative position of the current frame in the voice signal. Therefore, the feature vector represented both voice features and information about where the features were extracted in time axis of the voice signal. This technique was necessary to use the sentence instead of the vowels, because the sentence included a variety of voice features in each frame, which should not be averaged.

The proposed method employed GMM for detailed analysis of every valid frame in voice signal. Each Gaussian

Table 3: Standard deviations of feature values from the sentence and vowels.

		Subject									
		1	2	3	4	5	6	7	8	9	10
Sentence features	MFCC1	0.290	1.287	0.535	0.414	0.333	0.317	0.432	0.269	0.395	0.245
	MFCC2	0.292	0.358	0.270	0.407	0.356	0.353	0.363	0.391	0.264	0.290
	MFCC3	0.325	0.597	0.302	0.350	0.635	0.413	0.511	0.205	0.313	0.259
	MFCC4	0.246	0.200	0.223	0.434	0.286	0.180	0.448	0.322	0.260	0.139
	MFCC5	0.451	0.320	0.352	0.423	0.479	0.309	0.708	0.470	0.288	0.280
	MFCC6	0.213	0.292	0.199	0.227	0.258	0.240	0.428	0.523	0.329	0.160
	MFCC7	0.336	0.287	0.428	0.266	0.341	0.294	0.311	0.278	0.262	0.307
	MFCC8	0.340	0.346	0.257	0.289	0.269	0.293	0.303	0.347	0.258	0.204
	MFCC9	0.268	0.399	0.279	0.521	0.374	0.307	0.480	0.420	0.362	0.211
	MFCC10	0.359	0.279	0.284	0.461	0.387	0.412	0.381	0.485	0.286	0.193
	MFCC11	0.251	0.334	0.304	0.412	0.375	0.411	0.432	0.410	0.251	0.235
	MFCC12	0.329	0.380	0.178	0.325	0.590	0.398	0.669	0.278	0.265	0.313
Vowel features	aENG	0.069	0.878	0.208	0.417	0.394	0.129	0.912	0.244	1.549	1.659
	aF1	0.634	0.336	0.453	0.380	0.282	0.552	0.489	0.652	0.366	0.346
	aSHIM	0.848	1.030	0.875	1.167	1.094	1.094	2.843	2.195	1.448	0.749
	eSHIM	1.127	1.397	0.986	1.555	0.873	1.120	2.870	3.048	1.393	0.541
	iDTF0	5.234	7.824	1.775	9.167	3.757	4.080	10.320	6.106	9.598	6.307
	iJITT	0.933	1.066	0.695	5.042	1.623	1.154	2.869	2.789	1.096	0.915
	oDTF0	2.330	6.399	1.296	3.616	3.767	3.623	9.513	8.807	1.316	1.178
	oPW	0.046	0.454	0.206	0.500	0.294	0.272	1.133	0.225	1.198	2.080
	uF1	0.263	0.286	0.874	0.580	0.188	0.356	0.422	0.273	0.216	0.659

Vowel features, xENG (energy), xF1 (1st formant), xSHIM (shimmer), xDTF0 (average difference of pitch over the time interval), xJITT (jitter), and xPW (power) were used in the study of Do et al. [4] $x \in \{a, e, i, o, u\}$.

probability model represented constitutional and individual characteristics by covering each part of the sentence. An input feature vector extracted from a certain part of the sentence could be mapped to Gaussian models that were trained using voice features extracted from similar parts of training data. Our method was compared to the previous study, which used both vowels and the sentence. The proposed method had an average repeatability of 91.6% in experimental results using 10 individuals' voice recordings with 50 repeated tests per each individual. The results showed that our method had better repeatability than the previous study. It proved that using features extracted from every valid frame was better than using averaged features of all valid frames.

Averaged features could be good for monotonic utterance like vowels. However, features from the vowels are not proper to characterize individual voice quality. It can be easily realized that most of speaker identification applications use sentences, rather than vowels, since sentences are better to distinguish each individual's voice characteristics. Therefore, we conclude that detailed analysis using every single feature in each frame of the sentence, rather than using averaged features, is helpful to improve stability of SC diagnosis.

The proposed method is a text-dependent voice diagnosis, which uses the predefined sentence, and the same sentence must be used for both training and test stages equally. The stability will vary greatly when a different sentence is used in training and test stages. For future research, text-independent voice diagnosis method is required, so that subjects can speak freely to the system.

Acknowledgment

This research was supported by the National Research Foundation of Korea (NRF) funded by the Ministry of Science, ICT and Future Planning (no. 2006-2005173).

References

[1] J. Lee, *Dongeuisusebowon-Chogo*, Translated by D.-R. Kim, Cheongdam, 1999.

[2] J. Y. Kim and D. D. Pham, "Sasang constitutional medicine as a holistic tailored medicine," *Evidence-Based Complementary and Alternative Medicine*, vol. 6, no. S1, pp. 11–19, 2009.

[3] I. B. Song, *An Introduction To Sasang Constitutional Medicine*, Jimoondang, Seoul, Republic of Korea, 2005.

[4] J.-H. Do, E. Jang, B. Ku, J.-S. Jang, H. Kim, and J. Y. Kim, "Development of integrated Sasang constitution diagnosis method using face, body shape, voice, and questionnaire information," *BMC Complementary and Alternative Medicine*, vol. 12, article 85, 2012.

[5] K. H. Kim, B. Ku, N. Kang, Y.-S. Kim, J.-S. Jang, and J. Y. Kim, "Study of a vocal feature selection method and vocal properties for discriminating four constitution types," *Evidence-Based Complementary and Alternative Medicine*, vol. 2012, Article ID 831543, 10 pages, 2012.

[6] E. Jang, J. Y. Kim, H. Lee, H. Kim, Y. Baek, and S. Lee, "A study on the reliability of Sasang constitutional body trunk measurement," *Evidence-Based Complementary and Alternative Medicine*, vol. 2012, Article ID 604842, 8 pages, 2012.

[7] E. J. Lee, E. H. Sohn, J. H. Yoo et al., "The study of Sasangin's face," *Journal of Sasang Constitutional Medicine*, vol. 17, no. 3, pp. 55–68, 2005.

[8] S. Yang and D. Kim, "A study on the correlation between sound spectrogram and Sasang constitution," *Journal of Sasang Constitutional Medicine*, vol. 8, no. 2, pp. 191–202, 1996.

[9] D. Kim, S. Park, and G. Gun, "An objective study of Sasang constitution diagnosis by sound analysis," *Journal of Sasang Constitutional Medicine*, vol. 10, no. 1, pp. 65–80, 1998.

[10] M. Shin and D. Kim, "A study on the correlation between sound characteristics and Sasang constitution by CSL," *Journal of Sasang Constitutional Medicine*, vol. 11, no. 1, pp. 137–157, 1999.

[11] S.-J. Park and D.-R. Kim, "A study on the correlation between Sasang constitution and sound characteristics used harmonics and formant bandwidth," *Journal of Sasang Constitutional Medicine*, vol. 16, no. 1, pp. 61–73, 2004.

[12] D.-J. Kim, W.-K. Jung, J.-W. Choi, D.-R. Kim, and J.-W. Jeon, "A study on the characteristics of the adult men sound as by Sasang constitution analyzed with PSSC-2004," *Journal of Sasang Constitutional Medicine*, vol. 17, no. 1, pp. 67–83, 2005.

[13] S.-H. Kim, D.-Y. Han, J.-Y. Youn, D.-R. Kim, and J.-W. Jeon, "A study on the characteristics of the Korea adult women sound as by Sasang constitution analysed with PSSC-2004," *Journal of Sasang Constitutional Medicine*, vol. 17, no. 1, pp. 84–102, 2005.

[14] J.-W. Choi, H.-S. Song, D.-Y. Han, and S.-E. Cho, "A study on the characteristics of the Korean adult male sound according to Sasang constitution using PSCC with a sentence," *Journal of Sasang Constitutional Medicine*, vol. 18, no. 3, pp. 64–74, 2006.

[15] J. H. Kang, J. H. Yoo, H. J. Lee, and J. Y. Kim, "Automated speech analysis applied to Sasang constitution classification," *Phonetics and Speech Sciences*, vol. 1, no. 3, pp. 155–161, 2009.

[16] J. H. Kang, J. H. Do, and J. Y. Kim, "Voice classification algorithm for sasang constitution using support vector machine," *Journal of Sasang Constitutional Medicine*, vol. 22, no. 1, pp. 17–25, 2010.

[17] K. H. Kim, J.-S. Jang, Y.-S. Kim, and J. Y. Kim, "Study of developing SOP for extracting stable vocal features for accurate diagnosis," *Korean Journal of Oriental Physiology & Pathology*, vol. 25, no. 6, pp. 1108–1112, 2011.

[18] K. H. Kim, S. G. Kim, N. S. Kang, and J. Y. Kim, "Study for extraction of stable vocal features and definition of the features," *Korea Journal of Oriental Medicine*, vol. 17, no. 3, pp. 97–104, 2011.

[19] K.-H. Song, S.-G. Yu, S. Cha, and J. Y. Kim, "Association of the apolipoprotein A5 Gene −1131T>C polymorphism with serum lipids in Korean subjects: impact of Sasang constitution," *Evidence-Based Complementary and Alternative Medicine*, vol. 2012, Article ID 598394, 8 pages, 2012.

[20] F. Castaldo, D. Colibro, C. Vair, S. Cumani, and P. Laface, "Loquendo-Politecnico di Torino's 2010 NIST speaker recognition evaluation system," in *Proceedings of the 36th IEEE International Conference on Acoustics, Speech, and Signal Processing (ICASSP '11)*, pp. 5464–5467, May 2011.

[21] T. Kinnunen and H. Li, "An overview of text-independent speaker recognition: from features to supervectors," *Speech Communication*, vol. 52, no. 1, pp. 12–40, 2010.

[22] http://en.wikipedia.org/wiki/Mel-frequency_cepstrum.

[23] R. Hasan, M. Jamil, G. Rabbani, and S. Rahman, "Speaker identification using mel frequency cepstral coefficients," in *Proceedings of the 3rd International Conference on Electrical & Computer Engineering (ICECE '12)*, pp. 565–568, 2004.

[24] http://htk.eng.cam.ac.uk.

[25] A. P. Dempster, N. M. Laird, and D. B. Rubin, "Maximum likelihood from incomplete data via the EM algorithm," *Journal of the Royal Statistical Society*, vol. 39, no. 1, pp. 1–38, 1977.

Hindawi Publishing Corporation
Evidence-Based Complementary and Alternative Medicine
Volume 2013, Article ID 402585, 5 pages
http://dx.doi.org/10.1155/2013/402585

Research Article

Autonomic Conditions in Tinnitus and Implications for Korean Medicine

Eun Ji Choi,[1] Younghee Yun,[1,2] Seungyeon Yoo,[3] Kyu Seok Kim,[2] Jeong-Su Park,[4,5] and Inhwa Choi[1,2]

[1] *Department of Otorhinolaryngology of Korean Medicine, Kyung Hee University Hospital at Gangdong, Seoul, Republic of Korea*
[2] *Department of Ophthalmology, Otorhinolaryngology and Dermatology of Korean Medicine, College of Korean Medicine, Kyung Hee University, Seoul, Republic of Korea*
[3] *Department of Human Informatics of Korean Medicine, Interdisciplinary Programs, Kyung Hee University, Seoul, Republic of Korea*
[4] *Kyung Hee Center for Clinical Research and Drug Development, Kyung Hee University, Seoul, Republic of Korea*
[5] *Department of Preventive Medicine, Korean Medical College, Kyung Hee University Graduate School, Seoul, Republic of Korea*

Correspondence should be addressed to Inhwa Choi; inhwajun@hanmail.net

Received 2 April 2013; Revised 7 June 2013; Accepted 17 June 2013

Academic Editor: Seong-Gyu Ko

Tinnitus patients suffer from not only auditory sensations but also physical, mental, and social difficulties. Even though tinnitus is believed to be associated with the autonomic nervous system, changes in autonomic conditions in tinnitus patients are not receiving much research attention. The aims of this study were to investigate the autonomic condition of tinnitus patients and to consider Korean medicine in the treatment of tinnitus with an evidence-based approach. We performed a retrospective chart review and compared the heart rate variability (HRV) parameters of 40 tinnitus patients (19 acute and 21 chronic) and 40 healthy controls. In tinnitus patients, the power of the high frequency component and total power of the HRV significantly decreased ($P < 0.05$), and the low frequency to high frequency ratio significantly increased ($P < 0.05$). There was no significant difference between the acute and chronic patients. When comparing each group with the controls, there was a tendency that the longer the duration of tinnitus was, the larger the observed HRV change was. In conclusion, tinnitus patients have vagal withdrawal and sympathetic overactivity, and chronic tinnitus more strongly affects autonomic conditions than acute tinnitus. This study provides evidence for Korean medical treatments of tinnitus, such as acupuncture and Qi-training, that cause modulation of cardiac autonomic function.

1. Introduction

Tinnitus is an auditory phantom sensation experienced when no external sound is present [1]. Its prevalence in Korea has been reported to be 10.5% of the non-noise-exposed population and increases with age [2, 3]. Tinnitus can be categorized according to the duration of the disease. Generally, acute tinnitus is defined as a condition lasting shorter than three months, and chronic tinnitus is considered as a condition lasting longer than three months [4]. Tinnitus is also classified as subjective or objective. In most cases, tinnitus is described as subjective, which cannot be heard by anyone other than the patient [5]. Therefore, subjective tinnitus was the focus of this study.

Patients who experience tinnitus often report associated symptoms, such as emotional difficulties, sleep deprivation, and interference with social interactions [6]. Additionally, the annoyance of tinnitus is not correlated with the acoustic characteristics, but there is a significant correlation with psychological symptoms [7]. Although there are some management options for tinnitus and associated difficulties [8], little high-level evidence exists regarding the efficacy and specificity of the various options currently in use. Therefore, the choice of treatment is now largely in the hands of the individual clinician [9].

The autonomic nervous system (ANS) is a major factor in the difference between simply perceiving tinnitus and being distressed by it [10]. Heart rate variability (HRV) is

a noninvasive quantitative and qualitative tool that can be used to evaluate the function of the ANS. HRV studies should enhance our understanding of the physiological phenomena and disease mechanisms of tinnitus. Also, these types of studies may be useful for selecting the most effective therapeutic interventions [11].

There are prior studies regarding tinnitus and the autonomic nervous system. One study reported that heart rate variability (HRV) is suppressed and the sympathetic activity of the ANS is predominant in tinnitus patients [12]. In another study regarding tinnitus severity and neural activity, tinnitus distress correlated positively with sympathetic markers and negatively with parasympathetic markers [13].

However, in previous studies, the number of patients enrolled was small, and the data from control patients did not compensate for age or sex. Also, few studies have evaluated the acute and chronic effects of tinnitus on the ANS. The aims of the present study were to investigate the clinical features of the ANS in tinnitus patients and to define the relationship between the duration of tinnitus and variations in the ANS.

2. Materials and Methods

2.1. Subjects

2.1.1. Tinnitus Patients. We performed a retrospective chart review of patients with tinnitus who presented at the Department of Otorhinolaryngology of Korean Medicine, Kyung Hee University Hospital in Gangdong, Seoul, Republic of Korea, from January 2008 to February 2012.

The eligibility criterion for inclusion was first-time Korean adult outpatients presenting for treatment of subjective tinnitus (both bilateral and unilateral). Exclusion criteria were (1) the presence of disease known to affect HRV (cardiovascular, endocrinologic, autoimmune, neurologic, and psychiatric disorders, including alcoholism and polytoxemia), (2) patients with a history of smoking, (3) anticholinergic, antidepressant, or contraceptive pill use for at least four weeks prior to the study, (4) hormone replacement therapy, and (5) pregnancy.

2.1.2. Healthy Controls. The control group was comprised of healthy people who presented for a health checkup at the Health Promotion Center, Kyung Hee University Hospital in Gangdong, Seoul, Republic of Korea, from March 2011 to December 2011.

Inclusion criteria were (1) Korean adults who underwent an overall health checkup and had a measured HRV and (2) whose age and sex were matched with those of the tinnitus patients. The exclusion criteria were the same as for the tinnitus patients. After screening the healthy controls, we extracted random samples equally matched to the age and sex distributions of the patient group.

2.2. HRV Analysis. Subjects removed any metal attachments from their bodies and were seated on comfortable chairs in a quiet room and then asked to relax for 15 minutes. After the relaxation period, electrocardiography recording was performed for 5 minutes and was then assessed by the SA-3000P (Medicore Inc., Seoul, Republic of Korea).

Table 1: Interpretation of HRV parameters.

HRV parameter	Interpretation
Total power of the HRV spectrum (TP)	Total strength of ANS (overall state of HRV)
Very low frequency component (VLF)	Sympathetic regulation
Low frequency component (LF)	Both sympathetic and parasympathetic activities
High frequency component (HF)	Parasympathetic activity and the frequency of respiration
Ratio of absolute LF to HF power (LF/HF)	Sympathetic-parasympathetic balance

The HRV spectrum contains three major components: a very low frequency (VLF, below 0.04 Hz), a low frequency (LF, 0.04–0.15 Hz), and a high frequency (HF, 0.15–0.4 Hz). Recommendations for interpretation of HRV parameters are summarized in Table 1. The HRV was assessed on the basis of the frequency domain measures performed with the use of fast Fourier transformation [11, 14].

2.3. Statistical Analysis. SPSS 15.0 for Windows (SPSS Inc., Chicago, IL, USA) was used for data management and statistical analysis. All continuous variables are expressed as mean ± standard deviation (SD). Sex distribution was analyzed using the Chi-square test, and age was evaluated by analysis of variance (ANOVA). HRV variables that were not normally distributed were log-transformed prior to statistical analysis for parametric statistical analysis of nonnormally distributed data by Duan's smearing equation [15]. Transformed HRV variables were analyzed using an independent sample t-test or one-way ANOVA between groups. If there were statistically significant differences between groups in ANOVA, the post hoc test was used to identify them. A P value less than 0.05 was considered statistically significant.

3. Results

3.1. Subjects. In the tinnitus patient group, 79 patients were screened, and, of these, 40 (19 acute and 21 chronic) were included in the study. The mean ages of the acute and chronic patients were 45.21 ± 12.46 (SD) years and 47.81 ± 15.87 (SD) years, respectively.

In the healthy control group, we screened 2,114 people, and 40 of these, aged 46.53 ± 14.23 (SD) years, were finally selected as healthy controls. There were no significant differences in the age or sex distribution of the groups. Clinical characteristics of the study participants are summarized in Table 2.

3.2. HRV Parameters for Healthy Controls and Tinnitus Patients. The mean values of the HRV measurements are listed in Table 3. In the tinnitus patients, TP and HF were

Table 2: Sex and age distributions of the study participants.

Variables	Healthy controls ($n = 40$)	Tinnitus patients		P value
		Acute ($n = 19$)	Chronic ($n = 21$)	
Sex				
Male	20	11	9	0.637
Female	20	8	12	
Age, y (mean ± SD)	46.53 ± 14.23	45.21 ± 12.46	47.81 ± 15.87	0.848
Age subgroup				
19–29 y	7	3	4	
30–39 y	3	2	1	
40–49 y	10	5	5	
50–59 y	13	7	6	
60–69 y	5	2	3	
>70 y	2	0	2	

Data are n or mean ± SD. Sex distribution was evaluated using the Chi-square test. Age was evaluated by analysis of variance (ANOVA). Statistical significance was set at a P value < 0.05.

Table 3: HRV parameters for healthy controls versus tinnitus patients.

HRV parameter	Healthy controls	Tinnitus patients	P value
TP (ms^2)	7.49 ± 0.99	6.92 ± 1.14	0.020*
VLF (ms^2)	6.37 ± 0.92	6.09 ± 1.21	0.256
LF (ms^2)	5.98 ± 1.19	5.54 ± 1.27	0.114
HF (ms^2)	6.41 ± 1.19	5.13 ± 1.43	0.000**
LF/HF	0.94 ± 0.11	2.48 ± 3.47	0.008**

HRV data were log-transformed prior to statistical analysis. The values given are the mean ± SD. Statistical significance was set at a P value < 0.05, using independent sample t-test. TP: total power; VLF: very low frequency; LF: low frequency; HF: high frequency; LF/HF: ratio of absolute LF to HF power; *$P < 0.05$; **$P < 0.01$.

Table 4: HRV parameters for healthy controls and acute and chronic tinnitus patients.

HRV parameter	Healthy controls	Tinnitus patients		P value
		Acute	Chronic	
TP (ms^2)	7.49 ± 0.99	6.99 ± 1.23	6.86 ± 1.09	0.063
VLF (ms^2)	6.37 ± 0.92	6.18 ± 1.32	6.01 ± 1.12	0.461
LF (ms^2)	5.98 ± 1.19	5.52 ± 1.36	5.56 ± 1.22	0.288
HF (ms^2)	6.41 ± 1.19[a]	5.31 ± 1.34[b]	4.97 ± 1.52[b]	0.000**
LF/HF	0.94 ± 0.11[a]	1.85 ± 2.13[a, b]	3.05 ± 4.32[b]	0.007*

HRV data were log-transformed prior to statistical analysis. The values given are the mean ± SD. Statistical significance was set at a P value < 0.05, using analysis of variance (ANOVA). If there were statistically significant differences between groups, the post hoc test (Duncan) was used to identify them with "[a, b]". TP: total power; VLF: very low frequency; LF: low frequency; HF: high frequency; LF/HF: ratio of absolute LF to HF power; *$P < 0.05$; **$P < 0.01$.

lower, and the LF/HF was significantly higher than in controls. However, VLF and LF were not significantly different between the groups.

3.3. HRV Parameters for Healthy Controls and Acute and Chronic Tinnitus Patients. The values of the HRV parameters, divided into acute and chronic tinnitus patients, are summarized in Table 4. No significant differences were found between the acute and chronic patients. When compared to controls, only the HF was significantly decreased in acute patients; however, in chronic patients, the HF was significantly, decreased and the LF/HF was significantly increased.

4. Discussion

We investigated the autonomic condition in tinnitus patients as compared with healthy controls, as well as the acute and chronic effects of tinnitus on the ANS. Considering the differences in autonomic conditions between tinnitus patients (combined acute and chronic tinnitus patients) and healthy controls, the TP and HF were significantly decreased, and the LF/HF was significantly increased in tinnitus patients. A decreased TP could reflect a depressed state of the overall HRV, which has also been reported in several diseases [11] and stressful conditions [16]. A reduced HF can indicate reduced parasympathetic activity. An increased LF/HF could be due to either increased sympathetic autonomic modulation or decreased parasympathetic activity [17]. In the current series, the LF was nearly unchanged, but the HF was decreased in tinnitus. Therefore, the increase of the LF/HF is mainly due to reduction of parasympathetic activity, and this may cause sympathomimetic symptoms to appear more dominant. This result indicates that overall HRV and parasympathetic functions are significantly depressed and sympathetic activity is relatively predominant in tinnitus patients. This is in agreement with a previous study reporting that overall HRV is suppressed and that the activity of the sympathetic branch of the ANS predominates in tinnitus patient [12]. However, the results cannot be adequately compared to prior research because studies on the relationship between tinnitus and

autonomic condition are rare. Therefore, understanding that tinnitus is a form of noise perception, we searched for studies regarding noise and HRV and found interesting reports. Previous studies demonstrated reduced parasympathetic activity when listening to a mechanical sound, as opposed to synthesizer music or bird twitters, which have very different frequency components [18]. Because the sound of tinnitus is often a simple frequency, this may be consistent with the results of the present study. In another study, sympathetic activity was increased under exposure to acute noise [19], similar to the current results.

When tinnitus patients were divided into acute and chronic groups, there were no significant differences in HRV parameters. When comparing each group with the controls, in acute tinnitus patients, only the HF was significantly decreased. However, in chronic tinnitus patients, HF was significantly decreased, and the LF/HF was significantly increased. This can be interpreted to mean that chronic tinnitus has a stronger effect on changes in autonomic conditions compared with acute tinnitus.

In Korean medicine, tinnitus patients are treated with various modalities, such as acupuncture, herbal medicine, counseling, and Qi-training [20–22]. Previous studies have revealed that acupuncture at the Sishencong points and Qi-training enhanced cardiac vagal and suppressed sympathetic activities in humans [22, 23]. In a recent study, epifascial acupunctural stimulation at CV17 also increased vagal activity, and the presence of a specific acupunctural point that causes the modulation of cardiac autonomic function is suggested [24].

There are several limitations of the current study. The current study was controlled for age- and sex-related differences but not variations in symptom severity. Also, the HRV data were not measured at the same time of the day, so a circadian variation of HRV cannot be excluded.

To our knowledge, this is one of only a few studies regarding the effects of tinnitus on the autonomic condition. The results of the current study should help to elucidate the associated symptoms leading to a progressive deterioration in quality of life for tinnitus patients and aid in selecting proper Korean medical treatment options for alleviating the accompanying symptoms.

5. Conclusions

According to the HRV analysis of tinnitus patients, we conclude that tinnitus patients have significantly altered HRV parameters compared to healthy controls. Tinnitus reduced parasympathetic activity and chronically induced sympathetic overactivity. Chronic tinnitus had a stronger effect on autonomic changes than acute tinnitus. These findings provide evidence supporting Korean medical treatments for tinnitus, including modalities such as acupuncture and Qi-training, which enhance cardiac vagal and suppress sympathetic activities in humans. The underlying mechanisms and potential applications of Korean medicine for tinnitus warrant further investigation.

Acknowledgment

This study was supported by a Grant from the Traditional Korean Medicine R&D Project, Ministry of Health and Welfare, Republic of Korea (B120014).

References

[1] J. J. Eggermont and L. E. Roberts, "The neuroscience of tinnitus," *Trends in Neurosciences*, vol. 27, no. 11, pp. 676–682, 2004.

[2] A. J. Heller, "Classification and epidemiology of tinnitus," *Otolaryngologic Clinics of North America*, vol. 36, no. 2, pp. 239–248, 2003.

[3] J. W. Koo, W. C. Lee, H. Kim et al., "Prevalence of tinnitus and hearing thresholds of a non-noise-exposed population with and without tinnitus," *Korean Journal of Occupational and Environmental Medicine*, vol. 11, no. 3, pp. 323–331, 1999.

[4] A. Davis and A. E. Rafaie, "Epidemiology of tinnitus," in *Tinnitus Handbook*, R. S. Tyler, Ed., pp. 1–23, Singular, Thomson Learning, San Diego, Calif, USA, 2000.

[5] P. Martinez Devesa, A. Waddell, R. Perera, and M. Theodoulou, "Cognitive behavioural therapy for tinnitus," *Cochrane Database of Systematic Reviews*, no. 1, Article ID CD005233, 2007.

[6] J. Shargorodsky, G. C. Curhan, and W. R. Farwell, "Prevalence and characteristics of tinnitus among US adults," *American Journal of Medicine*, vol. 123, no. 8, pp. 711–718, 2010.

[7] L. M. Luxon, "Tinnitus: its causes, diagnosis, and treatment," *British Medical Journal*, vol. 306, no. 6891, pp. 1490–1491, 1993.

[8] B. I. Han, H. W. Lee, T. Y. Kim, J. S. Lim, and K. S. Shin, "Tinnitus: characteristics, causes, mechanisms, and treatments," *Journal of Clinical Neurology*, vol. 5, no. 1, pp. 11–19, 2009.

[9] D. J. Hoare and D. A. Hall, "Clinical guidelines and practice: a commentary on the complexity of tinnitus management," *Evaluation and the Health Professions*, vol. 34, no. 4, pp. 413–420, 2011.

[10] P. J. Jastreboff and J. W. Hazell, *Tinnitus Retraining Therapy: Implementing the Neurophysiological Model*, Cambridge University Press, Cambridge, UK, 2004.

[11] M. Malik, J. T. Bigger, A. J. Camm et al., "Heart rate variability: standards of measurement, physiological interpretation, and clinical use," *Circulation*, vol. 93, no. 5, pp. 1043–1065, 1996.

[12] E. Datzov, S. Danev, H. Haralanov, V. Naidenova, T. Sachanska, and A. Savov, "Tinnitus, heart rate variability, and some biochemical indicators," *International Tinnitus Journal*, vol. 5, no. 1, pp. 20–23, 1999.

[13] E. van der Loo, M. Congedo, S. Vanneste, P. V. de Heyning, and D. de Ridder, "Insular lateralization in tinnitus distress," *Autonomic Neuroscience*, vol. 165, no. 2, pp. 191–194, 2011.

[14] F. Yasuma and J.-I. Hayano, "Respiratory sinus arrhythmia: why does the heartbeat synchronize with respiratory rhythm?" *Chest*, vol. 125, no. 2, pp. 683–690, 2004.

[15] N. Duan, "Smearing estimate: a nonparametric retransformation method," *Journal of the American Statistical Association*, vol. 78, no. 383, pp. 605–610, 1983.

[16] S. Matthews, H. Jelinek, S. Vafaeiafraz, and C. S. McLachlan, "Heart rate stability and decreased parasympathetic heart rate variability in healthy young adults during perceived stress," *International Journal of Cardiology*, vol. 156, no. 3, pp. 337–338, 2012.

[17] B. Björ, L. Burström, M. Karlsson, T. Nilsson, U. Näslund, and U. Wiklund, "Acute effects on heart rate variability when exposed to hand transmitted vibration and noise," *International Archives of Occupational and Environmental Health*, vol. 81, no. 2, pp. 193–199, 2007.

[18] R. Yanagihashi, M. Ohira, T. Kimura, and T. Fujiwara, "Physiological and psychological assessment of sound," *International Journal of Biometeorology*, vol. 40, no. 3, pp. 157–161, 1997.

[19] L. Tzaneva, S. Danev, and R. Nikolova, "Investigation of noise exposure effect on heart rate variability parameters," *Central European Journal of Public Health*, vol. 9, no. 3, pp. 130–132, 2001.

[20] Y. B. Kim, "Clinical observations for evaluation protocol on tinnitus," *Korean Journal of Oriental Physiology & Pathology*, vol. 16, no. 2, pp. 403–407, 2002.

[21] J. H. Jeon, E. H. Choi, and Y. I. Kim, "Acupuncture combined with herbal medicine for the treatment of tinnitus: clinical study in 11 cases," *The Journal of Korean Acupuncture & Moxibustion Society*, vol. 25, no. 3, pp. 197–203, 2008.

[22] M. S. Lee, H. J. Huh, B. G. Kim et al., "Effects of Qi-training on heart rate variability," *American Journal of Chinese Medicine*, vol. 30, no. 4, pp. 463–470, 2002.

[23] J. D. Wang, T. B. J. Kuo, and C. C. H. Yang, "An alternative method to enhance vagal activities and suppress sympathetic activities in humans," *Autonomic Neuroscience*, vol. 100, no. 1-2, pp. 90–95, 2002.

[24] Y. Kurono, M. Minagawa, T. Ishigami, A. Yamada, T. Kakamu, and J. Hayano, "Acupuncture to Danzhong but not to Zhongting increases the cardiac vagal component of heart rate variability," *Autonomic Neuroscience*, vol. 161, no. 1-2, pp. 116–120, 2011.

Hindawi Publishing Corporation
Evidence-Based Complementary and Alternative Medicine
Volume 2013, Article ID 936257, 10 pages
http://dx.doi.org/10.1155/2013/936257

Research Article

Saussurea lappa Clarke-Derived Costunolide Prevents TNFα-Induced Breast Cancer Cell Migration and Invasion by Inhibiting NF-κB Activity

Youn Kyung Choi, Sung-Gook Cho, Sang-Mi Woo, Yee Jin Yun, Jeakyung Jo, Wooyoung Kim, Yong Cheol Shin, and Seong-Gyu Ko

Laboratory of Clinical Biology and Pharmacogenomics, Center for Clinical Research and Genomics, Department of Preventive Medicine, College of Korean Medicine, Kyung Hee University, 1 Hoegi-dong, Seoul 130-701, Republic of Korea

Correspondence should be addressed to Seong-Gyu Ko; epiko@khu.ac.kr

Received 5 April 2013; Accepted 3 May 2013

Academic Editor: Bo-Hyoung Jang

Saussurea lappa Clarke (SLC) has been used as a traditional medicine in Korea, China, and Japan for the treatment of abdominal pain and tenesmus. Costunolide, a sesquiterpene lactone isolated from SLC, has diverse medicinal effects. However, the anticancer effects of costunolide are still unclear in breast cancer. In this study, we demonstrate that costunolide suppresses tumor growth and metastases of MDA-MB-231 highly metastatic human breast cancer cells via inhibiting TNFα-induced NF-κB activation. Costunolide inhibited MDA-MB-231 tumor growth and metastases without affecting body weights in the *in vivo* mouse orthotopic tumor growth assays. In addition, costunolide inhibited *in vitro* TNFα-induced invasion and migration of MDA-MB-231 cells. Costunolide further suppressed TNFα-induced NF-κB signaling activation, resulting in a reduced expression of MMP-9, a well-known NF-κB-dependent gene to mediate breast cancer cell growth and metastases. Therefore, we conclude that SLC and its derivative costunolide suppress breast cancer growth and metastases by inhibiting TNFα-induced NF-κB activation, suggesting that costunolide as well as SLC may be promising anticancer drugs, especially for metastatic breast cancer.

1. Introduction

Most breast cancer is an epithelial tumor that develops from mammary gland tissue and the inner lining of milk ducts [1]. Metastatic breast cancer is not well cured by surgery, radiotherapy, and chemotherapy [2–4]. Cancer metastasis is the spread of tumor cells from an original site to distant parts of the body. This event consists of multistep processes, which includes tumor cell dissemination, extracellular matrix (ECM) degradation, tumor cell invasion into the ECM, angiogenesis, and secondary metastatic tumor growth [5–7]. Interestingly, primary tumors metastasize to specific organs; for example, aggressive breast cancers selectively metastasize to lung, bone, and brain tissue. This organ tropism seems to be related to different gene expression patterns [8–10].

TNFα is frequently detected in many human cancer tissues including breast, ovarian, and renal cancers [11, 12]. In addition, tumor cells producing TNFα are correlated with poor prognoses [11]. TNFα signaling activation through TNF receptor leads to promoting a recruitment of adaptor proteins and to activating signal cascades including NF-κB pathway [13, 14]. NF-κB regulates diverse physiological and pathological processes including development, metabolism, inflammation, and tissue homeostasis by regulating expression of various genes. In particular, genes regulated by NF-κB play roles such as development, proliferation, survival, and metastasis in cancer [15–17]. NF-κB protein bound to IκBα in the cytoplasm is maintained as an inactive state [18]. In response to NF-κB activation signals, IKKα/β complex is activated, resulting in phosphorylation of IκBα on serine residues 32 and 35. Phosphorylated IκBα is then ubiquitinated, and polyubiquitinated IκBα is degraded through proteasomal pathway. As a result, free NF-κB translocates from the cytoplasm to the nucleus and binds to specific DNA

sequences to regulate expression of target genes, which are related to tumor development and metastases [19–21].

The dried root of *Saussurea lappa* Clarke (SLC) has transitionally been used as an ingredient in Korea, China and Japan for the treatment of either abdominal pain or tenesmus. Several earlier studies indicated that the root of SLC has anticancer effect in gastric cancer cells [22, 23]. Costunolide ($C_{15}H_{20}O_2$), a sesquiterpene lactone that is a major component of the root of SLC [24] has been reported to have diverse effects such as anti-inflammatory [25], anti-viral [26], and -fungal [27] effects. Furthermore, costunolide affected anti various cancers including melanoma [28], intestinal [29], leukemia [30], prostate [31], and breast cancers [32].

While anti-cancer effects of either SLC or costunolide have been reported as mentioned befor, antimetastatic effects of either SLC or costunolide on metastatic breast cancer are still poorly understood. In this study, we found that SLC and costunolide inhibit TNFα-mediated breast cancer cell migration and invasion by inhibiting NF-κB activation, thereby suggesting the antimetastatic property of costunolide using highly metastatic MDA-MB-231 breast cancer cells.

2. Materials and Methods

2.1. Reagents and Cell Lines. Costunolide (molecular weight of 232.32, purity > 99%, see Figure 2(a)) was purchased from Wako (Wako Pure Chemical Industries, Osaka, Japan). RPMI 1640, fetal bovine serum (FBS), antibiotic-antimycotic, and phosphate-buffered Saline (PBS) were purchased from Gibco-BRL (Rockville, MD, USA). EZ-western detection kit was obtained from Daeillab (Daeillab service, Co., Seoul, Korea). TNFα was purchased from R&D systems (Minneapolis, MN,USA).

2.2. Preparation of Saussurea lappa Clarke (SLC) Extract Saussurea lappa. Clarke was purchased from Omniherb (Gyeong Buk, Korea). The 100 g of root of SLC was dipped in 1 L of 80% ethanol and sonicated by using an ultrasonicator (Branson, MO, USA) for 30 min at room temperature. The sonicated extract was filtered through a 0.22 mm filter and concentrated. The ethanol extracts were dried in a 42°C by using a vacuum pump evaporator (Eyela, Tokyo, Japan). The 28.5 g of concentrated extract was dissolved in DMSO to prepare a stock solution of 100 mg/mL. The stock solution was stored at −80°C until use.

2.3. Cell Migration and Invasion. Cell migration was measured by wound healing assays. Cells were seeded in 6-well plates and scratched with a 200 μL pipette tip. 24 hours after treatments with *Saussurea lappa* Clarke and costunolide, migrated cell numbers were counted. For invasion assay, cells were seeded in the upper chambers precoated with Matrigel and treated with SLC and costunolide. Low chambers were filled with 10% FBS or TNFα-contained medium, and invasive cells were stained with hematoxylin and eosin to visualize and count. All experiments were performed in triplicate and student's t-test was performed to determine statistics. P values below 0.05 and 0.001 were considered statistically significant. All data was represented as the mean ± standard deviation.

2.4. Immunofluorescence Assays. Immunofluorescence assays were used for p-NFκB nuclear translocation in MDA-MB-231 cell. After treatment with SLC and costunolide for 6 hours, cells were fixed with 4% paraformaldehyde for 15 min and then permeabilized with 0.5% Triton X-100 for 10 min. The cells were washed with PBS, blocked with 5% FBS in PBS for 30 min, and then incubated with anti-p-NF-κB antibody overnight at 4°C and with anti-Alexa Fluor-488 secondary antibody (Invitrogen, Eugene, Oregon, USA) for 1 hour. Phalloidin (Sigma) and TO-PRO-3 (Invitrogen) were used to contain F-actin and the nucleus, respectively. Images were obtained with Olympus FV10i Self-Contained Confocal Laser System. The object was 20x, and scale bars on the image indicate 50 μm.

2.5. Luciferase Assays. Cells were seeded in 24-well plates and NF-κB-luc plasmid (Stratagene, La Jolla, CA, USA) transfected in MDA-MB-231 cells by using Lipofectamine reagent (Invitrogen, Carlsbad, CA, USA). Cells were treated with SLC and costunolide for 6 hours, and then the luciferase assays were done by using dual-luciferase reporter assay (Promega, Madison, WI, USA). All transfections included the RLTK-Luc (kindly provided by Sang Hoon Kim) for transfection efficiency. All experiments were performed in triplicate and student's t-test was performed to determine statistics. P values below 0.05 and 0.001 were considered statistically significant. All data was represented as the mean ± standard deviation.

2.6. Western Blot. Total protein (30 μg) was separated by SDS-PAGE. After electrophoresis, the proteins were transferred to a nitrocellulose membrane. The membrane was blocked, incubated overnight at 4°C with primary antibodies, washed with PBS-T (PBS with 0.1% Tween-20), and incubated with appropriate HRP-conjugated secondary antibodies at room temperature for 1 hour. Immunoreactive protein was developed using an EZ-western detection kit (Daeillab service, Co., Seoul, Korea). Anti-MMP-9, -p-IKK, -IKK, -p-IκB, -IκB, -p-NF-κB, and -NF-κB were purchased from Cell Signaling (Danvers, MA, USA). Anti-Tubulin was purchased from Sigma (Louis, MO, USA).

2.7. RNA Extraction and RT-PCR. Cellular total RNA was extracted with TRIzol reagent (Invitrogen). The RNA concentration and purity were measured using a spectrophotometer. cDNA was synthesized from total RNA (1 μg) by reverse transcription. The primer sequences and product size were as follows: MMP-9 (262 bp) forward: 5′-CACTGTCCACCCCTCAGAGC-3′, reverse: 5′-GCCACTTGTCGGCGATAAGG-3′, GAPDH (300 bp) forward: 5′-CGTCTTCACCACCATGGAG-A-3′, reverse: 5′-CGGCCATCACGCCACAGTTT-3′. The products were checked by agarose electrophoresis and analyzed using ChemiDoc imaging system (BioRad, Hercules, CA, USA).

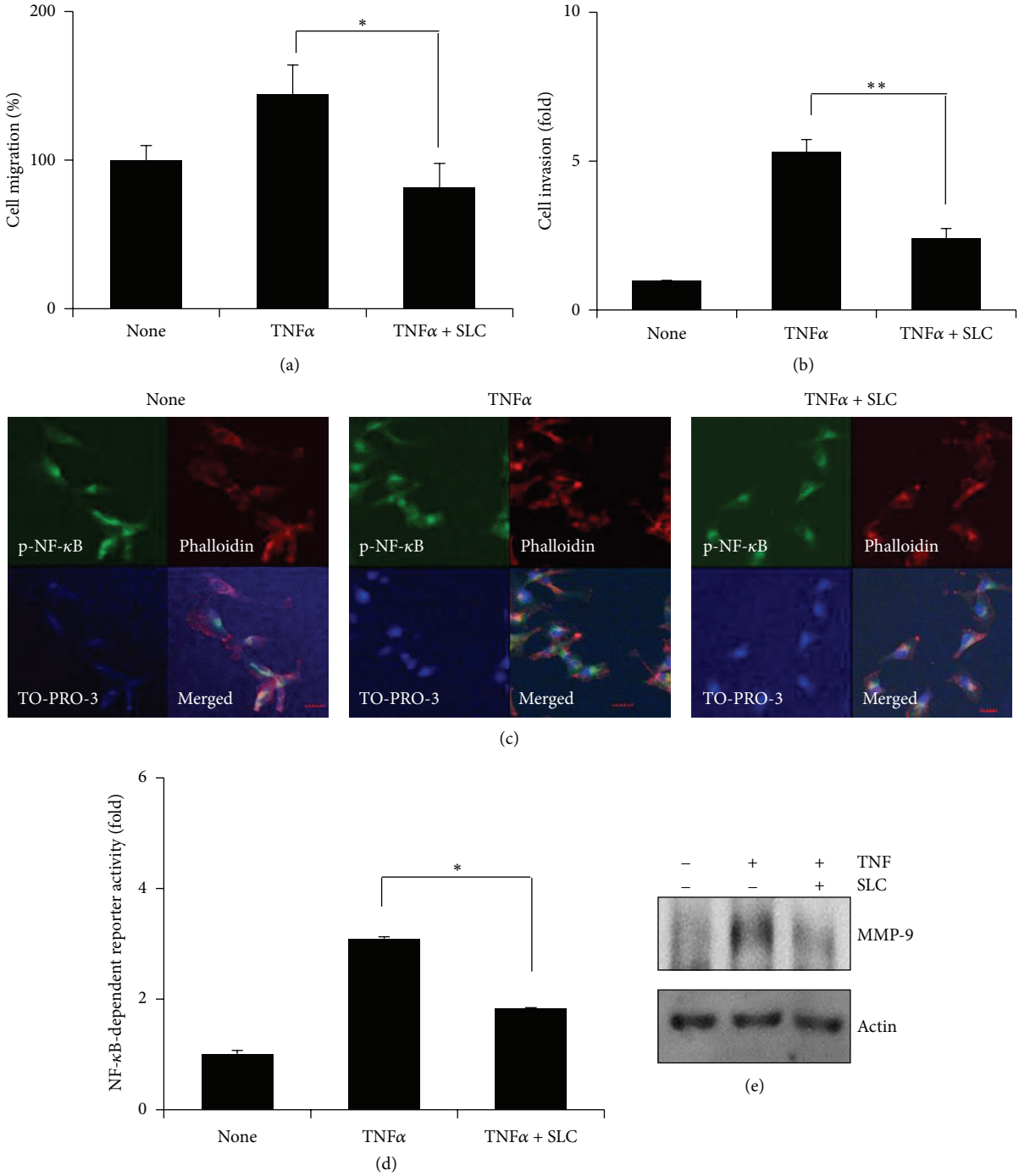

Figure 1: SLC inhibits TNFα-induced MDA-MB-231 cell migration and invasion by inhibiting NF-κB activation. (a) Cell migration was measured by wound healing assay. MDA-MB-231 cells were seeded and scratched, pretreated with SLC for 1 hour, and then exposed to TNFα for 24 hours. Cell migration was determined by counting cell numbers migrated from the wound healing region. $^{*}P < 0.05$. (b) MDA-MB-231 cells were seeded on the upper chambers and pretreated with SLC for 1 hour and then exposed to TNFα for 24 hours. Invading cells were stained with hematoxylin and eosin, and the cell numbers were measured. $^{**}P < 0.001$. (c) MDA-MB-231 cells were pretreated with SLC for 1 hour, then exposed to TNFα for 6 hours, and stained with p-NF-κB antibody. Phalloidin and TO-PRO-3 were for staining F-actin and the nucleus, respectively. The object was 20x, and scale bars on the image indicate 50 μm. (d) MDA-MB-231 cells were transfected with the NF-κB-dependent luciferase reporter, pretreated with SLC for 1 hour, and then exposed to TNFα for 6 hours. Luciferase assays were done by using dual-luciferase reporter assay. All transfections included the RLTK-Luc for transfection efficiency. $^{*}P < 0.05$. (e) MDA-MB-231 cells were pretreated with SLC for 1 hour and then exposed to TNFα for 24 hours. MMP-9 protein was measured by western blotting. Tubulin was used for the loading control.

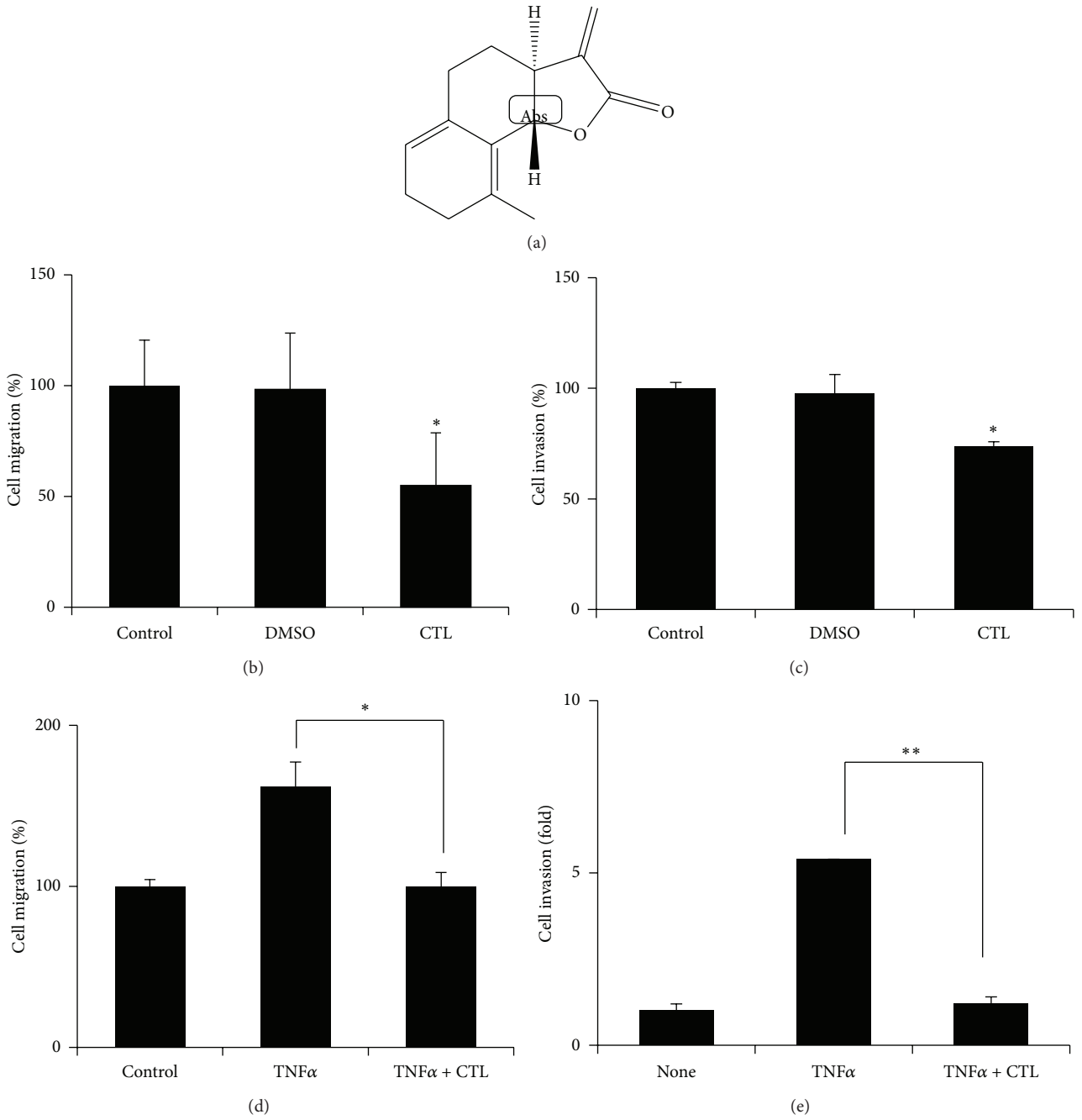

Figure 2: Costunolide inhibits TNFα-induced MDA-MB-231 cell migration and invasion. (a) Structure of costunolide. (b) MDA-MB-231 cells were seeded and scratched. Treatment with costunolide for 24 hours and counted. $^{*}P < 0.05$. (c) MDA-MB-231 cells were seeded on the upper chambers and treated with costunolide in 0% serum. Low chamber filed with 10% serum. $^{*}P < 0.05$. (d) Pretreated with costunolide for 1 hour and then exposed to TNFα for 24 hours. Cell migration was determined by counting numbers of cells migrated from the wound healing region. $^{*}P < 0.05$. (e) MDA-MB-231 cells were seeded on the upper chambers and treated with costunolide. Low chamber filed with TNFα. $^{*}P < 0.001$.

2.8. Gelatin Zymography Assay. Conditioned medium was harvested, concentrated, mixed with nonreducing sample buffer, and separated by SDS-PAGE electrophoresis containing 0.1% gelatin. After electrophoresis, the gel was washed with washing buffer (2.5% Triton X-100 in reaction buffer) and then incubated in reaction buffer (50 mM Tris-HCl, 5 mM $CaCL_2$, 1 μM $ZnCl_2$, and pH 7.4) for 18 h at 37°C. To visualize, the gel was stained with Coomassie brilliant blue R-250 and destained in 50% methanol, 40% distilled water, and 10% acetic acid.

2.9. In Vivo Studies. Animal studies were approved by Kyung Hee University Institutional Animal Care and Use Committee (KHU-IACUC). Six-week-old nude (Nu/Nu) mice were

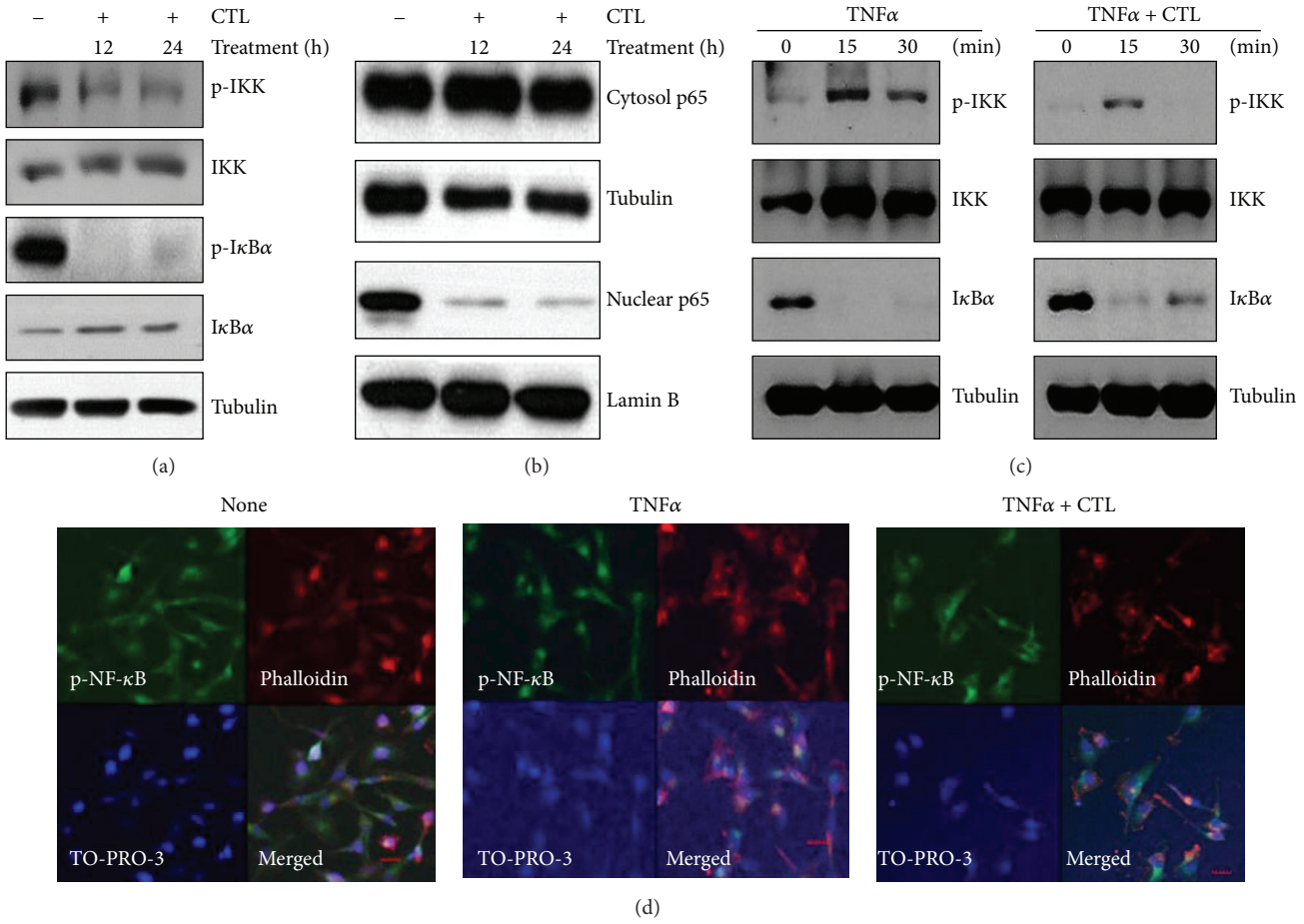

Figure 3: Costunolide inhibits TNFα-induced NF-κB pathway in MDA-MB-231 cells. (a) MDA-MB-231 cell were treated with costunolide for indicated time periods. Whole lysates were analyzed by western blotting with anti-pIKK, -IKK, -pIκBα, -IκBα, and Tubulin. (b) Cells were fractionated into cytoplasmic and nuclear compartment and western blotting for NF-κB. Tubulin and LaminB were used as loading control. (c) MDA-MB-231 cells were treated with TNFα and cotreated with TNFα and costunolide for 15 to 30 min. Whole lysates were analyzed by western blotting with anti-pIKK, -IKK, -IκBα, and Tubulin. (d) MDA-MB-231 cells were pretreated with costunolide for 1 hour, then exposed to TNFα for 6 hours, and stained with p-NF-Kb antibody. Phalloidin and TO-PRO-3 were for staining with F-actin and nucleus, respectively. The object was 20x, and the scale bars on the image indicate 50 μm.

purchased from Oriental Science and injected orthotopically into the 4th mammary fat fads with MDA-MB-231 cells (1×10^6 resuspended in a 1 : 1 mixture of PBS and growth factor-reduced matrigel (BD Biosciences, San Jose CA, USA)). A day after tumor cell injection, 20 μM of costunolide was injected into the mammary fat fads three times a week for 30 days. Tumor volumes were measured using calipers and calculated using the following formula: tumor volume (cubic millimeters) = width^2 × length/2. In addition, body weight was monitored.

2.10. Immunohistochemistry. Tumors were fixed with 4% formaldehyde for further analyses. Tumor tissues were embedded in paraffin, dissected with 5 μm, and deparaffinized in 100% xylene and ethanol series (100%, 95%,and 70%). Heat-induced antigen retrieval was 10 mM sodium citrate buffer for 5 min. Endogenous peroxidase was blocked with peroxidase blocking reagent containing 3.5% hydrogen peroxide. Nonspecific antigen was blocked with serum containing PBS followed by incubation with human ki-67 (5 μg/mL) (Abcam, MA, USA) and MMP-9 antibody (1 : 100) (Cell Signaling, Beverly, MA, USA) overnight at 4°C. It was incubated with biotin-labeled rabbit antibody for 1 hour at room temperature and incubated with ABC and DAB buffer substrate. Sections were visualized with DAB and hematoxylin, mounted, and analyzed using a bright field microscope. The object was 20x, and the scale bars on the image indicate 10 μm.

2.11. Statistics. Data were shown as the means and standard deviations. P values less than 0.05 in the two-tailed Student's t-test or one-way ANOVA were considered statistically significant.

3. Results

3.1. Saussurea lappa Clarke Suppresses TNFα-Induced Breast Cancer Cell Migration and Invasion via an Inhibition of NF-κB

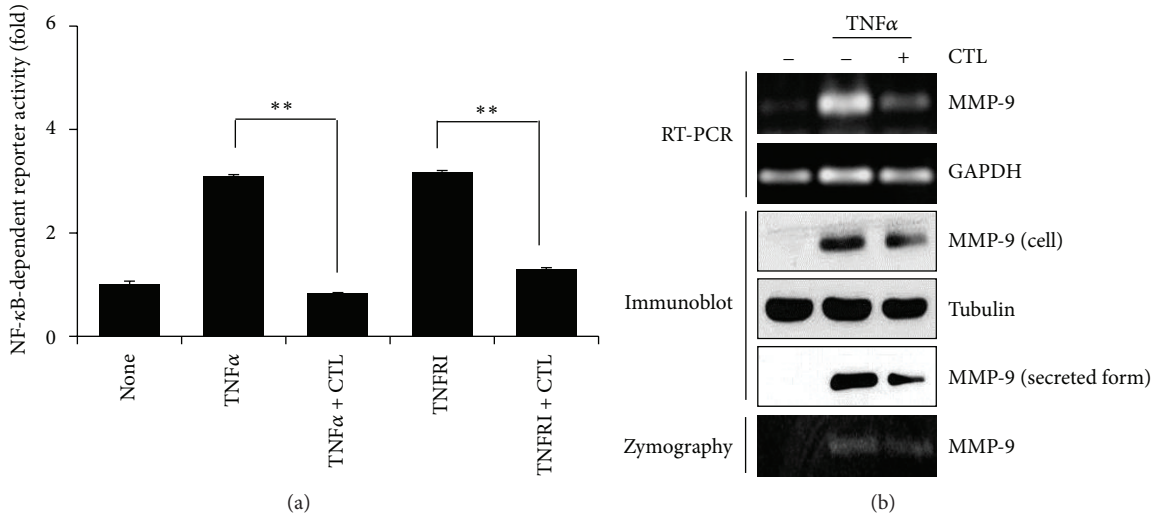

Figure 4: Costunolide inhibits TNFα-induced NF-κB activity and MMP-9 expression. (a) MDA-MB-231 cells were transfected with the NF-κB-dependent luciferase reporter, pretreated with costunolide for 1 hour, and then exposed to TNFα for 6 hours. In addition, after cotransfected with TNFRI and NF-κB-dependent luciferase reporter, treated with costunolide for 6 hours. Luciferase assay were done by using dual-luciferase reporter assays. All transfections included the RLTK-Luc for transfection efficiency. $^{**}P < 0.001$. (b) MDA-MB-231 cells were pretreated with costunolide for 1 hour and then exposed to TNFα for 6 hours. MMP-9 expression was analyzed by RT-PCR, western blotting, and zymography.

Activation. Because TNFα expression is abundant in tumor microenvironment, and its expression is correlated with poor prognoses [14, 15], we investigate effects of *Saussurea lappa* Clarke (SLC) on highly metastatic MDA-MB-231 cells. In normal culture condition, SLC treatment (50 μg/mL) inhibited MDA-MB-231 cell migration (data not shown). Next, TNFα increased the MDA-MB-231 cells migration compared to nontreated cells, and 50 μg/mL of SLC suppressed TNFα-induced MDA-MB-231 cells migration by approximately 63% (Figure 1(a)). In addition, 50 μg/mL of SLC significantly inhibited TNFα-induced cell invasion (Figure 1(b)). Next, to clarify the mechanism of SLC to inhibit cell migration and invasion, we performed the immunofluorescence assays to examine NF-κB pathway. As shown in Figure 1(c), TNFα induced nuclear translocation of phosphorylated NF-κB, which was blocked by SLC. In the luciferase assay, SLC inhibited TNFα-induced NF-κB-dependent transcriptional activity (Figure 1(d)). Accordingly, 50 μg/mL of SLC suppressed TNFα-induced mRNA and protein expression of MMP-9 that is well known as NF-κB-dependent gene (Figure 1(e)). Thus, our data indicate that SLC inhibits TNFα-induced highly metastatic MDA-MB-231 human breast cancer cell migration, invasion, and NF-κB activation.

3.2. Saussurea lappa Clarke-Derived Costunolide Suppresses Cell Migration and Invasion in Breast Cancer Cells. Since Costunolide ($C_{15}H_{20}O_2$) is a major component of SLC [22], we examined whether SLC-derived costunolide inhibits metastatic properties of breast cancer cells. Costunolide (20 μM) blocked cells migration in normal serum conditions by approximately 45% (Figure 2(a)). Next, to examine costunolide effect on cells invasion, MDA-MB-231 cells were seeded in the upper chambers precoated with matrigel and treated with costunolide in 1% serum contained media, and the low chambers were filled with 10% serum contained media. As shown in Figure 2(b), a treatment of breast cancer cells with 20 μM of costunolide for 24 hours reduced cells invasion.

Next we performed experiments to determine whether costunolide inhibits TNFα-induced cells migration and invasion. 20 μM of costunolide suppressed TNFα-induced MDA-MB-231 cell migration by approximately 62% (Figure 2(c)). In addition, whereas TNFα increased an invasiveness of MDA-MD-231 cells by approximately five folds, costunolide significantly inhibited TNFα-induced cell invasion by approximately five folds (Figure 2(d)).

3.3. Costunolide Inhibits NF-κB Pathway in Breast Cancer Cells. Next we examined costunolide effect on NF-κB signaling pathway in MDA-MB-231 cells. As shown in Figure 3(a), costunolide inhibited phosphorylation of IKK and IκBα, resulting in blocking IκBα degradation in a time-dependent manner. Accordingly, a treatment of the MDA-MB-231 cells with costunolide inhibited the nuclear translocation of p65 NF-κB subunit (Figure 3(b)).

Next, in order to examine whether costunolide suppresses TNFα-induced NF-κB pathway, we stimulated cells with TNFα for 15 to 30 min in the presence or absence of costunolide. As shown in Figure 3(c), TNFα-induced IKK phosphorylation was prolonged until 30 min, which was blocked by costunolide. Furthermore, while TNFα induced IκB degradation, costunolide slowly recovered IκBα expression at 15 min.

To confirm costunolide suppression of NF-κB nuclear translocation, we performed immunofluorescence assay using the anti-pNF-κB antibody. As shown in Figure 3(d),

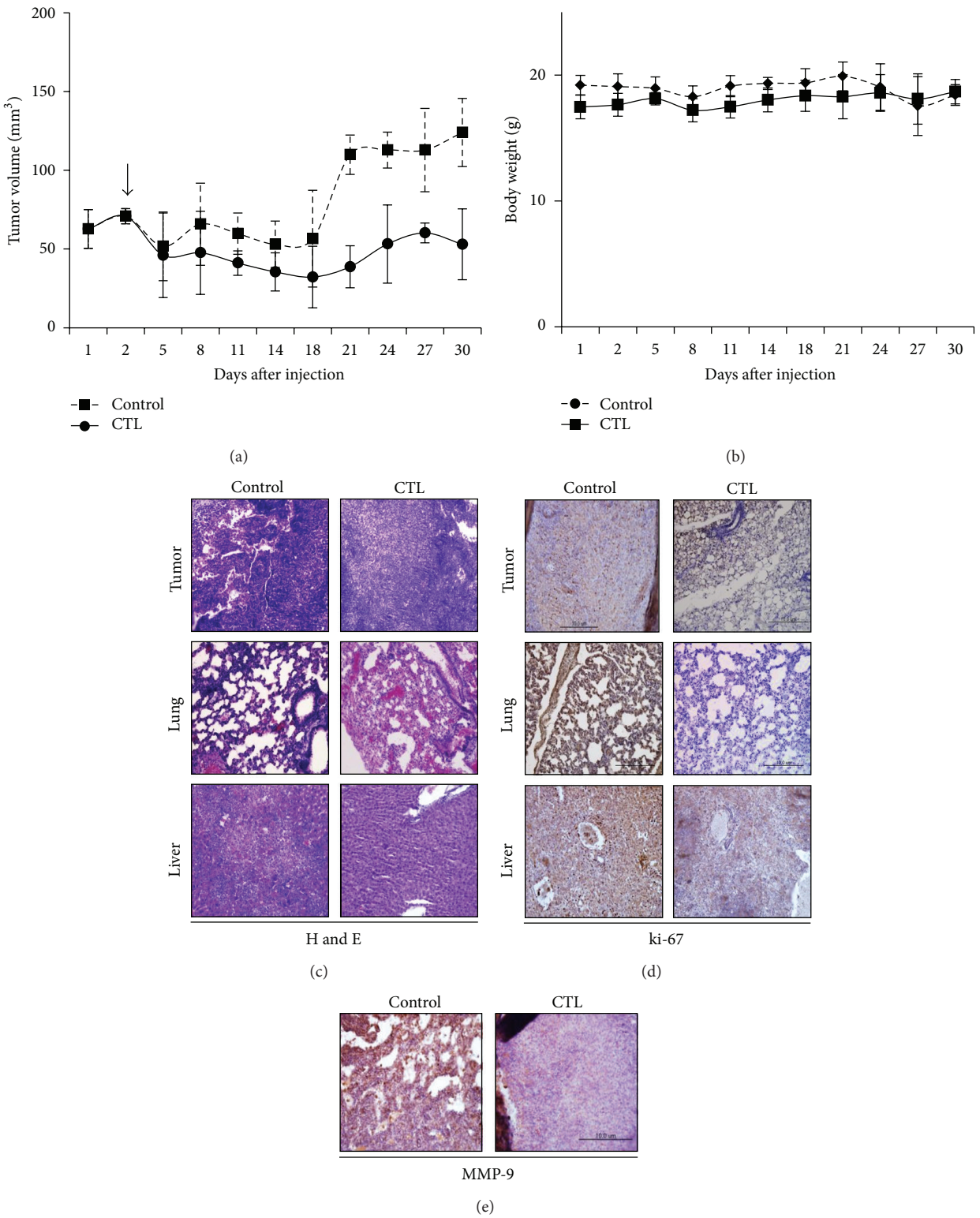

FIGURE 5: Costunolide inhibits orthotopically tumor growth and metastasis. (a) 1×10^6 MDA-MB-231 cells were orthotopically injected in nude mice (n = 5/group). Costunolide was injected into the mammary fat fad and repeated every three days for 30 days. Tumor volumes were measured using calipers. Tumor volume (cubic millimeters) = width^2 × length/2. (b) Body weight measured three times a week. (c) Tumor tissues were stained with hematoxylin and eosin. Photo images were taken at 20x magnification. (d) Tumor tissues were stained with anti-ki-67 antibody. (e) Tumor tissues were stained with anti-MMP-9 antibody. The object was 20x, and, scale bars on the image indicate 10 μm.

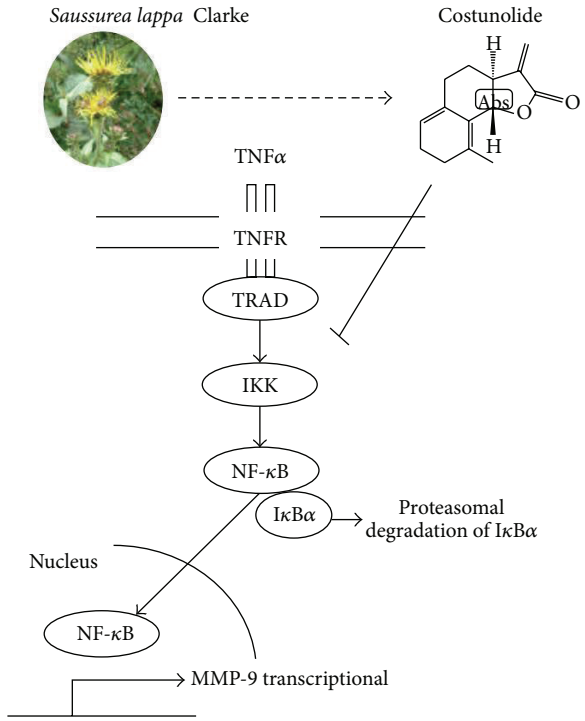

Figure 6: Schematic representation of the mechanism where costunolide inhibits TNFα-induced breast cancer cell migration and invasion by inhibiting NF-κB activity.

NF-κB was observed in the cytosol of the cells treated with costunolide. Thus, our data indicate that SLC-derived costunolide inhibits NF-κB pathway.

3.4. Costunolide Inhibits NF-κB Transcriptional Activity and MMP-9. To confirm the inhibition of NF-κB pathway by costunolide, we performed the transcriptional activation of NF-κB by using the luciferase assay. As shown in Figure 4(a), costunolide reduced TNFα-induced NF-κB transcriptional activation by 5-fold in MDA-MB-231 cells. We next examined whether costunolide affects upstream of IKK in TNFα-induced NF-κB pathway, MDA-MB-231 cells were cotransfected with NF-κB reporter gene and TNFRI and then cultured in the presence or absence of costunolide. Costunolide reduced TNFRI-induced NF-κB transcriptional activity by approximately 2.5-fold in MDA-MB-231 cells (Figure 4(a)).

It is known that MMP-9 is regulated by NF-κB, and the promoter region of MMP-9 gene contains binding sites for NF-κB. Thus, we examined whether costunolide inhibits MMP-9; we checked MMP-9 by using RT-RCR, western blot, and zymography. As shown in Figure 4(b), Costunolide inhibited TNFα-induced MMP-9 mRNA, protein, and enzyme activity, when cells were treated with costunolide for 24 hours.

3.5. Costunolide Inhibits Tumor Growth and Metastasis. To examine costunolide effect on breast cancer growth and metastases *in vivo*, MDA-MB-231 cells were orthotopically injected into the 4th mammary fat fads. A day after tumor cell injection, costunolide at 20 μM was injected into the mammary fat fad three times a week for 30 days. In addition, tumor volume and body weight of mice were also measured three times a week. As shown in Figure 5(a), costunolide reduced tumor volume ($P = 0.007628$), and no significant weight loss in mice treated with either costunolide or vehicle was observed (Figure 5(b)). When tumor tissues were stained with hematoxylin and eosin, we found that tumor cohort treated with costunolide compared to that with control was well differentiated (Figure 1(c)). In addition, tumor and organ (lung and liver) tissues were stained with anti-ki-67. Costunolide, compared to control reduced ki-67 positive cell in tumor, lung, and liver (Figure 1(d)). When tumor tissues were stained with MMP-9 antibody, costunolide inhibited a number of MMP-9 positive cells (Figure 1(e)). Thus, our data indicate that costunolide inhibits tumor growth and metastasis.

4. Discussion

TNFα-induced NF-κB pathway is a well-known molecular target for cancer therapy. Tumor cells released NF-κB-dependent MMPs by NF-κB-mediated TNFα production of immune cells in tumor microenvironment [33]. In this study, we found that *Saussurea lappa* Clarke-derived costunolide suppressed TNFα-induced MDA-MB-231 breast cancer cell migration and invasion by inhibiting NF-κB activity (Figure 5(c)). Thus, SLC as well as costunolide appears to be useful for treating highly metastatic breast cancer.

Matrix metalloproteinases (MMPs), a family of zinc-dependent endoproteinase is necessary for extracellular matrix (ECM) degradation among metastasis process. MMPs also affect many biological processes such as normal tissue remodeling, wound healing, angiogenesis, embryogenesis, and many diseases including cancer, atheroma, and arthritis [34]. MMP-9 is frequently overexpressed in many cancers and correlates with poor prognosis and survival in cancer patients [35–37]. In addition, MMP-9 is important for tumor metastasis by cleaving basement membranes, which allows migratory phenotype cells to be more invasive and motile [38–40]. MMP-9 is regulated by stimulators (phorbol 12-myristate 13-acetate, PMA; transforming necrosis factor alpha, TNFα; growth factor, UV; and stress) and transcription factors (nuclear factor kappaB; NF-κB and activator protein-1; AP-1) [39, 40]. In addition, MMP-9 is important for tumor metastasis by cleaving basement membranes, which allows migratory phenotype cells to be more invasive and motile. Thus, TNFα-induced MMP-9 expression via NF-κB is important for cancer growth and metastasis. In our study, TNFα-induced cell migration and invasion were inhibited by either SLC or costunolide. SLC and costunolide suppressed TNFα-induced NF-κB translocation to nucleus and transcriptional activity. In addition, costunolide specifically inhibited IKK phosphorylation and IκBα degradation. Those inhibitions further reduced NF-κB-dependent MMP-9 expression. As a result, costunolide suppressed *in vivo* tumor growth and metastasis.

This study concludes that (a) SLC suppresses TNFα-induced MDA-MB-231 cell migration and invasion by

inhibiting NF-κB-dependent MMP-9 expression, (b) SLC-derived costunolide inhibited serum or TNFα-induced MDA-MB-231 cell migration and invasion, (c) costunolide inhibited TNFα-induced NF-κB translocation resulting from the suppression phosphorylation and IκBα degradation (d) costunolide blocked TNFα-induced NF-κB transcription activity and TNFα-induced MMP-9 expression, and (e) costunolide decreased *in vivo* tumor growth and metastasis without weight loss (Figure 6). In sum, we provide evidence that the anti-cancer effect of both SLC and its component costunolide on MDA-MB-231 result from the inhibition of TNFα-induced NF-κB activation. Therefore, SLC-derived costunolide could be useful for treating highly metastatic breast cancer growth and metastases.

Acknowledgments

The authors thank Dr. Sang Hoon Kim (Department of Biology, Kyung Hee University) for sharing the luminometer and ChemiDoc imaging system. This study was supported by the National Research Foundation of Korea (NRF) grant funded by the Korea government (MSIP) (No. 2007-0054931), and by a Grant from the Korean Medicine R&D Project of the Ministry of Health and Welfare (B110043 and B120014).

References

[1] J. Sariego, "Breast cancer in the young patient," *The American Surgeon*, vol. 76, no. 12, pp. 1397–1400, 2010.

[2] K. I. Block, C. Gyllenhaal, D. Tripathy et al., "Survival impact of integrative cancer care in advanced metastatic breast cancer," *Breast Journal*, vol. 15, no. 4, pp. 357–366, 2009.

[3] P. A. C. Greenberg, G. N. Hortobagyi, T. L. Smith, L. D. Ziegler, D. K. Frye, and A. U. Buzdar, "Long-term follow-up of patients with complete remission following combination chemotherapy for metastatic breast cancer," *Journal of Clinical Oncology*, vol. 14, no. 8, pp. 2197–2205, 1996.

[4] E.-F. Solomayer, I. J. Diel, G. C. Meyberg, C. Gollan, and G. Bastert, "Metastatic breast cancer: clinical course, prognosis and therapy related to the first site of metastasis," *Breast Cancer Research and Treatment*, vol. 59, no. 3, pp. 271–278, 2000.

[5] D. Hanahan and R. A. Weinberg, "The hallmarks of cancer," *Cell*, vol. 100, no. 1, pp. 57–70, 2000.

[6] K. Pantel and R. H. Brakenhoff, "Dissecting the metastatic cascade," *Nature Reviews Cancer*, vol. 4, no. 6, pp. 448–456, 2004.

[7] P. S. Steeg, "Tumor metastasis: mechanistic insights and clinical challenges," *Nature Medicine*, vol. 12, no. 8, pp. 895–904, 2006.

[8] R. O. Hynes, "Metastatic potential: generic predisposition of the primary tumor or rare, metastatic variants: or both?" *Cell*, vol. 113, no. 7, pp. 821–823, 2003.

[9] Y. Kang, P. M. Siegel, W. Shu et al., "A multigenic program mediating breast cancer metastasis to bone," *Cancer Cell*, vol. 3, no. 6, pp. 537–549, 2003.

[10] A. J. Minn, G. P. Gupta, P. M. Siegel et al., "Genes that mediate breast cancer metastasis to lung," *Nature*, vol. 436, no. 7050, pp. 518–524, 2005.

[11] F. Balkwill, "Tumor necrosis factor or tumor promoting factor?" *Cytokine and Growth Factor Reviews*, vol. 13, no. 2, pp. 135–141, 2002.

[12] M. S. Naylor, G. W. H. Stamp, W. D. Foulkes, D. Eccles, and F. R. Balkwill, "Tumor necrosis factor and its receptors in human ovarian cancer: potential role in disease progression," *Journal of Clinical Investigation*, vol. 91, no. 5, pp. 2194–2206, 1993.

[13] T. Hehlgans and K. Pfeffer, "The intriguing biology of the tumour necrosis factor/tumour necrosis factor receptor superfamily: players, rules and the games," *Immunology*, vol. 115, no. 1, pp. 1–20, 2005.

[14] E. E. Varfolomeev and A. Ashkenazi, "Tumor necrosis factor: an apoptosis JuNKie?" *Cell*, vol. 116, no. 4, pp. 491–497, 2004.

[15] S. Shishodia and B. B. Aggarwal, "Nuclear factor-κB activation: a question of life or death," *Journal of Biochemistry and Molecular Biology*, vol. 35, no. 1, pp. 28–40, 2002.

[16] M. K. Pandey, B. Sung, A. B. Kunnumakkara, G. Sethi, M. M. Chaturvedi, and B. B. Aggarwal, "Berberine modifies cysteine 179 of IκBα kinase, suppresses nuclear factor-κB-regulated antiapoptotic gene products, and potentiates apoptosis," *Cancer Research*, vol. 68, no. 13, pp. 5370–5379, 2008.

[17] G. Helbig, K. W. Christopherson, P. Bhat-Nakshatri et al., "NF-κB promotes breast cancer cell migration and metastasis by inducing the expression of the chemokine receptor CXCR4," *Journal of Biological Chemistry*, vol. 278, no. 24, pp. 21631–21638, 2003.

[18] S. Ghosh, M. J. May, and E. B. Kopp, "NF-κB and rel proteins: evolutionarily conserved mediators of immune responses," *Annual Review of Immunology*, vol. 16, pp. 225–260, 1998.

[19] S. Janssens, A. Tinel, S. Lippens, and J. Tschopp, "PIDD Mediates NF-κB activation in response to DNA damage," *Cell*, vol. 123, no. 6, pp. 1079–1092, 2005.

[20] F. Balkwill, "TNF-α in promotion and progression of cancer," *Cancer and Metastasis Reviews*, vol. 25, no. 3, pp. 409–416, 2006.

[21] H. Häcker and M. Karin, "Regulation and function of IKK and IKK-related kinases," *Science's STKE*, vol. 2006, no. 357, p. re13, 2006.

[22] S. G. Ko, H.-P. Kim, D.-H. Jin et al., "*Saussurea lappa* induces G2-growth arrest and apoptosis in AGS gastric cancer cells," *Cancer Letters*, vol. 220, no. 1, pp. 11–19, 2005.

[23] S.-G. Ko, S.-H. Koh, C.-Y. Jun, C.-G. Nam, H.-S. Bae, and M.-K. Shin, "Induction of apoptosis by *Saussurea lappa* and Pharbitis nil on AGS gastric cancer cells," *Biological and Pharmaceutical Bulletin*, vol. 27, no. 10, pp. 1604–1610, 2004.

[24] A. Robinson, T. V. Kumar, E. Sreedhar et al., "A new sesquiterpene lactone from the roots of *Saussurea lappa*: structure-anticancer activity study," *Bioorganic and Medicinal Chemistry Letters*, vol. 18, no. 14, pp. 4015–4017, 2008.

[25] C. A. L. Kassuya, A. Cremoneze, L. F. L. Barros et al., "Antipyretic and anti-inflammatory properties of the ethanolic extract, dichloromethane fraction and costunolide from Magnolia ovata (Magnoliaceae)," *Journal of Ethnopharmacology*, vol. 124, no. 3, pp. 369–376, 2009.

[26] H.-C. Chen, C.-K. Chou, S.-D. Lee, J.-C. Wang, and S.-F. Yeh, "Active compounds from *Saussurea lappa* Clarks that suppress hepatitis B virus surface antigen gene expression in human hepatoma cells," *Antiviral Research*, vol. 27, no. 1-2, pp. 99–109, 1995.

[27] D. E. Wedge, J. C. G. Galindo, and F. A. Macías, "Fungicidal activity of natural and synthetic sesquiterpene lactone analogs," *Phytochemistry*, vol. 53, no. 7, pp. 747–757, 2000.

[28] C.-N. Chen, H.-H. Huang, C.-L. Wu et al., "Isocostunolide, a sesquiterpene lactone, induces mitochondrial membrane depolarization and caspase-dependent apoptosis in human

melanoma cells," *Cancer Letters*, vol. 246, no. 1-2, pp. 237–252, 2007.

[29] H. Mori, T. Kawamori, T. Tanaka, M. Ohnishi, and J. Yamahara, "Chemopreventive effect of costunolide, a constituent of oriental medicine, on azoxymethane-induced intestinal carcinogenesis in rats," *Cancer Letters*, vol. 83, no. 1-2, pp. 171–175, 1994.

[30] J.-H. Choi, J. Ha, J.-H. Park et al., "Costunolide triggers apoptosis in human leukemia U937 cells by depleting intracellular thiols," *Japanese Journal of Cancer Research*, vol. 93, no. 12, pp. 1327–1333, 2002.

[31] J.-L. Hsu, S.-L. Pan, Y.-F. Ho, T.-L. Hwang, F.-L. Kung, and J.-H. Guh, "Costunolide induces apoptosis through nuclear calcium2+ overload and DNA damage response in human prostate cancer," *Journal of Urology*, vol. 185, no. 5, pp. 1967–1974, 2011.

[32] Y. K. Choi, H. S. Seo, H. S. Choi et al., "Induction of Fas-mediated extrinsic apoptosis, p21WAF1-related G2/M cell cycle arrest and ROS generation by costunolide in estrogen receptor-negative breast cancer cells, MDA-MB-231," *Molecular and Cellular Biochemistry*, vol. 363, no. 1-2, pp. 119–128, 2012.

[33] P. Nyberg, T. Salo, and R. Kalluri, "Tumor microenvironment and angiogenesis," *Frontiers in Bioscience*, vol. 13, no. 17, pp. 6537–6553, 2008.

[34] C. M. Overall and C. López-Otín, "Strategies for MMP inhibition in cancer: innovations for the post-trial era," *Nature Reviews Cancer*, vol. 2, no. 9, pp. 657–672, 2002.

[35] L. M. Coussens and Z. Werb, "Matrix metalloproteinases and the development of cancer," *Chemistry and Biology*, vol. 3, no. 11, pp. 895–904, 1996.

[36] E. I. Deryugina, A. Zijlstra, J. J. Partridge et al., "Unexpected effect of matrix metalloproteinase down-regulation on vascular intravasation and metastasis of human fibrosarcoma cells selected in vivo for high rates of dissemination," *Cancer Research*, vol. 65, no. 23, pp. 10959–10969, 2005.

[37] M. E. Kupferman, M. E. Fini, W. J. Muller, R. Weber, Y. Cheng, and R. J. Muschel, "Matrix metalloproteinase 9 promoter activity is induced coincident with invasion during tumor progression," *The American Journal of Pathology*, vol. 157, no. 6, pp. 1777–1783, 2000.

[38] I. Stamenkovic, "Matrix metalloproteinases in tumor invasion and metastasis," *Seminars in Cancer Biology*, vol. 10, no. 6, pp. 415–433, 2000.

[39] M. Egeblad and Z. Werb, "New functions for the matrix metalloproteinases in cancer progression," *Nature Reviews Cancer*, vol. 2, no. 3, pp. 161–174, 2002.

[40] H. Sato and M. Seiki, "Regulatory mechanism of 92 kDa type IV collagenase gene expression which is associated with invasiveness of tumor cells," *Oncogene*, vol. 8, no. 2, pp. 395–405, 1993.

Hindawi Publishing Corporation
Evidence-Based Complementary and Alternative Medicine
Volume 2013, Article ID 561290, 5 pages
http://dx.doi.org/10.1155/2013/561290

Research Article

Detoxification Combining Fasting with Fluid Therapy for Refractory Cases of Severe Atopic Dermatitis

Kyu Seok Kim and Hae Jeong Nam

Department of Ophthalmology, Otorhinolaryngology and Dermatology of Korean Medicine, College of Korean Medicine, Kyung Hee University, 1 Hoegi-dong, Dongdaemun-gu, Seoul 130-701, Republic of Korea

Correspondence should be addressed to Hae Jeong Nam; ophthrl@khu.ac.kr

Received 27 March 2013; Accepted 14 July 2013

Academic Editor: Bo-Hyoung Jang

To introduce and determine the clinical benefits of a detoxification program that combines fasting with fluid therapy for refractory cases of severe atopic dermatitis (AD), we performed a retrospective chart review of inpatients with AD from March 2010 to February 2012 at the Department of Ophthalmology, Otorhinolaryngology and Dermatology of Korean Medicine in the Kyung Hee Medical Center. Patients were treated with the detoxification program, which combined fasting with fluid therapy, and herbal medicine, herbal wet wrap dressings, or acupuncture treatment when clinically necessary. The primary outcome was the SCORAD total index. The secondary outcome was the pruritus visual analogue scale (VAS) score in SCORAD as evaluated by a trained dermatology specialist. Among the 130 inpatients that have done detoxification, 7 patients met the inclusion criteria. The mean total SCORAD scores significantly decreased from 64.67 ± 11.72 to 26.26 ± 11.01 ($P = 0.018$) after the detoxification program. There was also a significant decrease in VAS score for pruritus from 8.00 ± 1.16 to 2.57 ± 0.98 ($P = 0.016$) between admission and discharge. We suggest that fasting with fluid therapy as a complementary and alternative treatment method may provide some benefits for patients with refractory cases of severe atopic dermatitis.

1. Introduction

Atopic dermatitis (AD) is a chronic relapsing inflammatory skin condition with extensive pruritus, erythema, excoriations, and scaly skin lesions [1]. Westernized medicine has conventionally used a combination of emollients, corticosteroids, antibiotics, calcineurin inhibitors, UV phototherapy, and systemic immunomodulating therapies like cyclosporine and interferon gamma-1b [1, 2]. Long-term conventional treatments for AD are occasionally difficult because of the chronic, recurrent nature of AD; thus, there is an increasing need to find better therapies that have minimal side effects [2, 3]. Lately, traditional Chinese medicine (TCM) with natural herbs and acupuncture has been regarded as a new therapy for AD that could minimize the use of corticosteroids and their side effects. However, TCM also has some problems, as some patients with severe AD who are refractory to conventional therapy developed significant side effects to TCM.

Detoxification, a part of complementary and alternative medicine, is described as working by releasing "toxins" from the body contaminated by metabolites and environmental toxins or by overindulgence and an insalubrious lifestyle [4]. Among the various methods for detoxification, fasting has an inhibitory effect on allergic dermatitis in experimental mouse models [5–7]. Furthermore, a clinical study has suggested a positive relationship between weight loss through repeated short-term fasting and symptom improvement in patients with AD [8]. Based on these previous studies, we applied the detoxification program, which combined fasting with fluid therapy, to refractory cases of severe AD.

The aim of this study was to introduce and evaluate the clinical benefits of this detoxification program on AD by performing a retrospective chart review of inpatients with severe AD.

2. Methods

2.1. Patients. We conducted a retrospective chart review of inpatients who have done detoxification program from

March 2010 to February 2012 at the Department of Ophthalmology, Otorhinolaryngology and Dermatology of Korean Medicine in the Kyung Hee Medical Center in Seoul and then selected refractory cases of severe AD. Eligibility criteria for inclusion were (1) a diagnosis of AD according to the UK Working Party's Diagnostic Criteria [9], (2) an age of 18 to 40 years, (3) admission required because of refractory pruritus or lifestyles that could exacerbate symptoms, and (4) a Scoring AD (SCORAD) index greater than 50. Verbal informed consent was obtained from each patient. Data was stored to safeguard confidentiality in password protected computer. Only one investigator had access to harvested patient data and when no longer needed data would be destroyed.

This study was approved by the Institutional Review Board of Kyung Hee Oriental Medical Center (IRB approval number KOMCIRB 2013-02).

2.2. Outcome Measurement. Primary outcome was the SCORAD total index at each admission and discharge day. Secondary outcomes were the pruritus self-assessment score changes of AD-related itching/scratching at each admission and discharge day, adverse changes in daily vital signs (BP, pulse, and temperature), and peripheral blood glucose level.

2.3. Adverse Events and Safety Monitoring. All unpredictable adverse events related to the detoxification program were reported to two Korean medical doctors (KMD and one medical doctor (MD) in the Department of East and West Integrated Medicine. Safety was assessed by the reporting of clinical laboratory tests, vital signs, and adverse events. Clinical laboratory tests, including AST/ALT, BUN/creatinine, red blood cell (RBC) count, white blood cell (WBC) count, hemoglobin, hematocrit, mean cell volume (MCV), mean cell hemoglobin (MCH), mean cell hemoglobin concentration (MCHC), number of platelets, and number of differentiated cells, were determined at each admission and discharge day. Vital signs of inpatients were checked with monitoring of adverse events (nausea/vomiting, fatigue, allergic reaction, and any adverse events related to the detoxification program) three times a day.

2.4. Intervention

2.4.1. Fasting. The detoxification program consists of three stages: (1) very low-calorie diet, (2) fasting, and (3) convalescence (Figure 1). On admission to the hospital, we confirmed that the detoxification program was appropriate for the patients with atopic dermatitis through examinations like blood tests or electrocardiograms. Before the fasting stage, patients were prescribed a very low-calorie diet for three meals. At that time, we recommended that patients take a vermicide to empty the intestines. If a patient did not have a bowel movement before the fasting stage, we administered an enema or prescribed herbal medicine to help with bowel movements. After a very low-calorie diet for three meals, no food was given to inpatients for three meals during the fasting stage. After the fasting stage, we again prescribed a very low-calorie diet for three meals. Two days before hospital discharge, we prescribed a general diet in order to examine the skin condition of patients to assess for signs like itching or scaling after being exposed to a general diet.

2.4.2. Fluid Therapy. From the day of admission to two days before discharge, we supplied about one liter of fluid per day (normal saline solution) to inpatients. If a patient complained of severely dry skin, it was possible to increase the amount of fluid. We examined the patients when fluid therapy was stopped.

2.4.3. Herbal Medicine and Acupuncture Treatment. We prescribed herbal medicine (types of decoction, ointment, or wet wrap dressing) or acupuncture treatment if necessary. Usually, acupuncture treatment was provided twice per day at acupuncture points both sides of LI4, LI11, SP10, SP6, and LR3 to control the skin inflammation of AD patients. The herbal medicine was a decoction of plant material, including *Rehmannia glutinosa, Angelica gigas, Paeonia japonica, Cnidium officinale* Makino, *Sophora flavescens* Solander ex Aiton, and *Spirodela polyrhiza*. We decocted 0 to 12 grams of each plant material with purified water as a daily dose according to patient progress. This daily dose was administered three times a day after each meal. We also used a decoction of plant material for the herbal wet dressings, including *Aloe vera*. Four or five layers of sterilized gauze were hydrated sufficiently with the decoction and were applied immediately to the AD lesions for 15 minutes. Herbal wet dressings were applied once or twice per day according to symptom severity. We applied the herbal medicine for AD only during the very low-calorie diet stage, not during the fasting stage. If some patients were sensitive, we did not apply acupuncture treatment to them during the fasting stage.

2.5. Statistical Analysis. Analyses were performed using SPSS version 17.0 for Windows. Data are presented as mean ± standard deviation (SD). The statistical calculation for Wilcoxon signed-rank test, a nonparametric method, was performed for the mean change of the SCORAD total index and the pruritus self-assessment score changes of AD-related itching/scratching between admission and discharge because assumptions of normality were violated. All differences were considered significant at $P < 0.05$.

3. Results

3.1. Patients. Among the 130 inpatients that have done detoxification, a total of 7 patients were included in this study (Figure 2). Clinical characteristics of patients on admission day are summarized in Table 1. The mean age of the 7 inpatients was 24 years (range 19–30). Hospitalization lasted an average of 9.29 days (range 7–15). Serum immunoglobulin E level was an average of 4934 IU/mL (range 18–14000). Eosinophil count was an average of 854.29 cells/mcl (range 130–1700). Antistreptolysin O titer level was an average of 183.29 IU/mL (range 101–284).

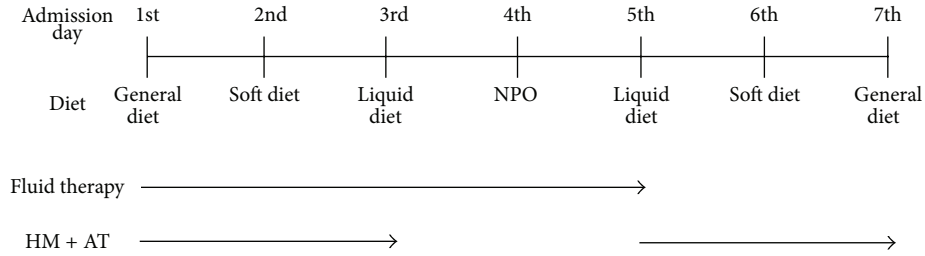

Figure 1: Flow chart of hospitalization program combining very low-calorie diet and fluid therapy. Abbreviation: HM, herbal medicine (decoction, ointment, or wet wrap dressing type); AT, acupuncture treatment; NPO, nothing per os.

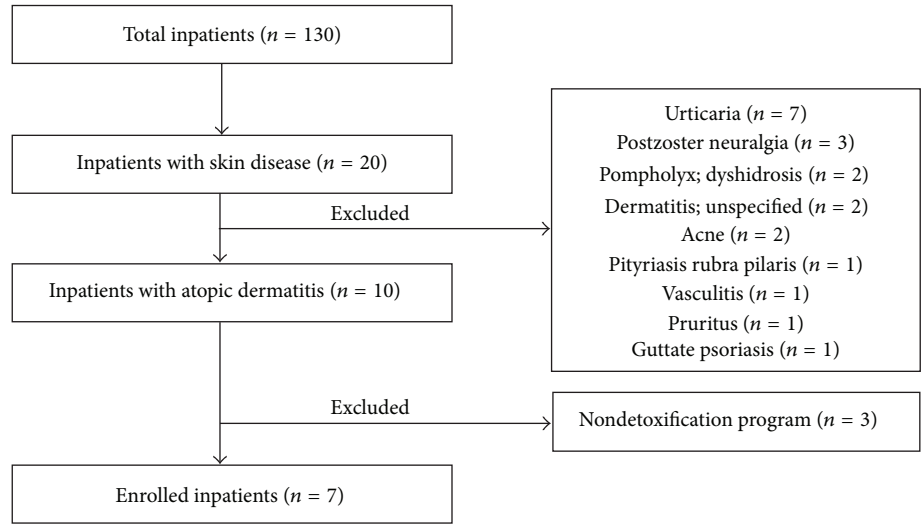

Figure 2: Flow chart of subjects' inclusion process.

3.2. Primary and Secondary Outcomes. The primary outcome, which was the SCORAD total index at each admission and discharge day, significantly decreased from 64.67 ± 11.72 (extent: 45.14 ± 29.32/intensity: 11.86 ± 1.95) to 26.26 ± 11.01 (extent: 34.14 ± 25.77/intensity: 5.57 ± 2.07) (P = 0.018). There was also a significant decrease in a secondary outcome, the pruritus self-assessment score changes of AD-related itching/scratching, from 8.00 ± 1.16 to 2.57 ± 0.98 (P = 0.016) between admission and discharge day (Figure 3).

3.3. Safety Evaluation. No adverse events were reported. Mean levels in systolic and diastolic blood pressure, respiratory rate, heart rate, and body temperature were similar at all measurement times. Also, clinical laboratory tests were similar between admission and discharge day.

4. Discussion

AD, especially when unmanageable, can be distressing and can reduce quality of life. Quick and effective treatments are necessary. Unfortunately, conventional treatments, whether western medicine or TCM, often fail to relieve symptoms of AD [10]. Therefore, we modified previous studies of fasting and developed the detoxification program, which combined fasting and fluid therapy, for inpatients with refractory cases of severe AD.

Fasting for a certain period of time can eliminate body waste, diminish gastrointestinal irritation, and refresh digestive and respiratory organs. In particular, inhibition of gastrointestinal irritation helps repair the mucous membrane and blocks any supply of unwholesome food, which can be allergens, for a certain period of time [11]. However, during the fasting stage, moisture and electrolytes can be lost. Accordingly, fluid therapy is needed to replenish the body with moisture and electrolytes [12]. A 0.9% hypertonic solution has some benefits because it is distributed first to the extracellular space. Although there is no scientific evidence on the pathophysiology, a large amount of fluid supply promoted recovery of postoperative or burn patients [13].

To apply detoxification to patients, careful attention is required in the following cases: (1) patients with gastric acid control disorders, (2) patients with hypoglycemia accompanied by vertigo or cold sweats, (3) patients with constipation, and (4) patients with anemia.

The typical period of detoxification is usually 7 days. If necessary, the period can be longer or shorter than 7 days, but the fasting state should not be longer than 3 consecutive days. Sidedishes have to be supplied to patients 1 or 2 days after a

Table 1: Patient summary.

Case	Age	Gender	Other atopy	Duration (unit: days)			Western medicine	HM type	AT	Serum IgE	Eosin count	ASO titer
				Hospitalization	VLCD Program	Fluid therapy						
1	19	Male	AR, AC, and food allergy (crab)	7	7	4	None	Decoction + ointment	Yes	1680	240	116
2	30	Male	AR, AC, and asthma	7	7	4	None	Decoction + ointment	Yes	14000	1340	273
3	20	Female	AR	12	8	5	Topical steroid	Decoction + ointment + wet wrap dressing	Yes	475	1510	284
4	22	Male	AR, food allergy (soybean)	8	8	4	None	Decoction + ointment	Yes	460	None	106
5	29	Male	ND	15	12	5	None	Decoction + ointment + wet wrap dressing	Yes	<18	130	202
6	25	Male	Food allergy	8	8	4	No response to topical and systemic steroid therapy	Decoction + ointment + wet wrap dressing	Yes	391	1700	101
7	23	Female	SD	8	8	4	None	Decoction + ointment	Yes	2400	210	201

*AR: allergic rhinitis; AC: allergic conjunctivitis; ND: nummular dermatitis; SD: seborrheic dermatitis; VLCD: very low calorie diet; HM: herbal medicine; AT: acupuncture treatment; IgE: immunoglobulin E; ASO: antistreptolysin O.

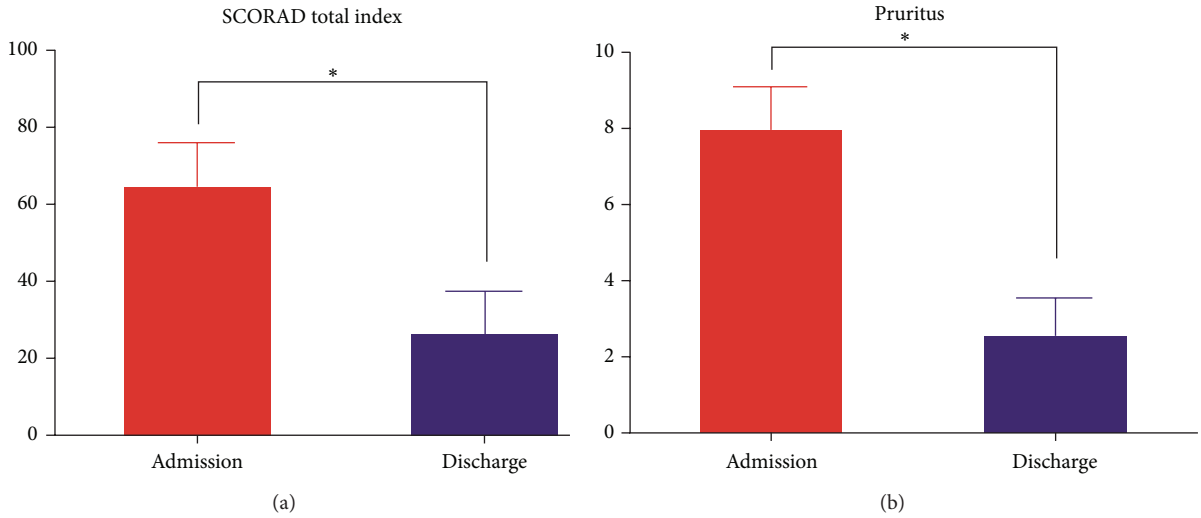

Figure 3: The mean change of SCORAD index and VAS score for pruritus after the detoxification program.

low-calorie diet not immediately after finishing fasting. Also, to calculate the fluid supply for patients, urinary and skin loss of water must be considered [14]. Although there were no cases in this study, based on experience in clinical practice, the symptoms of patients with AD, such as night-time itching, can be aggravated during the third very low-calorie meal or second fasting meal. However, these symptoms improve after about two to three days. Therefore, we should explain to patients that symptoms related to AD can deteriorate during the period of about seven days after the fasting diet. We also

have to explain to patients that symptoms related to AD can worsen if unwholesome foods, which can be allergens, are introduced after discharge from the hospital.

In experimental animal studies, fasting protected or diminished the distress level of autoimmune disease and allergy [5–7]. In clinical studies, fasting [15] and a low-calorie diet [16] have been reported to be effective in patients with rheumatoid arthritis. A review study found that one randomized trial concluded that weight loss may have some benefits for relieving asthma in overweight and obese patients [17]. Other studies indicated that fasting and DR can protect the increase of allergen-specific IL-4-producing T cells and suppress the allergic reaction [5] and in humans can ameliorate T-cell function [18].

A low-energy diet reduced inflammatory symptoms and oxidative damage in patients with AD [19]. A positive relationship between weight loss through short-term fasting and symptom improvement in patients with AD has also been reported [8]. These results are consistent with our findings after the detoxification program, which combined fasting with fluid therapy, for inpatients with AD.

However, there are still few data about fasting and fluid therapy in patients with AD. Numerous well-designed clinical studies, such as randomized controlled studies, are needed to acquire definite evidence on the effects of detoxification programs for inpatients with refractory cases of severe AD.

5. Conclusions

In this study, fasting with fluid therapy was effective for inpatients with refractory AD compared to conventional therapeutic modalities. The detoxification program, which combined fasting with fluid therapy, may be used as a novel treatment in refractory cases of severe AD.

Conflict of Interests

The authors declare that they have no conflict of interests.

References

[1] R. Berke, A. Singh, and M. Guralnick, "Atopic dermatitis: an overview," *The American Family Physician*, vol. 86, no. 1, pp. 35–42, 2012.

[2] C. Dinicola, A. Kekevian, and C. Chang, "Integrative medicine as adjunct therapy in the treatment of atopic dermatitis-the role of traditional Chinese Mmedicine, dietary supplements, and other modalities," *Clinical Reviews in Allergy and Immunology*, vol. 44, no. 3, pp. 242–253, 2013.

[3] M. Mizawa, T. Makino, H. Hikiami, Y. Shimada, and T. Shimizu, "Effectiveness of keishibukuryogan on chronic-stage lichenification associated with atopic dermatitis," *ISRN Dermatology*, vol. 2012, Article ID 158598, 6 pages, 2012.

[4] E. Ernst, "Alternative detox," *British Medical Bulletin*, vol. 101, no. 1, pp. 33–38, 2012.

[5] K.-I. Yamazaki, N. Kato-Nagaoka, T. Suzuki, K. Shida, and M. Nanno, "Immune deviation and alleviation of allergic reactions in mice subjected to dietary restriction," *Bioscience, Biotechnology and Biochemistry*, vol. 73, no. 12, pp. 2705–2711, 2009.

[6] K. Kouda and M. Iki, "Beneficial effects of mild stress (Hormetic Effects): dietary restriction and health," *Journal of Physiological Anthropology*, vol. 29, no. 4, pp. 127–132, 2010.

[7] H. Nakamura, K. Kouda, R. Tokunaga, and H. Takeuchi, "Suppressive effects on delayed type hypersensitivity by fasting and dietary restriction in ICR mice," *Toxicology Letters*, vol. 146, no. 3, pp. 259–267, 2004.

[8] H. Nakamura, K. Shimoji, K. Kouda, R. Tokunaga, and H. Takeuchi, "An adult with atopic dermatitis and repeated short-term fasting," *Journal of Physiological Anthropology and Applied Human Science*, vol. 22, no. 5, pp. 237–240, 2003.

[9] H. C. Williams, P. G. J. Burney, A. C. Pembroke, and R. J. Hay, "The U.K. Working Party's diagnostic criteria for atopic dermatitis. III. Independent hospital validation," *British Journal of Dermatology*, vol. 131, no. 3, pp. 406–416, 1994.

[10] A. Genois, M. Haig, A. D. Roches, A. Sirard, S. Le May, and C. C. McCuaig, "Case report of atopic dermatitis with refractory pruritus markedly improved with the novel use of clonidine and trimeprazine," *Pediatric Dermatology*, 2012.

[11] R. Weindruch and R. S. Sohal, "Caloric intake and aging," *the New England Journal of Medicine*, vol. 337, no. 14, pp. 986–994, 1997.

[12] G. Yagci, M. F. Can, E. Ozturk et al., "Effects of preoperative carbohydrate loading on glucose metabolism and gastric contents in patients undergoing moderate surgery: a randomized, controlled trial," *Nutrition*, vol. 24, no. 3, pp. 212–216, 2008.

[13] S. G. Oh and Y. H. Park, "Effect of fluid administration during the period of preoperative starvation on surgical patients," *Journal of the Korean Surgical Society*, vol. 18, no. 6, pp. 1–3, 1976.

[14] M. S. Oh, "Ten golden rules of fluid therapy," *Korean Journal of Hepatology*, vol. 7, no. 2, pp. 135–139, 2001.

[15] J. Kjeldsen-Kragh, M. Haugen, C. F. Borchgrevink et al., "Controlled trial of fasting and one-year vegetarian diet in rheumatoid arthritis," *The Lancet*, vol. 338, no. 8772, pp. 899–902, 1991.

[16] K. Iwashige, K. Kouda, M. Kouda et al., "Calorie restricted diet and urinary pentosidine in patients with rheumatoid arthritis," *Journal of Physiological Anthropology and Applied Human Science*, vol. 23, no. 1, pp. 19–24, 2004.

[17] F. B. Adeniyi and T. Young, "Weight loss interventions for chronic asthma," *Cochrane Database of Systematic Reviews*, vol. 7, Article ID CD009339, 2012.

[18] T. Ahmed, S. K. Das, J. K. Golden, E. Saltzman, S. B. Roberts, and S. N. Meydani, "Calorie restriction enhances T-cell-mediated immune response in adult overweight men and women," *Journals of Gerontology A*, vol. 64, no. 11, pp. 1107–1113, 2009.

[19] K. Kouda, T. Tanaka, M. Kouda et al., "Low-energy diet in atopic dermatitis patients: clinical findings and DNA damage," *Journal of Physiological Anthropology and Applied Human Science*, vol. 19, no. 5, pp. 225–228, 2000.

Hindawi Publishing Corporation
Evidence-Based Complementary and Alternative Medicine
Volume 2013, Article ID 527561, 12 pages
http://dx.doi.org/10.1155/2013/527561

Research Article

Cartilage Protective and Chondrogenic Capacity of WIN-34B, a New Herbal Agent, in the Collagenase-Induced Osteoarthritis Rabbit Model and in Progenitor Cells from Subchondral Bone

Jeong-Eun Huh,[1] Yeon-Cheol Park,[2] Byung-Kwan Seo,[2] Jae-Dong Lee,[3] Yong-Hyeon Baek,[2] Do-Young Choi,[3] and Dong-Suk Park[2]

[1] *East-West Bone & Joint Research Institute, Kyung Hee University, 149 Sangil-dong, Gangdong-gu, Seoul 134-727, Republic of Korea*
[2] *Department of Acupuncture & Moxibustion, Kang Dong Medical Center, Kyung Hee University, 149 Sangil-dong, Gangdong-gu, Seoul 134-727, Republic of Korea*
[3] *Department of Acupuncture & Moxibustion, College of Korean Medicine, Kyung Hee University, 1 Hoegidong, Dongdawmungu, Seoul 130-701, Republic of Korea*

Correspondence should be addressed to Dong-Suk Park; icarus08@hanmail.net

Received 29 March 2013; Revised 5 June 2013; Accepted 3 July 2013

Academic Editor: Bo-Hyoung Jang

We sought to determine the cartilage repair capacity of WIN-34B in the collagenase-induced osteoarthritis rabbit model and in progenitor cells from subchondral bone. The cartilage protective effect of WIN-34B was measured by clinical and histological scores, cartilage area, and proteoglycan and collagen contents in the collagenase-induced osteoarthritis rabbit model. The efficacy of chondrogenic differentiation of WIN-34B was assessed by expression of CD105, CD73, type II collagen, and aggrecan *in vivo* and was analyzed by the surface markers of progenitor cells, the mRNA levels of chondrogenic marker genes, and the level of proteoglycan, GAG, and type II collagen *in vitro*. Oral administration of WIN-34B significantly increased cartilage area, and this was associated with the recovery of proteoglycan and collagen content. Moreover, WIN-34B at 200 mg/kg significantly increased the expression of CD105, CD73, type II collagen, and aggrecan compared to the vehicle group. WIN-34B markedly enhanced the chondrogenic differentiation of CD105 and type II collagen in the progenitor cells from subchondral bone. Also, we confirmed that treatment with WIN-34B strongly increased the number of SH-2(CD105) cells and expression type II collagen in subchondral progenitor cells. Moreover, WIN-34B significantly increased proteoglycan, as measured by alcian blue staining; the mRNA level of type II α1 collagen, cartilage link protein, and aggrecan; and the inhibition of cartilage matrix molecules, such as GAG and type II collagen, in IL-1β-treated progenitor cells. These findings suggest that WIN-34B could be a potential candidate for effective anti-osteoarthritic therapy with cartilage repair as well as cartilage protection via enhancement of chondrogenic differentiation in the collagenase-induced osteoarthritis rabbit model and progenitor cells from subchondral bone.

1. Introduction

Osteoarthritis (OA) is a degenerative joint disease characterized by degradation and loss of articular cartilage, hypertrophic bone changes with osteophyte formation, and subchondral sclerosis [1, 2]. The disease results from homeostatic imbalance between matrix synthesis and degradation of joint tissue [3].

Currently, the subchondral bone is recognized as a key factor in normal joint protection and chondrogenic differentiation. Subchondral bone has been shown to exert important shock absorbing and supportive function. Subchondral bone can decrease the joint load and supplies nutrients to cartilage. Moreover, researchers believe that factors produced locally by subchondral bone tissue seep through the bone-cartilage interface [4]. These changes then lead to reactivation of the

secondary ossification centre and a decrease in cartilage thickness [5]. Cartilage defects that extend to the subchondral bone exhibit some ability to repair via the formation of neocartilage [6], probably due to the release of bone marrow-derived stem cells from the underlying subchondral bone [7].

OA has traditionally been seen as a primary articular cartilage disorder. However, recent observations have demonstrated that both early-stage increased remodeling and bone loss, and late-stage slow remodeling and subchondral densification are important components of the OA pathogenesis [8]. In addition, subchondral bone is thought to play a key role in OA pathogenesis. Subchondral bone changes in OA are potentially both a result and a cause of cartilage loss. Subchondral bone stiffness may decrease its viscoelastic properties and produce a loss of shock absorbing capacity, which in turn causes significant mechanical load and breakdown of the overlying cartilage [9]. Cartilage damage may in turn negatively influence the subchondral bone, thus perpetuating a pathogenic circle in the OA joint. Consequently, modulation of subchondral bone remodeling may become an attractive approach for OA treatment.

Current strategies for OA treatment include decreasing joint pain and stiffness, improving joint function, and delaying surgery. Commonly prescribed OA medications include nonsteroidal anti-inflammatory drugs, analgesics, locally administered corticosteroids, and viscosupplementation, which provide only symptomatic relief and eventually result in the need for surgical intervention [10]. Until now, effective agents have not been found that significantly prevent progression of disease and aid recovery of tissue damage. The search continues for reliable therapeutic agents that influence subchondral bone remodeling and establish their potential role as disease-modifying OA drugs (DMOADs). These agents include antiresorptives (estrogens, selective estrogen receptor modulators, bisphosphonates, calcitonins, and osteoprotegerin and blocking RANKL antibodies), bone-forming agents (parathormone and teriparatide), and antiosteoporotic agents with dual mechanism of action (strontium ranelate) [11]. However, there are still no DMOADs currently available to patients that can prevent disease progression and reverse the damage caused by OA [12].

To develop a novel antiosteoarthritis drug, we investigated the cartilage protection, analgesia, and anti-inflammation properties of 200 medicinal herbs used clinically for their anti-inflammatory and analgesic properties in traditional medicine. WIN-34B, a compound extracted from two herbs, the flowers of *Lonicera japonica* Thunb and roots of *Anemarrhena asphodeloides* BUNGE, was initially isolated through a comprehensive screening process. We standardized WIN-34B for quality control according to a previous report [13] and analyzed the major compounds of WIN-34B with the aim of standardizing its practical use and aiding in medicinal development. Data from several previous studies indicate that WIN-34B exhibits excellent analgesic and anti-inflammatory properties in the experimental models [13] and did not cause toxicity or gastric injury when orally administered to rats [14]. Also, WIN-34B showed that anti-inflammatory effect is mediate by reducing inflammatory mediators and regulating MMPs, ADAMTSs, and TIMPs via IκB-α and MAP kinases signal pathways in IL-1β-stimulated human OA fibroblast-like synoviocytes [15]. Furthermore, WIN-34B has cartilage protective effects in osteoarthritis human cartilage explants culture and chondrocytes [16]. These results suggest that WIN-34B could be a potential candidate for effective antiosteoarthritic therapy with cartilage protective properties and without toxicity instead of existing OA treatment. However, little is known about the effects of WIN-34B on chondrogenic differentiation.

In this study, we investigated the effects of WIN-34B on cartilage protection and chondrogenic differentiation in the collagenase-induced osteoarthritis rabbit model and progenitor cells from subchondral bone.

2. Materials and Methods

2.1. Preparation of WIN-34B Extract and Standardization. The dried flowers of *Lonicera japonica* and the dried root of *Anemarrhena asphodeloides* from Song Lim Pharmaceutical Company (Seoul, Republic of Korea) were purchased and identified by the Korea Pharmaceutical Trading Association (Seoul, Republic of Korea). Voucher specimens of *Lonicera japonica* Thunb. (no. OA-LOJ-15) and *Anemarrhena asphodeloides* Bunge (no. OA-ANA-11) were analyzed by HPLC analysis and deposited in the Central Research Institute, WhanIn Pharm. Co. Ltd. (Suwon, Republic of Korea).

WIN-34B was prepared by extracting a mixture of 2 kg of dried *Lonicera japonica* flowers and 1 kg of *Anemarrhena asphodeloides* root (2 : 1, w/w) with 10 L of 50% (v/v) ethanol for 4 h at 85°C. After the extracted solution was filtered and evaporated *in vacuo*, the resulting concentrate was dissolved in 225 mL distilled water and partitioned with 195 mL *n*-butanol. The *n*-butanol layer was evaporated *in vacuo* and lyophilized for complete removal of the residual solvent, resulting in a 7% yield of 11 g brown powder. We standardized WIN-34B for quality control according to a previous report [13], which we then analyzed by HPLC to find the standard compounds, mangiferin and chlorogenic acid.

2.2. In Vivo Study

2.2.1. Animals. Male New Zealand white rabbits (2.8–3.0 kg, nine to ten weeks) were obtained from the animal experimental center at Kyung Hee University Hospital (Seoul, Republic of Korea) and individually housed with water and food available ad libitum. The room was light/dark (08:00–20:00 h light, 20:00–08:00 h dark) controlled and kept at 21–24°C. All experiments were conducted according to the "Guiding Principles for the Care and Use of Laboratory Animals" and all procedures approved by the Animal Care and Use Committee of Kyung Hee University Medical Center.

2.2.2. Induction of Collagenase-Induced Osteoarthritis and Drug Treatment. Rabbits aged nine to ten weeks and weighing 2.8–3.0 kg at the start of the experiment (day 1) were anesthetized with an intramuscular injection of 0.5 mg/kg tiletamine-zolazepam (Zoletil50, Virbac, France). The shaved right knee joints of all rabbits were intra-articularly injected

with either 250 μL of 4 mg/mL collagenase solution (Clostridium histolyticum type II, 425 units/mL enzyme activity) or saline (control group). The same collagenase injection procedure was applied once more on day 4 according to methods described in Mankin [17]. Following the initial injection of collagenase (day 1), the rabbits were divided into groups (n = 10 per group). For four weeks, the vehicle groups were orally treated with 20 mL distilled water and the experimental groups were orally treated with WIN-34B (100, 200, and 400 mg/kg), joins (ETCP, SK chemicals, 400 mg/kg), celebrex (CEL, Pfizer, 100 mg/kg), and glucosamine (Gluco-Hcl, Sigma, 1500 mg/kg) on a daily basis using a feeding catheter (DJ2-284, Dae jong Ins. Korea).

2.2.3. Macroscopic Scoring of Stiffness. Stiffness was classified by movement, swelling, and reddening of knees. Each characteristic was subclassified as mild, moderate, and severe compared to the control group. The examination was performed by two independent observers who were blinded to the treatment groups.

2.2.4. Quantification of Global Histologic Score. After four weeks, the rabbits were sacrificed for histological examination. The right knee joints were then dissected and fixed in 10% phosphate-buffered formalin for two days, then decalcified in Calci-Clear Rapid solution (National Diagnostics, Atlanta, USA) for ten days, and then embedded in paraffin. Standard frontal sections of 5 μm were stained with hematoxylin and eosin (H&E) in the cartilage. Cartilage degradation features were analyzed using the scoring system developed by Colombo et al. [18] and modified by Kikuchi et al. [19]. The following six parameters were quantified: loss of superficial layer, erosion of cartilage, fibrillation and/or fissures, loss of stainable proteoglycan, disorganization of chondrocytes, and loss of chondrocytes. Each item was first graded from 1 to 4 (minimum to maximum damage) and the global histologic score was calculated as the total sum of each of the six parameters. All measurements were performed on the medial part of the tibial plateau, which is the region most affected by collagenase, and the femur condyle in the knee joint.

2.2.5. Quantification of Cartilage Area. All specimens were analyzed under bright-field microscopy (Axiovert 200, Carl Zeiss, Germany), and images were captured using a CCD camera (Axiocam MRc5, Carl Zeiss, Germany). The area of cartilage was measured in the whole of cartilage in the knee joints (100x magnification). All sections were evaluated by two independent observers blinded to the treatment groups. The results of these evaluations were then statistically analyzed.

2.2.6. Quantification of Proteoglycan by Safranin O Staining and Collagen by Masson's Trichrome Staining. These sections were also stained with Safranin O for detection of proteoglycan loss and Masson's trichrome for measurement of collagen in the cartilage. Cartilage depletion was indicated visually by diminished Safranin O staining and Masson's trichrome staining and was measured automatically with a Biocom microscope and AxioCam camera (Carl Zeiss, Germany). The proteoglycan content or collagen ratio of the cartilage was approximated by quantifying the staining intensity of the histologic sections [20, 21]. Intensity was measured in both the superficial and deep zone of the cartilage (100x magnification), and the ratio was calculated by dividing the Safranin O staining intensity (SOI) and the Masson's trichrome staining intensity (MTI) in the superficial zone by the SOI and MTI in the deep zone. All sections were evaluated by two independent observers blinded to the treatment groups. The results of these evaluations were then statistically analyzed.

2.2.7. Immunohistochemical Staining. Deparaffinized sections were pretreated with chondroitinase ABC (1 U/mL; SIGMA, St. Louis, MO, USA) at 37°C for 30 min. The endogenous peroxidase was blocked with 3% H_2O_2 in PBS at room temperature for 20 min and incubated in normal goat serum at room temperature for 30 min. Immunodetection of type II collagen was performed by raising a new polyclonal rabbit antibody (5 μg/mL; MP Biomedicals Inc., CA, USA) against the six amino-acid sequence (EKGPDP) of the C telopeptide of type II collagen at 4°C overnight. Rabbit anti-aggrecan antibody (10 μg/mL; Affinity BioReagents, Golden, CO, USA) was used to evaluate the aggrecan at 4°C overnight. Rabbit anti-CD105 antibody and rabbit anti-CD73 antibody (Santa Cruz Biotechnology, CA, USA) were treated to detect mesenchymal stem cells. After reaction of the biotinylated rabbit antibodies against goat immunoglobulin G (IgG) (DAKO, Glostrup, Denmark) at room temperature for 30 min, the sections were reacted with horseradish peroxidase-labeled streptavidin (DAKO) at room temperature for 15 min. The color was developed with 3,3-diaminobenzidine tetrahydrochloride (DAB) in 50 mmol/L of Tris-HCl, pH 7.6, 0.15 mol/L of NaCl, containing 0.05% Tween. Counterstaining was performed with hematoxylin. As a control, sections were reacted by replacing the first antibodies with nonimmune goat IgG (DAKO) at room temperature for 2 h before the immunostaining.

2.3. In Vitro Study

2.3.1. Isolation and Cultivation of Progenitor Cells from Rabbit Subchondral Bone. Subchondral bone was obtained from the knee joint of NewZealand white rabbit. To harvest progenitor cells from rabbit subchondral bone, bone was cut into small fragments, washed with phosphate buffered saline, and partially digested for 4 h at 37°C using 256 U/mL type I collagenase (Sigma-Aldrich, St Louis, MO, USA). The supernatant was discarded and the remaining fragments were placed in culture flasks and cultured in DMEM medium (Gibco-BRL, now part of Invitrogen Corporation, Carlsbad, CA, USA) containing 10% heat-inactivated FBS and an antibiotic mixture (100 units/mL penicillin base and 100 μg/mL streptomycin) at 37°C in the humidified atmosphere. This medium was replaced every 2 days until cells were observed in the Petri dishes. At this point, the culture medium was replaced with

fresh medium containing 10% FBS until confluence. Cells that reached 80%–90% confluence were passaged using trypsin-EDTA in PBS (0.05% v/v, Gibco-BRL) and expanded into plates as passage 1. Medium was exchanged every 3 days.

2.3.2. Flow Cytometry Analysis of Progenitor Cells and Chondrogenic Differentiation of Progenitor Cells from Rabbit Subchondral Bone. Mesenchymal progenitor cells from passage 2 of subchondral bone were washed in PBS/0.2% BSA and stained with fluorescence-isothiocyanate- (FITC-) conjugated mouse anti-human CD73, CD90, and CD45 (BD Biosciences, San Diego, CA, USA) phycoerythrin- (PE-) conjugated anti-human CD105(SH-2), the activated leukocyte cell adhesion molecule (ALCAM, CD166), CD34, and CD11b (BD Biosciences, San Diego, CA, USA) for 15 min on ice. For indirect staining, cells were incubated 30 min with either mouse anti-human STRO-1 or rabbit anti-human type II collagen (Col II)-IgG, washed with PBS/0.2% BSA, and stained with FITC-conjugated anti-mouse IgG (DAKO, Hamburg, Germany) for STOR-1 and PE-conjugated anti-rabbit IgG for Col II for 30 min at 4°C.

Mesenchymal progenitor cells from passage 2 of subchondral bone were seeded in 6-well plates at a concentration of 5×10^5cells/cm^2. After 24 h, cells were treated or nontreated with WIN-34B (10 μg/mL) and cultured for 7 days and 14 days. Cells were stained with CD45 FITC/CD105 PE or CD45 FITC/Col II PE for 30 min at 4°C. Cells were analyzed on FACScan (BD Biosciences, San Diego, CA, USA) using Cell Quest software (BD Biosciences San Diego, CA, USA).

2.3.3. Induction of Chondrogenic Differentiation in IL-1β-Stimulated Progenitor Cells of Rabbit Subchondral Bone. Mesenchymal progenitor cells from passage 2 were trypsinized (passage 3), and 2×10^5 cells in 1 mL standard media were centrifuged at 1000 rpm in 15 mL polypropylene. After overnight culture, media was changed to chondrogenic induction media. Chondrogenesis was induced by chondrogenic medium (high glucose DMEM medium supplemented with antibiotic mixture, 1% FBS, 50 μg/mL ascorbic acid-2-phosphate, 0.35 mM proline, 1% ITS$^+$, 10 ng/mL transforming growth factor-β3 (TGF-β3) [22]. Pellet of cells were treated with 5 ng/mL IL-1β (R&D Systems, Minneapolis, USA) in the absence or presence for 1 h and then added WIN-34B (1, 10 and 20 μg/mL). The medium was changed three times per week, and cells were maintained for up to 7 days.

(1) *Histological Analysis of Alcian Blue Staining.* Chondrogenic differentiation was histologically assessed by embedding micromasses in OCT compound and freezing, and cryosectioning at a thickness of 7 μm. Sections were stained with alcian blue, pH 1.0 (Rowley Biochemical, Danvers, MA, USA) to show proteoglycans.

(2) *Colorimetric Analysis of GAG and Type II Collagen.* GAG levels in the culture medium at seven days from onset of culture were determined by the amount of polyanionic material reacting with 1, 9-dimethylmethylene blue. Twenty microliter samples were mixed with 100 μL of DMB reagents (48 mg/mL DMB, 40 mM glycine, 40 mM NaCl, 10 mM HCl, pH 3.0) for 30 min at room temperature and quantified by measuring the absorbance at 590 nm (Spectramax, Molecular Devices, Sunnyvale, CA, USA). All measurements were performed in quadruplicate. Quantification was performed using a standard curve of chondroitin 6-sulfate from shark cartilage (Sigma) in the range of 0–35 μg/mL. Type II collagen levels were determined using the Sircol Collagen Assay (Biocolor Ltd., Valley Business Center, Northern Ireland). The culture medium at seven days from onset of culture was reacted with Sirius red dye containing sulfonic acid for 30 min at room temperature. The amount of type II collagen was calculated by measuring the absorbance at 540 nm and comparing that value to the standard concentration curve (0–200 μg/mL).

(3) *Analysis of Real-Time Quantitative Reverse Transcription-Polymerase Chain Reaction (qRT-PCR).* Total RNA was isolated using TRIzol reagent according to the manufacturer's protocol. Reverse transcription was performed by M-MLV Reverse Transcriptase (TaKaRa Biotechnology) according to the manufacturer's specifications. Briefly, first-strand cDNA was synthesized at 37°C for 1 h in 20 μL reaction mixture using 1 μg isolated mRNA. Real-time PCR (qRT-PCR) was carried out in a 25 μL volume container with SYBR Green PCR Master Mix (Roche Diagnostics). The template source was either 5 ng cDNA or purified DNA standard. The following primer sequences were used to amplify the type II α1 collagen, type I α1 collagen, cartilage link protein, and aggrecan (Table 1). β-actin was amplified as an internal control to standardize mRNA levels. Relative expression of the target genes in the study samples was obtained using the difference as calculated by the comparative threshold (C_t) method. The cycle of threshold (C_T) for each sample was averaged and normalized to GAPDH. The results were then analyzed by comparative $\Delta\Delta C_T$ method ($2^{(-\Delta\Delta C_T)}$) for relative quantification of gene expression.

2.4. Statistical Analysis. Data were expressed as mean ± SEM Differences among groups were analyzed by one-way ANOVA. In the case of two groups, a Student's t-test was used. Statistical significance was assessed at $P < 0.05$.

3. Results

3.1. Effects of WIN-34B on Stiffness and Cartilage Loss in the Collagenase-Induced Osteoarthritis Rabbit Model. Administration of WIN-34B dose dependently reduced knee stiffness in one week after treatment compared to the vehicle. In contrast, there was no significant improvement of stiffness in the CEL, ETCP, and Gluco-Hcl (Figure 1(a)). After three weeks, CEL at 200 mg/kg and ETCP at 400 mg/kg reduced these symptoms when compared to the vehicle. WIN-34B exhibited some mild changes such as structure or chondrocyte loss (Figure 1(b)). Morever, WIN-34B at 100, 200, and 400 mg/kg led to 1.8-, 2.0-, and 1.9-fold increases in cartilage area, respectively, compared to vehicle (Figure 1(c)). WIN-34B at 200 and 400 mg/kg significantly decreased cartilage degradation of the tibial plateau (2.3- and 2.4-fold) and femur

Table 1: Primers of targeted genes.

mRNA	Primers	Annealing Tm (cycle)
Type II α1 collagen	Fw: 5′-AAC ACT GCC AAC GTC CAG AT-3′ Rv: 5′-CTG CAG CAC GGT ATA GGT GA-3′	58°C (32)
Type I α1 collagen	Fw: 5′-TGA CCT CAA GAT GTG CCA CT-3′ Rv: 5′-GGG AGT TTC CAT GAA GCC-3′	58°C (32)
Cartilage link protein	Fw: 5′-GCG TCC GCT ACC CCA TCT CTA-3′ Rv: 5′-CTC TAA GGG CAC ATT CAC TT-3′	55°C (32)
Aggrecan	Fw: 5′-GAG GTC GTG GTG AAA GGT GT-3′ Rv: 5′-GTG TGG ATG GGG TAC CTG AC-3′	58°C (32)
GAPDH	Fw: 5′-GCT CTC CAG AAC ATC ACT CCT GCC-3′ Rv: 5′-CGT TGT CAT ACC AGG AAA TGA GCT T-3′	58°C (30)

Fw: forward; Rv: reverse; GAPDH: glyceraldehyde-3-phosphate dehydrogenase Tm: temperature.

condyle (1.8- and 2.2-fold), respectively, compared to the vehicle. Moreover, tibial plateau and femur condyle change tended to be higher in the WIN-34B at 200 and 400 mg/kg compared to other experimental groups (CEL, ETCP, and Gluco-Hcl) (Figure 1(d)).

3.2. Effects of WIN-34B on Cartilage Protection in the Collagenase-Induced Osteoarthritis Rabbit Model. Cartilage protective effects of WIN-34B were also evaluated by Safranin O staining for detection of proteoglycan loss and Masson's trichrome staining for measurement of collagen in the cartilage. In the normal, proteoglycan and collagen contents preserved in the knee joints, but not resulting in a marked loss of proteoglycan and collagen in the collagenase-induced knee joints (Figures 2(a) and 2(c)). WIN-34B at 100, 200, and 400 mg/kg increased the ratio of SOI (1.8-, 2.1-, and 2.0- fold) and MTI (2.2-, 4.2-, and 3.7-fold), respectively, compared to the vehicle. This ratio was also significantly higher in the WIN-34B at 100, 200, and 400 mg/kg compared to other experimental groups (CEL, ETCP, and Glugo-Hcl) (Figures 2(b) and 2(d)).

3.3. Effects of WIN-34B on Chondrogenic Differentiation in the Collagenase-Induced Osteoarthritis Rabbit Model. According to immunohistochemical analysis, WIN-34B at 200 mg/kg enhanced the expression of positive cells for CD105 (16.6-fold), CD73 (9.0-fold), type II collagen (13.1-fold), and aggrecan (7.9-fold) compared to cartilage area of vehicle (Figures 3(a) and 3(b)). Also, treatment with WIN-34B at 200 mg/kg enhanced the expression of CD105 (2.6-fold) and CD73 (2.7-fold) in the subchondral bone zone (Figures 3(c) and 3(d)).

3.4. Effects of WIN-34B on Chondrogenic Differentiation of Progenitor Cells from Rabbit Subchondral Bone. Expended progenitor cells showed typical cell surface antigens of mesenchymal stem and progenitor cells (Figure 4(a)). The antigens CD73, SH-2, CD90, and CD166 were present in progenitor cells from rabbit subchondral bone. Cells were positive for CD73 (44%), SH-2 (2–6%), CD90 (39%), CD166 (27%), and STRO-1 (31%). A population of cells were minority positive for SH-2, and negative for the hematopoietic antigen CD34 as well as for the leukocyte common antigen CD45 and macrophage antigen CD11b (Figure 4(a)). We also investigated the *in vitro* effects of WIN-34B on chondrogenic differentiation of progenitor cells derived from rabbit subchondral bone using flow cytometry analysis. The surface antigen for SH-2 was increased by 39% at 7 days and 52% at 14 days of culture in chondrogenic medium, and the expression of type II collagen was enhanced by 8–11% at 7 days and 14 days (Figure 5(b)). WIN-34B at 10 μg/mL increased the number of SH-2 cells (96% and 98%) and expression of type II collagen (23% and 19%) at 7 days and 14 days after cultivation, respectively (Figure 4(b)).

3.5. Effects of WIN-34B on Chondrogenic Differentiation of IL-1β-Treated Progenitor Cells from Rabbit Subchondral Bone. To evaluate the effects of WIN-34B on the chondrogenic differentiation of IL-1β-treated progenitor cells, cells were cultured in high-density pellets of chondrogenic conditions and added WIN-34B at 1, 10, and 20 μg/mL. According to histological analysis, IL-1β-treatment of subchondral progenitor cells led to an 8.0-fold reduction in proteoglycan expression compared to the control. However, treatment with WIN-34B at 1, 10, and 20 μg/mL led to 3.2-, 6.0-, and 9.7-fold increases, respectively, compared to the IL-1β-treated subchondral progenitor cells (Figure 5(a)). The level of chondrogenic markers was determined by qRT-PCR. IL-1β significantly decreased the mRNA expression of type II α1 collagen, cartilage link protein, and aggrecan. However, WIN-34B dose dependently increased the level of type II α1 collagen, cartilage link, and aggrecan compared to IL-1β-treated cells (Figure 5(b)). Moreover, WIN-34B dose dependently reduced the degradation of GAG and type II collagen induced by IL-1β compared to IL-1β-treated cells (Figure 5(c)).

4. Discussion

In this study, we investigated the effects of WIN-34B on cartilage protection and chondrogenic differentiation in the progress of OA. First, in the collagenase-induced osteoarthritis rabbit model, we evaluated the stiffness and cartilage loss to assess the effects of WIN-34B on disease progression. Cartilage protective effect was confirmed by determining

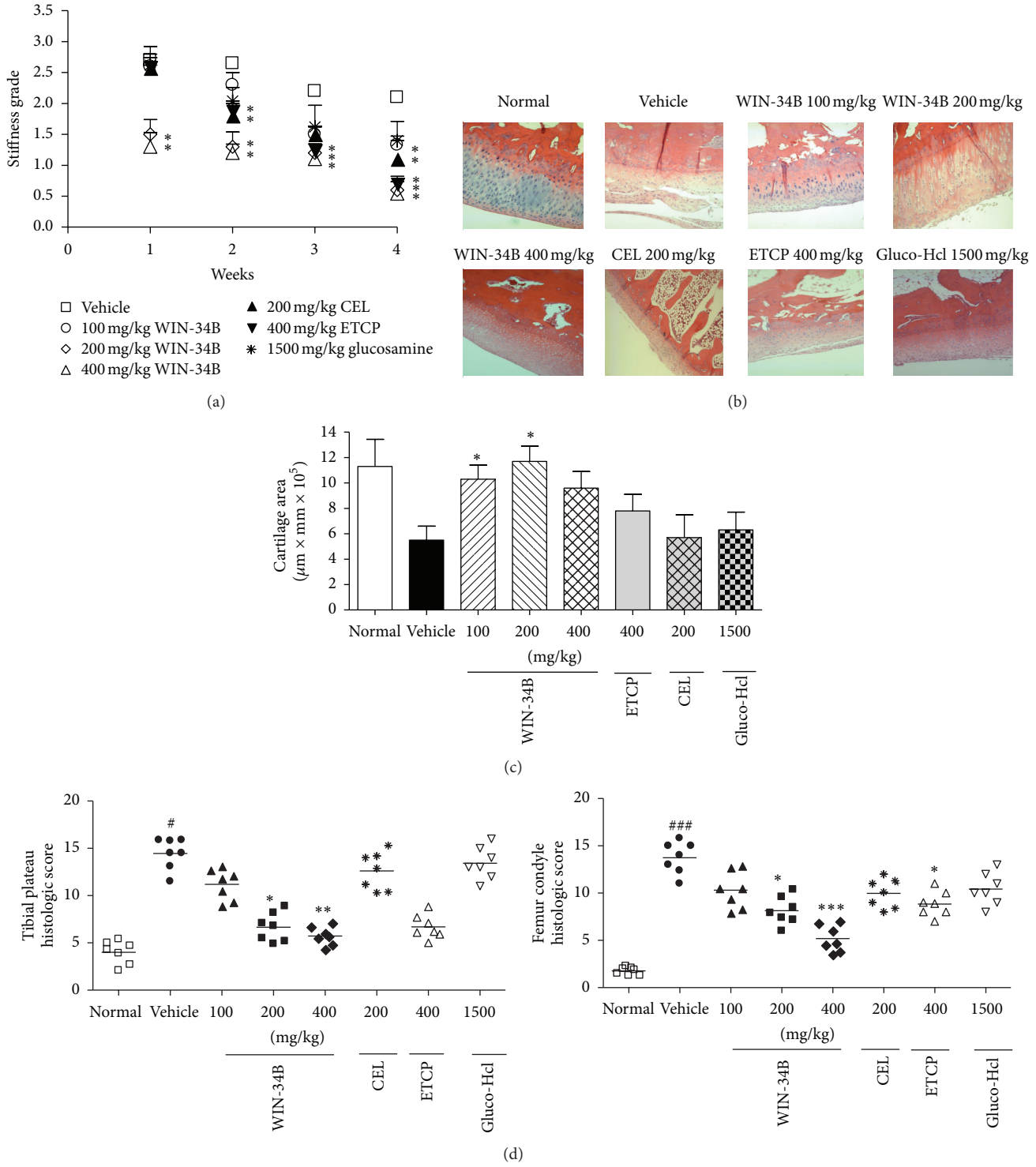

Figure 1: Effects of WIN-34B on disease progression in the collagenase-induced arthritis rabbit model. Right knees of rabbits were intra-articularly injected with collagenase on days 1 and 4. 100 mg/kg, 200 mg/kg, and 400 mg/kg WIN-34B; 200 mg/kg CEL; 400 mg/kg ETCP or 1500 mg/kg Gluco-Hcl were orally administered for four weeks. (a) Stiffness (b) Hematoxylin-Eosin stained sections of knee joints from the normal, vehicle, WIN-34B 100 mg/kg, WIN-34B 200 mg/kg, WIN-34B 400 mg/kg, CEL 200 mg/kg, ETCP 400 mg/kg, and Gluco-Hcl 1500 mg/kg. (c) Cartilage area and (d) histopathologic scores evaluated at the tibial plateau and femur condyle in animals with collagenase-induced arthritis. Values are the mean ± SEM. $^{\#}P < 0.05$ and $^{\#\#\#}P < 0.001$ compared to the normal group, $^{*}P < 0.05$, $^{**}P < 0.01$, and $^{***}P < 0.001$ compared to the vehicle group. Two independent experiments were performed with similar results.

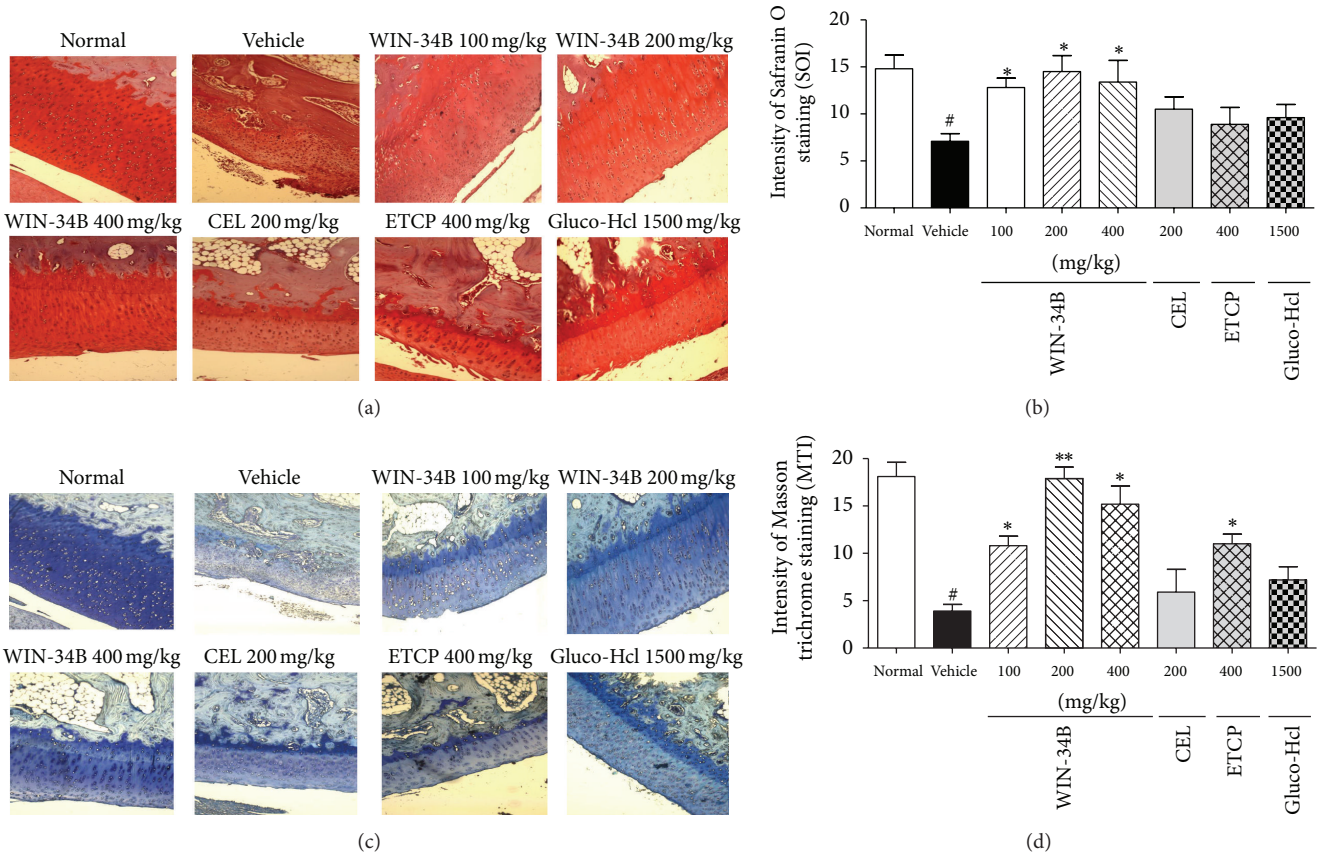

Figure 2: Effects of WIN-34B on cartilage protection in the knees of collagenase-induced arthritis rabbits. (a) Representative Safranin O stained sections of knee joints from the normal, vehicle, WIN-34B 100 mg/kg, WIN-34B 200 mg/kg, WIN-34B 400 mg/kg, CEL 200 mg/kg, ETCP 400 mg/kg, and Gluco-Hcl 1500 mg/kg group. (b) Proteoglycan content, expressed as a ratio, was calculated by dividing the Safranin O staining intensity (SOI) in the superficial zone (SOI-S) by SOI in the deep zone (SOI-D). (c) Representative Masson's trichrome stained sections of knee joints from the normal, vehicle, WIN-34B 100 mg/kg, WIN-34B 200 mg/kg, WIN-34B 400 mg/kg, CEL 200 mg/kg, ETCP 400 mg/kg and Gluco-Hcl 1500 mg/kg group. (d) Collagen content, expressed as a ratio, was calculated by dividing the Masson's trichrome staining intensity (MTI) in the superficial zone (MTI-S) by MTI in the deep zone (MTI-D). Values are mean ± SEM. $^{\#}P < 0.05$ compared to the normal group, $^{*}P < 0.05$ and $^{**}P < 0.01$ compared to the vehicle group. Two independent experiments were performed with similar results.

proteoglycan and collagen contents. Chondrogenic capacity of WIN-34B was assessed by the expression of CD105, CD73, type II collagen, and aggrecan using the immunohistochemical analysis. Second, we evaluated the expression of mesenchymal stem cell-related cell surface antigen to assess the chondrogenic induction of progenitor cells from subchondral bone by WIN-34B treatment in chondrogenic medium. The cartilage protective and chondrogenic capacity of WIN-34B was assessed by alcian blue staining of proteoglycan, the mRNA levels of chondrogenic maker genes, and the degradation of GAG and type II collagen in IL-1β-treated progenitor cells from rabbit subchondral bone.

Oral administration of WIN-34B resulted in a significant reduction of general clinical and histological scores. Also, WIN-34B significantly inhibited cartilage loss, as determined by measuring the proteoglycan and collagen. However, histopathology grading showed that CEL and Gluco-Hcl had no protective effect on cartilage, and ETCP resulted in significantly degraded cartilage in the femur condyle, but not the tibial plateau. These results suggest that WIN-34B is markedly more effective against cartilage destruction than the selective COX-2 inhibitor, ETCP, and Gluco-Hcl in the collagenase-induced osteoarthritis rabbit model. Our previous *in vitro* data on WIN-34B has shown cartilage protective effects through the regulation of matrix proteinases (aggrecanases and MMPs/TIMPs), inflammatory mediators (PGE2, NO, IL-1β, and TNF-α), and the MAPK pathways in osteoarthritis human cartilage explants culture and chondrocytes [15]. These results support the safety and therapeutic usefulness of WIN-34B for development as an OA treatment.

The ultimate goal of OA treatment is cartilage protection and repair but is not yet clear. Although, various surgical methods have been proposed to regenerate articular cartilage, including bone marrow stimulation [23], mosaicplasty [24], and autologous chondrocyte implantation [25], each of them has some disadvantage such as degeneration of repaired tissue, limitation of large defects, and long-term risk of developing OA [26].

There have been many reports of new DMOAD candidates with strong cartilage protective and chondrogenic

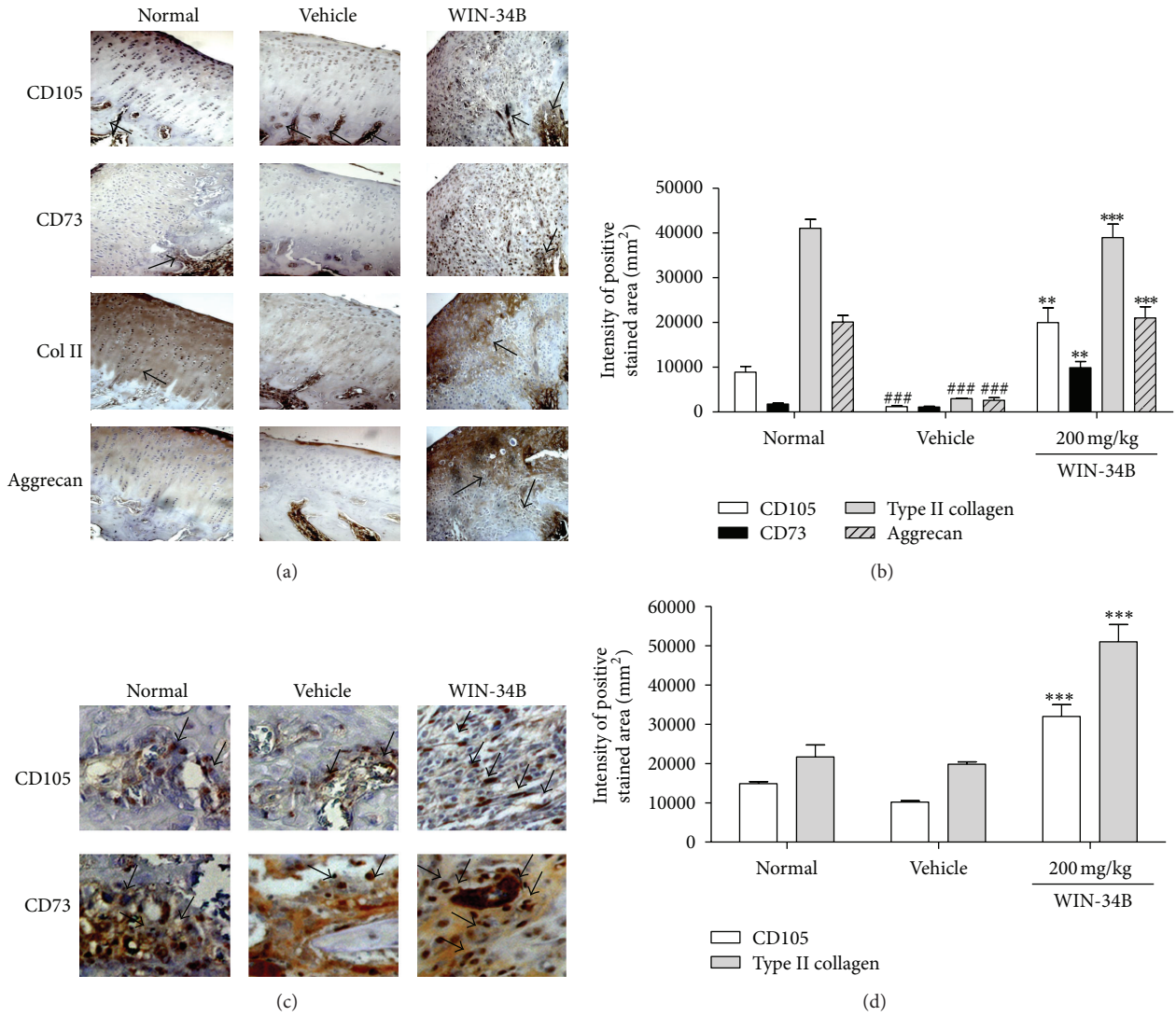

Figure 3: Effects of WIN-34B on chondrogenic differentiation in the knees of collagenase-induced arthritis rabbits. (a) Representative immunostained stained sections of cartilage from knee joints of animal in the normal, vehicle, and WIN-34B 200 mg/kg group. Lane 1: rabbit anti-CD105 antibody stained sections, lane 2: rabbit anti-CD73 antibody stained sections, lane 3: rabbit-anti-type II collagen (Col II) antibody stained sections, lane 4: rabbit-anti-aggrecan antibody stained sections. (b) Intensity of positive stained area of anti-CD105, anti-CD73, anti-type II collagen, and anti-aggrecan by immunostaining in the cartilage zone of knee joints. (c) Representative immunostained stained sections of subchondral bone from the knee joints of animals in the normal, vehicle, and WIN-34B 200 mg/kg groups. Lane 1: rabbit anti-CD105 antibody stained sections, lane 2: rabbit anti-CD73 antibody stained sections. (d) Intensity of positive stained area of anti-CD105 and anti-CD73 in the subchondral bone zone of knee joints. Values are the mean ± SEM. $^{\#\#}P < 0.01$ compared to the normal group, $^{**}P < 0.05$ and $^{***}P < 0.01$ compared to the vehicle group. Two independent experiments were performed with similar results.

activities. Antiresorptive agents, such as estrogens, and other bisphosphonates (BP) have been shown to have a chondroprotective function and a favorable effect in stopping OA progression in animal models [27–33]. Recently, selective estrogen receptor modulators (SERMs) have also demonstrated similar positive effects in OA treatment [27]. However, results from clinical trials using these drugs have been contradictory [34]. Bone-forming agents such as PTH (1–34) inhibited the terminal differentiation of human articular chondrocytes *in vitro* and reduced the progression of cartilage damage in a model of papain-induced OA in rats [35]. Strontium ranelate is an agent with dual mechanisms of action on bone metabolism, exerting antiresorptive and new bone forming effects [36]. However, there are few studies on the use of PTH (1–34) and strontium ranelate in animal models of OA, so more research need to be carried out. Therefore, it is reasonable to assume that drugs affecting subchondral bone remodeling may have a prominent role as DMOADs. While various attempts have been made to develop DMORDs, the results have been unsatisfactory regarding the effects and safety of these drugs [37].

Progenitor cells of subchondral bone were expected to be an alternative for cartilage repair of OA. Many researchers agree with the importance of subchondral bone healing in

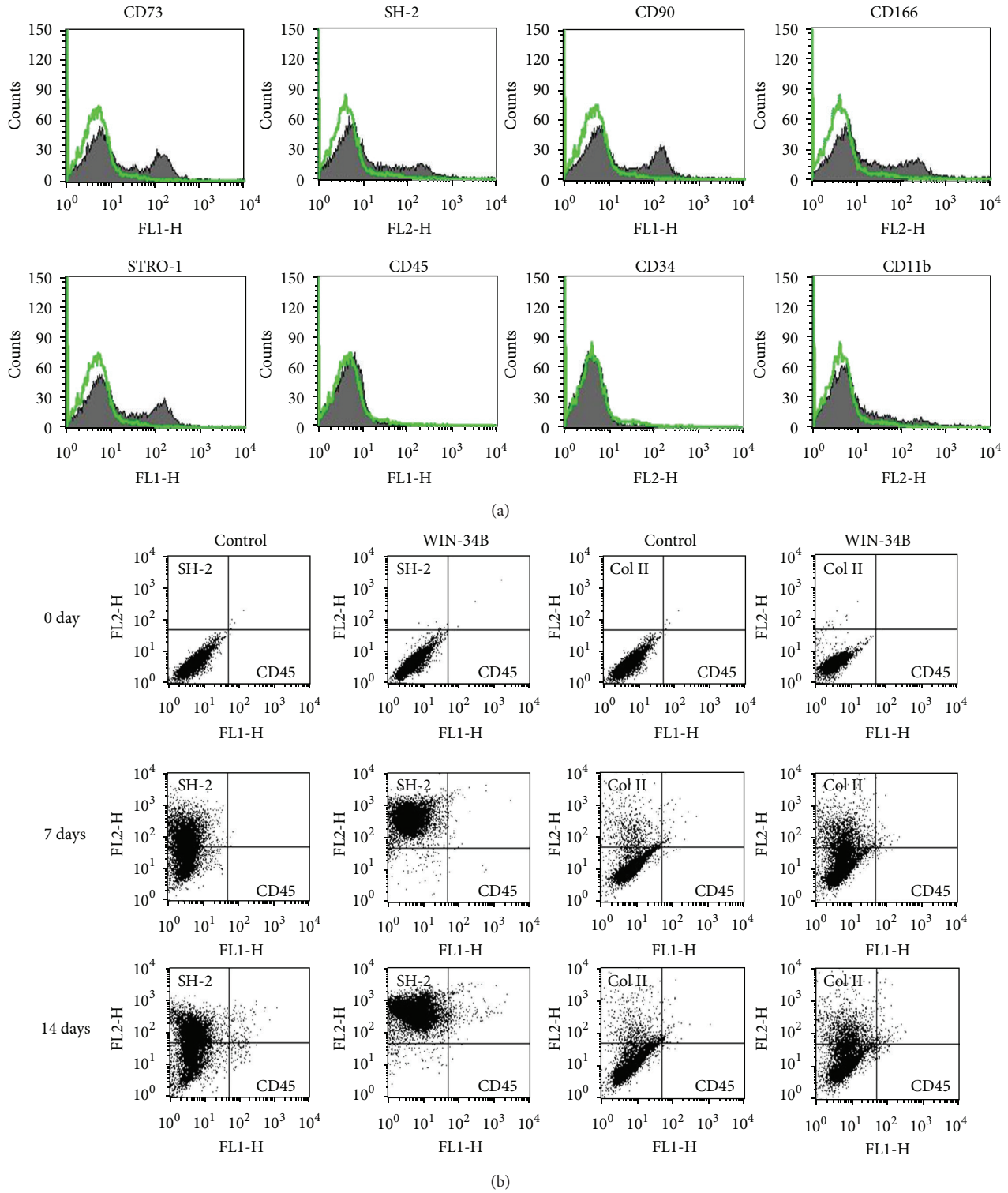

Figure 4: Effects of WIN-34B on chondrogenic differentiation of progenitor cells from rabbit subchondral bone. (a) Surface marker profiling of progenitor cells using flow cytometry. Cells were positive for CD73, SH-2, CD90, CD166, and STOR-1, and negative for CD45, CD34, and CD11b. (b) Chondrogenic induction of progenitor cells from subchondral bone cultured by WIN-34B treatment in chondrogenic medium. Progenitor cells from passage 2 of subchondral bone were seeded in 6-well plates at a concentration of 5×10^5 cells/cm^2. After 24 h, cells were treated or nontreated with WIN-34B (10 μg/mL) and cultured for 7 days and 14 days. Each of the three samples was measured for profiling markers.

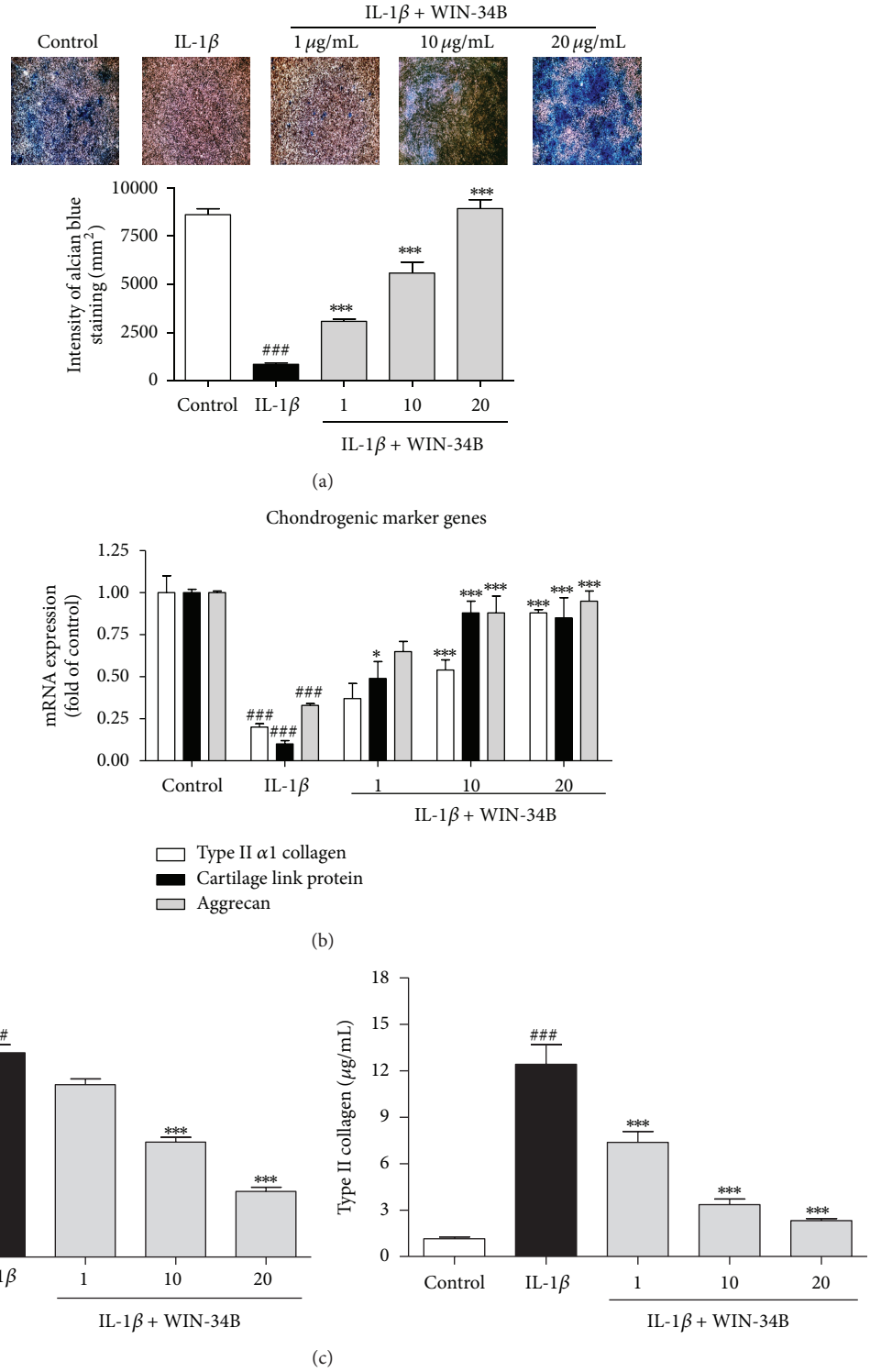

Figure 5: Effects of WIN-34B on chondrogenic differentiation of IL-1β-stimulated progenitor cells from rabbit subchondral bone. (a) Histological analysis of WIN-34B by alcian blue staining of chondrogenic differentiation in IL-1β-treated progenitor cells. Control, IL-1β, WIN-34B 1 μg/mL, WIN-34B 10 μg/mL, and WIN-34B 20 μg/mL after 7 days of culture in chondrogenic differentiation media. Magnified view (×100). (b) Dose response of WIN-34B on the mRNA expression of chondrogenic markers. Chondrogenic differentiation of subchondral progenitor cells that were incubated for seven days with 1, 10, and 20 μg/mL of WIN-34B in the presence of IL-1β. qRT-PCR was then performed for type II α1 collagen, cartilage link protein, and aggrecan. (c) Inhibitory effects of WIN-34B on GAG and type II collagen degradation on chondrogenic differentiation of IL-1β-stimulated subchondral progenitor cells. GAG and type II collagen degradation are shown as a cumulative release into the culture medium. Values are the mean ± SEM. $^{###}P < 0.001$ compared to the control group. $^{*}P < 0.05$, $^{***}P < 0.001$ compared to the IL-1β group. Data were obtained from at least three independent experiments.

the surgical and drug treatment of OA [38, 39]. Studies have attempted to find an effective combination of antigens in order to isolate a pure population of mesenchymal progenitor cells from various tissues [40]. One of these studies found that the coexpression of CD105 and CD73 could be sufficient in the adult human bone marrow cells [41]. Recently, micromass culture has been widely used to evaluate the chondrogenic potential of mesenchymal progenitor cells. Mesenchymal progenitor cells from human bone marrow increased the expression of type II and type X collagen in micromass culture [42]. Several studies reported that progenitor cells of human subchondral bone promoted the chondrogenic maker genes such as type II collagen, aggrecan, cartilage link protein, and cartilage oligomeric matrix protein [43–45]. In our study, WIN-34B increased the significant expression of CD105 and CD73 in the subchondral bone of collagenase-induced osteoarthritis rabbit model. Moreover, type II collagen and aggrecan fully recovered from damage by WIN-34B at 200 mg/kg. WIN-34B at 10 μg/mL increased the number of SH-2 cells and expression of type II collagen in subchondral progenitor cells. Furthermore, WIN-34B strongly induced proteoglycan, type II α1 collagen, cartilage link protein, and aggrecan and reduced the degradation of GAG and type II collagen in the IL-1β-treated subchondral progenitor cells. Therefore, we suggest that WIN-34B strongly induced chondrogenic differentiation by the induction of typical mesenchymal stem cell related cell surface antigen CD105 and CD73, and the enhancement of chondrogenic markers type II collagen and aggrecan *in vivo* and *in vitro*.

In summary, it was shown that WIN-34B exerted cartilage protection and chondrogenic differentiation in the collagenase-induced osteoarthritis rabbit model and progenitor cells from subchondral bone by stimulating chondrogenic differentiation of progenitor cells derived from subchondral bone. These results suggest that WIN-34B has potential for a new disease-modifying osteoarthritis drug (DMOAD) candidate in OA treatment.

Conflict of Interests

The authors have declared that there is no conflict of interests.

Authors' Contribution

Jeong-Eun Huh and Yeon-Cheol Park contributed equally to this work.

Acknowledgment

This work was supported by the Basic Science Research Program through the National Research Foundation of Korea (NRF), funded by the Ministry of Education, Science and Technology (2011-0012672 and 2011–0006033).

References

[1] A. R. Poole, "An introduction to the pathophysiology of osteoarthritis," *Frontiers in Bioscience*, vol. 4, pp. D662–D670, 1999.

[2] L. G. Ameye and W. S. S. Chee, "Osteoarthritis and nutrition. From nutraceuticals to functional foods: a systematic review of the scientific evidence," *Arthritis Research and Therapy*, vol. 8, no. 4, article R127, 2006.

[3] J. Martel-Pelletier, C. Boileau, J. Pelletier, and P. J. Roughley, "Cartilage in normal and osteoarthritis conditions," *Best Practice and Research: Clinical Rheumatology*, vol. 22, no. 2, pp. 351–384, 2008.

[4] A. M. Coats, P. Zioupos, and R. M. Aspden, "Material properties of subchondral bone from patients with osteoporosis or osteoarthritis by microindentation testing and electron probe microanalysis," *Calcified Tissue International*, vol. 73, no. 1, pp. 66–71, 2003.

[5] D. B. Burr, "Increased biological activity of subchondral mineralized tissues underlies the progressive deterioration of articular cartilage in osteoarthrosis," *Journal of Rheumatology*, vol. 32, no. 6, pp. 1156–1158, 2005.

[6] A. P. Newman, "Articular cartilage repair," *The American Journal of Sports Medicine*, vol. 26, no. 2, pp. 309–324, 1998.

[7] F. Shapiro, S. Koide, and M. J. Glimcher, "Cell origin and differentiation in the repair of full-thickness defects of articular cartilage," *Journal of Bone and Joint Surgery A*, vol. 75, no. 4, pp. 532–553, 1993.

[8] D. B. Burr and M. A. Gallant, "Bone remodelling in osteoarthritis," *Nature Review Rheumatology*, vol. 8, no. 11, pp. 665–673, 2012.

[9] E. L. Radin and R. M. Rose, "Role of subchondral bone in the initiation and progression of cartilage damage," *Clinical Orthopaedics and Related Research*, vol. 213, pp. 34–40, 1986.

[10] M. Merashly and I. Uthman, "Management of knee osteoarthritis: an evidence based review of treatment options," *The Lebanese Medical Journal*, vol. 60, no. 4, pp. 237–242, 2012.

[11] S. Castañeda, J. A. Roman-Blas, R. Largo, and G. Herrero-Beaumont, "Subchondral bone as a key target for osteoarthritis treatment," *Biochemical Pharmacology*, vol. 83, no. 3, pp. 315–323, 2012.

[12] F. Berenbaum, "Osteoarthritis year 2010 in review: pharmacological therapies," *Osteoarthritis and Cartilage*, vol. 19, no. 4, pp. 361–365, 2011.

[13] M. Kang, I. Jung, J. Hur et al., "The analgesic and anti-inflammatory effect of WIN-34B, a new herbal formula for osteoarthritis composed of *Lonicera japonica* Thunb and *Anemarrhena asphodeloides* BUNGE *in vivo*," *Journal of Ethnopharmacology*, vol. 131, no. 2, pp. 485–496, 2010.

[14] J. E. Huh, W. I. Lee, B. K. Seo et al., "Gastroprotective and safety effects of WIN-34B, a novel treatment for osteoarthritis, compared to NSAIDs," *Journal of Ethnopharmacology*, vol. 137, no. 2, pp. 1011–1017, 2011.

[15] J. E. Huh, B. K. Seo, Y. C. Park et al., "WIN-34B, a new herbal medicine, inhibits the inflammatory response by inactivating IκB-α phosphorylation and mitogen activated protein kinase pathways in fibroblast-like synoviocytes," *Journal of Ethnopharmacology*, vol. 143, no. 3, pp. 779–786, 2012.

[16] J. E. Huh, B. K. Seo, Y. H. Baek et al., "Standardized butanol fraction of WIN-34B suppresses cartilage destruction via inhibited production of matrix metalloproteinase and inflammatory mediator in osteoarthritis human cartilage explants culture and chondrocytes," *BMC Complementary and Alternative Medicine*, vol. 12, article 256, 2012.

[17] T. Kikuchi, T. Sakuta, and T. Yamaguchi, "Intra-articular injection of collagenase induces experimental osteoarthritis in

mature rabbits," *Osteoarthritis and Cartilage*, vol. 6, no. 3, pp. 177–186, 1998.

[18] C. Colombo, M. Butler, E. O'Byrne et al., "A new model of osteoarthritis in rabbits. I. Development of knee joint pathology following lateral meniscectomy and section of the fibular collateral and sesamoid ligaments," *Arthritis and Rheumatism*, vol. 26, no. 7, pp. 875–886, 1983.

[19] T. Kikuchi, H. Yamada, and M. Shimmei, "Effect of high molecular weight hyaluronan on cartilage degeneration in a rabbit model of osteoarthritis," *Osteoarthritis and Cartilage*, vol. 4, no. 2, pp. 99–110, 1996.

[20] P. Pastoureau, S. Leduc, A. Chomel, and F. de Ceuninck, "Quantitative assessment of articular cartilage and subchondral bone histology in the meniscectomized guinea pig model of osteoarthritis," *Osteoarthritis and Cartilage*, vol. 11, no. 6, pp. 412–423, 2003.

[21] M. Sabatini, C. Lesur, M. Thomas et al., "Effect of inhibition of matrix metalloproteinases on cartilage loss in vitro and in a guinea pig model of osteoarthritis," *Arthritis and Rheumatism*, vol. 52, no. 1, pp. 171–180, 2005.

[22] B. Johnstone, T. M. Hering, A. I. Caplan, V. M. Goldberg, and J. U. Yoo, "In vitro chondrogenesis of bone marrow-derived mesenchymal progenitor cells," *Experimental Cell Research*, vol. 238, no. 1, pp. 265–272, 1998.

[23] J. R. Steadman, K. K. Briggs, J. J. Rodrigo, M. S. Kocher, T. J. Gill, and W. G. Rodkey, "Outcomes of microfracture for traumatic chondral defects of the knee: average 11-year follow-up," *Arthroscopy*, vol. 19, no. 5, pp. 477–484, 2003.

[24] L. Hangody, P. Feczkó, L. Bartha, G. Bodó, and G. Kish, "Mosaicplasty for the treatment of articular defects of the knee and ankle," *Clinical Orthopaedics and Related Research*, no. 391, pp. S328–S336, 2001.

[25] J. D. Harris, R. A. Siston, X. Pan, and D. C. Flanigan, "Autologous chondrocyte implantation: a systematic review," *Journal of Bone and Joint Surgery A*, vol. 92, no. 12, pp. 2220–2233, 2010.

[26] H. Koga, L. Engebretsen, J. E. Brinchmann, T. Muneta, and I. Sekiya, "Mesenchymal stem cell-based therapy for cartilage repair: a review," *Knee Surgery, Sports Traumatology, Arthroscopy*, vol. 17, no. 11, pp. 1289–1297, 2009.

[27] K. D. Ham, R. F. Loeser, B. R. Lindgren, and C. S. Carlson, "Effects of long-term estrogen replacement therapy on osteoarthritis severity in cynomolgus monkeys," *Arthritis and Rheumatism*, vol. 46, no. 7, pp. 1956–1964, 2002.

[28] T. Y. Ho, K. Santora, J. C. Chen, A. L. Frankshun, and C. A. Bagnell, "Effects of relaxin and estrogens on bone remodeling markers, receptor activator of NF-kB ligand (RANKL) and osteoprotegerin (OPG), in rat adjuvant-induced arthritis," *Bone*, vol. 48, no. 6, pp. 1346–1353, 2011.

[29] M. Z. Yan, Y. Xu, Y. X. Gong et al., "Raloxifene inhibits bone loss and improves bone strength through an Opg-independent mechanism," *Endocrine*, vol. 37, no. 1, pp. 55–61, 2010.

[30] S. Canpolat, N. Tug, A. D. Seyran, S. Kumru, and B. Yilmaz, "Effects of raloxifene and estradiol on bone turnover parameters in intact and ovariectomized rats," *Journal of Physiology and Biochemistry*, vol. 66, no. 1, pp. 23–28, 2010.

[31] M. A. Karsdal, I. Byrjalsen, D. J. Leeming, and C. Christiansen, "Tibolone inhibits bone resorption without secondary positive effects on cartilage degradation," *BMC Musculoskeletal Disorders*, vol. 9, article 153, 2008.

[32] A. Kadri, T. Funck-Brentano, H. Lin et al., "Inhibition of bone resorption blunts osteoarthritis in mice with high bone remodelling," *Annals of the Rheumatic Diseases*, vol. 69, no. 8, pp. 1533–1538, 2010.

[33] M. Moreau, P. Rialland, J. Pelletier et al., "Tiludronate treatment improves structural changes and symptoms of osteoarthritis in the canine anterior cruciate ligament model," *Arthritis Research and Therapy*, vol. 13, no. 3, article R98, 2011.

[34] G. Herrero-Beaumont, J. A. Roman-Blas, S. Castañeda, and S. A. Jimenez, "Primary osteoarthritis no longer primary: three subsets with distinct etiological, clinical, and therapeutic characteristics," *Seminars in Arthritis and Rheumatism*, vol. 39, no. 2, pp. 71–80, 2009.

[35] J. K. Chang, L. H. Chang, S. H. Hung et al., "Parathyroid hormone 1–34 inhibits terminal differentiation of human articular chondrocytes and osteoarthritis progression in rats," *Arthritis and Rheumatism*, vol. 60, no. 10, pp. 3049–3060, 2009.

[36] O. Malaise, O. Bruyere, and J. Y. Reginster, "Strontium ranelate normalizes bone mineral density in osteopenic patients," *Aging—Clinical and Experimental Research*, vol. 19, no. 4, pp. 330–333, 2007.

[37] D. T. Felson, R. C. Lawrence, M. C. Hochberg et al., "Osteoarthritis: new insights—part 2: treatment approaches," *Annals of Internal Medicine*, vol. 133, no. 9, pp. 726–737, 2000.

[38] H. J. Mankin, "The response of articular cartilage to mechanical injury," *Journal of Bone and Joint Surgery A*, vol. 64, no. 3, pp. 460–466, 1982.

[39] W. S. Khan, D. S. Johnson, and T. E. Hardingham, "The potential of stem cells in the treatment of knee cartilage defects," *Knee*, vol. 17, no. 6, pp. 369–374, 2010.

[40] S. Bobis, D. Jarocha, and M. Majka, "Mesenchymal stem cells: characteristics and clinical applications," *Folia Histochemica et Cytobiologica*, vol. 44, no. 4, pp. 215–230, 2006.

[41] M. F. Pittenger, A. M. Mackay, S. C. Beck et al., "Multilineage potential of adult human mesenchymal stem cells," *Science*, vol. 284, no. 5411, pp. 143–147, 1999.

[42] S. Ichinose, K. Yamagata, I. Sekiya, T. Muneta, and M. Tagami, "Detailed examination of cartilage formation and endochondral ossification using human mesenchymal stem cells," *Clinical and Experimental Pharmacology and Physiology*, vol. 32, no. 7, pp. 561–570, 2005.

[43] J. E. Huh, Y. J. Ch, M. C. Yoo et al., "Induction of effective osteogenesis by mesenchymal stem cells from the human subchondral bone," *Journal of Korean Acupuncture and Moixibution Society*, vol. 23, no. 5, pp. 69–77, 2006.

[44] M. Endres, K. Neumann, T. Häupl et al., "Synovial fluid recruits human mesenchymal progenitors from subchondral spongious bone marrow," *Journal of Orthopaedic Research*, vol. 25, no. 10, pp. 1299–1307, 2007.

[45] K. Neumann, T. Dehne, M. Endres et al., "Chondrogenic differentiation capacity of human mesenchymal progenitor cells derived from subchondral cortico-spongious bone," *Journal of Orthopaedic Research*, vol. 26, no. 11, pp. 1449–1456, 2008.

Hindawi Publishing Corporation
Evidence-Based Complementary and Alternative Medicine
Volume 2013, Article ID 586741, 10 pages
http://dx.doi.org/10.1155/2013/586741

Research Article

Aconiti Lateralis Preparata Radix Activates the Proliferation of Mouse Bone Marrow Mesenchymal Stem Cells and Induces Osteogenic Lineage Differentiation through the Bone Morphogenetic Protein-2/Smad-Dependent Runx2 Pathway

Do Rim Kim, Ha Young Kim, Jae Kwang Park, Seong Kyu Park, and Mun Seog Chang

Department of Prescriptionology, College of Korean Medicine, Kyung Hee University, 26 Kyunghee Dae-ro, Dongdaemun-gu, Seoul 130-701, Republic of Korea

Correspondence should be addressed to Mun Seog Chang; mschang@khu.ac.kr

Received 2 April 2013; Accepted 1 July 2013

Academic Editor: Chang Shik Yin

Mesenchymal stem cells have the capacity for self-renewal and under appropriate stimulation give rise to osteogenic, adipogenic, and chondrogenic lineages. To advance the clinical use of stem cell therapy, such as stem cell transplantation, it is important to find substances that promote endogenous stem cell proliferation and differentiation. We investigated whether medicinal herbs have the potential to promote stem cell proliferation and differentiation, using a cell cycle analysis and differentiation assay. We found that Aconiti Lateralis Preparata Radix (ALR) promoted the proliferation rate of mouse bone marrow mesenchymal stem cells (mBMMSCs) up to 122.24% compared to untreated cells. Fluorescence-activated cell sorter analysis showed that the percentage of cells in the G2/M phase increased to 17.33% in ALR-treated cells compared to 5.65% in normal cells. Signaling pathway analysis indicated that this was mediated through the extracellular signal-regulated kinase 1/2 pathway. A differentiation assay showed that ALR induced differentiation of mBMMSCs into an osteogenic lineage 2 weeks after treatment, whereas traditional osteogenic induction medium treatment did not promote differentiation for 3 weeks. This osteogenic differentiation was signaled by the bone morphogenetic protein-2/Smad-dependent Runx2 pathway. We found that ALR could promote mBMMSC proliferation and differentiation into the osteogenic lineage.

1. Introduction

Adult stem cells are involved in the repair of tissue and in maintaining a balance between stem cell and differentiated cell populations by asymmetrical cell division [1]. Although adult stem cell populations are found in most adult tissue, the bone marrow is an ideal source of stem cells because it is easily accessible and can be used for cell and gene therapy [1, 2]. Mesenchymal stem cells (MSCs) are derived from bone marrow and represent a heterogeneous cell population of spindle-shaped cells that are characteristically adherent to plastic in culture [3]. MSCs have been isolated and cultured from many species including mice, rats, cats, dogs, rabbits, pigs, and baboons, albeit with varying success and with the expression of varied surface markers. MSCs have also been found to give rise to differentiated stromal cells belonging to the osteogenic, chondrogenic, adipogenic, myogenic, and fibroblastic lineages [4].

Some cytokine and growth factors involved in mitogen-activated protein kinase (MAPK) signaling are known to enhance MSC proliferation. Platelet-derived growth factor (PDGF) and fibroblast growth factor 2 (FGF2) have been known to enhance proliferation through c-Jun N-terminal kinase (JNK) signaling [5]. In addition, basic fibroblast growth factor (bFGF) is known to stimulate human bone marrow mesenchymal stem cell proliferation via extracellular signal-regulated kinase 1/2 pathway (ERK1/2). However, neither PDGF-BB nor bFGF-induced proliferation affects the osteogenic differentiation potential [6].

Cytokines and growth factors have important roles in stages ranging from self-renewal to differentiation; however, the molecular mechanisms involved in these processes are

still largely unknown and have practical limitations [7]. Furthermore, little is known about the involvement of medicinal herbs in the proliferation and differentiation of bone marrow mesenchymal stem cells. The involvement of a signal pathway that regulates proliferation and differentiation of MSCs by medicinal herbs in bone marrow has not been reported. A recent study has reported that Aconiti Ciliare Tuber extract promotes hair follicle morphogenesis by the activation of Wnt/β-catenin signaling to stimulate bulge stem cells [8].

The aim of the present study was to examine the possibility of ALR inducing proliferation and/or differentiation of mouse bone marrow mesenchymal stem cells (mBMMSCs) to replace the function of growth factors and cytokines and to elucidate the signaling pathways involved in these processes. To identify the effects of ALR on MSCs, we performed cell- and cell cycle-analysis, immunoblotting, immunohistochemistry, and differentiation assays.

2. Materials and Methods

2.1. Preparation of ALR Extract. ALR was purchased from Wonk Wang Herbal Drug Co. Ltd. (Seoul, Korea). We boiled 250 g of dried ALR in 5 L of water for 2 h at 100°C. The suspension was filtered and evaporated under reduced pressure. The yield of extraction was 17.1% (42.8 g). The filtrates were lyophilized and kept at 4°C. Before each experiment, dried extracts were dissolved in distilled deionized water (Millipore, Bedford, MA, USA) and vortexed for 2 min at room temperature.

2.2. Analysis ALR Sample Using Liquid Chromatography-Tandem Mass Spectrometry (LC-MS/MS). Stock solution of reference standards, aconitine, and benzoylaconine were prepared in 100% methanol at a concentration of 1 mg/mL. The working solutions for MS analysis were prepared in 100% methanol at a concentration of 1000 ng/mL. For standard curve, six calibration standards (at 10, 50, 100, 200, 500, and 1000 ng/mL) were analyzed. Lyophilized ALR extract was dissolved as 100 μg/mL in 100% methanol. The solution was separated by centrifugation at 2500 rpm for 15 min. The supernatant clear extract was filtered through 0.45 μm membrane filter prior to LC/MS/MS determination. Chromatography was performed on a liquid chromatography system (Agilent Technologies, CA, USA). A 500 μL aliquot of diluted ALR was injected into a 100 mm × 2.1 mm Atlantis DC18 column (Waters, USA). Mobile phases A and B consisted of 0.1% aqueous formic acid and acetonitrile, respectively. The elution followed a linear gradient of 5–95% for 20 min at a flow rate of 0.3 mL/min. QTRAP 3200 mass spectrometer system (ABSCIEX, MA, USA) operated in positive ionization modes was used in this study and processed multiple reactions monitoring (MRM) scanning. Mass spectrometer tuning parameters were optimized for each analyte by injecting a standard solution (0.001 mg/mL) and validated with several flow rates ranging from 0.1 to 0.5 mL/min. The mobile phase contains acetonitrile in water, adding 0.1% (v/v) formic acid. Under the optimized condition for positive mode, nitrogen was used as drying gas, 10 $Lmin^{-1}$, and nebulizer gas, 50 psi, while the voltage of ion spray in source was set at 5000 V and the gas temperature was 400°C.

2.3. Isolation of BMMSCs. Mouse stromal cells were isolated according to the methods of Nadri et al. [9], with some modification ion. Bone marrow cells were obtained by flushing the femurs and tibias of 8- to 12-week-old male C57BL/6 mice with Dulbecco's modified Eagle's medium (DMEM) (Gibco-BRL, Grand Island, NY, USA) supplemented with 15% fetal bovine serum (FBS, Gibco-BRL, Grand Island, NY, USA), 100 U/mL penicillin, and 100 μg/mL streptomycin. Single-cell suspensions were prepared from clumps of bone marrow by resuspending the cells using a mounted 26-gauge needle syringe and passing them through a 70 μm cell strainer (Falcon, Becton Dickinson and Company, Heidelberg, Germany). The cells were cultured in DMEM with 15% FBS, 100 U/mL penicillin, and 100 μg/mL streptomycin on 0.1% gelatin-coated 10 cm dishes at 37°C in a humidified atmosphere of 5% CO_2. After 3 days, nonadherent cells were removed, and adherent cells were expanded until 90% confluent (6 to 7 days). All animal procedures were performed in accordance with institutional guidelines.

2.4. Sorting of Sca-1-Positive and CD45-Negative BMMSCs Using Magnetic-Activated Cell Sorting (MACS). Enrichment of Sca-1-positive (+) BMMSCs was achieved by an MACS system (Miltenyi Biotec GmbH, Bergisch Gladbach, Germany). Following the third sorting passage, BMMSCs were incubated with phycoerythrin-(PE) conjugated anti-CD45 antibody (Miltenyi Biotec GmbH, Bergisch Gladbach, Germany) for 10 min at 4°C and washed with MACS buffer (phosphate-buffered saline (PBS) supplemented with 0.5% BSA and 2 mM EDTA). Anti-PE microbeads (Miltenyi Biotec GmbH, Bergisch Gladbach, Germany) were then incubated for 10 min at 4°C and washed once again with MACS buffer. The samples were passed through an MACS column in a Miltenyi magnet. The CD45 (−) BMMSCs were incubated with fluorescein isothiocyanate-(FITC) conjugated anti-Sca-1 antibody (Miltenyi Biotec) for 10 min at 4°C and then washed with MACS buffer. Anti-FITC microbeads (Miltenyi Biotec) were then incubated for 10 min at 4°C and again washed with MACS buffer. Samples were passed through an MACS column in a Miltenyi magnet and the Sca-1 (+) BMMSCs were eluted from the column by washing with the MACS buffer. The cells were stained with FITC-conjugated rat anti-mouse Sca-1, CD11b, and PE-conjugated rat anti-mouse CD105 (Miltenyi Biotec) at a concentration of 2 μg/mL at 4°C for 30 min. The cells were pelleted, washed twice with PBS, and fixed with 70% EtOH in PBS. Cells were analyzed with flow cytometry using a fluorescence-activated cell sorter (FACS) caliber flow cytometer (B&D Biosciences, Cell Quest software, San Jose, CA, USA).

2.5. BMMSCs Differentiation Assays. The potential for isolated cells to differentiate into osteogenic and adipogenic lineages was examined. For osteogenesis, the cultured cells were incubated in osteogenic conditioning medium as described previously [10]. Briefly, DMEM was supplemented with

10 mM β-glycerol phosphate (Sigma-Aldrich Co., St. Louis, MO, USA), 50 μg/mL ascorbate-2-phosphate (Sigma-Aldrich Co.), and 10^{-7} M dexamethasone (Sigma-Aldrich Co.). The culture medium was changed twice per week for up to 3 weeks. The cells were fixed with methanol for 10 min at room temperature and stained with Alizarin red (pH 4.0) for 5 min. Von Kossa staining was used for bone nodule formation. For adipogenesis, the cultured cells were incubated in adipogenic medium DMEM supplemented with 50 μg/mL indomethacin (Sigma-Aldrich Co.), 10^{-7} M dexamethasone, and 50 μg/ mL ascorbate-2-phosphate. The culture medium was changed twice per week for up to 3 weeks. The cells were then fixed in methanol for 45 min and stained with Oil Red O (Sigma-Aldrich Co.).

2.6. RNA Isolation and RT-PCR. One milliliter of phenozol was added to 1×10^6 cells, and total RNA was isolated according to the total RNA extraction kit protocol (INTRON Biotechnology, Seoul, Korea). First, strand cDNA synthesis was performed with 5 μg of total RNA using MMLV reverse transcriptase and oligo-dT primer for 1 h at 42°C. Subsequently, PCR amplification was performed using a modified method from that previously described [11]. The sequences of osteocalcin primers were as follows: 5′-GACCATCTTTCTGCTCACTCTG-3′ as forward primer and 5′-GTGATACCATAGATGTTTGTAG-3′ as reverse primer. The sequences of lipoprotein lipase primers were as follows: 5′-GAGGACACTTGTCATCTCATTC-3′ as forward primer and 5′-CCTTCT TATTGGTCAGACTTCC-3′ as reverse primer, whereas for the mouse β-actin, 5′-ACCGTGAAAAGATGACCCAG-3′ and 5′-TACGGATGTCAACGTCACAC-3′ were used. PCR products were separated on a 1.5% agarose gel, visualized using ethidium bromide and the i-MAX gel image analysis system (CoreBioSystem, Seoul, Korea), and then analyzed with Alpha Easy FC software (Alpha Innotech, San Leandro, CA, USA).

2.7. Cell Viability and Proliferation Assays. Cell proliferation was determined using an MTT assay. We starved mBMMSCs for 24 h and then treated them with ALR (1, 10, and 100 μg/mL). After 24 h, the medium was removed and the cells were incubated with the MTT to measure the metabolic activity. Spectrophotometric analysis at 450 nm was performed using a microtiter plate reader (Molecular Devices, Sunnyvale, CA, USA) to measure the metabolic activity.

2.8. Proliferating Cell Nuclear Antigen (PCNA) Detection. For PCNA detection, treated mBMMSCs were fixed and permeabilized in cold methanol, washed three times, and then blocked for 1 h at room temperature in a DMEM-based buffer containing 5% FCS. Samples were washed and incubated overnight with the antibody against PCNA. Following incubation, the cells were washed three more times and incubated for 4 h with goat anti-mouse Alexa 488 antibody (excitation 488 nm, emission 519 nm). For nuclei detection, the cells were incubated for 5 min with propidium iodide (PI) (3.75 μg/mL, excitation 540 nm, emission 630 nm). Imaging was performed using an Olympus BX-61 fluorescent microscope.

2.9. Cell Cycle Analysis. For the cell cycle analysis, mBMMSCs in starvation medium were incubated with ALR and various inhibitors for 24 h. The cells were harvested, washed with cold PBS, resuspended in PBS, and fixed in cold ethanol (70%) overnight at 4°C. The cell pellets were washed with ice cooled PBS, collected by centrifugation, and incubated at 37°C for 30 min in a 0.5 μg/mL RNase and PI solution (10 μg/mL). Fluorescence emitted from the PI-DNA complex was quantified after excitation of the fluorescent dye using a FACS (B&D Biosciences, Cell Quest software).

2.10. Western Blotting. Growth-arrested preconfluent mBMMSCs were incubated with various inhibitors and ALR for the indicated times. Cells were washed with PBS and lysed in a cell lysis buffer (Promega, Madison, WI, USA). The total cell lysates were separated using SDS-PAGE and were transferred to polyvinyl difluoride (PVDF) membranes (Millipore). The membranes were blocked with 5% skim milk and were washed with PBS-T buffer (PBS in 0.1% Tween 20). The membranes were blotted with primary antibodies: antiphosphoERK, antiphospho-p38 (Cell Signaling Technology, Beverly, MA, USA), antiphospho-Smad1/5 (Cell Signaling Technology), anti-ERK, anti-p38, anti-Runx2 (Santa Cruz Biotechnology Inc., Santa Cruz, CA, USA), and anti-β-tubulin (Santa Cruz Biotechnology). The blots were treated with appropriate secondary antibodies conjugated with horseradish peroxidase (Santa Cruz Biotechnology) and were then visualized by an enhanced chemiluminescence system (Amersham Biosciences, London, UK).

2.11. Statistical Analysis. Statistical analysis was performed using GraphPrism 4.0.3 software (GraphPad Software, Inc., San Diego, CA, USA). Data from MTT assay was presented using the mean, standard deviation (SD), and analyzed by the statistical software SPSS, version 12.0 (SPSS, Chicago, IL, USA).

3. Result

3.1. Detection and Quantification of ALR Indicator Compound Using LC-MS/MS. To identify and confirm the indicative compounds of ALR, 100 μg of lyophilized ALR was analyzed using an LC/MS/MS method. The MRM acquisition for benzoylaconine was detected at 105.1 with a retention time at 6.62 min (Figure 1(a)), but aconitine was not detected from 100 μg/mL of ALR extract. The result showed that 100 μg/mL of ALR extract contained 1.43 ng/mL of benzoylaconine (Figure 1(b)).

3.2. mBMMSCs Isolation and Characterization. To isolate and characterize the mBMMSCs, magnetic bead separation was carried out as described above. After negative and positive selections of bone marrow-derived cells with CD45 and Sca-1, collected cells were immunophenotyped for the detection of different mBMMSC surface antigens.

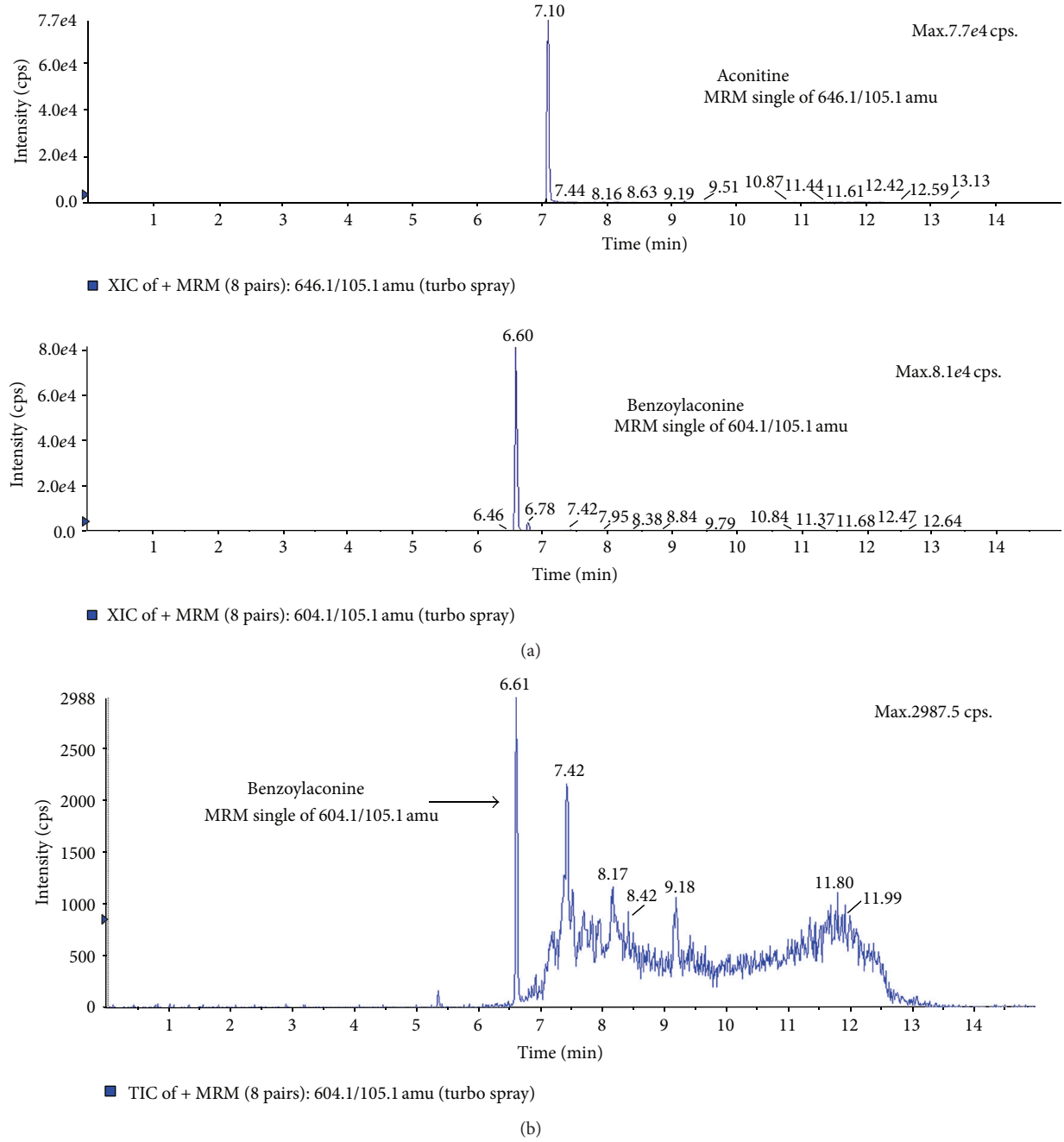

Figure 1: LC-MS/MS chromatograms of analytes in ALR extract. (a) Reference standards, aconitine, and benzoylaconine of ALR were detected at corresponding retention times. (b) Detection of indicative compound from 100 μg/mL of ALR extract. LC/MS/MS analysis showed that ALR extract contained benzoylaconine.

Cells were positively stained with FITC-conjugated rat anti-mouse Sca-1 and PE-conjugated rat anti-mouse CD105. Cells were also negatively stained with FITC-conjugated rat anti-mouse CD11b. The expressions of CD105, CD11b, and Sca-1 were characterized using FACS analysis. FACS analysis revealed that 97.06 and 90.10% of the selected cells expressed CD105 and Sca-1, respectively, (Figure 2(a)). Analysis of CD11b expression in cultured cells indicated that the level of its expression was 0.22%, which means that there was no contamination of hematopoietic cell lineage (Figure 2(a)).

To confirm the isolation of mBMMSCs, we examined the differentiation potential of mBMMSCs into multiple cell lineages. The BMMSCs were readily differentiated into osteocytes and adipocytes by culturing in appropriate induction media. In osteogenic cultures, nodule-like structures, which were stained with Alizarin red, were observed after 3 weeks

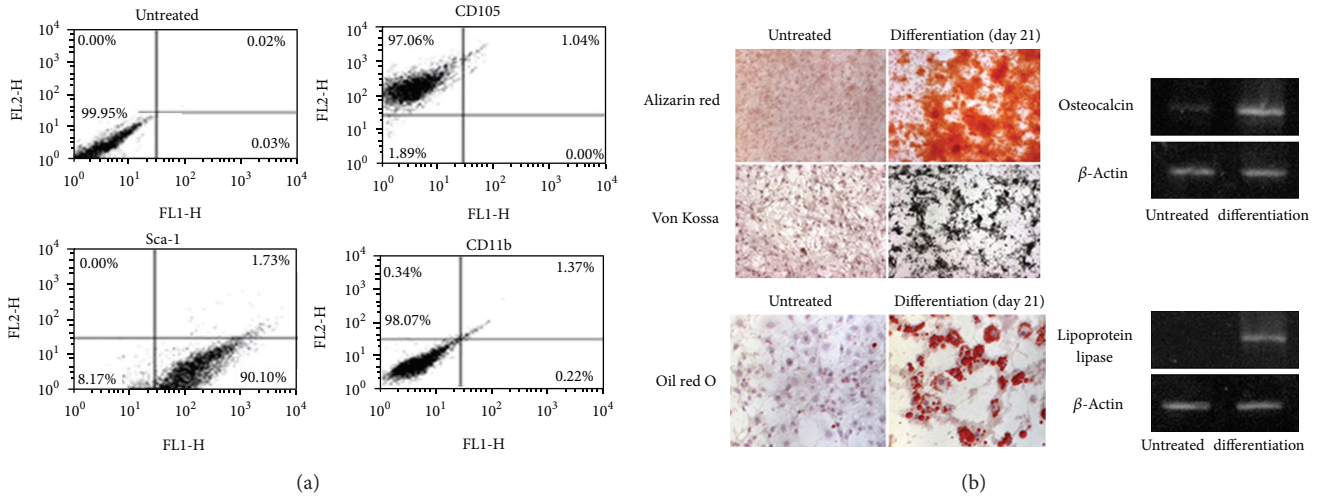

Figure 2: mBMMSC isolation and characterization using FACS analysis of surface markers and multilineage mesenchymal stem cell differentiation. (a) FACS analysis using positive (CD105, Sca-1) and negative (CD11b) selections. (b) The differentiation of mBMMSCs cells examined at 21 days following treatment shows the stimulation of osteogenesis and adipogenesis. Left panel: cells were stained with Alizarin red and von Kossa to identify osteogenic differentiation. To recognize adipogenic differentiation, lipid vesicles were stained with Oil Red: magnification, 40x. Right panel: mRNA levels of osteoblast- and adipocyte-specific markers such as osteocalcin and lipoprotein lipase were analyzed using RT-PCR.

of induction (Figure 2(b)). For the detection of calcium-phosphate deposits, a typical phenomenon for bone cells, osteogenic cultures were stained by the von Kossa method. As a result, cells showed calcium phosphate deposits equivalent to those observed in osteoblast cells. Likewise, after 2 to 3 weeks of mBMMSCs culture, the adipocytes were stained with Oil Red O. Adipose droplets were visible in adipogenic inductive medium (Figure 2(b)).

To further demonstrate the differentiation potential of mBMMSCs into multiple cell lineages, we analyzed the expression of osteoblast- and adipocyte-specific markers using RT-PCR. Expression levels of osteocalcin, an osteoblast specific marker, were elevated, and the lipoprotein lipase gene, an adipocyte-specific marker, was expressed in differentiation cells following 21 days of induction.

3.3. ALR Enhances mBMMSCs Proliferation through Progression of the Cell Cycle. The effects of ALR on the proliferation of mBMMSCs were determined from cell growth kinetics with an MTT assay measuring the metabolic activity of viable cells. Growth-arrested mBMMSCs cultured in a starvation medium for 24 h prior to the experiment were incubated for 24 h with ALR. ALR activated cell proliferation; specifically, 10 μg/mL ALR-treated cells increased by 122.24 $\pm$ 8.78% when compared with untreated cells ($P < 0.01$, Figure 3(a)). This suggests that ALR enhances the proliferation rate of mBMMSCs.

To further confirm the proliferating effects of ALR using cell cycle analysis, we examined the activity of PCNA, a protein that participates in DNA replication. Cells were grown in a medium treated with ALR (100 μg/mL, 24 h) in the presence or absence of SB202190 and PD98059, inhibitors of p38, and ERK1/2, respectively. Cells were then incubated with the fluorescent DNA binding dye, PI, for nuclear staining (red) and with an antibody directed against PCNA (green). ALR increased the level of PCNA staining compared to untreated cells, indicating that ALR activates BMMSC proliferation as observed in bFGF-treated cells (Figure 3(b)). Treatment with bFGF as a positive control is known to induce cell proliferation by activating the ERK1/2 pathway in many cell types. Pretreatment with SB202190 and PD98059 decreased the expression level of PCNA compared to cells treated with ALR alone. Taken together, from the FACS analysis, ALR promoted proliferation (G2/M) in mBMMSCs, whereas untreated cells remained in the G1 phase of the cell cycle (Figure 3(c)). Pre-treatment of mBMMSCs with PD98059 impaired this proliferation, inducing a G1 arrest as was also seen in treatment with SB202190. These results suggest that ALR enhances mBMMSC proliferation throughout the cell cycle by promoting pathways such as ERK1/2 and p38 cascades, which appear to be implicated in the G1 to S and S to G2/M switches.

3.4. ALR Activated mBMMSC Proliferation through the ERK1/2 Pathway. To elucidate the signaling events triggered by ALR treatment in mBMMSCs, western blot analyses were carried out. Growth-arrested mBMMSCs were incubated with ALR for 5, 10, and 30 min in the presence of PD98059 (30 μM, 2 h) prior to their incubation. Whole cell lysates were then immunoblotted using phospho-ERK1/2 antibodies. As shown in Figure 4, ALR treatment increased phosphorylation of ERK1/2, while ALR treatment in the presence of inhibitors led to decreased phosphorylation of ERK1/2. At the same time, growth-arrested mBMMSCs were incubated with ALR for 5, 10, and 30 min in the presence of SB202190 (30 μM, 2 h) prior to their incubation. Whole cell lysates were

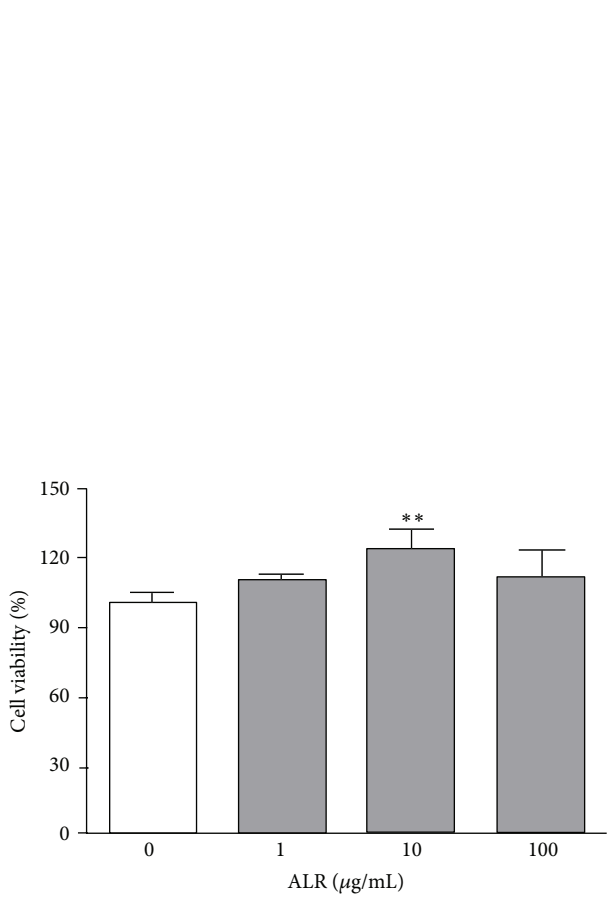

(a)

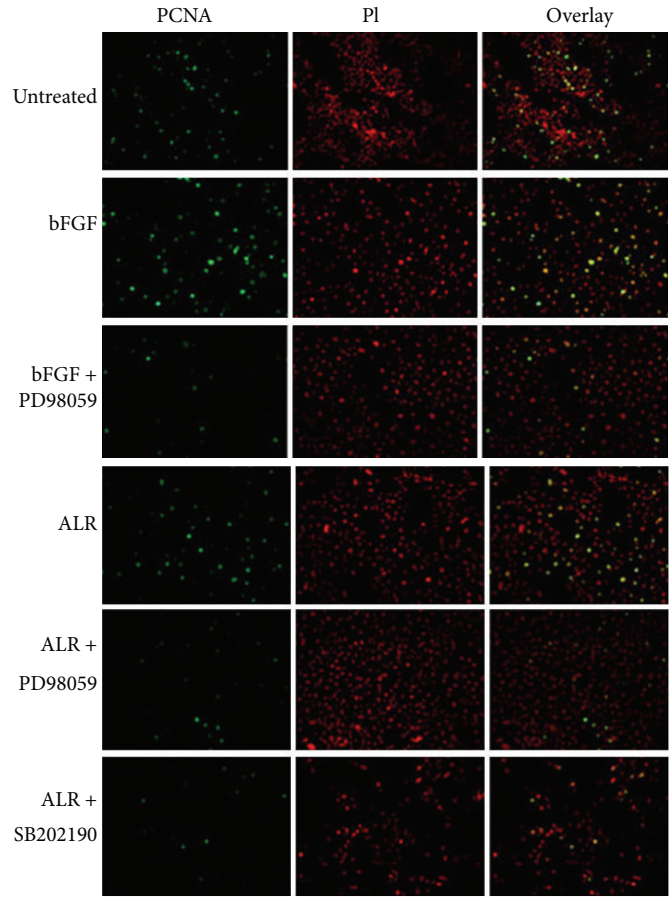

(b)

	Population (%)		
	G0/G1	S	G2/M
Untreated	84.80	9.55	5.65
ALR	76.06	6.61	17.33
ALR + PD98059	82.94	12.32	4.74
ALR + SB202190	86.77	8.99	4.24

(c)

Figure 3: (a) The effect of ALR on the growth of mBMMSCs. "Normal" represents PBS-treated cells, columns represent the mean ± SD ($n = 3$), and * indicates that the mean is significantly different from the control value ($^{**}P < 0.01$). (b) Proliferating cell nuclear antigen (PCNA) immunoreactivity measurements. Cells are stained with either anti-PCNA antibodies (green) or propidium iodide (red) for nuclear detection. Overlay images of both stains are also presented. bFGF was used as a positive control. All images were obtained using 20x magnification in an Olympus BX-61 fluorescent microscope. (c) The effect of ALR on the progression of mBMMSCs cell cycle. Results are the mean of three independent experiments.

immunoblotted using total p38 and phospho-p38 antibodies, but there was no change in the expression level of either protein (Figure 4). These results suggest that ALR activates the proliferation of mBMMSCs through the ERK1/2 pathway.

3.5. ALR Promoted Differentiation of mBMMSCs into the Osteogenic Lineage. An important feature of mBMMSCs is their ability to differentiate into osteoblasts, chondroblasts, and adipocytes. To examine whether ALR affected the osteogenic and adipogenic differentiation capacities of the cells, mBMMSCs were treated with ALR (100 μg/mL) for 3 weeks and were examined once per week. Both the Alizarin red and von Kossa assays showed a strong induction of mBMMSCs into the osteogenic lineage by ALR treatment. As shown in Figures 5(a) and 5(b), ALR induced osteogenic differentiation after 2 weeks of treatment, whereas induction by osteogenic medium did not begin for 3 weeks. In the adipogenic differentiation assay, lipid vacuoles were stained with

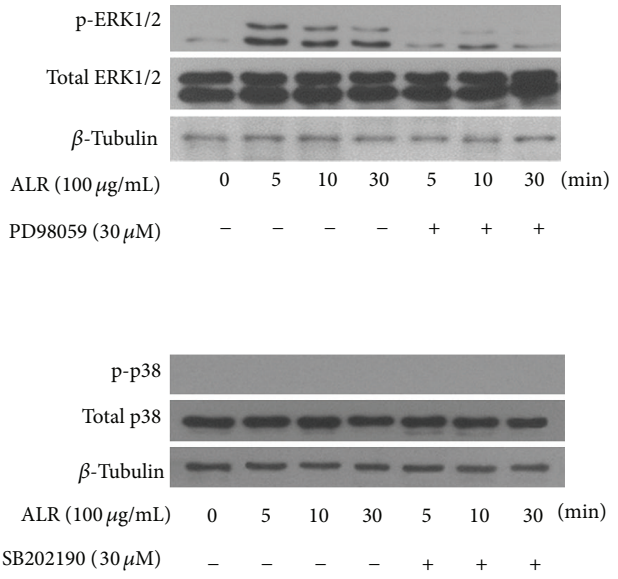

Figure 4: Immunoblots of ERKs and p38 detected with specific antibodies p-ERK1/2, p-p38, total ERK, and total p38 after ALR treatment with β-tubulin used as an internal control. mBMMSCs were incubated with ALR (100 μg/mL) over time in the presence or absence of inhibitors, SB202190 (30 μM, 2 h), and PD98059 (30 μM, 2 h).

Oil Red. Induction showed adipogenic differentiation at the end of 3 weeks; however, ALR treatment did not induce adipogenic lineage differentiation even after 3 weeks.

3.6. Signaling Pathway for ALR Stimulated Osteogenic Differentiation. To identify the signaling pathway that triggers the osteogenic differentiation of mBMMSCs by ALR, BMP-2/Smad and Wnt pathways were examined. For this, mBMMSCs were treated with either ALR (100 μg/mL) or osteogenic induction medium for 21 days. The BMP-2/Smad signal pathway was activated and Runx2 protein expression was increased by ALR treatment in osteogenic differentiation. Whole cell lysates were immunoblotted using phospho-Smad1/5, phospho-β-catenin, and Runx2 antibodies. As a result (Figure 6(a)), ALR treatment led to the increased phosphorylation of Smad1/5, while treatment with both ALR and osteogenic induction medium had no effect on the phosphorylation of Smad1/5. Phosphorylation of β-catenin was also increased by osteogenic induction medium treatment. However, ALR treatment decreased the phosphorylation of β-catenin. Subsequently, Runx2 protein levels were increased by ALR treatment and were decreased when treated with both ALR and osteogenic induction medium, when compared with untreated mBMMSCs (Figure 6(b)). These results suggest that ALR activates osteogenic differentiation through BMP-2/Smad-dependent Runx2 signaling pathway.

4. Discussion

The aim of this study was to investigate the effect of ALR on mBMMSC proliferation and differentiation and to elucidate the signaling pathways involved in these processes. ALR has been widely used for the improvement of symptoms such as, heart failure, inflammation, pain and diarrhea for thousands of years in Korea, China and Japan, but the toxicity of the ALR has been the subject of controversy in safety as medicinal herb. Major toxic ingredients were identified as some kinds of diester diterpenoid-type Aconitum alkaloids such as aconitine and mesaconitine [12]. Some processing techniques such as pressure-steaming were known to reduce the toxicity of Aconitum alkaloids, because alkaloids can hydrolyze the highly toxic diester-diterpene aconitum alkaloids to compounds of much lower toxicity such as benzoylaconine, benzoylmesaconine, benzoylhypaconine, and aconine [13]. LC/MS/MS results in this study showed that 100 μg/mL of ALR extract contained about 1.43 ng/mL of benzoylaconine, one of an indicative compound of ALR. However, aconitine was not detected from ALR extract. This could be interpreted in part by the hydrolysis of aconitine into other compounds during ALR extract preparation which includes the boiling step to extract active compounds. At least in cellular level, this was further confirmed through cell viability and cell cycle progression analysis. As shown in Figure 3, ALR did not show any cytotoxicity on mBMMSC growth and proliferation.

Bone marrow-derived adherent cell layers are composed of heterogeneous cells, including fibroblasts, hematopoietic progenitor cells, macrophages, endothelial cells, and adipocytes [9]. The purification of mBMMSCs has been more difficult than that of other species due to lack of specific surface markers for MSCs and the unwanted growth of non-MSCs in cell cultures [7, 9]. A more homogenous population of MSCs can be acquired after the third passage with frequent medium changes, in the absence of molecular markers [14, 15]. For successful MSC transplantation, it is important to obtain an established homogeneous MSC purification tool using surface markers [16].

Bone marrow was harvested from C57BL/c and maintained as described in the Materials and Methods section. During the *in vitro* expansion of mBMMSCs, cell morphology changed gradually from a fibroblast-like spindle shape to more flattened- and enlarged-shaped cells that were more homogeneous. The mouse mesenchymal stem cells expressed CD34, CD44, Sca-1, and Vcam-1 antigens (markers) but not CD11b and CD45. Therefore, the magnetic-activated cell sorting (MACS) method was used for the selection of mBMMSCs using positive (Sca1) and negative surface (CD11b) markers at passage 3, followed by confirmation with Sca-1-positive and CD11b-negative cells (Figure 2(a)) [9, 17]. The differentiation of mBMMSCs was confirmed by staining methods for both osteogenic and adipogenic lineage differentiations (Figure 2(b)).

MSCs can be applied in regenerative therapies such as the treatment of graft-versus-host disease and in cell therapies for their lack of strong immunogenicity [18]. Although MSCs are an appropriate tool in cell-based therapies, clinical application of MSCs is currently limited by the low number MSCs available for transplantation [19]. Thus, many researchers have been searching for a way to improve cell proliferation and/or differentiation by experimenting with various types of growth factors, despite the obscure molecular mechanisms of

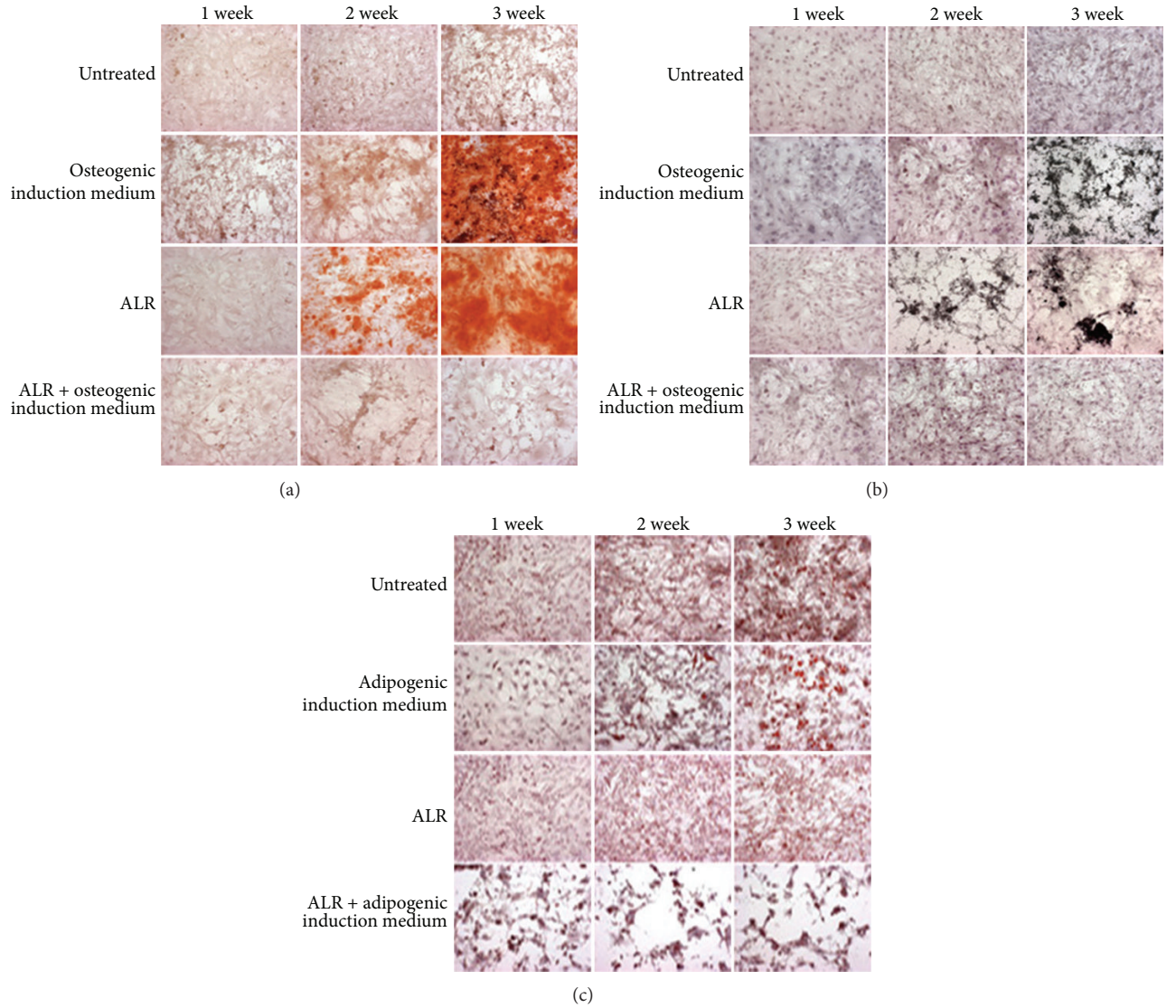

Figure 5: *In vitro* osteogenic and adipogenic differentiations of mBMMSCs by ALR. (a) Osteogenic cultures with Alizarin red staining for the detection of nodule-like structures; (b) osteogenic cultures stained with von Kossa for the detection of calcium-phosphate deposits; (c) adipogenic cultures stained with Oil Red for the detection of adipose droplets. Original magnification is 20x.

cell expansion. In this study, ALR promoted the proliferation of mBMMSCs. To detect mBMMSC proliferation by ALR treatment, we examined PCNA, a protein that participates in DNA replication. Results showed that ALR increased the level of positively stained PCNA when compared to that of untreated cells. In addition, the G1-to-S phase progression mechanism was found to be essential for cell cycle regulation. We performed a cell cycle analysis to examine the cell cycle transition in the ALR-treated proliferating cells. Results showed that ALR-treated cells expressed elevated G2/M progression compared to untreated cells.

To further understand ALR's effect on the cell cycle progression of mBMMSCs, the signaling pathways responsible for cell cycle progression were investigated. MAPK pathways are a continuative protein kinase cascade that regulates cell proliferation, differentiation, inflammatory response, and apoptotic cell death [20]. The ERK pathway (A-Raf, B-Raf, Raf-1 MEK1, and 2 ERK1/2) is activated by mitogens and growth factors, and activated ERK is translocated to the nucleus. Translocated ERK regulates transcription factors, changing gene expression to promote growth, differentiation, or mitosis. The p38 pathway is stimulated predominately by UV irradiation, heat shock, high osmotic stress, lipopolysaccharide, protein synthesis inhibitors, proinflammatory cytokines environmental stress, and inflammatory cytokines [21, 22]. In our results, ALR activated ERK1/2 phosphorylation in mBMMSCs but did not activate p38. These results strongly suggest that ALR enhances the proliferation of mBMMSCs though activating ERK1/2 pathway.

In terms of differentiation, ALR induced mBMMSCs differentiation into the osteogenic lineage, but not into the adipogenic lineage. Glucocorticoids, such as dexamethasone, are known to promote osteoblastic differentiation *in vitro* and to regulate the expression of osteoblast typifying genes such as

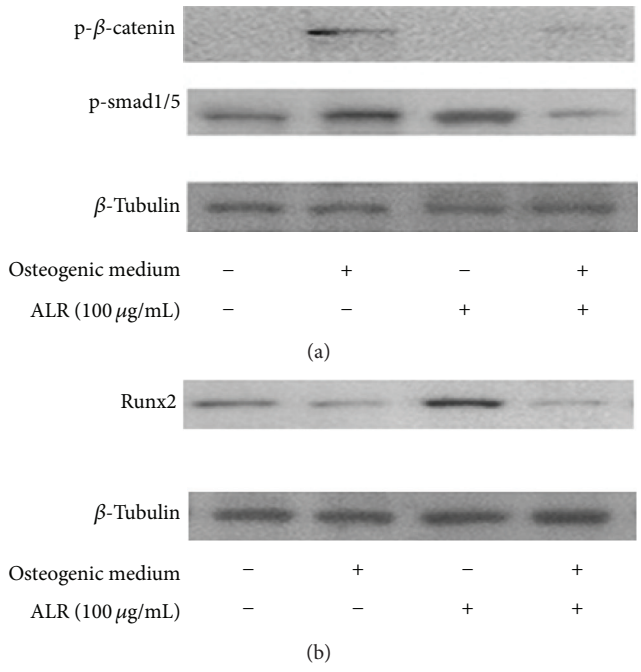

Figure 6: Immunoblots of p-Smad1/5, p-β-catenin, and total Runx2 after ALR treatment on mBMMSCs. β-tubulin was used as internal control. (a) Immunoblots conducted for the detection of Smad1/5 and p-β-catenin phosphorylation of using extract of mBMMSCs; (b) immunoblots carried out for the detection of Runx2on expression in mBMMSCs extract treated with ALR (100 μg/mL) or osteogenic induction medium.

Runx2, ALP, and osteocalcin in MSCs. Also, endogenous glucocorticoids have been found to differentiate MSCs through osteogenesis in mouse bone marrow [23]. Our results demonstrate that ALR promoted the differentiation of mBMMSCs into osteogenic lineage 2 weeks following treatment, as opposed to the osteogenic induction medium (including dexamethasone), which did not lead to differentiation for 3 weeks.

The regulation of osteoblast differentiation plays an important role in BMP-2 signaling and Wnt signaling pathways. In BMP-2 signaling, BMP-2 activates Smad1/5 and Smad4 and induces Runx2 expression. Subsequently, gene expression related to osteogenesis differentiation is promoted, as observed in the homeobox gene, msh homeobox homologue 2, or Osterix [24]. Wnt signaling has two different pathways, canonical and noncanonical pathway. The Wnt signal is transduced through Frizzled and Lrp5/6 and stabilizes β-catenin for translocation into the nucleus and for regulation of the expression of target genes. Wnt1, Wnt2, and Wnt3 induce alkaline phosphatase activity in mesenchymal cell lines. It has been reported that canonical Wnt β-catenin and BMP signaling induce osteogenic differentiation [24]. According to our results related with signaling pathways involved in osteogenic differentiation, ALR treatment for 3 weeks enhanced the phosphorylation of Smad1/5 without any effects on the Wnt/β-catenin pathway. Overall, Runx2 expression in ALR-treated cells increased in undifferentiated cells. However, the expression level of Runx2 was reduced in dexamethasone-induced osteogenic differentiation, and β-catenin expression was activated by dexamethasone. Similarly, the cotreatment of mBMMSCs with ALR and osteogenic induction medium showed decreased expression of Runx2.

Runx2, also known as Cbfa1, Osf2, AML3, and PEBP2γA, is a critical transcriptional factor in osteoblast differentiation and bone formation [25]. However, in terms of the signaling pathways involved in Runx2-mediated osteogenic differentiation, it has been suggested that FHL2, an LIM-domain protein with 4.5 LIM domains, interacts with β-catenin to increase Runx2 expression and to induce the osteogenic differentiation of mesenchymal stem cell [26]. However, Phillips et al. demonstrated that glucocorticoid-induced osteogenic differentiation decreased the phosphoserine levels associated with Runx2 and that exogenous Runx2 can antagonize the effect of dexamethasone [23, 25]. Thus, one explanation for our results is an antagonistic effect of dexamethasone and ALR-cotreated cells in regard to Runx2 expression.

In conclusion, this study demonstrated that after 2 weeks of treatment, ALR induced osteogenic differentiation and increased both cell proliferation and osteogenic differentiation in mBMMSCs, processes mediated by the BMP-2/Smad-dependent Runx2 signal pathway. Although the molecular mechanism of ALR action in stem cell regulation, growth, and differentiation requires further study, this study is an important step in overcoming the limitations to stem cell therapy in clinical uses such as transplantation, *in vitro* expansion, and endogenous induction of MSC proliferation and differentiation. Moreover, ALR may be considered as a medicinal herb for the treatment of bone-related diseases such as osteoporosis and osteopenia.

References

[1] A. van Damme, T. Vanden Driessche, D. Collen, and M. K. L. Chuah, "Bone marrow stromal cells as targets for gene therapy," *Current Gene Therapy*, vol. 2, no. 2, pp. 195–209, 2002.

[2] C. M. Kolf, E. Cho, and R. S. Tuan, "Mesenchymal stromal cells. Biology of adult mesenchymal stem cells: regulation of niche, self-renewal and differentiation," *Arthritis Research and Therapy*, vol. 9, no. 1, article 204, 2007.

[3] C. Tschöpe, K. Miteva, H.-P. Schultheiss, and S. van Linthout, "Mesenchymal stromal cells: a promising cell source for the treatment of inflammatory cardiomyopathy," *Current Pharmaceutical Design*, vol. 17, no. 30, pp. 3295–3307, 2011.

[4] G. Chamberlain, J. Fox, B. Ashton, and J. Middleton, "Concise review: mesenchymal stem cells: their phenotype, differentiation capacity, immunological features, and potential for homing," *Stem Cells*, vol. 25, no. 11, pp. 2739–2749, 2007.

[5] H.-J. Ahn, W.-J. Lee, K. Kwack, and Y. D. Kwon, "FGF2 stimulates the proliferation of human mesenchymal stem cells through the transient activation of JNK signaling," *FEBS Letters*, vol. 583, no. 17, pp. 2922–2926, 2009.

[6] O. Levy, T. Dvir, O. Tsur-Gang, Y. Granot, and S. Cohen, "Signal transducer and activator of transcription 3-A key molecular switch for human mesenchymal stem cell proliferation," *International Journal of Biochemistry and Cell Biology*, vol. 40, no. 11, pp. 2606–2618, 2008.

[7] R. Summer and A. Fine, "Mesenchymal progenitor cell research limitations and recommendations," *Proceedings of the American Thoracic Society*, vol. 5, no. 6, pp. 707–710, 2008.

[8] P. J. Park, B. S. Moon, S. H. Lee et al., "Hair growth-promoting effect of Aconiti Ciliare Tuber extract mediated by the activation of Wnt/β-catenin signaling," *Life Sciences*, vol. 91, pp. 935–943, 2012.

[9] S. Nadri, M. Soleimani, R. H. Hosseni, M. Massumi, A. Atashi, and R. Izadpanah, "An efficient method for isolation of murine bone marrow mesenchymal stem cells," *International Journal of Developmental Biology*, vol. 51, no. 8, pp. 723–729, 2007.

[10] M. B. Eslaminejad and S. Nadri, "Murine mesenchymal stem cell isolated and expanded in low and high density culture system: surface antigen expression and osteogenic culture mineralization," *In Vitro Cellular and Developmental Biology—Animal*, vol. 45, no. 8, pp. 451–459, 2009.

[11] R. K. Saiki, T. L. Bugawan, G. T. Horn, K. B. Mullis, and H. A. Erlich, "Analysis of enzymatically amplified β-globin and HLA-DQα DNA with allele-specific oligonucleotide probes," *Nature*, vol. 324, no. 6093, pp. 163–166, 1986.

[12] P. Tong, C. Wu, X. Wang et al., "Development and assessment of a complete-detoxi arthritis cation strategy for Fuzi (lateral root of Aconitum carmichaeli) and its application in rheumatoid therapy," *Journal of Ethnopharmacology*, vol. 146, no. 2, pp. 562–571, 2013.

[13] J. Singhuber, M. Zhu, S. Prinz, and B. Kopp, "Aconitum in traditional Chinese medicine: a valuable drug or an unpredictable risk?" *Journal of Ethnopharmacology*, vol. 126, no. 1, pp. 18–30, 2009.

[14] S. Nadri and M. Soleimani, "Isolation murine mesenchymal stem cells by positive selection," *In Vitro Cellular and Developmental Biology—Animal*, vol. 43, no. 8-9, pp. 276–282, 2007.

[15] M. Ohishi and E. Schipani, "Bone marrow mesenchymal stem cells," *Journal of Cellular Biochemistry*, vol. 109, no. 2, pp. 277–282, 2010.

[16] F. Tögel and C. Westenfelder, "Adult bone marrow-derived stem cells for organ regeneration and repair," *Developmental Dynamics*, vol. 236, no. 12, pp. 3321–3331, 2007.

[17] M. Baddoo, K. Hill, R. Wilkinson et al., "Characterization of mesenchymal stem cells isolated from murine bone marrow by negative selection," *Journal of Cellular Biochemistry*, vol. 89, no. 6, pp. 1235–1249, 2003.

[18] K. Ozawa, K. Sato, I. Oh et al., "Cell and gene therapy using mesenchymal stem cells (MSCs)," *Journal of Autoimmunity*, vol. 30, no. 3, pp. 121–127, 2008.

[19] R. S. Tuan, G. Boland, and R. Tuli, "Adult mesenchymal stem cells and cell-based tissue engineering," *Arthritis Research and Therapy*, vol. 5, no. 1, pp. 32–45, 2003.

[20] J.-F. Zhang, G. Li, C.-Y. Chan et al., "Flavonoids of Herba Epimedii regulate osteogenesis of human mesenchymal stem cells through BMP and Wnt/β-catenin signaling pathway," *Molecular and Cellular Endocrinology*, vol. 314, no. 1, pp. 70–74, 2010.

[21] M. R. Junttila, S.-P. Li, and J. Westermarck, "Phosphatase-mediated crosstalk between MAPK signaling pathways in the regulation of cell survival," *FASEB Journal*, vol. 22, no. 4, pp. 954–965, 2008.

[22] J. A. McCubrey, L. S. Steelman, S. L. Abrams et al., "Roles of the RAF/MEK/ERK and PI3K/PTEN/AKT pathways in malignant transformation and drug resistance," *Advances in Enzyme Regulation*, vol. 46, no. 1, pp. 249–279, 2006.

[23] L. Lin, S.-D. Dai, and G.-Y. Fan, "Glucocorticoid-induced differentiation of primary cultured bone marrow mesenchymal cells into adipocytes is antagonized by exogenous Runx2," *APMIS*, vol. 118, no. 8, pp. 595–605, 2010.

[24] R. Nishimura, K. Hata, F. Ikeda et al., "Signal transduction and transcriptional regulation during mesenchymal cell differentiation," *Journal of Bone and Mineral Metabolism*, vol. 26, no. 3, pp. 203–212, 2008.

[25] J. E. Phillips, C. A. Gersbach, A. M. Wojtowicz, and A. J. García, "Glucocorticoid-induced osteogenesis is negatively regulated by Runx2/Cbfa1 serine phosphorylation," *Journal of Cell Science*, vol. 119, no. 3, pp. 581–591, 2006.

[26] Z. Hamidouche, E. Haÿ, P. Vaudin et al., "FHL2 mediates dexamethasone-induced mesenchymal cell differentiation into osteoblasts by activating Wnt/β-catenin signaling-dependent Runx2 expression," *FASEB Journal*, vol. 22, no. 11, pp. 3813–3822, 2008.

Hindawi Publishing Corporation
Evidence-Based Complementary and Alternative Medicine
Volume 2013, Article ID 424313, 5 pages
http://dx.doi.org/10.1155/2013/424313

Research Article

Effect of Facial Cosmetic Acupuncture on Facial Elasticity: An Open-Label, Single-Arm Pilot Study

Younghee Yun,[1] Sehyun Kim,[2] Minhee Kim,[1] KyuSeok Kim,[1] Jeong-Su Park,[3,4] and Inhwa Choi[1]

[1] *Department of Dermatology of Korean Medicine, College of Korean Medicine, Kyung Hee University, No. 149 Sangil-dong, Gangdong-gu, Seoul 134-727, Republic of Korea*
[2] *Graduate School of East-West Medical Science, Kyung Hee University, Yongin, Gyeonggi-Do 446-701, Republic of Korea*
[3] *Kyung Hee Center for Clinical Research and Drug Development, Kyung Hee University, 1 Hoegidong, Dongdaemungu, Seoul 130-701, Republic of Korea*
[4] *Department of Preventive Medicine, Graduate School of Korean Medicine, Kyung Hee University, Seoul 130-701, Republic of Korea*

Correspondence should be addressed to Inhwa Choi; inhwajun@khnmc.or.kr

Received 5 April 2013; Accepted 4 July 2013

Academic Editor: Bo-Hyoung Jang

Background. The use of acupuncture for cosmetic purposes has gained popularity worldwide. Facial cosmetic acupuncture (FCA) is applied to the head, face, and neck. However, little evidence supports the efficacy and safety of FCA. We hypothesized that FCA affects facial elasticity by restoring resting mimetic muscle tone through the insertion of needles into the muscles of the head, face, and neck. *Methods*. This open-label, single-arm pilot study was implemented at Kyung Hee University Hospital at Gangdong from August through September 2011. Participants were women aged 40 to 59 years with a Glogau photoaging scale III. Participants received five treatment sessions over three weeks. Participants were measured before and after FCA. The primary outcome was the Moire topography criteria. The secondary outcome was a patient-oriented self-assessment scale of facial elasticity. *Results*. Among 50 women screened, 28 were eligible and 27 completed the five FCA treatment sessions. A significant improvement after FCA treatment was evident according to mean change in Moire topography criteria (from 1.70 ± 0.724 to 2.26 ± 1.059, $P < 0.0001$). The most common adverse event was mild bruising at the needle site. *Conclusions*. In this pilot study, FCA showed promising results as a therapy for facial elasticity. However, further large-scale trials with a controlled design and objective measurements are needed.

1. Introduction

With extended life expectancy, beauty and skin health are important factors in perceived quality of life. Currently, numerous interventions are offered for skin rejuvenation and anti-skin aging including treatments for facial wrinkles, facial muscle tone, and elasticity. Recently, cosmetic acupuncture has been introduced as an intervention for skin rejuvenation [1].

Facial cosmetic acupuncture (FCA) is the use of acupuncture on the head, face, and neck for cosmetic purposes. Several different types of FCA are currently practiced, and many possible mechanisms underlying these techniques have been proposed, including increasing or balancing qi, balancing internal Zang Fu organs, increasing blood flow by inserting needles at certain acupoints [2], and increasing muscle tone [3].

However, little evidence addresses the efficacy and safety of FCA. A recent case report describes the increased water and oil content of facial skin after FCA [4]; otherwise, there is only an introductory [1, 2] or non-English article [3]. To explore whether FCA has effects on facial elasticity, we designed an open-label, single-arm pilot study using the most frequently practiced FCA technique in Korea.

2. Participants and Methods

2.1. Ethics Approval. This study was performed in accordance with the International Committee on Harmonization Good

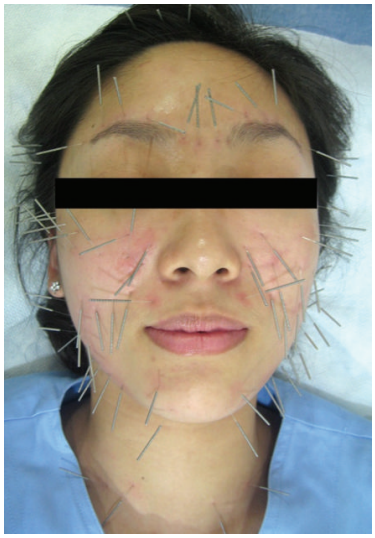

Figure 1: Facial cosmetic acupuncture applied in this study.

Clinical Practice guidelines and the revised version of the Declaration of Helsinki. The trial protocol was approved by the Institutional Review Board of Kyung Hee University Hospital at Gangdong (KHNMC-OH-IRB 2011-007). Written informed consent was obtained from all participants prior to enrollment, and participants were given ample time to decide about participating before signing the consent form.

2.2. Participant Recruitment and Inclusion/Exclusion Criteria. Participants were recruited by advertisements on bulletin boards at Kyung Hee University Hospital at Gangdong. Included were (a) women; (b) aged 40 to 59 years; (c) with a Glogau photoaging scale III [5]. We excluded individuals who (a) had dermabrasion, deep skin peels, laser resurfacing (ablative or nonablative), botulinum toxin, filler injection, or topical steroid treatment within the 6 months immediately prior to study entry; (b) had obvious skin disease or a history of chronic skin disease; (c) had a keloidal or hypertrophic scar tendency; or (d) were pregnant or breastfeeding. No other treatment for facial elasticity was permitted during the study period.

2.3. Study Protocol. This study was an open-label, single-arm pilot study at Kyung Hee University Hospital at Gangdong from August through September 2011. Five sessions of FCA treatment were given over three weeks. All participants received FCA twice a week for the first two weeks, then once a week for the last week, with three to four days between sessions. Participants were assessed based on changes in the Moire topography criteria [6].

2.4. Acupuncture Procedure. Acupuncture was applied (Figure 1) according to the Standards for Reporting Interventions in Clinical Trials of Acupuncture (STRICTA) [7].

(1) Acupuncture rationale

(a) A single practitioner inserted acupuncture needles into muscles of the face, head, and neck.

(b) All participants received the same FCA treatment at every treatment session.

(2) Needling details

(a) The total number of insertions per treatment ranged from approximately 100 to 110.

(b) The practitioner inserted acupuncture needles at the insertion, origin, belly and/or margin of

(i) head muscles including the temporalis and epicranial aponeurosis;

(ii) neck muscles including the sternocleidomastoid;

(iii) upper facial muscles including the frontalis, procerus, corrugator supercilii, and orbicularis oculi;

(iv) midfacial muscles including the auricularis, nasalis, levator labii superioris alaeque nasi, levator labii superioris, zygomaticus minor, and zygomaticus major;

(v) lower facial muscles including the orbicularis oris, risorius, depressor labii inferioris, depressor anguli oris, mentalis, and platysma.

(c) The depth of needle insertion varied with skin thickness and subcutaneous fatty tissue at the insertion site.

(d) The practitioner did not use any specific needling technique. However, the practitioner tried to insert needles into the contraction of muscles fibers over the muscle insertions, origins, bellies, and/or margins of muscles.

(e) Needles were retained for ten minutes.

(f) The practitioner used an acupuncture treatment aid, AcuPro (NEO Dr.), and stainless steel fine needles (0.2×15 mm, 0.25×30 mm) to reduce pain and to shorten treatment time (Figure 2).

(3) Treatment regimen

(a) All participants received five sessions FCA over the 3-week treatment period.

(b) All participants received FCA twice a week for the first two weeks, and then once a week for the last week.

(4) Other components of treatment

(a) No other treatments were given and participants were asked not to receive any other treatment for facial elasticity during the study period.

(b) All participants received FCA with an interval of three to four days between sessions.

(a) (b)

Figure 2: AcuPro and stainless steel fine needles used in this study.

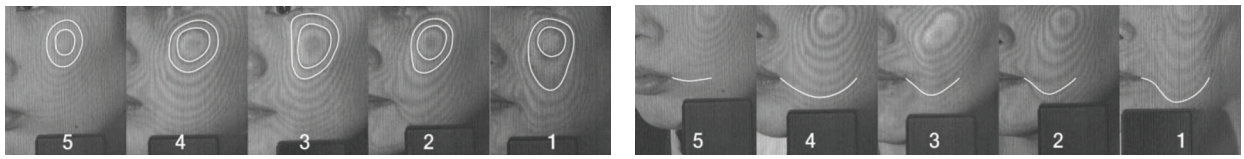

(a) (b)

Figure 3: Criteria for evaluating Moire topography.

2.5. Outcome Measurements. Outcomes were measured before and after the five sessions of FCA.

2.6. Primary Outcome. The primary outcome was a change in the Moire topography criteria after treatment compared with baseline. We generated contour lines on the face using a Moire topography system and took pictures with a digital camera Ixus750 (Canon, Tokyo, Japan). A single independent evaluator read the contour lines near the cheek and the perioral region in the printed digital image and graded the images based on the Moire topography criteria (Figure 3) [6].

2.7. Secondary Outcomes. A patient-oriented self-assessment scale of facial elasticity was performed with the same frequency as the primary measurements. Participants assessed their degrees of the facial elasticity using a 10 cm vertical line visual analog scale (VAS). The scale was marked at the top with "most severe condition," with the bottom labeled "fine condition."

2.8. Safety. The Institutional Review Board of Kyung Hee University Hospital at Gangdong reviewed the protocol, monitored patient safety, and investigated any adverse events independently of the investigators.

2.9. Statistical Analysis. All primary analyses were based on an intention-to-treat (ITT) population. End-of-study analyses were performed using the last observation carried forward for participants who did not complete the study. Patient characteristics were summarized using descriptive statistics. The nonparametric Wilcoxon signed-rank test was used for assessing clinical improvement. SPSS 15.0 for Windows (SPSS Inc., Chicago, IL, USA) was used for data management and statistical analysis. A P value less than 0.05 was considered statistically significant.

2.10. Quality Control. Before starting the trial, the acupuncture practitioner was trained and had been administering FCA at a clinic of Kyung Hee University Hospital at Gangdong for over a year. The investigator who assessed the outcomes received thorough training in assessing Moire topography.

3. Results

3.1. Participants. Of 50 participants screened, 28 were eligible for the study, 27 completed the five sessions of FCA treatment, and one dropped out because of pain after the first FCA treatment. The mean age was 50.04 ± 6.07 (range: 40–59) years, and all participants were Asian females with a Glogau photoaging scale III (Figure 4).

3.2. Primary Outcome. The primary outcome was mean change in Moire topography criteria from baseline to the end of the study in the ITT population. The Moire topography changed significantly ($P = 0.0001$) after FCA treatment (Table 1). Of the 27 participants who underwent all five sessions, 12 exhibited no change, while 15 showed a positive, single-level improvement (Table 2).

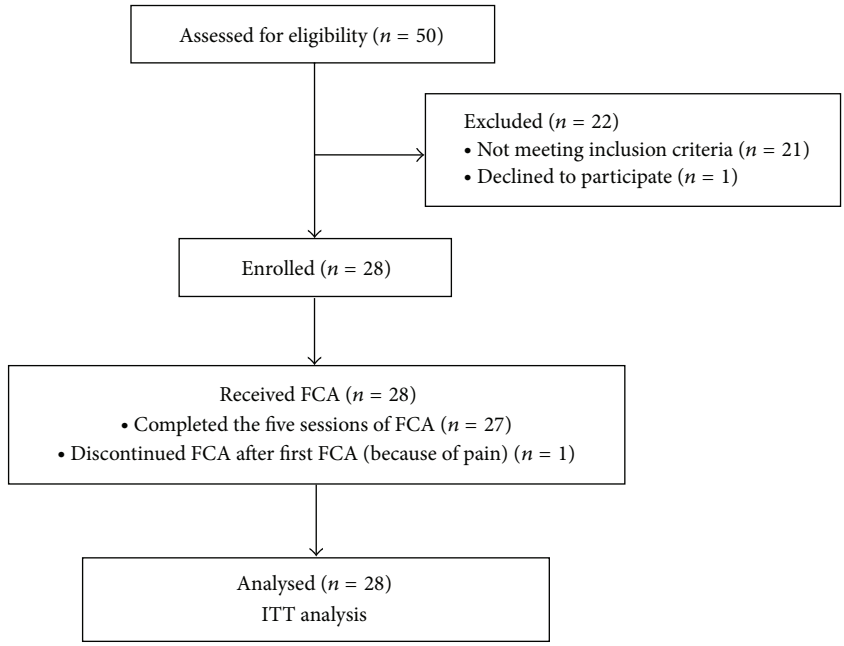

Figure 4: Progression of participants through the study.

Table 1: Mean change in Moire topography.

	Before FCA ($n = 28$)	After FCA ($n = 28$)	P value
Moire topography criteria	1.70 ± 0.724	2.26 ± 1.059	0.0001*

Data are mean ± standard deviation of percent change (95% confidence interval).
*Statistically significant difference, $P < 0.05$.

Table 2: Changes in Moire topography for participants who completed the study.

Negative change after FCA (n)	0
No change after FCA (n)	12
Single level improvement after FCA (n)	15
Total (n)	27

Table 3: Mean change in patient self-assessment of skin elasticity.

	Before FCA ($n = 28$)	After FCA ($n = 28$)	P value
Patient self-assessment Elasticity scale	6.15 ± 1.562	4.81 ± 1.942	0.006

Data are mean ± standard deviation of percent change (95% confidence interval).

3.3. Secondary Outcomes. Mean changes in a patient self-assessment of skin elasticity showed no significant differences (Table 3).

3.4. Safety Evaluation. The most commonly reported adverse event that was clearly attributable to FCA treatment was mild bruising (20/140 treatment sessions; 14.28%) at the needle site. Only one participant dropped out because of pain. No adverse events of scarring, nerve damage, or lengthy recovery periods were observed.

4. Discussion

This clinical open-label, single-arm pilot study investigated the efficacy and safety of FCA on facial elasticity. FCA has been increasing in use and popularity but few introductory articles [1, 2] were available until Donoyama et al. reported in 2012 on increased water and oil content for facial skin after cosmetic acupuncture [4].

Several different types of FCA are practiced. Recently, in Korea, clinicians have used FCA to enhance facial elasticity by restoring resting mimetic muscle tone by inserting needles into head, face, and neck muscles. Louarn et al. [8] conducted an MRI study on changes in the contour of facial mimetic muscles in patients of different ages. They found that facial mimetic muscles gradually straighten and shorten with age as a result of increased resting muscle tone. Based on these findings, we hypothesized that FCA could be used to improve facial elasticity with needles inserted into the muscles of the head, face, and neck, resulting in restored muscle tone.

Different methods for measuring facial elasticity range from manual examination to direct visualization. Moire topography is an optical measurement that does not require direct contact and allows high-precision visualization of facial shape in three dimensions, similar to a contour map [9]. Moire topography is used in studies of facial palsy, zygomatic fractures [10], facial morphology, and facial plastic surgery [11]. The Moire topography criteria were developed by Ahn et al. [6] for measuring facial elasticity. Moire topography

criteria show a very high correlation with age and the Cutometer, which evaluates skin elasticity.

In this study, we found that participants who underwent five FCA treatment sessions showed an improvement of about 0.5 by Moire topography. FCA also improved scores on a patient self-assessment of elasticity, but the changes were not significant. These results suggested that FCA improved facial elasticity in women aged 40 and 59 years with a Glogau photoaging scale III.

This study had several limitations. It is an open-label, single-arm pilot design. The sample size was small with no control group, and the trial duration was short compared to the actual clinical environment. For example, in the Cosmetic/Derma Clinic of Kyung Hee University Hospital at Gangdong, an FCA treatment course is generally eight treatment sessions over 4 weeks. The Moire topography criteria are an ordinal scale with wide intervals. The scale might not detect small changes and is highly dependent on the evaluator's judgment.

However, in spite of these limitations, this study could be helpful in providing clinicians with procedural details about FCA and could be the basis of future investigations aimed at elucidating the possible mechanisms of FCA including restoration of resting mimetic muscle tone. A larger study with a controlled design using different objective outcomes measure could be warranted.

Conflict of Interests

The authors state no conflict of interests. No financial support or benefits were received by the authors. The authors have no commercial associations or financial relationships to disclose.

Acknowledgments

The authors would like to thank Inho Jung for introducing the FCA procedure and Seungphil Cho for the helpful discussions. This study was supported by a grant from the Traditional Korean Medicine R&D Project, Ministry of Health & Welfare, Republic of Korea (B120014).

References

[1] J. B. Barrett, "Acupuncture and facial rejuvenation," *Aesthetic Surgery Journal*, vol. 25, no. 4, pp. 419–424, 2005.

[2] V. C. Doran, "An introduction to facial revitalisation acupuncture," *European Journal of Oriental Medicine*, vol. 5, no. 5, pp. 4–8, 2007.

[3] K. M. Lee, S. C. Lim, J. S. Kim, and B. H. Lee, "A clinical study on facial wrinkles treated with miso facial acupuncture—measured by the facial skin photographing system," *The Journal of Korean Acupuncture and Moxibustion Society*, vol. 27, no. 1, pp. 101–107, 2010.

[4] N. Donoyama, A. Kojima, S. Suoh, and N. Ohkoshi, "Cosmetic acupuncture to enhance facial skin appearance: a preliminary study," *Acupuncture in Medicine*, vol. 30, no. 2, pp. 152–153, 2012.

[5] R. G. Glogau, "Aesthetic and anatomic analysis of the aging skin," *Seminars in Cutaneous Medicine and Surgery*, vol. 15, no. 3, pp. 134–138, 1996.

[6] S. Ahn, S. Kim, H. Lee, S. Moon, and I. Chang, "Correlation between a Cutometer and quantitative evaluation using Moire topography in age-related skin elasticity," *Skin Research and Technology*, vol. 13, no. 3, pp. 280–284, 2007.

[7] H. MacPherson, D. G. Altman, R. Hammerschlag et al., "Revised standards for reporting interventions in clinical trials of acupuncture (STRICTA): extending the CONSORT statement," *Journal of Evidence-Based Medicine*, vol. 3, no. 3, pp. 140–155, 2010.

[8] C. L. Louarn, D. Buthiau, and J. Buis, "Structural aging: the facial recurve concept," *Aesthetic Plastic Surgery*, vol. 31, no. 3, pp. 213–218, 2007.

[9] K. Yuen, I. Inokuchi, M. Maeta, S.-I. Kawakami, and Y. Masuda, "Evaluation of facial palsy by moire topography index," *Otolaryngology—Head and Neck Surgery*, vol. 117, no. 5, pp. 567–572, 1997.

[10] Y. Kawano, "Three dimensional analysis of the face in respect of zygomatic fractures and evaluation of the surgery with the aid of Moiré topography," *Journal of Cranio-Maxillofacial Surgery*, vol. 15, pp. 68–74, 1987.

[11] C. P. Honrado and W. F. Larrabee Jr., "Update in three-dimensional imaging in facial plastic surgery," *Current Opinion in Otolaryngology and Head and Neck Surgery*, vol. 12, no. 4, pp. 327–331, 2004.

Hindawi Publishing Corporation
Evidence-Based Complementary and Alternative Medicine
Volume 2013, Article ID 741985, 10 pages
http://dx.doi.org/10.1155/2013/741985

Research Article

JNK1/2 Activation by an Extract from the Roots of *Morus alba* L. Reduces the Viability of Multidrug-Resistant MCF-7/Dox Cells by Inhibiting YB-1-Dependent MDR1 Expression

Youn Kyung Choi, Sung-Gook Cho, Hyeong Sim Choi, Sang-Mi Woo, Yee Jin Yun, Yong Cheol Shin, and Seong-Gyu Ko

Laboratory of Clinical Biology and Pharmacogenomics, Department of Preventive Medicine, College of Korean Medicine, Kyung Hee University, 1 Hoegi, Dongdaemun, Seoul 130-701, Republic of Korea

Correspondence should be addressed to Seong-Gyu Ko; epiko@khu.ac.kr

Received 5 April 2013; Revised 28 June 2013; Accepted 30 June 2013

Academic Editor: Bo-Hyoung Jang

Cancer cells acquire anticancer drug resistance during chemotherapy, which aggravates cancer disease. MDR1 encoded from multidrug resistance gene 1 mainly causes multidrug resistance phenotypes of different cancer cells. In this study, we demonstrate that JNK1/2 activation by an extract from the root of *Morus alba* L. (White mulberry) reduces doxorubicin-resistant MCF-7/Dox cell viability by inhibiting YB-1 regulation of *MDR1* gene expression. When MCF-7 or MCF-7/Dox cells, where MDR1 is highly expressed were treated with an extract from roots or leaves of *Morus alba* L., respectively, the root extract from the mulberry (REM) but not the leaf extract (LEM) reduced cell viabilities of both MCF-7 and MCF-7/Dox cells, which was enhanced by cotreatment with doxorubicin. REM but not LEM further inhibited YB-1 nuclear translocation and its regulation of *MDR1* gene expression. Moreover, REM promoted phosphorylation of c-Jun NH2-terminal kinase 1/2 (JNK1/2) and JNK1/2 inhibitor, SP600125 and rescued REM inhibition of both MDR1 expression and viabilities in MCF-7/Dox cells. Consistently, overexpression of JNK1, c-Jun, or c-Fos inhibited YB-1-dependent MDR1 expression and reduced viabilities in MCF-7/Dox cells. In conclusion, our data indicate that REM-activated JNK-cJun/c-Fos pathway decreases the viability of MCF-7/Dox cells by inhibiting YB-1-dependent *MDR1* gene expression. Thus, we suggest that REM may be useful for treating multidrug-resistant cancer cells.

1. Introduction

MDR1 (also called P-glycoprotein or ABCB1) encoded from a multidrug-resistant gene, *MDR1* (or *ABCB1*), mainly mediates multidrug resistance by an efflux of drugs [1–4]. Therapeutic approaches for treating cancer in clinics are hampered by MDR1-induced multidrug resistance [3–8]. Multidrug resistance of cancer cells acquired by MDR1 expression involves a transcriptional activity of Y-box binding protein 1 (YB-1) [9–15]. Doxorubicin-resistant MCF-7/Dox cells were constructed by consecutive treatment of doxorubicin (or adriamycin) [1]. This cell line highly expressing MDR1 is resistant to various anticancer drugs including doxorubicin, paclitaxel, vincristine, and etoposide, thereby being used widely for deciphering multidrug-resistant mechanisms *in vitro* [16].

It has been revealed that c-Jun NH2-terminal kinase 1/2 (JNK1/2) regulates MDR1 expression via c-Jun in multidrug-resistant gastric and pancreatic cell lines [17]. Likewise, JNK1/2 mediated hypoxia-induced MDR1 expression in HOP62 nonsmall lung cell carcinoma cell line [18]. In addition, AP-1 negatively regulated YB-1-mediated *MDR1* gene expression in MCF-7/Dox cell line [19]. In MCF-7 cells, MDR1 promoter activity was also negatively regulated by c-Fos [20]. Those findings suggest that JNK1/2-mediated signaling inhibits YB-1-dependent *MDR1* gene expression and causes a loss of multidrug-resistant phenotype to anticancer drugs. Furthermore, it is recently found that MDR1

silencing reduced the proliferation of multidrug-resistant cancer cells [21]. Therefore, while the inhibition of MDR1 channel function allows chemotherapeutic agents to be accumulated in the cells, the suppression of MDR1 expression itself is also likely to be enough to attenuate multidrug-resistant cancer cell growth.

Parts of *Morus alba* L. (white mulberry) including roots and leaves have been widely used in the traditional medicine for curing symptoms such as diabetes, edema, eczema, anemia, bleeding, dry constipation, fever, sore throat, headache, muscle aches and pain, and itching [22]. Recently, extracts from *Morus alba* L. have been revealed to affect cancer disease. REM caused apoptotic cell death of different types of cancer cells such as K562 and B380 human leukemia cells and B16 mouse melanoma cells [23]. Albanol A isolated from REM also induced apoptotic cell death of human leukemic HL-60 cells [24]. Likewise, LEM inhibited neuroblastoma cells [25]. 2-Arylbenzofuran derivatives isolated from LEM also showed cytotoxicity on different cancer cells: A549 (human lung cancer cells), BEL7402 (human liver cancer cells), BGC823 (human gastric cancer cells), HCT8 (human colon cancer cells), and A2780 (human oophoroma cells) [26]. Chalcone derivatives from LEM also showed cytotoxicity in HCT-8 and BGC823 [27]. In addition, lectin purified from LEM caused apoptotic cell death of both MCF-7 breast cancer cells and HCT-15 human colon cancer cells [28, 29]. Thus, REM, LEM, and their chemical components appear to have anticancer effects. However, it is unclear whether those have anticancer effect even in multidrug-resistant cancer cells.

In this study, we examined whether REM or LEM affects drug-resistant cancer cells. Our data present here that REM but not LEM reduces the viability of MCF-7/Dox cells highly expressing MDR1. This REM effect was due to JNK1/2 inhibition of YB-1-dependent MDR1 expression in multidrug-resistant cells. Thus, our present study provides knowledge for a role of REM against drug-resistant cancers.

2. Materials and Methods

Extract preparation, chemicals, and cell culture. Extracts from *Morus alba* L. (REM and LEM) were prepared by and obtained from Hanpoong Pharmaceutical Company (Jeonju, Korea) following the good manufacturing practices (GMP) procedures. In brief, herbs were boiled with 80% ethanol at 100°C, and filtered extracts were then concentrated and dried by vacuum at 60°C. The dried powers were lyophilized and then dissolved in distilled water. To qualify REM and LEM, HPLC analyses were performed by Hanpoong Pharmaceutical Company (Jeonju, Korea). MCF-7 and MCF-7/Dox cells were routinely cultured in DMEM with 10% fetal bovine serum and 1% antibiotics. For transient transfections, cells were transfected with mixtures of DNAs with Lipofectamine 2000 reagents (Invitrogen). SP600125, SB203580, PD98059, and LY294002 were obtained from Sigma.

Cell viability. Cells were cultured in 96-well plates and subjected to the Cell Proliferation assays (Promega). Cells were treated with the extracts for 72 hours and then subjected to the assays. All experiments were performed in triplicate. Data were represented by mean ± standard deviation. P values lower than 0.05 in Student's t-tests were considered statistically significant.

RT-PCR, Western Blot and Immunocytochemistry. Total RNAs were extracted with TRIzol (Invitrogen). Syntheses of cDNA were routinely performed by MMLV reverse transcriptase and random primers. PCR to detect *MDR1* mRNA was then performed. *GAPDH* was used for an internal control. Primers used are as follows: 5′-AAT-CCCATCACCATCTTCCA-3′ (*GAPDH* forward primer) and 5′-TGGACTCCACGACGTACTCA-3′ (*GAPDH* reverse primer). Protein was obtained by cell lysis with RIPA buffer, and total 30 μg of protein was loaded onto 6 to 10% SDS-PAGEs. Antibodies for pAKT, AKT, pERK1/2, ERK1, pJNK1/2, JNK1, pp38MAPK, p38MAPK, YB-1, and MDR1 were obtained from Cell Signaling. As an internal control, α-tubulin or actin was used. For the immunoprecipitation assays, anti-YB-1 or anti-JNK1/2 antibody was used. 50 μL of protein A/G bead slurry and 2 μg of the appropriate antibody were mixed with 200 μg of protein. 30 μg of protein was loaded as an input. For the nuclear fractionation, cells were lszed with buffer A (10 mM HEPES, 1.5 mM $MgCl_2$, 10 mM KCl, 0.5 mM DTT, and 0.05% NP-40), and then the supernatants were used for the cytosolic fractions. The pellets were mixed with buffer B (5 mM HEPES, 1.5 mM $MgCl_2$, 0.2 mM EDTA, 0.5 mM DTT, and 26% glycerol) and 300 mM NaCl and homogenized with 20 full strokes in Dounce homogenizer on ice. After centrifugation, the supernatants were used for the nuclear fractions. For the immunocytochemistry, cells were fixed with 4% formaldehyde, permeabilized with 0.5% Triton X-100, incubated in phosphate buffered saline containing 10% FBS, and then incubated with the anti-YB-1 antibody (Cell Signaling) and Alexa Fluor-488 goat anti-rabbit IgG antibody (Invitrogen). For the counter staining, phalloidin (Sigma) and TOPRO-3 (Invitrogen) were used to detect actin (especially, F-actin) and the nucleus. The object was 20x, and scale bars in the image indicate 50 μm.

Rhodamine 123 Efflux Assay. Cells were treated with the extracts for 30 hours and incubated for another 1 hour with 1 μg/mL of the rhodamine 123. Accumulation of Rhodamine 123 in cells was analyzed by flow cytometry.

Chromatin Immunoprecipitation (ChIP) Assays. To analyze YB1 interaction with MDR1 promoter region, we performed ChIP assays according to the manufacturer's procedures (Abcam). Briefly, nuclear fractions from the cells fixed with 1% formaldehyde were sonicated, and then anti-YB-1 antibody (Cell Signaling) was used for chromatin immunoprecipitation. For the positive control, anti-histone H3 antibody provided from the manufacturer (Abcam) was used. For the negative control, bead-only samples were used according to the manufacturer's procedure. YB-1-bound DNAs were then amplified with primers for MDR1 promoter region and *GAPDH* primers as the internal control. Data were obtained by normalizing ddCT from real-time PCR. The values

indicate the mean ± standard deviation from the experiments done in triplicate. P-value below 0.05 was considered statistically significant. ChIP primers used are as follows: YB-1 binding sites on MDR1 promoter, 5′-CAGTAGTGAAGCTGTAGGAC-3′, 5′-ATCAGAACTTGCTGTTCTGC-3′, GAPDH 5′-AATCCCATCACCATCTTCCA-3′, and 5′-TGGACTCCACGACGTACTCA-3′.

Luciferase Assays. Cells were transfected with MDR1-luc plasmid (pMDR1-1202, Addgene plasmid 37627) [30] and subjected to the luciferase assays (Promega). Extracts were treated for 6 hours. All experiments were performed in triplicate, and Student's t-test was performed to determine statistics. P value below 0.05 was considered statistically significant. All data were represented as the mean ± standard deviation.

3. Results

3.1. REM but Not LEM Reduces Cell Viabilities of MCF-7 and MCF-7/Dox. We first examined both mRNA and protein levels of MDR1, a key mediator of multidrug-resistant phenotype, in MCF-7 and MCF-7/Dox cells. MCF-7/Dox cells resistant to doxorubicin expressed MDR1 mRNA and protein, while MCF-7 cells did not (Figure 1(a)). Thus, we next examined whether our herbal extracts, REM and LEM, affect viabilities of MCF-7 and MCF-7/Dox cells. REM but not LEM reduced MCF-7 cell viability in a dose-dependent manner (Figure 1(b), left). In addition, REM at 100 μg/mL also decreased MCF-7/Dox cell viability by approximately 30% (Figure 1(b), right).

Thus, we further examined whether a combinatorial treatment of doxorubicin with REM or LEM causes a decrease of cell viability. Doxorubicin (Dox) alone strongly reduced the viability of MCF-7 cells, and its combination with various concentrations of REM or LEM appeared to more reduce it when higher concentrations of REM or LEM was combined (Figure 1(c), left). In MCF-7/Dox cells, REM at 100 μg/mL, when combined with 1 μg/mL of doxorubicin, decreased the viability by approximately 50% (Figure 1(c), right). However, we could not observe any reduction of multidrug-resistant cell viability in a combined treatment of doxorubicin with LEM. Subsequently, the MCF-7/DOX cells were treated with various concentrations of doxorubicin (10^{-3} to 1 μg/mL) in the presence or absence of either 100 μg/mL of REM or LEM. When combined with doxorubicin at 1 μg/mL, REM at 100 μg/mL but not LEM more reduced the viability by approximately 27%.

3.2. REM-Induced JNK1/2 Activation Inhibits MDR1 Expression. To decipher REM-mediated intracellular signaling pathways on MCF-7/Dox cells, MAPKs, and AKT, proteins known for cell proliferation and survival were examined. While REM and LEM did not alter phosphorylation of AKT and ERK1/2 in MCF-7/Dox cells, both extracts increased phosphorylation of p38MAPK. Furthermore, REM but not LEM increased JNK1/2 phosphorylation of (Figure 2(a)). Thus, REM is likely to selectively regulate JNK1/2 phosphorylation.

As JNK1/2 has been revealed to regulate MDR1 expression [17], we next examined whether REM affects MDR1 expression in MCF-7/Dox cells via JNK1/2. When MCF-7/Dox cells were treated with 100 μg/mL of either REM or LEM for 24 hours, REM but not LEM reduced mRNA and protein levels of MDR1 (Figure 2(b)). Thus, we further examined whether REM affects MDR1 expression in a transcription level. MCF-7/Dox cells were transfected with MDR1-luc construct and then treated with REM or LEM for 6 hours. While LEM did not affect MDR1 promoter-mediated luciferase activity, REM reduced it by approximately 70% (Figure 2(c)). In addition, REM but not LEM increased accumulation rate of rhodamine 123 in the cells (Figure 2(d)).

When MCF-7/Dox cells were pretreated with JNK1/2 inhibitor, SP600125, prior to REM treatment, REM inhibition of MDR1 expression was rescued by JNK1/2 inhibition (Figure 2(d)). Furthermore, JNK1/2 inhibition also rescued REM inhibition of MDR1 promoter activity (Figure 2(e)), indicating that REM-mediated JNK1/2 activation is likely important for the inhibition of MDR1 expression.

3.3. REM Inhibits YB1-Dependent MDR1 Expression. We next examined if REM inhibits nuclear translocation of YB-1, a key transcription factor regulating *MDR1* gene expression. MCF-7/Dox cells were treated with LEM or REM for 6 hours and then examined a localization of endogenous YB-1 in the cells. Although YB-1 was diffusely found in the cells, it mostly localized in the nucleus. While LEM treatment did not affect YB-1 localization pattern, REM disrupted nuclear localization of YB-1 (Figure 3(a)).

Accordingly, to examine if REM inhibits YB-1 interaction with MDR1 promoter, we performed the chromatin immunoprecipitation assays with the anti-YB-1 antibody. Our data from the chromatin immunoprecipitation assays showed that REM but not LEM inhibited YB-1 binding onto MDR1 promoter region (Figure 3(b)), which indicates that REM inhibits YB-1 interaction with MDR1 promoter.

Thus, we further examined if REM effect was mediated by inhibiting transcriptional activity of YB-1. When MCF-7/Dox cells were cotransfected with MDR1-luc and YB-1 and then treated with REM for 6 hours, REM treatment reduced YB-1-induced luciferase activity (Figure 3(c)).

3.4. REM-Activated JNK1/2 Inhibits YB-1-Dependent MDR1 Expression. Thus, we examined whether JNK1/2 inhibition rescues REM reduction of YB-1-dependent MDR1 expression. In the luciferase assays, SP600125 blocked REM inhibition of YB-1-dependent MDR1 promoter activity (Figure 4(a)). Thus, we further examined whether JNK1/2 signaling to c-Jun/c-Fos mediates REM inhibition of YB-1-dependent MDR1 expression. In the luciferase assays, we found that overexpression of JNK1, c-Jun, or c-Fos significantly reduces basal and YB-1-dependent MDR1 promoter activity (Figure 4(b)).

So, we further examined whether JNK1/2 directly inhibits YB-1 transcriptional activity by repressing YB-1 nuclear translocation. In our immunoprecipitation assays with anti-YB-1 antibody, we found that REM causes pJNK1/2

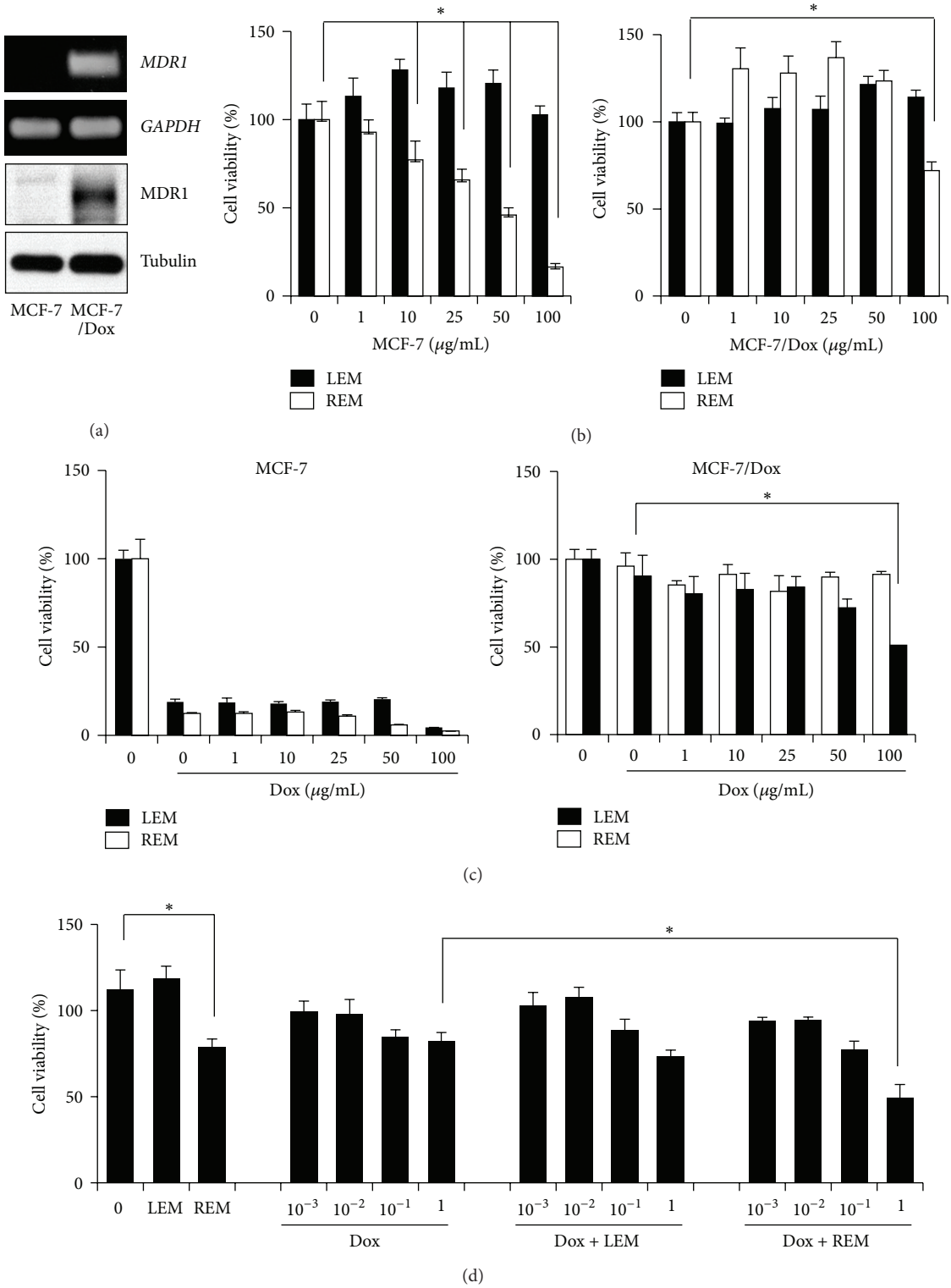

Figure 1: REM reduces cell viabilities of MCF-7/Dox cells. (a) MDR1 mRNA and protein levels were examined in MCF-7 and MCF-7/Dox cells. *GAPDH* and tubulin were used as internal controls. (b–d) MCF-7 and MCF-7/Dox cells were treated with the indicatives for 72 hours and then subjected to the MTT assays. The experiments were performed in triplicate, and P-value less than 0.05 (marked with asterisks, $*$) was considered statistically significant.

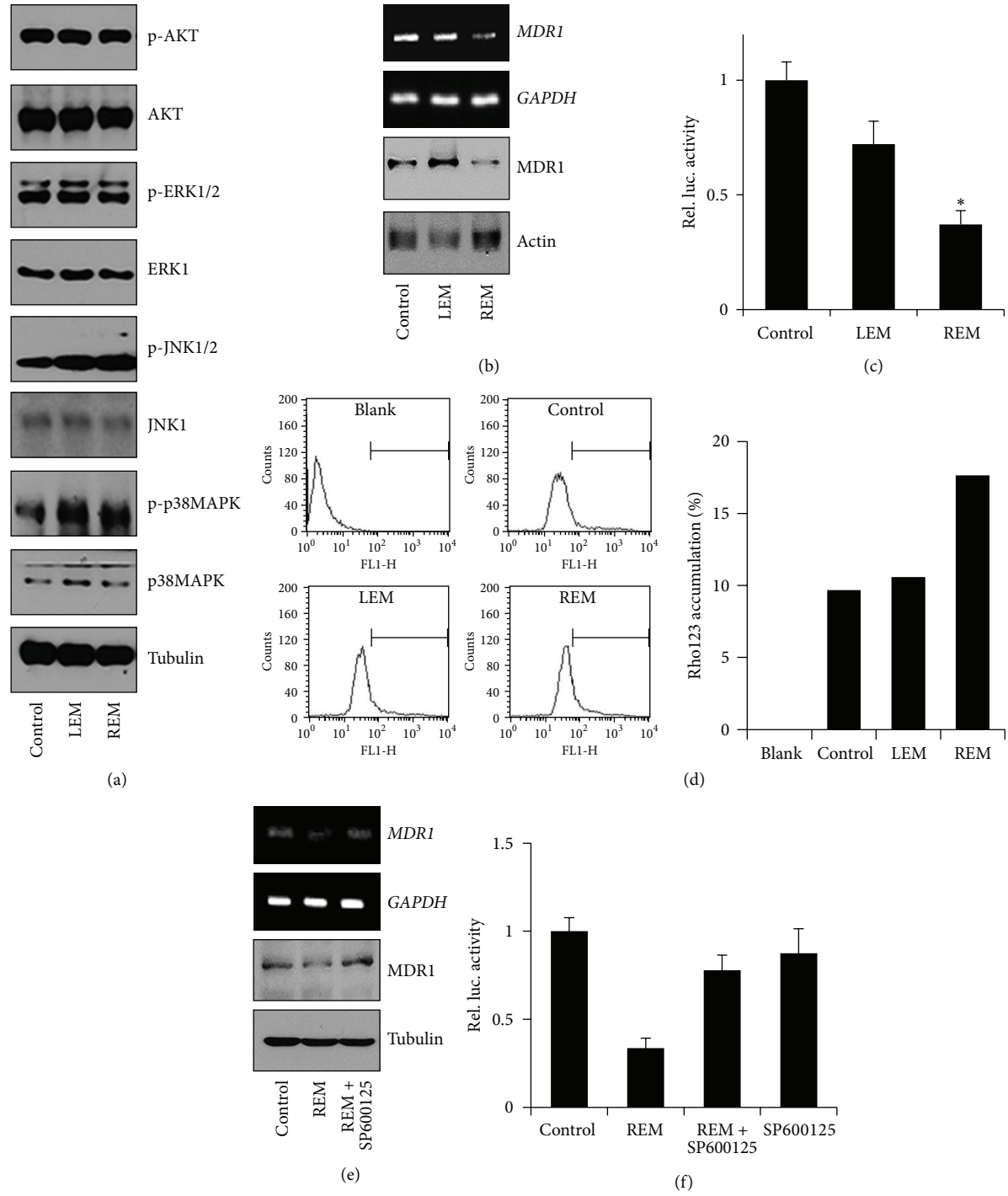

Figure 2: REM-induced JNK1/2 activation inhibits MDR1 expression. (a) Cells were treated with 100 μg/mL of either LEM or REM for 15 minutes. Tubulin was detected as an internal control. (b) Cells were treated with the indicatives for 24 hours, and then MDR1 mRNA and protein levels were examined. *GAPDH* and actin were used as internal controls. (c) To analyze the MDR1 promoter activities, MCF-7/Dox cells were transfected with MDR1-luc construct for 24 hours and then treated with the indicatives for another 6 hours. The luciferase assays were performed in triplicate, and P value less than 0.05 (marked with an asterisk, $*$) was considered statistically significant. (d) MCF-7/Dox cells were treated with the indicatives for 30 hours and then incubated with rhodamine 123 for another 1 hour. Rhodamine 123 accumulation rate was analyzed by flow cytometry. (e) Cells were pretreated with SP600125 for 30 minutes and then treated with 100 μg/mL of REM. 24 hours after treatment, MDR1 mRNA and protein levels were examined. *GAPDH* and tubulin were used as internal controls. (f) To examine MDR1 promoter activities, MCF-7/Dox cells were transfected with MDR1-luc construct for 24 hours and then treated with REM for another 6 hours. SP600125 was treated 30 minutes before REM treatment. The luciferase assays were performed in triplicate and P-value less than 0.05 (marked with an asterisk, $*$) was considered statistically significant.

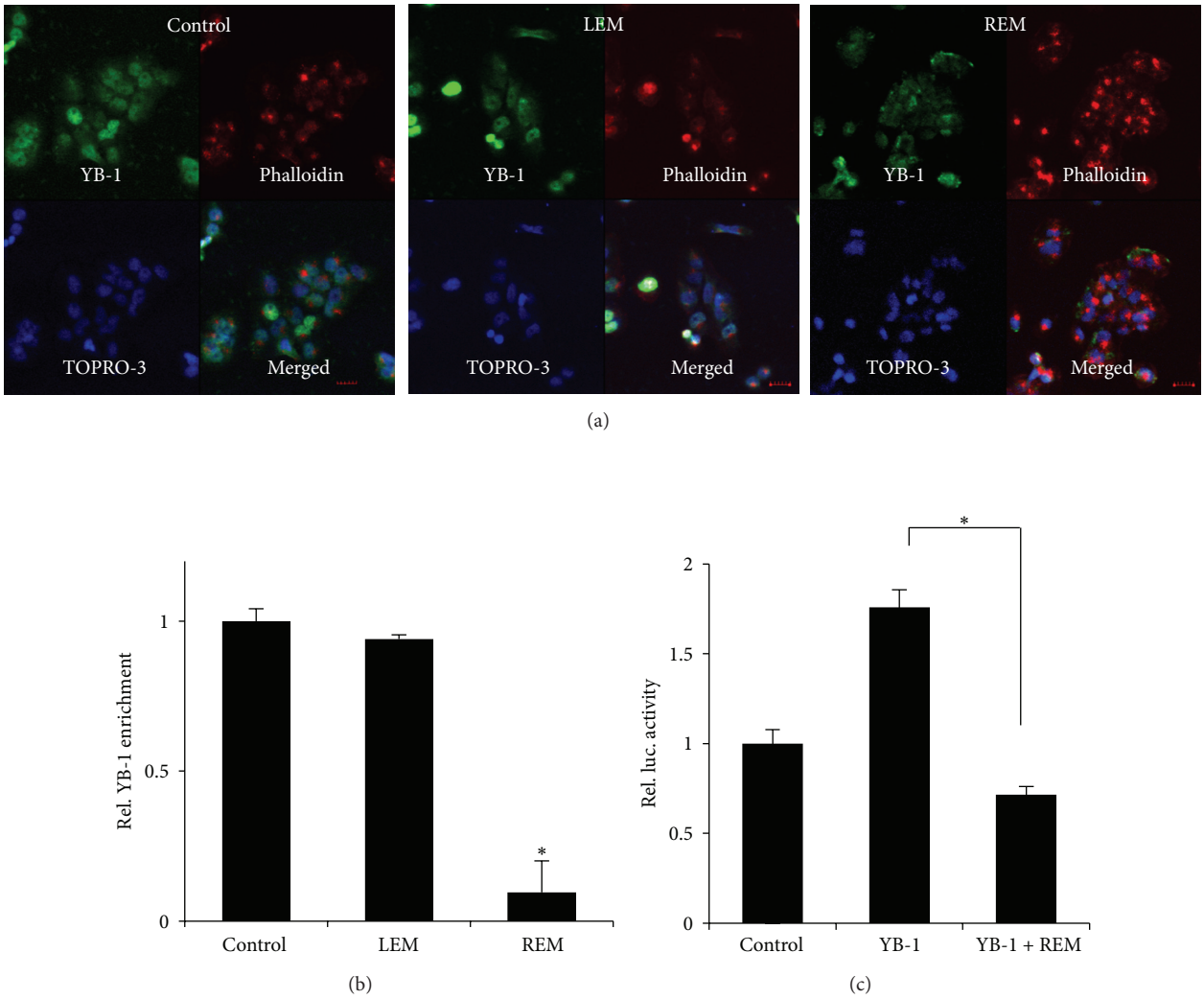

Figure 3: REM inhibits YB-1-dependent MDR1 expression. (a) YB-1 localization. Cells were stained with anti-YB-1 antibody (green), phalloidin (red), and TOPRO-3 (blue) to visualize YB-1 intracellular localization, actin, and nucleus. Scale bars, 50 μm. The objective, 20X. (b) MCF-7/Dox cells were treated with the indicatives for 6 hours and then fixed with 1% formaldehyde. Fragmented DNAs were incubated with the appropriate antibodies, and then PCR was routinely performed. *GAPDH* was used as an internal control. Relative values of YB-1 enrichment normalized by ddCT were obtained by experiments performed in triplicate. *P*-value less than 0.05 (marked with an asterisk, $*$) was considered statistically significant. (c) MCF-7/Dox cells were cotransfected with MDR1-luc and YB-1 constructs for 24 hours and then treated with the indicatives for another 6 hours. Assays were performed in triplicate, and *P* value less than 0.05 (marked with an asterisk, $*$) was considered statistically significant.

interaction with YB-1 in the cytosol and a reduction of YB-1 level in the nucleus, while YB-1 is distributed in both the cytosol and nucleus of the untreated cells (Figure 4(c)). Thus, our data indicate that REM-induced JNK1/2 activation may lead to malfunction of YB-1 through a direct interaction in the cytosol.

3.5. REM-Activated JNK1/2 Reduces Viabilities of Multidrug-Resistant Cells. Our serial data hypothesize that REM-activated JNK1/2 inhibition of YB-1-dependent MDR1 expression may result in the reduction of cell viability. Thus, we further examined whether REM inhibits the viability of cells overexpressing YB-1. When cells were transfected with YB-1 and treated with REM for 48 hours, YB-1 overexpression itself did not significantly alter cell viability. However, REM reduced the viability of cells overexpressing YB-1 by approximately 61 % (Figure 5(a)).

So, we next examined whether JNK1/2 inhibition rescued REM reduction of cell viabilitypagebreak When cells were pretreated with SP600125 for 30 minutes and then treated with REM for another 48 hours, REM did not affect cell viability. Furthermore, a combination of REM with doxorubicin also did not affect the viability of the cells pretreated with SP600125 (Figure 5(b)).

As REM activation of JNK1/2 reduced MDR1 expression level, we further examined whether JNK1/2 affects cell viability. When MCF-7/Dox cells were transiently transfected with JNK1, c-Jun, or c-Fos and then subjected to the MTT

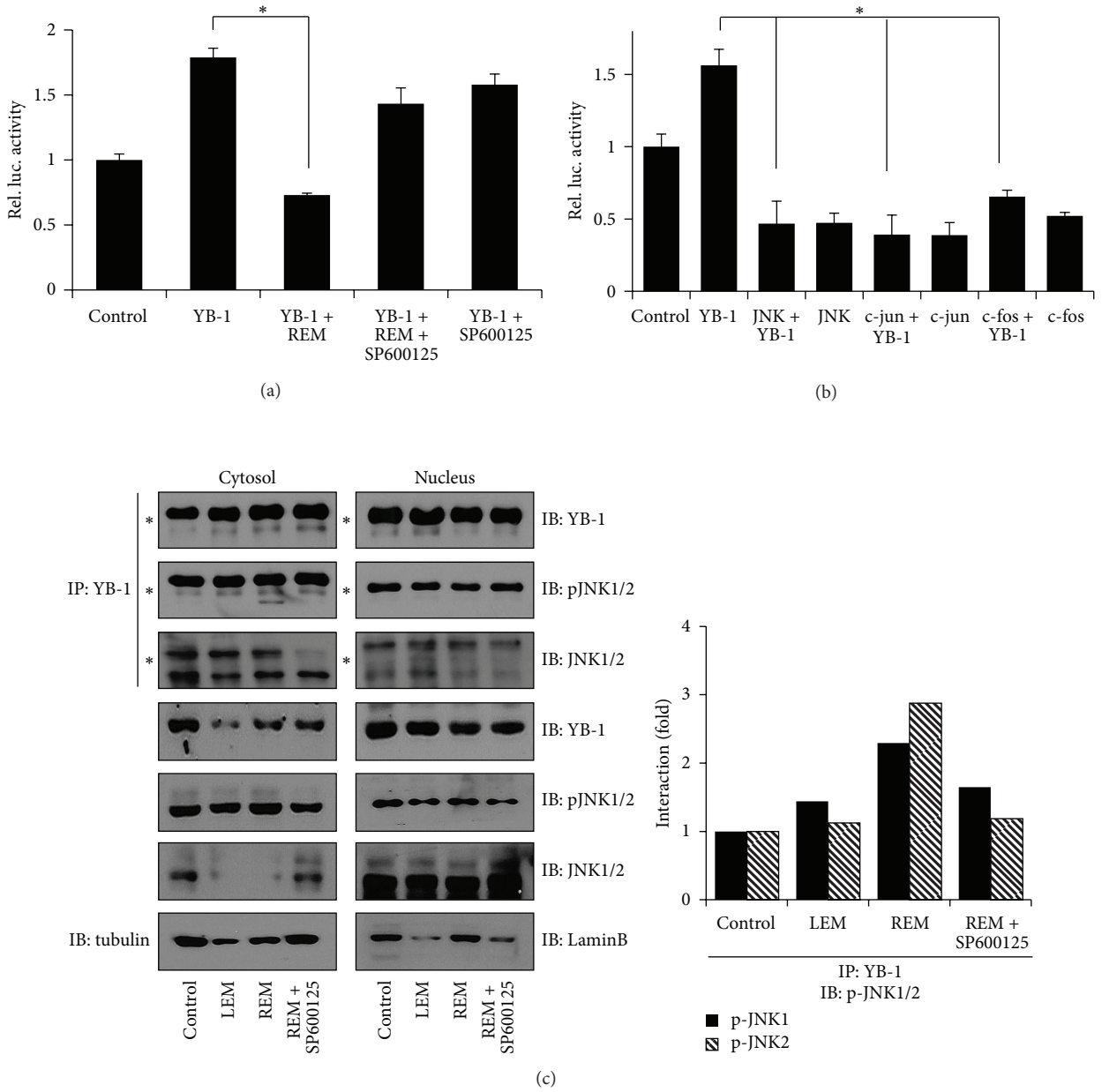

Figure 4: REM activation of JNK inhibits YB-1-dependent MDR1 expression. (a-b) MCF-7/Dox cells were transfected with MDR1-luc and constructs indicated for 24 hours. REM ± SP600125 was treated for 6 hours. Assays were performed in triplicate, and P value less than 0.05 (marked with an asterisk, $*$) was considered statistically significant. (c) YB-1 interaction with pJNK1/2. Cytosolic and nuclear proteins were immunoprecipitated with anti-YB-1 antibody. The immunoprecipitants and input proteins were then blotted with the antibodies for pJNK1/2, YB-1, JNK1, and actin. Asterisks indicate heavy chains from the immunoprecipitation. Quantitative analyses of protein interactions were performed using the Image J software.

assays, the overexpression of JNK, c-Jun, or c-Fos reduced the viabilities by approximately 30% to 50% (Figure 5(c)).

4. Discussion

Multidrug resistance of cancer cells results in poor prognoses. MDR1 expression upon a treatment of chemotherapeutic agents gains that phenotype [5, 8, 31, 32]. In this study, we provide knowledge that REM, the extract from white mulberry roots, reduces the viabilities of multidrug-resistant MCF-7/Dox cells by inhibiting YB-1-dependent MDR1 expression via JNK1/2 activation.

Inhibitions of drug efflux function of MDR1 have been issued in treatment of multidrug-resistant cancer cells expressing MDR1. In our study, REM reduced both MCF-7 and MCF-7/Dox cells, which were enhanced by doxorubicin addition. This additive effect is likely due to REM reduction of MDR1 expression, as this reduced MDR1 level causing

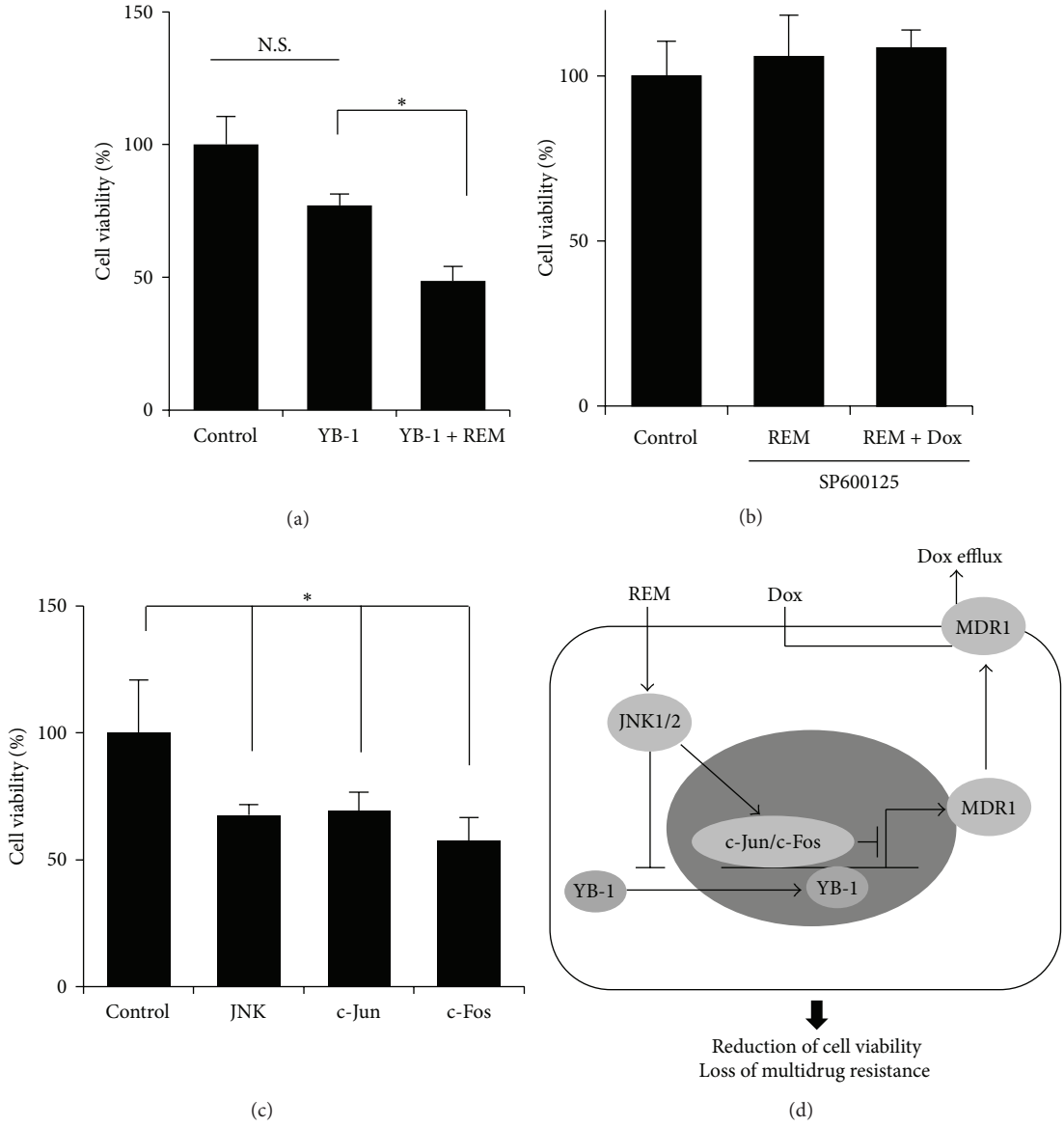

Figure 5: REM-induced JNK reduces MCF-7/Dox cell viability. (a) Cells were transfected with YB-1 and treated with REM 48 hours. The MTT experiments were performed in triplicate. N.S. indicates no significance in statistics. $*$, $P < 0.05$. (b) Cells were pretreated with SP600125 for 30 minutes and then treated with REM alone or REM plus doxorubicin for another 48 hours. The MTT assays were done in triplicate. (c) Cells were transfected with the indicatives for 48 hours and then subjected to the MTT assays. The experiments were performed in triplicate. $*$, $P < 0.05$. (d) Schematic illustration. YB-1-dependent MDR1 expression results in multidrug resistance by drug efflux (herein, doxorubicin). REM treatment activates JNK1/2, which blocks YB-1 nuclear translocation and induces c-Jun/c-Fos inhibition of YB-1-dependent MDR1 expression. Thus, REM results in the decrease of multidrug-resistant cancer cell viability with a loss of multidrug-resistant phenotype.

doxorubicin accumulation in the cells (Figure 5(d)). Furthermore, REM-induced JNK1/2 pathway caused the reduction of MDR1 expression and cell viability, which was rescued by SP600125 but not by SB203580, PD98059, and LY294002 (data not shown). Consistently, we found that MCF-7/Dox cell viability was reduced by overexpression of JNK1, c-Jun, or c-Fos. Recently, it has been found that MDR1 silencing with MDR1 shRNA reduces multidrug-resistant tumor cell proliferation [21], which indicates that a direct inhibition of MDR1 expression could be another option for treating multidrug-resistant cancer cells. Thus, the activation of JNK1/2 pathway to inhibit MDR1 expression is likely to be another option for treating multidrug-resistant cancer cells. In our preliminary cytotoxicity studies, multidrug-resistant leukemic cells were also sensitive to REM. Furthermore, REM repressed YB-1 transcriptional activity for MDR1 expression in those cell types (data not shown). Accordingly, REM but not LEM may affect viabilities of different types of drug-resistant cancer cells. Meanwhile, REM protected doxorubicin-induced cell death of H9c2 cardiac myoblast cells [33]. Thus, it is likely that REM effectively kill drug-resistant cancer cells with no or less side effect of doxorubicin *in vivo*.

JNK1/2 has been shown to negatively regulate different types of multidrug-resistant cancer cells such as multidrug-resistant EPG85-257RDB gastric cancer cells and EPP85-181RDB pancreatic cancer cells [17]. JNK1/2 activity was also negatively correlated with MDR1 expression in hepatocarcinoma cell lines [34]. Consistently, photosensitizer pheophorbide a based photodynamic therapy induced the apoptosis multidrug-resistant R-HepG2 cells via JNK1/2 activation [35]. Similarly, JNK1/2 activation by PSC833, a cyclosporine analogue, inhibited MDR1 expression in doxorubicin-resistant SK-MES-1/DX1000 lung cancer cell line [36]. It was recently shown that JNK1/2 involves DKK-3 in the apoptosis of MCF-7/Dox cells [37]. In addition, JNK1/2-mediated c-Jun activation inhibited MDR1 expression in multidrug-resistant K562/A02 cells [38]. Furthermore, c-Fos inhibited MDR1 expression in MCF-7 cells [20]. Thus, our data that REM-induced JNK1/2 inhibits MDR1 expression and multidrug-resistant cell viability is relevant to recent findings. However, JNK1/2 mediated hypoxia-induced MDR1 expression in HeLa cells [39]. Likewise, COX2-mediated JNK1/2-c-Jun activation appears to contribute multidrug resistance of HCT8/V colorectal cancer cells [40]. Therefore, it is likely that JNK1/2 regulation of multidrug-resistant cancer cells is dependent on mechanisms acquiring multidrug-resistant phenotype. Thus, the effect of REM remains to be tested in particular mechanisms such as hypoxia-induced MDR1 expression. Nevertheless, our findings here strongly suggest that REM regulation of JNK1/2 inhibits YB-1-dependent MDR1 expression in multidrug-resistant cancer cells.

In this study, we first provide evidence that REM activation of JNK1/2 reduces multidrug-resistant cancer cells by targeting YB-1-dependent MDR1 expression. Nevertheless, remains functions of REM against multidrug-resistant cancer cells in the *in vivo* experiments to be verified. Traditional medicines have long been used, suggesting that prescriptions based on traditional medicines work well in particular disease conditions. However, we still do not know what chemical components in REM uniquely play roles for JNK1/2 inhibition of YB-1-dependent MDR1 expression in multidrug-resistant cancer cells. Thus, it is required to understand the exact biochemical and molecular mechanisms by which REM works against multidrug-resistant cancer cells. That effort will improve the quality of traditional medicines with view of biomedical sciences.

5. Conclusion

This study demonstrates that REM but not LEM causes the reduction of multidrug-resistant cancer cell viability by JNK inhibition of YB-1-dependent MDR1 expression. Although we still explore to find the active chemical compounds that make the unique REM function against multidrug-resistant cancer cells, our study is expected to provide knowledge for REM effect against cancer disease.

Authors' Contribution

Youn Kyung Choi and Sung-Gook Cho contributed equally to this work.

Acknowledgments

The authors thank Dr. Sang-Hoon Kim and his colleagues (Kyung Hee University, Seoul, Korea) for sharing the luminometer. This research was supported by Basic Science Research Program through the National Research Foundation of Korea (NRF) funded by the Ministry of Education, Science and Technology (2011-0022382) and by a grant from Korean Medicine R&D project of the Ministry of Health and Welfare (B110043 and B120014).

References

[1] C. R. Fairchild, J. A. Moscow, E. E. O'Brien, and K. H. Cowan, "Multidrug resistance in cells transfected with human genes encoding a variant P-glycoprotein and glutathione S-transferase-π," *Molecular Pharmacology*, vol. 37, no. 6, pp. 801–809, 1990.

[2] J. W. Jaroszewski, O. Kaplan, and J. S. Cohen, "Action of gossypol and rhodamine 123 on wild type and multidrug-resistant MCF-7 human breast cancer cells: 31P nuclear magnetic resonance and toxicity studies," *Cancer Research*, vol. 50, no. 21, pp. 6936–6943, 1990.

[3] L. J. Goldstein, H. Galski, A. Fojo et al., "Expression of a multidrug resistance gene in human cancers," *Journal of the National Cancer Institute*, vol. 81, no. 2, pp. 116–124, 1989.

[4] G. D. Leonard, T. Fojo, and S. E. Bates, "The role of ABC transporters in clinical practice," *Oncologist*, vol. 8, no. 5, pp. 411–424, 2003.

[5] B. C. Shaffer, J.-P. Gillet, C. Patel, M. R. Baer, S. E. Bates, and M. M. Gottesman, "Drug resistance: still a daunting challenge to the successful treatment of AML," *Drug Resistance Updates*, vol. 15, pp. 62–69, 2012.

[6] R. de Souza, P. Zahedi, R. M. Badame, C. Allen, and M. Piquette-Miller, "Chemotherapy dosing schedule influences drug resistance development in ovarian cancer," *Molecular Cancer Therapeutics*, vol. 10, no. 7, pp. 1289–1299, 2011.

[7] A.-C. Hoffmann, P. Wild, C. Leicht et al., "MDR1 and ERCC1 expression predict outcome of patients with locally advanced bladder cancer receiving adjuvant chemotheraphy," *Neoplasia*, vol. 12, no. 8, pp. 628–636, 2010.

[8] J. Bourhis, J. Benard, O. Hartmann, L. Boccon-Gibod, J. Lemerle, and G. Riou, "Correlation of *MDR1 gene* expression with chemotherapy in neuroblastoma," *Journal of the National Cancer Institute*, vol. 81, no. 18, pp. 1401–1405, 1989.

[9] R. C. Bargou, K. Jürchott, C. Wagener et al., "Nuclear localization and increased levels of transcription factor YB-1 in primary human breast cancers are associated with intrinsic *MDR1 gene* expression," *Nature Medicine*, vol. 3, no. 4, pp. 447–450, 1997.

[10] Y. Basaki, F. Hosoi, Y. Oda et al., "Akt-dependent nuclear localization of Y-box-binding protein 1 in acquisition of malignant characteristics by human ovarian cancer cells," *Oncogene*, vol. 26, no. 19, pp. 2736–2746, 2007.

[11] M. Kuwano, Y. Oda, H. Izumi et al., "The role of nuclear Y-box binding protein 1 as a global marker in drug resistance," *Molecular Cancer Therapeutics*, vol. 3, no. 11, pp. 1485–1492, 2004.

[12] T. Ohga, K. Koike, M. Ono et al., "Role of the human Y box-binding protein YB-1 in cellular sensitivity to the DNA-damaging agents cisplatin, mitomycin C, and ultraviolet light," *Cancer Research*, vol. 56, no. 18, pp. 4224–4228, 1996.

[13] V. Evdokimova, P. Ruzanov, M. S. Anglesio et al., "Akt-mediated YB-1 phosphorylation activates translation of silent mRNA species," *Molecular and Cellular Biology*, vol. 26, no. 1, pp. 277–292, 2006.

[14] B. W. Sutherland, J. Kucab, J. Wu et al., "Akt phosphorylates the Y-box binding protein 1 at Ser102 located in the cold shock domain and affects the anchorage-independent growth of breast cancer cells," *Oncogene*, vol. 24, no. 26, pp. 4281–4292, 2005.

[15] A. G. Bader, K. A. Felts, N. Jiang, H. W. Chang, and P. K. Vogt, "Y box-binding protein 1 induces resistance to oncogenic transformation by the phosphatidylinositol 3-kinase pathway," *Proceedings of the National Academy of Sciences of the United States of America*, vol. 100, no. 21, pp. 12384–12389, 2003.

[16] G. Chen, B. A. Teicher, and E. Frei III, "Differential interactions of Pgp inhibitor thaliblastine with adriamycin, etoposide, taxol and anthrapyrazole CI941 in sensitive and multidrug-resistant human MCF-7 breast cancer cells," *Anticancer Research*, vol. 16, no. 6, pp. 3499–3506, 1996.

[17] J. Zhou, M. Liu, R. Aneja, R. Chandra, H. Lage, and H. C. Joshi, "Reversal of P-glycoprotein-mediated multidrug resistance in cancer cells by the c-Jun NH2-terminal kinase," *Cancer Research*, vol. 66, no. 1, pp. 445–452, 2006.

[18] M. Liu, D. Li, R. Aneja et al., "PO2-dependent differential regulation of multidrug resistance 1 gene expression by the c-Jun NH2-terminal kinase pathway," *Journal of Biological Chemistry*, vol. 282, no. 24, pp. 17581–17586, 2007.

[19] G. K. Chen, S. Sale, T. Tan, R. P. Ermoian, and B. I. Sikic, "CCAAT/enhancer-binding protein beta (nuclear factor for interleukin 6) transactivates the human *MDR1 gene* by interaction with an inverted CCAAT box in human cancer cells," *Molecular Pharmacology*, vol. 65, no. 4, pp. 906–916, 2004.

[20] B. Ogretmen and A. R. Safa, "Negative regulation of MDR1 promoter activity in MCF-7, but not in multidrug resistant MCF-7/Adr, cells by cross-coupled NF-κb/p65 and c-Fos transcription factors and their interaction with the CAAT region," *Biochemistry*, vol. 38, no. 7, pp. 2189–2199, 1999.

[21] S.-Y. Katoh, M. Ueno, and N. Takakura, "Involvement of MDR1 function in proliferation of tumour cells," *Journal of Biochemistry*, vol. 143, no. 4, pp. 517–524, 2008.

[22] Y. Yamatake, M. Shibata, and M. Nagai, "Pharmacological studies on root bark of mulberry tree (*Morus alba* L.)," *Japanese Journal of Pharmacology*, vol. 26, no. 4, pp. 461–469, 1976.

[23] S.-Y. Nam, H.-K. Yi, C. L. Jung et al., "Cortex Mori extract induces cancer cell apoptosis through inhibition of microtubule assembly," *Archives of Pharmacal Research*, vol. 25, no. 2, pp. 191–196, 2002.

[24] T. Kikuchi, M. Nihei, H. Nagai et al., "Albanol a from the root bark of *Morus alba* L. induces apoptotic cell death in HL60 human leukemia cell line," *Chemical and Pharmaceutical Bulletin*, vol. 58, no. 4, pp. 568–571, 2010.

[25] S. Park, J. Kim, and Y. Kim, "Mulberry leaf extract inhibits cancer cell stemness in neuroblastoma," *Nutrition and Cancer*, vol. 64, pp. 889–898, 2012.

[26] Y. Yang, T. Gong, C. Liu, and R.-Y. Chen, "Four new 2-arylbenzofuran derivatives from leaves of *Morus alba* L.," *Chemical and Pharmaceutical Bulletin*, vol. 58, no. 2, pp. 257–260, 2010.

[27] Y. Yang, T. Zhang, L. Xiao, L. Yang, and R. Chen, "Two new chalcones from leaves of *Morus alba* L.," *Fitoterapia*, vol. 81, no. 6, pp. 614–616, 2010.

[28] M. Deepa and S. Priya, "Purification and characterization of a novel anti-proliferative lectin from *Morus alba* L. leaves," *Protein & Peptide Letters*, vol. 19, pp. 839–845, 2012.

[29] M. Deepa, T. Sureshkumar, P. K. Satheeshkumar, and S. Priya, "Purified mulberry leaf lectin (MLL) induces apoptosis and cell cycle arrest in human breast cancer and colon cancer cells," *Chemico-Biological Interactions*, vol. 200, pp. 38–44, 2012.

[30] Z. Hu, S. Jin, and K. W. Scotto, "Transcriptional activation of the *MDR1 gene* by UV irradiation: role of NF-Y and Sp1," *Journal of Biological Chemistry*, vol. 275, no. 4, pp. 2979–2985, 2000.

[31] K. Nooter, A. M. Westerman, M. J. Flens et al., "Expression of the multidrug resistance-associated protein (MRP) gene in human cancers," *Clinical Cancer Research*, vol. 1, no. 11, pp. 1301–1310, 1995.

[32] T. Oue, A. Yoneda, S. Uehara, H. Yamanaka, and M. Fukuzawa, "Increased expression of multidrug resistance-associated genes after chemotherapy in pediatric solid malignancies," *Journal of Pediatric Surgery*, vol. 44, no. 2, pp. 377–380, 2009.

[33] S. K. Wattanapitayakul, L. Chularojmontri, A. Herunsalee, S. Charuchongkolwongse, S. Niumsakul, and J. A. Bauer, "Screening of antioxidants from medicinal plants for cardioprotective effect against doxorubicin toxicity," *Basic and Clinical Pharmacology and Toxicology*, vol. 96, no. 1, pp. 80–87, 2005.

[34] F. Yan, X.-M. Wang, Z.-C. Liu, C. Pan, S.-B. Yuan, and Q.-M. Ma, "JNK1, JNK2, and JNK3 are involved in P-glycoprotein-mediated multidrugresistance of hepatocellular carcinoma cells," *Hepatobiliary and Pancreatic Diseases International*, vol. 9, no. 3, pp. 287–295, 2010.

[35] P. M.-K. Tang, D.-M. Zhang, B. N.-H. Xuan et al., "Photodynamic therapy inhibits p-glycoprotein mediated multidrug resistance via JNK activation in human hepatocellular carcinoma using the photosensitizer pheophorbide a," *Molecular Cancer*, vol. 8, article 56, 2009.

[36] H. Bark and C.-H. Choi, "Psc833, cyclosporine analogue, downregulates MDR1 expression by activating JNK/c-Jun/AP-1 and suppressing NF-κB," *Cancer Chemotherapy and Pharmacology*, vol. 65, no. 6, pp. 1131–1136, 2010.

[37] K. Kawasaki, M. Watanabe, M. Sakaguchi et al., "REIC/Dkk-3 overexpression downregulates P-glycoprotein in multidrug-resistant MCF7/ADR cells and induces apoptosis in breast cancer," *Cancer Gene Therapy*, vol. 16, no. 1, pp. 65–72, 2009.

[38] Z.-H. Miao and J. Ding, "Transcription factor c-Jun activation represses mdr-1 gene expression," *Cancer Research*, vol. 63, no. 15, pp. 4527–4532, 2003.

[39] K. M. Comerford, E. P. Cummins, and C. T. Taylor, "c-Jun NH2-terminal kinase activation contributes to hypoxia-inducible factor 1α-dependent P-glycoprotein expression in hypoxia," *Cancer Research*, vol. 64, no. 24, pp. 9057–9061, 2004.

[40] H. Sui, S. Zhou, Y. Wang et al., "COX-2 contributes to P-glycoprotein-mediated multidrug resistance via phosphorylation of c-Jun at Ser63/73 in colorectal cancer," *Carcinogenesis*, vol. 32, no. 5, pp. 667–675, 2011.

Hindawi Publishing Corporation
Evidence-Based Complementary and Alternative Medicine
Volume 2013, Article ID 570428, 8 pages
http://dx.doi.org/10.1155/2013/570428

Research Article

Cervical Coupling Motion Characteristics in Healthy People Using a Wireless Inertial Measurement Unit

Hyunho Kim,[1] Sang-Hoon Shin,[2] Jeong-Kyun Kim,[3] Young-Jae Park,[1,3] Hwan-Sup Oh,[3,4] and Young-Bae Park[1,3]

[1] *Department of Biofunctional Medicine & Diagnostics, College of Korean Medicine, Kyung Hee University, Seoul 130-702, Republic of Korea*
[2] *Department of Oriental Biomedical Engineering, College of Health Science, Sangji University, Wonju 220-702, Republic of Korea*
[3] *Department of Human Informatics of Korean Medicine, Interdisciplinary Programs, Kyung Hee University, Seoul 130-701, Republic of Korea*
[4] *Department of Mechanical Engineering, College of Engineering, Kyung Hee University, Yongin 446-701, Republic of Korea*

Correspondence should be addressed to Young-Bae Park; bmppark@khu.ac.kr

Received 3 April 2013; Accepted 18 June 2013

Academic Editor: Bo-Hyoung Jang

Objective. The objectives were to show the feasibility of a wireless microelectromechanical system inertial measurement unit (MEMS-IMU) to assess the time-domain characteristics of cervical motion that are clinically useful to evaluate cervical spine movement. *Methods*. Cervical spine movements were measured in 18 subjects with wireless IMUs. All rotation data are presented in the Euler angle system. Amount of coupling motions was evaluated by calculating the average angle ratio and the maximum angle ratio of the coupling motion to the primary motion. Reliability is presented with intraclass correlation coefficients (ICC). *Results*. Entire time-domain characteristics of cervical motion were measured with developed MEMS-IMU system. Cervical range of motion (CROM) and coupling motion range were measured with high ICCs. The acquired data and calculated parameters had similar tendency with the previous studies. *Conclusions*. We evaluated cervical motion with economic system using a wireless IMU of high reliability. We could directly measure the three-dimensional cervical motion in degrees in realtime. The characteristics measured by this system may provide a diagnostic basis for structural or functional dysfunction of cervical spine. This system is also useful to demonstrate the effectiveness of any intervention such as conventional medical treatment, and Korean medical treatment, exercise therapy.

1. Introduction

Musculoskeletal disorder is one of the most suitable fields which Korean medicine interventions such as acupuncture or moxibustion can be applied to. Although a myriad of studies have been conducted on the efficacy and effectiveness of complementary and alternative medicine to the acute or chronic musculoskeletal disorders [1–5], studies on the evaluation tools for musculoskeletal motion are very rare. Among the various motions, in particular, cervical motion is biomechanically and neurophysiologically complex and depends on various nonskeletal conditions such as muscular, neuromuscular, proprioceptive, and perceptional conditions [6]. By observing cervical range of motion (CROM) and coupling motion, which occurs on the secondary planes relative to the primary plane, we can examine the stability of the cervical function [6–13]. They are also believed to reflect central nervous motor control strategy [14]. CROM and cervical coupling motion have been studied as important elements to diagnose pathological disorders such as clinical instability due to degeneration, disease, or trauma [6, 7, 10, 15, 16]. But, most studies have only measured the maximum coupling motion angles and did not assess the time-domain characteristics, despite their importance.

A motion capture and analysis device is necessary to analyze the time-domain motion characteristic of a subject.

These measurements traditionally relied on the naked eye, goniometers, inclinometers, and potentiometers; thus, inaccuracies and limitations have existed [17, 18]. But, with highly developed technology, many studies have been attempted with more accurate devices, such as optoelectronic devices [19, 20], electromagnetic field systems [7], or ultrasonic devices [21, 22]. However, these instruments have some disadvantages. First, they require additional space to fix transmitters and receivers in several strictly calculated spots [20]. Second, these devices require a postmeasurement process to interpolate the data or an error-adjusting system because of disturbance or perturbation of signal by obstacles, and this makes it impossible to acquire real-time data, which is one of the most important disadvantages [23]. Third, these devices are too expensive to be used in clinics or hospitals, as they require several types of transmitters and receivers [24]. Furthermore, the transmitters and receivers can be a physical burden to subjects due to their size and mass.

Many studies have been conducted on body-attached inertial measurement units (IMU) to solve these disadvantages. An IMU is a complex-sensor device consisting of a few accelerometers, gyroscopes, magnetometers, and Kalman filters [25–27]. The IMU allows for an easy analysis of rotation movement because it provides the rotation matrix directly, whereas other instruments should calculate the rotation matrix from the absolute coordinates, so the IMU has been used mainly for animation, game design, or in the gait analysis field. The IMU had initial limitations for measuring minute movements of the human body because of its large size, mass, and wired condition [24, 28–30]. But, size and mass have been reduced dramatically to a few cubic millimeters and a few grams with the development of the microelectromechanical system (MEMS) technology, and it is now possible to measure minute movements without disturbance and to obtain precise human body motion data [31–33]. After the IMU was used for motion analysis, many studies about its validity [34, 35], and reliability [23, 36, 37] in comparison with optoelectronic electromagnetic, and ultrasonic instruments were published. Furthermore, the IMU has become more convenient to use after combining the technology with radio frequency (RF) or Bluetooth wireless systems.

The aim of this study is to show the feasibility of the IMU as a measurement device for analyzing CROM and cervical coupling motion by reporting cervical motion time-domain characteristics in healthy subjects judged by the Neck Disability Index (NDI) questionnaire. We also defined and calculated some parameters to assess cervical motion stability. Previous studies have reported the feasibility of the IMU to measure CROM [38, 39], and other studies have reported coupling motion using the electromagnetic tracking system [14, 40], but few or no study has attempted to measure and analyze cervical motion time-domain characteristics with a wireless IMU.

2. Methods

2.1. Equipment. Two wireless IMU modules (model EBIMU24G, E2BOX, Seoul, Republic Korea) and one RF receiver (model EBRF24G3CH, E2BOX) were used to measure cervical motion. This IMU module is very small (32 mm × 21 mm × 6.5 mm), and its mass is 7.85 g with a lithium polymer battery attached. The module consists of a 2.4 GHz ISM band wireless transceiver and nine MEMS sensors (three gyroscopes, three accelerometers, and three magnetometers), with nine degrees of freedom. The sensitivities of the sensors are 250–2000 dps (gyroscope), 2–8 g (accelerometer), and 1.3–8.1 gauss (magnetometer). The static accuracy is $<0.5^{\circ}$, and dynamic accuracy is $<2^{\circ}$ according to the 2012 datasheet provided.

2.2. NDI Questionnaire. NDI is an adaptation of the Oswestry Low Back Pain questionnaire and consists of ten items, including items for evaluating pain, sleep quality, work ability, driving, and daily living ability. A high score indicates high neck function disability. Test-retest reliability for the NDI is 0.89 [41].

2.3. Subjects. Eighteen healthy volunteers were recruited (eight males, eleven females; age, 25–35 years; mean age 27.44 ± 1.89). The subjects were limited to the no- or mild-disability groups as scored by the NDI questionnaire. Subjects were excluded if they had undergone a recent cervical operation or had a disease that could disturb cervical movements. Subjects with 0–4 NDI scores were allocated to the no-disability group, and subjects with 5–14 NDI scores were allocated to the mild-disability group. The mean NDI score of the subjects is 5.65, and the standard deviation is 3.52. The subjects were recruited via advertisements at Kyung Hee University, Oriental Medicine Hospital. This study was approved by the Institutional Review Board of Kyung Hee University, Oriental Medicine Hospital, and all procedures were conducted after informed consent was provided.

2.4. Procedure. Subjects were seated on a fixed chair and cervical movement was measured using two wireless MEMS-IMUs at a sampling frequency of 20 Hz. One sensor was placed on the center of the forehead, and the other was placed on the upper one-third point between the suprasternal notch and the xiphoid process. The sensors were fixed with Velcro straps. The sensor located on the forehead measured head motion, and the other sensor was used to compensate for body trunk movement. Device installation is presented in Figure 1.

After instructed to gaze forward naturally, the subjects were instructed to perform three parts of the test. The first part was an exercise. They were instructed how to rotate their heads on three rotation planes such as the transverse plane for left and right axial rotation, the sagittal plane for extension and flexion, and the coronal plane for left and right bending. Subjects were told that all motions should be performed with an almost fixed speed and to rotate or tilt their head as much as possible. The second part was the natural test. Subjects were asked to perform a very natural motion without thinking about adjusting their motion. The last part was the neutral test. Subjects were asked to try not to create a coupling motion, but to move with their head

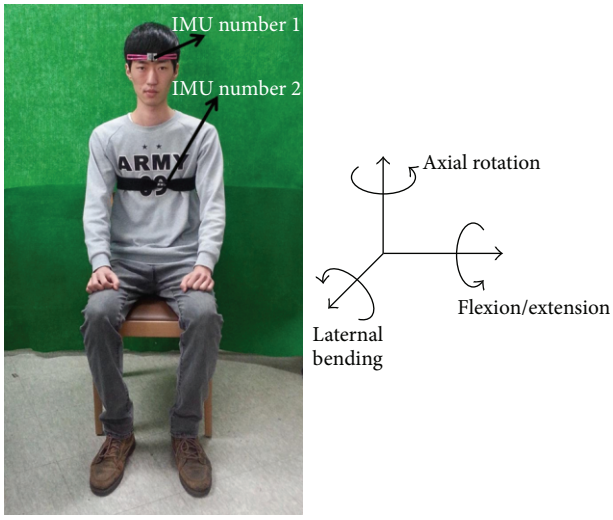

Figure 1: Inertial measurement unit installation and axis presentation.

strictly adjusted. All motions were repeated five times. The subjects were asked to close their eyes during all procedures to remove visual stimulation or auto orientation cues. The sequence of tests and movements were fixed, and verbal instructions were recored once and replayed by a computer system for removing the bias induced by instructors. Data were recorded automatically throughout the testing via an RF wireless system. Calibration was performed before each test and measurement.

2.5. Data Analysis. Cervical motion data were acquired using Lab VIEW 2010 (National Instruments Inc., Austin, TX, USA) in Euler form for the physical intuitiveness of the Euler angle coordinate system. The sequence of Euler angles is roll-pitch-yaw. All statistical calculations were performed using SPSS Statistics 19 (SPSS, Inc., Chicago, IL, USA).

Data from the sensor attached to the thorax were used to compensate for head movements. We normalized the data along the time axis and calculated the area under curve to estimate the amount of motion. We also calculated intraclass correlation coefficients (ICCs) of CROM and maximum angle of coupling motion by using analysis of variance (ANOVA) to assess reliability of the measurement system.

3. Results

3.1. The Cervical Motion Time-Domain Characteristics of One Subject. Figure 2 shows an example of the cervical motion time-domain characteristics on the natural test. The three curves in the graph are each Euler angle components. The red curve in Figure 2(a) indicates extension and flexion on the sagittal plane, which are primary motions, and the blue and green curves indicate rotation on the coronal and transverse planes, which are the coupling motions in this case. The colored curves in Figures 2(b) and 2(c) represent the same motions as shown in Figure 2(a). Positive values indicate flexion, right lateral bending, and right axial rotation, whereas

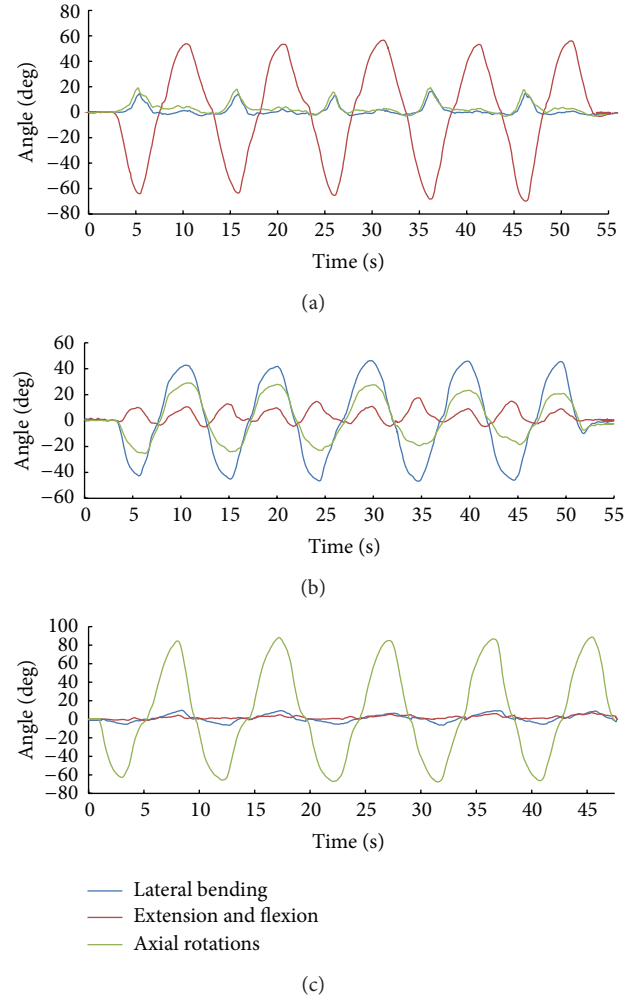

Figure 2: An example of three-dimensional cervical motion patterns described in the Euler rotation coordinates. (a) Measurement when extension and flexion are primary motions. (b) Measurement when lateral bending is primary motions. (c) Measurement when axial rotations are primary motions. Positive values represent flexion, right side bending, and right axial rotation.

negative values indicate extension, left lateral bending, and left axial rotation. As shown in Figure 2(a), this subject shows right axial rotation and right lateral bending of about 20 degrees during an extension, whereas almost no rotation or side bending during a flexion. He shows large and complex coupling movement during side bending (Figure 2(b)) but shows little coupling motion of under 10 degrees during axial rotation (Figure 2(c)).

3.2. CROM and Maximum Coupling Motion. Similar to traditional instruments, this system can measure the CROM and maximum coupling motion angle. Table 1 shows the means and standard deviations of the measured CROMs on the natural and neutral tests. We can observe a tendency that the CROMs on the neutral test are less than the CROMs on the natural test. The calculated ICCs of measuring CROM are high (>0.95). The maximum coupling motion angles on the

Table 1: Cervical range of motion on the natural test and the neutral test.

Plane	Movement	Natural test (°)		Neutral test (°)	
		Mean ± SD	ICC (95% CI)	Mean ± SD	ICC (95% CI)
Sagittal	Total	116.70 ± 17.26	0.98 (0.96–0.99)	106.76 ± 20.33	0.99 (0.97–1.00)
	Extension	57.23 ± 8.80	0.97 (0.93–0.99)	52.75 ± 9.25	0.95 (0.90–0.98)
	Flexion	58.48 ± 11.83	0.98 (0.96–0.99)	54.02 ± 13.46	0.98 (0.97–0.99)
Coronal	Total	89.42 ± 10.11	0.97 (0.95–0.99)	83.69 ± 13.79	0.99 (0.98–1.00)
	Left	44.15 ± 6.72	0.97 (0.93–0.99)	42.17 ± 7.33	0.98 (0.96–0.99)
	Right	45.28 ± 4.97	0.98 (0.95–0.99)	41.52 ± 7.11	0.98 (0.97–0.99)
Transverse	Total	143.29 ± 17.02	0.99 (0.97–0.99)	134.87 ± 22.43	0.98 (0.97–0.99)
	Left	69.67 ± 10.87	0.99 (0.97–0.99)	64.89 ± 11.74	0.98 (0.96–0.99)
	Right	73.62 ± 10.81	0.99 (0.97–0.99)	69.98 ± 13.99	0.99 (0.98–1.00)

SD: standard deviation; ICC: intraclass correlation coefficient; CI: confidence interval.

Table 2: Maximum angle of coupling motions on the natural test and the neutral test.

Primary	Coupling	Natural test (°)		Neutral test (°)	
		Mean ± SD	ICC (95% CI)	Mean ± SD	ICC (95% CI)
Extension	Lateral bending	7.50 ± 4.93	0.95 (0.90–0.98)	5.79 ± 3.60	0.97 (0.93–0.99)
	Axial rotations	8.44 ± 4.56	0.94 (0.88–0.98)	6.52 ± 2.75	0.83 (0.65–0.94)
Flexion	Lateral bending	7.63 ± 5.56	0.98 (0.97–0.99)	5.61 ± 3.08	0.94 (0.87–0.98)
	Axial rotations	7.89 ± 4.31	0.97 (0.94–0.99)	6.18 ± 2.63	0.86 (0.70–0.95)
Left bending	Extension and flexion	13.14 ± 6.22	0.95 (0.90–0.98)	9.93 ± 4.86	0.96 (0.93–0.99)
	Axial rotations	12.21 ± 5.78	0.93 (0.85–0.97)	12.35 ± 5.71	0.95 (0.90–0.98)
Right bending	Extension and flexion	7.72 ± 3.25	0.90 (0.78–0.96)	6.22 ± 2.74	0.93 (0.86–0.97)
	Axial rotations	14.92 ± 6.86	0.97 (0.94–0.99)	14.19 ± 7.34	0.97 (0.95–0.99)
Left rotation	Lateral bending	7.59 ± 4.20	0.97 (0.94–0.99)	5.59 ± 3.12	0.95 (0.91–0.98)
	Extension and flexion	7.38 ± 3.78	0.96 (0.92–0.98)	6.40 ± 3.05	0.94 (0.88–0.98)
Right rotation	Lateral bending	7.09 ± 3.31	0.97 (0.94–0.99)	6.34 ± 3.58	0.96 (0.92–0.99)
	Extension and flexion	7.52 ± 3.32	0.97 (0.93–0.99)	6.22 ± 3.52	0.96 (0.91–0.98)

SD: standard deviation; ICC: intraclass correlation coefficient; CI: confidence interval.

two tests are presented in Table 2 with their ICCs. The average ICC of measuring coupling motion on the natural test is 0.96, and that on the neutral test is 0.94.

3.3. Average Angle Ratio and Maximum Angle Ratio of Coupling Motion. We set up a parameter, amount of motion, as area under curve. We can calculate the average angle ratio of coupling motion to the primary motion with this amount of motion. This concept is shown in Figure 3. The amount of motion was thought to be proportional to the area under curve from the initial position to the maximum angle because returning from the maximum rotation point is affected by the previously occurred coupling motion. After the area was calculated, it was normalized along the time axis for adjusting the duration difference in each measurement. By normalization along the time axis, we obtained the average coupling motion angle and calculated the average angle ratio of coupling motion to the primary motion. The average angle ratio and maximum angle ratio of coupling motion are shown in Table 3.

4. Discussion

4.1. Measurements with the Wireless IMU System. We designed and constructed a wireless IMU system to measure cervical motion to overcome the physical, time, and economic disadvantages of prior instruments [20, 23, 24]. The objective of this study was to demonstrate the feasibility of this wireless IMU system to evaluate stability and describe cervical motion. Tables 1 and 2 show the ICCs of this measurement system. The ICCs of the CROM measurements are >0.97 except for one case, and those of the coupling motions are >0.90 except for two cases. This indicates the high reliability of this measurement system and this methodology to measure the cervical motions. ICCs of the coupling motion measurement are generally slightly less than those of the CROM measurements. This could mean that coupling motions cannot be controlled strictly, or a little fluctuation of coupling motion may be occurred in every trial. Nevertheless, the reliability of this system is still high.

Previous studies reported the ICCs of prior instruments. ICC values were >0.791 for measuring CROM and were >0.40

Table 3: Average angle ratio and maximum angle ratio of coupling motions on the natural test and the neutral test.

Primary	Coupling	AAR (mean ± SD)		MAR (mean ± SD)	
		Natural test	Neutral test	Natural test	Neutral test
Extension	Lateral bending	0.09 ± 0.05	0.09 ± 0.06	0.13 ± 0.09	0.11 ± 0.07
	Axial rotations	0.14 ± 0.09	0.13 ± 0.07	0.15 ± 0.08	0.13 ± 0.06
Flexion	Lateral bending	0.10 ± 0.06	0.09 ± 0.04	0.12 ± 0.08	0.10 ± 0.05
	Axial rotations	0.12 ± 0.07	0.12 ± 0.09	0.13 ± 0.06	0.12 ± 0.06
Left bending	Extension and flexion	0.27 ± 0.13	0.22 ± 0.13	0.30 ± 0.14	0.24 ± 0.12
	Axial rotations	0.29 ± 0.16	0.16 ± 0.11	0.28 ± 0.12	0.30 ± 0.13
Right bending	Extension and flexion	0.16 ± 0.09	0.29 ± 0.15	0.17 ± 0.07	0.15 ± 0.07
	Axial rotations	0.34 ± 0.18	0.37 ± 0.25	0.34 ± 0.16	0.35 ± 0.19
Left rotation	Extension and flexion	0.09 ± 0.06	0.08 ± 0.04	0.11 ± 0.06	0.08 ± 0.04
	Lateral bending	0.11 ± 0.06	0.12 ± 0.09	0.10 ± 0.05	0.10 ± 0.05
Right rotation	Extension and flexion	0.09 ± 0.05	0.08 ± 0.04	0.09 ± 0.04	0.09 ± 0.04
	Lateral bending	0.13 ± 0.08	0.12 ± 0.09	0.10 ± 0.05	0.09 ± 0.06

SD: standard deviation; AAR: average angle ratio; MAR: Maximum angle ratio.

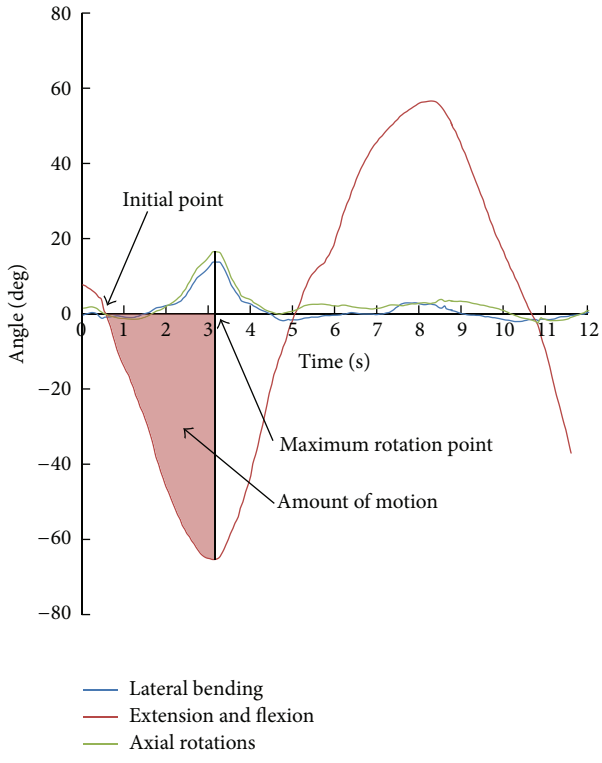

Figure 3: Amount of motion as area under curve. The amount of rotation is defined as the area under curve from the initial point to the maximum rotation point. This area was used to calculate the average angle of coupling motion. Positive values represent flexion, right side bending, and right axial rotation. In this case, there is little coupling motion in flexion.

for measuring coupling motions using a three-dimensional electromagnetic motion tracking device [13]. In some cases, almost all ICC values were <0.75 when coupling motion was measured using a three-dimensional electromagnetic motion tracking device [40]. ICCs using the three-dimensional kinematic method were reported >0.74 [42]. A study that measured CROMs with a wired IMU reported ICCs of 0.79–0.99 [38]. Comparing the ICCs of the IMU systems and the prior instruments, the test-retest reliability of the IMU system is relatively very high whether wired or wireless condition. This shows the potential possibility of a wireless IMU system in measuring and evaluating stability or function of the various musculoskeletal joint systems.

4.2. Parameters to Analyze the Time-Domain Characteristics. CROM is one of the most well-investigated physical parameter [9] and measuring CROM is important clinically [7, 43]. Additionally, the coupling motion behavioral pattern is also clinically important to diagnose disorders such as degeneration, disease, trauma, or dislocation [6–13]. CROMs in healthy subjects were measured in our study (Table 1), and there is a similar tendency with the previous studies [6, 40]. This result may suggest the possibility of high concurrent validity of this system.

Previous studies reported only maximum values of coupling motion and did not discuss the entire pattern or the time-domain characteristics of coupling motion. Discussion about the entire coupling motion pattern is essential, because the starting point, increasing slope, average coupling angles, and its fluctuation also have clinical information that which muscles are recruited, which nerves are activated, and what pattern the motor control is fulfilled in. The time-domain characteristics of coupling motion can give qualitative and clinical clues about these questions. For example, if coupling motions simultaneously occur with the primary rotation, this case has clinically obvious difference from the case that coupling motions occur after some primary rotation or especially near the maximum point of the primary rotation. But if only maximum angles of coupling motions are reported, the two different cases cannot be distinguished. Likewise, amount of the coupling motion must be considered with amount of the primary motion, because cases of same amount of coupling motion with different maximum range of primary motions

must be discussed separately. Cervical movement with more primary ROM in normal range can be understood to have better function or motor control strategy than one with less primary ROM in case that those two have the same amount of coupling motion.

We defined and calculated amount of motion with area under curve to consider the time-domain characteristic including rotation angle and time duration. In addition, to consider the primary motion amount, we defined average angle ratio as the ratio of average coupling motion angle to average primary motion angle. Therefore, one primary motion has two angle ratios according to the two secondary planes (Table 3). Average angle ratios of the coupling motion are large when the primary motion is lateral bending. Maximum angle ratios in primary lateral bending are approximate 30%, and those in primary axial rotations are approximate 10%. These values resemble the results of the previous study that used the prior instruments [10, 44].

4.3. Clinical Values of Evaluating the Coupling Motion. Coupling motion generally occurs in healthy subjects, because one motion recruit various muscles. For example, the rectus capitis posterior major, oblique capitis inferior and superior, and splenius muscles are recruited as intrinsic rotators when rotating the head, and the sternocleidomastoid, scalene, upper trapezius, and levator scapular muscles are recruited as extrinsic rotators. Among these, sternocleidomastoid muscle, anterior and middle scalene muscles act as extrinsic flexor muscles. Similarly, the upper trapezius and levator scapular muscles are also extrinsic extensor muscles. So, flexion or extension can occur simultaneously during axial rotation, according to the central nervous system motor control strategies. Coupling motion on the neutral test reflects these inevitably integrated muscle movements because subjects intended to make rotations strictly on only one plane in neutral test. Excessive or distorted coupling motion can occur in asymptotic subjects, who have no clinical symptom such as pain or ROM limitation, because the coupling motion can be a protective postural strategy to avoid pain [14].

We should not directly diagnose muscle or nerve problems only using the amount of coupling motion. Instead, we could observe the entire cervical motion with this measurement system, and by doing so, we could calculate parameters including time-domain information and consider the entire curve for diagnosing diseases or observing progress. A direct correlation between coupling motion pattern and specific musculoskeletal or nervous problem can be estimated if the coupling motion patterns are analyzed by pattern analysis or other data-mining methods, or if imaging studies such as X-ray, computed tomography, or magnetic resonance imaging are combined with this system.

This technique can also be applied to various joint systems, which enables clinicians or physical therapists to evaluate various joint functions, to examine the effect of clinical interventions including complementary and alternative medical treatments, and to preventively care for patients by correcting movement habits. If the proper biofeedback systems are combined with this real-time evaluation, therapeutic approach can be made in the musculoskeletal or neurological rehabilitation fields.

4.4. Limitations. We used the NDI index to include only the no- and mild-disability group, but this questionnaire has limitation of being unable to filter out pain-avoidance by creating excessive or limited cervical coupling motion. Although other studies reported an age effect on cervical motion [44, 45], we could not reproduce this effect because the subjects were 25–35 years of age.

5. Conclusion

We developed a measurement system using a wireless IMU to evaluate cervical motion quantitatively and qualitatively. Using this system, we were able to measure CROM and coupling motion in real time, so we could observe the entire characteristics of the coupling motions. We calculated the average angle ratios and maximum angle ratio of coupling motions to evaluate the time-domain motion characteristics. These parameters may provide accurate rotation movement data and diagnostic basis for structural or functional dysfunction of the cervical spine with further studies. High test-retest reliability, the resemblance of the results with the previous studies, and the economic advantages of this system may present the potential utility of this system in many aspects.

Conflict of Interests

The authors have declared that no competing interests exist.

Authors' Contribution

Hyunho Kim and Sang-Hoon Shin equally contributed to this paper.

References

[1] H. Lee, J. H. Lee, T. Y. Choi, M. S. Lee, H. Lee, and B. C. Shin, "Acupuncture for acute low back pain: a systematic review," *Clinical Journal of Pain*, vol. 29, no. 2, pp. 172–185, 2013.

[2] M. Xu, S. Yan, X. Yin et al., "Acupuncture for chronic low back pain in long-term follow-up: a meta-analysis of 13 randomized controlled trials," *American Journal of Chinese Medicine*, vol. 41, no. 1, pp. 1–19, 2013.

[3] H. Kwak, J. Kim, J. Park et al., "Acupuncture for Whiplash-associated disorder: a randomized, waiting-list controlled, pilot trial," *European Journal of Integrative Medicine*, vol. 4, no. 2, pp. e151–e158, 2012.

[4] Y. Tobbackx, M. Meeus, L. Wauters et al., "Does acupuncture activate endogenous analgesia in chronic whiplash-associated disorders? A randomized crossover trial," *European Journal of Pain*, vol. 17, no. 2, pp. 279–289, 2013.

[5] A. J. P. Hutchinson, S. Ball, J. C. H. Andrews, and G. G. Jones, "The effectiveness of acupuncture in treating chronic non-specific low back pain: a systematic review of the literature," *Journal of Orthopaedic Surgery and Research*, vol. 7, no. 1, article 36, 2012.

[6] E. Malmström, M. Karlberg, P. A. Fransson, A. Melander, and M. Magnusson, "Primary and coupled cervical movements: the effect of age, gender, and body mass index. A 3-dimensional movement analysis of a population without symptoms of neck disorders," *Spine*, vol. 31, no. 2, pp. E44–E50, 2006.

[7] C. L. Koerhuis, J. C. Winters, F. C. T. van der Helm, and A. L. Hof, "Neck mobility measurement by means of the "Flock of Birds" electromagnetic tracking system," *Clinical Biomechanics*, vol. 18, no. 1, pp. 14–18, 2003.

[8] K. M. Hermann, C. S. Reese, and A. M. Jette, "Relationships among selected measures of impairment, functional limitation, and disability in patients with cervical spine disorders," *Physical Therapy*, vol. 81, no. 3, pp. 903–912, 2001.

[9] N. Strimpakos, V. Sakellari, G. Gioftsos et al., "Cervical spine ROM measurements: optimizing the testing protocol by using a 3D ultrasound-based motion analysis system," *Cephalalgia*, vol. 25, no. 12, pp. 1133–1145, 2005.

[10] V. Feipel, B. Rondelet, J. Le Pallec, and M. Rooze, "Normal global motion of the cervical spine: an electrogoniometric study," *Clinical Biomechanics*, vol. 14, no. 7, pp. 462–470, 1999.

[11] S. Lee, E. R. C. Draper, and S. P. F. Hughes, "Instantaneous center of rotation and instability of the cervical spine: a clinical study," *Spine*, vol. 22, no. 6, pp. 641–648, 1997.

[12] C. Cook, E. Hegedus, C. Showalter, and P. S. Sizer Jr., "Coupling behavior of the cervical spine: a systematic review of the literature," *Journal of Manipulative and Physiological Therapeutics*, vol. 29, no. 7, pp. 570–575, 2006.

[13] L. Guo, S. Lee, C. Lin et al., "Three-dimensional characteristics of neck movements in subjects with mechanical neck disorder," *Journal of Back and Musculoskeletal Rehabilitation*, vol. 25, no. 1, pp. 47–53, 2012.

[14] A. Woodhouse and O. Vasseljen, "Altered motor control patterns in whiplash and chronic neck pain," *BMC Musculoskeletal Disorders*, vol. 9, article 90, 2008.

[15] M. J. Pearcy and S. B. Tibrewal, "Axial rotation and lateral bending in the normal lumbar spine measured by three-dimensional radiography," *Spine*, vol. 9, no. 6, pp. 582–587, 1984.

[16] M. M. Panjabi, T. Oda, J. J. Crisco III, J. Dvorak, and D. Grob, "Posture affects motion coupling patterns of the upper cervical spine," *Journal of Orthopaedic Research*, vol. 11, no. 4, pp. 525–536, 1993.

[17] C. A. Buck, F. B. Dameron, M. J. Dow, and H. V. Skowlund, "Study of normal range of motion in the neck utilizing a bubble goniometer," *Archives of Physical Medicine and Rehabilitation*, vol. 40, pp. 390–392, 1959.

[18] D. Capuano-Pucci, W. Rheault, J. Aukai, M. Bracke, R. Day, and M. Pastrick, "Intratester and intertester reliability of the cervical range of motion device," *Archives of Physical Medicine and Rehabilitation*, vol. 72, no. 5, pp. 338–340, 1991.

[19] K. Canseco, C. Albert, J. Long, M. Khazzam, R. Marks, and G. F. Harris, "Postoperative foot and ankle kinematics in rheumatoid arthritis," *Journal of Experimental and Clinical Medicine*, vol. 3, no. 5, pp. 233–238, 2011.

[20] A. A. A. Rahni and I. Yahya, "Obtaining translation from a 6-DOF MEMS IMU—an overview," in *Proceedings of the Asia-Pacific Conference on Applied Electromagnetics (APACE '07)*, article 4603861, December 2007.

[21] W. H. M. Castro, A. Sautmann, M. Schilgen, and M. Sautmann, "Noninvasive three-dimensional analysis of cervical spine motion in normal subjects in relation to age and sex: an experimental examination," *Spine*, vol. 25, no. 4, pp. 443–449, 2000.

[22] K. Park, H. Cynn, O. Kwon et al., "Effects of the abdominal drawing-in maneuver on muscle activity, pelvic motions, and knee flexion during active prone knee flexion in patients with lumbar extension rotation syndrome," *Archives of Physical Medicine and Rehabilitation*, vol. 92, no. 9, pp. 1477–1483, 2011.

[23] P. Y. M. Chung and G. Y. F. Ng, "Comparison between an accelerometer and a three-dimensional motion analysis system for the detection of movement," *Physiotherapy*, vol. 98, no. 3, pp. 256–259, 2011.

[24] T. Liu, Y. Inoue, K. Shibata, and X. Tang, "A wearable inertial sensor system for human motion analysis," in *Proceedings of the IEEE International Symposium on Computational Intelligence in Robotics and Automation (CIRA '05)*, pp. 409–413, June 2005.

[25] S. Sessa, M. Zecca, Z. Lin et al., "Ultra-miniaturized WB-3 Inertial Measurement Unit: performance evaluation of the attitude estimation," in *Proceedings of the IEEE International Conference on Robotics and Biomimetics (ROBIO '10)*, article 5723462, pp. 998–1003, December 2010.

[26] Z. Lin, M. Zecca, S. Sessa et al., "Development of an ultra-miniaturized inertial measurement unit WB-3 for human body motion tracking," in *Proceedings of the 3rd IEEE/SICE International Symposium on System Integration (SII '10)*, article 5708361, pp. 414–419, December 2010.

[27] A. M. Sabatini, C. Martelloni, S. Scapellato, and F. Cavallo, "Assessment of walking features from foot inertial sensing," *IEEE Transactions on Biomedical Engineering*, vol. 52, no. 3, pp. 486–494, 2005.

[28] A. Godfrey, R. Conway, D. Meagher, and G. ÓLaighin, "Direct measurement of human movement by accelerometry," *Medical Engineering and Physics*, vol. 30, no. 10, pp. 1364–1386, 2008.

[29] F. Ochi, K. Abe, S. Ishigami, K. Otsu, and H. Tomita, "Trunk motion analysis in walking using gyro sensors," in *Proceedings of the 1997 19th Annual International Conference of the IEEE Engineering in Medicine and Biology Society*, vol. 4, pp. 1824–1825, November 1997.

[30] L. Tao, Y. Inoue, K. Shibata, and H. Morioka, "Development of wearable sensor combinations for human lower extremity motion analysis," in *Proceedings of the IEEE International Conference on Robotics and Automation (ICRA '06)*, article 1641944, pp. 1655–1660, May 2006.

[31] K. Saber-Sheikh, E. C. Bryant, C. Glazzard, A. Hamel, and R. Y. W. Lee, "Feasibility of using inertial sensors to assess human movement," *Manual Therapy*, vol. 15, no. 1, pp. 122–125, 2010.

[32] D. Cardarelli, "An integrated MEMS inertial measurement unit," in *Proceedings of the 2002 IEEE Position Location and Navigation Symposium*, pp. 314–319, Palm Springs, Calif, USA, April 2002.

[33] A. Warnasch and A. Killen, "Low cost, high G, Micro Electro-Mechanical Systems (MEMS), Inertial Measurements Unit (IMU) program," in *Proceedings of the 2002 IEEE Position Location and Navigation Symposium*, pp. 299–305, April 2002.

[34] T. Ito, "Walking motion analysis using 3D acceleration sensors," in *Proceedings of the 2nd UKSim European Symposium on Computer Modelling and Simulation (EMS '08)*, article 4625258, pp. 123–128, September 2008.

[35] J. J. Kavanagh and H. B. Menz, "Accelerometry: a technique for quantifying movement patterns during walking," *Gait and Posture*, vol. 28, no. 1, pp. 1–15, 2008.

[36] R. Moe-Nilssen, "Test-retest reliability of trunk accelerometry during standing and walking," *Archives of Physical Medicine and Rehabilitation*, vol. 79, no. 11, pp. 1377–1385, 1998.

[37] M. Henriksen, H. Lund, R. Moe-Nilssen, H. Bliddal, and B. Danneskiod-Samsøe, "Test-retest reliability of trunk accelerometric gait analysis," *Gait and Posture*, vol. 19, no. 3, pp. 288–297, 2004.

[38] P. S. Theobald, M. D. Jones, and J. M. Williams, "Do inertial sensors represent a viable method to reliably measure cervical spine range of motion?" *Manual Therapy*, vol. 17, no. 1, pp. 92–96, 2012.

[39] J. M. Jasiewicz, J. Treleaven, P. Condie, and G. Jull, "Wireless orientation sensors: their suitability to measure head movement for neck pain assessment," *Manual Therapy*, vol. 12, no. 4, pp. 380–385, 2007.

[40] L. Guo, C. Yang, C. Yang, Y. Hou, J. Chang, and W. Wu, "The feasibility of using electromagnetic motion capture system to measure primary and coupled movements of cervical spine," *Journal of Medical and Biological Engineering*, vol. 31, no. 4, pp. 245–254, 2011.

[41] H. Vernon and S. Mior, "The neck disability index: a study of reliability and validity," *Journal of Manipulative and Physiological Therapeutics*, vol. 14, no. 7, pp. 409–415, 1991.

[42] M. V. Bulgheroni, F. Antonaci, S. Ghirmai, G. Sandrini, G. Nappi, and A. Pedotti, "A 3D kinematic method for evaluating voluntary movements of the cervical spine in humans," *Functional Neurology*, vol. 13, no. 3, pp. 239–245, 1998.

[43] H. Lee, L. L. Nicholson, and R. D. Adams, "Cervical range of motion associations with subclinical neck pain," *Spine*, vol. 29, no. 1, pp. 33–40, 2004.

[44] C. Sforza, G. Grassi, N. Fragnito, M. Turci, and V. F. Ferrario, "Three-dimensional analysis of active head and cervical spine range of motion: effect of age in healthy male subjects," *Clinical Biomechanics*, vol. 17, no. 8, pp. 611–614, 2002.

[45] J. W. Youdas, T. R. Garrett, V. J. Suman, C. L. Bogard, H. O. Hallman, and J. R. Carey, "Normal range of motion of the cervical spine: an initial goniometric study," *Physical Therapy*, vol. 72, no. 11, pp. 770–780, 1992.

Hindawi Publishing Corporation
Evidence-Based Complementary and Alternative Medicine
Volume 2013, Article ID 824270, 4 pages
http://dx.doi.org/10.1155/2013/824270

Research Article

The Evaluation of CP-001 (a Standardized Herbal Mixture of *Houttuynia cordata*, *Rehmannia glutinosa*, *Betula platyphylla*, and *Rubus coreanus*) for Cytochrome P450-Related Herb-Drug Interactions

Hye Hyun Yoo,[1] Sun-A Kim,[1] In Sook Kim,[1] and Seong-Gyu Ko[2]

[1] *Institute of Pharmaceutical Science and Technology and College of Pharmacy, Hanyang University, Ansan, Gyeonggi-do 426-791, Republic of Korea*
[2] *Laboratory of Clinical Biology and Pharmacogenomics, Department of Preventive Medicine, College of Oriental Medicine, Kyung Hee University, Seoul 130-701, Republic of Korea*

Correspondence should be addressed to Seong-Gyu Ko; epiko@khu.ac.kr

Received 5 April 2013; Revised 11 June 2013; Accepted 13 June 2013

Academic Editor: Bo-Hyoung Jang

In the present study, the effect of CP-001, a standardized herbal mixture of *Houttuynia cordata*, *Rehmannia glutinosa*, *Betula platyphylla*, and *Rubus coreanus*, on cytochrome P450 (CYP) enzyme-mediated drug metabolism was investigated *in vitro* to evaluate the potential for herb-drug interactions. CP-001 was tested at concentrations of 1, 3, 10, 30, and 100 μg/mL. A CYP-specific substrate mixture was incubated with CP-001 in human liver microsomes, and the metabolites generated by each CYP-specific metabolic reaction were measured by liquid chromatography-tandem mass spectrometry. CP-001 seemed to slightly inhibit some CYP isozymes, but the IC_{50} values for all CYP isozymes were greater than 100 μg/mL. Furthermore, CP-001 did not exhibit time-dependent CYP inhibitory activities, indicating that it does not act as a mechanism-based inactivator of CYP enzymes. In conclusion, the effects of CP-001 on CYP isozyme activities were negligible at the concentrations tested. Therefore, the likelihood of herbal mixture-drug interaction is considered minimal.

1. Introduction

Herbal medicines are increasingly being used as alternative medicines worldwide. Consequently, it is very likely that some patients will take herbal medicines in combination with prescription or conventional medications, which may lead to unexpected adverse effects caused by herb-drug interactions. There may be many mechanisms underlying various herb-drug interactions, but the representative mechanism is an alteration of the absorption, metabolism, or clearance of coadministered drugs by the herb. Many herbs can induce or inhibit drug metabolizing enzymes such as cytochrome P450 (CYP450), altering the pharmacokinetics of the coadministered drugs and subsequently reducing their pharmacological effects or causing toxicity [1, 2]. For these reasons, evaluations of herb-drug interactions associated with drug metabolizing enzymes are necessary to ensure the safety of the concomitant use of herbal medicines.

CP-001 is a standardized herbal mixture of *Rehmannia glutinosa, Houttuynia cordata, Rubus coreanus,* and *Betula platyphylla*. *R. glutinosa* has traditionally been used to treat hemostasis, activate blood circulation, and improve kidney function in East Asian countries [2]. It has been reported that *R. glutinosa* has antiallergy effects [3] and anti-inflammatory functions [4–6]. *H. cordata* has been used to treat inflammatory diseases in traditional oriental medicine, and it has been reported to possess several pharmacological activities such as anti-inflammatory, antiviral, and anticancer effects [7–9]. *R. coreanus* is a type of raspberry, the fruits of which have traditionally been used for the treatment of asthma and allergy in Asian countries and have anti-inflammatory and antioxidative activities.

Table 1: Information on the CYP-specific substrates used and the metabolites monitored in this study.

P450 isozyme	Marker substrate	Concentration	Metabolites monitored	Q1/Q3
CYP 1A2	Phenacetin	40 μM	Acetaminophen	152.1/110.1
CYP 2A6	Coumarin	2.5 μM	7-OH-Coumarin	162.9/106.9
CYP 2D6	Dextromethorphan	5 μM	Dextrorphan	258.3/157.1
CYP 2C9	Diclofenac	10 μM	4-OH-Diclofenac	312.2/230.9
CYP 2C19	(±)-Mephenytoin	160 μM	4-OH-Mephenytoin	235/150.1
CYP 3A4	Midazolam	2.5 μM	1-OH-Madazolam	343.1/325.1
Internal standard			Terfenadine	472.4/436.4

Recently, in our pharmacological assay, CP-001 exhibited a synergistic therapeutic effect on atopic dermatitis (AD). This herbal mixture is currently under development as a therapeutic agent for the treatment of AD. Therefore, a preclinical evaluation of potential herb-drug interactions was required. In this study, the effects of CP-001 on CYP450-mediated drug metabolism was evaluated to predict the CYP450-related herb-drug interactions.

2. Materials and Methods

2.1. Chemicals and Reagents. CP-001 was provided by Hanpoong Pharm & Foods Co., Ltd. (Jeonju, Rebiblic of Korea). CP-001 was standardized to contain 1.25% catalpol, 0.26% quercitrin, and 0.42% ellagic acid. Pooled human liver microsomes were purchased from BD Gentest (Woburn, MA, USA). Glucose-6-phospate, β-NADP$^+$, glucose-6-phospate dehydrogenase, phenacetin, coumarin, diclofenac, mephenytoin, dextromethorphan, midazolam, furafylline, methoxsalen, sulfaphenazole, ticlopidine, quinidine, ketoconazole, and terfenadine were obtained from Sigma Chemical Co. (St. Louis, MO, USA). Formic acid was purchased from Merck (Darmstadt, Germany). All other solvents used were of HPLC grade and were purchased from J. T. Baker (Phillipsburg, NJ, USA). Distilled water was prepared using a MilliQ purification system (Millipore, Billerica, MA, USA).

2.2. CYP Inhibition Assay. The CYP inhibition assay was performed with 0.5 mg/mL human liver microsomes in a final incubation volume of 0.2 mL. The incubation mixtures consisted of various concentrations of CP-001 (1, 3, 10, 30, and 100 μg/mL in methanol), an NADPH-generating system (NGS) containing 0.1 M glucose-6-phosphate, 10 mg/mL β-NADP$^+$, and 1.0 U/mL glucose-6-phosphate dehydrogenase and a substrate mixture (Table 1) in 0.1 M potassium phosphate buffer (pH 7.4). The incubation mixture was incubated at 37°C without NGS for 5 min and then continuously incubated for 30 min with NGS in a water bath. Well-known selective CYP inhibitors were tested as positive controls (10 μM furafylline for CYP1A2; 20 μM methoxsalen for CYP2A6; 50 μM sulfaphenazole for CYP2C9; 20 μM ticlopidine for CYP2C19; 50 μM quinidine for CYP2D6; 5 μM ketoconazole for CYP3A4). After the incubation, the reaction was stopped by adding 400 μL of 0.1% acetic acid containing 4 μL of an internal standard solution (16 μM terfenadine in DMSO). To test the possibility of mechanism-based inactivation, 0.5 mg/mL human liver microsomes was preincubated with various concentrations of CP-001 (1, 3, 10, 30, and 100 μg/mL) in 0.1 M potassium phosphate buffer (pH 7.4) for 30 min in the presence of NGS. After the preincubation, the substrate mixture was added, and the solution was continuously incubated for 30 min. The rest of the procedure was performed as described previously.

2.3. Sample Preparation. The incubation mixtures were passed through activated Sep-Pak C_{18} cartridges (96-well OASIS HLB extraction cartridge, Waters, Milford, MA, USA). The cartridges were activated with methanol (1 mL) and 0.1% acetic acid in distilled water (2 mL). After sample loading, the cartridges were washed twice with 1 mL 0.1% acetic acid in distilled water and eluted with 1 mL methanol. After the evaporation of the eluates under nitrogen gas, the residue was redissolved in 100 μL of reconstitution buffer (0.1% formic acid in distilled water : acetonitrile = 85 : 15), and 5 μL aliquots were subjected to liquid chromatography-tandem mass spectrometry (LC-MS/MS).

2.4. LC-MS/MS Analysis. The LC-MS/MS system consisted of an Agilent 1260 series binary pump HPLC system (Agilent Technologies, Palo Alto, CA, USA) and an Agilent 6460 triple quad mass spectrometer (Agilent Technologies, Palo Alto, CA, USA) equipped with an electrospray ionization (ESI) source. A Fortis C_8 column (2.1 mm × 100 mm, 5 μm; Fortis Technologies Ltd., Cheshire, England, UK) was used for the separation. The column temperature was maintained at a constant 40°C using a thermostatically controlled column oven. The HPLC mobile phases consisted of 0.1% formic acid in distilled water (A) and 90% acetonitrile in 0.1% formic acid (B). A gradient program was used for the HPLC separation with a flow rate of 0.2 mL/min. The solvent composition was initially set at 15% B, gradually increased to 85% Bover 3 min, and maintained for 1.5 min, and then the column was reequilibrated for 3.5 min. The entire column eluent was introduced directly into the mass spectrometer. Nitrogen was used both as the nebulizing gas at 20 psi and as the drying gas at a flow rate of 10 L/min at 300°C. The mass spectrometer was operated in positive ion mode. Multiple reaction monitoring (MRM) detection was employed. The precursor-product ion pairs (Q1/Q3) used in MRM mode were presented in Table 1.

Table 2: The effects of CP-001 on the CYP enzyme activities without preincubation.

P450 isozyme	Remaining activities (% of control) CP-001 (μg/mL)					IC50
	1	3	10	30	100	
CYP1A2	101.6	116.1	87.5	95.6	78.3	>100
CYP2A6	83.9	81.4	85.4	88.8	94.2	>100
CYP2D6	84.5	90.1	88.1	80.4	75.2	>100
CYP2C9	122.0	130.1	93.6	111.5	108.0	>100
CYP2C19	79.4	87.1	81.8	76.8	62.0	>100
CYP3A4	87.8	96.1	86.3	88.8	85.2	>100

Table 3: The effects of CP-001 on the CYP enzyme activities with preincubation.

P450 isozyme	Remaining activities (% of control) CP-001 (μg/mL)					IC50
	1	3	10	30	100	
CYP1A2	111.4	98.8	79.3	83.5	70.6	>100
CYP2A6	116.1	106.8	104.9	101.5	96.9	>100
CYP2D6	107.3	109.6	129.2	109.3	98.7	>100
CYP2C9	83.7	96.8	75.5	76.4	69.8	>100
CYP2C19	117.5	109.7	106.3	94.2	75.1	>100
CYP3A4	111.6	109.9	102.3	89.9	75.7	>100

3. Results and Discussion

The inhibitory effects of CP-001 on CYP-specific metabolic activities were evaluated in human liver microsomes. The assay system was tested with well-known selective inhibitors of CYP isozyme (positive controls). The remaining activity of the CYP isozymes after the treatment of each selective inhibitor was as follows: 5.0% for CYP1A2 (furafylline); 8.2% for CYP2A6 (methoxsalen); 5.3% for CYP2C9 (sulfaphenazole); 12.7% for CYP2C19 (ticlopidine); 2.5% for CYP2D6 (quinidine); and 4.5% for CYP3A4 (ketoconazole). All the inhibitors selectively inhibited the corresponding CYP marker activity. When CP-001 was evaluated at concentrations of 1, 3, 10, 30, and 100 μg/mL, CP-001 showed minimal inhibitory effects on all CYP isozymes tested (Table 2), with estimated IC_{50} values above 100 μg/mL, although the enzyme activity of CYP2C19 was slightly inhibited in a concentration-dependent manner. When CP-001 was tested after preincubation with human liver microsomes, the extent of inhibition on several CYP isozyme activities was somewhat different, but the IC_{50} values were all above 100 μg/mL (Table 3), comparable to those without pre-incubation. Therefore, CP-001 is considered to have negligible effects on CYP-mediated drug metabolism as a mechanism-base inhibitor as well as a competitive inhibitor.

There have been several reports on the effects of the herbs contained in CP-001 on CYP catalytic activities [10–12]. Regarding *H. cordata*, decreases in the activities of CYP1A1, CYP2C11, and CYP2E1 were observed in 24 h oxidized frying oil-fed rats after feeding with a diet containing *H. cordata* [10]. However, this study was not conducted to evaluate the herb-drug interaction but rather to evaluate chemopreventive potential as those CYP enzymes could be involved in the activation of precarcinogens or other chronic diseases. *R. glutinosa* was reported to inhibit CYP1A2, CYP2C9, CYP2D6, CYP2E1, and CYP3A4 *in vitro* in a concentration-dependent manner, but significant inhibition was only observed at a relatively high concentration (1 mg/mL), which is difficult to reach in a clinical setting [11]. There was a report on the effects of *R. coreanus* on CYP3A activity, but the effect was not so considerable [12]. The effects of *B. platyphylla* on CYP-mediated drug metabolism have not yet been reported.

In conclusion, we have evaluated the inhibitory potential of CP-001 on human CYP enzyme activities *in vitro* as a part of preclinical ADME studies. The present results indicate that CP-001 may not interact with coadministered drugs by modulating CYP-mediated metabolism. However, the results of *in vitro* tests are not necessarily consistent with *in vivo* findings. Therefore, continuous monitoring of herb-drug interactions along with pharmacokinetics studies may be required through subsequent clinical stages.

Acknowledgment

This study was supported by a Grant of the Traditional Korean Medicine R&D Project of the Ministry for Health and Welfare, Republic of Korea (B110017 and B110043).

References

[1] B. J. Gurley, S. F. Gardner, M. A. Hubbard et al., "Cytochrome P450 phenotypic ratios for predicting herb-drug interactions in humans," *Clinical Pharmacology and Therapeutics*, vol. 72, no. 3, pp. 276–287, 2002.

[2] R.-X. Zhang, M.-X. Li, and Z.-P. Jia, "*Rehmannia glutinosa*: review of botany, chemistry and pharmacology," *Journal of Ethnopharmacology*, vol. 117, no. 2, pp. 199–214, 2008.

[3] Y.-Y. Sung, T. Yoon, J. Y. Jang, S.-J. Park, and H. K. Kim, "Topical application of *Rehmannia glutinosa* extract inhibits mite allergen-induced atopic dermatitis in NC/Nga mice," *Journal of Ethnopharmacology*, vol. 134, no. 1, pp. 37–44, 2011.

[4] P.-S. Wu, S.-J. Wu, Y.-H. Tsai, Y.-H. Lin, and J. C.-J. Chao, "Hot water extracted *Lycium barbarum* and *Rehmannia glutinosa* inhibit liver inflammation and fibrosis in rats," *The American Journal of Chinese Medicine*, vol. 39, no. 6, pp. 1173–1191, 2011.

[5] H. Kim, E. Lee, S. Lee, T. Shin, Y. Kim, and J. Kim, "Effect of *Rehmannia glutinosa* on immediate type allergic reaction," *International Journal of Immunopharmacology*, vol. 20, no. 4-5, pp. 231–240, 1998.

[6] H.-M. Kim, C.-S. An, K.-Y. Jung, Y.-K. Choo, J.-K. Park, and S.-Y. Nam, "*Rehmannia glutinosa* inhibits tumour necrosis factor-α and interleukin-1 secretion from mouse astrocytes," *Pharmacological Research*, vol. 40, no. 2, pp. 171–176, 1999.

[7] H. M. Lu, Y. Z. Liang, L. Z. Yi, and X. J. Wu, "Anti-inflammatory effect of *Houttuynia cordata* injection," *Journal of Ethnopharmacology*, vol. 104, no. 1-2, pp. 245–249, 2006.

[8] W. Li, P. Zhou, Y. Zhang, and L. He, "*Houttuynia cordata*, a novel and selective COX-2 inhibitor with anti-inflammatory activity," *Journal of Ethnopharmacology*, vol. 133, no. 2, pp. 922–927, 2011.

[9] T.-Y. Lin, Y.-C. Liu, J.-R. Jheng et al., "Anti-enterovirus 71 activity screening of Chinese herbs with anti-infection and inflammation activities," *The American Journal of Chinese Medicine*, vol. 37, no. 1, pp. 143–158, 2009.

[10] Y.-Y. Chen, C.-M. Chen, P.-Y. Chao, T.-J. Chang, and J.-F. Liu, "Effects of frying oil and *Houttuynia cordata* thunb on xenobiotic-metabolizing enzyme system of rodents," *World Journal of Gastroenterology*, vol. 11, no. 3, pp. 389–392, 2005.

[11] P. M. Y. Or, F. F. Y. Lam, Y. W. Kwan et al., "Effects of Radix Astragali and Radix Rehmanniae, the components of an anti-diabetic foot ulcer herbal formula, on metabolism of model CYP1A2, CYP2C9, CYP2D6, CYP2E1 and CYP3A4 probe substrates in pooled human liver microsomes and specific CYP isoforms," *Phytomedicine*, vol. 19, no. 6, pp. 535–544, 2012.

[12] H. Kim, Y.-J. Yoon, J.-H. Shon, I.-J. Cha, J.-G. Shin, and K.-H. Liu, "Inhibitory effects of fruit juices on CYP3A activity," *Drug Metabolism and Disposition*, vol. 34, no. 4, pp. 521–523, 2006.

Hindawi Publishing Corporation
Evidence-Based Complementary and Alternative Medicine
Volume 2013, Article ID 181769, 7 pages
http://dx.doi.org/10.1155/2013/181769

Research Article

Case Series of an Intraoral Balancing Appliance Therapy on Subjective Symptom Severity and Cervical Spine Alignment

Young Jun Lee,[1] Joo Kang Lee,[2] Soo Chang Jung,[3] Hwang-woo Lee,[4] Chang Shik Yin,[5] and Young Jin Lee[6]

[1] *Department of FCST, Graduate School of Integrated Medicine, CHA University, Seoul 135-081, Republic of Korea*
[2] *Spine Research Center, Gimcheon University, Gimcheon 740-704, Republic of Korea*
[3] *Department of Dentistry, Graduate School of Integrated Medicine, CHA University, Seoul 135-081, Republic of Korea*
[4] *Department of Diagnostic Radiology, Graduate School of Integrated Medicine, CHA University, Seoul 135-081, Republic of Korea*
[5] *Acupuncture and Meridian Science Research Center, College of Korean Medicine, Kyung Hee University, Seoul 130-701, Republic of Korea*
[6] *Graduate School of Integrated Medicine, School of Medicine, CHA University, Seoul 135-081, Republic of Korea*

Correspondence should be addressed to Chang Shik Yin; acuyin@khu.ac.kr and Young Jin Lee; leeyjsd@gmail.com

Received 8 April 2013; Accepted 7 June 2013

Academic Editor: Bo-Hyoung Jang

Objective. The objective of this study was to investigate the effect of a holistic intraoral appliance (OA) on cervical spine alignment and subjective symptom severity. *Design*. An observational study on case series with holistic OA therapy. *Setting*. An outpatient clinic for holistic temporomandibular joint (TMJ) therapy under the supervision of the Pain Center, CHA Biomedical center, CHA University. *Subjects*. Ambulatory patients presenting with diverse chief complaints in the holistic TMJ clinic. *Main Measures*. Any immediate change in the curvature of cervical spine and the degree of atlantoaxial rotation was investigated in the images of simple X-ray and computed tomography of cervical spine with or without OA. Changes of subjective symptom severity were also analyzed for the holistic OA therapy cases. *Results*. A total of 59 cases were reviewed. Alignment of upper cervical spine rotation showed an immediate improvement ($P < 0.001$). Changes of subjective symptom severity also showed significant improvement ($P < 0.05$). *Conclusion*. These cases revealed rudimentary clinical evidence that holistic OA therapy may be related to an alleviated symptom severity and an improved cervical spinal alignment. These results show that further researches may warrant for the holistic TMJ therapy.

1. Introduction

Temporomandibular disorders (TMDs) are not only a potential cause of nondental pain in the orofacial region such as the temporomandibular joint (TMJ) [1], but they may contribute to various symptoms, including neck pain, depression, chronic fatigue, sleep disorders, decreased productivity, and mood disorder [2]. Among these TMD-associated symptoms, coexistence of neck or head pain and TMDs is very common [3]. The close correlation of TMDs with cervical spine disorders has been reported by several researches [4–7]. One study reported that patients who have TMDs report neck symptoms more frequently than patients who do not have TMDs. At the same time, patients who have neck pain report more signs and symptoms of TMD than those who have no neck pain [8]. Cervical spine disorders were reported in 71% of the TMD patients group and only 40% of the non-TMD group [9]. Limitations in the upper cervical region (C0–C3 level) were reported to be present significantly more in the 31 TMD patients than in the 30 controls [10].

Although there has been a debate about the exact role of intraoral appliances (OA) in management of TMDs, OA can be used as one of the important therapeutic modalities for TMD or related disorders [11]. Several studies have shown that functional disturbances in the cervical vertebrae were significantly reduced through acting upon the muscles of the

mouth and jaw with OA or other TMD treatments [12, 13], although another study using radiographic and photographic findings reported no significant change in head and neck posture after intraoral splint use [14]. OA has been one of the main modalities of holistic TMJ therapy with a perspective of balance in the nervous system and whole-body structure [15, 16]. This study aimed to investigate an effect of OA on subjective symptom severity and cervical spine alignment in holistic TMJ therapy cases.

2. Materials and Methods

2.1. Subjects and Design. This study was designed as a within-subject prepost comparison observational study with one group. Ambulatory patients who newly visited the outpatient clinic of holistic TMJ therapy were prescribed with their first OA, volunteered to participate in this study, provided an informed consent, and were asked to receive radiologic assessment twice: once with OA and once without OA. Patients may be included if they showed somatic dysfunction in the region of TMJ with manifestations of tissue texture abnormality, asymmetry, restriction of motion, or tenderness, or showed positive sign on applied kinesiology-type manual muscle testing in relation to TMJ. Those patients have been considered as possible candidates for holistic OA therapy [15]. Positive sign on manual muscle testing means a response of change in isometric muscle contraction in relation to a touch to the skin of TMJ area. Chief complaint of patients may vary significantly. This study was performed under the supervision of Pain Center, CHA Biomedical center, CHA University, during the period from December 2006 to November 2007 (Table 1). Records were analyzed for 59 outpatient cases (27 females, 32 males). Mean age was 35.2 (SD 13.3). The study protocol was approved by the institutional review board of the CHA university (IRB no. 08-32).

2.2. Intervention: Holistic Intraoral Appliance Therapy. An OA was individually fabricated and fitted on the spot. OA fabrication was based on the so-called functional cerebrospinal therapy (FCST), originally developed by one of the authors of this paper (Young J. Lee) [15]. As an impression material, vinyl polysilane was used (Exafine putty type, GC Corporation, Japan). On trial-and-error basis, the height and shape of an OA was gradually adjusted for the very individual under examination with continuous monitoring of changes in sign/symptom manifestations, somatic dysfunction, or manual muscle testing. The final height and shape of OA in a given session of treatment was determined on the spot based on the immediate improvement of somatic dysfunction or manual muscle testing (Figure 1) [15]. Thus fabricated OA was intraorally fitted on the spot. The OA thus fabricated was periodically applied by the patient in daily life, as long as symptomatic improvement was maintained. At a follow-up visit, the previous OA might be discarded and a new one be fabricated.

2.3. Radiologic Examination. A CT scan and simple X-ray of cervical spine were taken twice: without application of the OA, followed by with application of the OA. Any significant change in the alignment of the occiput-atlas axis or the cervical spine was explored in relation to the OA. Examination was done within several days (maximum 3 days) after prescribing the first OA for the participant. The patients assumed a supine position facing straight ahead during the examination procedure. The degree of rotational misalignment between the atlas and the axis was measured

Table 1: General characteristics of the patients.

	No. (%)
Gender	
Male	32 (54.2%)
Female	27 (45.8%)
Chief complaints	
Pain disorder	33 (55.9%)
Temporomandibular joint pain	9 (15.3%)
Neck pain	8 (13.6%)
Headache	6 (10.2%)
Others	10 (16.9%)
Idiopathic torticollis	9 (15.3%)
Others	17 (28.8%)
Duration of symptoms (years)	
0–2	20 (33.9%)
2–4	15 (25.4%)
4–10	12 (20.3%)
10–16	8 (13.6%)
16–22	2 (3.4%)
22–38	2 (3.4%)
Outpatient treatment	
Period (months)*	1.5 ± 1.7 (0.1–8.1)
No. of treatments*	20.7 ± 33.4 (3–229)

*Data are presented as mean ± SD (range).

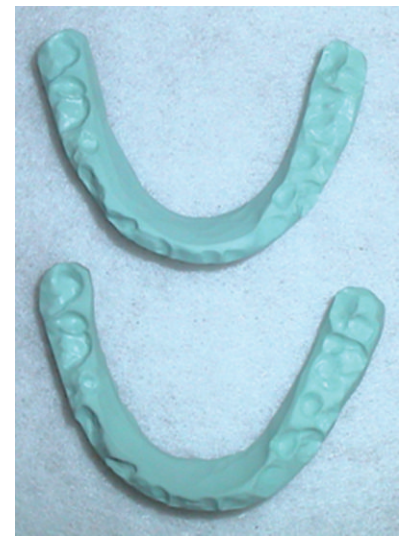

Figure 1: Custom-made intraoral appliance used for holistic temporomandibular therapy.

according to the method of Patijn et al. [17]. Absolute degree of the rotation misalignment between the atlas and the axis was compared in relation to the OA. The patient assumed an erect posture facing straight ahead (paralleling the bite line to the floor) for the lateral X-ray imaging. Degree of lordosis of the cervical spine was measured according to the Cobb technique [18]. The entire CT scan and X-ray imaging were performed by the same radiologist with the same method for all the cases.

2.4. Subjective Symptom Severity. The symptom severity data, which were repeatedly documented by the method of a visual analogue scale (VAS) ranging from 0 to 10, where 10 represents unbearable discomfort and 0 represents no discomfort, were additionally reviewed. The VAS severities on the first and last visit were analyzed as a measurement of the clinical picture of the participants without any assumption of direct correlation between cervical alignment and symptom severity.

2.5. Statistical Analysis. Statistical comparisons were performed using SPSS statistical software (version 17 for Windows, SPSS Inc.). Degree of rotational misalignment and severity of subjective symptoms were compared using the Wilcoxon signed-ranks test. Values were presented as mean ± standard deviation with a significance level of 0.05.

3. Results

3.1. Immediate Changes in Rotational Misalignment Following Use of the Intraoral Appliance. Rotational misalignment in upper cervical spine showed immediate change in 72.4% of the patients. Predominant change was decreased in rotational misalignment after OA's use ($P < 0.01$). When grouped according to type of the change, 62.1% of the patients showed a 2.8-degree decrease (Figure 2), and 10.3% of the patients showed a 2.7-degree increase (Table 2).

3.2. Immediate Changes in Cervical Lordosis Following Use of the Intraoral Appliance. Degree of cervical lordosis showed immediate change in 80.0% of the patients. When grouped according to type of the change, 38.2% of the patients showed a 5.1-degree decrease, and 41.8% of the patients showed a 5.5-degree increase (Table 3).

3.3. Changes in the Severity of Subjective Symptoms. The patients showed improvement in the severity of subjective symptoms such as neck pain and chronic fatigue (Table 4, Figure 3) after a mean treatment period of 1.5 months with 20.7 treatments (Table 1).

4. Discussion

In this study, we found that immediate change in cervical alignment seems to be related with an OA therapy: the degree of rotational misalignment between the atlas and axis was reduced. In addition to that, the participants showed an improvement in subjective symptom severities after 1.5 months, even though this change may not be associated with the OA therapy. Wearing an intraoral appliance seemed to accompany reduced degree of cervical lordosis in those with greater-than-average degrees of lordosis or increased degree of cervical lordosis in those with lesser-than-average degrees of lordosis, coming closer to the average degree of lordosis. However, the average degree of lordosis was not different between the two conditions. We cannot exclude the possibility that these changes in cervical lordosis may just reflect a random variation or the statistical phenomenon of regression to the mean.

Positive relationship between TMD and cervical spine was reported in previous reports [4, 6]. Although the relationship between TMD and head and neck posture or cervical spine alignment has not been shown clearly [5, 19], clinical or muscular aspects of such relationship may not be so ambiguous, considering increased muscular fatigability of cervical extensor muscles in TMD patients [20] and close correlation between TMD and spinal pain in clinical practice [7]. Increased or decreased lordosis of cervical alignment may be related to increased stress or vulnerability to stress in cervical spine [21–23]. In this study, we found that wearing the intraoral balancing appliance appeared to be related to such change in cervical alignment that increased or decreased cervical lordosis turning into a close-to-average angle of lordosis. This may be related to decrease in stress or vulnerability to stress of cervical spine. It is suggested that the change into more close-to-average lordosis from decreased lordosis, rather than from increased lordosis, may be more closely related to stress reduction considering that flexion deformity and decreased lordotic curve is a well-described type of aberration in cervical curvature [23].

The close correlation of TMD with cervical spine disorders has been reported previously, and there are several explanations in terms of biomechanical, neuroanatomical, and neurophysiological aspects for these close relations [24]. Neurophysiologically, there is convergence and central excitatory connection between the trigeminal nerve and the trigeminocervical nucleus. For example, afferent input from neck muscles and the cervical spine results in masticatory muscle contraction through the excitation of motor neurons in the trigeminal nerve [25, 26]. Experimental trapezius muscle pain was observed to spread most often to the infraauricular zone and was also accompanied by a temporary reduction of mouth opening [27]. While sensory information from trigeminal primary afferent neurons descends down to C2-C3 and even C6 [28–30], experimentation has shown that electrical stimulation of the infraorbital nerve, a branch of the trigeminal nerve, activates interneurons in the ventral horns of C1 to C4, readily exciting neck muscle motoneurons [31]. In the case of TMD, transmission of nociception from the TMJ by means of the auriculotemporal nerve, the posterior trunk of the mandibular nerve, to the spinal tract of the trigeminal nerve, the trigeminocervical nucleus, and the motoneurons of the cervical spine is the one mechanism through which TMD causes cervical pain and muscle tension changes [32]. Biomechanically, the temporomandibular system and cervical spine behave as one functional unit. Thus, not only could changes in head posture result in cervical spine dysfunction,

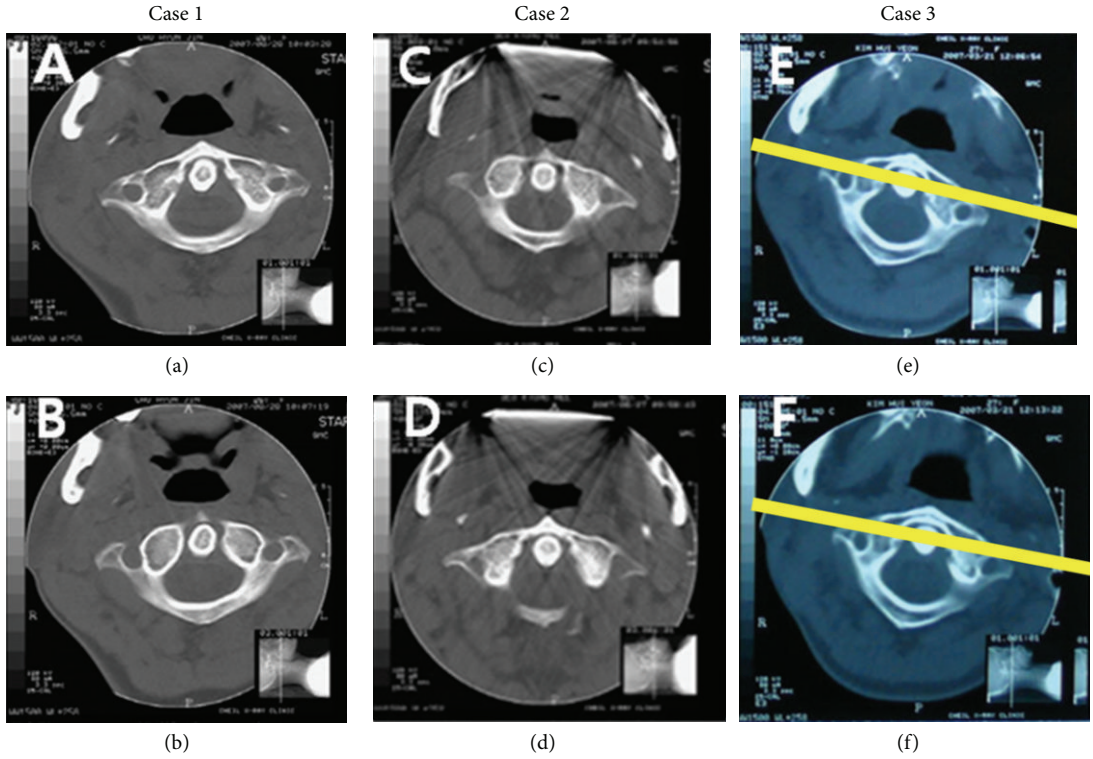

Figure 2: Exemplary CT image of 3 patients. Comparison shows an immediate change in the degree of rotational misalignment in the atlas while wearing the oral appliance. (a), (c), and (e) CT image while not wearing the oral appliance. (b), (d), and (f) CT image while wearing the oral appliance. Lines drawn over figures (e) and (f) indicate ameasuring method of atlas rotation angle with a line passing the anterior border of foramen transversarium of the atlas.

Table 2: Immediate change in degree of rotational misalignment between C1 and C2 vertebrae on a computed tomography image.

	No. (%)*	Degree of the rotational misalignment		Immediate change
		Without an intraoral appliance	With an intraoral appliance	
Groups based on type of the change				
Decrease	36 (62.1)	6.1 ± 5.0	3.3 ± 4.1	−2.8 ± 2.0***
No change	16 (27.6)	2.4 ± 2.2	2.4 ± 2.2	0
Increase	6 (10.3)	2.7 ± 2.1	5.3 ± 3.5	2.7 ± 2.7**
Total	58 (100.0)	4.7 ± 4.5	3.3 ± 3.6	−1.4 ± 2.5***

*There were missing data in one case. Values are presented as number (%) or mean ± SD.
**$P < 0.05$, ***$P < 0.001$ by Wilcoxon signed-rank test.

Table 3: Immediate change in degree of cervical lordosis calculated by Cobb technique on a simple X-ray image.

	No. (%)*	Mean ± SD		Degree of change
		Without an intraoral appliance	With an intraoral appliance	
Groups based on the type of the change				
Decrease	21 (38.2)	45.3 ± 11.4	40.5 ± 11.0	−5.1 ± 3.7**
No change	11 (20.0)	41.6 ± 3.32	41.6 ± 3.3	0
Increase	23 (41.8)	35.8 ± 10.4	41.4 ± 11.4	5.5 ± 4.7**
Total	55 (100.0)	40.6 ± 12.0	41.1 ± 11.4	0.4 ± 6.1

*There were missing data in four cases. Values are presented as number (%) or mean ± SD.
**$P < 0.001$ by Wilcoxon signed-rank test.

Table 4: Frequent subjective symptom groups and treatment sessions of each group.

Subjective symptoms	No. (%)*	Treatment sessions
Neck pain	39 (70.9)	18.4 ± 20.5
Chronic fatigue	17 (30.9)	21.6 ± 19.3
Headache	14 (25.5)	16.4 ± 23.7
Temporomandibular joint pain	13 (23.6)	15.0 ± 14.3
Shoulder pain	11 (20.0)	6.9 ± 3.6
Temporomandibular joint noise	11 (20.0)	30.8 ± 66.2
Chronic dyspepsia	8 (14.5)	19.3 ± 17.5
Cervical dystonia	8 (14.5)	51.8 ± 75.2
Low back pain	8 (14.5)	19.3 ± 20.1

*There were missing data in four cases. Values are presented as number (%) or mean ± SD.

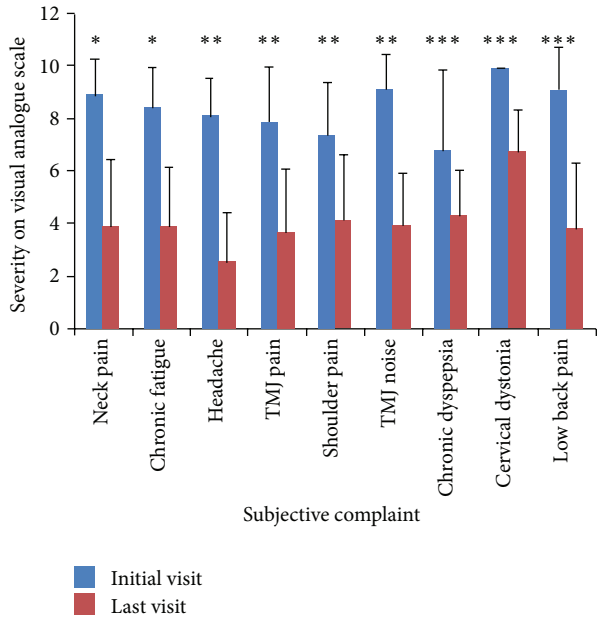

Figure 3: Severity of subjective symptoms compared between initial and last visits. TMJ: temporomandibular joint. $^{*}P < 0.05$, $^{**}P < 0.01$, $^{***}P < 0.001$ by Wilcoxon signed-rank test.

but cervical spine movement could also result in changes in TMJ movement [33]. With forward head posture, the posterior cervical muscles are shortened isometrically, while the anterior submandibular muscles are stretched to cause retrusive forces on the mandible [34]. Increase in the vertical dimension of the resting mandible was reported to occur with an increase in the angle of habitual head posture and a decrease in the retrusion of the mandible [35]. Simultaneous functional movements in the temporomandibular, atlantooccipital, and cervical spine joints were also reported [36]. Several studies have shown that functional disturbances in the cervical vertebra were significantly reduced by acting upon the muscles of the mouth and jaw as a result of OA or other TMD treatments [12, 13]. The successful correction of unbalanced TMJ position is suggested to be dependent on the health of the cervical and other spine musculature as well as the head position [37, 38]. And OA can possibly reduce the loading inside the TMJ by reducing the intensity of muscle activity or shifting the condylar loading area [39].

This study adopted a CT scanning and simple X-ray imaging for analysis of the cervical spine alignment. For analysis of the positioning of the cervical spinal curve in individuals with TMD, many studies have evaluated cervical spine alignment using cephalometric X-rays. However, evaluation based upon cephalometric X-rays has some limitations, such as artificial positioning. The lateral cervical spine X-ray is also difficult to interpret due to head tilt. In the present study, X-rays were taken with individuals in a natural standing position, with no modifications of the cervical curve. In spite of the reported interexaminer and intraexaminer reliability [40, 41], there exist possible limitations of plain radiography [42–44], which can be overcome using CT assessment. An axial CT through the upper cervical spine demonstrates the rotated position of the atlas on the axis and associated forward or backward displacement of the atlas [45].

There has been debate about the exact role of OA in the management of TMDs, although many types of OA have been used for over 50 years to treat TMDs. In the last 20 years, changes in the pathophysiology of TMDs from simple mechanical and structural concepts to complex neurophysiologic concepts have forced a reconsideration of traditional idea about using OA [46]. But the OA may still be a valuable adjuvant modality in the management of TMDs [11]. There are various OA designs, such as the flat plane stabilization appliance (Michigan splint) [47], the traditional anterior bite plane appliance, the minianterior appliances [48], the anterior repositioning appliance [49], the neuromuscular appliances [50], the posterior bite plane appliances [51], and the hydrostatic appliance [52].

The indication of an OA therapy in this study was not that of the conventional TMD criteria. The indication includes any of the somatic dysfunction signs or positive applied kinesiology-style manual muscle testing, which may actually be said as including even any functional (nonpathologic) imbalance in the TMJ and nearby muscles or static posture or joint movement trajectory. We may not tell that the participants in this study belong to TMD. However, the objective of this study was to explore any relationship between OA therapy and cervical alignment, not the effect on TMD. And we tried to make an approach to OA therapy from perspectives of complementary and alternative medicine rather than the more strict conventional TMD concept or OA therapy. So, we adopted a new type of OA therapy that is developed in the Republic of Korea and is applied for diverse chief complaints with a functional imbalance in the TMJ region from perspectives of balance enhancing in the nervous system [15, 16, 53]. The design of this OA reflects mixed concepts of the flat plane stabilization appliance and neuromuscular appliances.

This study is an observational study on case series without control group. This limitation prevents definite comparison or inference. Further investigation adopting controlled study and more rigid design is warranted. This study only evaluated the immediate change of cervical alignment in relation to an application of OA in one group. So we cannot state definitely

any correlation between such a change of cervical alignment and the clinical symptom change. However, the immediate cervical alignment change observed in this study may warrant further investigation into the correlations between the TMJ, OA, subjective symptoms, and cervical alignment. Future studies may also be needed to investigate the dynamic relationship between the cervical spine and TMDs [53]. In order to clarify the dynamic relationship between the movements of the cervical spine and neck muscles and the mandibular opening or closing and masticatory muscles, the complex dynamics of TMJ and the cervical spine need to be analyzed through the use of reliable clinical instrumentation. Through such studies, clinical application of OA therapies will be developed as a therapy with an evidence base.

This kind of holistic TMJ balancing approach is based on Yin-yang's balance concept as an application of meridian balance concept [15]. It was originally developed in Korean medicine in the 1990s [54]. TMJ posture is adjusted with intraoral TMJ balancing appliance that was tailor made based on verification using such functional assessments as palpation on meridian-muscular system, applied kinesiology, and functional neurological examination [15]. Postural training of TMJ using intraoral TMJ balancing appliance may lead to positive whole-body response. Unlike previous reports on episodic cases treated with this holistic approach [55], this study analyzed cases series in which diverse chief complaints are distributed from pain to dyspepsia with additional analysis on possible mechanism of this holistic approach, a close linkage between TMJ postural intervention and change in upper cervical alignment. However, it is unclear if this treatment keeps prolonged effects. Further studies are warranted to convince the effect of intraoral appliance for therapeutics.

In conclusion, this study revealed a significant correlation between OA in holistic TMJ therapy and an immediate change of cervical spine alignment and symptom severity.

References

[1] J. P. Okeson, *The American Academy of Orofascial Pain: Guidelines for Assessment, Diagnosis, and Management*, Quintessence, Chicago, Ill, USA, 1996.

[2] R. C. Auvenshine, "Acute vs. chronic pain," *Texas Dental Journal*, vol. 117, no. 7, pp. 14–20, 2000.

[3] D. A. Cacchiotti, O. Plesh, P. Bianchi, and C. McNeill, "Signs and symptoms in samples with and without temporomandibular disorders," *Journal of Craniomandibular Disorders*, vol. 5, no. 3, pp. 167–172, 1991.

[4] R. la Touche, C. Fernández-de-las-Peñas, J. Fernández-Carnero et al., "The effects of manual therapy and exercise directed at the cervical spine on pain and pressure pain sensitivity in patients with myofascial temporomandibular disorders," *Journal of Oral Rehabilitation*, vol. 36, no. 9, pp. 644–652, 2009.

[5] J. P. de Farias Neto, J. M. de Santana, V. J. de Santana-Filho, L. J. Quintans-Junior, A. P. de Lima Ferreira, and L. R. Bonjardim, "Radiographic measurement of the cervical spine in patients with temporomandibular dysfunction," *Archives of Oral Biology*, vol. 55, no. 9, pp. 670–678, 2010.

[6] S. A. Olivo, J. Fuentes, P. W. Major, S. Warren, N. M. R. Thie, and D. J. Magee, "The association between neck disability and jaw disability," *Journal of Oral Rehabilitation*, vol. 37, no. 9, pp. 670–679, 2010.

[7] K. Walczyńska-Dragon and S. Baron, "The biomechanical and functional relationship between temporomandibular dysfunction and cervical spine pain," *Acta of Bioengineering and Biomechanics*, vol. 13, no. 4, pp. 93–98, 2011.

[8] A. de Wijer, J. R. J. de Leeuw, M. H. Steenks, and F. Bosman, "Temporomandibular and cervical spine disorders: self-reported signs and symptoms," *Spine*, vol. 21, no. 14, pp. 1638–1646, 1996.

[9] P. J. Alanen and P. K. Kirveskari, "Occupational cervicobrachial disorder and temporomandibular joint dysfunction," *Cranio*, vol. 3, no. 1, pp. 69–72, 1984.

[10] A. de Laat, H. Meuleman, A. Stevens, and G. Verbeke, "Correlation between cervical spine and temporomandibular disorders," *Clinical Oral Investigations*, vol. 2, no. 2, pp. 54–57, 1998.

[11] T. T. T. Dao and G. J. Lavigne, "Oral splints: the crutches for temporomandibular disorders and bruxism," *Critical Reviews in Oral Biology and Medicine*, vol. 9, no. 3, pp. 345–361, 1998.

[12] L. Cane, M. P. Schieroni, G. Ribero, M. Ferrero, and S. Carossa, "Effectiveness of the Michigan splint in reducing functional cervical disturbances: a preliminary study," *Cranio*, vol. 15, no. 2, pp. 132–135, 1997.

[13] L. F. Vernon and D. C. Ehrenfeld, "Treatment of temporomandibular joint syndrome for relief of cervical spine pain: case report," *Journal of Manipulative and Physiological Therapeutics*, vol. 5, no. 2, pp. 79–81, 1982.

[14] G. R. Root, S. L. Kraus, S. J. Razook, and G. S. Samson, "Effect of an intraoral splint on head and neck posture," *The Journal of Prosthetic Dentistry*, vol. 58, no. 1, pp. 90–95, 1987.

[15] C. S. Yin, H. G. Koh, Y. J. Lee, S. I. Chun, and Y. J. Lee, "Functional Cerebrospinal Therapy (FCST), a new physiologic therapeutics developed as meridian yin-yang balance approach," *Korean Journal of Acupuncture*, vol. 22, pp. 169–174, 2005.

[16] C. S. Yin, Y. J. Lee, and Y. J. Lee, "Neurological influences of the temporomandibular joint," *Journal of Bodywork and Movement Therapies*, vol. 11, no. 4, pp. 285–294, 2007.

[17] J. Patijn, J. Wilmink, F. H. J. ter Linden, and H. Kingma, "CT study of craniovertebral rotation in whiplash injury," *European Spine Journal*, vol. 10, no. 1, pp. 38–43, 2001.

[18] D. Malfair, A. K. Flemming, M. F. Dvorak et al., "Radiographic evaluation of scoliosis: review," *American Journal of Roentgenology*, vol. 194, no. 3, pp. S8–S22, 2010.

[19] S. Armijo-Olivo, K. Rappoport, J. Fuentes et al., "Head and cervical posture in patients with temporomandibular disorders," *Journal of Orofacial Pain*, vol. 25, no. 3, pp. 199–209, 2011.

[20] S. Armijo-Olivo, R. A. Silvestre, J. P. Fuentes et al., "Patients with temporomandibular disorders have increased fatigability of the cervical extensor muscles," *Clinical Journal of Pain*, vol. 28, no. 1, pp. 55–64, 2012.

[21] P. Korovessis, G. Koureas, S. Zacharatos, and Z. Papazisis, "Backpacks, back pain, sagittal spinal curves and trunk alignment in adolescents: a logistic and multinomial logistic analysis," *Spine*, vol. 30, no. 2, pp. 247–255, 2005.

[22] W. Wei, S. Liao, S. Shi, J. Fei, Y. Wang, and C. Chen, "Straightened cervical lordosis causes stress concentration: a finite element model study," *Australasian Physical & Engineering Sciences in Medicine*, vol. 36, no. 1, pp. 27–33, 2013.

[23] T. Öktenoğlu, A. F. Özer, L. A. Ferrara, N. Andalkar, A. C. Sarioğlu, and E. C. Benzel, "Effects of cervical spine posture

on axial load bearing ability: a biomechanical study," *Journal of Neurosurgery*, vol. 94, no. 1, pp. 108–114, 2001.

[24] A. de Laat, "Reflexes elicitable in jaw muscles and their role during jaw function and dysfunction: a review of the literature—part II: central connections of orofacial afferent fibers," *Cranio*, vol. 5, no. 3, pp. 246–253, 1987.

[25] J. W. Hu, X.-M. Yu, H. Vernon, and B. J. Sessle, "Excitatory effects on neck and jaw muscle activity of inflammatory irritant applied to cervical paraspinal tissues," *Pain*, vol. 55, no. 2, pp. 243–250, 1993.

[26] P. Svensson, L. Arendt-Nielsen, and L. Houe, "Muscle pain modulates mastication: an experimental study in humans," *Journal of Orofacial Pain*, vol. 12, no. 1, pp. 7–16, 1998.

[27] O. Komiyama, M. Arai, M. Kawara, K. Kobayashi, and A. de Laat, "Pain patterns and mandibular dysfunction following experimental trapezius muscle pain," *Journal of Orofacial Pain*, vol. 19, no. 2, pp. 119–126, 2005.

[28] N. Bogduk, "The anatomical basis for cervicogenic headache," *Journal of Manipulative and Physiological Therapeutics*, vol. 15, no. 1, pp. 67–70, 1992.

[29] M. F. Jacquin, R. W. Rhoades, H. L. Enfiejian, and M. D. Egger, "Organization and morphology of masticatory neurons in the rat: a retrograde HRP study," *Journal of Comparative Neurology*, vol. 218, no. 3, pp. 239–256, 1983.

[30] C. F. Marfurt, "The central projections of trigeminal primary afferent neurons in the cat as determined by the transganglionic transport of horseradish peroxidase," *Journal of Comparative Neurology*, vol. 203, no. 4, pp. 785–798, 1981.

[31] V. Di Lazzaro, A. Quartaroue, K. Higuchi, and J. C. Rothwell, "Short-latency trigemino-cervical reflexes in man," *Experimental Brain Research*, vol. 102, no. 3, pp. 474–482, 1995.

[32] J. S. Mannheimer and R. M. Rosenthal, "Acute and chronic postural abnormalities as related to craniofacial pain and temporomandibular disorders," *Dental Clinics of North America*, vol. 35, no. 1, pp. 185–208, 1991.

[33] S. L. Krauss, "Cervical spine influences on the management of TMD," in *Temporomandibular Disorders*, S. L. Kraus, Ed., Churchill Livingstone, New York, NY, USA, 1994.

[34] R. Cailliet, *Soft Tissue Pain and Disability*, F.A. Davis Co., Philadelphia, Pa, USA, 1979.

[35] D. W. Darling, S. Kraus, and M. B. Glasheen-Wray, "Relationship of head posture and the rest position of the mandible," *The Journal of Prosthetic Dentistry*, vol. 52, no. 1, pp. 111–115, 1984.

[36] P.-O. Eriksson, B. Häggman-Henrikson, E. Nordh, and H. Zafar, "Co-ordinated mandibular and head-neck movements during rhythmic jaw activities in man," *Journal of Dental Research*, vol. 79, no. 6, pp. 1378–1384, 2000.

[37] P. Check and D. Curl, "Posture and craniofacial pain," in *Chiropractic Approach to Head Pain*, D. D. Curl, Ed., Williams & Wilkins, Baltimore, Md, USA, 1994.

[38] T. M. Gregory, "Temporomandibular disorder associated with sacroiliac sprain," *Journal of Manipulative and Physiological Therapeutics*, vol. 16, no. 4, pp. 256–265, 1993.

[39] G. D. Klasser and C. S. Greene, "Oral appliances in the management of temporomandibular disorders," *Oral Surgery, Oral Medicine, Oral Pathology, Oral Radiology and Endodontology*, vol. 107, no. 2, pp. 212–223, 2009.

[40] B. L. Jackson, W. Barker, J. Bentz, and A. G. Gambale, "Inter- and intra-examiner reliability of the upper cervical X-ray marking system: a second look," *Journal of Manipulative and Physiological Therapeutics*, vol. 10, no. 4, pp. 157–163, 1987.

[41] E. F. Owens Jr., "Line drawing analyses of static cervical X ray used in chiropractic," *Journal of Manipulative and Physiological Therapeutics*, vol. 15, no. 7, pp. 442–449, 1992.

[42] D. C. Sigler and J. W. Howe, "Inter- and intra-examiner reliability of the upper cervical X-ray marking system," *Journal of Manipulative and Physiological Therapeutics*, vol. 8, no. 2, pp. 75–80, 1985.

[43] H. M. Kowalski, W. A. Cohen, P. Cooper, and J. H. Wisoff, "Pitfalls in the CT diagnosis of atlantoaxial rotary subluxation," *American Journal of Roentgenology*, vol. 149, no. 3, pp. 595–600, 1987.

[44] M. Lukhele, "Atlanto-axial rotatory fixation," *South African Medical Journal*, vol. 86, no. 12, pp. 1549–1552, 1996.

[45] J. W. Fielding, W. T. Stillwell, K. Y. Chynn, and E. C. Spyropoulos, "Use of computed tomography for the diagnosis of atlanto-axial rotatory fixation. A case report," *Journal of Bone and Joint Surgery. American*, vol. 60, no. 8, pp. 1102–1104, 1978.

[46] B. J. Sessle, "The neural basis of temporomandibular joint and masticatory muscle pain," *Journal of Orofacial Pain*, vol. 13, no. 4, pp. 238–245, 1999.

[47] American Academy of Orofacial Pain, *Guidelines for Assessment, Diagnosis, and Management*, Quintessence, Chicago, Ill, USA, 1996.

[48] W. E. Shankland II, "Migraine and tension-type headache reduction through pericranial muscular suppression: a preliminary report," *Cranio*, vol. 19, no. 4, pp. 269–278, 2001.

[49] W. B. Farrar, "Differentiation of temporomandibular joint dysfunction to simplify treatment," *The Journal of Prosthetic Dentistry*, vol. 28, no. 6, pp. 629–636, 1972.

[50] B. C. Cooper, "The role of bioelectronic instrumentation in the documentation and management of temporomandibular disorders," *Oral Surgery, Oral Medicine, Oral Pathology, Oral Radiology, and Endodontics*, vol. 83, no. 1, pp. 91–100, 1997.

[51] M. L. Gelb and H. Gelb, "Gelb appliance: mandibular orthopedic repositioning therapy," *Cranio Clinics International*, vol. 1, no. 2, pp. 81–98, 1991.

[52] M. D. Lerman, "The hydrostatic appliance: a new approach to treatment of the TMJ pain-dysfunction syndrome," *The Journal of the American Dental Association*, vol. 89, no. 6, pp. 1343–1350, 1974.

[53] Y. J. Lee, *Cerebrospinal Functional Medicine*, Medical Book Publisher, Seoul, Republic of Korea, 2007.

[54] C. S. Yin and Y. J. Lee, "FCST, its foundation and early history," *Jorunal of TMJ Balancing Medicine*, vol. 1, pp. 9–12, 2011.

[55] I. C. Shon, K. S. Ahn, K. S. Sohn et al., "Two cases of spasmodic torticollis managed by yinyang balance appliance of FCST for the meridian and neurologic balance," *The Korean Journal of Maridian & Acupoint*, vol. 23, pp. 111–123, 2006.

Hindawi Publishing Corporation
Evidence-Based Complementary and Alternative Medicine
Volume 2013, Article ID 584604, 13 pages
http://dx.doi.org/10.1155/2013/584604

Research Article

Gene Expression Profile of the A549 Human Non-Small Cell Lung Carcinoma Cell Line following Treatment with the Seeds of *Descurainia sophia*, a Potential Anticancer Drug

Bu-Yeo Kim, Jun Lee, Sung Joon Park, Ok-Sun Bang, and No Soo Kim

KM-Based Herbal Drug Research Group, Herbal Medicine Research Division, Korea Institute of Oriental Medicine, Daejeon 305-811, Republic of Korea

Correspondence should be addressed to No Soo Kim; nosookim@kiom.re.kr

Received 3 April 2013; Revised 27 May 2013; Accepted 5 June 2013

Academic Editor: Bo-Hyoung Jang

Descurainia sophia has been traditionally used in Korean medicine for treatment of diverse diseases and their symptoms, such as cough, asthma, and edema. Our previous results showed that ethanol extract of the seeds of *D. sophia* (EEDS) has a potent cytotoxic effect on human cancer cells. In this study, we reveal the molecular events that are induced by EEDS treatment in A549 human lung cancer cells. The dose-dependent effect of EEDS on gene expression was measured via a microarray analysis. Gene ontology and pathway analyses were performed to identify functional involvement of genes regulated by EEDS. From gene expression analyses, two major dose-dependent patterns were observed after EEDS treatment. One pattern consisted of 1,680 downregulated genes primarily involved in metabolic processes (FDR < 0.01). The second pattern consisted of 1,673 upregulated genes primarily involved in signaling processes (FDR < 0.01). Pathway activity analyses revealed that the metabolism-related pathways and signaling-related pathways were regulated by the EEDS in dose-dependent and reciprocal manners. In conclusion, the identified biphasic regulatory mechanism involving activation of signaling pathways may provide molecular evidence to explain the inhibitory effect of EEDS on A549 cell growth.

1. Introduction

Public health statistics indicate that neoplastic disease (commonly referred to as cancer) is a leading cause of death in the Republic of Korea, where more than 142 cancer-related deaths per 100,000 people occurred in 2011 (http://kostat.go.kr). Although a wide-range of anticancer drugs that target cancer-related molecules have been developed, the five-year relative survival rate of cancer patients, especially those with lung cancer, has not improved significantly (http://www.cancerresearchuk.org/cancer-info/cancerstats/survival/common-cancers/). This disappointing clinical outcome may be a consequence of the multifactorial nature of cancer and the acquisition of drug resistance by tumor cells [1, 2]. For these reasons, anticancer chemotherapy is now shifting from mono-substance therapy to combination therapy [3–5]. Extracts of medicinal herbs represent promising sources of novel multi-substance anticancer drugs [3].

Descurainia sophia (L.) Webb ex Prantl (Flixweed) is widely distributed in northeastern China and belongs to the family Brassicaceae (Cruciferae). In traditional Korean medicine (KM), the seeds of *D. sophia* have been used for the treatment of diverse diseases and their symptoms, such as cough, asthma, and edema [6]. According to the results of previous studies, *D. sophia* possesses biologically active secondary metabolites, such as cardiac glycosides [7], sulfur glycoside [8], nor-lignan [9], and lactones [10]. In our *in vitro* cytotoxic pre-screening system, the ethanol extract of *D. sophia* seeds (EEDS) displayed potent cytotoxicity against diverse human cancer cells. In addition, cytotoxic (helveticoside) and anti-inflammatory (quercetin and syringaresinol) active constituents were isolated from the EEDS [6].

Although the therapeutic constituents we identified in the EEDS have been well-characterized, the diverse composition of herbal extracts makes it difficult to elucidate their exact molecular mechanisms. Moreover, considering that a number

of genes regulated by herbal extracts exert combined effects on various biological pathways, it is important to study the effects of herbal extracts at the genomic and molecular levels rather than at the individual gene level. Recent advances in the multi-target/multi-substance therapeutic approach have underscored the importance of using high-throughput analyses to identify the therapeutic mechanisms of complex drugs, such as herbal extracts [11]. Therefore, in the present study, we measured the *in vitro* anti-proliferative effects of the EEDS on human lung cancer cells and developed a gene expression profile using a microarray analysis. Dose-dependent analyses of the microarray data revealed that biological functions associated with signal transduction, such as apoptosis, were significantly elevated after EEDS treatment.

2. Materials and Methods

2.1. Plant Materials. The dried seeds of *D. sophia* were purchased from the Kwangmyungdang Medicinal Herbs Co. (Ulsan, Republic of Korea) and identified by Dr. Go Ya Choi, Basic Herbal Medicine Research Group, Herbal Medicine Research Division, Korea Institute of Oriental Medicine, Republic of Korea. A voucher specimen (KIOM-CRC-5) was deposited at the Cancer Research Center, Herbal Medicine Research Division, Korea Institute of Oriental Medicine, Republic of Korea.

2.2. Preparation of EEDS. The dried seeds (9.0 kg) of *D. sophia* were ground and extracted by maceration (40 L of 80% EtOH for 48 h, 3 times) at room temperature. The combined extracts were filtered through Whatman filter paper (No. 2, Whatman International, Maidstone, UK) and concentrated using an EYELA rotary evaporation system (20 L, Tokyo Rikakikai, Tokyo, Japan) at 40°C to yield a two-phase extract (766.1 g), which consisted of an upper oil phase and a lower solid phase. The oil phase did not affect the proliferation of A549 cells. Therefore, we did not test the oil phase for further studies. The solid lower extract (535.7 g) was dried in a WiseVen vacuum oven (WOW-70, Daihan Scientific, Seoul, Republic of Korea) at 40°C for 24 h prior to use. The dried solid ethanol extract, that is EEDS, was dissolved in 100% dimethylsulfoxide (DMSO, Sigma, St Louis, MO, USA) at a concentration of 20 mg/mL and stored at −80°C.

2.3. Cell Lines and Culture Conditions. All human lung cancer cell lines, including the A549 cells, and the IMR-90 normal lung fibroblast cells used in this study were obtained from the American Type Culture Collection (ATCC, Manassas, VA, USA). All cells, with the exception of IMR-90 (DMEM), were grown in RPMI1640 (Invitrogen, Carlsbad, CA, USA) that had been supplemented with 10% (v/v) fetal bovine serum (FBS) (Invitrogen), 100 U/mL of penicillin, and 100 μg/mL of streptomycin (Invitrogen) in 5% CO_2 humidified air at 37°C.

2.4. Cell Proliferation Assays. Cell viability was quantified in a 96-well tissue culture plate using the Ez-Cytox cell proliferation assay kit (Daeil Lab Service, Seoul, Republic of Korea), as previously described [12]. Briefly, 5×10^3 cells were seeded on culture plates containing 100 μL/well of culture medium. After 24 h, the cells were exposed to various concentrations of the EEDS and maintained for the indicated time periods. The maximum concentration of DMSO vehicle was 0.5% (v/v). Following drug treatment, the cells were washed with phosphate-buffered saline (PBS) to minimize the interference of the EEDS with the Ez-Cytox reaction. Color development in the Ez-Cytox solution by live cells was monitored at 450 nm using the Emax microplate reader (Molecular Devices, Sunnyvale, CA, USA).

2.5. Colony Forming Assays. A549 cells were seeded on 6-well culture plates at a density of 200 cells/well and grown for 24 h. The cells were exposed to various concentrations of the EEDS or the vehicle control for 72 h. The culture medium was removed, and after a brief wash with PBS, the cells were grown for 10 days in fresh medium that did not contain the EEDS. After a brief wash with ice-cold PBS, the cells were fixed using an ice-cold neutralized 4% (w/v) paraformaldehyde solution (Biosesang, Seongnam, Republic of Korea) for 10 min. After removing the fixation solution, the colonies were stained with a 0.05% (w/v) crystal violet (Sigma) cell staining solution for 30 min. The free crystal violet solution was removed, and the cells were washed two times with tap water. The stained colonies were photographed, and the number of colonies was manually counted.

2.6. FACS Analysis. Apoptotic cell death was determined using the fluorescein isothiocyanate (FITC)-Annexin V apoptosis detection kit (BD Biosciences, San Jose, CA, USA) according to the manufacturer's instruction. In brief, A549 cells were seeded on 6-well culture plates at a density of 2×10^5 cells/well. After 24 h, cells were exposed to EEDS (0 or 20 μg/mL) for the indicated time periods. Cells were harvested, washed two times with ice-cold PBS, and resuspended in 100 μL of 1x binding buffer. Then, 5 μL of FITC-Annexin V and 5 μL of propidium iodide (PI) solution were added to the cells, and the mixture was incubated at room temperature for 15 min in the dark. After addition of 400 μL of 1x binding buffer, the cells were analyzed by flow cytometry (FACSCalibur, BD Biosciences).

2.7. Microarray Experiment. Total RNA from A549 cells that had been treated with either the EEDS or the vehicle control was prepared using the Easy-Spin total RNA extraction kit (iNtRON Biotechnology, Seoul, Republic of Korea) in accordance with the manufacturer's instructions. Before performing the microarray experiment, the quality of the isolated total RNA was confirmed by electropherogram. RNA integrity number (RIN) = 9.8–10.0, $OD_{260/280}$ (>2.0), and $OD_{260/230}$ (>2.2) were determined (see Supplementary Figure 1 and Supplementary Table 1 of the Supplementary Material online at http://dx.doi.org/10.1155/2013/584604), as previously described [13], by Genomictree, Inc. (Daejeon, Republic of Korea). Total RNA was amplified and labeled using the Low RNA Input Linear Amplification kit PLUS (Agilent Technologies, Santa Clara, CA, USA) and then hybridized to a microarray (Agilent Human whole genome

44 K, Agilent Technologies) containing approximately 44,000 probes (~21,600 unique genes), in accordance with the manufacturer's instructions. The arrays were scanned using an Agilent DNA Microarray Scanner.

2.8. Semiquantitative PCR (qPCR). Single-stranded cDNA was synthesized from 1 μg of total RNA using the SuperScript III first-strand synthesis system (Invitrogen) according to the manufacturer's instruction. The concentration of cDNA was quantified using the ND-1000 NanoDrop spectrophotometer (Thermo Scientific, Wilmington, DE, USA), and 100 ng of cDNA was used as a template for semi-qPCR reaction. The PCR products were analyzed by 1.5% agarose gel electrophoresis. The information of primer sequences and PCR reaction conditions are summarized in the Supplementary Table 3.

2.9. Dose-Dependent Microarray Analyses. The raw signal intensities were obtained using Agilent Feature Extraction Software (Agilent Technologies). Array elements with signal intensities below 1.4-fold of the local background were eliminated, and then the remaining elements were normalized using the quantile method [14]. After averaging the ratio of duplicated spots, the expression ratios were hierarchically clustered using the CLUSTER program (http://rana.lbl.gov/). The short time series expression miner (STEM) program, which was originally developed for the temporal analysis of gene expression [15], was used to identify dose-dependently expressed genes. The statistical significance of the resultant expression pattern was calculated as a false discovery rate (FDR) using 1,000 random permutations.

2.10. Public Microarray Dataset. The publically available microarray dataset with accession number of GSE4573, archived in the Gene Expression Omnibus (http://www.ncbi.nlm.nih.gov/geo), was used in the present study [16]. The dataset was composed of 130 squamous lung carcinoma tissues with survival information. We normalized the probe intensities of each array using the quantile method [14]. After averaging multiple probes, genes that were associated with survival were selected using BRB ArrayTools (version 4.2.1, http://linus.nci.nih.gov/BRB-ArrayTools.html), which compute a statistical significance for each gene using a Cox proportional hazard regression model with a univariate permutation test number of 10,000.

2.11. Gene Ontology (GO) Analyses. The Functional Annotation Tool of DAVID [17] and the High-Throughput GoMiner algorithm [18] were used for simple and dose-dependent GO analyses, respectively. Only the list of genes was used for DAVID, while both the list of genes and the expression ratios were applied as inputs for the GoMiner. In both cases, the P value of each GO-term was calculated using Fisher's exact test. For adjustments of multiple comparisons, the Benjamini-Hochberg procedure was used for DAVID [17]. For the GoMiner analysis, a random sampling-based FDR was calculated from 1,000 iterations. The resultant significant GO-terms from the GO analysis were entered into the REVIGO program to construct a network structure composed of nonredundant subsets of GO terms, where the distance between GO terms was measured based on the semantic similarity [19].

2.12. Pathway Analyses. A pathway enrichment analysis based on Fisher's exact test was performed using DAVID [17]. As with GO analysis, significantly enriched pathways were identified from an input list of genes and statistically adjusted using FDR. For a more systematic pathway analysis, we conducted a Signaling Pathway Impact Analysis (SPIA) [20], which identifies pathways relevant to the experimental conditions using a list of differentially expressed genes and their expression ratios combined with signaling pathway topology. By randomly bootstrapping the pathway topology (n = 3,000), two statistical measurements, P_{NDE} and P_{PERT}, were calculated, which measure the overrepresentation of input genes in a pathway and the abnormal perturbation of a specific pathway, respectively. The global P value (P_{G}) calculated from P_{NDE} and P_{PERT} was used as the selection criteria for significant pathways.

The pathway analysis methods outlined above primarily focused on the identification of enriched pathways using differentially expressed genes. We then measured dose-dependent changes in pathway activity by calculating a linear combination of the logarithmic value of the expression of all of the genes in each pathway, with a weight of 1. When the genes acted as repressors, the weight was multiplied by −1. The measured activities were normalized and hierarchically clustered. The statistical significance for each pathway was estimated using the random permutation-based method (n = 1, 000) [21] in which the FDR was determined by comparing the activity values with randomly permutated values. Only pathways with an FDR below 0.05 were included in the clustering analysis. The pathway information used in the present study was obtained from the Kyoto Encyclopedia of Genes and Genomes (KEGG, http://www.genome.jp/kegg/) database.

2.13. Pathway Similarity Matrix. Pathway similarity was measured based on the number of common genes between pathways. Briefly, a matrix of the number of common genes in distinct pathways was constructed and the relative similarity was measured using the Jaccard algorithm [22] in which the fraction of common genes between two pathways was used to calculate similarity. Therefore, the absence of a common gene in two pathways was not considered in measuring similarity. Finally, the relative similarity matrix was hierarchically clustered, and the pathway activity values obtained by linear combinations of the expression ratio, as described above, were merged into a similarity matrix.

3. Results

3.1. Cytotoxic Effects of the EEDS on Human Lung Cancer Cells. To determine the cytotoxic effects of the EEDS, A549 human lung cancer cells were exposed to increasing concentrations of the EEDS or the vehicle control for indicated time periods.

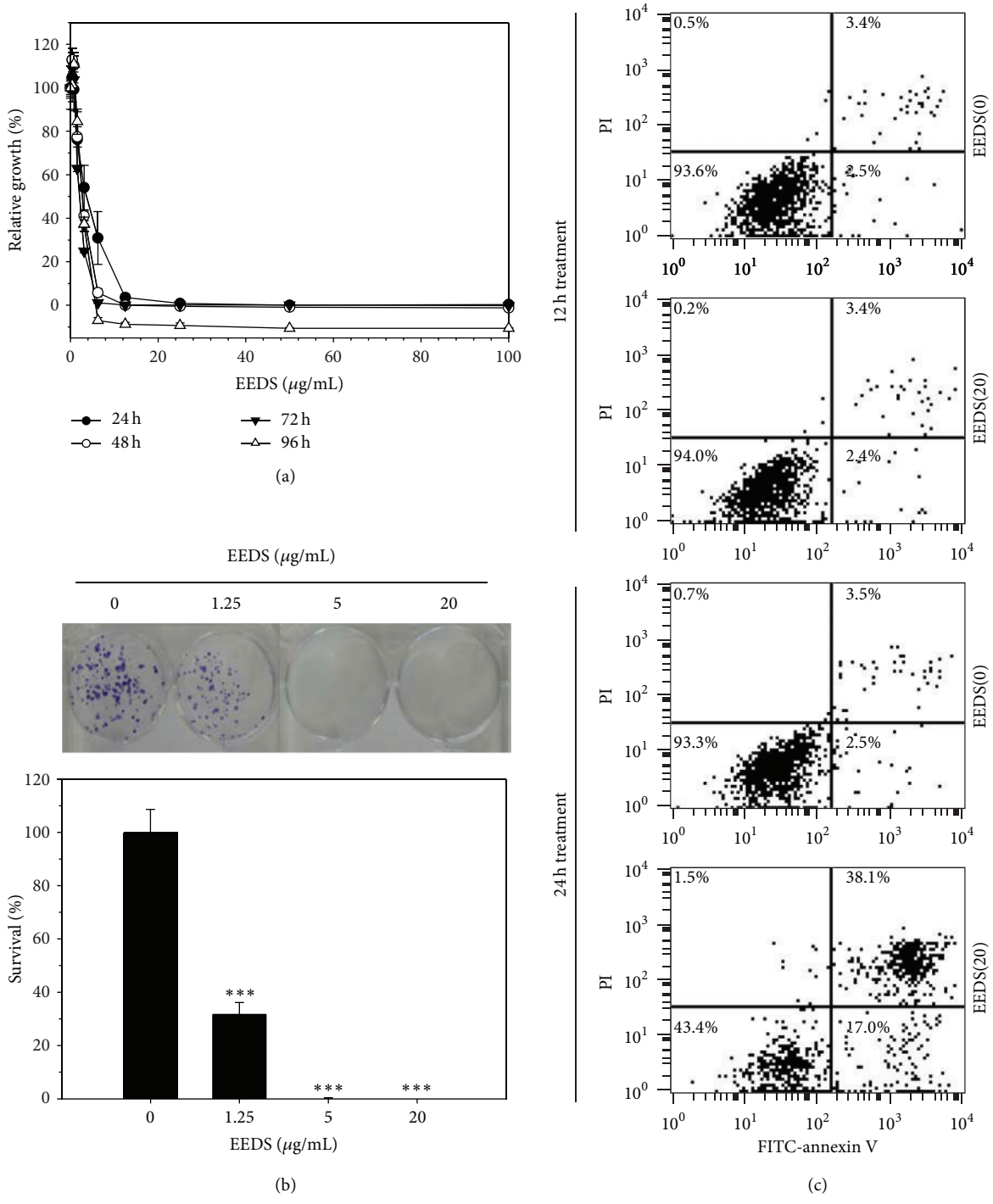

Figure 1: Cytotoxic effect of EEDS on A549 human lung cancer cells. (a) A549 was exposed to increasing concentrations (0–100 μg/mL) of EEDS for various time periods (24–96 h). Cell viability was determined based on mitochondrial enzyme activity as described in the Materials and Methods section. The relative cell growth at each drug dose was calculated by comparison with the vehicle control (0 μg/mL of EEDS, 0.5% DMSO) treatment. (b) A549 cells were exposed to increasing concentrations (0–20 μg/mL) of EEDS for 72 h and then incubated for an additional 10 days in the absence of EEDS (upper panel). Colonies stained with crystal violet were counted and expressed as relative survival (%) compared to the vehicle control (0.5% DMSO) treatment (lower panel). All data are presented as the mean ± S.D. of triplicate experiments. The differences between the vehicle control and treated groups were determined using Student's t-test. $^{***}P < 0.001$. (c) Representative FITC-Annexin V/PI scatter plots for A549 cells following the EEDS treatment. A549 cells were exposed to EEDS (0 or 20 μg/mL) for 12 h or 24 h, and then subjected to FACS analysis of FITC-Annexin V and PI.

Table 1: IC_{50} of EEDS in human lung cancer cell lines.

Cell lines	NCI60 panel	Disease	Drug expose (h)	IC_{50}	
				EEDS (μg/mL)	Dox (μM)[a]
A549	Yes	Lung cancer	24	3.72 ± 1.12	n.d.
			48	2.81 ± 0.19	0.04 ± 0.00
			72	2.15 ± 0.01	n.d.
			96	2.59 ± 0.16	n.d.
NCI-H23	Yes	Lung cancer	48	6.60 ± 0.18	0.22 ± 0.04
NCI-H226	Yes	Lung cancer	48	13.18 ± 0.77	0.33 ± 0.04
NCI-H460	Yes	Lung cancer	48	8.08 ± 0.01	0.31 ± 0.04
IMR-90	—	Normal lung	48	10.54 ± 0.79	0.40 ± 0.04

[a]Dox, doxorubicin, was included as a reference anticancer drug [12].

As shown in Figure 1(a), the EEDS efficiently inhibited A549 cell growth in a dose-dependent manner. Three other human lung cancer cell lines (NCI-H23, NCI-H226, and NCI-H460) and the IMR-90 normal human lung fibroblast cell line were also exposed to increasing concentrations of the EEDS for 48 h. The half maximal inhibitory concentrations (IC50s) of the EEDS against different cells lines were calculated and are summarized in Table 1. Among the tested cell lines, A549 (2.81 ± 0.19 μg/mL) cells were the most sensitive, while NCI-H226 (13.18 ± 0.77 μg/mL) and IMR-90 (10.54 ± 0.79 μg/mL) were relatively resistant to EEDS. We also performed colony forming assays to determine whether the EEDS could affect the tumorigenic ability of A549 cells. The results indicated that treatment with 5 and 20 μg/mL of the EEDS for 72 h completely inhibited colony formation from single cells, whereas cells treated with the vehicle control (0 μg/mL of EEDS, 0.5% DMSO) were able to form colonies (Figure 1(b), upper panel). Relatively lower colony numbers were observed in A549 cells treated with a low concentration of the EEDS (1.25 μg/mL) (Figure 1(b), lower panel). In order to elucidate how EEDS can inhibit cell proliferation, we assessed apoptotic cell death of A549 cells following EEDS treatment. Relative to the vehicle control, the percentage of A549 cells undergoing early (Annexin V positive and PI negative) and late (Annexin V positive and PI positive) apoptotic cell death was increased after 24 h treatment of 20 μg/mL of EEDS. Taken together, these data suggest that the EEDS can inhibit cell proliferation and reduce the tumorigenicity of A549 cells through induction of apoptotic cell death. We selected A549 cells that had been treated with the EEDS for further analyses of gene expression profiling.

3.2. Gene Expression Profiles. The overall pattern of gene expression in A549 cells after EEDS treatment is shown in Figure 2(a). Two subgroups of genes that were upregulated and downregulated in dose-dependent manners were identified. To obtain more quantitative analysis, we applied a dose-dependency analysis to the gene expression values. In accordance with the clustering profile of the genes, two significantly different patterns (Down- and Up-patterns) were observed (FDR < 0.001). The Down-pattern consisted of 1,680 genes that were downregulated in a dose-dependent manner, and the Up-pattern consisted of 1,673 genes that were upregulated in a dose-dependent manner. Expression plots of the two patterns are presented in Figure 2(b). The top 20 genes that displayed the greatest amount of variations in each pattern are listed in Table 2. In addition, the expression ratios for all of the genes included in Figure 2(a) are indicated in Supplementary Table 2. The results of the expression chip analysis were validated using semi-qPCR reactions of 10 selected genes displaying UP- and Down-patterns (Figure 2(c)).

3.3. Prognostic Implications. We investigated whether dose-dependent alteration in gene expression is implicated in clinical outcomes of lung cancer. First, using publically available lung cancer data (GSE4573), we identified survival-related genes (log-rank P value < 0.05). We then examined the relationship between these prognostic genes and UP- or Down-pattern genes. As shown in Table 3, 48 Down-pattern and 50 Up-pattern genes were among the survival-related genes identified from lung cancer patients. Among the 48 Down-pattern genes, 32 Down-pattern genes displayed high-hazard ratios (>1), and 16 genes displayed low-hazard ratios (<1). However, there were a greater number of Up-pattern genes with low-hazard ratios (26 genes) than those with high-hazard ratios (24 genes). Although this reciprocal distribution of genes was marginally significant (P value of 0.069 in Fisher Exact test), considering that genes with high-hazard ratios were downregulated, while genes with low-hazard ratios were upregulated, we hypothesized that EEDS treatment may enhance antitumorigenic effects.

3.4. GO Analysis. To identify the biological function of the two patterns, a GO analysis was performed. The Down-pattern gene set was enriched with metabolic GO terms, including cofactor biosynthesis, heterocycle biosynthesis, and nitrogen compound biosynthesis. In contrast, signaling-related GO terms, including transcription regulation, protein kinase regulation, and apoptosis regulation, were enriched in the Up-pattern gene set. The top 10 statistically significant categories of GO terms (FDR < 0.01) are shown in Table 4 (for the full list of enriched GO terms, please see Supplementary Table 4).

3.5. Profiling of GO Terms. The simple GO analysis considered only genes included in the Down- or Up-pattern

Table 2: Top 20 list of genes mostly down-regulated or up-regulated by EEDS.

Down-pattern				Up-pattern			
Symbol	EEDS (μg/mL)			Symbol	EEDS (μg/mL)		
	1.25	5	20		1.25	5	20
CSRP2BP	−1.35*	−3.05	−6.16	HBEGF	0.86	1.58	4.44
SCARA5	−0.28	−2.58	−5.71	C7orf53	2.86	2.73	4.46
HOXB13	−0.66	−2.42	−5.06	SERPINE1	1.54	3.50	4.59
FOXS1	0.12	−2.40	−4.92	CD274	2.59	3.23	4.60
SNORA12	−2.24	−4.44	−4.91	NOG	1.16	3.91	4.67
RIMBP3	−2.00	−2.74	−4.89	PER1	2.22	1.52	4.68
ST6GAL1	−1.82	−2.20	−4.88	ARC	0.78	1.69	4.79
DACT2	−2.47	−4.08	−4.87	GADD45B	1.23	1.95	4.82
TMEM37	−1.42	−4.37	−4.85	LTB	1.37	4.06	4.85
EEF2K	−1.55	−2.50	−4.84	FOS	1.25	0.52	4.87
GPRIN2	−2.57	−3.41	−4.79	DDIT3	1.66	2.78	4.90
SALL2	−2.08	−4.10	−4.76	C3orf52	1.04	2.26	4.96
CBR3	−1.56	−3.26	−4.57	MAFF	1.62	2.70	5.07
FANCF	−1.30	−1.88	−4.56	IL8	2.94	4.52	5.55
CCR7	−0.58	−1.72	−4.47	PPP1R15A	1.42	2.61	5.59
C5orf58	−0.90	−1.72	−4.38	LOC387763	3.52	4.33	5.67
VAV3	−0.91	−3.48	−4.36	ATF3	1.02	2.49	5.69
C14orf93	−0.64	−2.00	−4.31	EGR2	0.11	0.72	6.46
NTHL1	−0.57	−2.05	−4.31	FOSB	1.36	3.75	7.85
VASH1	−1.31	−3.69	−4.28	EGR1	1.44	4.10	10.02

*Fold induction represents $\log_2$ expression ratio of gene compared with that of control.

gene sets. To identify dose-dependent changes in GO terms, all differentially expressed genes were considered in the analysis. As shown in Figure 3(a), most GO terms were altered by treatment with the highest EEDS concentration tested (20 μg/mL; FDR < 0.01). Consistent with the results of the simple GO analysis, the major functions altered were associated with apoptosis and signaling processes.

The enriched GO categories included redundant terms, however, and it was therefore necessary to remove duplicate terms. We used the REVIGO program to obtain nonredundant GO terms (FDR < 0.01) that were altered by EEDS treatment and to measure the functional relationship of these terms in the network structure. Figure 3(b) shows that signaling-related GO terms, including apoptosis, the MAPK cascade, protein kinase regulation, and phosphorylation regulation, were connected with each other as a cluster, suggesting an interrelationship of biological processes after EEDS treatment in A549 cells.

3.6. Pathway Analyses. In addition to the GO analysis, we also examined the functional changes induced by EEDS treatment by performing pathway analyses. Enriched pathways (FDR < 0.01) identified from the Down- and the Up-pattern gene sets are listed in Table 5. Although only the base excision repair pathway (KEGG 03410) and pentose phosphate pathway (KEGG 00030) were significantly enriched in the Down-pattern gene set, signaling-related pathways, including the MAPK pathway (KEGG 4010), the apoptosis pathway (KEGG 4210), the p53 pathway (KEGG 4155), and the TGF-beta pathway, were enriched in the Up-pattern gene set. The list and positions of the Up- or Down-pattern genes in the pathways are depicted in Supplementary Figure 2. For more systematic analyses of the pathways, we conducted SPIA pathway analyses, which calculate a P value for a pathway based on random perturbations to the pathway network topology. In the Down-pattern gene set (Figure 4(a)), only the sulfur relay system pathway (KEGG 4211) was significant ($P_G < 0.01$), whereas in the Up-pattern gene set (Figure 4(b)), the MAPK pathway (KEGG 4010), the apoptosis pathway (KEGG 4210), the p53 pathway (KEGG 4155), and the TGF-beta pathway were significant ($P_G < 0.01$). These results are consistent with those of the simple pathway enrichment analysis (Table 5). We also obtained similarly enriched pathways using the combined Down- and Up-pattern gene sets (Figure 4(c)).

3.7. Pathway Activity Analyses. Sequential changes in pathway activities based on the EEDS treatment dose were measured using a linear combination of the expression values of all genes in each pathway. Two major subclusters of pathways were grouped based on the statistically significant (FDR < 0.01) similarity of pathway activities (Figure 5(a)). Sub-cluster 1, which is composed of pathways with activities that decreased in a dose-dependent manner, is associated with several metabolism-related pathways. Sub-cluster 2, which is composed of pathways with activities that increased in a

Table 3: Clinical association of Down- or Up-pattern genes regulated by the EEDS with survival from lung cancer.

Down-pattern				Up-pattern			
Symbol	Fold induction*	*P* value**	Hazard ratio**	Symbol	Fold induction	*P* value	Hazard ratio
HMBS	−2.06	0.00225	1.41	YPEL5	1.99	0.000577	0.62
GMPPA	−2.80	0.00283	1.46	MNT	1.56	0.00344	1.42
CD79A	−1.27	0.00431	0.72	GGA3	1.11	0.00421	1.40
HSPA12A	−1.18	0.00759	1.43	MGC29506	1.00	0.00471	0.72
RUNX3	−1.19	0.00818	0.71	CHD7	1.63	0.00763	1.49
RBKS	−1.17	0.0123	1.47	ERCC6	1.52	0.00887	1.37
LRRC20	−2.88	0.0132	1.47	SSBP2	1.61	0.0122	0.72
RNF144A	−1.37	0.0136	0.75	NUFIP1	1.41	0.0129	1.33
C11orf60	−1.30	0.0148	1.36	CLK3	1.04	0.0159	1.37
BCS1L	−1.12	0.0149	1.32	PPP1R13L	2.74	0.0160	1.35
CHST12	−2.05	0.0155	0.75	TNFSF9	1.92	0.0162	1.34
CRYBB2P1	−1.09	0.0172	0.75	DDX52	1.80	0.0163	1.36
APITD1	−2.35	0.0176	1.35	FAM108B1	1.33	0.0192	0.73
AP1G2	−1.62	0.0177	1.39	ZMYM5	1.23	0.0203	1.32
ALDH3B1	−1.77	0.0185	1.36	PTPRH	1.89	0.0217	1.34
AUTS2	−1.89	0.0210	0.74	BTG2	3.33	0.0231	0.74
NIPSNAP1	−1.64	0.0229	1.29	ARHGEF15	1.52	0.0233	1.3
LCMT1	−1.69	0.0240	1.29	SPATA2L	1.68	0.0244	1.30
HERC6	−1.18	0.0250	0.75	PRKRIP1	1.56	0.0245	0.76
DYRK4	−1.21	0.0261	0.77	KIFC1	1.47	0.0247	1.32
TPD52L1	−1.30	0.0262	1.35	RUNX1	2.83	0.0247	1.32
VPS33B	−1.05	0.0274	1.32	GOLGA8A	2.02	0.0249	0.72
DHRS1	−1.83	0.0280	1.28	ABL1	1.15	0.0254	0.76
WDR61	−1.26	0.0292	1.32	CRABP2	2.34	0.0258	0.75
PYGL	−1.62	0.0314	1.31	DDIT3	4.91	0.0260	1.34
MKS1	−1.08	0.0316	1.29	IP6K2	2.19	0.0273	0.76
VASH1	−4.29	0.0336	0.77	LOC729806	1.2	0.0275	1.36
MRPL46	−1.52	0.0338	1.29	ELL	2.63	0.0284	0.79
APBA2	−2.56	0.0340	0.75	TRAF4	1.00	0.0294	1.39
LARGE	−2.96	0.0341	0.76	SEMA7A	1.16	0.0297	1.31
IMP3	−1.40	0.0354	1.28	PRNP	1.51	0.0303	0.75
AAAS	−1.55	0.0354	0.78	GADD45A	4.03	0.0314	0.76
TGIF1	−1.41	0.0359	1.26	GLIPR1	1.94	0.0330	0.77
C11orf80	−1.03	0.0363	1.32	PAPOLG	1.93	0.0331	0.75
AGAP11	−1.51	0.0387	1.33	ZNF484	2.81	0.0336	1.36
CCR7	−4.47	0.0390	0.78	RAP2C	1.46	0.0336	0.76
RRBP1	−1.05	0.0395	0.77	MED1	1.25	0.0389	1.24
CDC123	−1.09	0.0422	1.29	HERPUD1	1.01	0.0392	0.79
REEP4	−1.48	0.0433	1.28	DDR2	1.11	0.0404	0.79
PFKFB1	−1.40	0.0433	0.78	PLK4	1.59	0.0417	1.30
ZNF839	−2.28	0.0440	1.3	CDC42SE1	2.29	0.0417	0.76
CCDC53	−1.88	0.0460	0.80	AOC2	1.09	0.0430	1.29
RDX	−1.22	0.0466	1.29	RUNX2	1.80	0.0438	1.29
EIF2B3	−2.05	0.0470	1.27	SFRS12IP1	1.81	0.0451	0.76
PAAF1	−1.81	0.0471	1.35	INPP1	1.40	0.0456	0.76
PITPNC1	−1.39	0.0483	1.29	MCAM	1.57	0.0458	0.79
ATIC	−1.31	0.0492	1.27	LTB	4.85	0.0470	0.77
DDX28	−1.63	0.0498	1.28	ZCCHC10	1.13	0.0480	0.79
				SP2	1.59	0.0489	0.79
				PTHLH	2.81	0.0499	0.79

*Fold induction represents $\log_2$ expression ratio of gene at treatment with 20 μg/mL of EEDS.

**Log-rank *P* value and hazard ratio were measured in Cox-proportional hazard regression model performed in public lung cancer data [16].

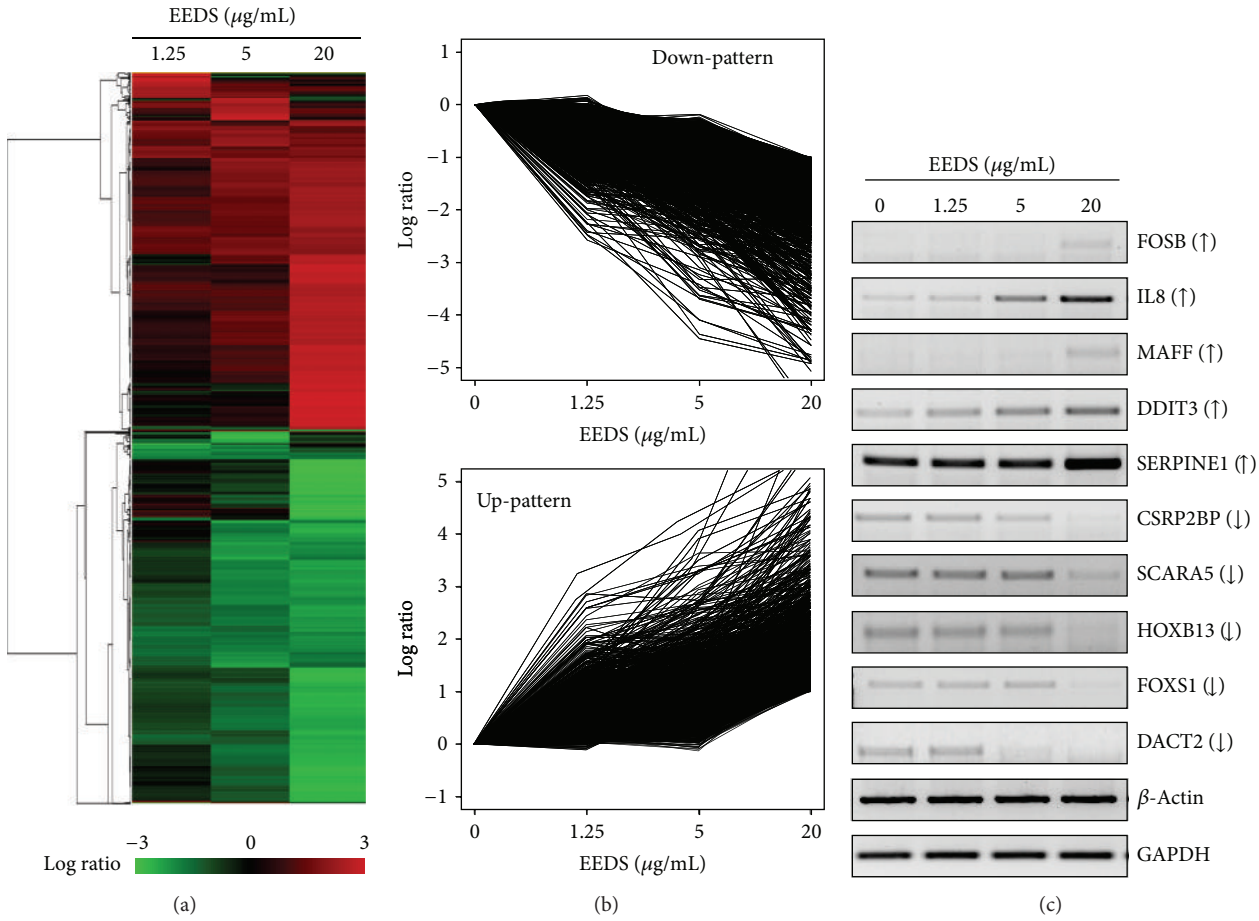

Figure 2: Dose-dependent gene expression by EEDS treatment in A549 cells. (a) Approximately 5,400 differentially expressed genes with a fold ratio greater than 2 or less than 0.5 (for up- and down-regulation, resp.) compared to the vehicle control group in at least one sample were clustered hierarchically. Columns and rows represent individual samples and genes, respectively. The expression ratio color scale ranges from red (high) to green (low), as indicated by the scale bar. Genes exhibiting statistically significant dose-dependent alterations were identified via the STEM program (FDR < 0.001). (b) The Down-pattern is composed of 1,680 genes and the Up-pattern is composed of 1,673 genes. (c) Data acquired from expression chip analysis was confirmed by semi-qPCR. Ten selected genes displaying Up- (↑) and Down- (↓) patterns were amplified using gene specific primers. β-actin and GAPDH were used as loading controls.

dose-dependent manner, is associated with signaling-related pathways as well as immune- and disease-related pathways. To identify the relationship between the statistically significant pathways, we constructed a similarity matrix of pathways based on component genes and pathway activities. As shown in Figure 5(b), subgroups of pathways were clustered based on the similarities of their component genes. Among them, one large subgroup was composed of signaling- and immune-related pathways. The full list of pathways is presented in Supplementary Figure 3. The pathway activities, depicted on a diagonal line or "Activity" on the right panel, indicate that pathways clustered in a subgroup have common levels of activity. For example, the signaling- and immune-related pathways that clustered in the same subgroup show similarly increased activities, suggesting that the interconnection of these diverse pathways may be involved in the response mechanism of A549 cells to EEDS treatment.

4. Discussion

Our previous study demonstrated that the EEDS is cytotoxic to human cancer cell lines and that a cardiac glycoside (helveticoside) is an active cytotoxic constituent of the EEDS [6]. In accordance with our previous work, the EEDS significantly inhibited cell growth and tumorigenicity in A549 human non-small cell lung carcinoma cells through induction of apoptotic cell death (Figure 1). Although the major cytotoxic constituent (helveticoside) of the EEDS was previously identified, the cellular mechanism underlying the therapeutic effects of the EEDS was not. One of the main limitations in elucidating the therapeutic mechanism of whole extracts is the complexity of the biological processes affected by the diverse components of extracts. Therefore, it is difficult to reveal the biological pathways associated with herbal drug treatment using a conventional approach based on the

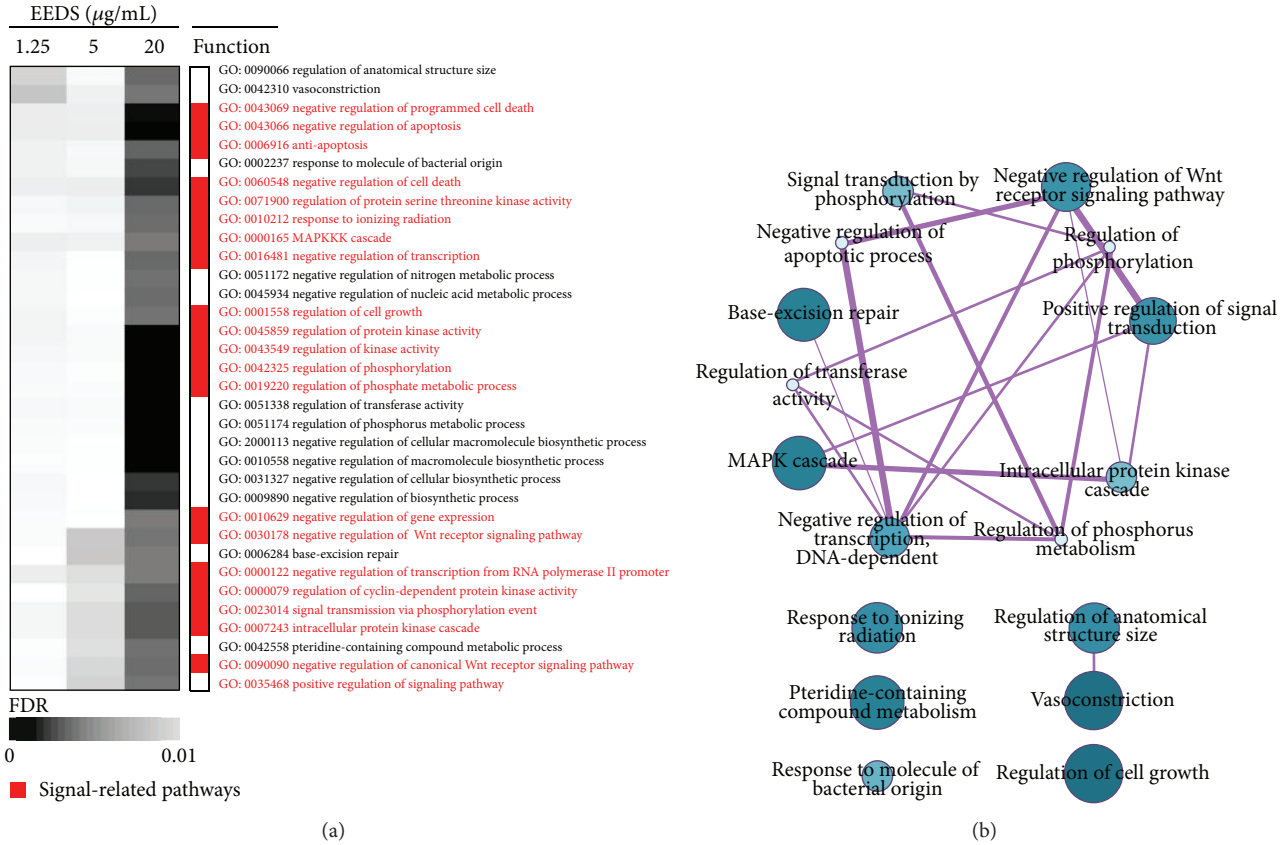

Figure 3: Distribution of GO terms altered by EEDS treatment in A549 cells. (a) GO terms associated with differentially expressed genes that had a fold ratio greater than 2 or less than 0.5 (for up- and down-regulation, resp.) were analyzed at each dose of EEDS using the High-Throughput GoMiner tool. Columns represent individual samples, and rows represents statistically significant GO terms (FDR < 0.01). The positions of signaling-related pathways are colored red. Statistical significance is represented by a gray color gradient, as indicated by the scale bar. (b) A network composed of all nonredundant statistically significant GO terms (FDR < 0.01) after EEDS treatment (20 μg/mL) was constructed using the REVIGO program. The size and color density of each GO term are proportional to its statistical significance, and edge thickness represents the relatedness between two nodes.

analysis of a handful of genes. In general, administration of herbal drugs induces or represses a large number of genes across the whole genome. In the present study, roughly 5,400 genes (approximately 25% of all genes) were found to be differentially expressed following EEDS treatment, as shown in Figure 2(a). Given that treatment with 20 μg/mL of the EEDS significant inhibited cell growth, we also investigated whether the genes regulated by the EEDS are involved in cell growth signaling functions.

Among the differentially expressed genes, two statistically significant patterns of gene expression were observed (Figure 2(b)). The functional segregation of the two gene expression patterns was then validated in two manners. First, we investigated the clinical associations of the two patterns by comparing the gene sets with survival-related genes that were obtained from a public lung cancer dataset. Interestingly, there was a tendency for high-risk genes in lung cancer to be more heavily distributed in the Down-pattern gene set (32 versus 16), while low-risk genes were more heavily distributed in the Up-pattern gene set (26 versus 24), with marginal statistical significance (P value of 0.069). Although the number of genes that were common to the Up- or Down-pattern gene sets and survival-related genes was small, our results suggest that the EEDS could be effective in prolonging survival by inhibiting high-risk genes and activating low-risk genes. Second, differences in functional involvement between the Down-pattern and Up-pattern gene sets were measured using GO and pathway analyses. For example, genes grouped in the Down-pattern gene set, which exhibited dose-dependent decrease in expression, were involved in heterogeneous functions, such as metabolic processes or the base excision repair pathway, while genes in the Up-pattern gene set were predominately associated with cell growth signaling functions (Figure 4 and Table 5). Previous reports indicated that energy metabolism involving the pentose phosphate pathway can regulate lung cancer cells [23] and polymorphisms in the base excision repair pathway are related to lung cancer risk [24] and can modulate the effectiveness of chemotherapy in lung cancer patients [25]. Cell growth-related pathways including the MAPK pathway (KEGG 4010), the apoptosis pathway (KEGG 4210), the p53 pathway (KEGG 4155), and the TGF-beta pathway

Table 4: Top 10 GO terms associated with Up- and Down-patterns by EEDS treatment.

GO ID	GO terms	P value*	FDR**
Down-pattern			
GO:0051188	Cofactor biosynthetic process	$9.26E-08$	$2.57E-04$
GO:0051186	Cofactor metabolic process	$1.79E-07$	$2.49E-04$
GO:0018130	Heterocycle biosynthetic process	$8.03E-07$	$7.42E-04$
GO:0044271	Nitrogen compound biosynthetic process	$6.15E-06$	$4.25E-03$
GO:0006399	tRNA metabolic process	$1.65E-05$	$9.12E-03$
Up-pattern			
GO:0045449	Regulation of transcription	$4.21E-26$	$1.55E-22$
GO:0006350	Transcription	$3.75E-21$	$6.91E-18$
GO:0006355	Regulation of transcription, DNA-dependent	$3.11E-14$	$3.82E-11$
GO:0051252	Regulation of RNA metabolic process	$3.78E-14$	$3.49E-11$
GO:0006357	Regulation of transcription from RNA polymerase II promoter	$2.05E-13$	$1.51E-10$
GO:0042325	Regulation of phosphorylation	$2.03E-11$	$1.25E-08$
GO:0051173	Positive regulation of nitrogen compound metabolic process	$2.39E-11$	$1.26E-08$
GO:0045859	Regulation of protein kinase activity	$2.44E-11$	$1.12E-08$
GO:0019220	Regulation of phosphate metabolic process	$2.68E-11$	$1.10E-08$
GO:0051174	Regulation of phosphorus metabolic process	$2.68E-11$	$1.10E-08$

*P values were calculated using Fischer's test.
**FDR corrections were calculated using the Benjamini-Hochberg procedure in DAVID program [17].

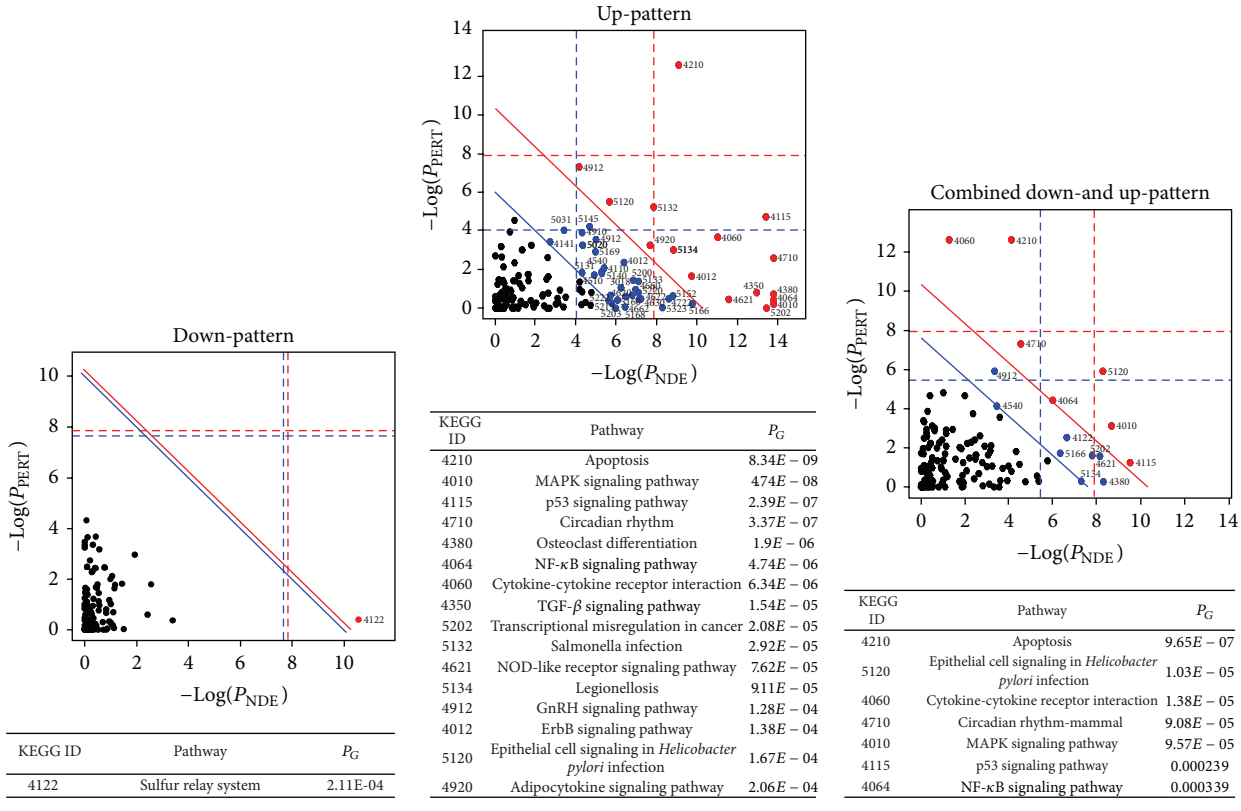

KEGG ID	Pathway	P_G
4122	Sulfur relay system	2.11E-04

(a)

KEGG ID	Pathway	P_G
4210	Apoptosis	$8.34E-09$
4010	MAPK signaling pathway	$474E-08$
4115	p53 signaling pathway	$2.39E-07$
4710	Circadian rhythm	$3.37E-07$
4380	Osteoclast differentiation	$1.9E-06$
4064	NF-κB signaling pathway	$4.74E-06$
4060	Cytokine-cytokine receptor interaction	$6.34E-06$
4350	TGF-β signaling pathway	$1.54E-05$
5202	Transcriptional misregulation in cancer	$2.08E-05$
5132	Salmonella infection	$2.92E-05$
4621	NOD-like receptor signaling pathway	$7.62E-05$
5134	Legionellosis	$9.11E-05$
4912	GnRH signaling pathway	$1.28E-04$
4012	ErbB signaling pathway	$1.38E-04$
5120	Epithelial cell signaling in *Helicobacter pylori* infection	$1.67E-04$
4920	Adipocytokine signaling pathway	$2.06E-04$

(b)

KEGG ID	Pathway	P_G
4210	Apoptosis	$9.65E-07$
5120	Epithelial cell signaling in *Helicobacter pylori* infection	$1.03E-05$
4060	Cytokine-cytokine receptor interaction	$1.38E-05$
4710	Circadian rhythm-mammal	$9.08E-05$
4010	MAPK signaling pathway	$9.57E-05$
4115	p53 signaling pathway	0.000239
4064	NF-κB signaling pathway	0.000339

(c)

Figure 4: Pathways altered by EEDS treatment in A549 cells. Statistically significant pathways in (a) the Down-pattern, (b) the Up-pattern, and (c) the combined Down- and Up-patterns were analyzed by implementing the SPIA program. The horizontal or vertical axis represents the overrepresentation of a pathway (P_{NDE}) or the perturbation of a pathway (P_{PERT}), respectively. Red or blue dotted lines represent the Bonferroni- or FDR- corrected thresholds of significance (1%), respectively, for each axis value. Red and blue circles are significant pathways after Bonferroni and FDR correction (1%) of the global P values (P_G), respectively. A list of pathways consisting of red circles (Bonferroni corrected $P_G < 0.01$) is shown below.

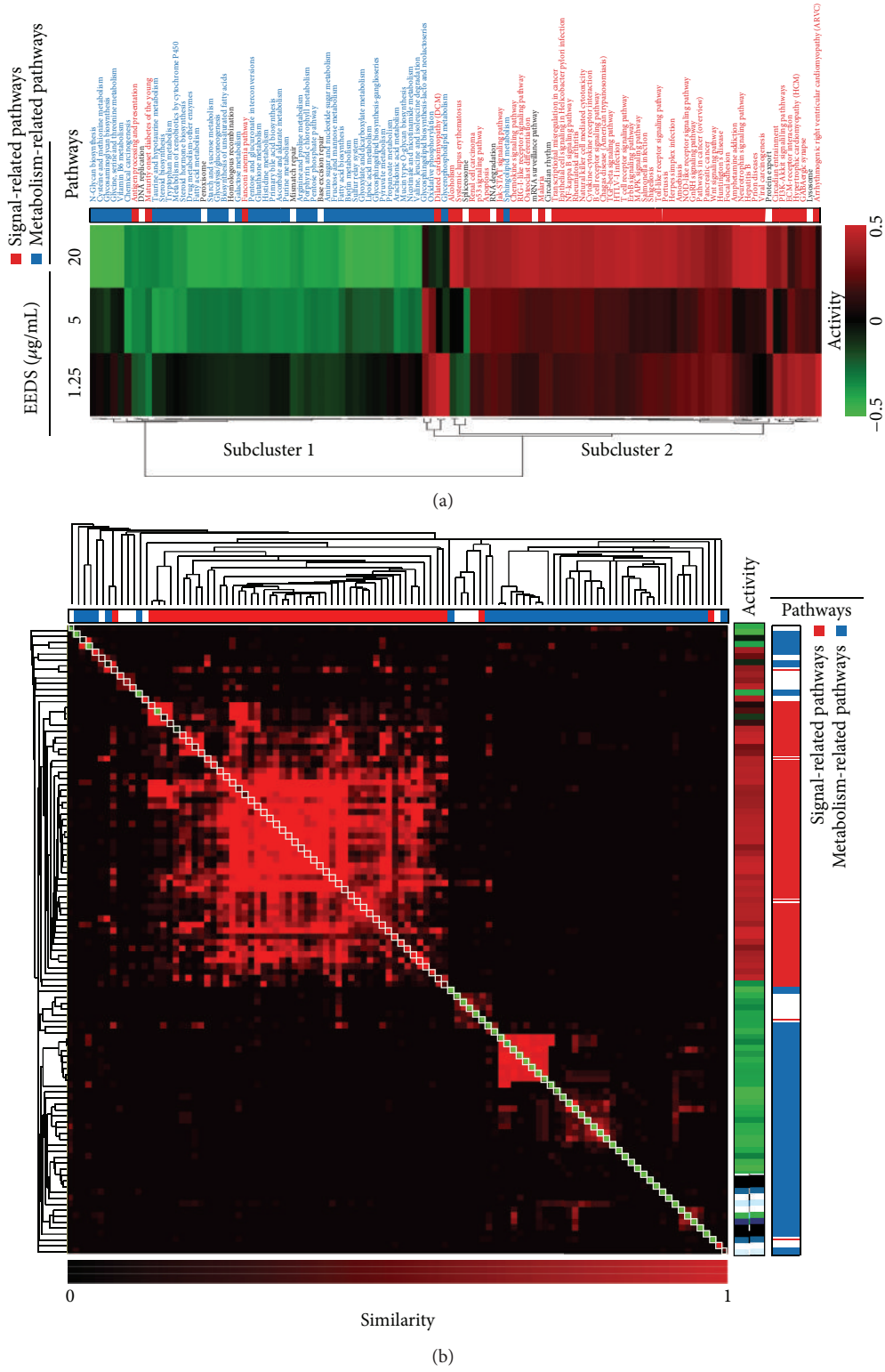

Figure 5: Pathway activities altered by EEDS treatment in A549 cells. (a) The dose-dependent change in pathway activities was measured and clustered hierarchically. Columns represent individual samples, and rows represent activities of pathways. The pathway activity color scale ranges from red (high) to green (low), as indicated by scale bars with arbitrary units. The pathway positions are colored green to indicate metabolic pathways and red to indicate signaling-related pathways. (b) After measurement of the similarity between pathways, the matrix of similarity was clustered hierarchically and merged with activities of pathways. The level of similarity is represented in red with a scale bar. The color in the box of a diagonal line or "Activity" on the right panel represents the activity of the pathway. The positions of signaling-related pathways are colored red and the metabolism-related pathways are colored blue.

Table 5: Pathways associated with Up- and Down-patterns by EEDS treatment.

KEGG ID	Pathway	P value*	FDR**
Down-pattern			
03410	Base excision repair	$3.90E{-}04$	$6.66E{-}03$
00030	Pentose phosphate pathway	$1.47E{-}04$	$1.22E{-}03$
Up-pattern			
04010	MAPK signaling pathway	$1.16E{-}07$	$1.83E{-}05$
04210	Apoptosis	$4.99E{-}06$	$3.94E{-}04$
04115	p53 signaling pathway	$2.46E{-}05$	$1.29E{-}03$
04350	TGF-beta signaling pathway	$5.36E{-}05$	$2.11E{-}03$
04060	Cytokine-cytokine receptor interaction	$1.14E{-}04$	$3.60E{-}03$
04710	Circadian rhythm	$3.20E{-}04$	$8.38E{-}03$
04621	NOD-like receptor signaling pathway	$3.39E{-}04$	$7.61E{-}03$

*P values were calculated using Fischer's test.
**FDR corrections were calculated using the Benjamini-Hochberg procedure [17].

were also significantly enriched in the Up-pattern gene set ($P_G < 0.01$), raising the possibility that the EEDS stimulates functionally related biological pathways (Figure 4(b)). The MAPK pathway has been widely reported to be involved in the growth and invasion of lung cancer, and this pathway has been used for the development of anti-lung cancer drugs [26–28]. Activation of the apoptosis and p53 pathways is also one of the main targets of anti-lung cancer drugs, including herbal extracts [29–31]. Other functionally related pathways identified in the Up-pattern gene set included immune system- or infectious disease-related pathways, including cytokine-cytokine receptor interaction (KEGG 04060), NOD-like receptor signaling pathway (KEGG 04621), Helicobacter pylori infection (KEGG 05120), and Salmonella infection (KEGG 05132). Interestingly, immune-system regulation has been reported to improve lung cancer patient outcomes [32, 33]. Similar functional involvement was also observed when we performed a pathway analysis using all of the differentially expressed genes contained in the Down- or the Up-pattern gene sets (Figure 4(c)).

In addition to the Down- and Up-pattern gene sets, we used the expression values from all genes to measure changes in pathway activities. Intriguingly, the results of this analysis clearly demonstrated that metabolism-related pathways and signaling-related pathways were regulated in dose-dependent and reciprocal manners (Figure 5(a)). The activities of a group of metabolism-related pathways were significantly diminished, whereas a group of signaling pathways, including apoptosis and immune-related pathways, were significantly activated in a dose-dependent manner. The regulatory pattern observed in our system is in agreement with the postulated anti-carcinogenic effects of the EEDS, as previously proposed by many reports in which the inhibition of metabolic pathways and the activation of apoptosis or immune-related pathways were the main targets of lung cancer drug development [23, 26, 29, 31, 32]. The observation that the activities of diverse signaling and metabolic pathways appeared in separate clusters implies the existence of a common reciprocal regulatory mechanism. Therefore, we also measured the relationships between pathways based on the similarities of pathway component genes and integrated pathway activities. The results of this analysis indicate that signaling pathways with increased activity are grouped in a large cluster, suggesting that diverse signaling pathways are similarly affected by EEDS treatment (Figure 5(b)). In contrast, the results show that metabolic pathways with decreased activity are grouped in a small cluster. Our results show that the signaling and metabolic pathways were interconnected through the complex network structure.

Despite these data, the growth inhibitory effect of the EEDS is difficult to explain. To fully elucidate the molecular mechanism underlying the activity of the EEDS, the biological implication of the reciprocal regulation of two biologically distinct groups of pathways must be determined and the exact relationships between the diverse pathways should be verified in more detail. Moreover, further rigorous studies should be done to determine whether the observed reciprocal regulation of biological functions is a general mechanism of herbal extracts. Nonetheless, our present results provide evidence in support of the importance of using whole genome approaches to elucidate pharmaceutical mechanisms.

5. Conclusion

In conclusion, the results of the present study indicate that EEDS treatment induces dose-dependent responses in A549 human non-small cell lung carcinoma cells that involve the up-regulation of a large group of genes associated with cell growth-related signaling pathways and the downregulation of genes associated with metabolic function. This reciprocal regulatory mechanism may provide clues to further our understanding of the mechanism driving growth inhibition in human cancer cells treated with the EEDS, especially in A549 human lung cancer cells.

Conflict of Interests

The authors have declared that there are no competing interests associated with this paper.

Acknowledgments

The authors wish to thank Ms. Deok Rim Heo for her technical assistance in acquiring FACS data. This research was supported by a Grant from the Korea Institute of Oriental Medicine (KIOM, K13061).

References

[1] G. Ghavami, M. R. Kazemali, and S. Sardari, "Informatics of drug synergism in naturally occurring anticancer agents," *Recent Patents on Anti-Cancer Drug Discovery*, vol. 6, no. 1, pp. 26–44, 2011.

[2] J.-S. Chia, J.-L. Du, W.-B. Hsu, A. Sun, C.-P. Chiang, and W.-B. Wang, "Inhibition of metastasis, angiogenesis, and tumor

growth by Chinese herbal cocktail Tien-Hsien Liquid," *BMC Cancer*, vol. 10, article 175, 2010.

[3] H. Wagner and G. Ulrich-Merzenich, "Synergy research: approaching a new generation of phytopharmaceuticals," *Phytomedicine*, vol. 16, no. 2-3, pp. 97–110, 2009.

[4] S. Faivre, S. Djelloul, and E. Raymond, "New paradigms in anticancer therapy: targeting multiple signaling pathways with kinase inhibitors," *Seminars in Oncology*, vol. 33, no. 4, pp. 407–420, 2006.

[5] S. Sathornsumetee, "Therapeutic strategies to target multiple kinases in glioblastoma," *Anti-Cancer Agents in Medicinal Chemistry*, vol. 11, no. 8, pp. 700–711, 2011.

[6] Y. J. Lee, N. S. Kim, H. Kim et al., "Cytotoxic and anti-inflammatory constituents from the seeds of *Descurainia sophia*," *Archives of Pharmacal Ressearch*, vol. 36, no. 5, pp. 536–541, 2013.

[7] Y. Q. Chen, R. Z. Li, and Y. W. Wang, "Identification of cardiac glycosides from the seeds of *Descurainia sophia* L. Webb," *Acta Pharmaceutica Sinica*, vol. 16, no. 1, pp. 62–64, 1981.

[8] K. Sun, X. Li, J.-M. Liu, J.-H. Wang, W. Li, and Y. Sha, "A novel sulphur glycoside from the seeds of *Descurainia sophia* (L.)," *Journal of Asian Natural Products Research*, vol. 7, no. 6, pp. 853–856, 2005.

[9] K. Sun, X. Li, W. Li, J.-M. Liu, J.-H. Wang, and Y. Sha, "A new nor-lignan from the seeds of *Descurainia sophia*," *Natural Product Research*, vol. 20, no. 6, pp. 519–522, 2006.

[10] K. Sun, X. Li, W. Li, J. Wang, J. Liu, and Y. Sha, "Two new lactones and one new aryl-8-oxa-bicyclo[3,2,1]oct-3-en-2-one from *Descurainia sophia*," *Chemical and Pharmaceutical Bulletin*, vol. 52, no. 12, pp. 1483–1486, 2004.

[11] T. M. Ehrman, D. J. Barlow, and P. J. Hylands, "In silico search for multi-target anti-inflammatories in Chinese herbs and formulas," *Bioorganic and Medicinal Chemistry*, vol. 18, no. 6, pp. 2204–2218, 2010.

[12] Y. J. Lee, J. Kim, J. M. Yi et al., "Anti-proliferative neolignans from *Saururus chinensis* against human cancer cell lines," *Biological & Pharmaceutical Bulletin*, vol. 35, no. 8, pp. 1361–1366, 2012.

[13] A. Schroeder, O. Mueller, S. Stocker et al., "The RIN: an RNA integrity number for assigning integrity values to RNA measurements," *BMC Molecular Biology*, vol. 7, article 3, 2006.

[14] B. M. Bolstad, R. A. Irizarry, M. Åstrand, and T. P. Speed, "A comparison of normalization methods for high density oligonucleotide array data based on variance and bias," *Bioinformatics*, vol. 19, no. 2, pp. 185–193, 2003.

[15] J. Ernst and Z. Bar-Joseph, "STEM: a tool for the analysis of short time series gene expression data," *BMC Bioinformatics*, vol. 7, article 191, 2006.

[16] M. Raponi, Y. Zhang, J. Yu et al., "Gene expression signatures for predicting prognosis of squamous cell and adenocarcinomas of the lung," *Cancer Research*, vol. 66, no. 15, pp. 7466–7472, 2006.

[17] G. Dennis Jr., B. T. Sherman, D. A. Hosack et al., "DAVID: database for annotation, visualization, and integrated discovery," *Genome Biology*, vol. 4, no. 5, article P3, 2003.

[18] B. R. Zeeberg, H. Qin, S. Narasimhan et al., "High-throughput GoMiner, an "industrial-strength" integrative gene ontology tool for interpretation of multiple-microarray experiments, with application to studies of Common Variable Immune Deficiency (CVID)," *BMC Bioinformatics*, vol. 6, article 168, 2005.

[19] F. Supek, M. Bošnjak, N. Škunca, and T. Šmuc, "Revigo summarizes and visualizes long lists of gene ontology terms," *PLoS ONE*, vol. 6, no. 7, Article ID e21800, 2011.

[20] A. L. Tarca, S. Draghici, P. Khatri et al., "A novel signaling pathway impact analysis," *Bioinformatics*, vol. 25, no. 1, pp. 75–82, 2009.

[21] S. Y. Lee, K. H. Song, I. Koo et al., "Comparison of pathways associated with hepatitis B- and C-infected hepatocellular carcinoma using pathway-based class discrimination method," *Genomics*, vol. 99, no. 6, pp. 347–354, 2012.

[22] S. Veerla and M. Höglund, "Analysis of promoter regions of co-expressed genes identified by microarray analysis," *BMC Bioinformatics*, vol. 7, article 384, 2006.

[23] V. P. Sukhatme and B. Chan, "Glycolytic cancer cells lacking 6-phosphogluconate dehydrogenase metabolize glucose to induce senescence," *FEBS Letters*, vol. 586, no. 16, pp. 2389–2395, 2012.

[24] W. Zhao, L. Hu, J. Xu et al., "Polymorphisms in the base excision repair pathway modulate prognosis of platinum-based chemotherapy in advanced non-small cell lung cancer," *Cancer Chemotherpy and Pharmacology*, vol. 71, no. 5, pp. 1287–1295, 2013.

[25] C. Kiyohara, K. Takayama, and Y. Nakanishi, "Association of genetic polymorphisms in the base excision repair pathway with lung cancer risk: a meta-analysis," *Lung Cancer*, vol. 54, no. 3, pp. 267–283, 2006.

[26] Z. Lu, L. Ding, H. Hong, J. Hoggard, Q. Lu, and Y.-H. Chen, "Claudin-7 inhibits human lung cancer cell migration and invasion through ERK/MAPK signaling pathway," *Experimental Cell Research*, vol. 317, no. 13, pp. 1935–1946, 2011.

[27] H. Ji, Z. Wang, S. A. Perera et al., "Mutations in BRAF and KRAS converge on activation of the mitogen-activated protein kinase pathway in lung cancer mouse models," *Cancer Research*, vol. 67, no. 10, pp. 4933–4939, 2007.

[28] A. A. Adjei, "The role of mitogen-activated ERK-kinase inhibitors in lung cancer therapy," *Clinical Lung Cancer*, vol. 7, no. 3, pp. 221–223, 2005.

[29] S. Mohan, S. I. Abdelwahab, S. C. Cheah et al., "Apoptosis effect of girinimbine isolated from *Murraya koenigii* on lung cancer cells *in vitro*," *Evididence-Based Complementary and Alternative Medicine*, vol. 2013, Article ID 689865, 12 pages, 2013.

[30] Y. F. Ho, S. A. Karsani, W. K. Yong, and S. N. Abd Malek, "Induction of apoptosis and cell cycle blockade by helichrysetin in a549 human lung adenocarcinoma cells," *Evididence-Based Complementary and Alternative Medicine*, vol. 2013, Article ID 857257, 10 pages, 2013.

[31] T. Choedon, D. Dolma, and V. Kumar, "Pro-apoptotic and anti-cancer properties of thapring—a Tibetan herbal formulation," *Journal of Ethnopharmacology*, vol. 137, no. 1, pp. 320–326, 2011.

[32] F. A. Shepherd, J.-Y. Douillard, and G. R. Blumenschein Jr., "Immunotherapy for non-small cell lung cancer: novel approaches to improve patient outcome," *Journal of Thoracic Oncology*, vol. 6, no. 10, pp. 1763–1773, 2011.

[33] G. Mazzoccoli, M. Grilli, S. Carughi et al., "Immune system alterations in lung cancer patients," *International Journal of Immunopathology and Pharmacology*, vol. 16, no. 2, pp. 167–174, 2003.

Hindawi Publishing Corporation
Evidence-Based Complementary and Alternative Medicine
Volume 2013, Article ID 765914, 10 pages
http://dx.doi.org/10.1155/2013/765914

Research Article

Efficacy and Safety of *Gwakhyangjeonggi-San* Retention Enema in Normal Rats and Spontaneously Hypertensive Rats

Eunyoung Song,[1] Euiju Lee,[2] Yongmin Bu,[3] Junhee Lee,[2] Seungwon Shin,[2] Junghee Yoo,[2] Jaewoo Park,[4] and Jinhyeok Kwon[1]

[1] *Department of Sasang Consitutional Medicine, Graduate School of Clinical Korean Medicine, Kyung Hee University, Seoul 130-702, Republic of Korea*
[2] *Department of Sasang Constitutional Medicine, College of Korean Medicine, Kyung Hee University, Seoul 130-702, Republic of Korea*
[3] *Department of Herbal Pharmacology, College of Korean Medicine, Kyung Hee University, Seoul 130-702, Republic of Korea*
[4] *Department of Spleen System, College of Korean Medicine, Kyung Hee University, Seoul 130-702, Republic of Korea*

Correspondence should be addressed to Euiju Lee; sasangin@daum.net

Received 5 April 2013; Accepted 30 May 2013

Academic Editor: Bo-Hyoung Jang

The purpose of this study is to establish a protocol of retention-enema experiments and evaluate the antihypertensive effect and the safety of *Gwakhyangjeonggi-san* retention enema. Normal and spontaneously hypertensive rats (SHRs) were divided into treatment and control groups, respectively. We applied the *Gwakhyangjeonggi-san* extract by decoction and 0.9% NaCl in each group, estimated the blood pressure and body weight, and performed HPLC analysis. ALT, AST, BUN, and creatinine were examined. The systolic blood pressure within each group in normal rats differed significantly in time effect, and so did the diastolic blood pressure in the treatment group of normal rats. The systolic, diastolic, and mean blood pressure showed significant differences in group effect in the treatment group of the SHRs. The time effect of the body weight in both groups of normal rats differed significantly, so did group × time and time effects in both groups of SHRs. AST, ALT, BUN, and creatinine showed no significant difference between groups. We concluded that the *Gwakhyangjeonggi-san* retention enema has a hypotensive effect in normal rats within the regular range of blood pressure, but an antihypertensive effect in SHRs. Also, the intervention is safe and does not affect the liver and kidney functions in normal rats.

1. Introduction

An enema is a procedure to infuse or drip medication into the rectum through the anus. Decoctions or liquids of medication are usually used as the external treatment. Especially, retention enema is the way to keep drugs (normal saline, herbal medicine, or coffee, etc.) in the rectum for a relatively long time [1].

Bloemen et al. showed that butyrate enemas enhance anastomotic strength of the intestine [2], de Sounza et al. investigated the budesonide and probiotics enemas which are effective to diminish colitis [3], and Bae et al. suggested the anal therapy using Syzygium aromaticum could regulate immediate-type hypersensitivity or anaphylaxis [4].

Only a few investigations involved in retention enema have been conducted. According to the preceding experimental researches, Sprague-Dawley rats [5], mice [6], and Wister rats [7, 8] were used in the experiments of retention enema. And pediatric foley catheters [5], stomach nodes [9], or nylon hoses [7] were used to insert test liquids. The retention time was 15 seconds [7], 30 seconds [3, 10], or 10 minutes [6]. The target disease of most researches was colitis [3, 5, 7, 10]. These show that the method of the retention enema experiments is not unified, nor systematic.

Retention enema is applied to a broader range of diseases including colon-related disorders, cancers, hypertension, and prehypertension in Asian counties. Recently, retention enema was reported as an effective treatment to prevent

prehypertension patients from hypertension [11]. However, it is necessary to find out the efficacy and the safety of retention enema adopted in patients with prehypertension or hypertension.

Korea National Health & Nutrition Examination Survey announced that, among the Korean adults over 30 years, 21.8% of prehypertensive patients and 28.9% of hypertensive patients were reported in 2010, which means that a half of the people over age 30 had hypertension or the risk of developing hypertension [12]. According to another research, 16.6% of individuals of normal blood pressure progressed to hypertension in 5 years, whereas 32.7% of those of prehypertension did so [13]. A cohort research including 169, 871 Chinese people over 40 years old revealed that the risk to develop cardiovascular disorders is higher in the prehypertension group than in normal blood pressure group (relative risk = 1.34), and it is effective to treat prehypertension in patients with diabetes or cardiovascular disorders [14]. This means that it is necessary to detect and regulate the prehypertension early because it progresses easily to hypertension and elevates the occurrence risk of cardiovascular disorders.

In Kim's manual that investigated the clinical effectiveness of retention enema in the hypertension and prehypertension groups, *Gwakhyangjeonggi-san* was used as a test liquid. *Gwakhyangjeonggi-san* is known to block the Ca^{2+} inflow, which results in the vasorelaxant effect by NO action isolated from blood vessels [15]. Expecting that *Gwakhyangjeonggi-san* could act as a vasorelaxant effector in vasoconstrictive diseases such as hypertension [15], we used *Gwakhyangjeonggi-san* as a test liquid, too.

The aim of this study is to establish a protocol of retention-enema experiments and evaluate the antihypertensive effect and the safety of retention enema using *Gwakhyangjeonggi-san*.

2. Materials and Methods

This study was carried out following National Institutes of Health Guide for the Care and Use of Laboratory Animals (NIH Publications no. 80-23, 1996, revised edition) and approved by Kyung Hee University Institutional Animal Care and Use Committee (KHUASP(SE)-12-039).

2.1. Plant Materials. A herbarium voucher sample (KHKH-2013-HK-118) that consists of *Gwakhyangjeonggi-san* was manufactured by Kyung Hee Herb Pharm and examined and deposited in the Korean Medicine Pharmaceutical Operation team, Department of Pharmacy, Kyung Hee University Korean Medicine Hospital (Seoul, Republic of Korea). And constituting components were analyzed in the Pharmaceutical Manufacturing Team, Department of Pharmacy, Kyung Hee University Korean Medicine Hospital (Seoul, Republic of Korea).

The herbs that compose *Gwakhyangjeonggi-san* are *Agastachis Herba* (above-ground parts) 6.0 g, *Perillae Herba* (leaves and twigs) 4.0 g, *Angelicae Dahuricae Radix* (root) 2.0 g, *Arecae Pericarpium* (peel) 2.0 g, *Hoelen* (sclerotium) 2.0 g, *Magnoliae Cortex* (bark) 2.0 g, *Atractylodis Rhizoma Alba* (rhizome) 2.0 g, *Citri Unshii Pericarpium* (peel) 2.0 g, *Pinelliae Tuber Cum Z. R. Crudus et Alumen* (tuber) 2.0 g, *Platycodi Radix* (root) 2.0 g, and *Glycyrrhizae Radix Preparata* (rhizome) 2.0 g. The total amount of the herbs is 28 g.

2.2. Extraction. We put all of the 11 chopped herbs into a felt pouch, then immersed the pouch into Pressure Oriental Herb Medicine Extractor (Handle-Type, KSNP B1130 - 240L, Kyungseo Machine, Incheon, Republic of Korea), and added 120 mL of water to submerge the herbs in the water. Using decocting method, it was concentrated for more than 2 hours until the volume reached 100 mL. The concentrated liquid was mixed with 0.9% saline and the proportion of the final test liquid used was 9 : 1 (concentrates : saline).

2.3. High Performance Liquid Chromatography (HPLC) Analysis. The HPLC system used consisted of Alliance 2690 Separation Module, a Waters 996 Photodiode Array Detector, and a Millenium 32 Chromatography Manager Version 3.2. Chromatographic separations were carried out on a Nucleosil C18 column (4.0 mm × 250 mm I.D. Waters Corporation, Milford, MA, USA) for glycyrrhizin, hesperidin, honokiol, and magnolol at ambient temperature.

Glycyrrhizin, honokiol, and magnolol were purchased from Wako pure chemicals industries, Ltd. (Osaka, Japan). Hesperidin was purchased from Sigma Co. (St. Louis, MO, USA).

Acetonitrile (ACN) and water were used in the product of J. T. Baker (Phillipsburg, NJ, USA). Acetic acid and monopotassium phosphate were used in the product of Duksan pure chemicals Co., Ltd. (Ansan, Kyungki-do, Republic of Korea).

The mobile phase on glycyrrhizin was water-ACN-acetic acid (620 : 380 : 5, v/v) with a flow rate of 1.2 mL/min. The mobile phase on hesperidin was 1/15 M monopotassium phosphate-ACN (815 : 185, v/v) with a flow rate of 1.0 mL/min. The mobile phase on honokiol and magnolol was ACN-water-acetic acid (500 : 500 : 10, v/v) with a flow rate of 1.5 mL/min. The mobile phase was filtered through a 0.45 μm membrane filter (Millipore, Bedford, MA, USA) and was then degassed before use.

GJS was used in the product of Kyung Hee University Korean Medicine Hospital. Each sample was extracted with 50% ethanol for glycyrrhizin, methanol for hesperidin, and ethyl ether for magnolol and honokiol and filtered.

2.4. Animals. Male Sprague-Dawley rats (body weight = 300 ± 20 g) were used as normal and spontaneously hypertensive rats (SHRs). The normal rats were 7–9 weeks old, while the SHRs were 8 weeks old. Both were purchased from Samtaco Animal Corporation (Seoul, Republic of Korea). We adapted the experimental rats to the environment of laboratory for 7 days before the procedure. Less than 5 rats were raised in a plastic cage. We maintained the temperature (22°C ± 2°C) and the humidity (55% ± 15 %) in the laboratory, giving the artificial sunlight for 12 hours every day. Distilled water

Table 1: The setting of drug retention enema.

	The kind, quality of the material and diameter of catheter	The insertion length of catheter	Sample volume	Retention time	Instillation speed
Setting	8 Fr suction catheter	8 cm	6 mL/300 g	10 min	4 mL/min
Procedure	(i) S.D rat (280–320 g) (ii) Measuring BW (iii) Anesthetizing by 2% isoflurane (iv) Ventral position, angle (45°) (v) Connecting syringe which is filled with sample or 0.9% saline to catheter and inserting it into the anal of S.D rat (8 fr suction catheter, 8 cm) (vi) Plastering baseline in catheter (vii) Instillation sample or 0.9% saline (6 mL/300, 4 mL/min) (viii) Retaining sample or 0.9% saline during 10 min (ix) Recovering S.D rat during 10 min (defecation) (x) Measuring BW				

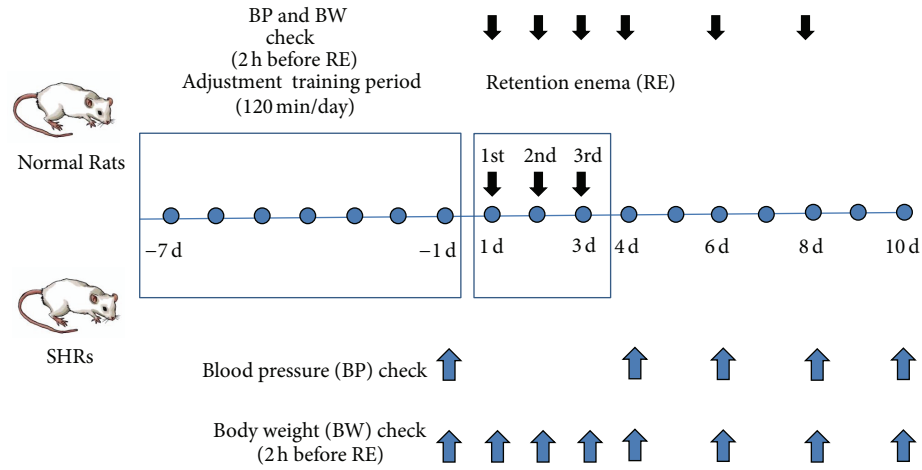

Figure 1: Experimental procedure.

and solid feed were given freely to rats for the experimental period.

We divided 2 groups. The control group was defined as CON group (0.9% NaCl, 6 mL/300 g, $n = 10$), where retention enema with saline was performed. The other was GJS group (*Gwakhyangjeonggi-san*, 6 mL/300 g, $n = 10$), where retention enema with *Gwakhyangjeonggi-san* was performed. Ten rats were randomly allocated to each group in normal rats and SHR rats, respectively.

2.5. Final Protocol through a Preliminary Experiment. The training procedure was carried out 4 times a day and 30 minutes per time for 7 days to adapt the rats in the animal containment (Kent Scientific Corporation, USA) for measuring blood pressure. After the adaptive training, the normal rats and SHRs were relieved in a thermostat for 10~15 minutes. And we measured the body weight of the normal rats and SHRs, anesthetized the rats with isoflurane, fixed them on the operating table, and put them on anaesthetic masks in order. The syringe that contains test liquids, 0.9% of saline, was linked to an 8 Fr suction catheter and fastened up to a tube-connected insertion pump. With the anaesthetic masks worn, we reserved the test liquids for 10 minutes and then relived the rats again (Table 1).

2.6. Blood Pressure Measurement. We measured the rat blood pressure indirectly using a noninvasive blood pressure system (Kent Scientific Corporation, USA). By the tail-cuff method, the blood pressure was measured when not anesthetized after incubating at 36°C ± 0.2°C for 15 minutes [16]. Enema was performed 3 times in all of the rats. In normal rats, blood pressure was measured 2 hours before each enema and first, third, and fifth days after the last enema, whereas, in SHRs, on the day before the first enema and first, third, fifth, and seventh days after the last enema (Figure 1).

2.7. Body Weight Measurement. We measured body weight 3 times at 2 hours before each enema and at the same time on

the first, third, and fifth days after the third enema in normal rats, whereas on the day before the first enema and on the first, third, fifth, and seventh days after the third enema in SHRs.

2.8. Safety

2.8.1. Experimental Group Allocation. We divided 3 groups, which are normal group (no intervention, $n = 8$), CON group (0.9% NaCl, 6 mL/300 g, $n = 8$), and GJS group (*Gwakhyangjeonggi-san*, 6 mL/300, $n = 8$), and randomly allocated 8 rats in each group.

2.8.2. Blood Sample Analysis. After 7-day adaptive training, we carried out a retention enema every day for 3 days. And we anesthetized the rats with isoflurane 2 hours after the third enema and collected 5 mL blood using a 26G disposable syringe by cardiac puncture method. The collected blood was put into SST bottle (BD vacutainer SST tube, BD Korea, USA) and analyzed. We requested aspartate aminotransferase (AST), alanine aminotransferase (ALT), blood urea nitrogen (BUN), and creatinine analysis to Eone Reference Laboratory (Incheon, Republic of Korea).

2.9. Statistical Analysis. We used the PASW Statistics 18.0 for Windows (Chicago, IL). Using generalized estimating equation, we tested group effect, time effect, and group × time effect between groups, as well as time effect within a group with the change of blood pressure and body weight, respectively. As of the safety, we applied Kruskal-Wallis test for a three-group analysis on variables with single assessment. And multiple comparisons using Mann-Whitney U test were performed with the differences of AST, ALT, BUN, and creatinine, respectively, between groups (employing two-tailed Bonferroni-corrected P value of <0.017 to minimize type I error). We calculated mean error and standard error and considered the errors significant when $P < 0.05$.

3. Result

3.1. Blood Pressure in Normal Rats. Figure 1 shows the blood pressure measured in the whole period. The systolic blood pressure decreased in CON group, while it increased in the beginning and decreased gradually after all in GJS group (Figure 2(a)). The diastolic blood pressure showed the same tendency in both groups, respectively (Figure 2(b)).

We calculated the difference of blood pressures daily, based on the baseline blood pressure day. The change of systolic blood pressure was negative in CON group but mostly positive on GJS group. And the absolute value of the systolic blood pressure increased in CON group, while it tended to decrease in GJS group during the whole period (Figure 2(c)). In the change of the diastolic blood pressure, the similar patterns appeared in both groups, respectively (Figure 2(d)).

In comparison of the systolic blood pressure between CON and GJS groups, there was no significant group × time effect ($P = 0.374$) nor significant group effect ($P = 0.179$). But there was statistically significant time effect within CON group ($P = 0.001$) and GJS group ($P < 0.001$).

In comparison of the diastolic blood pressure between CON and GJS groups, there was no significant group × time effect ($P = 0.180$) nor significant group effect ($P = 0.131$). However, there was statistically significant time effect in GJS group ($P = 0.001$), but no significant time effect in CON group ($P = 0.202$).

3.2. Blood Pressure in SHRs. The systolic blood pressure increased during the whole period in CON group, while it decreased, except on the fifth day after 3 enemas, in GJS group (Figure 3(a)). The diastolic blood pressure in CON group increased overall, while it decreased, except on the third and fifth days after 3 enemas, in GJS group (Figure 3(b)). The mean blood pressure in CON group increased overall, while it fluctuated similarly with the pattern of the diastolic blood pressure in GJS group (Figure 3(c)).

The systolic blood pressure between CON and GJS groups did not show any significant difference in group × time effect ($P = 0.396$) but showed significant difference in the group effect ($P = 0.012$). And the time effect did not differ significantly in CON group ($P = 0.471$), while it differed significantly in GJS group ($P < 0.001$).

The diastolic blood pressure between CON and GJS groups did not show any significant difference in group × time effect ($P = 0.572$) but showed significant difference in group effect ($P = 0.009$). And the time effect did not differ significantly in CON group ($P = 0.779$), while it differed significantly in GJS group ($P < 0.001$).

The mean blood pressure between CON and GJS groups did not show any significant difference in group × time effect ($P = 0.436$) but showed significant difference in group effect ($P = 0.012$). And the time effect did not differ significantly in CON group ($P = 0.956$), while it differed significantly in GJS group ($P < 0.001$).

3.3. Body Weight in Normal Rats and SHRs. The body weight in CON and GJS groups of normal rats decreased a little for 3 days when the enema was performed, maintained until the sixth day after the third enema, and increased after the eighth day (Figure 4(a)). No significant group × time effect existed ($P = 0.715$), and no group effect either ($P = 0.363$). However, the time effect appeared statistically significant in CON ($P < 0.001$) and GJS ($P < 0.001$) groups.

The body weight of SHRs increased overall during the whole period in both CON and GJS groups (Figure 4(b)). The group × time effect differed significantly ($P = 0.001$), so as the time effect within both groups ($P < 0.001$).

3.4. AST, ALT, BUN, and Creatinine. The measured AST was 112.25 ± 6.51 IU/L (normal group), 136.12 ± 20.09 IU/L (CON group), and 97.25 ± 3.94 IU/L (GJS group). The ALT was 33.25 ± 1.81 IU/L (normal group), 38.50 ± 2.16 IU/L (CON group), and 35.00 ± 1.31 IU/L (GJS group). The BUN was 14.55 ± 1.24 mg/dL (normal group), 16.83 ± 0.97 mg/dL (CON group), and 13.38 ± 0.94 mg/dL (GJS group). The creatinine was 0.27 ± 0.01 mg/dL (normal group), 0.27 ± 0.01 mg/dL (CON group),

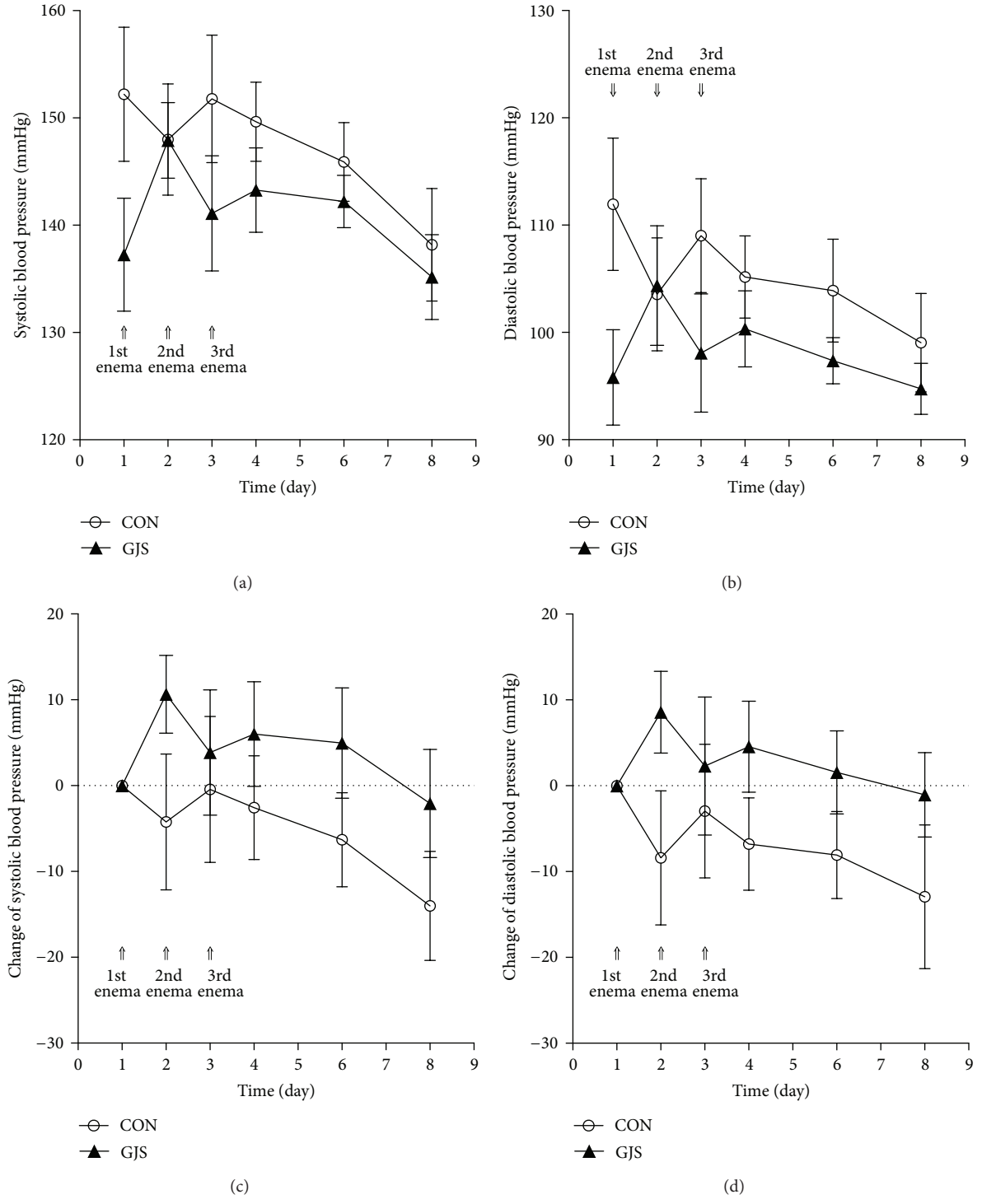

Figure 2: The blood pressure in the whole period. (a) Systolic blood pressure. (b) Diastolic blood pressure. (c) The change of systolic blood pressure. (d) The change of diastolic blood pressure.

and 0.24 ± 0.01 mg/dL (GJS group). AST, ALT, BUN, and creatinine showed no significant difference between groups.

3.5. HPLC Analysis. Figure 5 shows the typical chromatogram of glycyrrhizin (a), *Glycyrrhizae Radix* (b), and GJS (c). The peak time of glycyrrhizin was about 10.6 minutes and the content was 3.27% and 0.46% in *Glycyrrhizae Radix* and GJS, respectively.

Figure 6 shows the typical chromatogram of hesperidin (a), *Citri pericarpium* (b), and GJS (c). The peak time of hesperidin was about 25.5 minutes and the content was 4.7% and 0.6% in *Citri pericarpium* and GJS, respectively.

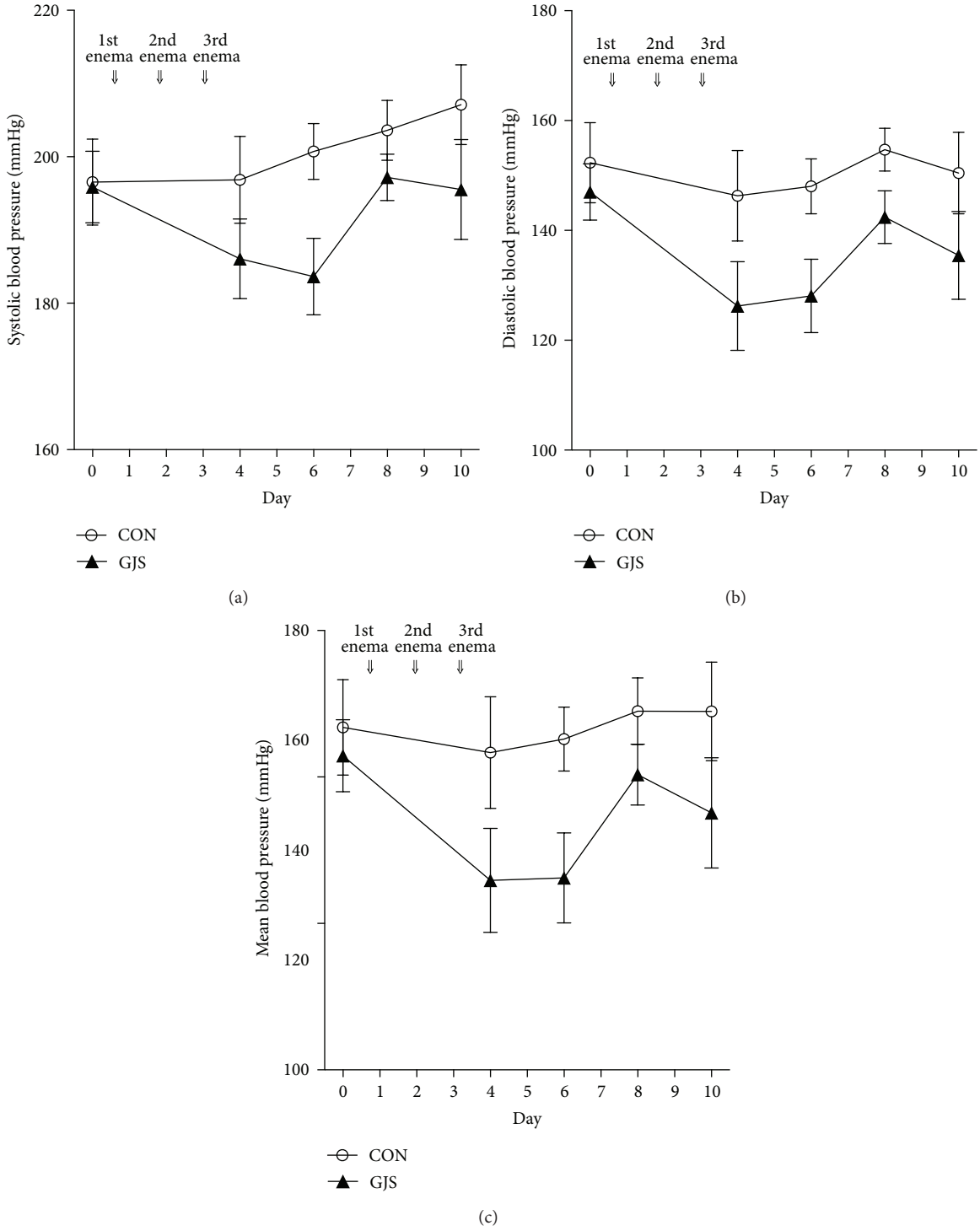

Figure 3: The blood pressure in the whole period. (a) Systolic blood pressure. (b) Diastolic blood pressure. (c) Mean blood pressure.

Figure 7 shows the typical chromatogram of honokiol and magnolol (a), *Magnoliae Cortex* (b), and GJS (c). The peak time of honokiol was about 9.1 minutes and the content was 2.16% and 0.005% in *Magnoliae Cortex* and GJS, respectively. The peak time of magnolol was about 12.6 minutes and the content was 6.24% and 0.01% in *Magnoliae Cortex* and GJS, respectively.

4. Discussion

We drew the protocol of retention enema through a pilot study and clinical experiences. The pilot study could make us confirm the efficacy and safety of the method. We used Sprague-Dawley rats because they are known to endure shock caused by enema and be easy to insert test liquids. As of

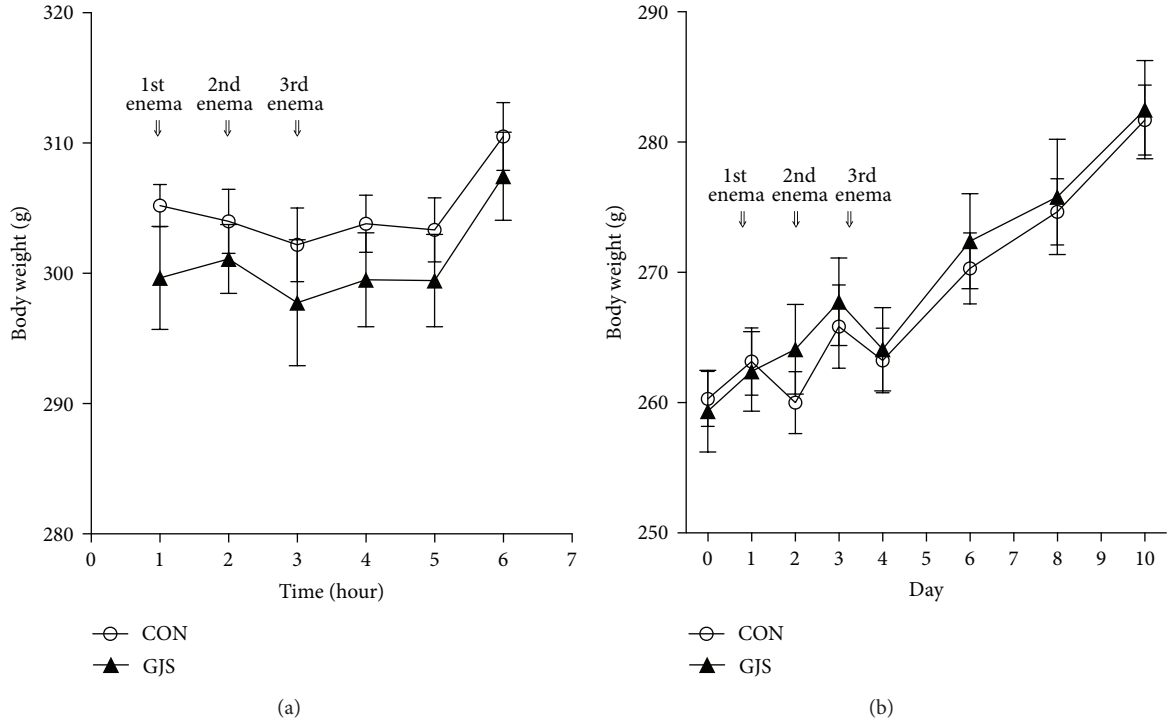

Figure 4: The body weight change in the whole period. (a) Normal rats. (b) SHRs.

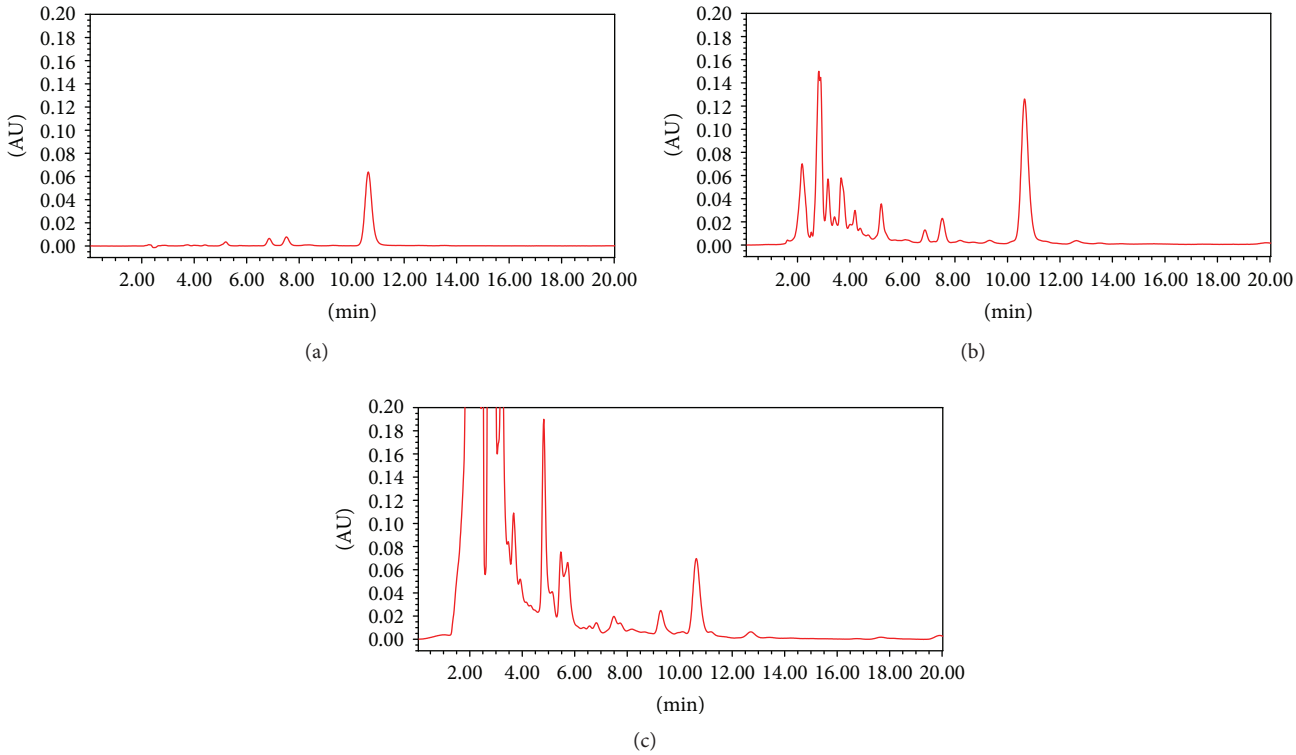

Figure 5: Chromatograms of (a) glycyrrhizin, (b) *Glycyrrhizae Radix*, and (c) GJS.

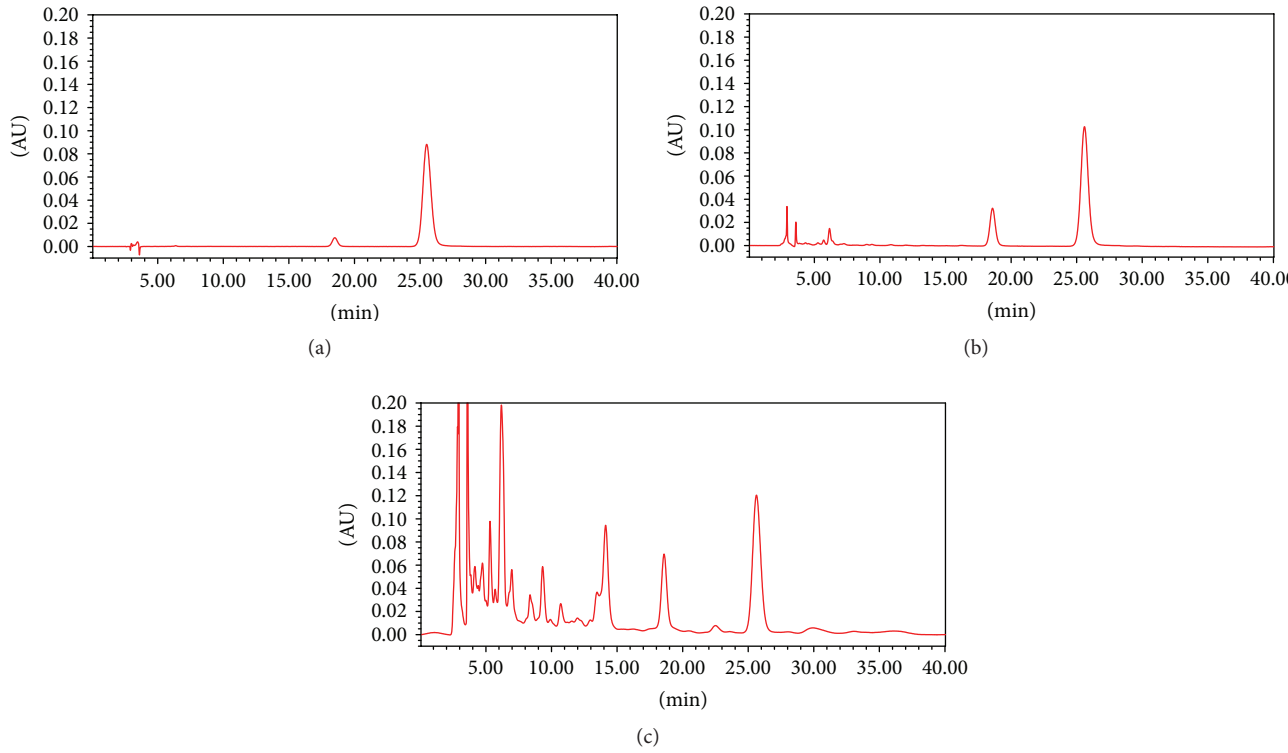

Figure 6: Chromatograms of (a) hesperidin, (b) *Citri pericarpium*, and (c) GJS.

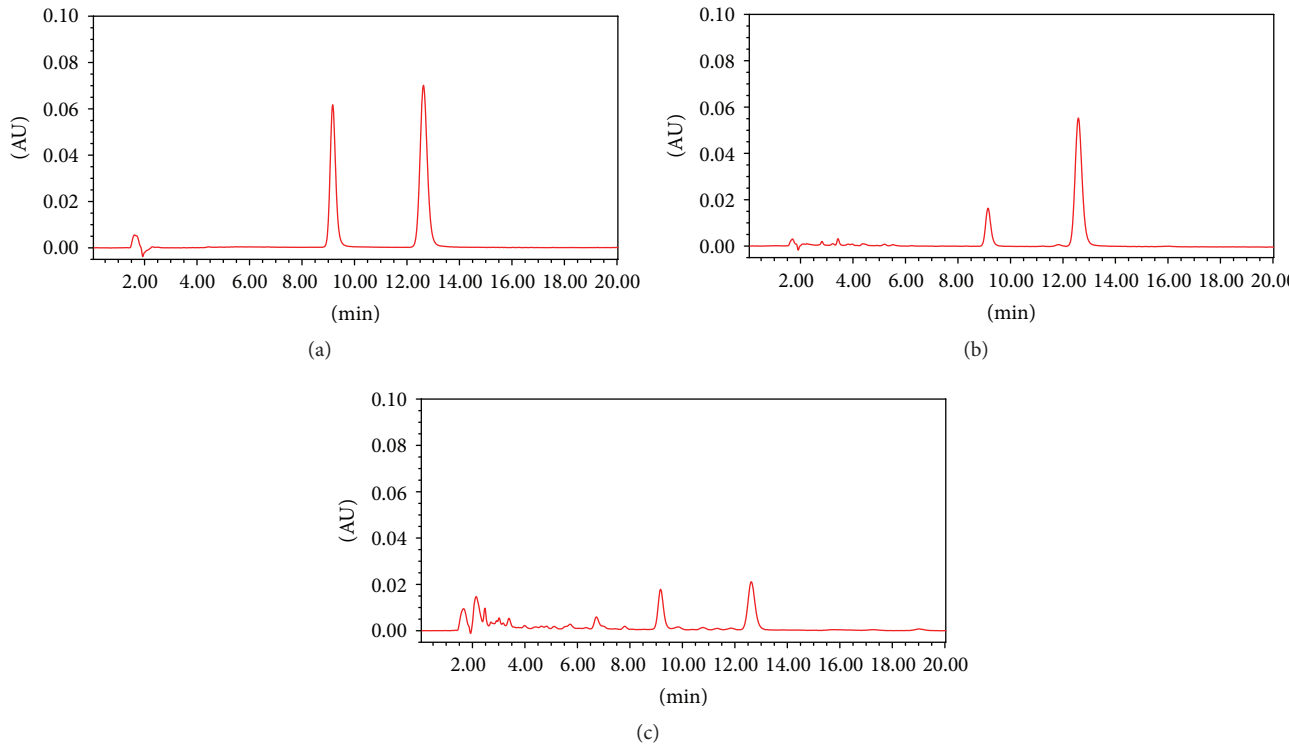

Figure 7: Chromatograms of (a) honokiol and magnolol, (b) *Magnoliae Cortex*, and (c) GJS.

the insertion tool and diameter, 6 Fr polyethylene catheter (male Wistar rats 250–300 g) [3] and 8 Fr pediatric foley catheter (S.D rat, 220–320 g) [5] have been applied. As of the insertion length, 6 cm [17] and 8 cm [7] have been used. About the retention time, the absorption concentration peaked around 10 minutes after the insertion in a study [18], and another researcher kept the test liquid for 10 minutes [6]. And the insertion velocity was 4 mL/min deprived from the running-fluid velocity, 1000 mL per 90 seconds, based on Kim's manual. The method applied in this study is very similar to the way used in the clinical practice.

A study reported that the test liquid made of *Gwakhyangjeonggi-san* is absorbed in the transverse colon during the retention [19]. However, the change of blood pressure did not differ between the CON groups and GJS groups in normal rats. This is because the normal rats do not have any disorders to be influenced by test liquids. On the other hand, the changes of systolic and diastolic blood pressure differed significantly with time in GJS group, and the changes of systolic blood pressure did in CON group too. This means that retention enema has hypotensive effect in normal rats.

The systolic, diastolic, and mean blood pressure had no interactions between the group and time in CON and GJS groups of SHRs. However, the blood pressure decreased significantly with time only in GJS group, which indicates there is a meaningful antihypertensive effect when the *Gwakhyangjeonggi-san* retention enema is applied. This can be explained by a few reasons. First, *Gwakhyangjeonggi-san* is reported to have the vasodilator effect, which leads to the antihypertensive effect [15]. Second, pharmacologically, glycyrrhizin in *Glycyrrhizae Radix* can lower blood cholesterol level and blood pressure, hesperidin in *Citri pericarpium* has a hypotensive effect acting on smooth muscles in the blood vessel directly, and honokiol and magnolol in *Magnoliae Cortex* reduced the blood pressure of rats and cats by intravenous injection [20–22]. All of these components were analyzed by HLPC method in this study. Also it is known that angelic acid in *Angelicae Dahuricae Radix* stimulates the vasomotor center in medulla oblongata, the ether extract of *Hoelen* strengthens cardiac contraction, and *Platycodi Radix* lowers blood pressure for a short time [20–22], even though we could not measure 3 of these in our HPLC analysis. Third, the large intestine can absorb fats and oils components easily, which are contained a lot in herbs of *Gwakhyangjeonggi-san* [17]. Lastly, the test-liquid concentration absorbed in large intestine peaked in 10 minutes after the retention [18], which is applied to this study too.

It is usually believed that the weight loss lower the blood pressure; however, the blood pressure decreased significantly in GJS group, even though the change of body weight increased in SHRs. This indicates the antihypertensive effect is from the test liquids, not from the weight loss.

There was no significant difference in AST, ALT, BUN, and creatinine between groups. We found out that the retention enema by *Gwakhyangjeonggi-san*, which does not affect liver and kidney function, is a safe way.

The importance of this study is that the protocol of retention enema has been established at first through the preliminary experiment and the clinical practice. Secondly, we have confirmed the safety of retention enema by *Gwakhyangjeonggi-san*, which means it does not affect the liver and kidney functions. Finally the antihypertensive effect has been revealed in *Gwakhyangjeonggi-san* retention enema. The effect maintained 7 days after the enema in SHRs.

The limitations are as follows. First, the baseline values of blood pressure were different between groups because of the different levels of adaptation by group in normal rats. We analyzed the change of blood pressures to correct the difference. Second, the observation time after the enema was too short. A long-term experiment is necessary to find out the continuous effect. Third, blood test to assess hepatic and renal enzymes, histological test to examine colonic mucosal changes, and additional test to identify intestinal bacteria are usually carried out in a safety study. However, only simple blood tests were performed with normal rats in this study. In the future, overall safety study will proceed including SHRs. Fourth, the HPLC results did not reveal every active component of every herb instituting *Gwakhyangjeonggi-san*. This could be because the lag of the HPLC machine or little mass of some herbs in *Gwakhyangjeonggi-san*. Fifth, considering the usual duration of drug activity, the maintenance of lowered blood pressure for 5 or 7 days could be due to the enema itself, not the enema with *Gwakhyangjeonggi-san*. Further studies are needed to investigate the precise mechanisms under the enema without any specific drugs. Lastly, the variation was too big because of the small sample. The sample size should be increased in the future study.

This study suggests that the retention enema with *Gwakhyangjeonggi-san* is safe when performed in normal people, preventive of hypertension in prehypertension patients, and antihypertensive in hypertension patients.

A long-term observation should be carried out in the future, based on which we can estimate the active duration of retention enema with *Gwakhyangjeonggi-san*. Secondly, the effect of the *Gwakhyangjeonggi-san* enema should be compared with that of the *Gwakhyangjeonggi-san* oral intake as a hypotensive effector. Finally, a randomized controlled trial should be performed to confirm the clinical effectiveness and safety.

5. Conclusions

The retention enema with *Gwakhyangjeonggi-san* has a hypotensive effect in normal rats within the regular range of blood pressure, but an antihypertensive effect in SHRs. The retention enema is safe and does not affect the liver and kidney functions in normal rats.

Conflict of Interests

The authors declare that they have no conflict of interests.

Acknowledgment

This study was supported by a Grant of the Traditional Korean Medicine R&D Project, Ministry of Health & Welfare, Republic of Korea (B120043).

References

[1] M. J. Lee, "The study of enema therapy as one of the detoxification therapy," *Journal of Oriental Neuropsychiatry*, vol. 15, no. 2, pp. 23–36, 2004.

[2] J. G. Bloemen, M. H. Schreinemacher, A. P. De Bruine, W. A. Buurman, N. D. Bouvy, and C. H. Dejong, "Butyrate enemas improve intestinal anastomotic strength in a rat model," *Diseases of the Colon and Rectum*, vol. 53, no. 7, pp. 1069–1075, 2010.

[3] M. M. de Sounza, J. E. De Aguilar-Nascimento, and D. B. Dock-Nascimento, "Effects of budesonide and probiotics enemas on the systemic inflammatory response of rats with experimental colitis," *Acta Cirurgica Brasileira*, vol. 22, no. 1, pp. 40–45, 2007.

[4] S. H. Bae, G. Moon, and J. H. Won, "Inhibitory effect of immediate-type hypersensitivity of Syzygium aromaticum extract by anal therapy," *The Journal of Oriental Medical Surgery, Ophthalmology and Otolaryngology*, vol. 13, no. 1, pp. 142–156, 2000.

[5] R. H. Rolandelli, S. H. Saul, R. G. Settle, D. O. Jacobs, S. O. Trerotola, and J. L. Rombeau, "Comparison of parenteral nutrition and enteral feeding with pectin in experimental colitis in the rat," *American Journal of Clinical Nutrition*, vol. 47, no. 4, pp. 715–721, 1988.

[6] E. Gaudier, M. Rival, M.-P. Buisine, I. Robineau, and C. Hoebler, "Butyrate enemas Upregulate Muc genes expression but decrease adherent mucus thickness in mice colon," *Physiological Research*, vol. 58, no. 1, pp. 111–119, 2009.

[7] S.-M. Guo, H.-B. Tong, L.-S. Bai, and W. Yang, "Effect of traditional Chinese medicinal enemas on ulcerative colitis of rats," *World Journal of Gastroenterology*, vol. 10, no. 13, pp. 1914–1917, 2004.

[8] T. Takagi, Y. Naito, T. Okuda et al., "Ecabet sodium promotes the healing of trinitrobenzene-sulfonic-acid-induced ulceration by enhanced restitution of intestinal epithelial cells," *Journal of Gastroenterology and Hepatology*, vol. 25, no. 7, pp. 1259–1265, 2010.

[9] G. U. Lee, S. J. Moon, G. Moon, and J. H. Won, "Inhibitory effects of allergic reaction of Sochungyongtang," *The Journal of Traditional Korean Medicine*, vol. 8, no. 2, pp. 227–238, 1998.

[10] H. Yuceyar, O. Ozutemiz, A. Huseyinov et al., "Is administration of n-3 fatty acids by mucosal enema protective against trinitrobenzene-induced colitis in rats?" *Prostaglandins Leukotrienes and Essential Fatty Acids*, vol. 61, no. 6, pp. 339–345, 1999.

[11] H. J. Kim, *Detoxification-Liveliness Therapy*, Sallim Korean Medicine Clinic, Busan, Republic of Korea, 2011.

[12] Ministry of Health, *Report on 2010 National Health and Nutrition Survey*, Ministry of Health and Welfare, Seoul, Republic of Korea, 2011.

[13] Ministry of Health Welfare and Family Affairs; Korea Centers for Disease Control & Prevention, *KHyDDI (Korea Hypertension Diabetes Daegu Initiative) Project Report*, Kyungpook National University, Daegu, Repulic of Korea, 2008.

[14] D. Gu, J. Chen, X. Wu et al., "Prehypertension and risk of cardiovascular disease in Chinese adults," *Journal of Hypertension*, vol. 27, no. 4, pp. 721–729, 2009.

[15] C. M. Koo, J. K. Sun, H. H. Kim, and C. G. Nam, "Effects of Gwakhyangjungisan on the arterial contraction in rabbit," *Korean Journal of Oriental Internal Medicine*, vol. 24, no. 2, pp. 260–268, 2003.

[16] Korea Food & Drug Administration, *A Guideline to Test the Efficacy of Herbal Medicine for Hypertension*, Korea Food & Drug Administration, Seoul, Republic of Korea, 2007.

[17] T. Nakashima, T. Maeda, H. Nagamoto, T. Kumakura, M. Takai, and T. Mori, "Rebamipide enema is effective for treatment of experimental dextran sulfate sodium induced colitis in rats," *Digestive Diseases and Sciences*, vol. 50, no. 1, pp. S124–S131, 2005.

[18] H. S. Lee, S. K. Jin, J. H. Choi, and Y. S. Ku, "Rectal absorption of acetaminophen from polyethylene glycol and witepsol suppositories," *Korean Journal of Clinical Pharmacy*, vol. 8, no. 2, pp. 143–146, 1998.

[19] S. J. Lee, "The movement of large intesine," *Chungbuk Medical Journal*, vol. 7, no. 2, pp. 157–167, 1997.

[20] S. Y. Lee, D. G. An, and M. G. Shin, *Clinical Applications of Herbal Medicines*, Seongbosa, Seoul, Republic of Korea, 1981.

[21] S. Y. Lee, *Herbology*, Seongbosa, Seoul, Republic of Korea, 1981.

[22] G. J. Jin, *The Interpretation of Bonchogangmok*, Hakwon, Beijing, China, 1992.

Hindawi Publishing Corporation
Evidence-Based Complementary and Alternative Medicine
Volume 2013, Article ID 617302, 7 pages
http://dx.doi.org/10.1155/2013/617302

Research Article

Water Extract of Deer Bones Activates Macrophages and Alleviates Neutropenia

Han-Seok Choi, Soon Re Kim, Se Hyang Hong, Jin Mo Ku, Min Kyoung Kim, Hye Sook Seo, Sung-Gook Cho, Sangtae Shin, Yong Cheol Shin, and Seong-Gyu Ko

Department of Preventive Medicine, College of Korean Medicine, Kyung Hee University, Seoul 130-701, Republic of Korea

Correspondence should be addressed to Seong-Gyu Ko; epiko@khu.ac.kr

Received 4 April 2013; Accepted 11 May 2013

Academic Editor: Bo-Hyoung Jang

Extracts from deer bones, called nok-gol in Korean, have long been used to invigorate Qi. While neutropenia is not well detected in normal physiological condition, it could be a cause of severe problems to develop diseases such as infectious and cancerous diseases. Thus, a prevention of neutropenia in normal physiology and pathophysiological states is important for maintaining Qi and preventing disease progress. In cell biological aspects, activated macrophages are known to prevent neutropenia. In this study, we demonstrate that water extract of deer bone (herein, NG) prevents neutropenia by activating macrophages. In mouse neutropenia model system *in vivo* where ICR mice were treated with cyclophosphamide to immunosuppress, an oral administration of NG altered the number of blood cells including lymphocytes, neutrophils, basophils, and eosinophils. This *in vivo* effect of NG was relevant to that of granulocyte colony stimulating factor (G-CSF) that was known to improve neutropenia. Our *in vitro* studies further showed that NG treatment increased intracellular reactive oxygen species (ROS) and promoted macrophagic differentiation of mouse monocytic Raw264.7 cells in a dose-dependent manner. In addition, NG enhanced nitric oxide (NO) synthesis and secretions of cytokines including IL-6 and TNF-α. Consistently, NG treatment induced phosphorylation of ERK, JNK, IKK, IκBα, and NF-κB in Raw264.7 cells. Thus, our data suggest that NG is helpful for alleviating neutropenia.

1. Introduction

Neutropenia is characterized by a low neutrophil number, which could be a risk of disease development including infectious and cancerous diseases [1–6]. Thus, therapeutic approaches such as administration with G-CSF or GM-CSF have been applied to prevent neutropenic phenomenon, while no trials are completely worked yet [7–10]. Macrophages, one of the players in the innate immune system, modulate immune response through inflammatory cytokines and reactive oxygen species (ROS) [11–13]. In neutropenic situation, macrophages could not be involved in inflammation because neutrophil depletion results in no reaction of monocytes and macrophages [14]. As macrophages produce CSF, an activation of macrophages is crucial for preventing neutropenia and secondary diseases [15–17].

Extracts from deer bones, called nok-gol in Korean, have been traditionally used as a drug invigorating Qi. Recent researches further reported various therapeutic effects of this traditional medicine on inflammatory disease [18, 19], bone resorption [20], and aging [21]. Furthermore, extracts of deer bones affected macrophagic activation in *S. aureus*-infected mice [22]. In this study, we demonstrate that water extract of deer bones (hereafter, NG) alleviates neutropenia through activating macrophages.

2. Materials and Methods

2.1. Cell Culture and Deer Bone Extract Preparation. Raw264.7 mouse monocytic/macrophagic cells were grown in Dulbecco's Modified Eagle's Medium (DMEM) supplemented with 10% heat-inactivated fetal bovine serum (FBS) and 1% antibiotics at 37°C in a 5% CO_2 humidified incubator. Water extract of deer bones (NG) was provided by Nongshim Corporation (Republic of Korea). More information on NG production processes could be requested from the company.

Table 1: The sequence of PCR primers.

Primer name	Sequences
IL-6	
Forward	5′-CAA GAG ACT TCC ATC CAG TTG C-3′
Reverse	5′-TTG CCG AGT TCT CAA AGT GAC-3′
TNF-α	
Forward	5′-ATG AGC ACA GAA AGC ATG ATC-3′
Reverse	5′-TAC AGG CTT GTC ACT GGA ATT-3′
COX-2	
Forward	5′-AAG ACT TGC CAG GCT GAA CT-3′
Reverse	5′-CTT CTG CAG TCC CAG GTT CAA-3′
iNOS	
Forward	5′-AAT GGC AAC ATC AGG TCG GCC ATC ACT-3′
Reverse	5′-GCT GTG TGT CAC AGA AGT CTC GAA CTC-3′
GAPDH	
Forward	5′-GAG GGG CCA TCC ACA GTC TTC-3′
Reverse	5′-CAT CAC CAT CTT CCA GGA GCG-3′

Table 2: The number of WBC, lymphocytes, neutrophils, monocytes, and eosinophils in mice blood. Each value presents the mean ± SD ($^{*}P < 0.05$, $^{**}P < 0.01$, and $^{***}P < 0.001$).

(a)

	Normal	Negative Con	Positive Con	NG
WBC (K/uL)	10.89 ± 1.57	2.49 ± 1.48***	4.93 ± 0.71***	5.10 ± 1.48**
Lymphocytes (K/uL)	6.21 ± 1.27	0.76 ± 0.27***	1.77 ± 0.39**	2.00 ± 0.56**
Neutrophils (K/uL)	2.81 ± 0.77	1.07 ± 0.72*	2.75 ± 0.67	2.91 ± 0.79
Monocytes (K/uL)	0.59 ± 0.16	0.18 ± 0.07**	0.15 ± 0.07***	0.12 ± 0.04**
Eosinophils (K/uL)	0.22 ± 0.07	0.37 ± 0.06*	0.38 ± 0.06*	0.30 ± 0.13
Basophils (K/uL)	0.05 ± 0.02	0.04 ± 0.02	0.05 ± 0.02	0.07 ± 0.04

(b)

	Normal	Negative Con	Positive Con	NG
Lymphocytes (%)	60.01 ± 6.85	41.93 ± 9.20*	41.64 ± 9.18*	31.05 ± 7.25***
Neutrophils (%)	29.87 ± 8.26	35.15 ± 19.12	55.95 ± 11.12**	60.31 ± 7.88***
Monocytes (%)	5.59 ± 0.64	5.21 ± 1.97	6.77 ± 1.62	4.06 ± 2.73
Eosinophils (%)	2.79 ± 1.33	8.99 ± 2.58**	7.12 ± 2.04**	4.68 ± 0.73*
Basophils (%)	0.50 ± 0.10	1.78 ± 0.89*	1.54 ± 0.23***	1.07 ± 0.62

2.2. In Vivo Studies. Six-week-old male ICR mice were purchased from Orient (Sungnam, Republic of Korea). All procedures were performed on the approval of the animal care center of Kyung Hee University (Approval no. KHUASP (SE)-12-042). To induce neutropenia, mice were intraperitoneally injected with 150 mg/kg of cyclophosphamide twice in one week and then treated with cyclophosphamide (100 mg/kg) two times in another week. Mice were rested for one week with no treatment when treatments were switched. In addition, mice were randomized into 4 groups (normal, control, G-CSF, and NG; five mice per group) during resting time points. G-CSF (1 μg/kg) or NG (200 mg/kg) was orally administered every day for the last procedure. At the end of the experiment, mice were sacrificed by CO_2 inhalation, and cardiac blood was collected.

2.3. Cell Surface Observation. Cells seeded into 60 mm culture dish at a density of 3×10^5 cells/dish were treated with NG (25, 250, 500 μg/mL) for 24 h. Cell surfaces were observed by taking images using a camera (Olympus, Japan) connected to a light microscope.

2.4. Cell Viability Assay. Cell viability was determined using WST assay (Dogen, Republic of Korea). RAW264.7 cells (1×10^4 cells/well) were seeded into 96-well plates and incubated overnight. Cells were then treated with different concentrations of NG and incubated for another 24 hours. 10 μL of WST solution was added to 100 μL cell culture medium, and plates were incubated for 2 hours. Optical density (OD) was determined at 450 nm using a microplate reader (Versa Max, Molecular Devices, CA, USA).

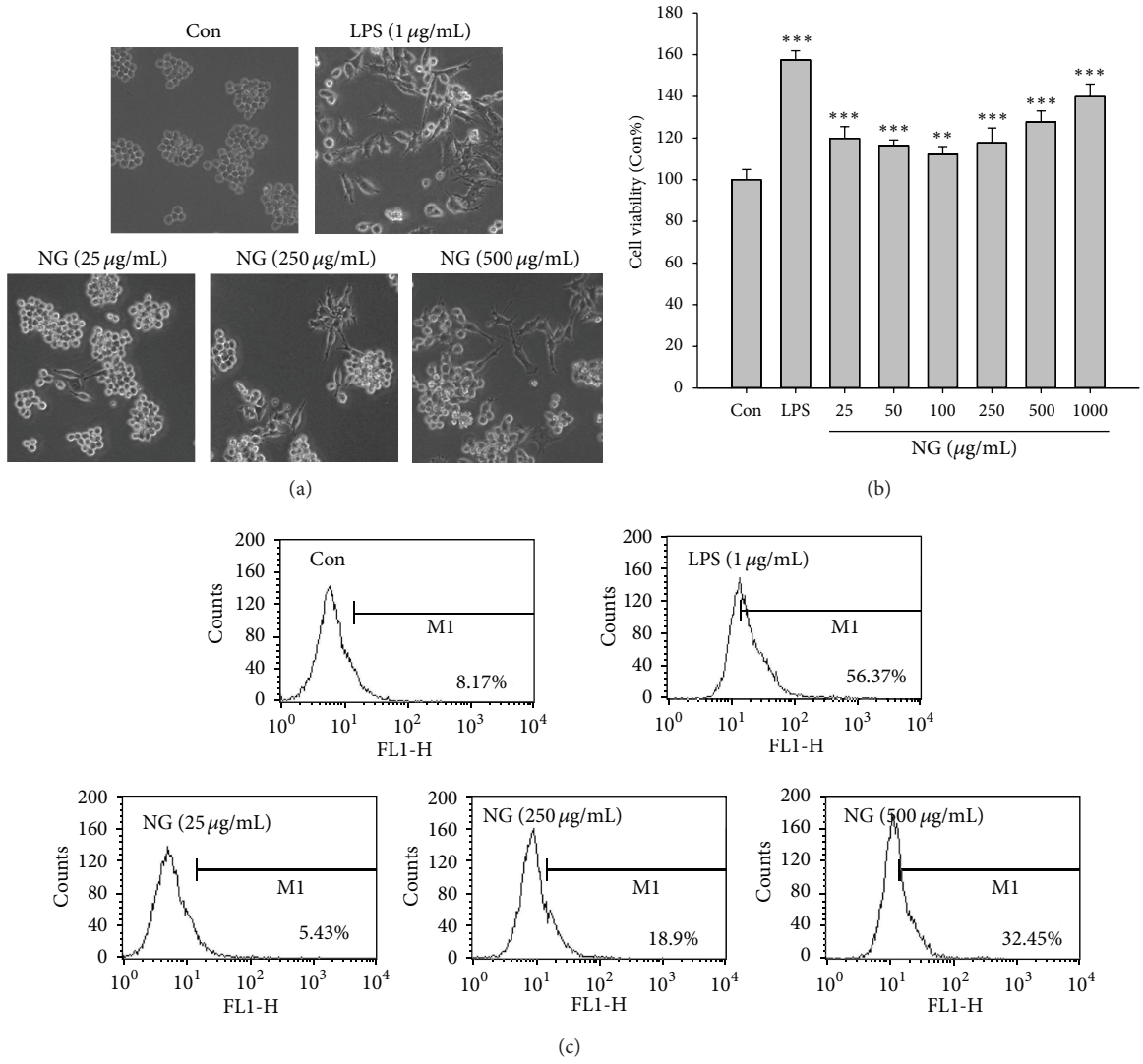

Figure 1: NG activates RAW264.7 cells. (a) Cells were seeded into 60 mm culture dish at a density of 3×10^5 cells/dish. The next day, cells were treated with NG for 24 h. Cell surface was observed by taking a photograph using a camera attached to a microscope. (b) Cell viability was determined using WST assay after NG treatment. (c) ROS level was measured using DCFH-DA. Data are shown as the mean of three independent experiments (error bars are mean ± standard deviation (SD)) ($^*P < 0.05$, $^{**}P < 0.01$, and $^{***}P < 0.001$).

2.5. Intracellular ROS Level Measurement. Raw264.7 cell pellets were washed with PBS and incubated with 20 μM DCFH-DA for 1 hour at 37°C in the dark. After washing with PBS, green fluorescence (480 nm excitation/530 nm emission) was measured by flow cytometry (BD FACSCalibur).

2.6. Detection of Nitric Oxide (NO). NO production was measured by adding Griess reagent in culture medium (Welgene, Republic of Korea). In detail, 150 μL of supernatant from each well was transferred to 96-well plate and then mixed with 150 μL of Griess reagent solution. Mixtures were then incubated for 30 min at room temperature. OD was determined at 570 nm using a microplate reader.

2.7. RT-PCR. Raw264.7 cell pellets were washed with ice-cold PBS, and RNAs were extracted using the easy-blue RNA extraction kit (Intron Biotech, Korea) according to the manufacturer's instructions. Total RNAs were quantified using NanoDrop ND-1000 spectrophotometer (NanoDrop Technologies Inc.) and subjected to reverse transcriptions using cDNA synthesis kit (TaKaRa, Japan). Conventional PCRs were then performed using appropriate primers. GAPDH was used as an internal control. Primer information was described in Table 1.

2.8. IL-6 and TNF-α Measurement. IL-6 and TNF-α levels from Raw264.7 were measured by sandwich ELISA using BD Pharmingen mouse ELISA set. Cells in 6-well plates were treated with different concentrations of NG and incubated for 24 h. Cytokine levels were measured at 450 nm using a microplate reader.

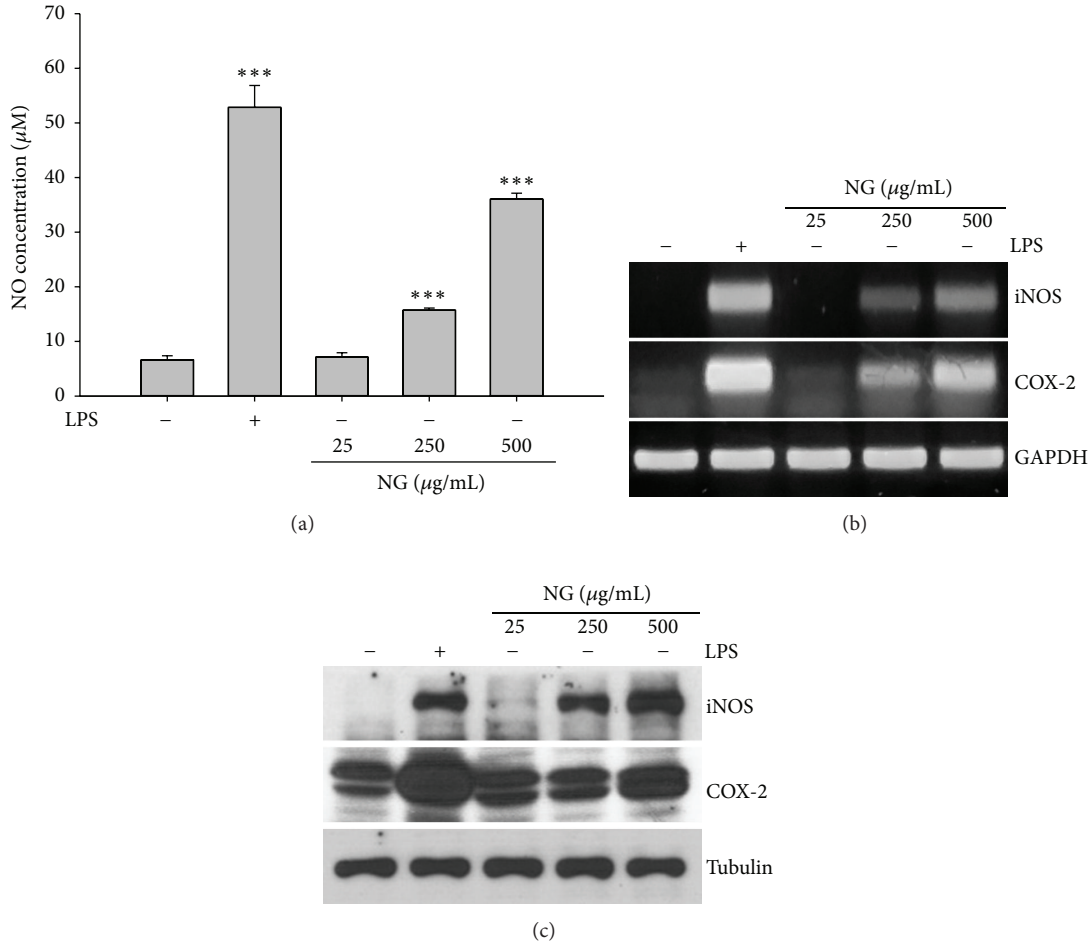

Figure 2: NG augmented NO concentration and iNOS and COX-2 expression. (a) NO production was measured using Griess reagent. (b) iNOS and COX-2 mRNA expression was measured by RT-PCR. (c) iNOS and COX-2 protein expression was measured by Western blot. Data are shown as the mean of three independent experiments (error bars are mean ± standard deviation (SD)) ($^{*}P < 0.05$, $^{**}P < 0.01$, and $^{***}P < 0.001$).

2.9. Western Blot Analysis. Whole cell lysates were washed with ice-cold PBS and lysed with RIPA buffer. Equal amount of protein (30 μg) was run on 10% SDS-PAGE and transferred to nitrocellulose membranes. Blotted membranes were then incubated overnight at 4°C with appropriate primary antibodies. After washing in PBS-tween 20 for 1 hour, membranes were incubated with appropriate HRP-conjugated secondary antibodies and bands were visualized with the enhanced chemiluminescence detection system (Amersham-Pharmacia Biotech, Buckinghamshire, UK).

2.10. Analyses of Cardiac Blood. Whole blood samples from mice were collected by cardiac punctures. Blood was loaded in Vacutainer tubes containing EDTA (BD Biosciences, USA). Analyses of WBC, neutrophil, and monocyte in blood were done using blood analyzer (Hemavet 950, Drew Scientific, Germany).

2.11. Statistical Analysis. Data from experiments performed in triplicate presented mean ± standard deviation. Statistical significance was obtained by Student's t-test, and a P value less than 0.05 was considered statistically significant.

3. Results and Discussion

3.1. Water Extract of Deer Bone (NG) Induces RAW264.7 Cell Differentiation. LPS has been known to induce a differentiation of monocytic Raw264.7 cells to macrophages. Consistently, LPS (1 μg/mL) induced Raw264.7 differentiation in our experiment. Likewise, NG treatment also resulted in Raw264.7 cell differentiation in a dose-dependent manner (Figure 1(a)). In addition, both LPS and NG increased WST activities in RAW264.7 cells, indicating that NG induced activities of dehydrogenases (Figure 1(b)). Macrophages secrete ROS, when being activated [23]. So, we further measured ROS levels in Raw264.7 cells treated with different concentrations of NG or LPS. As seen in Figure 1(c), NG augmented ROS level in a dose-dependent manner. Thus, our data indicate that NG induces Raw264.7 cell differentiation to macrophages.

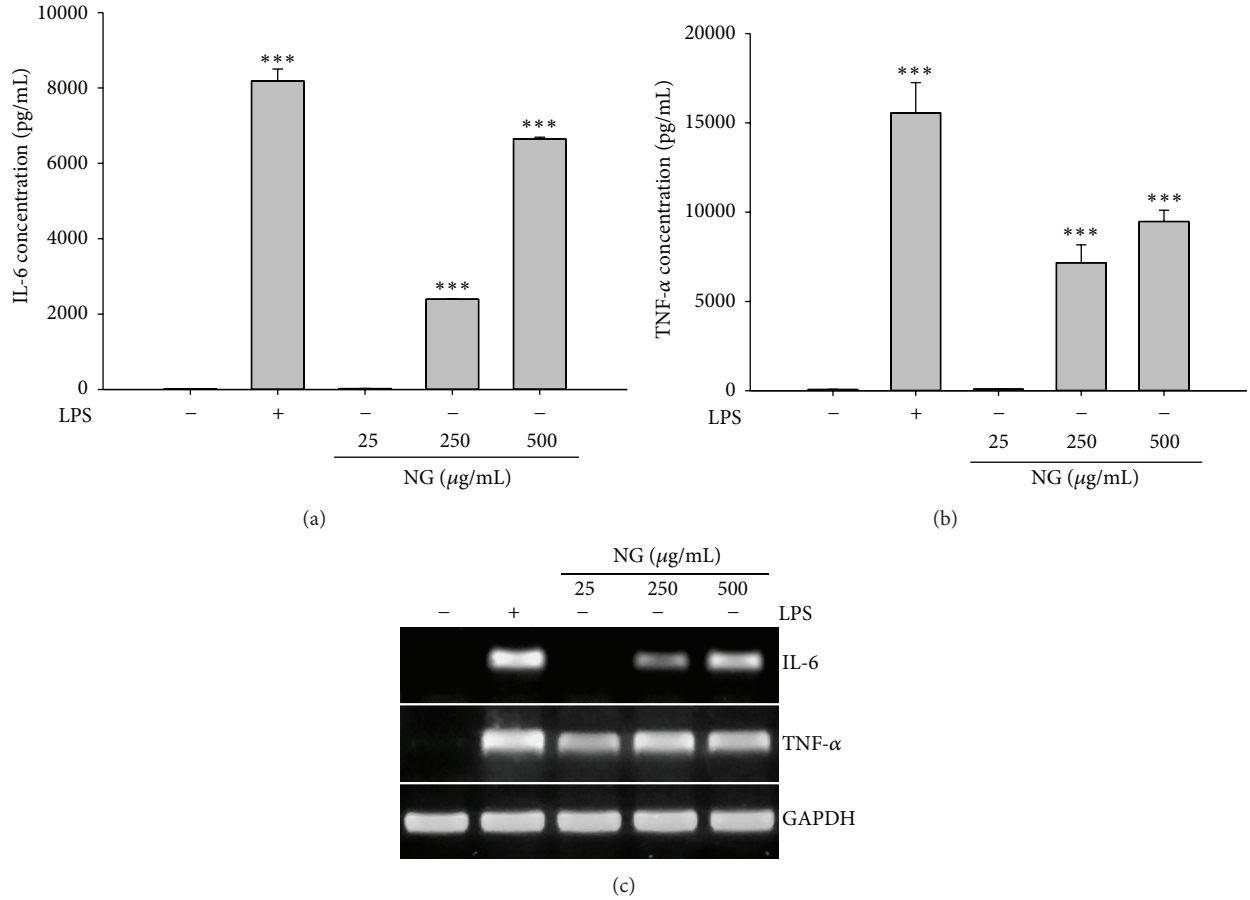

Figure 3: NG increased cytokines production. The release of IL-6 and TNF-α was measured by sandwich ELISA assay. Data are shown as the mean of three independent experiments (error bars are mean ± standard deviation (SD)) ($^{*}P < 0.05$, $^{**}P < 0.01$, and $^{***}P < 0.001$).

3.2. NG Increases NO Concentration and Induces Expression of iNOS and COX-2. We next examined whether NG affects intracellular NO contents in Raw264.7 cells. When Raw264.7 cells were treated with different concentrations of NG or LPS as a positive control, both NG and LPS increased NO production (Figure 2(a)). As NO generation is associated with iNOS and COX-2, we further examined whether NG affects iNOS and COX-2. NG treatment increased expression of both iNOS and COX-2 (Figures 2(b) and 2(c)).

3.3. NG Produces IL-6 and TNF-α. Macrophages react to microbial invasion through IL-6 and TNF-α secretion [17, 24]. Therefore, we measured the levels of IL-6 and TNF-α in Raw264.7 cells treated with different concentrations of NG for 24 hours. NG as well as LPS significantly increased levels of IL-6 and TNF-α (Figures 3(a) and 3(b)). This NG effect on IL-6 and TNF-α resulted from transcriptional regulation of both cytokines because NG treatment induced mRNA expression of either IL-6 or TNF-α (Figure 3(c)).

3.4. NG Induces Activation of MAPKs and NF-κB. It has been reported that LPS activates macrophages through activation of MAPKs and NF-κB [25]. So, we examined whether NG affects signaling pathways of MAPKs and NF-κB in Raw264.7 cells. When Raw264.7 cells were treated with 250 μg/mL of NG for 360 minutes, ERK phosphorylation was increased at 10 minutes after NG treatment and sustained until 30 minutes after NG treatment. JNK phosphorylation was increased at 10 minutes after NG treatment and peaked up at 30 minutes. However, NG appeared not to affect p38 phosphorylation (Figure 4(a)). We also found that NG activates NF-κB pathway. IKK phosphorylation was gradually increased from 10 minutes and peaked up at 30 minutes after NG treatment. Likewise, IκB phosphorylation was increased during that time points and total IκB level was consistently reduced (Figure 4(b)). Accordingly, NG resulted in nuclear accumulation of phosphorylated form of NF-κB, when phosphorylated form of NF-κB in cytoplasmic and nuclear fractions were analyzed (Figure 4(c)). Thus, our data indicate that NG activates MAPK and NF-kB pathways as like LPS (Figure 5).

3.5. NG Alleviates in Mouse Neutropenia Model System. To verify NG effect in immune systems *in vivo*, we applied mouse neutropenia model system. In mice treated with NG, blood analyses presented a decrease of lymphocyte numbers and an increase of either neutrophils or eosinophils (Table 2). In NG-treated mice compared to normal mice, lymphocyte numbers

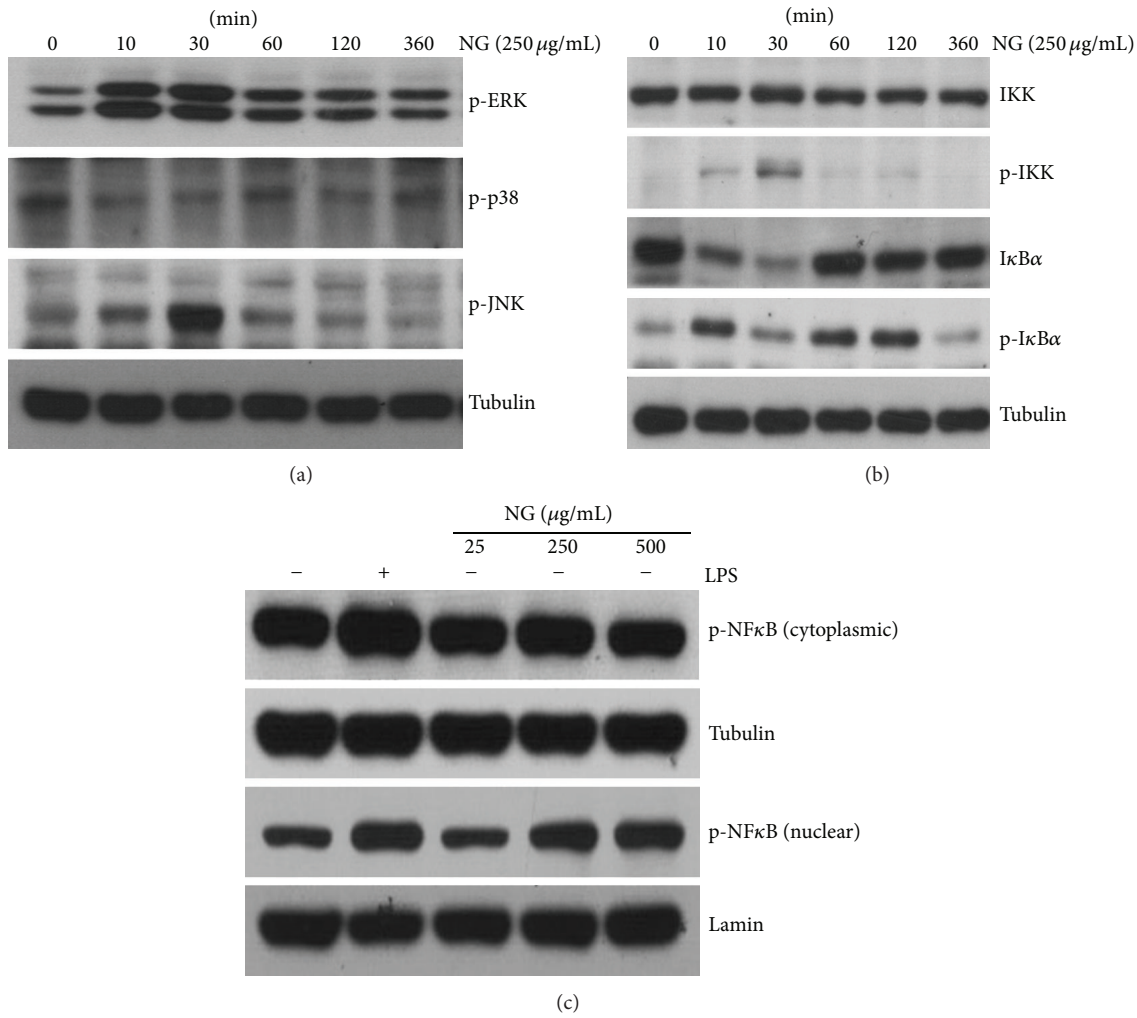

Figure 4: NG induced activation of MAPK and NF-κB. (a) Whole-cell lysates were analyzed by Western blot for the detection of specific proteins, as indicated (p-ERK, p-p38, p-JNK, and tubulin). (b)Whole-cell lysates were analyzed by Western blot for the detection of specific proteins, as indicated (IKK, p-IKK, IκBα, p-IκBα, and tubulin). (c) Nuclear and cytosolic extracts were analyzed by Western blot for the detection of specific proteins, as indicated (p-NF-κB, tubulin, and lamin).

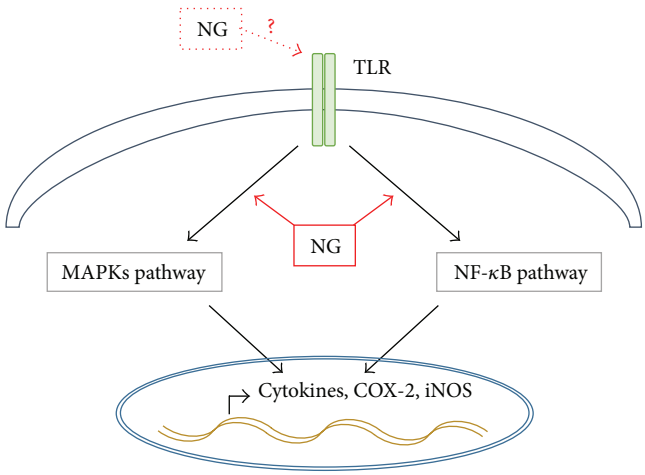

Figure 5: NG induces immune responses through MAPKs and NF-κB activation (schematic diagram).

were diminished by approximately 30% and neutrophil numbers were increased by approximately 30%. While numbers of monocytes and basophils were not altered significantly, eosinophil numbers were also significantly increased from 2.79% to 4.68%. Thus, our *in vivo* data indicate that NG treatment may improve immune defects including neutropenia.

4. Conclusion

Our purpose of the study is to know whether NG has an immunomodulating effect. We confirmed that NG treatment increased ROS and promoted macrophagic differentiation of mouse monocytic Raw264.7 cells. In the *in vivo* study, we confirmed that NG improved immune defects including neutropenia. Hence, we conclude that NG is helpful for alleviating neutropenia.

Authors' Contribution

H.-S. Choi and S. R. Kim equally contributed to this work.

Acknowledgments

This study was supported by Nongshim Corporation (no. 20121086), the Korea Science and Engineering Foundation (KOSEF) Grant funded by the Korea Government (MEST) (no. 2009-0063466), and a Grant from Korea Medicine R&D Project of the Ministry of Health and Welfare (no. B120014).

References

[1] A. Safdar and D. Armstrong, "Infections in patients with hematologic neoplasms and hematopoietic stem cell transplantation: neutropenia, humoral, and splenic defects," *Clinical Infectious Diseases*, vol. 53, pp. 798–806, 2011.

[2] R. Sokolic, "Neutropenia in primary immunodeficiency," *Current Opinion in Hematology*, vol. 20, pp. 55–65, 2013.

[3] Z. Paz, M. Nails, and E. Ziv, "The genetics of benign neutropenia," *The Israel Medical Association Journal*, vol. 13, pp. 625–629, 2011.

[4] V. Kouranos, G. Dimopoulos, A. Vassias, and K. N. Syrigos, "Chemotherapy-induced neutropenia in lung cancer patients: the role of antibiotic prophylaxis," *Cancer Letters*, vol. 313, pp. 9–14, 2011.

[5] M. J. Kaplan, "Neutrophils in the pathogenesis and manifestations of SLE," *Nature Reviews Rheumatology*, vol. 7, pp. 691–699, 2011.

[6] M. Akhtari, B. Curtis, and E. K. Waller, "Autoimmune neutropenia in adults," *Autoimmunity Reviews*, vol. 9, no. 1, pp. 62–66, 2009.

[7] O. Frankfurt and M. S. Tallman, "Growth factors in leukemia," *Journal of the National Comprehensive Cancer Network*, vol. 5, pp. 203–215, 2007.

[8] A. W. Roberts, "G-CSF: a key regulator of neutrophil production, but that's not all!," *Growth Factors*, vol. 23, no. 1, pp. 33–41, 2005.

[9] G. He and M. Karin, "NF-κB and STAT3- key players in liver inflammation and cancer," *Cell Research*, vol. 21, no. 1, pp. 159–168, 2011.

[10] P. S. Becker, "Growth factor priming in therapy of acute myelogenous leukemia," *Current Hematology Reports*, vol. 3, no. 6, pp. 413–418, 2004.

[11] M. E. Spurlock, "Regulation of metabolism and growth during immune challenge: an overview of cytokine function," *Journal of Animal Science*, vol. 75, no. 7, pp. 1773–1783, 1997.

[12] H. M. Lo, C. L. Chen, C. M. Yang et al., "The carotenoid lutein enhances matrix metalloproteinase-9 production and phagocytosis through intracellular ROS generation and ERK1/2, p38 MAPK, and RARbeta activation in murine macrophages," *Journal of Leukocyte Biology*, vol. 93, no. 5, pp. 723–735, 2013.

[13] Y. H. Kuan, Y. C. Li, F. M. Huang, and Y. C. Chang, "The upregulation of tumour necrosis factor-alpha and surface antigens expression on macrophages by bisphenol A-glycidyl-methacrylate," *International Endodontic Journal*, vol. 45, pp. 619–626, 2012.

[14] K. S. Janardhan, S. K. Sandhu, and B. Singh, "Neutrophil depletion inhibits early and late monocyte/macrophage increase in lung inflammation," *Frontiers in Bioscience*, vol. 11, no. 2, pp. 1569–1576, 2006.

[15] J. Bohlius, M. Reiser, G. Schwarzer, and A. Engert, "Impact of granulocyte colony-stimulating factor (CSF) and granulocyte-macrophage CSF in patients with malignant lymphoma: a systematic review," *British Journal of Haematology*, vol. 122, no. 3, pp. 413–423, 2003.

[16] D. C. Dale, "Colony-stimulating factors for the management of neutropenia in cancer patients," *Drugs*, vol. 62, supplement 1, pp. 1–15, 2002.

[17] S. Gordon, "Alternative activation of macrophages," *Nature Reviews Immunology*, vol. 3, pp. 23–35, 2003.

[18] S. K. Kang, K. S. Kim, S. I. Kim, K. H. Chung, I. S. Lee, and C. H. Kim, "Immunosuppressive activity of deer antler extracts of Cervus korean TEMMINCK var. mantchuricus Swinhoe, on type II collagen-induced arthritis," *In Vitro Cellular and Developmental Biology—Animal*, vol. 42, no. 3-4, pp. 100–107, 2006.

[19] K. S. Kim, Y. H. Choi, K. H. Kim et al., "Protective and anti-arthritic effects of deer antler aqua-acupuncture (DAA), inhibiting dihydroorotate dehydrogenase, on phosphate ions-mediated chondrocyte apoptosis and rat collagen-induced arthritis," *International Immunopharmacology*, vol. 4, no. 7, pp. 963–973, 2004.

[20] Y. J. Li, T. H. Kim, H. B. Kwak, Z. H. Lee, S. Y. Lee, and G. J. Jhon, "Chloroform extract of deer antler inhibits osteoclast differentiation and bone resorption," *Journal of Ethnopharmacology*, vol. 113, no. 2, pp. 191–198, 2007.

[21] C. Y. Kuo, T. Wang, T. Y. Dai et al., "Effect of the velvet antler of formosan sambar deer (Cervus unicolor swinhoei) on the prevention of anllergic airway response in mice," *Evidence-Based Complementary and Alternative Medicine*, vol. 2012, Article ID 481318, 10 pages, 2012.

[22] T. Y. Dai, C. H. Wang, K. N. Chen et al., "The antiinfective effects of velvet antler of Formosan sambar deer (Cervus unicolor swinhoei) on staphylococcus aureus-infected mice," *Evidence-Based Complementary and Alternative Medicine*, vol. 2011, Article ID 534069, 9 pages, 2011.

[23] E. Szliszka, D. Skaba, Z. P. Czuba, and W. Krol, "Inhibition of inflammatory mediators by neobavaisoflavone in activated RAW264.7 macrophages," *Molecules*, vol. 16, no. 5, pp. 3701–3712, 2011.

[24] J. Ma, T. Chen, J. Mandelin et al., "Regulation of macrophage activation," *Cellular and Molecular Life Sciences*, vol. 60, no. 11, pp. 2334–2346, 2003.

[25] S. M. Dauphinee and A. Karsan, "Lipopolysaccharide signaling in endothelial cells," *Laboratory Investigation*, vol. 86, no. 1, pp. 9–22, 2006.

Hindawi Publishing Corporation
Evidence-Based Complementary and Alternative Medicine
Volume 2013, Article ID 385219, 9 pages
http://dx.doi.org/10.1155/2013/385219

Research Article

Anthricin Isolated from *Anthriscus sylvestris* (L.) Hoffm. Inhibits the Growth of Breast Cancer Cells by Inhibiting Akt/mTOR Signaling, and Its Apoptotic Effects Are Enhanced by Autophagy Inhibition

Chang Hwa Jung,[1,2] Heemun Kim,[1] Jiyun Ahn,[1,2] Sung Keun Jung,[1] Min Young Um,[1] Kun-Ho Son,[3] Tae Wan Kim,[4] and Tae Youl Ha[1,2]

[1] *Department of Food Biotechnology, University of Science and Technology, Daejon 305-806, Republic of Korea*
[2] *Division of Metabolism and Functionality Research, Korea Food Research Institute, 1201 Anyangpangyo-ro, Seongnam 463-746, Republic of Korea*
[3] *Department of Food Science and Nutrition, Andong National University, Kyungbuk 760-749, Republic of Korea*
[4] *Department of Food Science and Biotechnology, Andong National University, Kyungbuk 760-749, Republic of Korea*

Correspondence should be addressed to Tae Youl Ha; tyhap@kfri.re.kr

Received 5 March 2013; Revised 8 May 2013; Accepted 8 May 2013

Academic Editor: Bo-Hyoung Jang

Anthricin (deoxypodophyllotoxin) is a natural product isolated from *Anthriscus sylvestris* (L.) Hoffm. (Apiaceae). Here, we investigated the effect of anthricin on autophagy and mammalian target of rapamycin (mTOR) signaling as anticancer actions in breast cancer cells. Many studies have supported the contention that the phosphoinositide 3-kinase (PI3K)/Akt/mTORC1 pathway is considerably deregulated in breast cancer and that autophagy plays important roles in the development of this type of cancer, although the exact underlying mechanisms remain unknown. Our data confirmed that anthricin markedly induced apoptosis in 2 breast cancer cell lines, MCF7 (estrogen receptor positive) and MDA-MB-231 (estrogen receptor, progesterone receptor, and Her2/Neu receptor negative). Anthricin treatment decreased the levels of phosphorylated Akt and mTORC1, followed by inhibition of cell growth. Interestingly, blockage of autophagy by a pharmacological inhibitor or genetic deletion of ULK1 and Atg13 accelerated anthricin-induced apoptosis, suggesting that autophagy has cytoprotective effects. Taken together, our results indicate that anthricin is an inhibitor of mTOR and that a combination of an autophagy inhibitor and anthricin may serve as a new promising strategy for the treatment of breast cancer cells.

1. Introduction

Breast cancer is the most common type of cancer in women, accounting for 22.9% of invasive cancers in this population and 16% of all female cancers [1]. Among the various therapeutic approaches that have been used to reduce the mortality from breast cancer, chemoprevention may be the most effective in reducing the risk of, or eradicating, cancer in healthy people or in patients with earlystage invasive breast cancer. Numerous studies have supported the contention that natural compounds can function as cancer-prevention and therapeutic agents. Several studies on breast cancer have revealed the potential of naturally occurring chemopreventive agents, such as eupatorin, oleuropein, genistein, and resveratrol, as anti-breast cancer drugs [2–6]. Chemoprevention is attractive for cancer therapy because it represents an easy and low-cost cancer-control method, mainly for individuals with an inherited predisposition to certain cancers.

Anthriscus sylvestris (L.) Hoffm. (Apiaceae) is a common wild plant that is indigenous to Europe, North America, Africa, Asia, and New Zealand [7]. The dried root of *A. sylvestris* has been used in Korean traditional drugs for the treatment of various diseases, including bronchitis, and as an antipyretic, a cough remedy, and an analgesic herbal

drug. This plant accumulates the anthricin (deoxypodophyllotoxin), which has anticancer activity against lung cancer, lymphomas, and genital tumors [8–12]. The inhibitory effect of anthricin on a variety of cancer cells is related to the induction of G2/M cell-cycle arrest and caspase-dependent apoptosis [11]; however, the mechanism underlying this biological phenomenon remains unknown. Here, we sought to determine if the Akt/mammalian target of rapamycin (mTOR) pathway and the autophagic process play any specific role in the regulation of the anticancer properties of anthricin in breast cancer cell lines.

The Akt/mTOR pathway has been identified as an important target in breast cancer research over the past 20 years. This pathway is integral to various cellular functions, including cellular metabolism, proliferation, and survival [13, 14]. More specifically, this pathway overcomes drug resistance in hormone-receptor-positive breast cancer [13]. Although autophagy, which is a lysosome-mediated degradation system, may be important in the regulation of cancer development and progression and in determining the response of tumor cells to anticancer therapy, its role in cancer therapy remains controversial [15]. Autophagy is controlled by Akt/mTOR signaling in the regulation of nutrient-sensing pathways. mTOR represses the ULK1/2 complex, which recruits other autophagy-related proteins (Atg) for the formation of the autophagosome [16]. A recent report has suggested that autophagy acts as a prosurvival process that regulates apoptosis in breast cancer cells [17]. Therefore, we hypothesized that anthricin regulates Akt/mTOR signaling and autophagy to modulate cell death or cell survival. In this study, we evaluated the mechanism of cell death induced by anthricin isolated from *A. sylvestris* in MCF-7 and MDA-MB-231 breast cancer cell lines.

2. Materials and Methods

2.1. Isolation of Anthricin from A. sylvestris (L.) Hoffm. The dried roots of *A. sylvestris* (8.25 kg) were refluxed with hot MeOH (3 times) and concentrated to give a residue (959.25 g), which was suspended in H_2O and was partitioned with hexane (89.41 g), CH_2Cl_2 (28.66 g), EtOAc (8.15 g), and BuOH (42.58 g). The hexane fraction (73.62 g) was loaded onto a silica-gel column (80 × 15 cm) and eluted with a gradient of hexane : EtOAc (10 : 0.2 to 10 : 1) to give 16 subfractions. Among these, subfraction 14 was recrystallized from MeOH to afford anthricin (2.9 g). The CH_2Cl_2 fraction (27.57 g) was loaded onto a silica-gel column (80 × 10 cm) and eluted with a gradient of hexane : EtOAc (10 : 1 to 10 : 2) to give 14 subfractions. Subfraction 12 was recrystallized from MeOH to afford anthricin (5.4 g). The molecular weight and fragment ions of the compound were identified using liquid chromatography-tandem mass spectrometry (LC-MS/MS) and nuclear magnetic resonance (NMR). The molecular weight and the fragment ions are summarized as follows: anthricin, $C_{22}H_{22}O_7$; mp, 168–170°C; ^{1}H-NMR (300 MHz, $CDCl_3$): δ 6.65 (1H, s, H-2), 6.50 (1H, s, H-5), 6.32 (2H, s, H-2′, 6′), 5.93 (1H, d, J = 1.2 Hz, OCH_2O), 5.91 (1H, d, J = 1.2 Hz, OCH_2O), 4.58 (1H, d, J = 2.7 Hz, H-7′), 4.43 (1H, m, H-9), 3.90 (1H, m, H-9), 3.78 (3H, s, $C_{4'}$-OCH_3), 3.73 (6H, s, $C_{3'}$-OCH_3, $C_{5'}$-OCH_3), 3.05 (1H, m, H-7), 2.75 (2H, m, H-8, 8′); ^{13}C-NMR (75.5 MHz, $CDCl_3$) δ: 174.9 (C-9′), 152.5 (C-3′), 147.0 (C-3), 146.7 (C-4), 137.0 (C-4′), 136.3 (C-1′), 130.6 (C-6), 128.3 (C-1), 110.4 (C-5), 108.4 (C-6′), 108.2 (C-2), 101.2 (OCH_2O), 72.0 (C-9), 60.7 ($C_{4'}$-OCH_3), 56.2 ($C_{3'}$-OCH_3, $C_{5'}$-OCH_3), 47.5 (C-8′), 43.7 (C-7′), 33.1 (C-7), 32.7 (C-8); EI-MS m/z: 398 $[M]^+$.

2.2. Reagents. RPMI-1640 medium, fetal bovine serum (FBS), bovine calf serum (CS), sodium pyruvate, and penicillin-streptomycin were obtained from Gibco BRL (Grand Island, NY, USA). Anti-p62 (sc-28359), anti-mTOR (sc-1549), anti-ULK1 (sc-33182), anti-β-actin (sc-47778), anti-raptor (sc-81537), TSC2 (sc-893), and secondary antibodies were purchased from Santa Cruz Biotechnology (Santa Cruz, CA, USA). Antibodies against p-mTOR (no. 5536s), mTOR (no. 9272), p-S6K1 (no. 9205), S6K1 (no. 9202), p-Akt (no. 9271), Akt (no. 9272), LC3B (no. 2775s), PARP (no. 9542s), cleaved caspase-3 (no. 9661s), cleaved caspase-7 (no. 9491), cleaved caspase-9 (no. 9501), cyclin B1 (no. 4138), p-chk2 (no. 2661s), and Bax (no. 2772) were from Cell Signaling (Danvers, MA, USA). The anti-Atg13 antibody has been described in our previous report [16]. Glutathione 4B beads were obtained from GE Healthcare (Piscataway, NJ, USA). Chloroquine (CQ) and rapamycin were purchased from Sigma-Aldrich (Saint Louis, MO, USA) and Calbiochem (San Diego, CA, USA), respectively.

2.3. Cell Culture and Transfection. MCF7 and MDA-MB-231 cells were cultured in RPMI with 1% penicillin-streptomycin and 10% FBS at 37°C in 5% CO_2. For transient transfection, cells were transfected with GFP-LC3 using FuGENE 6 (Roche Applied Science, Indianapolis, IN) according to the manufacturer's protocol.

2.4. RNA Interference. RNA silencing was achieved using the ON-TARGETplus SMART human TSC2 pool or ON-TARGETplus siCONTROL nontargeting pool (Dharmacon, Lafayette, CO, USA). MCF-7 cells were seeded in 60-mm plates and transiently transfected with negative control siRNA or TSC2 siRNA using Lipofectamine RNAiMAX (Invitrogen) according to the manufacturer's instructions. Cells were treated with 25 μg/mL anthricin for 12 h at 24 h after transfection and analyzed by Western blotting.

2.5. Lentiviral Preparation and Viral Infection. Lentiviral shRNA transduction was assessed as described previously [16]. Briefly, the PLKO.1 vectors encoding shRNAs were transfected into HEK 293T cells with the lentiviral packaging vectors pHR8.2ΔR and pCMV-VSV-G using FuGENE 6. Viruses were collected 72 h after transfection, and MCF-7 cells were infected with the collected viruses for 8 h in the presence of polybrene. Stably transduced cells were selected using puromycin. The target sequences for the Atg13 shRNA were 5′-gaatttggagctggaggat-3′ and 5′-agtttcctacacggtgtac-3′, and those for the ULK1 shRNA were 5′-gacttccaggaaatggctaat-3′ and 5′-acatcgagaacgtcaccaagt-3′. Knockdown of *Atg13* and *ULK1* was confirmed by immunoblotting.

2.6. Cell Viability Assay. The human breast cancer cell lines were seeded in a 96-well plate at a concentration of 2×10^3 cells/well. After 24 h of preconditioning, the cells were exposed to various concentrations of anthricin for 12 or 24 h, respectively. Subsequently, 50 μL of cell counting kit-8 (no. CK04, Dojindo, Kumamoto, Japan) solution was added into each well and the plate was incubated for an additional 3 h at 37°C, to detect cell survival. Cell viability was calculated by measuring the absorbance on a microplate reader (Tecan, Infinite M200) at 450 nm.

2.7. Cell Proliferation Assay. The breast cancer cell lines were treated with anthricin and cells were counted on days 1, 2, and 3. On each of these days, cells were trypsinized and harvested with RPMI medium. Cells were diluted 10 times with Isoton II diluent and loaded onto a Z2 counter. Three independent measurements were analyzed quantitatively.

2.8. Western Blot Assay. The breast cancer cell lines were treated with anthricin for the indicated times. After treatment, cells were harvested with 1% Triton-X100 buffer, run on SDS-PAGE, transferred to a PVDF membrane, and probed with polyclonal or monoclonal antibodies.

2.9. Coimmunoprecipitation. For coimmunoprecipitation, whole-cell lysates were prepared in a buffer containing 0.3% Chaps buffer, as described by Kim et al. [18], and immunoprecipitated with an mTOR antibody. Immunoprecipitated proteins were washed 4 times using lysis buffer, loaded onto 8% gels, transferred onto a PVDF membrane, and detected.

2.10. Immunostaining. MCF7 cells were seeded and transfected with GFP-LC3 on a Lab-TEK Chamber Slide (no. 177437, Thermo Fisher Scientific, Rochester, NY). Cells were treated with anthricin for 8 h at 2 d after transfection and fixed with 3.7% formaldehyde, permeabilized with 0.3% Triton X-100, and stained with DAPI (4′-6-diamidino-2-phenylindole; D-1306, Invitrogen). Images from stained cells were acquired using a confocal microscope (Nikon, DIGITAL ECLIPSE C1 plus, Japan).

2.11. Annexin V Apoptosis Analyses. Cells (1×10^3) were plated in 60 mm plates and treated with vehicle, anthricin, or chloroquine for 12 h. Cells were then fixed in 70% ethanol and stored at −20°C for 24 h. After staining with annexin V, apoptosis was determined using a BD FACS Calibur Flow Cytometer (BD Biosciences, San Jose, CA).

2.12. Statistical Analyses. Differences between groups were evaluated using one-way analysis of variance (ANOVA) with the GraphPad Prism5 software (San Diego, CA, USA). The Bonferroni post hoc test was used if differences were significant after ANOVA. Data are expressed as the mean ± SD.

3. Results

3.1. Anthricin from A. sylvestris (L.) Hoffm. Induces Apoptosis and Cell-Cycle Arrest in Breast Cancer Cells. To investigate the inhibitory effect of anthricin on breast cancer cell growth, we first determined cell viability in 2 breast cancer cell lines: MCF7 (estrogen receptor positive) and MDA-MB-231 (estrogen receptor, progesterone receptor, and Her2/Neu receptor negative). The cells were treated with various concentrations of anthricin for the indicated time, and cell viability was analyzed using a cell counting kit-8. Anthricin significantly inhibited cell growth and proliferation in both cancer cell lines in a dose-dependent manner without toxicity in normal cells (Figures 1(a) and 1(b), Supplementary 1 available online at http://dx.doi.org/10.1155/2013/385219). The IC50 concentrations at 24 h in anthricin-treated MDA-MB-231 and MCF7 cells were 40.9±2.1 and 41.1±1.5 nM, respectively. A previous study showed that anthricin induces apoptosis in HeLa cells, suggesting the possible involvement of the induction of apoptosis in different cancer cell lines [11, 12]. To confirm the effect of anthricin on the induction of apoptosis, the cells were treated with anthricin and apoptosis-related signals were analyzed by immunoblotting. Anthricin treatment in both cancer cell lines promoted the time-dependent cleavage of caspase-3, caspase-7, or caspase-9 (Figure 1(c)). We also observed that PARP cleavage was augmented by increasing the concentration of anthricin. The drug also induced Bax accumulation in a dose-dependent manner. Previous studies showed that anthricin induces cell cycle arrest at G(2)/M phase in HeLa cells [11, 12]. To elucidate the mechanism of G2/M phase arrest in anthricin-treated breast cancer cells, we investigated the expression of G2/M phase-related factor. Our results confirmed that anthricin induced G(2)/M phase cell-cycle arrest in breast cancer cells by enhancing the expression of p53 and the phosphorylation of chk2 and downregulating Cyclin B1, cdc25c, and CDC2 (Figure 1(d)). G2/M phase arrest is linked in the activation of ATM, chk2, p53, and p21 as well as the inactivation of CDC2 [19]. Collectively, these data suggest that anthricin treatment exhibited potent growth suppressive activity in breast cancer through induction of apoptosis and G(2)/M phase cell-cycle arrest.

3.2. Anthricin Induces Autophagy. Autophagy is a lysosomal degradation pathway for quality control of cytoplasm by eliminating dysfunctional subcellular structures [20]. Recently, autophagy has been suggested to be responsible for the maintenance of intracellular homeostasis and for enabling cell survival under stress conditions. This process is involved in the pathogenesis of various diseases, including cancer [15]. Recent studies on autophagy seem to be controversial regarding its dual role as a mechanism that is responsible for protecting or killing cells [21]. We examined whether anthricin induces autophagy and whether autophagy subsequently promotes or prevents apoptosis in anthricin-treated cells. We first evaluated the level of p62, a ubiquitin-binding protein that is involved in autophagy and the levels of which are decreased by lysosomal hydrolases during autophagic process [22]. Anthricin treatment downregulated p62 in MDA-MB-231 and MCF7 cells in a dose-dependent manner (Figure 2(a)). We confirmed this result by evaluating the lipidation of microtubule-associated protein 1 light chain 3 (LC3) via immunoblotting. During autophagy, cytosolic LC3-I conjugates covalently to phosphatidylethanolamine to yield a lipidated form of LC3 (LC3-II) [23]. The combination with the lysosomal inhibitors, CQ, is increased in LC3-II levels

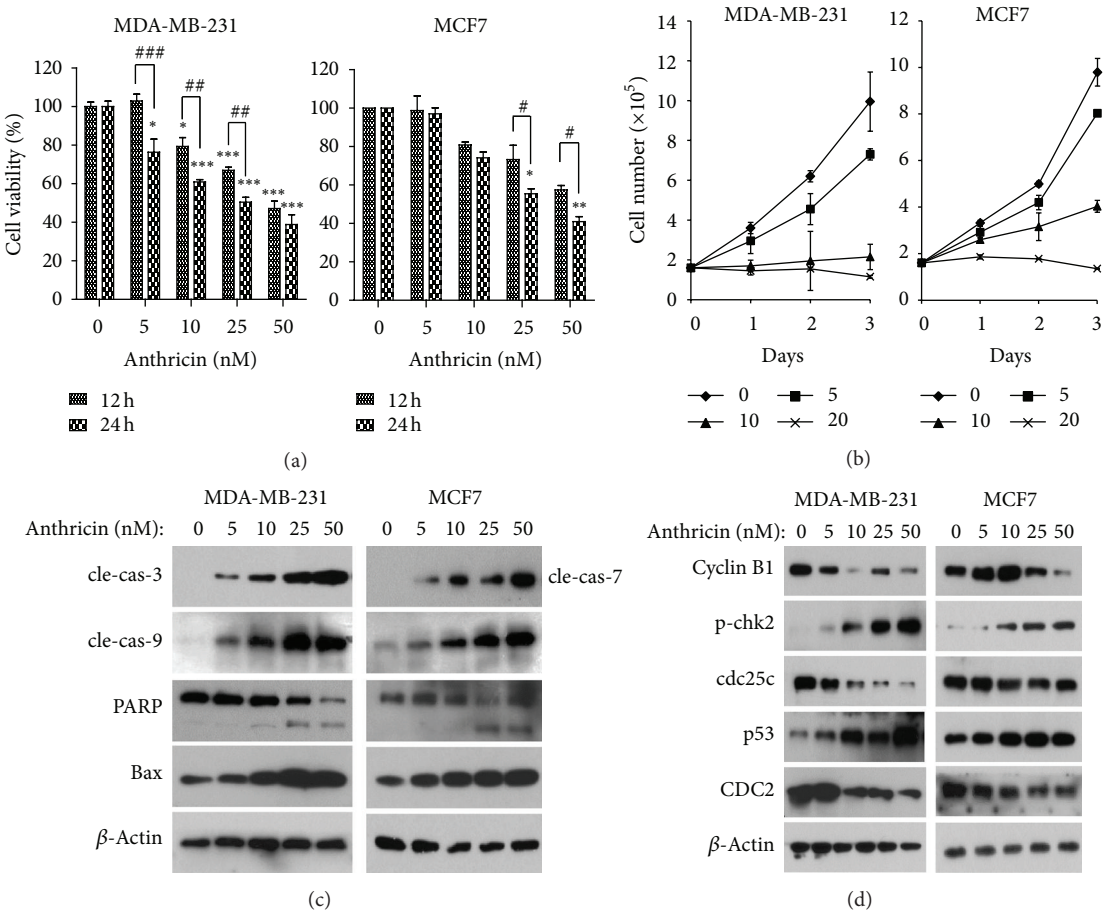

Figure 1: Anthricin isolated from *Anthriscus sylvestris* (L.) Hoffm. inhibits cell growth and proliferation. (a) Analysis of cell viability in anthricin-treated MDA-MB-231 and MCF7 cells. Cells were treated with varying concentrations of anthricin for 12 or 24 h. Cell viability was evaluated using the cell counting kit-8 (CCK-8). Data are expressed as a percentage of the control and shown as mean ± SD ($n = 3$) values. $^{*}P < 0.05$; $^{**}P < 0.01$; $^{***}P < 0.001$ compared with vehicle-treated cells. $^{\#}P < 0.05$; $^{\#\#}P < 0.01$; $^{\#\#\#}P < 0.001$ compared with the group treated with anthricin for 12 h. (b) Reduced cell proliferation rate of breast cancer cells. The error bars represent the mean ± SD ($n = 4$). (c) Induction of apoptosis by anthricin in breast cancer cells. The extent of apoptosis in MDA-MB-231 and MCF-7 cells treated with varying concentrations of anthricin for 24 h was analyzed by immunoblotting. (d) Cell cycle arrest by anthricin in breast cancer cells. The expression of cell-cycle-related proteins was analyzed by immunoblotting.

due to the inhibition of LC3-II degradation by lysosomes [23]. CQ inhibits late step of autophagy pathway as it raises the lysosomal pH, which leads to inhibition of both fusion of autophagosome with lysosome [24]. This indicates that an increase in the total amount of LC3-II in the presence of lysosomal inhibitor indicates an increase of autophagic influx. Anthricin treatment gradually increased the LC3-II form in a dose-dependent manner in the presence of CQ (Figure 2(b)), suggesting that anthricin plays a role in inducing autophagy. We also investigated the formation of endogenous LC3 puncta in MDA-MB-231 cells using fluorescence microscopy. Our confocal images showed that LC3 puncta formation was abundant in cells treated for 8 h (Figure 2(c)). We obtained similar results in MCF-7 cells, as anthricin treatment increased the formation of LC3 puncta in MCF-7 cells transiently transfected with GFP-LC3 (Figures 2(d) and 2(e)).

3.3. Autophagy Plays a Cytoprotective Role in Anthricin-Treated Breast Cancer Cells. Although the results described earlier suggest that anthricin induces autophagy, it remains to be determined whether the inhibition of autophagy promotes or prevents apoptosis after breast cancer cells are treated with anthricin. To address this question, we blocked autophagy via pharmacological or genetic inhibition. The blockage of autophagy using CQ enhanced cell death in MCF7 and MDA-MB-231 cells without any change in CQ-induced cell death (Figures 3(a) and 3(b), Supplementary 2). We also confirmed that cotreatment with CQ enhanced apoptosis as detected by annexin V staining (Figure 3(c)). However, apoptotic effect was not enhanced by cotreatment with rapamycin (Supplementary 3). These results suggest that mTOR activity may directly affect the cell growth in breast cancer cells. To validate the finding that the inhibition of autophagy promotes cell death in MCF-7 cells, the autophagy-related proteins ULK1

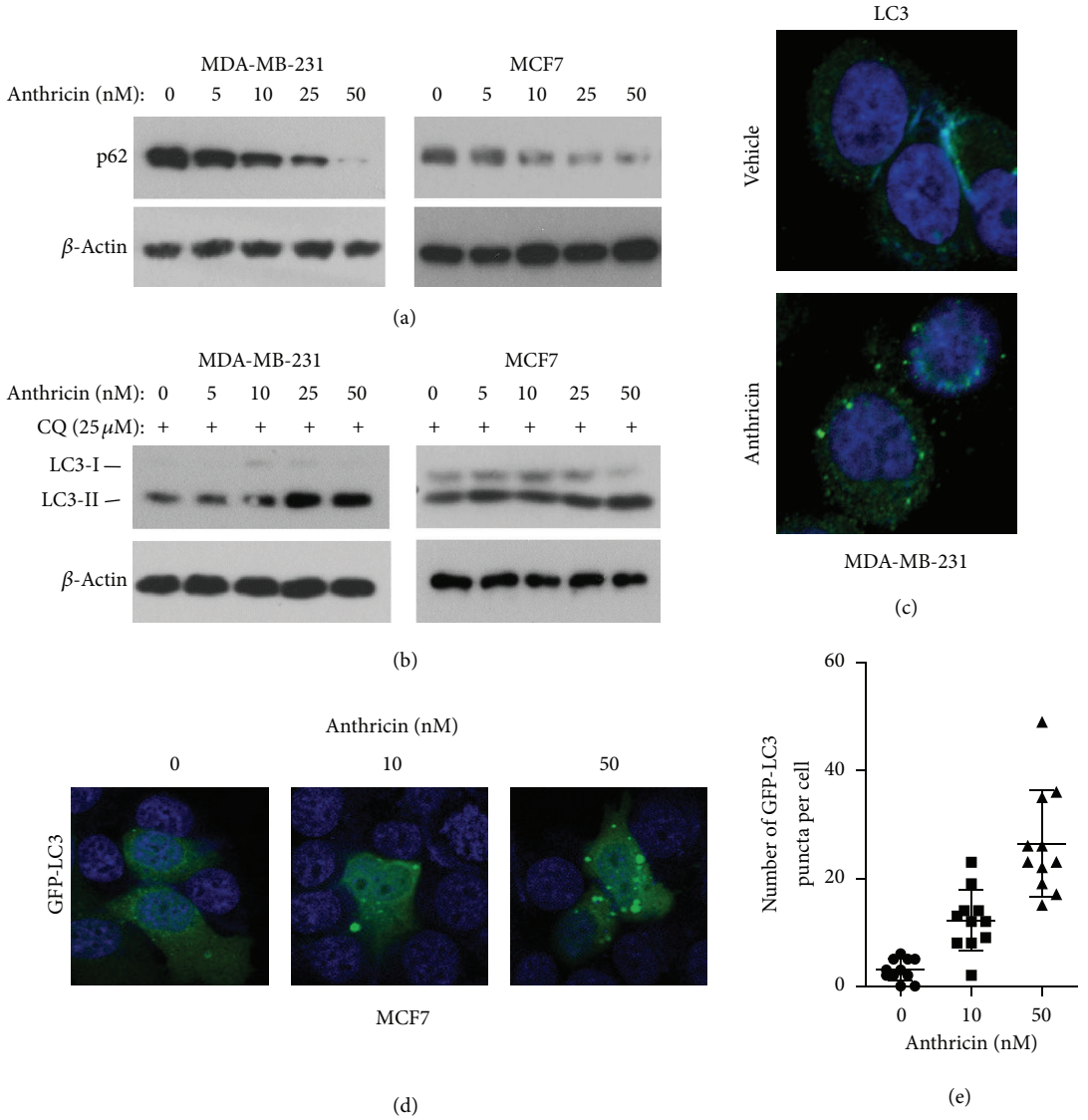

Figure 2: Anthricin induces autophagy. (a) p62 levels in anthricin-treated breast cancer cells. Cells were treated with varying concentrations of anthricin for 8 h. Protein levels were analyzed by immunoblotting. (b) Immunoblot analysis of the LC3 protein. The levels of endogenous LC3-II increased in breast cancer cells treated with anthricin. The cells were cotreated with anthricin and chloroquine (CQ) for 8 h. (c) Immunostaining of LC3 in MDA-MB-231 cells. The cells were treated with CQ for 8 h to induce autophagosome accumulation. After fixation and permeabilization, autophagosomes were stained with an anti-LC3B rabbit polyclonal antibody and visualized with Alexa Fluor 488 goat anti-rabbit IgG. (d) MCF-7 cells were transduced with GFP-LC3. Two days later, cells were cotreated with anthricin and CQ for 8 h. (e) Quantitative analysis of the formation of GFP-LC3 puncta.

and Atg13 were silenced in MCF-7 cells using lentiviral infection. The Atg13- and ULK1-silenced cells exhibited a significant increase in cell death after exposure to anthricin (Figure 3(d)). Western blotting also indicated that the expression levels of cleaved caspase-7 and PARP cleavage increased in ULK1 and Atg13 knockdown cells compared with wild-type cells (Figure 3(e)). Atg13 plays a positive role in the regulation of ULK1 activity and is important for the stability of ULK1 [16]. Figure 3(e) also supports that Atg13 is important for ULK1 stabilization in MCF7 cells. Collectively, these results suggest that blockage of autophagy enhances anthricin-induced apoptosis in breast cancer cells.

3.4. Anthricin Inhibits Akt-mTOR Signaling. The mTOR pathway promotes tumor growth and survival, while suppressing autophagy [25, 26]. Anthricin treatment strongly inhibited mTOR kinase activity in a time- and dose-dependent manner, as measured by the phosphorylation of S6K1 (Figures 4(a) and 4(b)). The reduced mTOR kinase activity seems to be due to the inhibition of Akt. The siRNA knockdown of TSC2 in MCF-7 cells affected mTOR activity slightly after anthricin treatment, suggesting that anthricin may directly inhibit both Akt and mTOR signals (Figure 4(c)). Raptor is an mTOR-binding protein; its deletion or the disruption of its binding to mTOR appears to increase apoptosis [27]. We also observed

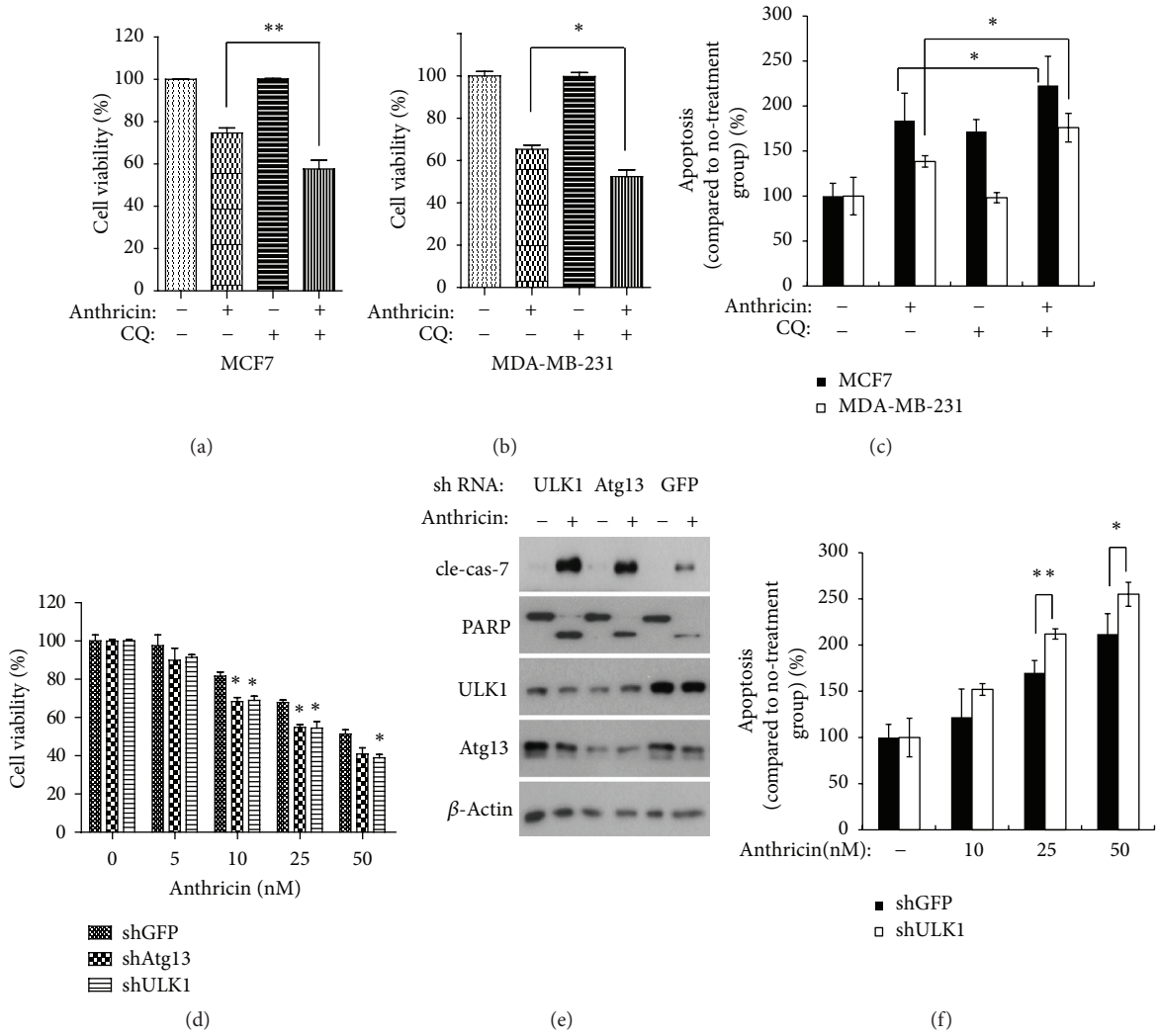

Figure 3: Autophagy plays a cytoprotective role in anthricin-treated breast cancer cells. (a and b) Autophagy inhibition promotes cell death. Cells were treated with 25 nM anthricin and/or 25 μM CQ for 12 h. Data are expressed as a percentage of the control and shown as mean ± SD ($n = 3$). $^{*}P < 0.05$; $^{**}P < 0.01$ compared to vehicle-treated cells. (c) Cotreatment of anthricin and CQ is more sensitive to the apoptotic cell death in MCF-7 and MDA-MB-231. Apoptosis was analyzed by flow cytometry and annexin V staining as described in Materials and Methods. Data are represented as means ± S.D. as determined from 3 independent experiments. $^{*}P < 0.05$ compared to anthricin alone. (d) Anthricin enhances cell death in ULK1 or Atg13 knockdown cells. MCF-7 cells stably transduced with lentiviral shRNA were treated with anthricin (25 nM) for 12 h. Data are expressed as a percentage of the control and shown as the mean ± SD ($n = 3$). $^{*}P < 0.05$; $^{**}P < 0.01$ compared with shGFP control cells within the same concentration. (e) Apoptosis increased in ULK1- and Atg13-silenced MCF-7 cells after anthricin treatment. The extent of apoptosis in cells treated with 25 nM anthricin for 12 h was analyzed by immunoblotting. (f) Anthricin is more sensitive to the apoptotic cell death in ULK1-silenced MCF-7 cells. Apoptosis was analyzed by flow cytometry and annexin V staining. $^{*}P < 0.05$ compared with shGFP control cells within the same concentration.

that anthricin disrupted the association between raptor and mTOR. These results indicate that anthricin treatment to breast cancer cells induces apoptosis via the inhibition of Akt-mTOR signals, whereas autophagy induction may act as a cell-survival mechanism in MCF-7 cells.

4. Discussion

Anthriscus sylvestris (L.) Hoffm. has been used in traditional medicine for the treatment of various diseases, such as bronchitis, as well as an antipyretic and analgesic herbal drug [7]. *A. sylvestris* contains lignans such as anthricin (deoxypodophyllotoxin) that are responsible for its various biological effects. In this study, we isolated anthricin from *A. sylvestris* and evaluated the mechanism underlying the apoptosis induced by treatment with this compound in breast cancer cells. We found that mTOR signaling and autophagy play important roles in the balance between cell death and cell survival induced by anthricin in breast cancer cells.

Several groups have reported that anthricin has antitumor activity against prostate, cervical, and lung cancer cells [10, 11, 28]. Our data showed that anthricin was effective in inducing apoptosis in the MCF-7 and MDA-MB-231 breast cancer cell lines. Anthricin treatment induced autophagy,

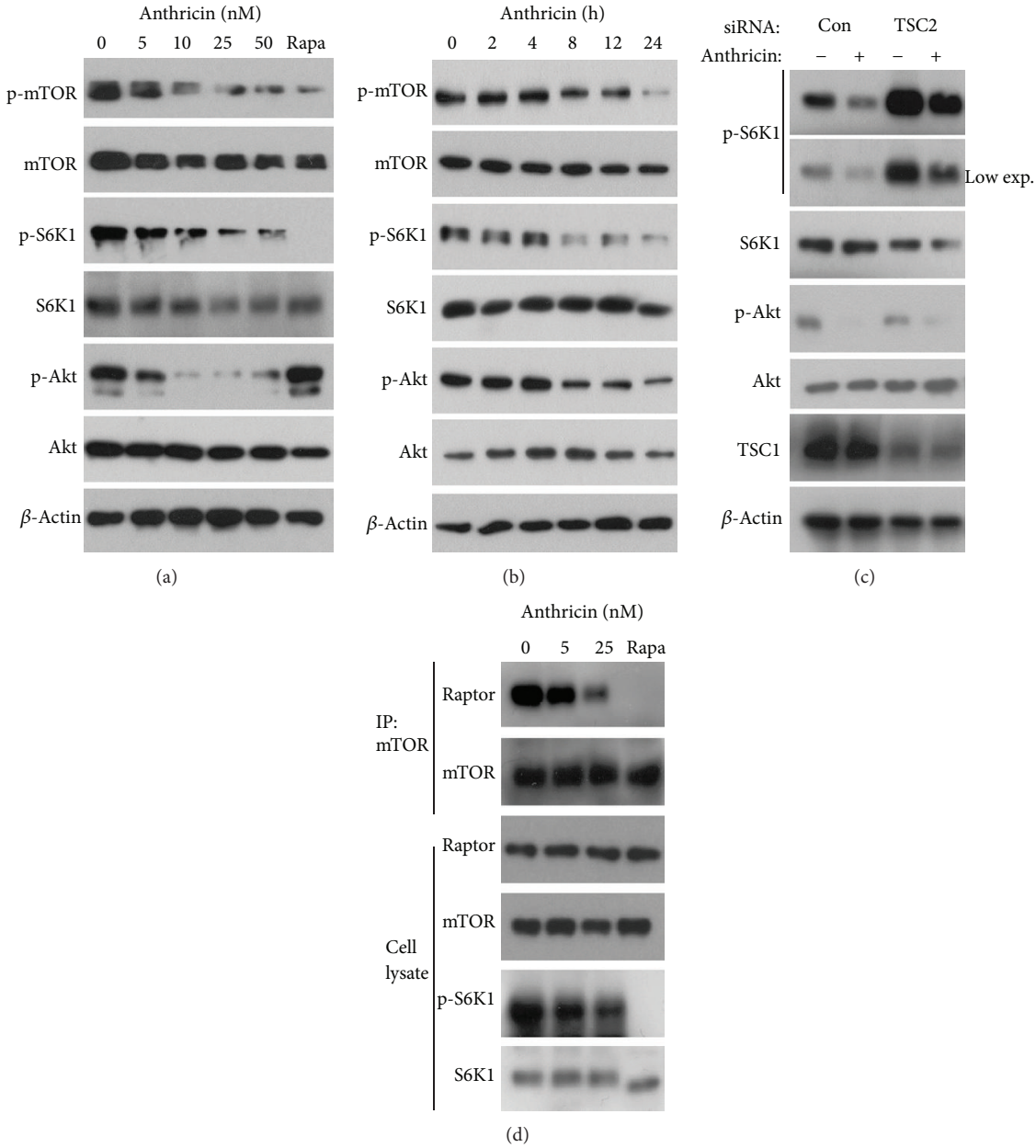

Figure 4: Anthricin inhibits Akt/mTOR signaling. (a) Anthricin inhibits the phosphorylation of mTOR, S6K1, and Akt in a dose-dependent manner. MCF-7 cells were treated with varying concentrations of the drug for 12 h or 100 nM rapamycin for 1 h, and the phosphorylation states of mTOR (p-Ser2448), S6K1 (p-Thr389), and Akt (p-Ser473) were analyzed by immunoblotting. (b) Anthricin inhibits the phosphorylation of mTOR, S6K1, and Akt in a time-dependent manner. MCF-7 cells were treated with 25 nM anthricin for the time period specified. (c) Anthricin is a potential target of mTOR and Akt. MCF-7 cells were transduced with TSC2 siRNA or scrambled siRNA (control). Cells were treated with or without 25 nM anthricin, and the proteins were analyzed by immunoblotting. (d) Anthricin disrupts the association between mTOR and raptor. mTOR immunoprecipitates were isolated from anthricin-treated MCF-7 cells by using an anti-mTOR antibody, and the amounts of raptor and mTOR in the immune complexes were analyzed by immunoblotting.

which has a dual function in cancer cell lines (death and survival). Recent studies have suggested that autophagy plays a cytoprotective role in breast cancer cells [29, 30]. Our data for autophagy flux assays and immunostaining demonstrated that anthricin induced autophagy. An increase in autophagosome accumulation may be caused either by increased autophagosome formation or by the blockage of autophagic degradation after fusion of the autophagosome with a lysosome. In the autophagy flux assay, we observed a decrease in the levels of p62, which is degraded in the autolysosome. The formation of endogenous LC3 or GFP-LC3 puncta was increased in anthricin-treated breast cancer cells. Collectively, these data demonstrate that anthricin is a positive regulator of the autophagic process.

Our study provided strong evidence that anthricin induces apoptosis and autophagy. According to our results,

autophagy plays an important role in the survival of breast cancer cells. Notably, apoptosis increased on cotreatment with anthricin and a pharmacological autophagy inhibitor, CQ. We also investigated whether the genetic knockdown of autophagy-related proteins enhanced apoptosis in MCF-7 cells. MCF-7 cells were silenced using shULK1 and shAtg13; these proteins play a critical role in the autophagic process [16]. The knockdown of ULK1 and Atg13 enhanced cell death in MCF-7 cells after treatment with anthricin. These results suggest that autophagy inhibition can be an apoptosis-enhancing pathway in breast cancer cells. Cells have developed a defense mechanism in response to changes in the intracellular environment. During stress, prosurvival and prodeath processes are concomitantly activated in cells. The final outcome depends on the balance between life and death during stress. If exposure to stress results in damage to organelles, then the cell can clear the damaged organelles via autophagy, but if the cell is beyond rescue, apoptosis will become.

Accumulating data suggest that mTOR is an attractive target for the development of novel anticancer molecules. More specifically, the phosphatidylinositol-3-kinase (PI3K)/Akt/mTOR pathway plays a critical role in multiple cellular functions, including proliferation, growth, and metabolism, and this pathway is highly activated in many types of cancer [13, 25]. Our data showed that anthricin treatment reduced the phosphorylation of Akt, S6K1, and mTOR, suggesting that anthricin inhibits the Akt/mTOR signaling pathway, thus inhibiting breast cancer growth. In fact, this pathway can modulate estrogen-independent growth, which may lead to endocrine resistance [31]. Anthricin also induced autophagy, which is directly regulated by mTOR. Autophagy induction under unfavorable conditions may play a cytoprotective role in breast cancer cells. Recent data suggest that coordinate inhibition of the mTOR and autophagy pathways promotes apoptosis [32], and these findings may require further preclinical and clinical study of coordinate autophagy and Akt/mTOR inhibition as a rational approach to improve therapeutic outcomes in breast cancer is warranted.

In conclusion, our most significant finding is that anthricin isolated from *A. sylvestris* inhibits Akt/mTOR signaling in breast cancer cells. Thus, anthricin inhibits the growth of breast cancer cells and its apoptotic effects are enhanced by autophagy inhibition. The current study shows that anthricin may be an effective as an anti-breast cancer agent. Our data predict that both autophagy and mTOR inhibition may be useful therapeutic approaches for breast cancer.

Authors' Contribution

Chang Hwa Jung and Heemun Kim contributed equally to the work.

Acknowledgments

This study was supported by a grant from the Korea Food Research Institute and by the R&D Program of MKE/KEIT-10033818.

References

[1] Society AC, *Cancer Facts & Figures 2011–2013*, American Cancer Society, Atlanta, Ga, USA, 2013.

[2] V. Androutsopoulos, R. R. J. Arroo, J. F. Hall, S. Surichan, and G. A. Potter, "Antiproliferative and cytostatic effects of the natural product eupatorin on MDA-MB-468 human breast cancer cells due to CYP1-mediated metabolism," *Breast Cancer Research*, vol. 10, no. 3, article R39, 2008.

[3] M. H. Elamin, M. H. Daghestani, S. A. Omer et al., "Olive oil oleuropein has anti-breast cancer properties with higher efficiency on ER-negative cells," *Food and Chemical Toxicology*, vol. 53, pp. 310–316, 2013.

[4] E. J. Choi and G. H. Kim, "Antiproliferative activity of daidzein and genistein may be related to ERα/c-erbB-2 expression in human breast cancer cells," *Molecular Medicine Reports*, vol. 7, no. 3, pp. 781–784, 2013.

[5] Y. Li, H. Chen, T. M. Hardy, and T. O. Tollefsbol, "Epigenetic regulation of multiple tumor-related genes leads to suppression of breast tumorigenesis by dietary genistein," *PLoS ONE*, vol. 8, no. 1, Article ID e54369, 2013.

[6] M. Athar, J. H. Back, L. Kopelovich, D. R. Bickers, and A. L. Kim, "Multiple molecular targets of resveratrol: anti-carcinogenic mechanisms," *Archives of Biochemistry and Biophysics*, vol. 486, no. 2, pp. 95–102, 2009.

[7] O. Hendrawati, H. J. Woerdenbag, J. Hille, W. J. Quax, and O. Kayser, "Seasonal variations in the deoxypodophyllotoxin content and yield of Anthriscus sylvestris L. (Hoffm.) grown in the field and under controlled conditions," *Journal of Agricultural and Food Chemistry*, vol. 59, no. 15, pp. 8132–8139, 2011.

[8] G. Jeong, O. Kwon, B. Park et al., "Lignans and coumarins from the roots of *Anthriscus sylvestris* and their increase of caspase-3 activity in HL-60 cells," *Biological and Pharmaceutical Bulletin*, vol. 30, no. 7, pp. 1340–1343, 2007.

[9] K. Y. Kim, H. J. Cho, S. N. Yu et al., "Interplay of reactive oxygen species, intracellular Ca(2+) surge and loss of mitochondrial homeostasis in the apoptotic ablation of prostate cancer cells by deoxypodophyllotoxin," *Journal of Cellular Biochemistry*, 2012.

[10] N. Muto, T. Tomokuni, M. Haramoto et al., "Isolation of apoptosis- and differentiation-inducing substances toward human promyelocytic leukemia HL-60 cells from leaves of Juniperus taxifolia," *Bioscience, Biotechnology and Biochemistry*, vol. 72, no. 2, pp. 477–484, 2008.

[11] S. Y. Shin, Y. Yong, C. G. Kim, Y. H. Lee, and Y. Lim, "Deoxypodophyllotoxin induces G2/M cell cycle arrest and apoptosis in HeLa cells," *Cancer Letters*, vol. 287, no. 2, pp. 231–239, 2010.

[12] Y. Yong, S. Y. Shin, Y. H. Lee, and Y. Lim, "Antitumor activity of deoxypodophyllotoxin isolated from *Anthriscus sylvestris*: induction of G2/M cell cycle arrest and caspase-dependent apoptosis," *Bioorganic and Medicinal Chemistry Letters*, vol. 19, no. 15, pp. 4367–4371, 2009.

[13] J. Baselga, "Targeting the phosphoinositide-3 (PI3) kinase pathway in breast cancer.," *The oncologist*, vol. 16, supplement, pp. 12–19, 2011.

[14] C. García-García, Y. H. Ibrahim, V. Serra et al., "Dual mTORC1/2 and HER2 blockade results in antitumor activity in preclinical models of breast cancer resistant to anti-HER2 therapy," *Clinical Cancer Research*, vol. 18, no. 9, pp. 2603–2612, 2012.

[15] P. Maycotte and A. Thorburn, "Autophagy and cancer therapy," *Cancer Biology and Therapy*, vol. 11, no. 2, pp. 127–137, 2011.

[16] C. H. Jung, C. B. Jun, S. Ro et al., "ULK-Atg13-FIP200 complexes mediate mTOR signaling to the autophagy machinery," *Molecular Biology of the Cell*, vol. 20, no. 7, pp. 1992–2003, 2009.

[17] C. Amaral, M. Borges, S. Melo et al., "Apoptosis and autophagy in breast cancer cells following exemestane treatment," *PLoS ONE*, vol. 7, no. 8, Article ID e42398, 2012.

[18] D.-H. Kim, D. D. Sarbassov, S. M. Ali et al., "mTOR interacts with raptor to form a nutrient-sensitive complex that signals to the cell growth machinery," *Cell*, vol. 110, no. 2, pp. 163–175, 2002.

[19] G. R. Stark and W. R. Taylor, "Control of the G2/M transition," *Molecular Biotechnology*, vol. 32, no. 3, pp. 227–248, 2006.

[20] S. A. Tooze, H. B. J. Jefferies, E. Kalie et al., "Trafficking and signaling in mammalian autophagy," *IUBMB Life*, vol. 62, no. 7, pp. 503–508, 2010.

[21] S. Zhou, L. Zhao, M. Kuang et al., "Autophagy in tumorigenesis and cancer therapy: Dr. Jekyll or Mr. Hyde?" *Cancer Letters*, vol. 323, no. 2, pp. 115–127, 2012.

[22] D. J. Klionsky, F. C. Abdalla, H. Abeliovich et al., "Guidelines for the use and interpretation of assays for monitoring autophagy," *Autophagy*, vol. 8, no. 4, pp. 445–544, 2012.

[23] N. Mizushima and T. Yoshimori, "How to interpret LC3 immunoblotting," *Autophagy*, vol. 3, no. 6, pp. 542–545, 2007.

[24] R. Xie, S. Nguyen, W. L. McKeehan, and L. Liu, "Acetylated microtubules are required for fusion of autophagosomes with lysosomes," *BMC Cell Biology*, vol. 11, article 89, 2010.

[25] T. W. Grunt and G. L. Mariani, "Novel approaches for molecular targeted therapy of breast cancer: interfering with PI3K/AKT/mTOR signaling," *Curr Cancer Drug Targets*, vol. 13, no. 2, pp. 188–204, 2013.

[26] M. P. Ghadimi, G. Lopez, K. E. Torres et al., "Targeting the PI3K/mTOR axis, alone and in combination with autophagy blockade, for the treatment of malignant peripheral nerve sheath tumors," *Molecular Cancer Therapeutics*, vol. 11, no. 8, pp. 1758–1769, 2012.

[27] Y. Zhang, S. Xu, J. Lin et al., "mTORC1 is a target of nordihydroguaiaretic acid to prevent breast tumor growth in vitro and in vivo," *Breast Cancer Research and Treatment*, vol. 136, no. 2, pp. 379–388, 2012.

[28] Y. Kim, S. Kim, Y. You, and B. Ahn, "Deoxypodophyllotoxin; the cytotoxic and antiangiogenic component from *Pulsatilla koreana*," *Planta Medica*, vol. 68, no. 3, pp. 271–274, 2002.

[29] S. Kanematsu, N. Uehara, H. Miki et al., "Autophagy inhibition enhances sulforaphane-induced apoptosis in human breast cancer cells," *Anticancer Research*, vol. 30, no. 9, pp. 3381–3390, 2010.

[30] V. Prabhu, P. Srivastava, N. Yadav et al., "Resveratrol depletes mitochondrial DNA and inhibition of autophagy enhances resveratrol-induced caspase activation," *Mitochondrion*, 2012.

[31] P. Malaguti, S. Vari, F. Cognetti, and A. Fabi, "The Mammalian target of rapamycin inhibitors in breast cancer: current evidence and future directions," *Anticancer Research*, vol. 33, no. 1, pp. 21–28, 2013.

[32] X. Xie, E. P. White, and J. M. Mehnert, "Coordinate autophagy and mTOR pathway inhibition enhances cell death in melanoma," *PLoS ONE*, vol. 8, no. 1, Article ID e55096, 2013.